UNITED STATES
DEPARTMENT OF THE INTERIOR
GEOLOGICAL SURVEY

NATIONAL EARTHQUAKE HAZARDS REDUCTION PROGRAM, SUMMARIES OF TECHNICAL REPORTS VOLUME XXI

Prepared by Participants in

NATIONAL EARTHQUAKE HAZARDS REDUCTION PROGRAM

Compiled by

Muriel L. Jacobson

Thelma R. Rodriguez

The research results described in the following summaries were submitted by the investigators on October 16, 1985 and cover the 6-months period from May 1, 1985 through October 31, 1985. These reports include both work performed under contracts administered by the Geological Survey and work by members of the Geological Survey. The report summaries are grouped into the three major elements of the National Earthquake Hazards Reduction Program.

Open File Report No. 86-31

The data and interpretations in these progress reports may be reevaluated by the investigators upon completion of the research. Readers who wish to cite findings described herein should confirm their accuracy with the author.

CONTENTS

Earthquake Hazards Reduction Program

Page

ELEMENT I - Recent Tectonics and Earthquake Potential

Determine the tectonic framework and earthquake potential of U.S. seismogenic zones with significant hazard potential.

Objective (I-2): Source zone characteristics

Identify and map active crustal faults, using geophysical and geological data to interpret the structure and geometry of seismogenic zones.

1. Identify and map active faults in seismic regions.
2. Combine geophysical and geologic data to interpret tectonic setting of seismogenic zones.................. 57

Objective (I-3): Earthquake potential

Estimate fault slip rates, earthquake magnitudes, and recurrence intervals for seismogenic zones and faults disclosed by research under Objectives T-1 and T-2, using geological and geophysical data.

1. Earthquake potential estimates for regions of the U.S. west of 100°W.
2. Earthquake potential estimates for regions of the U.S. east of 100°W.
3. Support studies in geochemistry, geology, and soils science that enable fault movements to be accurately dated... 103

ELEMENT II. Earthquake Prediction Research

Collect observational data and develop the instrumentation, methodologies, and physical understanding needed to predict damaging earthquakes.

Page

Objective (II-1): Prediction Methodology and Evaluation

Develop methods to provide a rational basis for estimates of increased earthquake potential. Evaluate the relevance of various geophysical, geochemical, and hydrological data for earthquake prediction.

1. Develop, operate and evaluate instrumentation for monitoring potential earthquake precursors.
2. Analyze and evaluate seismicity data collected prior to medium and large earthquakes.
3. Obtain and analyze data from seismically active regions of foreign countries through cooperative projects with the host countries.
4. Systematically evaluate data and develop statistics that relate observations of specific phenomena to earthquake occurrence.
5. Develop, study and test prediction methods that can be used to proceed from estimates of long-range earthquake potential to specific short-term predictions.. 157

Objective (II-2): Earthquake Prediction Experiments

Conduct data collection and analysis experiments in areas of California capable of great earthquakes, where large populations are at risk. The experiments will emphasize improved coordination of data collection, data reporting, review and analysis according to set schedules and standards.

1. Collect and analyze data for an earthquake prediction experiment in southern California, concentrating on the southern San Andreas fault from Parkfield, California to the Salton Sea.
2. Collect and analyze data for an earthquake prediction experiment in central California, concentrating on the San Andreas fault north of Parkfield, California........ 266

Objective (II-3): Theoretical, Laboratory and Fault Zone Studies

Improve our understanding of the physics of earthquake processes through theoretical and laboratory studies to guide and test earthquake prediction observations and data analysis. Measure physical properties of those zones selected for earthquake experiments, including stress, temperature, elastic and anelastic characteristics, pore pressure, and material properties.

Objective (II-4): Induced Seismicity Studies

Determine the physical mechanism responsible for reservoir-induced seismicity and develop techniques for predicting and mitigating this phenomena.

ELEMENT III Evaluation of Regional and Urban Earthquake Hazards

Delineate, evaluate, and document earthquake hazards and risk in urban regions at seismic risk. Regions of interest, in order of priority, are:

1) The Wasatch Front
2) Southern California
3) Northern California
4) Anchorage Region
5) Puget Sound
6) Mississippi Valley
7) Charleston Region

ELEMENT IV Earthquake Data and Information Services

Most of the technical summaries contained in this volume are for research contracts solicited by RFP-1485. The description in the previous table of contents corresponds to respective Elements and Objectives of that RFP. Additionally some of the summaries are for research objectives that were initiated in earlier years. These objectives are covered in the descriptions found in the following table of contents.

Initiated before FY83

I. Earthquake Hazards and Risk Assessment (H)

II. Earthquake Prediction (P)

Southern California Seismic Arrays

Contract No. 14-08-0001-21854

Clarence R. Allen
Seismological Laboratory, California Institute of Technology
Pasadena, California 91125 (818-356-6904)

Investigations

This semi-annual Technical Report Summary covers the six-month period from 1 April 1985 to 30 September 1985. The contract's purpose is the partial support of the joint USGS-Caltech Southern California Seismographic Network, which is also supported by other groups, as well as by direct USGS funding of its own employees at Caltech. According to the contract, the primary visible product will be a joint Caltech-USGS catalog of earthquakes in the southern California region; quarterly epicenter maps and preliminary catalogs are also required and have been submitted as due during the contract period. About 250 preliminary catalogs are routinely distributed to interested parties.

Results

Figure 1 shows the epicenters of all cataloged shocks that were located during the six-month reporting period. Some of the seismic highlights during this period were:

Number of earthquakes processed: 6590
Number of earthquakes of M = 3.0 and greater: 166
Number of earthquakes of M = 4.0 and greater: 20
Largest event within network area: M = 4.6 (22 August, near China Lake)
Largest nearby shock: M = 6.0 (4 August, near Coalinga)
Smallest reported felt earthquake: M = 1.4 (16 September, San Diego)

The most interesting earthquake sequences during the reporting period were: (1) the Coalinga sequence in early August, which extended the earlier activity somewhat farther southeast; (2) the mid-August swarm near China Lake, continuing long-lasting swarm activity there; and (3) the mid-June series of widely felt shocks centered just south of downtown San Diego (Fig. 2). The largest of these San Diego events are now assigned magnitudes of 3.9, 4.0, and 3.9; they led to California's first "earthquake alert," owing to the judged possibility that they might be followed by still larger events in the same area. Although this was a somewhat "new" location for seismic activity, a glance at Figure 1 shows that other seismic activity during the period was fairly typical of that of the past few years.

A significant improvement in data-analysis capabilities of the joint network took place during the reporting period with the replacement of the aging PDP 11/70 computer with a new VAX 750 system. This system is used in off-line data processing, and the new VAX computer should not only make routine analysis more efficient, but, importantly, will also allow much easier access to array data by research users. Appropriate software for the new computer system is currently under active development.

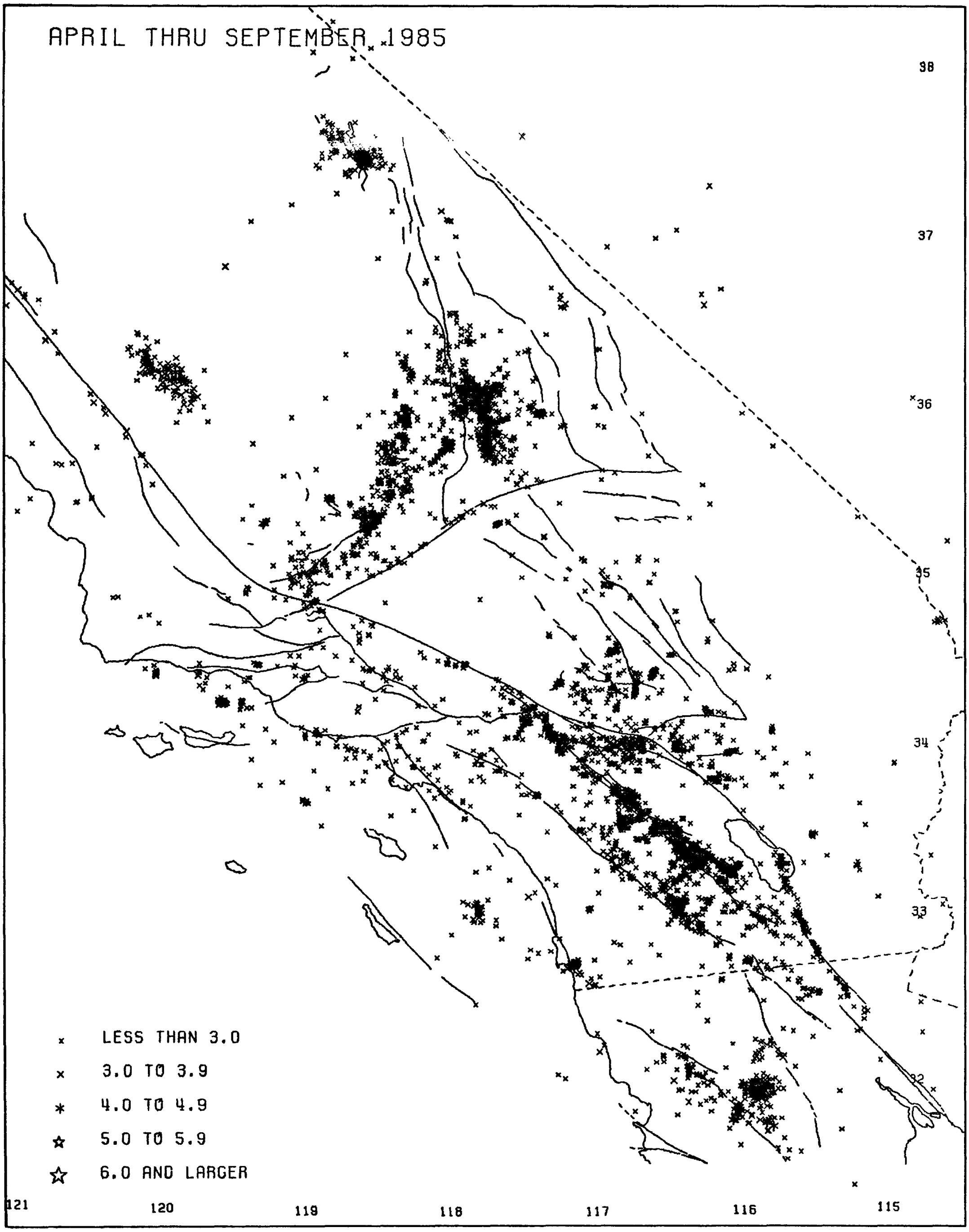

Figure 1.--Epicenters of larger earthquakes in the southern California region, 1 April 1985 to 30 September 1985.

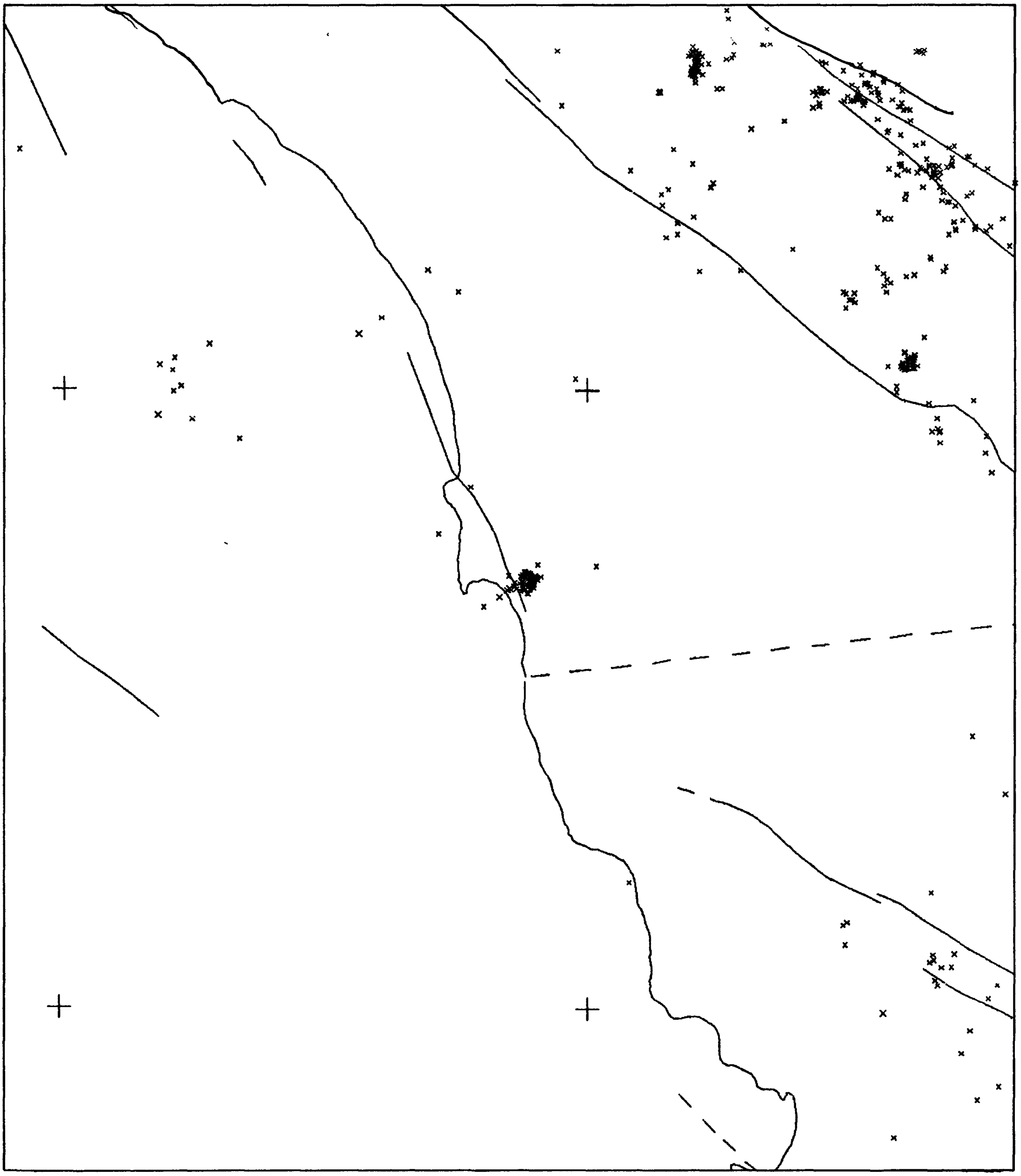

Figure 2.--Epicenters near San Diego during June 1985. Data are preliminary, and locations may be biased.

REGIONAL SEISMIC MONITORING ALONG THE WASATCH FRONT URBAN CORRIDOR AND ADJACENT INTERMOUNTAIN SEISMIC BELT

14-08-0001-21857

W. J. ARABASZ, R.B. SMITH, and J.C. PECHMANN
Department of Geology and Geophysics
University of Utah
Salt Lake City, Utah 84112
(801)581-6274

Investigations

This contract supports "network operations" (including a computerized central recording laboratory) associated with the University of Utah 80-station regional seismic telemetry network. USGS support focuses on the seismically hazardous Wasatch Front urban corridor of north-central Utah but also encompasses neighboring areas of the Intermountain seismic belt (ISB). The University of Utah maintains de facto responsibility for earthquake surveillance, including emergency response and direct public interface, for an 800-km-long segment of the ISB between Yellowstone Park and southernmost Utah. The State of Utah, the U.S. Bureau of Reclamation, the National Park Service and the U.S. Geological Survey (Geothermal Research Program) also contributed support to operation of the University of Utah network during the report period.

Primary products of this USGS contract are quarterly earthquake catalogs and a semi-annual data submission, in magnetic-tape form, to the USGS Data Archive.

Results

Figure 1 shows the epicenters of 221 earthquakes ($M \leqslant 3.2$) located in part of the University of Utah study area designated the "Utah region" (lat. 36.75°-42.5°N, long. 108.75°-114.25°W) during the six-month period April 1 to September 30, 1985. The seismicity includes three shocks of M3.0 or greater and two felt earthquakes. Spatial clustering in Figure 1 relates, in part, to three swarms ($M \leqslant 2.6$) at the northern end and to the north of the Great Salt Lake, and to mining-related earthquakes in the vicinity of active underground coal mining near Price in east-central Utah.

North of the Utah region, four felt earthquakes of M4.1 to M4.6 (together with numerous smaller earthquakes) occurred between August 21 and September 7, 1985, in a small source region (43.2°N, 110.9°W) 30 km south of Jackson, Wyoming, near Palisades Reservoir. Figure 2 (from Richins and Arabasz, 1985) indicates that the source region does not simply coincide with a zone of major active faulting, but does lie within a belt of diffuse background seismicity trending northeastward through the SE Idaho-western Wyoming region. The epicenter map shown in Figure 2 represents an unpublished compilation available from the University of Utah and reported by Richins and Arabasz (1985). The catalog is for the nine-year period 1976 to

1984 and includes approximately 2,200 earthquakes ($M \leqslant 4.7$). It should be noted that the catalog reflects major efforts to collect seismographic data from diverse sources in the region, and to discriminate frequent surface blasting at large phosphate mines in SE Idaho. The NEIS/NGDC data file for the same area and time period consists of 80 earthquakes.

Reports and Publications

Pechmann, J.C., Utah earthquake activity January through March 1985, Wasatch Front Forum, v. 1, no. 4, 1, 1985.

Pechmann, J.C., Utah earthquake activity April through June 1985, Wasatch Front Forum, v. 2, no. 1, 6, 1985.

Pechmann, J.C., W.D. Richins, and W.J. Arabasz, Utah Earthquakes, 1983, submitted for inclusion in U.S. Earthquakes, 1983.

Richins, W.D., and W.J. Arabasz, Seismicity of southeastern Idaho based on seismic monitoring using regional and temporary local networks, Geol. Soc. Am., Abstracts with Programs, 17, 261, 1985.

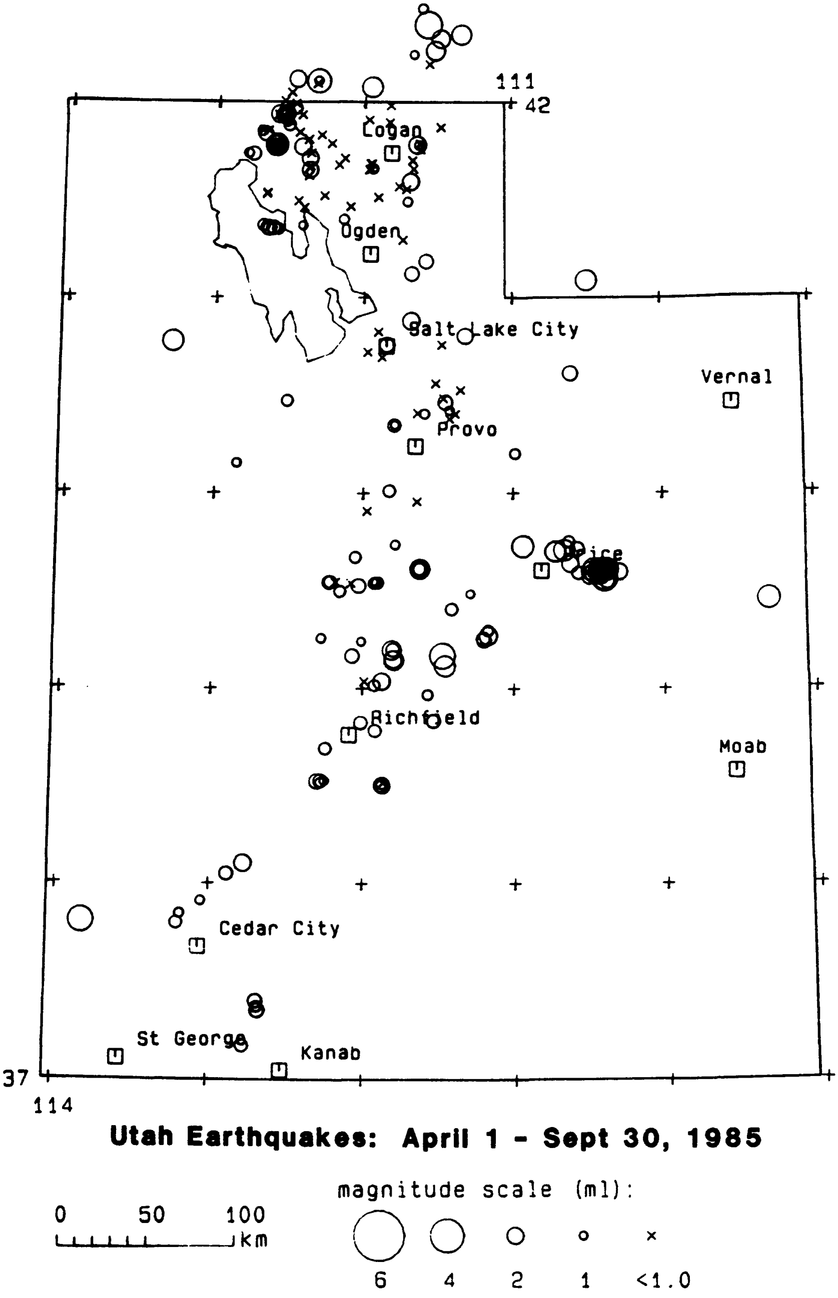

Utah Earthquakes: April 1 - Sept 30, 1985

Figure 1.

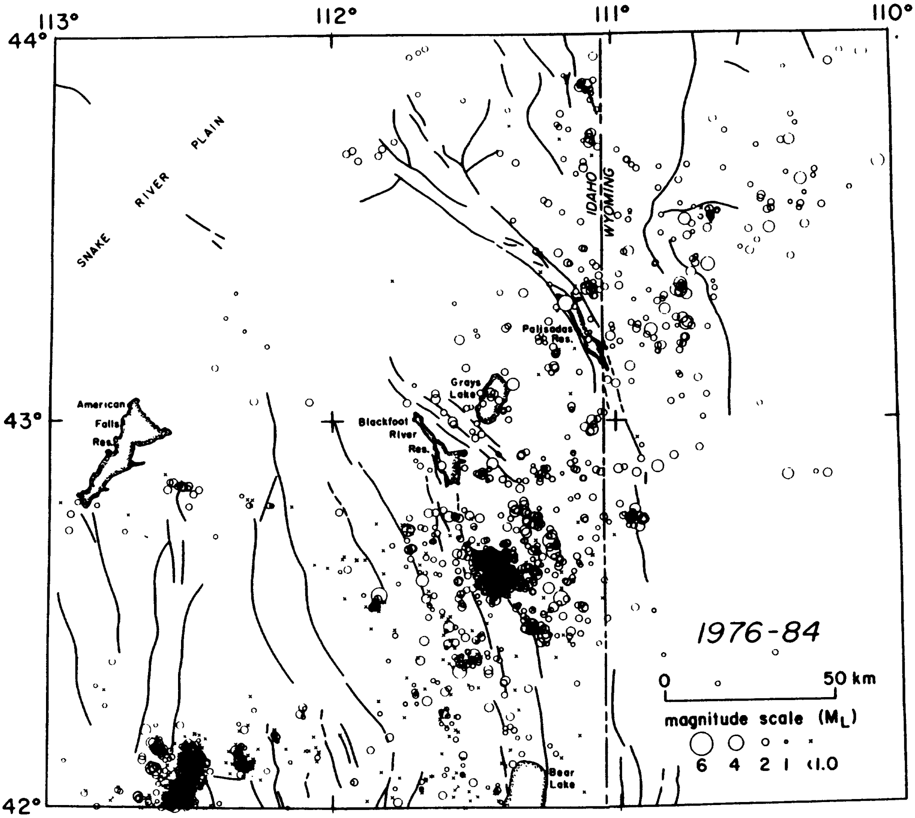

Figure 2. Epicenter map for SE Idaho/western Wyoming for 1976-84.

Seismological Data Processing

9930-03354

Barbara Bekins and Thomas Jackson

Branch of Seismology
U.S. Geological Survey
345 Middlefield Rd. MS 977
Menlo Park, California, 94025
(415) 323-8111 ext. 2965

Investigations

Computer data processing is now an integral part of seismological research. The purpose of this project is to provide a simple, powerful, computer data processing system to meet the needs of scientists in the earthquake prediction program and monitor earthquakes in northern California. This goal includes maintaining the ability to transfer data and programs over a network and the ability to share data and programs with USGS external contractors.

Results

The PDP11-70 UNIX system has continued to operate smoothly, and performs a large amount of computing for program projects. Some current statistics:

168	registered users
464730	1024-byte disk storage blocks used
75	login sessions per weekday

An Integrated Solutions Optimum System has been ordered to replace the PDP11-70. This is a so-called super micro system based on the Motorola 68020 micro-processor. The system has 24 terminal ports, a fast graphics subsystem, an SMD disk controller, a nine track 6250-1600 bpi tape drive, an ethernet controller, the 68881 floating point coprocessor, two million bytes of memory and a 16 bit parallel input device. It runs the 4.2BSD UNIX system and with demand paged virtual memory. Delivery of this system is expected in late October, 1985.

The Seismology Branch Vax 11/750 is now running under VMS version 4.2. Development is proceeding on combining data from the real time Ppicker, the CUSP system, and Calnet group processing into one unified database. These data will be accessed through the CUSP database system. In addition there are plans to bring up the SAC system written at Lawrence Livermore Labs. This system provides interactive analysis of seismic waveforms.

Work is proceeding on plans to replace the current system for digitizing of selected earthquakes recorded on FM tapes. This digitizing is presently performed on Data General Eclipse systems. Plans call for an IBM PC/XT for positioning the tape and a Tustin digitizer to digitize the data. These data will then be sent to the Vax 750 for storage and analysis using the CUSP system.

This project also handles one third of the support for the office Vax 780 operation. This support consisted of weekly and monthly disk backups to tape, authorizing new users, redistributing Seismology branch disk quotas, assisting users, and occasional miscellaneous activities related to computer operations and system management.

In the next few months all existing and terminal to computer connections by branch computer users will be changed over to the new Rolm PABX system. This will allow users to access several different computers at 9600 baud, or dial computers offsite from a terminal connection though their phone.

SEISMIC SOURCE MECHANISM STUDIES IN THE ANZA–COYOTE SEISMIC GAP

14-08-0001-21893

Jonathan Berger and James N. Brune
Institute of Geophysics and Planetary Physics
Scripps Institution of Oceanography
University of California, San Diego
La Jolla, CA 92093

Investigations:

This report covers the progress of the research investigating the Anza–Coyote Canyon seismic gap for the period of the first half of 1985. The objectives of this research are: 1) to study the mechanisms and seismic characteristics of small and moderate earthquakes, and 2) to determine if there are premonitory changes in seismic observables preceeding small and moderate earthquakes. This work is carried out in cooperation with Tom Hanks, Joe Fletcher and Linda Haar of the U.S. Geological Survey, Menlo Park.

Network Status:

During the period of this report, ten stations of the Anza Seismic Network were telemetering three-component data. The network was set at a low gain to try to record earthquakes up to magnitude 4 occurring inside the array.

The winter and spring of 1985 was relatively mild and did not impact the operation of the Anza Seismic Network. The thermal dependence of the remote radio transmitters has been eliminated so that future seasonal frequency adjustments of each station will not be necessary. There were no changes or modifications made to the data acquisition systems.

Seismicity:

In the six months of winter and spring, the Anza network recorded over 60 events which were large enough to locate and determine source parameters. These events had moments ranging from 5.5×10^{18} to 6.4×10^{20} dyne-cm, and stress drops ranging from about 1 to 100 bars (Brune model). The seismicity pattern seems unchanged from what has been observed before (Figure 1). The seismicity does not appear to be associated with the main trace of the San Jacinto fault on the north-west end of the array. These events in this area tend to be between the Hot Springs fault at depths of 12 to 19 km. The events on the south-east end of the array near the trifurcation of the San Jacinto fault also do not have any obvious associations with the identified fault traces. These earthquakes are occurring at depths between 8 and 12 km. The shallowest events are still occurring in the Cahuilla area.

Coherence Studies :

We installed an array of 9 portable digitizers to investigate the spatial coherence of seismic waves from local earthquakes. The stations are installed in a pattern of nested triangles with radii of 30 meters, 100 meters, and 300 meters. These portable recorders are all operated off of one master clock signal to give a common time base and to eliminate the relative drift between each recorder. We recorded 10 events during the period of this report on 5 or more recorders simultaneously. These events range in hypocentral distance from 16 to 60 kilometers. The programs needed to analyze this data were also being developed during this period of time. We will be calculating coherences and frequency-wavenumber diagrams for this data set, as well as examining the local variations of seismic source estimates.

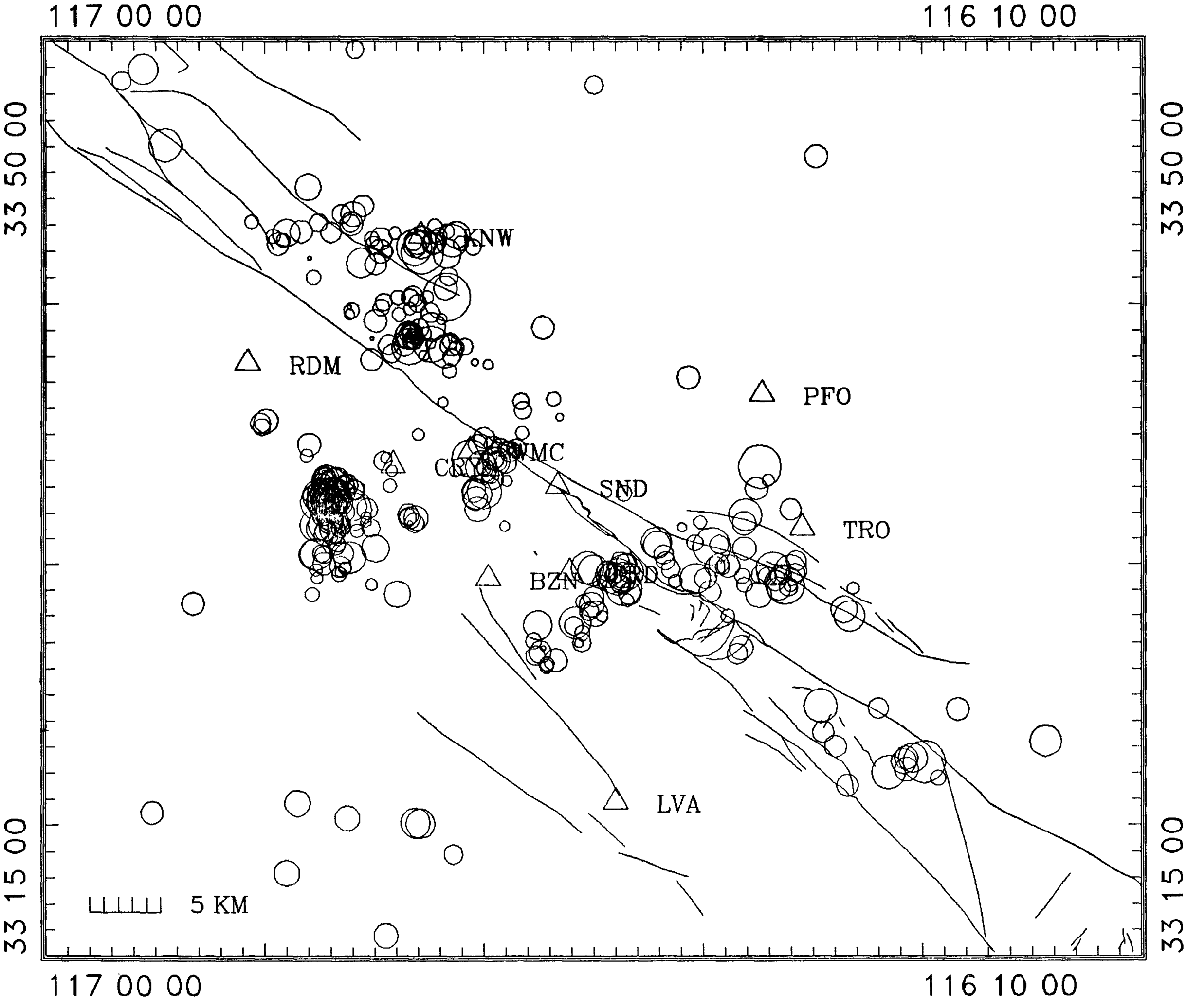
117 00 00
116 10 00
33 50 00
33 15 00
KNW
RDM
PFO
WMC
CR
SND
TRO
BZN
LVA
5 KM

Central Aleutian Islands Seismic Network

Contract No. 14-08-0001-21896

Selena Billington and Carl Kisslinger
Cooperative Institute for Research in Environmental Sciences
Campus Box 449, University of Colorado
Boulder, Colorado 80309

(303) 492-8028

Brief Description of Instrumentation and Data Reduction Methods

The Adak seismic network consists of 13 high-gain, high-frequency, two-component seismic systems and one six-component system (ADK) located at the Adak Naval Base. Station ADK has been in operation since the mid-1960s; nine of the additional stations were installed in 1974, three in 1975, and one each in 1976 and 1977.

Data from the stations are FM-telemetered to recording sites near the Naval Base, and are then transferred by cable to the Observatory on the Base. Data were originally recorded by Develocorder on 16 mm film; since 1980 the film recordings are back-up and the primary form of data recording has been on analog magnetic tape. The tapes are mailed to CIRES once a week.

At CIRES the analog tapes are played back at four-times the speed at which they were recorded into a computer which digitizes the data, automatically detects events, and writes an initial digital event tape. This tape is edited to eliminate spurious triggers, and a demultiplexed tape containing only seismic events is created. All subsequent processing is done on this tape. Times of arrival and wave amplitudes are read from an interactive graphics display terminal. The earthquakes are located using a program developed for this project by E. R. Engdahl, which uses corrections to the arrival times which are a function of the station and the source region of the earthquake.

Data Annotations

Earthquake locations are complete through June 1985. Our normal lag time for hypocenter locations is six-to-eight weeks, dependent on the postal service from Adak. The last major field trip to service the network was in July and August, 1984. Because of logistic problems, the westernmost station could not be reached at that time, and we were also unable to make needed return trips to two other far-west stations. Of the 28 short-period vertical and horizontal components, 20 were operating for the period of January through June, 1985. (A minor field trip in August, 1985, recovered one of the "down" components.)

Current Observations

277 earthquakes were located with data from the network during the six-month time period from January through June, 1985. Epicenters of these events are shown in Figure 1 and a vertical cross-section is given in Figure 2. Seven of the events located within the past six months were large enough to be located teleseismically (USGS PDEs), although one of the seven was not assigned a value of body-wave magnitude by the USGS and therefore does not show up as a square in Figures 1 and 2. Two events had m_b greater than or equal to 5.0, including an m_b 5.8 earthquake on May 24, seen at 178.271 ° W in Figure 1.

More detailed information about the network status and a catalog of the hypocenters determined for the time period reported here are included in our semi-annual data report to the U.S.G.S. Recent research using these data is reported in the Technical Summary for U.S.G.S. Grant No. 14-08-001-G881 in this volume.

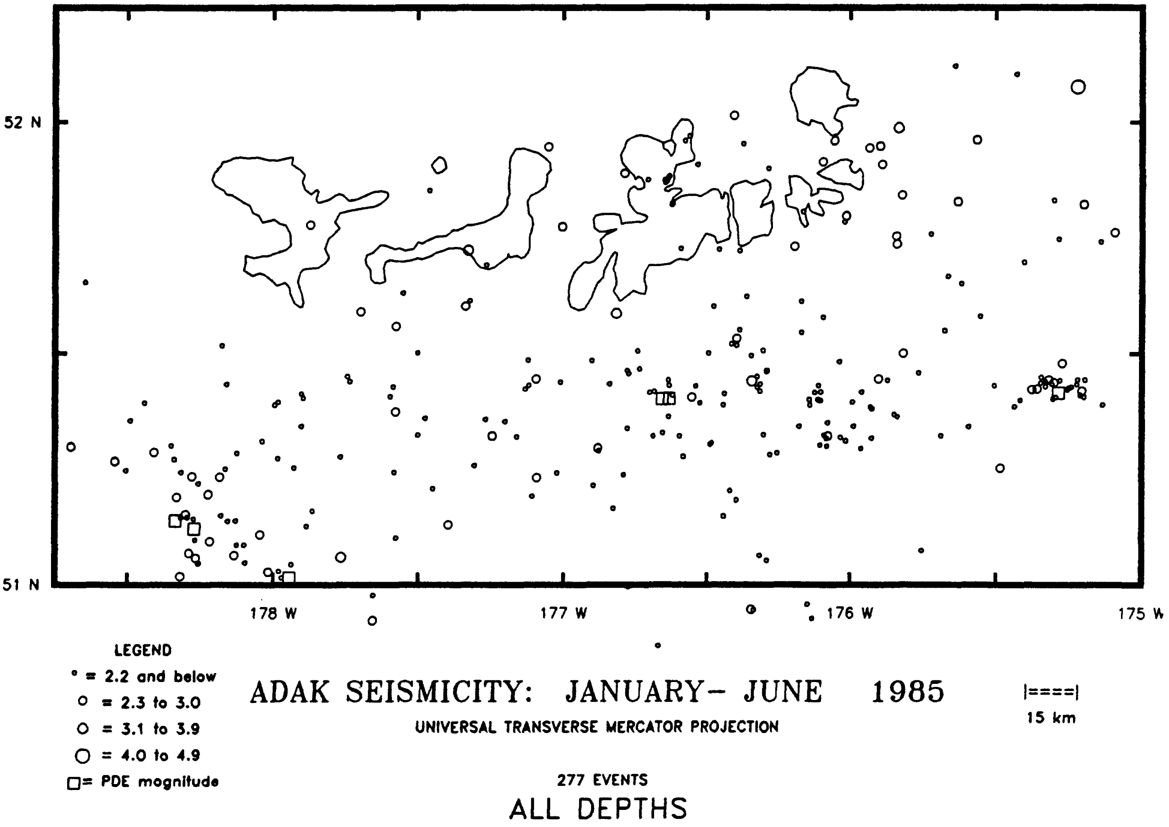

Figure 1: Map of seismicity which occurred from January 1 through June 30, 1985. All epicenters were determined from Adak network data. Events marked with squares are those for which a teleseismic body-wave magnitude has been determined by the USGS; all other events are shown by symbols which indicate the duration magnitude determined from Adak network data. The islands mapped (from Tanaga on the west to Great Sitkin on the east) indicate the geographic extent of the Adak seismic network.

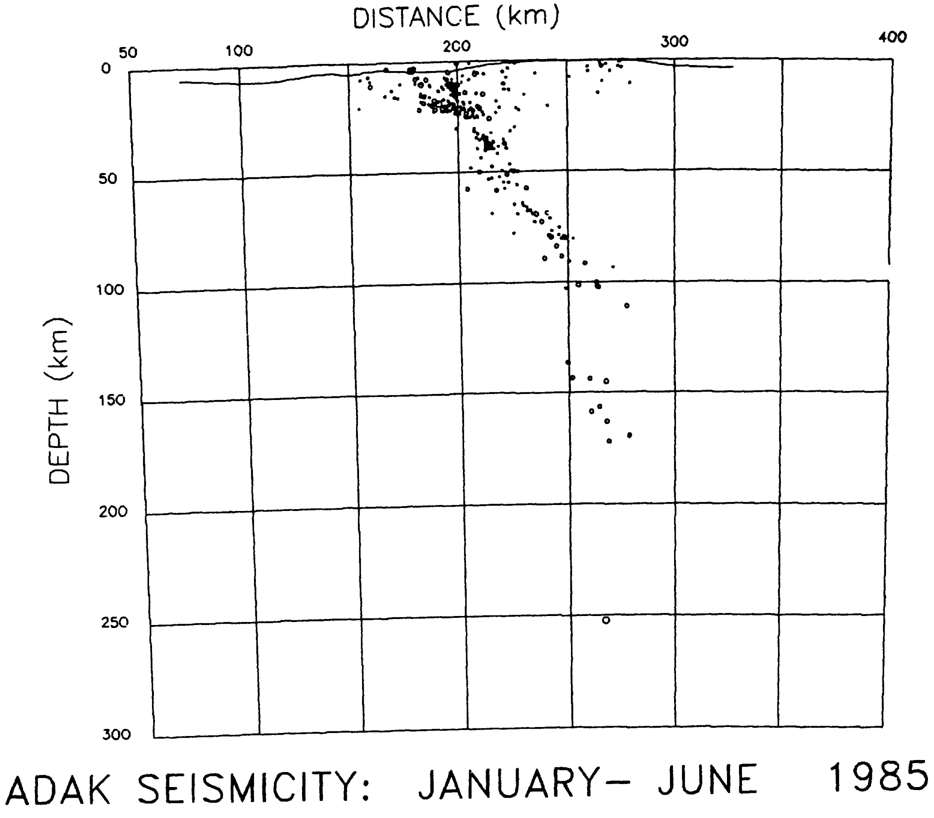

Figure 2: Vertical cross section of seismicity which occurred from January 1 through June 30, 1985. Events are projected according to their depth (corresponding roughly to vertical on the plot) and distance from the pole of the Aleutian volcanic line. The zero-point for the distance scale marked on the roughly-horizontal axis of the plot is arbitrary. Events marked with squares are those for which a teleseismic body-wave magnitude has been determined by the USGS; all other events are shown by symbols which indicate the duration magnitude determined from Adak network data. The irregular curve near the top of the section is bathymetry. Earthquakes deeper than about 100 km depth are mislocated too far south (left) as an effect of the slab on their ray paths to the local stations.

WESTERN GREAT BASIN-EASTERN SIERRA NEVADA SEISMIC NETWORK

Contract 14-08-0001-21867

E.J. Corbett, W.F. Nicks, and U.R. Vetter
Seismological Laboratory
University of Nevada
Reno, NV 89557
(702) 784-4975

Investigations

This program supports continued operation of a seismographic network in the western Great Basin of Nevada and eastern California, with the purpose of recording and location of earthquakes occurring in the western Great Basin, and acquiring a data base of phase times and analog and digital seismograms from these earthquakes. These data are used for research on: (1) ongoing seismicity in the western Great Basin with emphasis on the Long Valley caldera; (2) source mechanisms studies of these earthquakes; (3) possible precursory seismicity patterns in the White Mountains gap; (4) seismicity near reservoirs in the Lake Tahoe region; and (5) evaluation of the contribution that high-quality digital broad-band seismic stations can make to regional network-seismic studies.

Results

A. *Seismic Network Operation*

A number of changes have been made to our analog network. In May 1985, our Battle Mountain station (BMN) was converted to a digital station. This freed up one telemetry channel which allowed us to begin recording another phone line from the USGS Mammoth network. The new stations being recorded on-line are TUN, FBR, GRP, and MDP (3-comp) and are indicated on the figure. In late September 1985, DOE in conjunction with USC, attempted to make a change in instrumentation at DLH, the downhole seismometer in Long Valley caldera. While attempting to raise the 3-component seismometer package, the cable snapped and the instruments were lost. Consequently, UNR no longer records this station.

In summary, the University of Nevada is now operating 56 short-period analog seismographic stations, four of which are multi-component. In addition we are recording signals from 15 USGS stations, 2 U.C. Berkeley stations, and 1 from the California Division of Water Resources. All 74 of these stations are being recorded on analog magnetic tape at Reno as well as digitally by our on-line system.

In addition to the analog stations, the University of Nevada operates 3 remote digital seismographic stations. The digital stations provide broad-band (0.05-30 Hz), wide dynamic-range (96 dB) digitization of signals from a 3-component set of seismometers, and telemeter the data to the Reno facility where it is continuously recorded. The data is currently being recorded at 25 samples per second, but we are in the process of upgrading the system to 50 sps. In addition, the vertical components of these stations are also being recorded on our on-line recording system. In May 1985, the station at Bodie was moved to Battle Mountain, so that the three stations are now operating in mine tunnels at Mina, Battle Mountain, and Washoe Lake (MNA, BMN, and WCN). An additional station planned for the Las Vegas area has been delayed due the fact that the most desirable site is in a Bighorn sheep wilderness area, which requires an involved permitting process. Instead, we have begun construction of the fourth site at a location in northwestern Nevada (Donnelly Peak).

We are in the process of acquiring a microwave system to replace some of our major VHF radio links. Although the initial investment is substantial, the savings in telephone line costs will offset the expense in about 2 years. The principal advantages of the microwave system are increased reliability, especially during the winter months, less susceptibility to nearby lightning ground strikes, reduced radio interference, and a substantial increase in the number of signals we can transmit. The project has continued on schedule, with construction of our Slide Mountain microwave site nearing completion. As of mid-October the blockhouse has been completed, wired for power, the tower erected, and the transmission dish has been hung. What remains is the installation of the electronics on Slide Mountain and the receiver site on campus.

B. *On-line System*

A computer-based earthquake recording system has been operating successfully since May 1984. It provides on-line event detection and digitization of the analog seismic signals transmitted to the Reno data facility. This system facilitates analysis of large numbers of earthquakes and will allow waveform analysis of the network data. The triggering algorithm has been tuned sufficiently so that false triggers are now reduced to about 10%. We are still plagued by noise triggers during lightning storms, due to our dependence on VHF radio telemetry, but we expect this problem to be alleviated by the installation of the microwave system. We are currently recording 84 seismic signals and 4 time signals on the 96-channel on-line system. For the period May 11, 1984 to September 30, 1985, we have recorded and archived digital seismograms for 8,150 seismic events. Of this number 4,491 (55%) are local earthquakes that we have located and cataloged. The remainder of the data are teleseisms, regional events, nuclear tests, and local events of less than 10 seconds duration, (roughly magnitude < 1.5 M_L), for which we save the traces but do not time the arrivals.

C. *Data Analysis*

Our earthquake data have been timed and located through September 30, 1985. This is with the exception of some data gaps that exist between November 23 and December 31, 1984. These gaps resulted from our analysis staff being swamped by the large number of aftershocks following the magnitude 6 earthquake at Round Valley, and are being filled as time permits. Since the beginning of the contract period on November 1, 1984, the University of Nevada Seismological Laboratory registered 2,413 earthquakes. Of these events:

930 were magnitude 2 or greater;
109 were magnitude 3 or greater;
15 were magnitude 4 or greater;
3 were magnitude 5 or greater;
1 was magnitude 6 or greater.

As the figure shows, most of the activity since May has been continuing aftershocks of the November 23, 1984 Round Valley earthquake. In addition, a high level of seismic activity continues in the mountain block south of the Long Valley Caldera.

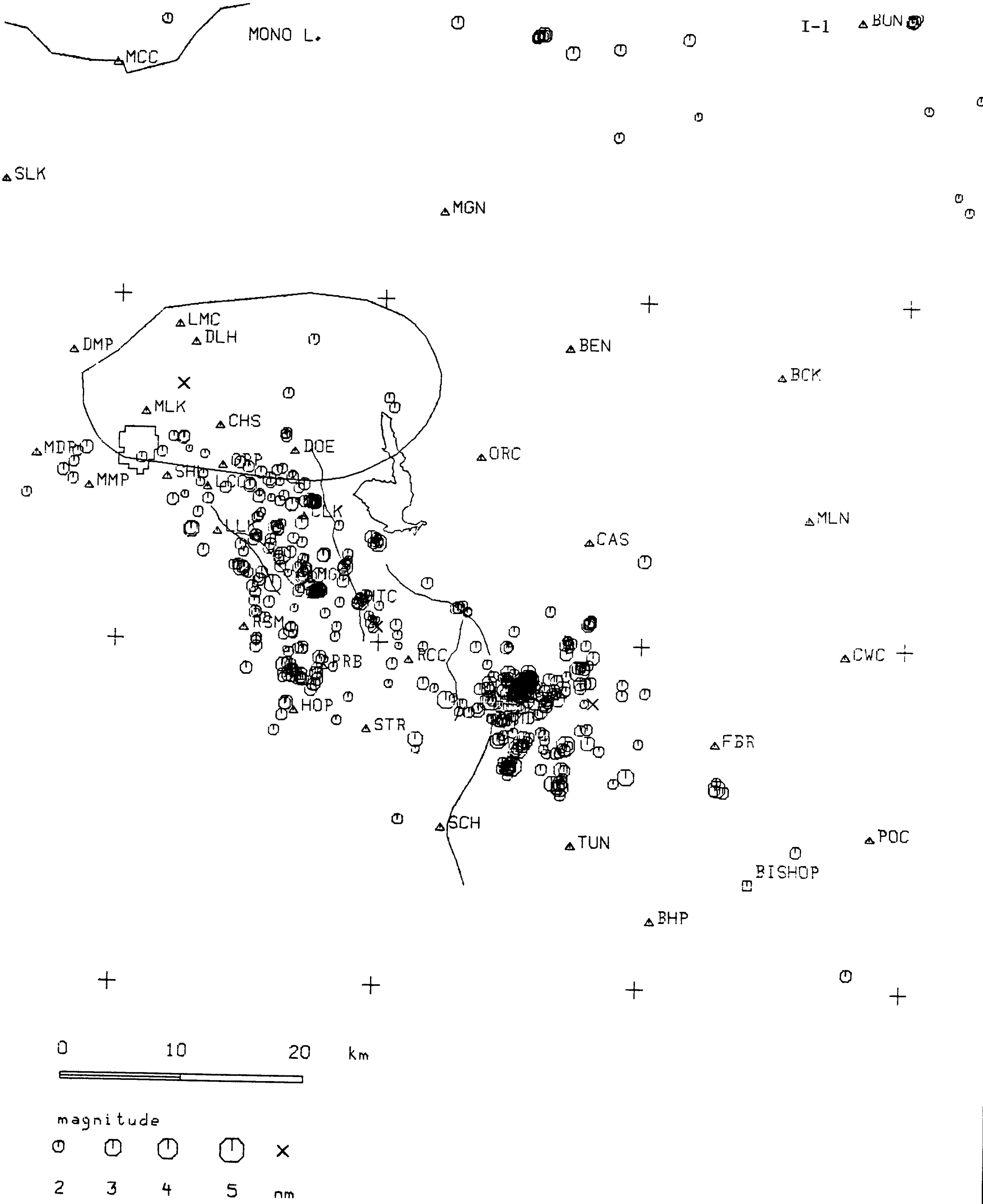

Mammoth seismicity -- May - Sept 1985

Regional Seismic Monitoring in Western Washington

14-08-0001-21861

R.S. Crosson and S.D. Malone
Geophysics Program
University of Washington
Seattle, WA 98195
(202) 543-8020

Investigations

Operation of the western Washington regional seismograph network and routine preliminary analysis of earthquakes in western Washington are carried out under this contract. Quarterly catalogs of seismic activity in Washington and Northern Oregon are available for 1984 and for the first two quarters of 1985, and are funded jointly by this contract and others. The time period covered by this summary is the six months from April 1, 1985 through September 30, 1985. Data are provided for USGS contract 14-08-0001-22007 as well as for other research programs. Network calibration and data assembly efforts are closely related to and overlap objectives under contract 22007, also summarized in this volume. Publications are listed in the 22007 summary.

Results

Network operation for stations in western Washington continued normally. No unusual regional earthquake activity was recorded. In late May and early June Mount St. Helens underwent a non-explosive eruptive phase accompanied by energetic seismicity. A new station (PGW) sited on the Kitsap Peninsula near Port Gamble began operation on April 12, 1985. This station, along with station MEW on McNeil Island, provide improved coverage of the central Puget Sound Basin. Station RPW in the Skagit Valley, lost in 1982, was reinstalled and began operation in September. An additional station in this region is being planned. A temporary station in the same area, BLS, was discontinued due to noise problems.

Since early 1982, some stations in the telemetered network have been calibrated so that recovery of absolute ground motion is possible. Figure 1 shows sites at which calibrated equipment is currently operating. Additional calibrated equipment will gradually be installed at selected stations as part of our program to upgrade data quality and increase operational reliability.

Equipment at each calibrated station consists of a Geotech S-13 seismometer and a Morrissey-Interface Technology amplifier/VCO package. Standard damping is 0.70 critical. Most calibrated stations use a Morrissey-Interface Technology discriminator, but some use Emtel discriminators which have similar response characteristics. The complete systems should all have similarly-shaped response curves differing only in absolute gain level. Figure 2 shows an approximate response curve for the whole system (with a 1-second seismometer free period) as recorded on the digital system at the University of Washington.

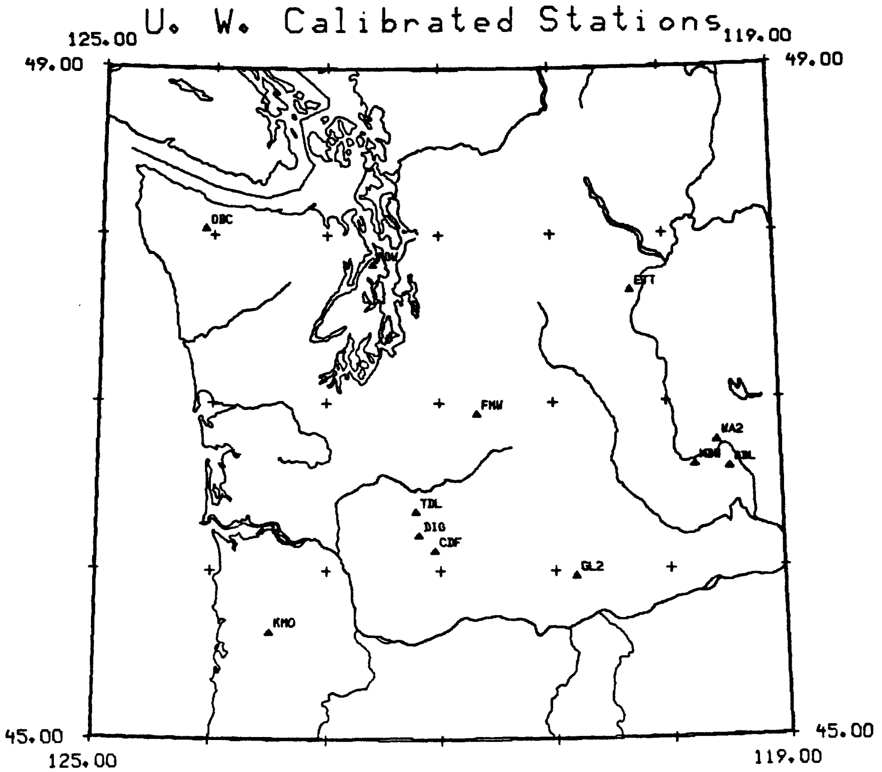

Figure 1. Calibrated stations currently in operation. Station DIG is a three component station. Other stations consist of one vertical S-13 seismometer, a "SLU" type VCO and use Emtel or Morrissey-Interface Technology discriminators.

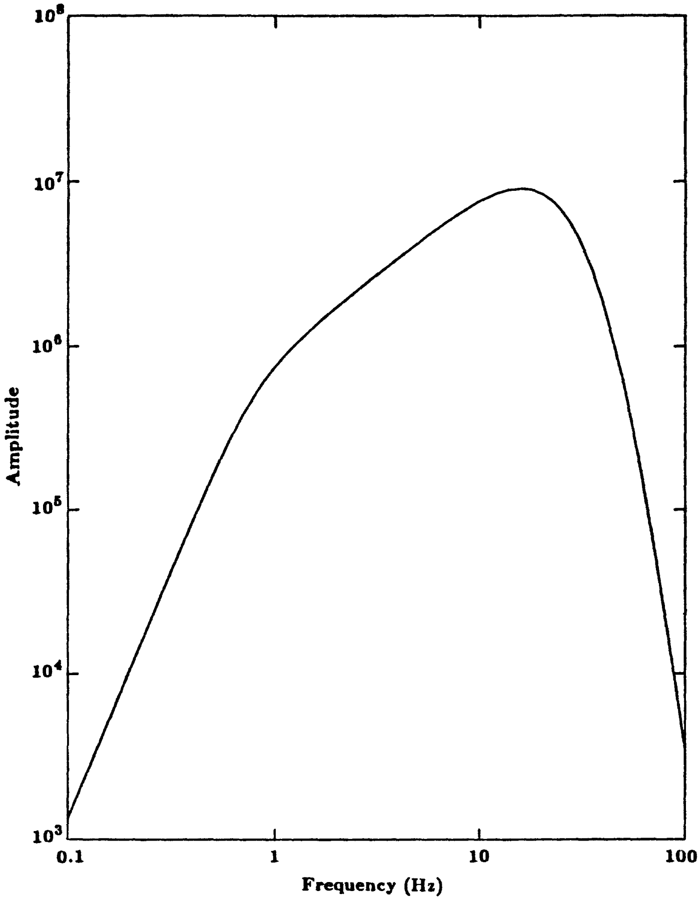

Figure 2. Approximate relative amplitude magnification curve for complete calibrated short-period system into online computer.

Figure 2. Approximate relative amplitude magnification curve for complete calibrated short-period system into online computer.

Figure 1. Calibrated stations currently in operation. Station DIG is a three component station. Other stations consist of one vertical S-13 seismometer, a "SLU" type VCO and use Emtel or Morrissey-Interface Technology discriminators.

Central California Network Operations

9930-01891

Wes Hall
Branch of Seismology
U.S. Geological Survey
345 Middlefield Raod, Mail Stop 977
Menlo Park, California 94025
(415) 323-8111, Ext. 2509

Investigations

Maintenance and recording of 329 seismograph stations (391 components) located in Northern and Central California. Also recording 72 components from other agencies. The area covered is from the Oregon border south to Santa Maria.

Results

1. Modified eighteen (18) J302M VCO/AMP. The improved version was designed to exhibit a temperature coefficient of less than 50 PPM/degree centigrade. (This is equivalent to 2Hz per 1000 Hz/40 degree centigrade).

2. Fremont Peak to Mission Peak - Installed a second 6' parabolic microwave antenna at Mission Peak for space diversity to alleviate fade problem.

3. Williams Hill to Fremont Peak - Installed a second 10' parabolic microwave antenna at Fremont Peak for space diversity to alleviate fade problem.

4. KAR to Hog Canyon - Installed a second 6' parabolic antenna at Hog Canyon to receive microwave signals from KAR.

5. Installed a 10' parabolic antenna at 60' level on an existing tower at Edwards AFB.

6. Constructed the footing and erected a 40' tower; mounted a 10' and 6' parabolic antenna at Strawberry Peak, Rim National Forest, San Bernadino, California. Tower and antennas are part of the Edward AFB-Strawberry Peak - Santigo Peak portion of the Southern California microwave system.

7. Currently, the Northern and Central California seismic network microwave system is carrying 31 phone lines (this equates to 240 signal channels).

Telemetry Networks

A number of modifications have been made to the Central California Seismic Network telemetry system to reduce telemetry costs. Approximately 200 stations are being carried on the microwave network. This network has been installed between Mount Tamalpias and San Luis Obispo with a branch to Parkfield and Menlo Park being the receiving point. At the present time additions are being made which will allow the system to be used in a full duplex mode.

ALASKA SEISMIC STUDIES

9930-01162

John C. Lahr, Christopher D. Stephens, Robert A. Page
Branch of Seismology
U. S. Geological Survey
345 Middlefield Road, MS 977
Menlo Park, California 94025
(415)323-8111, Ext. 2510

Investigations

1)Continued collection and analysis of data from the high-gain, short-period seismic network extending across southern Alaska from Juneau to Cook Inlet and inland across the Chugach mountains. Due to funding constraints, seismographs at fifteen sites, including all but two east of Icy Bay, were closed down during the summer field season. Three new seismographs were installed in the vicinity of Knight Island in western Prince William Sound to investigate the nature of a cluster of shallow seismicity that has persisted beneath the island since at least 1972. We plan to operate the three stations for one or two years and then move them to another special study area.

2) Continued monitoring in the region of the proposed Bradley Lake hydroelectric project on the southern Kenai Peninsula, a cooperative effort with the Alaska Power Authority.

3) Cooperated with the Branch of Engineering Seismology and Geology in operating 19 strong-motion accelerographs in southern Alaska, including 13 between Icy Bay and Cordova in the area of the Yakataga seismic gap.

Results

1) During the past six months preliminary hypocenters were determined for 1691 earthquakes that occurred between February and July, 1985 (Figure 1). Nineteen moderate-sized events with magnitudes ranging from 4.1 to 4.8 m_b were located during this period. Thirteen of these larger events were located within the Benioff-Wadati zone of the subducted Pacific plate beneath and west of Cook Inlet; the others were located at shallower depths, including one along the Denali fault near the U.S.-Canadian border, two beneath Prince William Sound, two offshore near the edge of the continental margin, and one near Mt. Katmai on the Alaska Peninsula. In and around the Yakataga seismic gap the pattern of shallow microearthquake activity (Figure 2) was similar to that observed over the past several years, with concentrations of events occurring beneath Waxell Ridge near the center of the gap, beneath the Copper River Delta, and within the aftershock zone of the 1979 St Elias earthquake north and east of Icy Bay. Nearly all of these events had coda-duration magnitudes of 2.5 or less. Within the aftershock zone of the St. Elias earthquake, the two largest events had coda-duration magnitudes of only 2.5 and 2.7. This is unusual compared to preceding six-month periods in which several events of at least magnitude 3 occurred, but it may simply reflect a continuing decrease in the rate of aftershock activity. Aftershocks from the 1983 Columbia Bay earthquake north of Prince William Sound and the 1984 Sutton earthquake on the Castle Mountain fault form distinct clusters within the

distribution of shallow events. The cluster of events located beneath the northern tip of Knight Island reflects an emphasis placed on locating smaller events in this area following the installation of three local seismographs in July. Other features in the distribution of shallow seismicity, such as the concentrations along the volcanic arc west of Cook Inlet, beneath the Talkeetna Mountains north of the Castle Mountain fault, and along the Duke River fault system, are similar those observed over the past several years.

2) Earthquakes located within the Benioff-Wadati zone beneath the Bradley Lake sub-array on the southen Kenai Peninsula were studied to investigate the distribution of seismicity and orientation of stresses within the upper part of the subducted plate. By considering only events located with a homogeneous phase set, high-quality relative locations were obtained. The distribution of hypocenters indicate that locally the seismic zone is about 20 to 25 km thick with its upper surface at a depth of about 35 km. P-wave polarities for rays leaving the source in an upward direction indicate that the orientations of the principal stress axes change systematically with increasing depth within the subducted plate. Although the nodal planes are not well constrained due to a combination of poor coverage of the focal sphere and uncertainties in emergence angles for rays traveling to more distant regional stations, the patterns of P-wave polarities for upward-leaving rays are compatible with downdip tension in the upper 12 km of the seismic zone in this area and downdip compression deeper within the zone.

3) Five ELOG (remote earthquake detection and logging instrument) systems were deployed in seismically active areas within the Talkeetna mountains, including the aftershock zone of the 1984 Sutton earthquake. Two units were installed adjacent to a seismograph of the regional network to provide a basis for checking the detection capabilities of the ELOG units. Data recovered from two months of recording during the summer have not yet been analyzed to identify possible earthquake triggers. Three of the units will remain in operation during the winter.

A prototype of the analog telemetry interface (ATI) was tested successfully for a short period in Alaska this summer. These units will be installed at telephone exchanges where signals are multiplexed. The ATI incorporates many new features, such as periodically sending test tones to verify correct phone operation, sending information on the squelch status of radio receivers, measuring signal level in db's with a built-in digital meter, and translating one center frequency to another.

Reports

Lahr, J. C., Page, R. A., Stephens, C. D., and Fogleman, K. A., 1985, The 1984 Sutton, Alaska, earthquake: Evidence for activity on the Talkeetna segment of the Castle Mountain fault system, (Director's approval, 09/85).

Page, R. A., 1985, Comment on "Earthquake frequency and prediction", by Z.-R. Liu, Bulletin of the Seismological Society of America, (submitted 06/85).

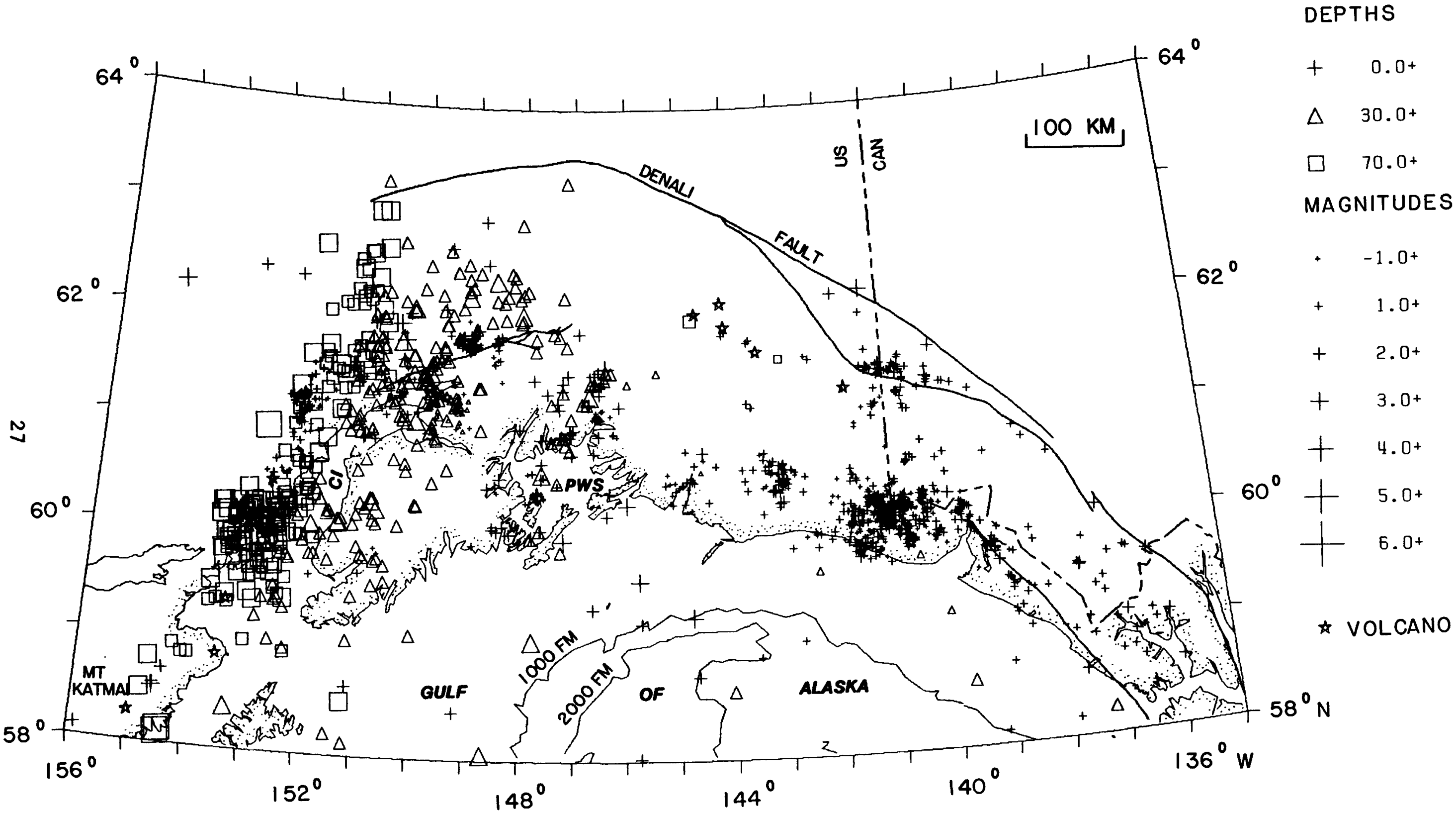

Figure 1. Earthquakes located by the USGS southern Alaska seismograph network during February - July, 1985. Epicenters of 1691 events are plotted. Magnitudes are determined from coda-duration or maximum amplitude, and for events of magnitude 3 and larger can be as much as one unit smaller than the teleseismic m_b magnitude. The lowest level to which data is processed varies across the mapped area due to uneven station distribution and to criteria used to select earthquakes for processing. Abbreviations are: CI - Cook Inlet, PWS - Prince William Sound. See Figure 2 for more detailed information about place names.

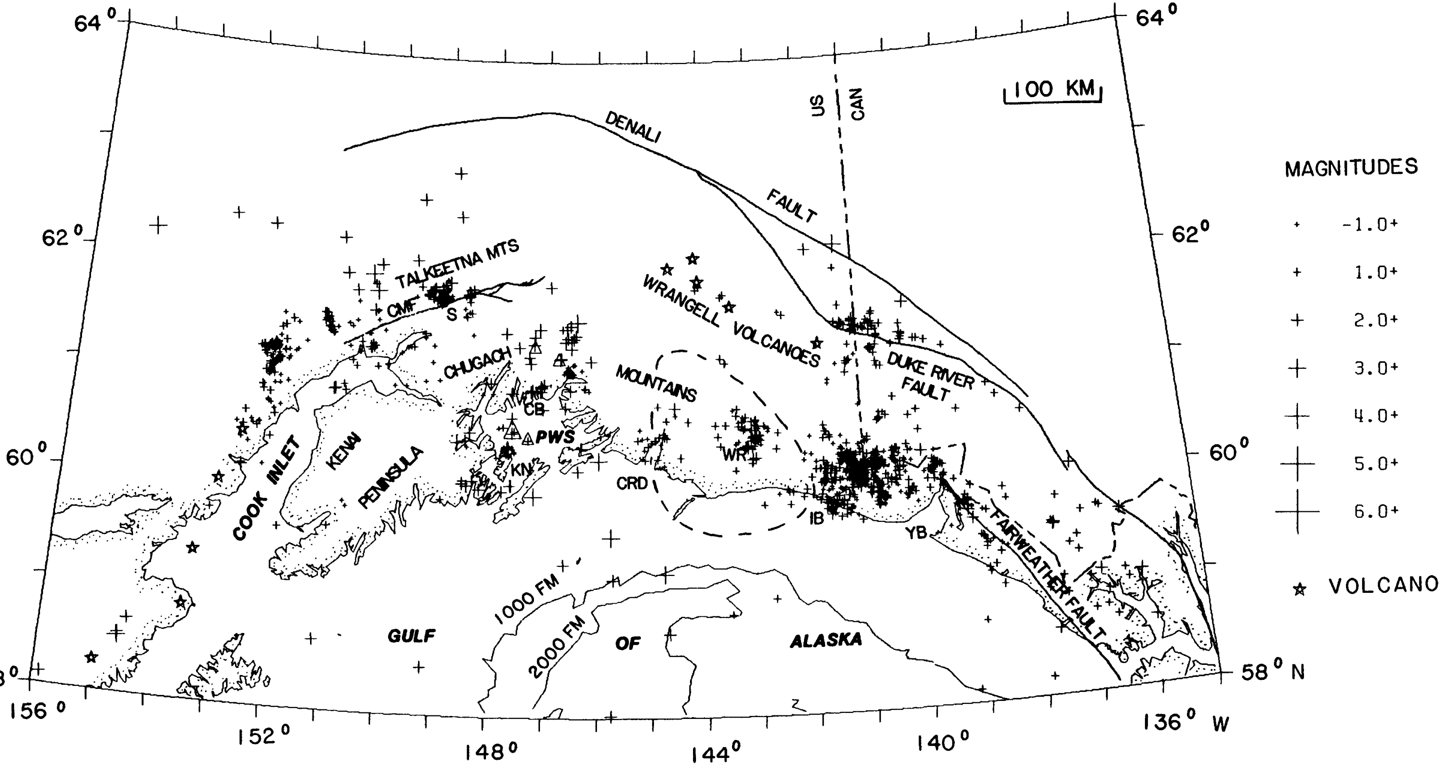

Figure 2. Epicenters of earthquakes from Figure 1 which were located at depths of 30 km or less. Dashed contour indicates inferred approximate extent of Yakataga seismic gap. Abbreviations are: CB - Columbia Bay, CMF - Castle Mountain fault, CRD - Copper River Delta, IB - Icy Bay, KN - Knight Island, PWS - Prince William Sound, S - Sutton, WR - Waxell Ridge, YB - Yakutat Bay.

Seismic Data Library

9930-01501

W. H. K. Lee
U. S. Geological Survey
Branch of Seismology
345 Middlefield Road, Mail Stop 977
Menlo Park, California 94025
(415) 323-8111, Ext. 2630

This is a non-research project and its main objective is to provide access of seismic data to the seismological community. This Seismic Data Library was started by Jack Pfluke at the Earthquake Mechanism Laboratory before it was merged with the Geological Survey. Over the past ten years, we have built up one of the world's largest collections of seismograms (almost all of them on microfilm) and related materials. Our collection includes approximately 4.5 million WWNSS seismograms (1962 - present), 1 million USGS local earthquake seismograms (1966-1979), 0.5 million historical seismograms (1900-1962), and 20,000 earthquake bulletins, reports and reprints.

Recently, we received a few thousand magnetic tapes containing a complete set of digital waveform data of the Global Digital Seismic Network. We plan to make these valuable data available to the seismological community. The extent of our service will depend on the available funding, which is yet to be approved.

In conjunction with the Microearthquake Data Analysis Project (9930-01173), we completed a general earthquake data management system called "USGS Earthquake Archiving and Retrieval System". A description of this system was given in the previous Semi-Annual Report. During the last few months, we documented archived data sets in the following two reports.

Reports

Messier, T. M., Oneill, M. E., and Lee, W. H. K., USGS Earthquake Data Archiving and Retrieval System: Archived data sets in the General Library--GL000001 to GL000200, USGS Open-File Report 85-436, 316 pp., 1985.

Tottingham, D. M., Newberry, J. T., and Lee, W. H. K., USGS Earthquake Data Archiving and Retrieval System: Archived data sets in the Standardized Library--SL000001 to SL000100, USGS Open-File Report, 85-397, 290 pp., 1985.

Northern and Central California Seismic Network Processing

9930-01160

Fredrick W. Lester
Branch of Seismology
U.S. Geological Survey
345 Middlefeld Road M/S 977
Menlo Park, California 94025
(415) 323-8111, ext. 2149

Investigations

1. Signals from 454 stations of the multipurpose Northern and Central California Seismic Network (Calnet) are telemetered continuously to the central laboratory facility in Menlo Park. They are supplemented with signals from up to 54 stations from other institutions. The data are recorded, reduced, and analyzed to determine the origin times, magnitudes, and hypocenters of the earthquakes that occur in or near the network. Data on these events are presented in the forms of lists, computer tape and mass data files, and maps to summarize the seismic history of the region and to provide basic data for further research in seismicity, earthquake hazards, and earthquake mechanics and prediction. A magnetic tape library of "dubbed" unprocessed analog tape records of the network for significant local earthquakes and teleseisms is maintained to facilitate futher detailed studies of crust and upper mantle structure and physical properties, and of the mechanics of earthquake sources.

Results

1. Figure 1 shows the seismic activity of Northern and Central California for the period April 1 through September 30, 1985. The 9481 earthquakes plotted are all reliable locations using 4 or more phase readings in the solution. The phase readings were obtained either by the Caltech-USGS Seismic Processing System (CUSP), or by the automatic Real Time Picker (RTP), or by hand timing, or they are a combination of these sources. The data have been screened for blasts and those found have been eliminated. Identification of quarries in the Sierra Nevada Foothills is a constant problem so that all quarry data may not have yet been eliminated from the catalog. We feel that the catalog of location data maintained by Calnet is complete for earthquakes magnitude 1.5 and larger.

   Currently all data are processed through the CUSP system and are available from the CUSP data base, including the digitial seismograms. Events that are detected on Develocorder films or by the RTP that are not detected by CUSP are added to the data base as quickly as time permits. This is being accomplished by digitizing the earthquakes from the analog magnetic tapes on another computer. These digital data are then input into the CUSP system and processed to completion using standard CUSP timing and analysis techniques. Any events missed by CUSP and not available for digitizing from the magnetic tapes are processed by hand from Develocorder films and the final location and phase data are added to the data base. These hand processed events are the only ones for which there are no digital seismograms in the data base. At the present time less than 10 percent of the earthquakes located go undetected by CUSP. For a more complete description of the CUSP system see the project description "Consolidated Digital Recording and Analysis" by Sam W. Stewart.

Personnel from the project are currently involved in all facets of the processing of network data. Currently, however, the main focus of the project is to finalize and publish old network data, scan seismograms for back-up event detection, suppliment CUSP data with data that were detected either visually or by the RTP, and assist in the loading of pre-1985 network data into the CUSP data base.

2. Final processing of data for the first half of calendar year 1978 is complete and those data are ready for publication. Work is currently underway on the final processing of the 1982 data. It is expected that data from the second half of 1982 will be published by the end of 1985.

3. On August 4, 1985 we recorded a magnitude 5.5 earthquake that occurred approximately 20km east of Coalinga, California, along the northern end of the Kettleman Hills. This earthquake was preceded by five foreshocks, the largest of which was magnitude 4.5. In the two months following the main shock we have located more than 380 aftershocks, the largest of which occurred on August 5 and was magnitude 4.4. The aftershock zone for this sequence is roughly coincident with the Kettleman Hills and borders on the east, with little or no overlap, the Coalinga aftershock zone. Table 1 contains the locations of all magnitude 4.0 and larger earthquakes in this sequence.

4. Quarterly reports were prepared on seismic activity around Lake Shasta, Warm Springs Dam, the Auburn Dam site and Melones Dam for the appropriate funding agencies. Quarterly reports on seismic activity in the Mount Shasta area and in Lassen Volcanic National Park were also prepared and distributed to interested agencies and individuals.

5. Work is currently underway on a paper by Mari Kauffmann, Steve Walter, and Rick Lester describing the seismicity in the Klamath Mountains-southern Cascades - northern Sierra Nevada region of California for the years 1977-1984. This paper should be completed in 1986

Reports

Walter, S. R., Intermediate - focus earthquakes associated with Gorda Plate subduction in northern California, submitted to BSSA.

TABLE 1

MAGNITUDE 4.0 AND LARGER EARTHQUAKES IN THE KETTLEMAN HILLS AREA - AUGUST 4-OCTOBER 9, 1985

DATE	HRMN	SEC	LAT	LONG	DEPTH	MAG
850804	1129	15.07	36- 8.42	120- 9.43	12.34	4.5
850804	1201	55.80	36- 8.63	120- 9.20	11.91	5.5
850804	1515	39.62	36- 2.67	120- 5.75	11.59	4.3
850805	1445	37.92	36- 7.41	120- 5.87	7.69	4.4
850807	016	3.40	36- 0.96	120- 8.73	13.98	4.3

NORTHERN CALIFORNIA SEISMICITY

APRIL - SEPTEMBER 1985

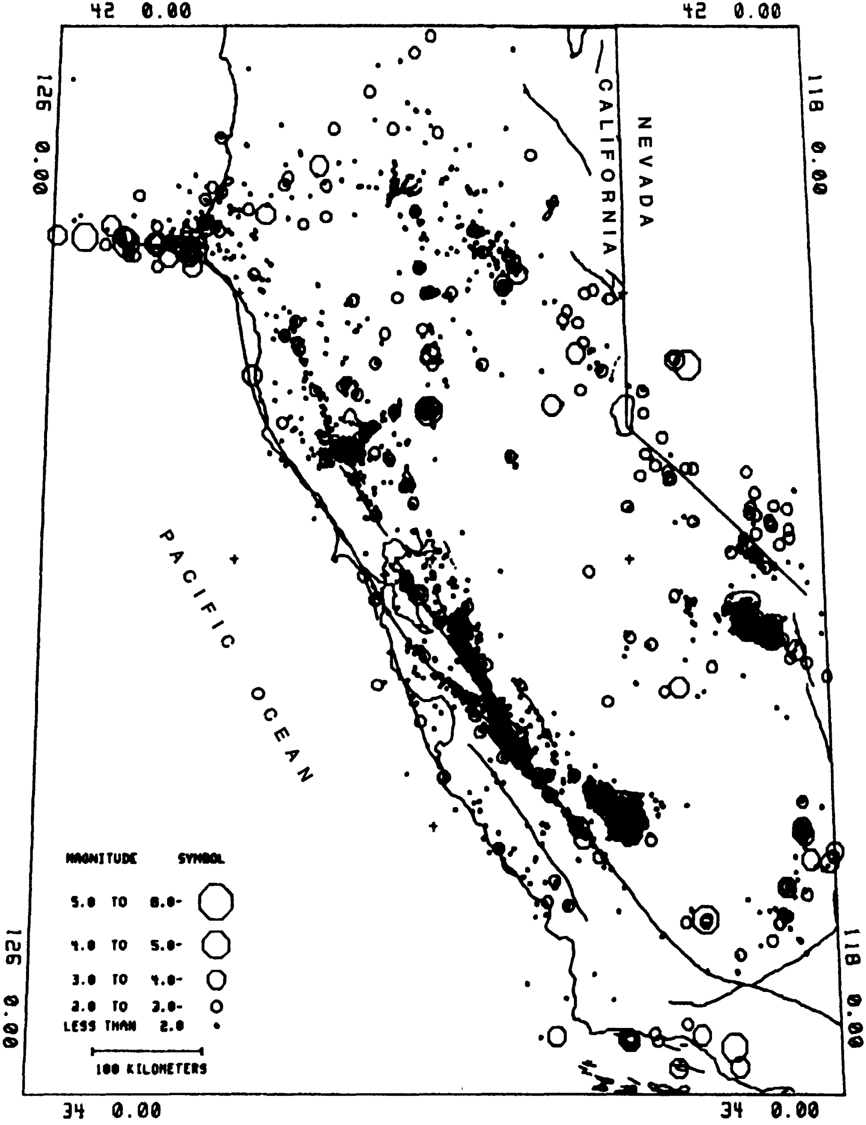

FIGURE 1

Array Studies of Seismicity

9930-02106

David H. Oppenheimer
Branch of Seismology
United States Geological Survey
345 Middlefield Road - MS 977
Menlo Park, California 94025
(415) 323-8111, ext. 2791

Investigations

1. Continue testing and enhancement of computer algorithms to compute and display earthquake fault-plane solutions.

2. Complete investigation of fault-plane solutions at The Geysers, California for inferences on state of stress and mechanism of induced seismicity.

3. Begin analysis of earthquake doublets at Morgan Hill and Coyote Lake regions of California for investigation of temporal changes in crustal properties in the seismogenic zone.

Results

1. Algorithms for computing and displaying double-couple earthquake fault plane solutions from first motion polarities were implemented and tested. The inversion is accomplished through a two-stage grid-search procedure that finds the source model minimizing a normalized, weighted sum of first-motion polarity discrepancies. Two weighting factors are incorporated in the minimization: one reflecting the estimated variance of the data, and one based on the absolute value of the theoretical P wave radiation amplitude. The latter weighting gives greater (lesser) weight to observations near radiation lobes (nodal planes). Recent enhancements include reporting of multiple fault plane solutions for a given earthquake through detection of discrete minimas in the coarse grid search procedure. The fault plane solution uncertainties are now computed as a function of the data uncertainty and reported both as the uncertainity in the model parameters (strike, dip, and rake) of the solution and as nearby mechanisms for which the solution misfit is less than the 95% confidence estimate of the best solution. An Open-file report which describes the inversion and lists the source code and companion code for displaying the fault plane solutions is in the review process and should be completed shortly.

2. Fault plane solutions for 210 earthquakes of magnitude 1.1 to 3.3 at The Geysers exhibit normal and strike-slip behavior at all depths, and reverse faulting at depths shallower than 1.0 km. Large variations in fault mechanisms occur over epicentral distances as small as 1.0 km, precluding the identification of the slip plane from the auxiliary. Inversion of the focal mechanisms for the orientation of principal components of deviatoric stress tensor indicates that within the upper three km depth the greatest and least principal stress axes are nearly horizontal (strike-slip faulting stress regime) and in the direction NNE-SSW and ESE-WNW, respectively. The plunge of the principle stress axis increases to near

vertical below 3 km (normal faulting stress regime), while the least principle stress axis remains oriented ESE-WNW. The inversion also shows that the state of stress at depth at The Geysers approaches uniaxial extension. These results are compatible with regional geodetic and leveling data, indicating that the earthquakes represent failure on fault planes in response to the regional stress field.

Local geodetic measurements suggest that geothermal steam extraction generates stress perturbations no greater than a few bars per year, but these stress changes are believed to be sufficient to induce earthquakes. The proximity of earthquake locations with respect to producing steam well locations and surface subsidence suggest that the most likely inducing mechanism involves stresses induced by reservoir contraction due either to pore collapse of the reservoir rock as water migrates out into the permeable fractures, or to thermal contraction which results from production-related pressure declines in the reservoir.

The presence of large depositional basins to the north-northeast of The Geysers, together with extension at The Geysers suggests that the extension occurs over the entire region between the Maacama and Bartlett Springs fault strike-slip zones. It is difficult to attribute this extension to tectonics associated with typical pull-apart basins due to the lack of regional topographic expression and definition of the extent of the master strike-slip faults. However, it appears that the regional extension accounts for the wide-spread presence of Quaternary volcanism in the Clear Lake area. A manuscript describing this work is in the review process.

3. Phase data for earthquakes recorded in the Morgan Hill and Coyote Lake regions of California were assembled for the time period 1/69 through 9/85. Current efforts are directed towards ensuring the data sets are complete, mapping old stations names to current names, and detecting temporal multiplets through comparison of arrival time patterns at stations common to pairs of earthquakes.

Reports

Zandt, G., S. K. Park, C. Ammon, and D. Oppenheimer, 1985, P-delays in northern California: evidence on the southern edge of the subducting Gorda plate, Trans. Am. Geophys. Union (abs.), in press.

Regional Microearthquake Network in the Central Mississippi Valley

14-08-0001-21887

Willaim V. Stauder and Robert B. Herrmann
Department of Earth and Atmospheric Sciences
Saint Louis University
P.O. Box 8099 Laclede Station
St. Louis, MO 63156
(314) 658-3131

Investigations

The purpose of the network is to monitor seismic activity in the Central Mississippi Valley Seismic zone, in which the large 1811-1812 New Madrid earthquakes occurred. The following section gives a summary of network observations during the year 1984.

Results

In 1984, 357 earthquakes were located and 77 other nonlocatable earthquakes were detected by the 38 station regional telemetered microearthquake network operated by Saint Louis University for the U. S. Geological Survey and the Nuclear Regulatory Commission. Figure 1 shows 336 earthquakes located within a 4° x 5° region centered on 36.5°N and 89.5°W. Seismograph stations are denoted by triangles and are labeled by the station code. The magnitudes are indicated by the size of the open symbols. Figure 2 shows the locations and magnitudes of 121 earthquakes located within a 1.5° x 1.5° region centered at 36.25°N and 89.75°W. Figures 3 and 4 are similar to Figures 1 and 2, but the epicenter symbols(squares) are scaled to focal depth.

165 teleseisms were recorded by the PDP 11/34 microcomputer in 1984. Epicentral coordinates were determined by assuming a plane wavefront propagating across the network and using the travel-time curves to determine back azimuth and slowness, and by assuming a focal depth of 15 kilometers using spherical geometry. Arrival-time information for teleseismic P and PkP phases has been published in the quarterly earthquake bulletin.

The significant earthquakes occurring in 1984 include the following:

1 12 January 1984, UTC 0248, 37.59°N, 89.75°W: felt in an area about 10 miles south of Perryville, Missouri. m_{Lg}(10Hz) = 3.0(SLM).

2 28 January 1984, UTC 2129, 36.61°N, 89.92°W: felt (IV) in Malden and Gideon, Missouri. m_{Lg}(10Hz) = 3.2(SLM).

3 An earthquake swarm began in November 1983 in southern Illinois near Ohio River Lock and Dam No. 53 and continued through this year. Over 200 events were detected. Peak activity occurred in February with the event on February 13, UTC 2242, 37.21°N, 89.02°W, felt (IV) at Bandana, Kentucky. Felt (III) at Kevil and La Center, Kentucky and also felt (III) at Belknap, Cairo, Grand Chain, Mounds, Tamms, and Ullin, Illinois. m_{Lg}(10Hz) = 3.2(SLM), m_{Lg}(3Hz) = 3.0 <FVM>, m_{bLg} = 3.3(BLA).

A slightly larger event occurred on 14 February 1984, UTC 2256, 37.21°N, 89.00°W: felt (IV) at Belknap, Cairo, Karnak, Olmstead, and Perks, Illinois. Also felt (IV) at Bandana and Kevil, Kentucky. Felt (III) in parts of western Kentucky, southeastern Missouri, and southern Illinois. m_{Lg}(10Hz) = 3.6 (SLM), m_{bLg} = 3.8(BLA).

4 17 April 1984, UTC 0444, 38.41°N, 88.48°W: felt (IV) at Fairfield, Ellery, Dix, Griffin, Keenes and Mill Shoals, Illinois. Felt (III) at Barnhill, Bluford, Geff, Macedonia, and Mount Erie, Illinois. $m_{Lg}(10\text{Hz}) = 3.2$ (SLM), $m_{Lg}(3\text{Hz}) = 2.7$<FVM>, $m_D = 2.8$(TEIC).

5 26 June 1984, UTC 1515, 36.10°N, 89.39°W: felt in the Dyersburg, Tennessee area. $m_{Lg}(10\text{Hz}) = 3.2$(SLM), $m_D = 3.0$(TEIC).

6 29 June 1984, UTC 0758, 37.70°N, 88.47°W: slight damage (VI) at Harrisburg, Illinois. Felt (V) at Raleigh and (IV) at Equality, Herod, Karbers Ridge, Muddy, and Shawneetown. Felt in Gallatin, Hamilton, Hardin, Johnson, Saline, and Williamson counties. Also felt in several communities in northwestern Kentucky. $m_{Lg}(10\text{Hz}) = 3.8$(SLM), $m_{bLg} = 4.1$ (NEIS), $m_D = 3.3$(TEIC).

7 28 July 1984, UTC 2339, 39.22°N, 87.07°W: felt (V) at Clay City and Coal City, Indiana. Felt (IV) at Bloomfield, Bowling Green, Carlisle, Coalmont, Cory, Freedom, Hymera, Jasonville, Lewis, Linton, Midland, Patricksburg, and Worthington, Indiana. $m_{Lg}(10\text{Hz}) = 4.0$(SLM), $m_D = 3.8$(TEIC).

8 30 July 1984, UTC 0733, 37.82°N, 90.92°W: felt at Bonne Terre, Farmington, and Flat River, Missouri. Also felt at Carbondale, Illinois. $m_{Lg}(10\text{Hz}) = 3.0$(SLM), $m_D = 2.6$(TEIC).

9 29 August 1984, UTC 0650, 39.11°N, 87.45°W: felt (V) at Clay City, Indiana. Felt (III) at Bowling Green, Crane, Fairbanks, and Lewis, Indiana. $m_{Lg}(10\text{Hz}) = 3.1$(SLM), $m_D = 2.7$(TEIC).

10 6 September 1984, UTC 1606, 36.10°N, 89.35°W: felt at Brazil, Tennessee. $m_{Lg}(10\text{Hz}) = 2.9$(SLM), $m_D = 2.4$(TEIC).

11 27 September 1984, UTC 1303, 35.25°N, 92.21°W: felt (IV) at Enola, Arkansas. $m_{Lg}(10\text{Hz}) = 3.4$(SLM), $m_{bLg} = 3.3$ (TUL), $m_D = 3.2$(TEIC).

A second event occurred at UTC 1316: $m_{Lg}(10\text{Hz}) = 3.0$(SLM), $m_{bLg} = 2.4$(TUL), $m_D = 2.7$(TEIC).

12 9 October 1984, UTC 1154, 34.74°N, 85.16°W: slight damage (VI) south of Ringgold, Georgia. Minor damage reported in the Chattanooga, Tennessee area. Felt (V) at La Fayette, Chickamauga, and Trenton, Georgia. Felt in northwestern Georgia, northeastern Alabama and parts of south central Tennessee. $m_{Lg}(10\text{Hz}) = 4.2$(SLM), $m_{bLg} = 4.0$(NEIS), $m_D = 3.8$(TEIC). Consult TEIC, Memphis, for further information.

13 3 December 1984, UTC 1155, 36.15°N, 89.70°W: felt (IV) at Cooter, Missouri, and (III) at Gabler, Missouri and Miston, Tennessee. Also felt at Caruthersville, Missouri. $m_{Lg}(10\text{Hz}) = 3.0$(SLM), $m_{Lg}(3\text{Hz}) = 3.2$ <FVM>, $m_D = 3.0$(TEIC).

ACKNOWLEDGEMENTS

The cooperation of the Tennessee Earthquake Information Center, National Earthquake Information Service, and the University of Kentucky is gratefully acknowledged for providing station readings, magnitude data, and felt information. The results reported were a result of the support form the Department of the Interior, U.S. Geological Survey, under Contract 14-08-0001-19751 and the U.S. Nuclear Regulatory Commission under Contract NRC-04-81-195-03.

REFERENCES

Central Mississippi Valley Earthquake Bulletin, Department of Earth and Atmospheric Sciences, Saint Louis University. 1984, Nos. 39-42.

PDE Preliminary Determination of Epicenters, Monthly Listings, U. S. Geological Survey, 1984.

TEIC Quarterly Seismological Bulletin, Tennessee Earthquake Information Center, Memphis State University. 1984, Vol. 5, Nos. 1-4.

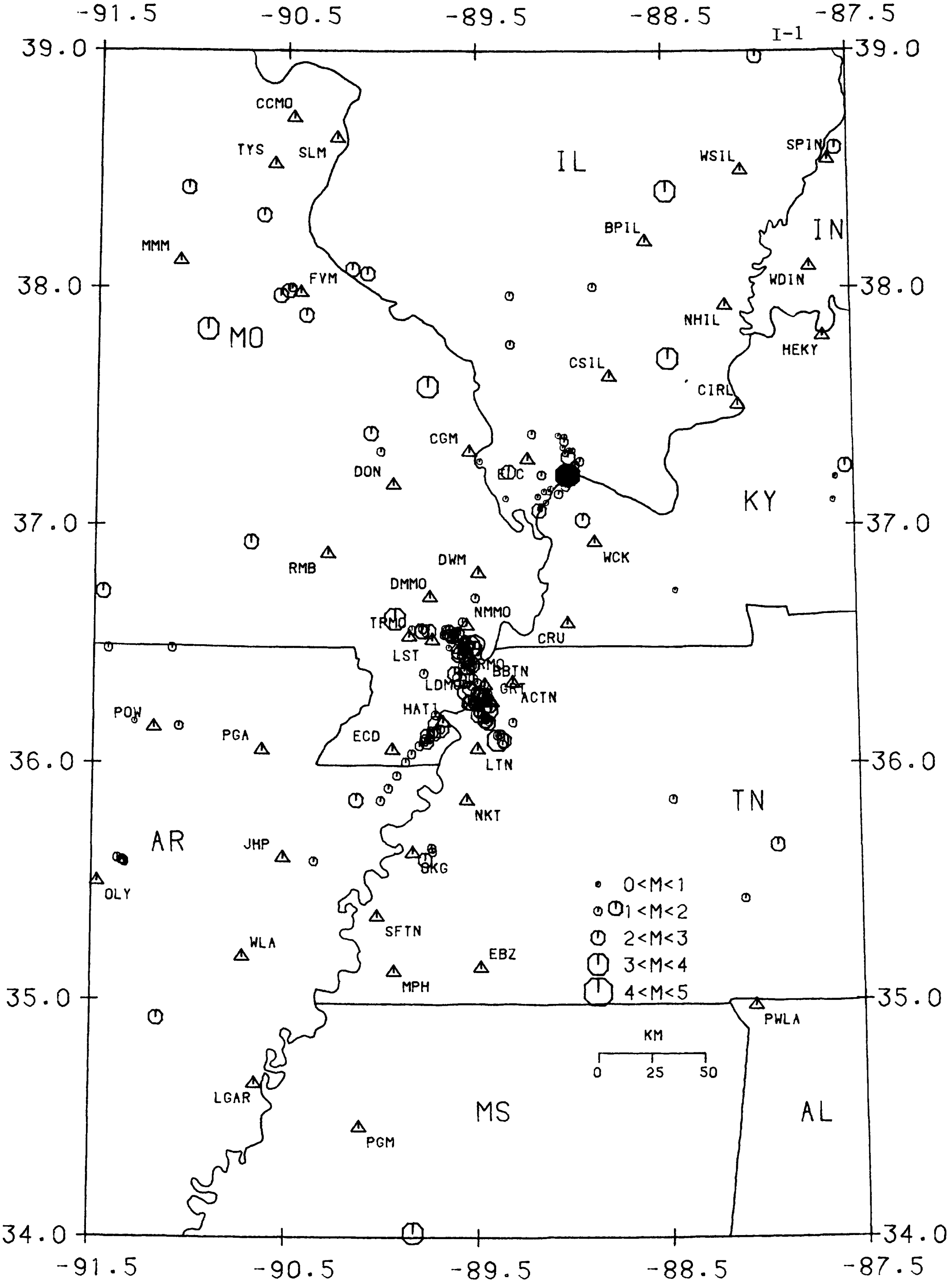

FIGURE 1

REPORTING PERIOD 01 JAN 1984 TO 31 DEC 1984

LEGEND . △ STATION ⊙ EPICENTER

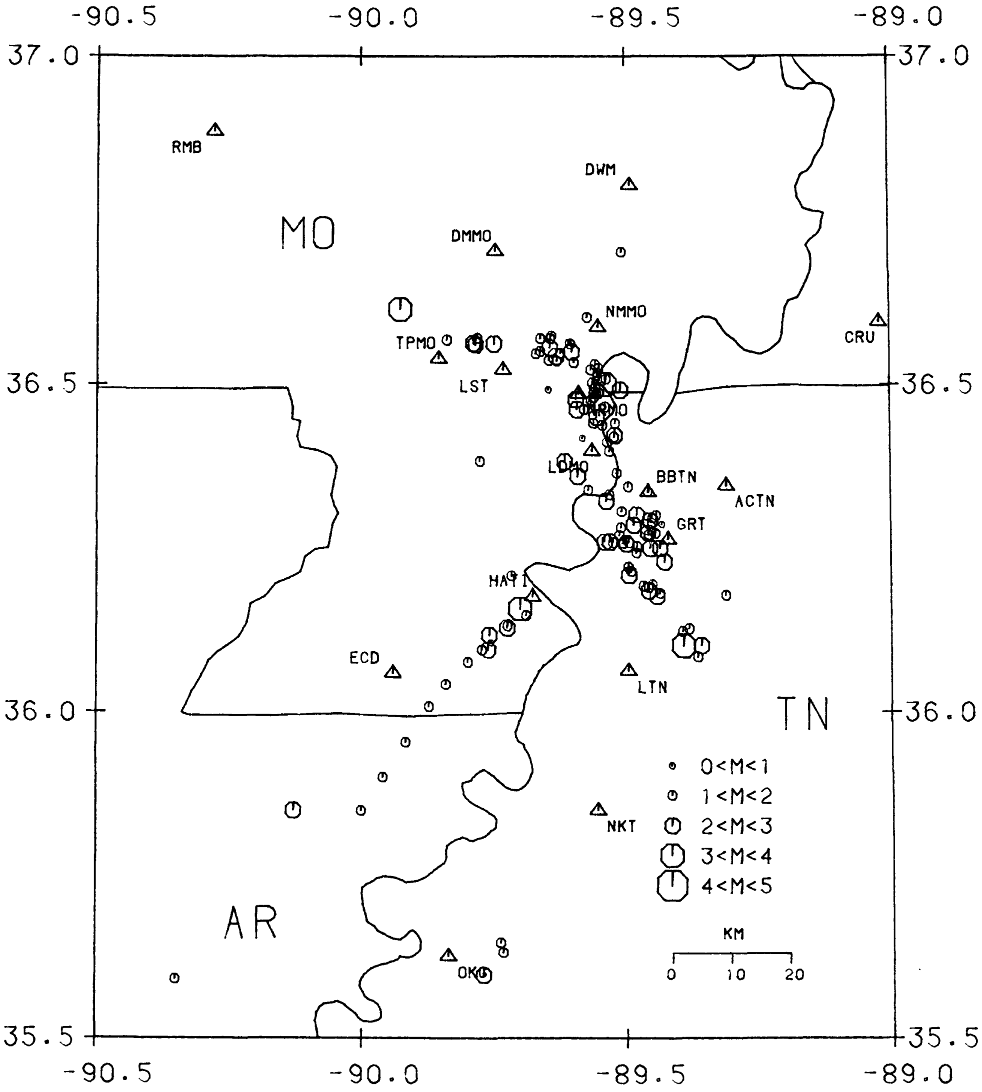

FIGURE 2

REPORTING PERIOD 01 JAN 1984 TO 31 DEC 1984

LEGEND . ⚠ STATION ⊙ EPICENTER

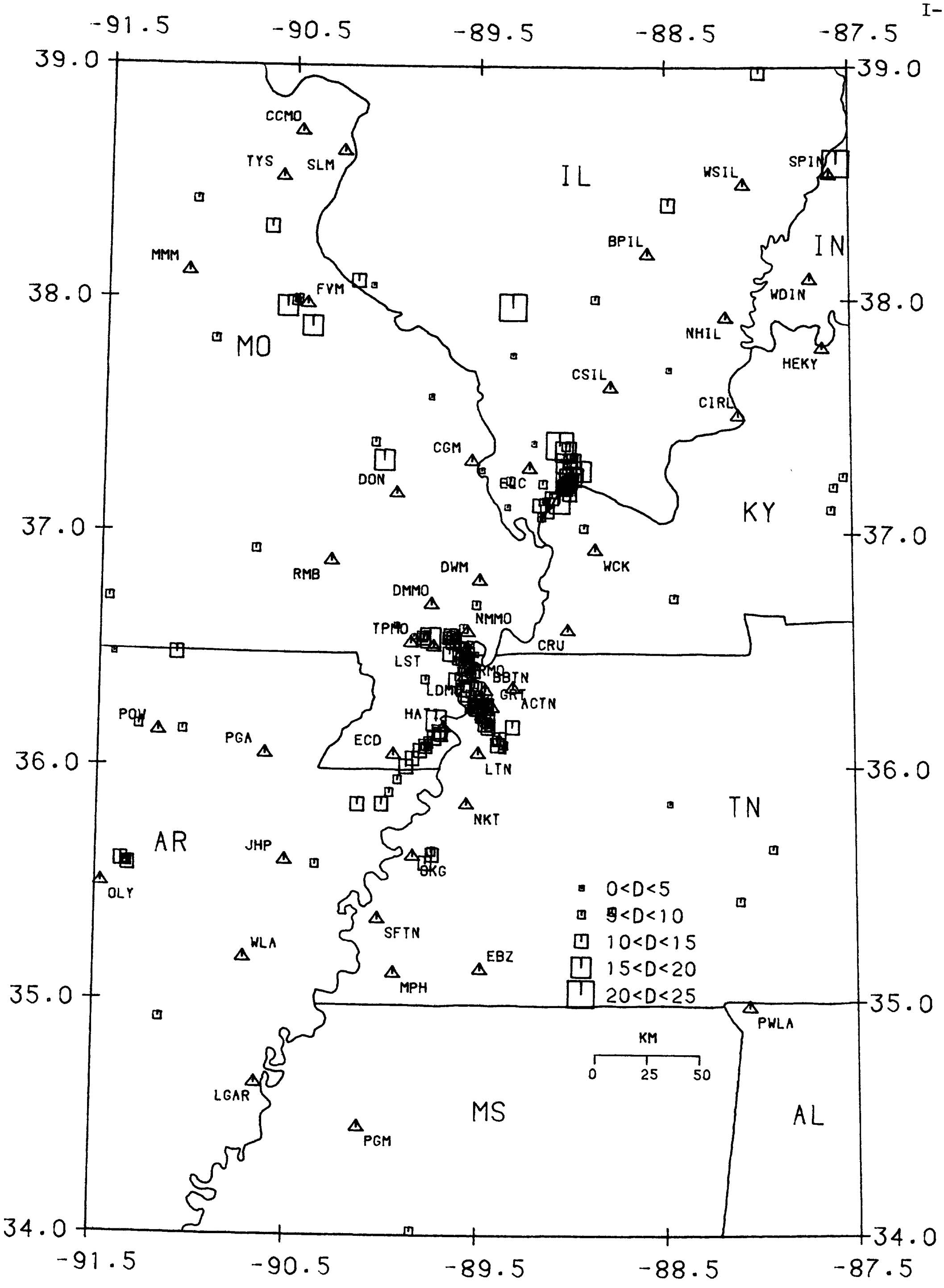

FIGURE 3

REPORTING PERIOD 01 JAN 1984 TO 31 DEC 1984

LEGEND . △ STATION □ EPICENTER

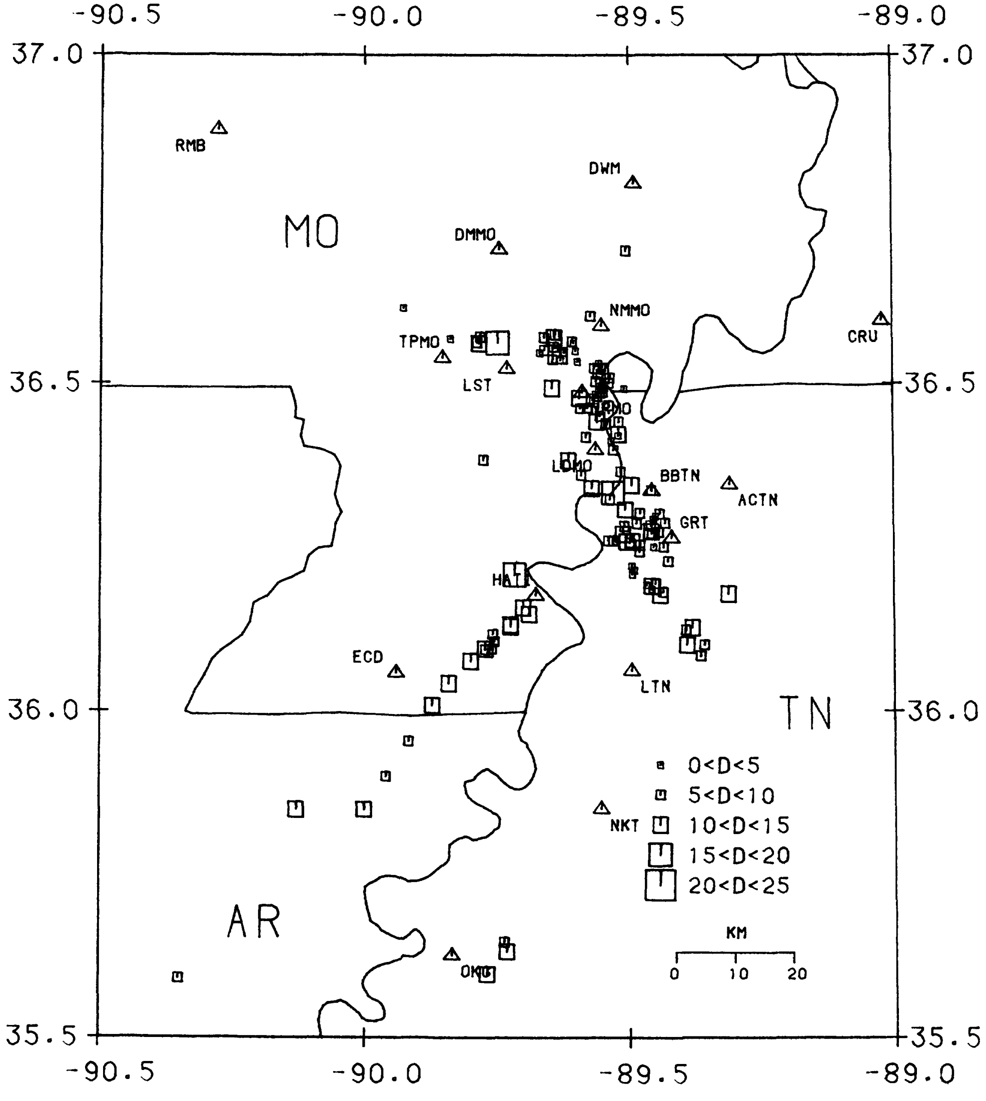

FIGURE 4

REPORTING PERIOD 01 JAN 1984 TO 31 DEC 1984

LEGEND . △ STATION ◘ EPICENTER

Consolidated Digital Recording and Analysis

9930-03412

Sam W. Stewart
Branch of Seismology
U.S. Geological Survey
345 Middlefield Road M/S 977
Menlo Park, California 94025
(415) 323-8111 Ext. 2577

Investigations

The goal is to operate, on a routine and reliable basis, a computer-automated system that will detect and process earthquakes occurring within the USGS Central California Earthquake Network (also known as CALNET). Presently, the output from more than 450 short-period seismic stations is telemetered to a central recording point in Menlo Park, California. Two DEC PDP11/44 computers, and a VAX/750, are used on this project. The 11/44A is dedicated to the task of online, realtime detection of earthquakes and storing the waveforms for later analysis. The 11/44B is used for offline processing and archiving of earthquakes. Both computers have a 512 channel analog-to-digital converter, so the 11/44B can serve as backup to the online system whenever necessary. The two computers can communicate with each other via a simple digital-bit I/O "semaphore" system, and can transfer large amounts of data via a dual-ported disk subsystem or a dual-ported magnetic tape subsystem. The VAX/750 is a general purpose computer used by the Branch of Seismology. We use it as the primary "research" computer for the CUSP system. It holds the primary data base of earthquake summary data and phase card data, which is available for research pruposes. We update and maintain the CALNET data on this computer.

Both 11/44 computers use the RSX11M-PLUS (v2.1) operating system. The VAX/750 uses the DEC VMS operating system. Software has been developed largely by Carl Johnson in Pasadena, but with considerable modification by Peter Johnson, Bob Dollar and Sam Stewart, to meet Menlo Park's specific needs. Our applications are all written in Fortran-77, but with heavy use of system functions unique to the RSX or VMS operating systems.

Results

1. During the period April 1985 thru September 1985 approximately 7000 events were processed through the CUSP system. This includes 6100 events that were classified as 'LOCAL' events, i.e., they occurred within or near enough to the network that hypocenters were calculated and the data entered into the catalogs. The remaining 900 events were either regional or teleseismic events, or unprocessed copies of local events that were too small ($M < 1.0$) to be timed, or copies of very large events that had to be 'split' in order to be accomodated by the 11/44 hardware limitations. In addition, a few thousand non-seismic, noise events detected by the online 11/44A computer had to be examined and deleted. Considering only the seismic events, this projects to an annual rate of processing about 14,000 events per year.

2. In the last report, we mentioned that conversion of the seismic telemetry

transmission systems from leased telephone lines to our own microwave transmission system had resulted in some serious noise problems. The new microwave system was plagued with fading or complete dropouts, resulting in loss of data by the 11/44A online detection system. During the current report period these problems continued to be attacked vigorously by Branch personnel. These problems have diminished greatly, particularly during the last month or two (Aug-Sept 1985). It remains to be seen what happens when the winter rain and snow begins.

3. We have continued to develop programs on the Branch VAX/750 to facilitate CUSP processing needs in Menlo Park. Some of this effort has been to transfer programs working under RSX on the 11/44 systems to the equivalent programs working under VMS on the VAX/750 system. For example, data tapes digitized on the ECLIPSE system can now be read into and processed directly on the 750. This allows users to make extensive use of the large analog dubbed tape library of earthquakes, extending back about 10 years.

   Other programs have been developed directly for 750 use. For example, the original CALNET phase card data can be entered directly into the CUSP data base. This has been done for the 1969 data, and conversion of subsequent years will soon be underway.

4. Although we are 'current' in processing and archiving earthquake data from the Central California Earthquake Network (CALNET), until now we have not had the procedures and programs to make the data 'easily' available to other researchers. During this report period such procedures were developed and carried out. When the data for a particular month are 'finished', then we write various binary and ASCII tapes containing event summary data and phase data in various forms. The tapes of interest to the user are (i) binary monthly 'FREEZE' tapes, readable by CUSP, containing everything CUSP knows about each earthquake (except the digitized traces), (ii) binary, cumulative 'ARKIVE' tapes, readable by CUSP, that contain the digitized traces, and (iii) ASCII monthly tapes in standard ANSI format, readable by VMS 'COPY' command, by the UNIX 'TPANSI' command, or by FORTRAN programs, that contain summary and phase data in HYPO71 format.

Reports

None

Seismic Monitoring of the Shumagin Seismic Gap, Alaska

USGS 14-08-0001-21919

John Taber and Klaus H. Jacob
Lamont-Doherty Geological Observatory of Columbia University
Palisades, New York 10964
(914) 359-2900

Investigations

Seismic data from the Shumagin seismic network were processed to obtain origin times, hypocenters, and magnitudes for local and regional events. The processing resulted in files of hypocenter solutions and phase data, and archive tapes of digital data. These files are used for the analysis of possible earthquake precursors, seismic hazard evaluation, and studies of regional tectonics and volcanicity (see Analysis Report, this volume). A published bulletin for 1984 data is available.

Results

The seismicity of the Shumagin Islands region from January 1 to June 30, 1985 is shown in map view and cross section in figure 1. The overall pattern over this time period is similar to the long term seismicity. High concentrations of events occur at the base of the main thrust zone and in the shallow crust directly above it. The continuation of the thrust zone towards the trench is poorly defined. West of the network the seismicity is more diffuse in map view. Below the base of the main thrust zone (~45 km) the dip of the Benioff zone steepens. The double planed nature of the lower Benioff zone is barely evident over this short time period.

The yearly network servicing was successfully completed in June. The network is capable of digitally recording and locating events as small as Ml = 0.4 with uniform coverage at the 2.0 level. Onscale recording is possible to at least Ml = 5.0 on a telemetered 3 component force-balance accelerometer. Larger events are recorded by one digitally recording accelerometer and on photographic film by 12 strong-motion accelerometers.

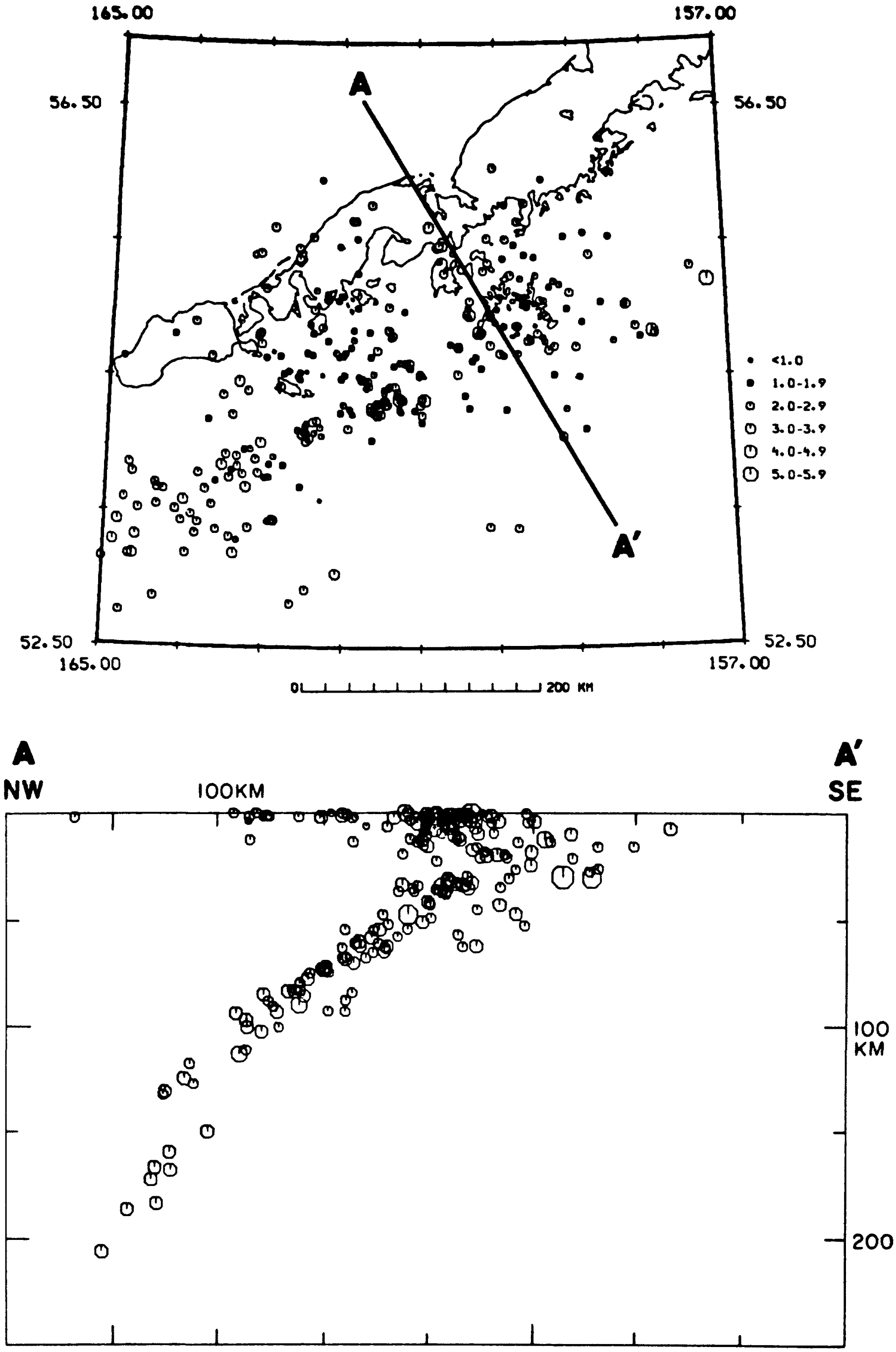

Figure 1. Top: Seismicity recorded by the Shumagin Island seismic network from January 1 to June 30, 1985. Bottom: Cross section of seismicity projected along the line A-A' in the upper figure.

Earthquake Hazard Research in the Greater Los Angeles Basin and Its Offshore Area

#14-08-0001-21858

Ta-liang Teng
Thomas L. Henyey
Egill Hauksson

Center for Earth Sciences
University of Southern California
Los Angeles, CA 90089-0741
(213) 743-6124

INVESTIGATIONS

(1) Monitor earthquake activity in the Los Angeles Basin and the adjacent offshore area.

(2) Upgrade of telemetry electronics used by remote field stations. The microprocessor-based Optimal Telemetry System has been deployed for field testing at three seismic stations.

RESULTS

(1) The earthquake activity that occured in the Los Angeles basin and the southern California coastal zone from January 1 to October 8, 1985 is shown in Figure 1. The seismicity rate during 1985 is similar to the rate that was recorded during the previous three years. The earthquake activity in the Los Angeles basin is characterized by single shocks that are scattered throughout the region. Two clusters of activity are observed; one near the northern end of the Palos Verdes fault and a second near Point Mugu on the Malibu coastal fault. The seismicity in the Santa Barbara region is characterized by several different spatial clusters. Continued activity is observed in the vicinity of the April 1984 swarm, which was located on the offshore extension of the Oak Ridge fault. A high level of activity is also observed near the eastern part of the Santa Ynez fault.

(2) Major progress in seismic instrumentation has recently been made at U.S.C. in connection with the completion of a new optimal telemetry system (OTS). It resolves a serious difficulty in the present-day seismic network operation. In a modern seismic network, the sensor and the digital recorder both have adequate dynamic range. However, the telemetry links with VCO's degrade the overall dynamic range down to 45 dB or less. This serious difficulty reduces the usefulness of a digital seismogram only to the two bits of information at the very beginning of the wave train (bottom of Figure 2), namely, the P arrival and the polarity. We have successfully developed the OTS and are implementing the system in a number of U.S.C. stations. This OTS has 120 dB effective dynamic range and 60 dB resolution. For the same off-scaled signal shown

at the bottom of Figure 2, the corresponding unclipped signal is given on the top of the same figure. Not only are the P and S arrivals clearly seen, the entire waveform is well recorded, which provides more information than the mere two bits mentioned above. The OTS can gain range up to three components at the same station. Controlled by a microprocessor, if events are not occurring in quick successions, the OTS can transmit in series all three channels back to the recording center through a standard one channel (±125 Hz) of voice-grade telephone circuit. This function enables all network stations to be converted into 3-component stations without additional telemetry cost and still at 120 dB effective dynamic range. We plan to utilize the waveform data to study source parameters (e.g. stress drop, source radius and seismic moment) of local earthquakes as well as unusual path effects in the Los Angeles basin. The waveform analysis will contribute both to earthquake hazards evaluations as well as earthquake prediction research.

REPORTS

Hauksson, E. and G. Saldivar, Recent seismicity (1970-1984) along the Newport-Inglewood fault, Los Angeles Basin, southern California, EOS, vol. 65, no. 45, p. 996, 1984.

Hauksson, E., T. L. Teng, T. L. Henyey, J. K. McRaney, L. Hsu and G. Saldivar, Earthquake Hazard Research in the Los Angeles Basin and its Offshore Area, U.S.C. Geophysics Laboratory Technical Report #8501, 1985.

Hauksson, E., T. L. Teng and J. McRaney, The Santa Barbara Channel Easter Swarm of April 1984, USGS Semi-Annual Data Review Meeting in Santa Barbara, California, September, 1984.

Teng, T. L., Application Results of an Optimal Telemetry System, submitted to AGU Fall Meeting, 1985.

Saldivar, G., E. Hauksson and T. L. Teng, The Malibu Earthquake (M=5.0) and Its Aftershock Sequence, southern California, January, 1979, submitted to AGU Fall Meeting, 1985.

Hauksson, E., Constraints on the Velocity Structure of the Crust in the Los Angeles Basin and the Central Transverse Ranges, southern California, submitted to AGU Fall Meeting, 1985.

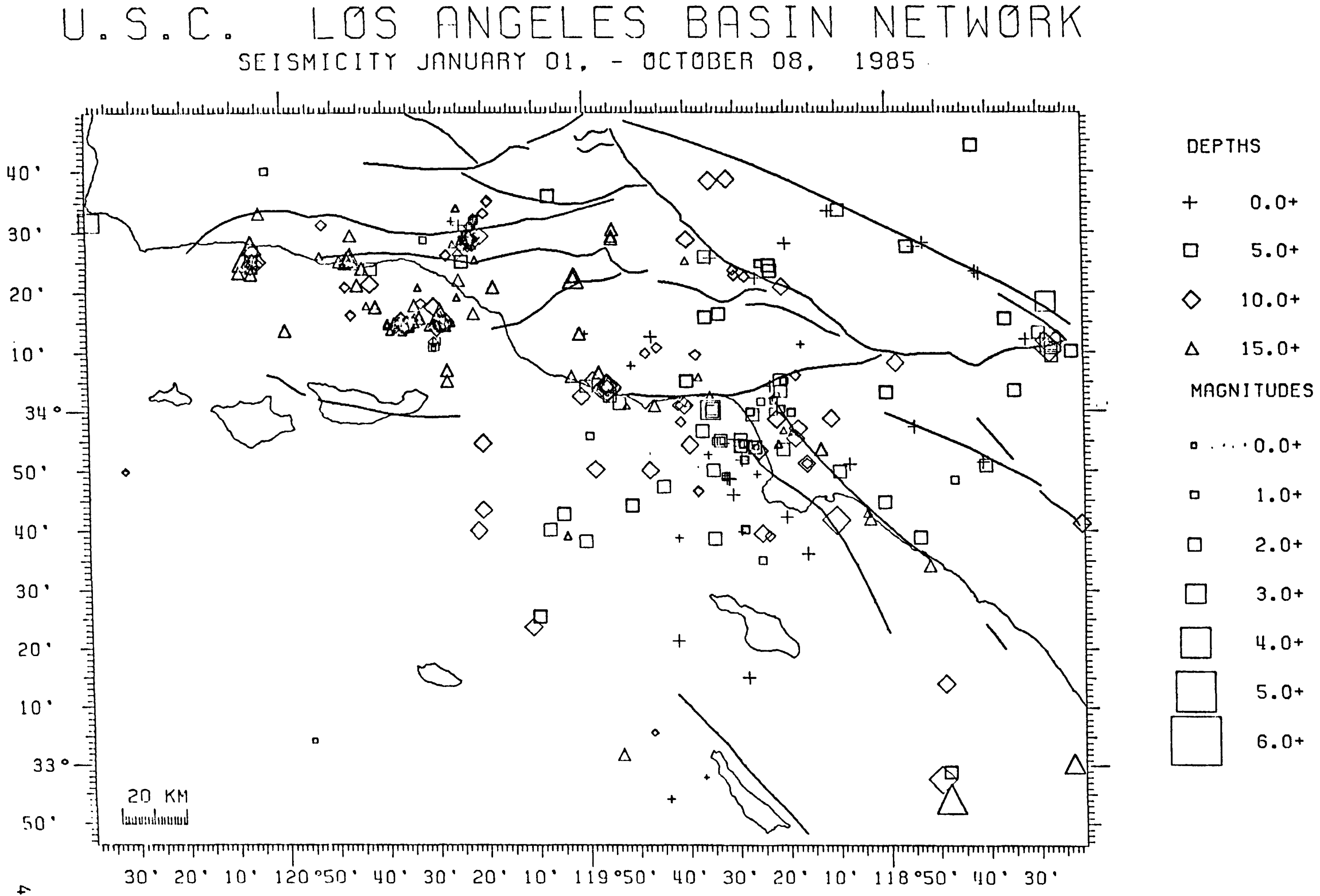

Figure 1. Seismicity in the southern California coastal zone recorded by the U.S.C. network.

Figure 2. (Above) seismogram gain ranged at the station by OTS. (Below) the corresponding clipped seismogram that passed through an analog amplifier/VCO.

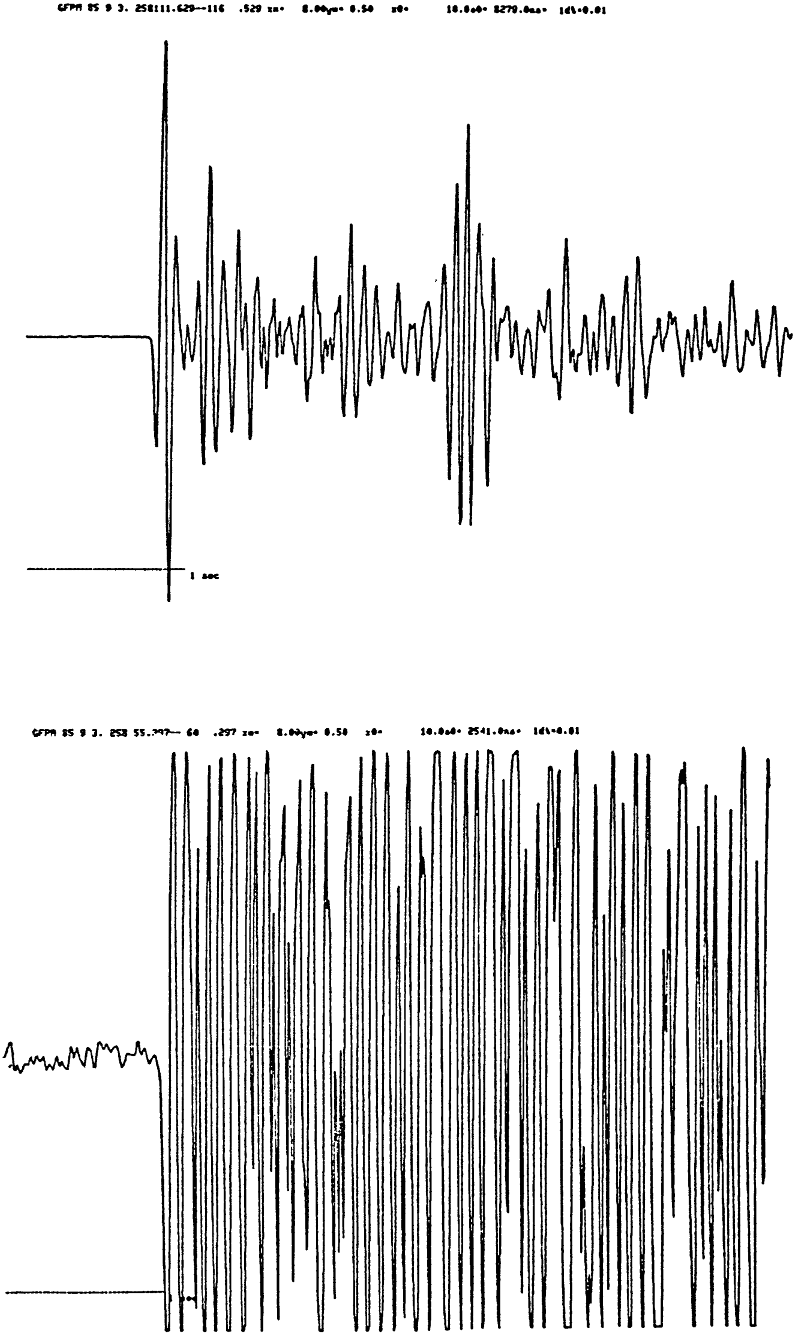

Field Experiment Operations

9930-01170

John VanSchaack
Branch of Seismology
U.S. Geological Survey
345 Middlefield Road MS-977
Menlo Park, California 94025
(415) 323-8111, ext. 2584

Investigations

This project performs a broad range of management, maintenance, field operation, and record keeping tasks in support of seismology and tectonophysics networks and field experiments. Seismic field systems that it maintains in a state of readiness and deploys and operates in the field (in cooperation with user projects) include:

a. 5-day recorder portable seismic systems.
b. "Cassette" seismic refraction systems.
c. Portable digital event recorders.
d. Smoked paper recorder portable seismic systems.

This project is responsible for obtaining the required permits from private landowners and public agencies for installation and operation of network sensors and for the conduct of a variety of field experiments including seismic refraction profiling, aftershock recording, teleseism P-delay studies, volcano monitoring, etc.

This project also has the responsibility for managing all radio telemetry frequency authorizations for the Office of Earthquakes, Volcanoes, and Engineering and its contractors.

Results

Seismic Refraction

One hundred twenty seismic cassette recorders were used in 2 separate experiments to gather deep crustal velocity and structural data. Record sections were produced and preliminary analysis was done in the field for the first experiment. These 2 experiments were:

1. Alaska; Three deployments were completed with a total of 360 recording sites. The first deployment ran from Glen Allen, AK northeast about 120 km along the Tok Cutoff. The second deployment ran from the southwest tip of Montegue Island to a point just north of Cordova, AK. The third deployment ran from the mouth of the Copper River to a point just north of Tsaina Lodge on the Richardson Highway. The instruments operated at about 95% yield.

2. Medicine Lake, CA; One hundred twenty instruments were deployed in a grid with 1 km spacing at Medicine Lake. Eight shots were fired into the grid; four at a radial distance of about 40 km and four at a radial distance of about 100 km.

Data Processing Center Operations

9930-01499

John Van Schaack
Branch of Seismology
U. S. Geological Survey
345 Middlefield Road- Mail Stop 977
Menlo Park, California 94025
(415) 323-8111, Ext. 2584

Investigations

This project has the general housekeeping, maintenance and management authority over the Earthquake Prediction Data Processing Center. Its specific responsibilities include:

1. Day to day operation and performance quality assurance of 5 network magnetic tape recorders.
2. Day to day management, operation, maintenance, and performance quality assurance of 2 analog tape playback stations.
3. Day to day management, operation, maintenance and performance quality assurance of the U.S.G.S. telemetered seismic network event library tape dubbing facility (for California, Alaska, and Hawaii).
4. Projection of usage of critical supplies, replacement parts, etc., maintenance of accurate inventories of supplies and parts on hand, uninterrupted operation of the Data Processing Center.

Results

Procedures and staff for fulfilling assigned responsibilities have been developed and the Data Processing Center is operating smoothly and serving a large variety of scientific user projects.

Geothermal Seismotectonic Studies

9930-02097

Craig S. Weaver
Branch of Seismology
U. S. Geological Survey
at Geophysics Program AK-50
University of Washington
Seattle, Washington 98195
(206) 442-0627

Investigations

1. Continued analysis of the seismicity and volcanism patterns of the Pacific Northwest in an effort to develop an improved tectonic model that will be useful in updating earthquake hazards in the region. (Weaver, Baker, Michaelson, Yelin)

2. Continued acquisition of seismicity data along the Washington coast, directly above the interface between the North American plate and the subducting Juan de Fuca plate. (Weaver, UW contract)

3. Continued seismic monitoring of the Mount St. Helens area, including Spirit Lake (where the stability of the debris dam formed on May 18, 1980 is an issue) and Elk Lake, and the southern Washington-northern Oregon Cascade Range. The data from this monitoring is being used in the development of seismotectonic models for southwestern Washington. (Weaver, Grant, Shemeta, UW contract)

4. Study of Washington seismicity, 1938-1970. Available helicorder records are being scanned in an effort to determine the completeness of existing earthquake catalogs for the time period that predates the establishment of the existing short-period network. Although the entire period is being examined, emphasis is being placed on three time periods: 1) 1944-1949 (possible foreshocks to the 1949 south Puget Sound earthquake), 2) 1960-1965 (possible foreshocks to the 1965 south Seattle earthquake), and 3) study of an earthquake sequence between 1958-1962 that occurred near Swift Reservoir (the largest event has an M_L=5.1). The events near Swift Reservoir were probably on the southern segment of the SHZ. (Yelin, Grant, Weaver)

5. Detailed analysis of the seismicity sequence accompanying the May 18, 1980 eruption of Mount St. Helens. Earthquakes are being located in the ten hours immediately following the onset of the eruption, and the seismic sequence is being compared with the detailed geologic observations made on May 18. (Weaver, Shemeta, UW contract)

Results

1. Work has been completed on determining a focal mechanism for the 1949 South Puget Sound earthquake (M=7.1). This earthquake is the largest magnitude event recorded in Washington, and the results have implications for earthquake hazards in the Pacific Northwest (eight people were killed during the earthquake) and in defining the regional tectonic framework. The focal mechanism analysis used P, SH, and SV first motions as well as the SH/SV amplitude

ratio from eight, long-period, three-component teleseismic records and three records from regional distances.

Identification of the pP phase on each of the teleseismic record indicates that the source depth is 54 km, rather than the depth of 70 km commonly cited. The focal mechanism for this event (Figure 1) was computed using a combination of manual fitting of fault planes and a grid testing routine. Both forward and inverse body wave modeling were utilized to further define source parameters. Distinct pulses, that are assumed to be source effects, were observed in the far-field waveforms, and these pulses have been modeled for the effects of directivity. This analysis made it possible to discriminate between the fault and the auxiliary plane. Our preferred fault plane strikes east-west +/-15°, dips N45°E +/-15°, and has nearly pure left-lateral strike-slip motion. The fault length is estimated to be about 40 km.

2. Earthquake hypocenters and the focal mechanisms from three large earthquakes that are interpreted as being within the Juan de Fuca plate, have been used to infer the geometry of the upper portion of the subducting plate. Using the data from the University of Washington seismic catalogs, there is a westward displacement of earthquake hypocentral depths beneath southwestern Washington as compared to northwestern Washington (Figure 2). We infer from this distribution that in the depth range of 35-60+ kilometers, the Juan de Fuca plate is dipping more steeply beneath southwestern Washington than to the north. Plotting the hypocenters south of the 1965 earthquake in a cross-section along line B-B' (Figure 3) indicates that these events are in a very thin, southeast-dipping distribution. The orientation of the T-axis, calculated from the 1949 earthquake is in very good agreement with the dip of the hypocenters. We conclude that beneath southwestern Washington the geometry of the Juan de Fuca plate is complex and has a component of plate dip to the southeast.

Reports

Weaver, C. S. and C. A. Michaelson, Seismicity and volcanism in the Pacific Northwest: evidence for the segmentation of the Juan de Fuca plate, *Geophysical Research Letters, v. 12,* 215-218, 1985.

Michaelson, C. A., and C. S. Weaver, Upper mantle structure from teleseismic P-wave arrivals in Washington and northern Oregon, submitted to *Journal Geophysical Research,* (Director's approval, 2/85).

Baker, G. E., *Source parameters of the magnitude 7.1, 1949, South Puget Sound, Washington earthquake determined from long-period body waves,* M.S. thesis, University of Washington, 68 pp., 1985.

Weaver, C. S., G. E. Baker, and S. W. Smith, Complex plate geometry beneath Washington: Evidence from seismicity and the 1949 South Puget Sound earthquake, submitted to *Science,* (Director's approval, 8/85).

Weaver, C. S., Combined regional seismotectonics and the extent of Cenozoic volcanism: An improved first-order geothermal assessment of the Cascade Range? (abs), in, *U. S. Geological Survey Open-File Report,* in preparation, (Director's approval, 7/85).

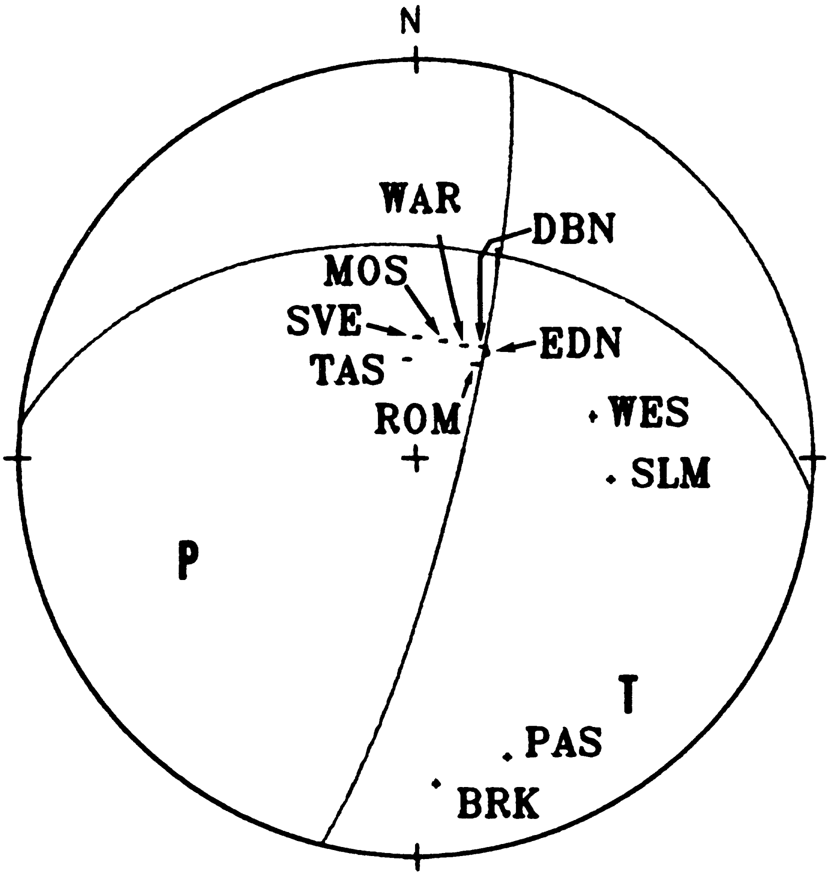

Figure 1: Long-period focal mechanism for the 1949 south Puget Sound, Washington earthquake (M=7.1). Shown in this figure are the P-wave polarities, with "-" being dilatation, "+" being compressional, and "0" (at EDN) nodal. The east-west striking plane is the preferred fault plane. Plot is equal area, lower hemisphere.

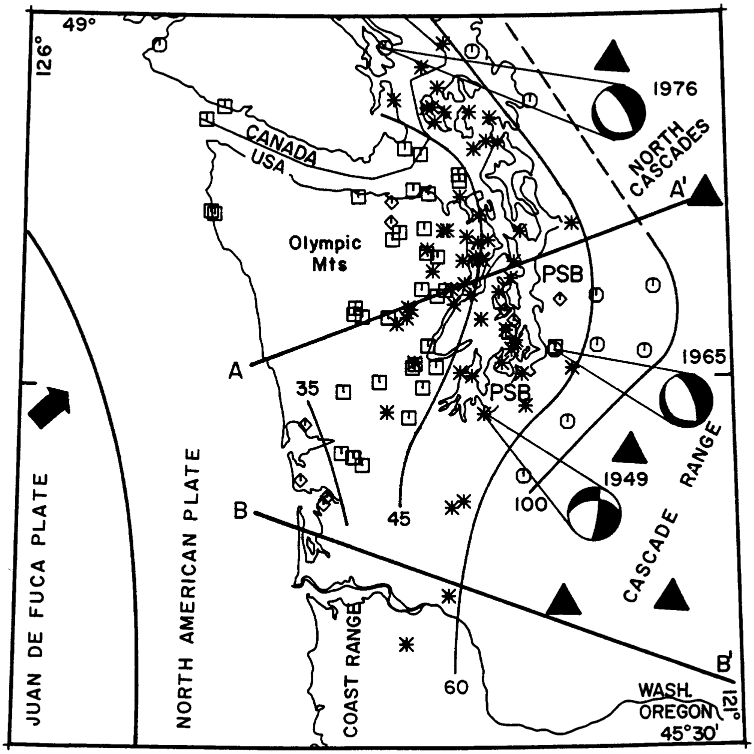

Figure 2: Hypocenters for earthquakes within the Juan de Fuca Plate. Symbols represent depth range, with diamonds being 30-35 km, squares 35-45 km, asterisks 45-60 km, and circles 60-100 km. Contours are hand-drawn, dashed where more poorly constrained. Focal mechanisms are shown for three large magnitude events; the 1965 and 1976 events have been studied by others, the 1949 event focal mechanism is taken from Figure 1.

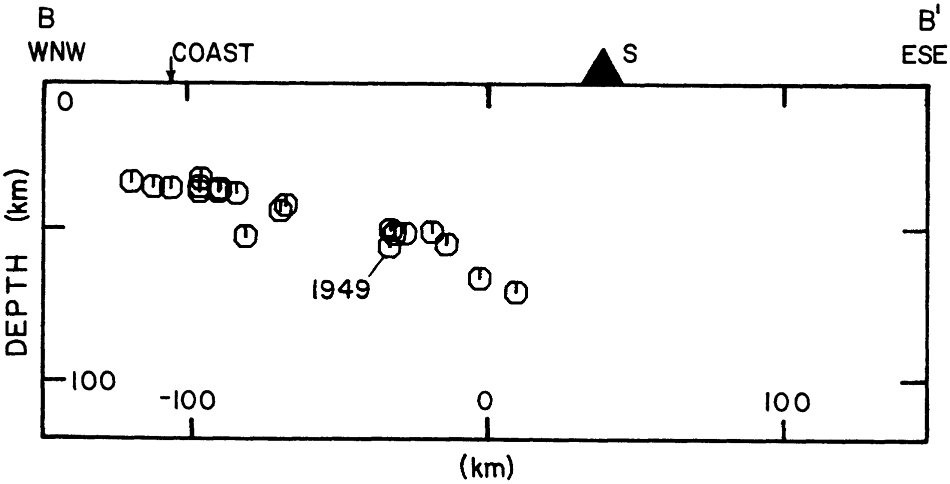

Figure 3: Cross-section of earthquakes located south of the 1965 event. Cross-section is oriented along the strike of line B-B' in Figure 2, view is to the north-northeast. No vertical exaggeration.

Holocene deformation near Coalinga, California

9540-02190

Brian F. Atwater, Project Chief
Branch of Western Regional Geology
c/o Department of Geological Sciences AJ-20
University of Washington
Seattle, WA 98195
(206) 543-0804

Investigations and Results

The investigations and results described for this project in Summaries of Technical Reports, volume 20, were written up as a chapter for the Coalinga Professional Paper. This chapter has been revised following peer review.

Reports

Atwater, B.F., Tinsley, J.C., Stein, R.S., Trumm, D.A., Tucker, A.B. Donahue, D.J., and Jull, A.J.T., 1985, Progress toward estimation of earthquake recurrence at Coalinga Anticline, California: EOS (abstract EOS, in press)

QUATERNARY DEFORMATION STUDIES IN THE REGION OF THE MENDOCINO TRIPPLE JUNCTION

Contract No. 14-08-0001-22009

Gary A. Carver and Raymond M. Burke
Dept. of Geology
Humboldt State University
Arcata, California 95521
(707) 826-3931
and
Harvey M. Kelsey
Dept. of Geology
Western Washington University
Bellingham, Washington
(206) 676-3582

Investigations

1. Marine terrace mapping and deformation investigation.
2. Marina terrace soils and terrace remnant correlation studies.
3. Mapping and structure analysis of San Andreas system-Coastal thrust zone transition faulting.

Results

1. Remnants of raised marine terraces are present along most of the coast between Cape Mendocino and Big Lagoon (Fig. 1 and Fig. 2). The terrace remnants are displaced by northwest trending northeast dipping thrust and reverse faults, folded by northwest trending anticlines and synclines, and tilted on rotated fault bounded blocks (Carver et. al. 1983). Terrace remnants are best developed and preserved on uplifted headlands, especially the Trinidad headland and Table Bluff, where at least 5 emergent surfaces are present.

The style of deformation recorded in the terraces changes from south to north along this section of the coast. Late Quaternary growth of large folds, including the Eel River syncline and the Humboldt Hill and Table Bluff anticlines dominate the deformation recorded in the terraces between Cape Mendocino and Eureka. The first (lowest) emergent terrace at Table Bluff is tilted 2 to 3 degrees in the limbs of the Table Bluff anticline and uplifted 55 meters above present sea level at the fold axis. The second and third emergent terraces at Table Bluff are inclined 5 and 8 degrees in the fold limbs and uplifted 60 and 113 meters above present sea level at the axis. Similar folded terrace remnants are present at Humboldt Hill.

The terraces at Eureka are nearly horizontal and show little evidence of tilting or faulting. The prominent Eureka surface has been uplifted 35 meters above present sea level.

North of Eureka, terrace remnants record late Quaternary deformation resulting principally from displacement on thrust and reverse faults and northeast tilting on fault bounded blocks. Vertical displacements of the first emergent terrace of 28 to 37 meters across each of four major faults, the Fickle Hill, Mad River, McKinleyville, and Trinidad faults, have been measured. Tilting of the first emergent terrace remnants on blocks bounded by these faults ranges from less than 1 to 3 degrees. Small folds and warps are apparent in the terraces near the faults.

The first emergent terrace has been uplifted a maximum of 68 meters above present sea level near Trinidad, and tilted 3 degrees to the northeast at Big Lagoon where the terrace extends below present sea level.

2. Soils developed on marine terrace remnants have been studied at 29 sites along the coast between Table Bluff and Big Lagoon (Fig. 1 and 2). To date soil profiles have been described and sampled and particle size analysis has been completed. Preliminary interperation of the soils data suggests terrace remnants along the coast between Table Bluff and Big Lagoon represent at least 4 soil age classes, and that remnants of the same age class can be correlated on the basis of their soil characteristics (Fig.3). The first emergent terrace remnants at Trinidad, McKinleyville, and Table Bluff are capped by thin (<120 cm) weakly developed soils which lack argillic (Bt) horizons. The second emergent terrace remnants at Trinidad and Table Bluff and the first emergent remnants at Eureka and Humboldt Hill are characterized by soils with moderately thick (150 to 185 cm) profiles and argillic (Bt) horizons containing 30 to 40 percent clay. The third soil age class is represented by thick (>200cm) profiles with thick argillic horisons containing 38 to 42 percent clay and occurs on the third emergent terrace at Table Bluff, the second emergent terrace at Humboldt Hill, and the first terrace at Arcata. The oldest terrace soil examined in this investigation is present on the fourth terrace at Trinidad. This soil has an argillic (Bt) horizon 120 cm. thick containing 43 to 47 percent clay.

3. Field studies of late Cenozoic structures at four areas on or near the boundray between the San Andreas fault system and the coastal thrust and fold zone have been initiated. The study areas, located near Garberville, Bridgeville, Maple Creek, and Gold Bluffs, include faulted, folded, and tilted sequences of late Cenozoic sediments at or near the northern end of the Maacama, Eaton Roughs, Lake Mountain, and Grogan faults (Herd, 1978; Upp, 1982; Kelsey and Cashman, 1983; Kelsey and Allwardt 1983). Field investigations are directed toward measurment and mapping of deformation structures, especially faults and folds, in the late Cenozoic sediments.

References

Carver, G. A., Stephens, T. A., and Young, J. C., 1983, Quaternary thrust and reverse faulting on the Mad River fault zone, coastal northern California, Geol. Soc. Am. abs. with program, v.15, no. 5.

Herd, D. G., 1978, Intracontinental plate boundray east of Cape Mendocino, Geology, v. 6, p 721-725.

Kelsey, H. M. and Allwardt, A. O., 1983, Evidence for a major Quaternary fault zone in the Central Belt Franciscan melange, northern California; Geol. Soc. Am. abs with program, v. 15, no. 5.

Kelsey, H. M. and Cashman, S. M., 1983, Wrench faulting in northern California and its tectonic implications; Tectonics, v.2, p. 565-576.

Upp, R. R., 1982, Holocene activity on the Maacama fault, Mendocino County, California; [PhD dissertation] Stanford University 112 p.

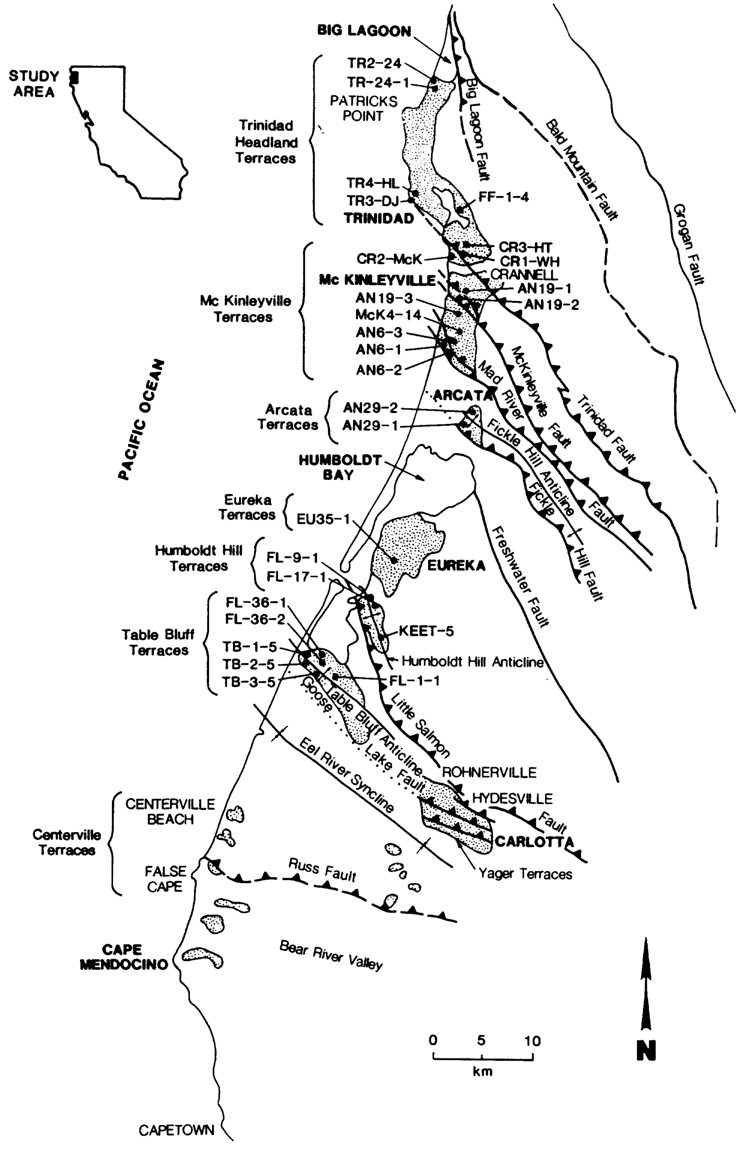

Figure 1. Map of coastal California between Cape Mendocino and Big Lagoon showing principal late Quaternary Quaternary tectonic structures, terrace remnants (shaded), an soil analysis sites.

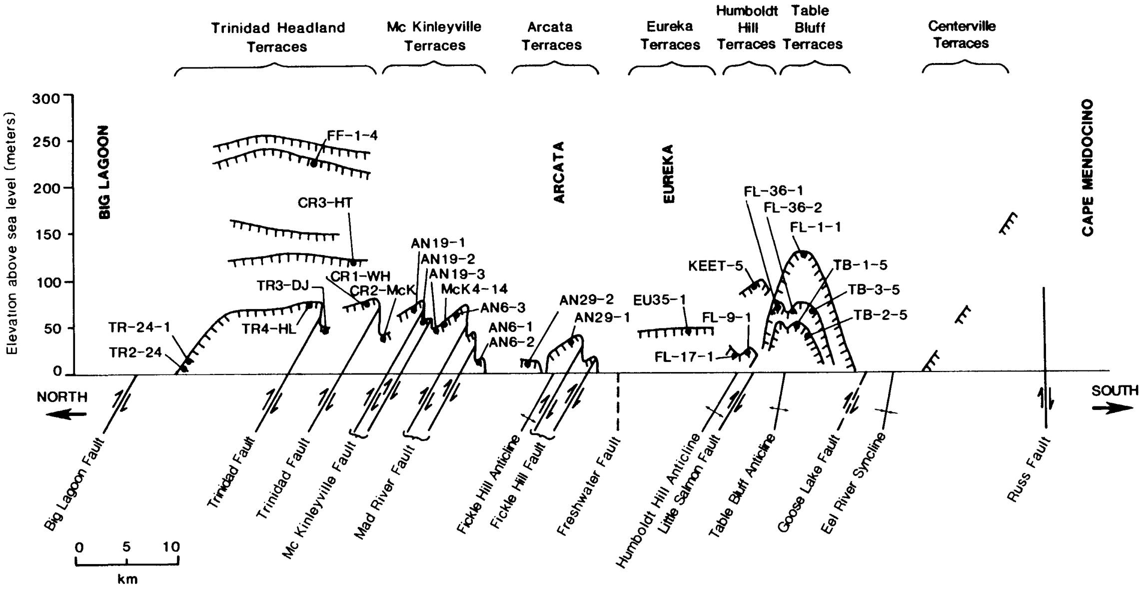

Figure 2. North-south section along the coast between Big Lagoon and Cape Mendocino showing principal late Quaternary tectonic structures, terrace remnants (hachered lines), and soil analysis sites.

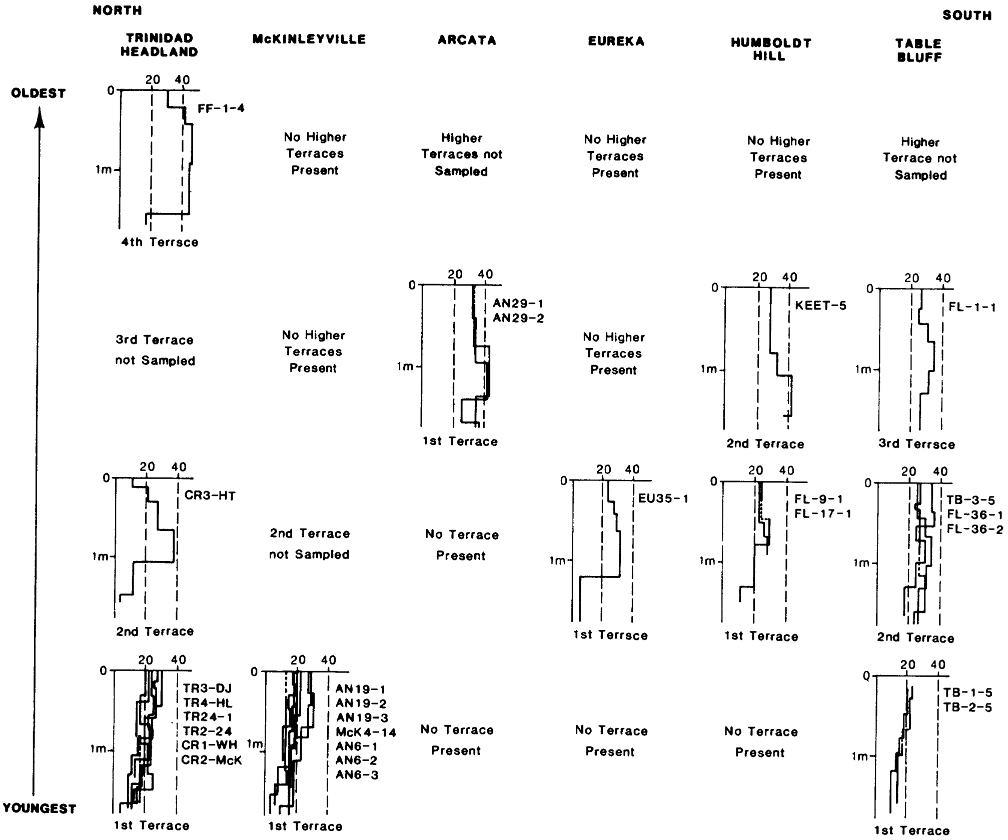

Figure 3. Clay-size particle distribution (profile depth - vertical axis - vs. percent clay - horizontal axis) for soils on terraces between Cape Mendocino and Big Lagoon. Profiles are arranged on the diagram according to preliminary interpretation of four age classes, youngest at the bottom.

Comparative Earthquake and Tsunami Potential for Zones in the Circum-Pacific Region

9600-98700

George L. Choy
Stuart P. Nishenko
William Spence
Branch of Global Seismology and Geomagnetism
Denver Federal Center
Box 25046, Mail Stop 967
Denver, Colorado 80225
(303) 236-1506

Investigations

1. Prepare detailed maps and text of comparative earthquake potential for the west coasts of Mexico, Central America, and South America.

2. Conduct investigations of the historic repeal-time data for great earthquakes in the northern Pacific Ocean margin.

3. Develop a working model for the interaction between forces that drive plate motions and the occurrence of great subduction zone earthquakes. Develop a rapid method for the estimation of the source properties of significant earthquakes.

4. Conduct investigations into the tectonic mechanisms of major earthquakes in Peru and the central Sunda arc in order to assess the likelihood of possible major subduction zone events in those locations.

Results

1. The probabilistic work for the west coast of Chile and southern Peru has been done. The corresponding paper was published in the April 1985 issue of the Journal of Geophysical Research. In collaboration with scientists of CERESIS, data are being gathered for the probabilistic analysis of the rest of the west coast of South America and Central America. Dr. Mendoza is completing a study of the great earthquake of Colombia, 1979. The probabilistic work for northern Mexico is largely completed, and the results will be submitted for publication towards the end of the year by Drs. Nishenko and K. Singh (University of Mexico). Two seismic gaps stand out as having high probabilities for recurrence of large earthquakes within the next two decades: the central Oaxaca gap and the Acapulco-San Marcos gap. The Michoacan earthquake of September 1985 occurred in a known gap, but insufficient repeat-time data precluded a reliable probabilistic evaluation. An analysis of the 1932 Jalisco earthquake, which until 1985 was the largest event in Mexico this century, has been published in the Bulletin of the Seismological Society of America.

2. Data on the occurrence of great earthquakes and tsunamis from the Queen Charlotte Islands through the Aleutians have been collected. Evaluation of the probabilistic recurrences in this region will be done by Dr. Nishenko in collaboration with Dr. K. Jacob (LDGO).

3. An evaluation of the ridge push and slab pull forces in the context of the stress that leads to great subduction zone earthquakes has been completed and a paper submitted to the Journal of Geophysical Research. We are developing and testing an algorithm to automate processing of broadband digital data which will permit rapid estimation of important source properties of all earthquakes with $m_b > 5.8$.

4. Research has been completed on the 1974 central Peru earthquake (M_S 7.8). One conclusion is that the maximum likely earthquake to occur in central Peru is M_S 8.4. A study on the central Sunda arc earthquake of 1977 (M_S 7.9) is complete. A primary conclusion is that a great thrust earthquake will not occur at the arc, but that a great normal-faulting earthquake is possible.

Reports

Choy, G. L., Broadband body-wave analysis of the complex rupture process of the Samoa earthquake of September 1, 1981: Journal of Geophysical Research, submitted.

Nishenko, Stuart P., 1985, Seismic potential for large and great interplate earthquakes along the Chilean and southern Peruvian margins of South America: A quantitative reappraisal: Journal of Geophysical Research, v. 90, p. 3589-3615.

Nishenko, S. P., and Singh, S. K., Conditional probabilities for the occurrence of large plate boundary earthquakes along the Mexican subduction zone: 1985-2005, in preparation.

Singh, S. K., Ponce, L., and Nishenko, S. P., 1985, The great Jalisco, Mexico earthquakes of 1932 and the Rivera subduction zone: Bulletin of the Seismological Society of America, in press.

Spence, William, The 1977 Sumba earthquake series: Direct evidence for slab pull: Journal of Geophysical Research, submitted.

Earthquake Hazard Investigations in the Pacific Northwest

14-08-0001-22007

R.S. Crosson
Geophysics Program
University of Washington
Seattle, WA 98195
(202) 543-8020

Investigations

The objectives of this research are to provide fundamental data and interpretations for earthquake hazard investigations. Currently, we are focusing on seismicity, structure, and tectonic questions related to the occurrence of a hypothetical major subduction earthquake on the Juan de Fuca - North American plate boundary. Specific tasks which we have worked on in this contract period are:

1. Compiling a uniform data-base of all arrival time data available for Washington and northern Oregon from 1970 to the present.

2. Calibration of computer determined codas for magnitude determination.

3. Initial studies of tomographic inversion of travel times to determine three-dimensional earth structure.

4. Locations, focal mechanisms and occurrence characteristics of crustal and subcrustal earthquakes beneath western Washington and their relationship to subduction processes.

5. Re-examination of teleseismic travel-times of large events in the Pacific Northwest for evidence of slab location and orientation.

6. Analysis and interpretation of Pn observations.

7. Study of three-dimensional seismic attenuation (Q) structure of the Puget Sound area (primarily funded under another project).

Results

1. We are establishing a uniform base of arrival time data for all network data from 1970 to the present. From 1970 through 1979, data were archived in several different formats, at several sites. 'Pickfiles' of arrival times have been reformatted and events relocated using updated velocity models and location routines. The western Washington data from 1970-1979 are complete, and are being used in research. Eastern Washington data from 1975-1979 have been reformatted, and are being checked for completeness.

2. We have completed calibration of our compute coda magnitude determination algorithm using 18 earthquakes for which M_L was available. Routine use of this procedure may improve the consistency of magnitude estimates.

3. We are investigating the feasibility of a tomographic inversion of arrival-time data to determine the velocity structure of the Puget Sound area using P and S-wave data recorded by the

University of Washington seismic network. We hope to use local events to determine crustal velocity structure shallower than about 40 km. We are presently exploring the effect of a non-isotropic data set, and calculating the approximate resolution which could be achieved with this method.

4. A data base of focal mechanisms is being established. We have plotted stereographic projections of first-arrival polarities for about 60 of the largest earthquakes in Washington. These projections are being checked against data traces, and focal mechanisms determined when possible. A grading scheme will be implemented to indicate the quality of focal mechanism solutions. Such a grading scheme will consider inconsistent or ambiguous arrivals, and the range of feasible focal mechanisms. Once completed, the data base will be used to determine the most probable set of regional tectonic stresses in western Washington.

5. Teleseismic residuals from the 1965 Puget Sound earthquake were interpreted by McKenzie and Julian (1971) to indicate a north-south striking slab dipping 50 degrees East. These residuals were calculated using the Jeffreys-Bullen travel-time tables. We are redoing these calculations using several travel-time models and additional earthquakes in an attempt to determine if slab effects are indeed detectable.

6. Previously reported results from Pn analysis have been submitted to the BSSA in an article by C. Zervas and R. S. Crosson.

7. Under another contract, we are undertaking an evaluation of seismic attenuation in western Washington. In cooperation with Dr. W.H.K. Lee of the USGS, we are using spectral estimates of coda waves to determine regional coda Q. A preliminary data set of fifty events has been processed, and results are being analyzed.

Articles

Ludwin, R.S., S.D. Malone, R.S. Crosson, 1985 (in press), Washington Earthquakes, 1983, National Earthquake Information Service

Zervas, C.E. , and R.S. Crosson, 1985 (submitted to BSSA), Pn Observations and Interpretations in Washington

Reports

Univ. of Wash. Geophysics Program, 1984, Quarterly Network Report 85-A on Seismicity of Washington and Northern Oregon

Univ. of Wash. Geophysics Program, 1984, Quarterly Network Report 85-B on Seismicity of Washington and Northern Oregon

Investigation of Seismic-Wave Propagation for Determination of Crustal Structure

9950-01896

Samuel T. Harding
Branch of Engineering Geology and Tectonics
U.S. Geological Survey
Box 25046, MS 966, Denver Federal Center
Denver, CO 80225
(303) 236-1572

Investigations

1. Finished processing and interpreting the seismic-reflection lines across the Beatty scarp, Beatty, Nevada.

2. Finished processing of all the 48-fold seismic-reflection surveys available to the USGS in the New Madrid seismic zone and began to the interpret the deeper structures.

Results

1. Two high-resolution seismic-reflection surveys were conducted across two scarps near Beatty, Nev., by employing the MINI-SOSIE system technique. The first survey was run across the scarp southeast of Beatty over a feature mapped as the Beatty fault. Reflection profiles from this area indicated the absence of faulting where the line was run. The next profile that was run across a fault scarp on the east side of Crater Flats showed one fault with a throw of approximately 30 m. This fault appeared on a reflector at 160-m depth and was located east of the fault scarp. This fault, if associated with the scarp, represents a strike-slip fault or a reverse fault, or perhaps a combination of the two. No hint of normal faulting could be seen from the data collected.

2. From reprocessed seismic-reflection data west of Caruthersville, Mo., along the trend of the New Madrid seismic zone, a large-scale fault has been found that is coincident with the earthquake activity. This fault has many of the characteristics of a large strike-slip fault which is consistent with the fault-plane solutions determined for this part of the New Madrid seismic zone. The largest displacement is seen on sub-basement reflectors with a throw of 380 m and a net slip of 400 m. As the fault approaches the surface, the fault dies out into folds which are characteristic of flower structures attributed to strike-slip faulting. This fault has a west dip of approximately 75° and terminates at 12.8 km in the midcrustal reflections. The maximum fault downdip dimension (width) seen on this profile is 7.5 km.

Report

Dwyer, R. A., and Harding, S. T., 1985, New Madrid fault from seismic-reflection data [abs.]: Eastern Section Seismological Society of America, Knoxville, Tennessee.

Seismic Source Characteristics of Western States Earthquakes

Contract No. 14-08-0001-21912

Donald V. Helmberger

Seismological Laboratory,
California Institute of Technology
Pasadena, California 91125
(818)-356-6998

Investigation

There are strong suggestions that earthquakes occurring at particular locations tend to reproduce nearly identical signals, for example see Richter (1958). The phenomenon of certain regions having higher stress drop than others has been discussed for many years, Thatcher (1971) and more recently Nava and Brune (1983). Thus, we suggest that a good appreciation of the characteristics of faulting in the various regions should be included along with the seismicity patterns in hazard appraisal. We address the problem of determining the source parameters with magnitudes greater than about 4.5 by applying a semi-automated inversion technique. Many of the earthquakes in this magnitude class are not well suited to the waveform analysis of the teleseismic body waves or surface waves because they are not large enough to produce usable records at large distances. On the other hand, the earthquakes are small enough to produce on-scale recordings at regional distances (2° to 30°). Recently, we have shown that it is possible to retrieve the source parameters of moderate size earthquakes from long-period seismograms at these distances, for example see Figure 1.

We plan to analyze the waveforms of 30 to 40 WUS and Northern Mexico earthquakes (Baja) which were recorded on the LRSM and WWSS networks during the post-1962 years. We hope that these results will provide the ground work (reference events and paths) for extending the waveform analysis to pre-1962 data.

Results

This project has just begun and most of the efforts have gone into data collection and digitization. A six-month no-cost extension has been requested because of the slow rate of obtaining the LRSM data. Complete data sets for about 10 events have been assembled and will be reported on shortly. The particular results for one of these events, namely the Walker Pass earthquake of 1962, will be briefly discussed in this summary.

The Walker Pass earthquake ($M_L = 6.3$) of 15 March 1946 occurred near the 16 September 1962 event ($M_L = 4.9$), thus the latter can be used as a Master event in later analysis of the larger event. The 1946 event produced significant strong motions in Pasadena and is well-recorded. Both earthquakes are located on the eastern edge of the southern Sierra Nevada mountains at approximately 35.75° north latitude and 118.05° west longitude. P_{nl} modeling of the WWSSN data (rather sparce at this early date) and the LRSM data for the 62 event is displayed in figure 1 following the procedure discussed by Wallace et. al (1981). The solution has been constrained to fit the first motion information from the Berkeley and Caltech arrays as well, see Dollar and Helmberger (1985). The orientation and the moment are well constrained but not the depth or time history. The latter parameters are obtained from the short-period information, see figure 2, where the depth phase pP is especially clear. Assuming a $t_\alpha^* = .6$, we obtain a triangular source time history with a rise time of .4 secs and a decay time of .4. The epicenter depth is determined to be 16 km which is significantly deeper than assigned to this event by the standard short-period network, namely 4 to 7 km.

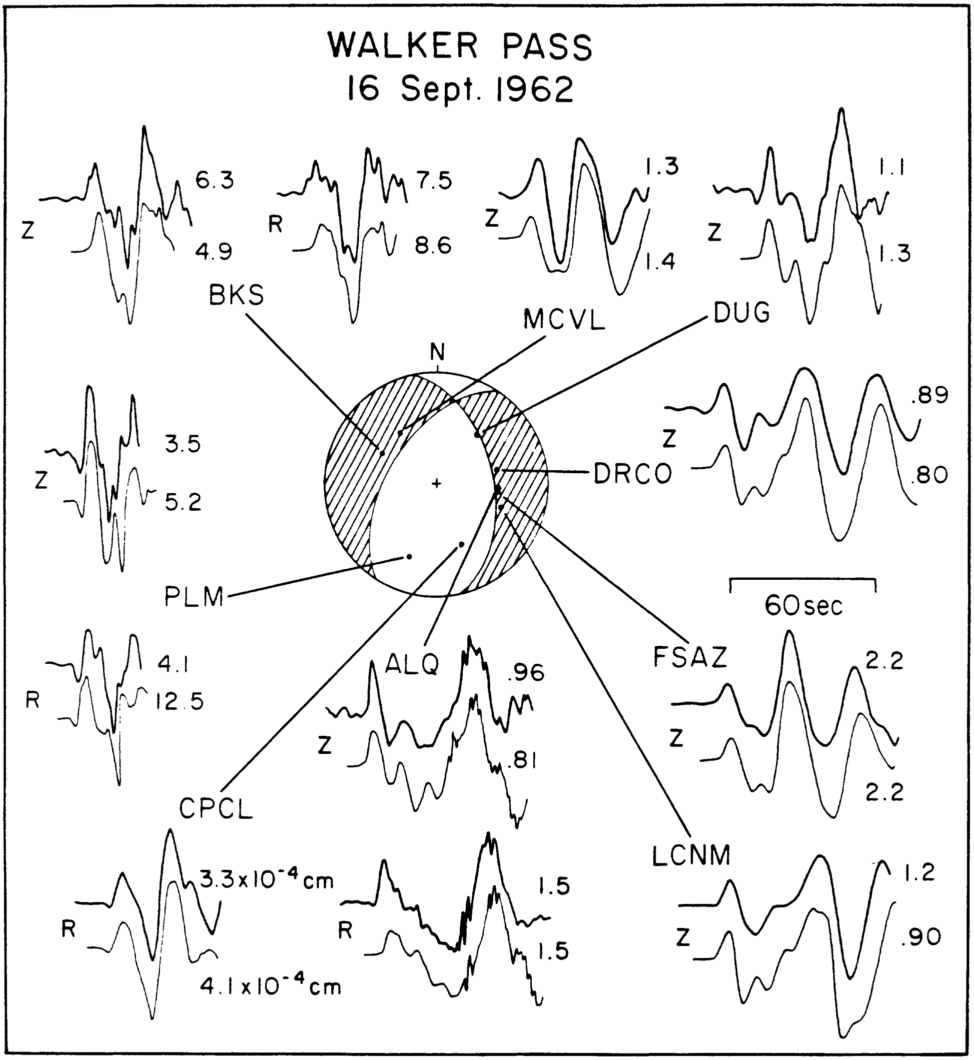

Figure 1: Comparison between P_{nl} observations (upper trace) and synthetics (lower trace). The stations with four letters belong to the LRSM network while the three letter designation indicates WWSSN stations. The orientation parameters are: strike $= 346^o$, dip $= 45^o$, and rake $= 243^o$. The moment estimate is $.51x\,10^{24}$ dyne-cm.

This WUS (Western United States) event appears to have a relatively short duration ($\tau = .8$) compared to its' moment ($M_0 = .65 \times 10^{24}$) and would be considered to be a high-stress drop event. Secondly, events with similar moments and durations in the eastern United States, as reported by Somerville (1985) and LeFevre (1985), produce short periods back in California of the same magnitude indicated in figure 2.

The P_{nl} comparisons for the New Brunswick earthquake of January 9, 1982 are displayed in figure 3 where the orientation was constrained by first-motions and the study by Nabelek (1984). He, also, assumed a $t_\alpha^* = .6$ in modeling a small telesiesmic data set and obtained a moment estimate of 1.3×10^{24} dyne-cm which agrees well with the P_{nl} results. However, the New Brunswick event has a magnitude of 5.7 while Walker Pass has a magnitude of 4.9. This mismatch in magnitude, but with comparable physical parameters, will be addressed with larger data sets as this study progresses. Also, the question of stress-drop versus depth needs to be examined since we generally do not see teleseismic short periods from WUS events with moment of (10^{24} dyne-cm) shallower than 6 kms unless they are at NTS.

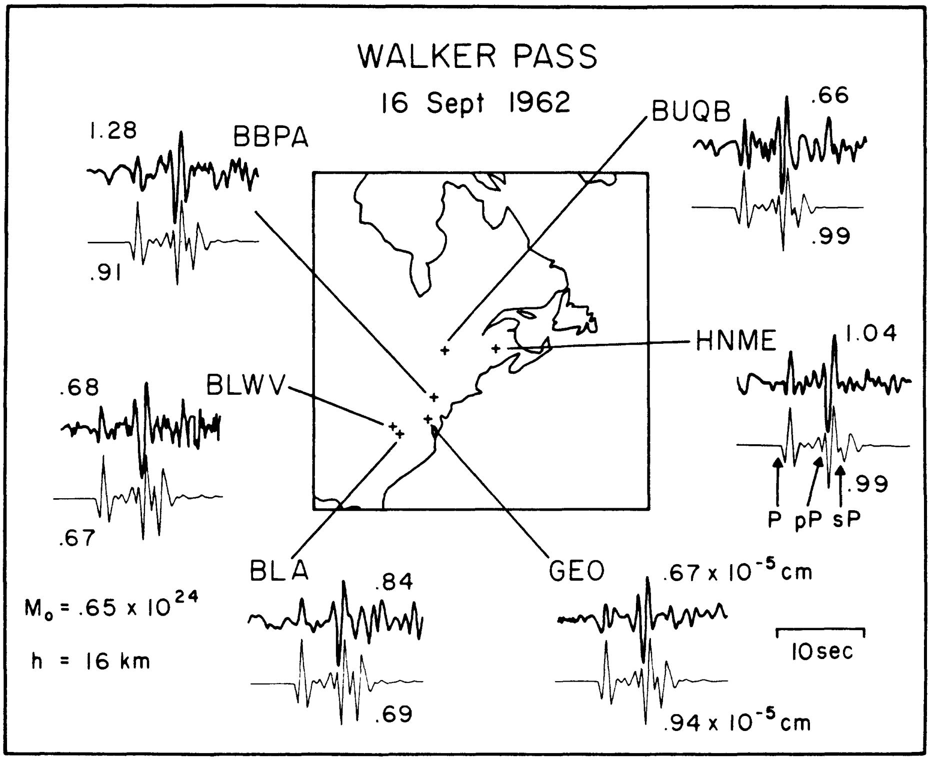

Figure 2: Comparison of teleseismic short-period seismograms and synthetics assuming $t_\alpha^* = .6$ with a duration of .8 secs. The numbers indicate the displacement amplitude.

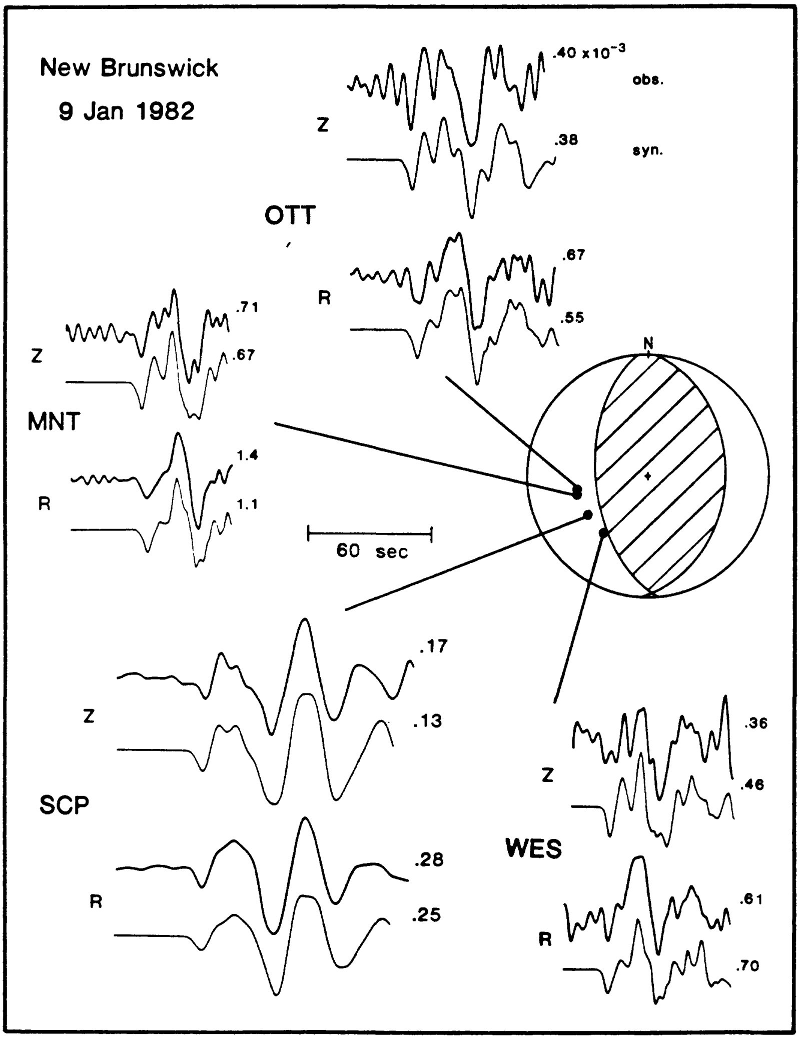

Figure 3: Comparison of P_{nl} synthetics and observations with the solution proposed by Nabelek (1984). The numbers indicate the displacement amplitude in cm assuming a moment of $1.6x\,10^{24}$ dyne-cm.

References

Dollar, R. S. and D. V. Helmberger, 1985, Body wave modeling using a master event for the sparsely recorded 1946 Walker Pass, California earthquake, AGU abstract.

Helmberger, D. V. and G. R. Engen, 1980, Modeling the long-period body waves from shallow earthquakes at regional distances, Seismol. Soc. Amer., Bull., 70, pp. 16 1714.

LeFevre, L. V., 1985, Seismic moments of intraplate earthquakes from seismograms at regional distances, AGU abstract.

Nabelek, J. L., 1984, Determination of earthquake source parameters from inversion of body waves, Ph.D. thesis, Massachusetts Institute of Technology.

Nava, F. A. and J. N. Brune, 1983, Source mechanism and surface wave excitation for two earthquakes in Northern Baja, California, Mexico, Seismol. Soc. Amer., Bull., in press.

Richter, C. R., 1958, Elementary Seismology, W. H. Freeman and Company, San Francisco, California.

Somerville, P., 1985, Constant stress-drop scaling at large eastern north American earthquakes, AGU abstract.

Thatcher, W., 1971, Surface wave propagation and source studies in the Gulf of California region, Ph.D. thesis, Caltech, Pasadena, California.

Wallace, T. C., D. V. Helmberger and G. R. Mellman, 1981, A technique for the inversion of regional data in source parameter studies, J. Geophys. Res., 86, pp. 1679-1685.

Earthquake Hazard Research in the Central Mississippi Valley

14-08-0001-21999

Robert B. Herrmann
Department of Earth and Atmospheric Sciences
Saint Louis University
P.O. Box 8099 Laclede Station
St. Louis, MO 63156
(314) 658-3131

Goals

1. Perform research on the earthquake process in the New Madrid Seismic Zone to delineate the active tectonic processes. 2. Perform more general research relating to the problems of the eastern U. S. earthquake process and of the nature of eastern U. S. earthquakes compared to western U. S. earthquakes.

Investigations

1. A reinvestigation of spectral scaling of earthquakes in the Central Mississippi Valley Seismic zone is being initiated. Care will be taken to determine a corner frequency versus seismic moment scaling which is obtained from vertical component Lg recordings that have been corrected properly for anelastic attenuation.

2. A theoretical study of the effect of local structure on Lg amplitude spectra shows that there is little bias in seismic moment estimates using vertical component data but substantial bias using horizontal component data when hard rock and Mississippi Embayment earth models are compared.

Results

The following theses have been completed. Copies of the theses have been forwarded to the External Program, Office of Earthquake, Volcanoes and Engineering, USGS at Reston, VA, Menlo Park, CA. Copies have also been sent to the Branch of Engineering Geology, and Tectonics, OEVE, USGS, Golden, CO.

Chulick, J. A. (1985). A comparison of M_L to m_{Lg} for large California earthquakes with scaling considerations for strong ground motion, M. S. Thesis, Saint Louis University, 76pp.

Nguyen, B. V. (1985). Surface-wave focal mechanisms, magnitudes, and energies for some Eastern North American earthquakes with tectonic implication, M. S. Thesis, Saint Louis University, 275pp.

Leu, P.-L. (1985). Magnitude corrections for the central Mississippi Valley seismic network, M. S. Thesis, Saint Louis University, 162pp.

Shin, T.-C. (1985). Lg and coda wave studies of Eastern Canada, Ph. D. Dissertation, Saint Louis University, 185pp.

The following papers have been submitted for publication or have been published:

Saikia, C. K. and R. B. Herrmann (1985). Application of waveform modeling to determine focal mechanisms of four 1982 Miramichi aftershocks, *Bull. Seism. Soc. Am.* **75,** 1021-1040.

Herrmann, R. B. (1985). An extension of random vibration theory estimates of strong ground motion to large distances, "Letter to the Editor," *Bull. Seism. Soc. Am.* **75,** (in press).

Herrmann, R. B. (1985). Surface-wave studies of some South Carolina earthquakes, *Bull. Seism.*

Soc. Am. **75,** (in press).

Saikia, C. K. (1986). Wave form modeling of two earthquakes (M ~ 1.1) of July, 1983 from Miramichi aftershock zone, *Bull. Seism. Soc. Am.* **76,** (in review).

Saikia, C. K. and R. B. Herrmann (1986). Determination of focal mechanisms of some earthquakes at Monticello, South Carolina, and earth structure by waveform modeling, *Geophys. J.* (in review).

Saikia, C. K. and R. B. Herrmann (1986). Moment-tensor solutions for three 1982 Arkansas swarm earthquakes by waveform modeling, *Bull. Seis. Soc. Am.* **76,** (in review).

Tectonics of Central and Northern California

9910-01290

William P. Irwin

Branch of Engineering Seismology and Geology
U.S. Geological Survey
345 Middlefield Road, MS 977
Menlo Park, CA 94025
(415) 323 8111, ext. 2065

Investigations

1. Continued preparation of a geologic map of Klamath Mountains and adjacent areas, California and Oregon (scale 1:500,000), for purposes of tectonic analysis of the region.

2. Compilation of the geology of the Redding 2-degree sheet, California (scale 1:250,000), in cooperation with J. P. Albers and others. Field work included reconnaissance of unmapped parts of Ironside Mountain 15-minute quadrangle to prepare map coverage suitable for compilation of the Redding sheet.

3. Paleomagnetic study to determine the rotational and translational histories of the accreted terranes of northern California, in collaboration with E.A. Mankinen and C.S. Gromme.

Results

During the report period, additional paleomagnetic work was done on the Shasta Bally plutonic belt and on the Ironside Mountain batholith. Our previous studies of the Klamath Mountains had indicated that the province consists of two major subdivisions which we called the northeastern and southwestern domains. Although the two domains are tectonically distinct, the boundary between them is a rather vague and imprecise northwest-trending zone. The paleomagnetic investigations previously reported are based on studies in the northeast domain, excepting those made on Shasta Bally batholith which lies along the boundary and may be in the southwest domain. These previous investigations have shown that the Paleozoic and pre-Cretaceous Mesozoic formations and plutons of the northeastern domain generally show strong clockwise rotation. However, the Early Cretaceous Shasta Bally batholith and related plutons show little or no clockwise rotation (13°±14.3°). We interpreted this virtual cessation of rotation to indicate the end of the tectonic accretion of the Klamath mountains to the North American continent. Paleomagnetic results we had obtained on the Great Valley overlap sequence at the south end of the province (12.7°±17.8°), and those that are reported for Tertiary volcanic rocks of the nearby southern Cascade Range (13.0°±8.6°), are remarkably similar to the results for the Shasta Bally plutonic belt. This strongly suggests that the Klamath Mountains province, the northern Great Valley sequence, and the southern Cascade Range rotated a small amount clockwise as a single rigid block during middle or late Tertiary time.

As most of the paleomagnetic information on the Klamath Mountains is from the northeast domain, we focused our most recent field work on the southwest domain in an effort to establish whether the tectonic histories of the two domains are similar. We core-drilled several widespread localities along the length of the Ironside Mountain batholith, but laboratory results from this latest sampling are not yet completed.

Reports

Irwin, W.P., 1985, Age and tectonics of plutonic belts in accreted terranes of the Klamath Mountains, California and Oregon, in D.G. Howell, ed., Tectonostratigraphic terranes of the circum-Pacific region: Circum-Pacific Council for Energy and Mineral Resources, Earth Science Series, no. 1, p. 187-199.

Blome, C.D., and Irwin, W.P., 1985, Significance of equivalent radiolarian ages from ophiolitic terranes of Cyprus and Oman: Geology, v. 13, p. 401-404.

Irwin, W.P., 1985, Reconnaissance geologic map of the Hyampom quadrangle, Trinity and Hummboldt Counties, California: U.S. Geological Survey, Miscellaneous Field Studies Map MF-1809, scale 1:62,500.

Irwin, W.P., Yule, J.D., Court, B.L., Snoke, A.W., Stern, L.A., and Copeland, W.B., 1985, Reconnaissance geologic map of the Dubakella Mountain quadrangle, Trinity, Shasta, and Tehama Counties, California: U.S. Geological Survey, Miscellaneous Field Studies Map MF-1808, scale 1:62,500.

Mankinen, E.A., Gromme, C.S., and Irwin. W.P., 1985, Paleomagnetic constraints on the accretionary history of the Klamath Mountains province, California and Oregon [abs.]: Eos (American Geophysical Union, Transactions), in press.

Postglacial uplift in northeastern United States
9510-3207

Carl Koteff
U.S. Geological Survey
National Center, MS 928
703/860-6503   FTS 928-6503

INVESTIGATIONS

Field investigations were conducted in coastal Maine and adjoining New Brunswick, Canada, this past half year. Glacio-marine deltas that were constructed at the retreating ice margin into the transgressing sea were examined, and several precise altitudes of the former sea level were obtained at the topset/foreset contact of these deltas. This method has been shown to be a very accurate way to depict former water levels in both lacustrine and marine environments. Much of the work this past field season was done in cooperation with the Maine Geological Survey, and in part helped to refine their previous studies. The age of the marine deltas in Maine range from about 14,000 B.P. in the southwestern part of the state to about 13,000 B.P. in the eastern part and in New Brunswick. Beach deposits formed during offlap were also examined. These features date from about 13,000 B.P. and younger, constructed after the rate of uplift exceeded the rate of sea level rise. Late glacial deposits inland from the marine limit were also examined to establish their relationship to the deglacial pattern.

RESULTS

The systematic nature of ice retreat (morphosequence concept) is now demonstrated by both the marine features and inland glacial deposits. Previously, regional stagnation was thought to be the prevalent mode of deglaciation that followed systematic ice retreat in the marine areas. This is important in establishing an uplift isobase model that has not been complicated by either major ice readvances (there were none) or a lingering regional stagnating ice mass. However, it appears that there are varying ages for retreatal ice-marginal positions, which were controlled by local topography as well as the presence of a local active ice cap in northern Maine and the Maritime Provinces of Canada. During the 14,000-13,000 B.P. time span represented by these ice-marginal positions, the postglacial uplift rate increased rapidly. Thus, the uplift isobases in southwestern Maine appear to be evenly spaced, with a relatively steep gradient (about 0.9 m/km up to the north northwest) which is similar to that established in the Connecticut Valley region of western New England; in eastern Maine however, the uplift isobases appear to be irregular and perhaps more broadly spaced. The combination of more rapid uplift about 13,000 B.P. and ice marginal positions closely controlled by local topography in eastern Maine may be a more reasonable solution to the irregular isobases there than suggestion that neotectonics was involved. More detailed field work along the coast in southwestern Maine, eastern New Hampshire, and eastern Massachusetts is planned to confirm this pattern.

REPORTS

Koteff, Carl, and Larsen, F. D., 1985, Postglacial uplift in the Connecticut Valley, western New England, (abs.): Geological Society of America Abstracts with Programs, v. 17, p. 29.

Koteff, Carl, and Larsen, F. D. (in press), Postglacial uplift in western New England: Evidence for delayed bedrock rebound. Quaternary Research.

Seismological Field Investigations

9950-01539

C. J. Langer
Branch of Engineering Geology and Tectonics
U.S. Geological Survey
Denver Federal Center, MS 966
Denver, CO 80225
(303) 236-1593

Investigations

1. Guinea, West Africa, earthquake -- local investigation of aftershocks resulting from M_s = 6.2 earthquake of December 22, 1983.

2. Borah Peak, Idaho, earthquake -- local investigation of aftershocks resulting from M_s = 7.3 earthquake of October 18, 1983.

3. Western Argentina (Caucete) earthquake -- local investigation of aftershocks resulting from M_s = 7.4 earthquake of November 23, 1977.

4. Western Argentina (Sierra Pie de Palo region) velocity model -- development of a P-wave velocity structure and station corrections.

5. Alpine, Wyoming, earthquake sequence -- local investigation of seismicity related to August, 1985 M = 4+ earthquakes.

6. North Yemen earthquake -- local investigation of aftershocks related to the M_s = 6.0 earthquake of December 23, 1982.

Results

1. Aftershocks of the Guinea, West Africa, earthquake show a system of three en echelon faults with a predominant right-lateral strike-slip motion. The complete draft of the manuscript "Aftershocks and surface faulting associated with the intraplate Guinea, West Africa, earthquake of December 22, 1983", reporting on the above results, has cleared internal review. It requires some, but not serious, revision before submittal to the BSSA.

2. A first draft of the manuscript "Tectonic aspects of the Willow Creek Hills Barrier: Aftershocks of the 1983 Borah Peak, Idaho, earthquake" is well underway (currently 48 pp including tables and illustrations). It will be included in the Borah Peak Bulletin edited by Bucknam and Stein.

3. A paper describing the aftershocks of the 1977 western Argentina earthquake was accepted for publication in August 1983 in the BSSA, subject to revision. It has finally been revised resulting in considerable improvement. The manuscript will be resubmitted to the BSSA after some final tweaking by the authors.

4. The manuscript giving details of how a velocity model was developed to locate aftershocks of the 1977 western Argentina earthquake has been totally rewritten. It has gone in for Branch Chief approval before being published as a USGS bulletin.

5. Preliminary locations of 14 earthquakes in a near north-south zone about 20 km long and 8 km wide and with depths between about 5 and 15 km have been located about 10 km east of Alpine, Wyoming. The above seismicity occurred during a four-day period in mid-September and was located by data from a nine-station temporary network of seismographs.

6. The first draft of a manuscript titled "Aftershocks of the December 13, 1982, North Yemen earthquake: conjugate normal faulting in an extensional near plate margin setting" is almost complete. Except for some drafting and a little more work on interpretation, it is ready for review.

Northeastern Seismicity and Tectonics
9510-02388

Nicholas M. Ratcliffe
U.S. Geological Survey, MS 925
Reston, Virginia 22092
(703) 860-6406

and

John K. Costain
R. M. D'Angelo
Virginia Polytechnic Institute and State University
Blacksburg, Virginia 24061

INVESTIGATIONS

1. Interpretation of VIBROSEIS reflection profiles of Ramapo seismic zone in New Jersey and eastern Pennsylvania.

2. Geologic mapping along VIBROSEIS profiles in New Jersey and Pennsylvania, and characterization of reflectors in basement rocks.

3. Core drilling of border faults of Newark basin in eastern Pennsylvania and p wave velocity determinations of fault zone rocks.

RESULTS

1. A 15 km-long 12 and 24 fold VIBROSEIS profile across the northwestern margin of the Newark basin (fig. 1) and adjacent Musconetcong thrust system in eastern Pennsylvania shows a gentle prominent reflection dipping 30° south at the basin margin (B in fig. 2). Reflectors in a 0.5 km thick zone in the footwall block, beneath and parallel with the Mesozoic border fault, correspond with the updip projection of the Musconetcong thrust of Drake and others, 1967 (M in fig. 2).

2. Continuous core from a 1,000 ft hole in gneiss of the footwall block (location 1, fig. 1) and field studies document fault intercalation of mylonitic middle Proterozoic gneiss and Cambrian dolostone in homoclinally southeast-dipping imbricate thrust faults in the zone of reflections in basement rocks.

3. Measurements of p wave velocity and density of cores of mylonitic gneiss and dolostone and on their nonmylonitized protoliths, from 0 to 9000 psi reveal marked changes in velocity ranging from 6.7 km/sec for nonmylonitic dolostone to 4.5 km/sec for phyllonitic mylonite derived from gneiss. Normal incidence reflection coefficients calculated for interfaces between gneiss, dolostone, and their mylonitic counterparts are sufficiently large (.127 to .105) to account for the prominent reflectors seen in the imbricate thrust faultled footwall block beneath the Newark basin border fault.

4. Two continuously cored holes across the border fault of the Newark basin (location 2, fig. 1) on the VIBROSEIS section were completed in June 1985. The results, summarized in figure 3, confirm the gentle 27° and 34° dips for faults at basin margin seen in the VIBROSEIS data.

5. The results cited above: (1) confirm gentle dips for the border fault of the Newark basin in eastern Pennsylvania and suggest strongly that reactivation of Paleozoic thrust faults controlled formation of the Mesozoic extensional faults and (2) indicate that mylonitic rocks associated with Paleozoic thrust faults west of and beneath the Newark basin have sufficiently large reflection coefficients to be reflectors in VIBROSEIS data. These results will be helpful in the interpretation of similar reflectors present in basement rocks in our other VIBROSEIS profiles of the Ramapo seismic zone.

REPORTS

D'Angelo, R. M., 1985, Correlation of seismic reflection data with seismicity over the Ramapo, New Jersey, fault zone: M.A. thesis, Virginia Polytechnic Institute and State University, 82 p.

Ratcliffe, N. M., and Burton, W. C., 1985a, Fault reactivation models for origin of the Newark basin and studies related to Eastern U.S. seismicity, *in* Robinson, G. P., and Froelich, A. J., eds., Proceedings of the Second U.S. Geological Survey Workshop on the Early Mesozoic basins of the Eastern United States: U.S. Geological Survey Circular No. 946, p. 36-45.

Ratcliffe, N. M., and Burton, W. C., 1985b, Preliminary results of core drilling of the Triassic border faults near Riegelsville, Pennsylvania: U.S. Geological Survey Open-File Report No. 85-573, 23 p.

Ratcliffe, N. M., D'Angelo, R. M., Costain, J. K., and Burton, W. C., in press, Low-angle extensional faulting, reactivated mylonites and seismic reflection geometry of the Newark basin margin in eastern Pennsylvania: (submitted to *Geology*).

Ratcliffe, N. M., Vidale, Rosemary, and Burton, W. C., 1985, Ordovician ductile deformation zones in the Hudson Highlands and their relationship to metamorphic zonation in cover rocks of Dutchess County, New York: *in* Tracy, R. J., ed., New England Intercollegiate Geological Conference, 77th Annual Meeting, Guidebook for field trips in Connecticut and adjacent areas of New York and Rhode Island, p. 25-60.

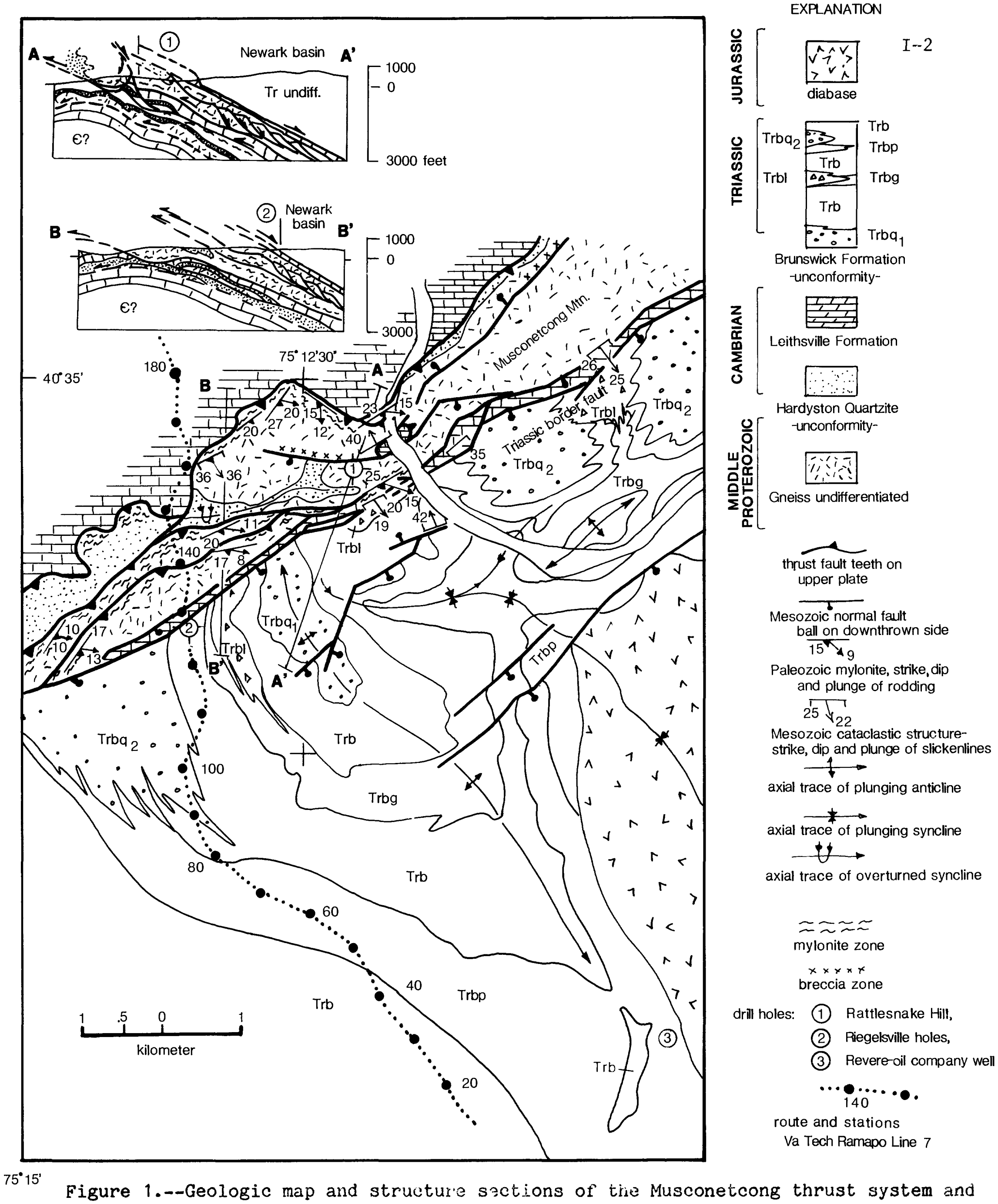

Figure 1.--Geologic map and structure sections of the Musconetcong thrust system and border faults of the Newark basin in eastern Pennsylvania showing location of drill sites 1 and 2, and location of VIBROSEIS profile, figure 2.

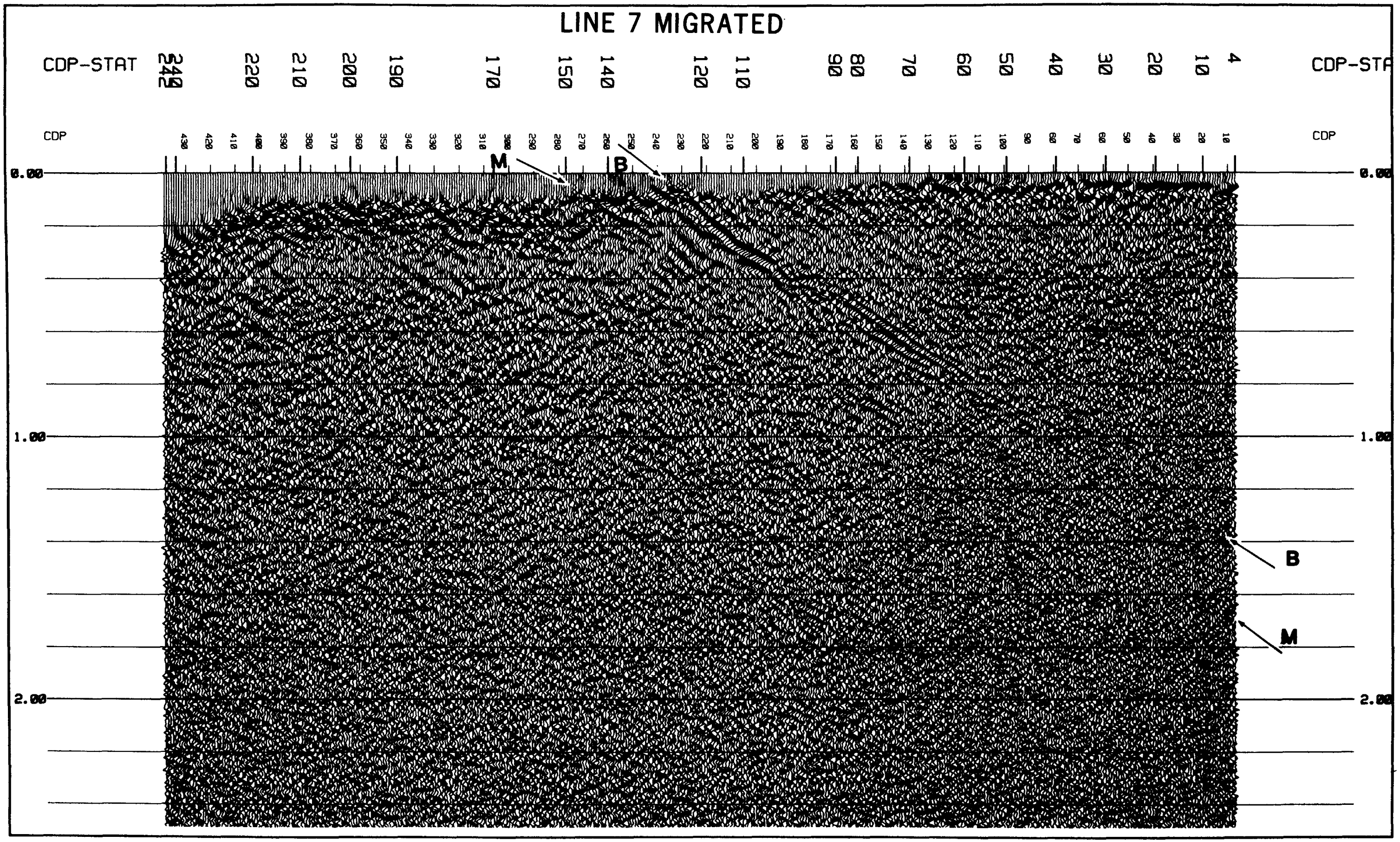

Figure 2.--Migrated version of VIBROSEIS profile, two-way travel time in seconds.

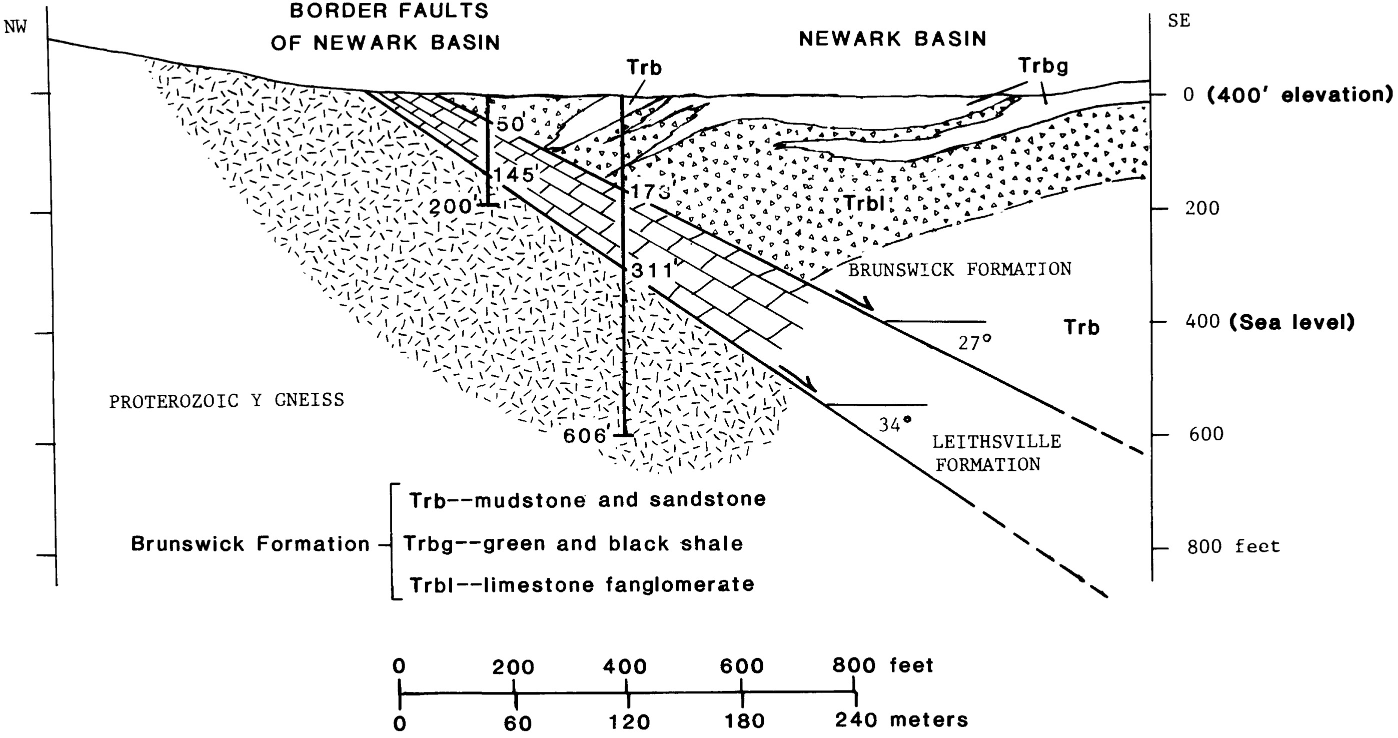

Figure 3.--Cross section illustrating results of coring at drill site 2 (fig. 1).

Basement Tectonic Framework Studies
Southern Sierra Nevada, California

9910-02191

Donald C. Ross

Branch of Engineering Seismology and Geology
U.S. Geological Survey
345 Middlefield Road, MS 977
Menlo Park, CA 94025
(415) 323-8111, ext. 2341

Investigations

1. Field studies of plutonic and metamorphic rocks along the eastern Sierra Nevada front from State Highway 178 (Freeman Canyon) north to the Little Lake area.

2. Synthesis of petrographic data for the metamorphic rocks of the southern Sierra Nevada between lat 35°30' and 36°00' north.

Results

1. Field studies in May 1985 delineated the southern and eastern limits of a large body of relatively mafic plutonic rock that is the probable extension of the "Sacatar" body that Miller and Webb (1940) described on the Kern Plateau to the west. These plutonic rocks are intruded by numerous fine-grained mafic dikes (spessartite lamprophyre and microdiorite), which are probably part of the Independence dike swarm (Moore and Hopson, 1961) that has been dated as about 148 m.y. (Chen and Moore, 1982). The dike swarm thus provides a datable "horizon" and enables the subdivision of the Cretaceous from the Jurassic plutons. This new mapping has now delineated two large probably Jurassic plutons that extend as far south as Walker Pass along the eastern front of the Sierra Nevada. Mafic scraps somewhat further south may also be Jurassic remnants. Rb-Sr studies of these two bodies are now underway by R.W. Kistler (Branch of Isotope Geology).

2. Preliminary study of samples and thin sections of an unusual gray gneissic rock along the southwest side of a long northwest-trending roof pendant of metasedimentary rocks south of Indian Wells Canyon suggests that the gneissic rocks may reflect a significant old (Mesozoic?) shear zone. The gneissic rocks, at least in part, are strongly deformed, but now rehealed and recrystallized granitic rock. The probable shear zone is "eaten through" by a felsic granitic body, which if dated, would place an upper limit on the age of the shearing.

3. The metamorphic rocks of the southern Sierra Nevada from lat 35°30' to 36°00' north can be grouped into four belts of somewhat related roof pendants. An eastern belt consists of generally thinly layered schist, pure to impure quartzite, with lesser, but locally conspicuous, layers of carbonate rocks. These metasedimentary rocks are reminiscent of some of the Paleozoic rocks of the Cordilleran miogeocline, but they contain an Upper Triassic-Lower Jurassic fossil locality. A strongly contrasting central belt consists largely of massive to thickly bedded, largely unsorted, rapidly deposited, gramule quartzite, and lesser highly argillaceous schist. Also characteristic of this belt is metavolcanic rock, including abundant ash flow tuff layers. A western belt of pendants is much like the eastern belt and would probably not be easily distinguished without the presence of the central belt. On the far west side of the batholith some, as yet only cursorily examined, roof pendants appear to contain more schist, and less quartzite and calcareous layers than the western belt.

Reports

Sims, J.D., Ross, D.C., and Irwin, W.P., 1985, Tectonic framework of the Parkfield-Cholame area, central San Andreas fault zone, California: Geological Society of America Abstracts with Programs, v. 17, p. 718.

Detailed Geologic Studies, Central San Andreas Fault Zone

9910-01294

John D. Sims
Branch of Engineering Seismology and Geology
U.S. Geological Survey
345 Middlefield Road, MS 977
Menlo Park, California 94025
(415) 323-8111, Ext. 2252

Investigations

1. Field investigations of structural and stratigraphic relationships between late Cenozoic sedimentary units and underlying Franciscan and Late Cretaceous units in the Parkfield-Cholame-Coalinga area of the southern Diablo Range.
2. Field investigations of Holocene and historic slip rates in the Parkfield-Cholame area.

Results

1. The final editing and construction of geologic maps of the San Andreas Fault Zone in the Parkfield, Cholame Hills, The Dark Hole, Cholame Valley and Tent Hills 7 1/2 - minute quadrangles was completed. The maps reveal the structural complexity of the area and illustrate that several (three) strands of the San Andreas have been active at different times. In the Parkfield area the complex movement history is evidenced by the relative position of a slice of Miocene volcanic rocks with the hornblende gabbro of Gold Hill. The volcanic rocks, the Lang Canyon volcanics, are correlated with the Pinnacles-Neenach volcanics. The gabbro of Gold Hill is correlated with the Logan-Eagle Rest Peak gabbro. In a palinspastic restoration the Eagle Rest Peak gabbro is 55 km NW of the Neenach Volcanics in the San Emidgio and Tehachipi Mountains. This relative position and distance is maintained between the Pinnacles volcanics and Logan Gabbro in the northern Gabilan Range. However, in the Parkfield area the relative position is reversed and the Lang Canyon volcanics lie 16 km NW of the gabbro of Gold Hill. This reversed position requires the movement of two different fragments of the Neenach volcanics. Such movement is accomplished by the first fragment, the Pinnacles mass, moving northwest about 95 km, at which time active faulting was transferred eastward and a second fragment separated from the Neenach volcanics, the Long Canyon volcanics. The Pinnacles and Lang Canyon volcanics maintained a constant 95 km distance as the Pacific plate moved NW to its present position.

   Petrographic analysis of framework grains in sandstones of the Miocene Temblor Formation of central California and in underlying and overlying rocks of Eocene and late Miocene age reveal a sudden influx of volcanic material into a sequence of quartzo-feldspathic sandstones. The quartz- and feldspar-rich sandstone of Eocene and Miocene age in the southern Diablo range and the Coalinga region consistently contains less than 5 percent volcanic detritus. However, intervals in the Temblor Formation of early Miocene (upper Saucesian to upper Luisian) age at Reef Ridge, the Kettleman Hills and Coalinga Anticline contain up to 46 percent volcanic detritus. Volcanic detritus is absent in sandstones of the Temblor Formation in the Cholame Hills which is probably of Lower Saucesian age. The fresh volcanic material, apparently derived from the same mafic source area, appears in the Temblor Formation at different time-stratigraphic horizons separated by about 1.5-2.5 m.y. over a distance of 40 to 50 km. Facies relationships, paleocurrent data, and paleogeography indicate that the volcanic source area was west of the present trace of the San Andreas Fault, and not a Sierran source as proposed by others. Paleogeographic interpretation of the provenance data suggest a volcanic source west of the present Temblor Range moved to a more northerly position during Late Saucesian time, implying that right-lateral movement in central California began at about 16 m.y. The volcanism is perhaps related to the northward migration of the Mendocino triple junction. Constraints as the source of the volcanic detritus are: 1) andesitic volcanism in the Sierra did not begin until late Miocene, 2) the presence of a bathyl to abyssal basin in the San Joaquin Valley requires Sierran detritus to be transported around the margins of the basin to the Coalinga array, 3) the early Miocean Valley Springs Formation to the north of Coalinga contains no fresh volcanic detritus, 4) granitic, sedimentary and metamorphic detritus was consistently supplied from the Salinian block from Eocene to Late Miocene time.

2. The history of slip for three sites in the Parkfield area were reconstructed with J.J. Lienkaemper and W.H. Prescott using data from creep meters, alignment arrays, short-range geodetic networks and offset cultural features. The fence near Water Tank, 3.1 km north of Highway 46, has been offset 69±3 cm since its construction in 1908. If the slip in the 1922, 1934, and 1966 events was the same and the interseismic rate of slip was constant, the data imply that coseismic slip is 15 cm per event and the rate of slip between events was 0.33 cm yr^{-1}. The offset of the Parkfield bridge is 126±2 cm since 1932. Geodetic surveys of a 1.6-km-long low-angle line that crosses the San Andreas fault at a low angle give an interseismic rate of 0.78±0.06 cm yr^{-1} for the interval 1974-1985. Together these data suggest 42 cm of slip per event. A fence on the Classen ranch, on Middle Mountain, indicates 106±3 cm of slip since 1946. Nearby alignment arrays give an interseismic rate of 2.26 cm yr^{-1}; and the data imply 17 cm of slip for the 1966 event.

Reports

Sims, J.D., Perkins, J.A., Wray, M.J., _____, Offset Late Holocene deposits in trenches across the San Andreas Fault at Parkfield, California: *U.S. Geological Survey Open-File Report.*

Perkins, J.A., and Robinson, S.W., _____, Uncertainty inherent in the application of radiocarbon dating to slip-rate studies: *Seismological Society of America Bulletin.*

Perkins, J.A., Sims, J.D., Sturgen, S.W., and Wray, M.S., _____, Late Holocene deposits in trenches across the San Andreas Fault at Melendy Ranch, San Benito County, California: *U.S. Geological Survey Open-File Report.*

Sims, J.D., Ross, D.C., and Irwin, W.P., 1985, Tectonic Framework of the Parkfield-Cholame area, central San Andreas Fault zone, California: *Geological Society of America Abstracts with Programs, v. 17, p. 718.*

Sims, J.D., _____, Geologic methods for the interpretation of paleoseismicity: *Seismological Society of America Bulletin.*

INTEGRATED STUDIES OF EARTHQUAKE SOURCE ZONE CHARACTERISTICS, HAZARDS, AND PREDICTION IN THE WASATCH FRONT URBAN CORRIDOR AND ADJACENT INTERMOUNTAIN SEISMIC BELT

14-08-0001-21983

R.B. SMITH, W. J. ARABASZ, and J.C. PECHMANN*
Department of Geology and Geophysics
University of Utah
Salt Lake City, Utah 84112
(801)581-6274

Investigations

1. Moment-magnitude relations in the Utah-Idaho region and stress drop-versus-moment behavior.
2. Waveform analysis of preshock-mainshock-aftershock sequences in Utah.
3. Kinematics of Great Basin intraplate extension.
4. Three-dimensional velocity structure of the 1983 Borah Peak, Idaho, earthquake area.
5. Seismicity of the Hansel Valley-Pocatello Valley area along the Utah-Idaho border.

Results

1. Moment-magnitude (M_o-M_L) data for the southern Intermountain seismic belt (ISB) have been investigated along with stress-drop versus seismic-moment behavior for the corresponding earthquakes, following the analysis of Hanks and Boore (1984). Using P-wave spectra, a M_o-M_L relation of $\log M_o = 0.99M_L + 17.8$ was determined for the magnitude range of $2.5 \leqslant M_L \leqslant 5.0$ from a set of 16 earthquakes in the southern ISB during 1981-1985 (Figure 1). Seismic moments were determined from a suite of 36 stations of the University of Utah seismic network that were calibrated indirectly using spectra of deep focus teleseismic earthquakes. The calibration was checked by comparison of moment values for 24 Borah Peak, Idaho, aftershocks ($\log M_o$ from 19.6 to 23.4) with those determined independently by Boatwright (1985). The slope of 0.99 is similar to that of the relation $\log M_o = 1.1M_L + 18.4$ of Doser and Smith (1982), determined for an independent set of events in the range $3.7 \leqslant M_L \leqslant 6.0$. In contrast, M_o-M_L relations for California in this magnitude range, such as the relation $\log M_o = 1.5M_L + 16.0$ for $3.5 \leqslant M_L \leqslant 7.0$ of Thatcher and Hanks (1973; see also Bakun, 1984), are generally steeper in slope than those for Utah. Slopes near unity are generally limited to smaller magnitudes for California events. This is a reflection of the essential non-linearity of M_o-M_L relations (Hanks and Boore, 1984).

Stress drops determined from P-wave pulse durations are basically constant with increasing M_o, whereas those determined from P-wave corner frequencies are affected by a non-instrumental frequency band limitation

---

*Graduate students J.F. Peinado, P.K. Eddington, L.L. Leu, and G.J. Chen also contributed significantly to this project during the report period.

(similar to an f-max effect) causing an apparent increase of stress drop with moment. Such a band limitation is used to explain the persistence of the shallow slope (0.99) in the M_o-M_L relation to higher magnitudes in the Intermountain seismic belt.

2. Cross correlations of filtered waveforms for closely-spaced local earthquakes can be used to place strong constraints on their relative locations under the assumption that events producing very similar waveforms occur within one quarter of the shortest wavelength for which the similarity is observed (Geller and Mueller, 1980). Tests using digital seismograms of quarry blasts with known locations, recorded by the University of Utah seismic network, support this "quarter wavelength" hypothesis. The waveform cross-correlation technique was applied to earthquakes during 1981-83 within 20 km of 1) an M_L 4.3 mainshock near Salt Lake City, Utah, on October 8, 1983, and 2) an M_L 4.0 mainshock that occurred on May 24, 1982 near Richfield, Utah. No unusual seismicity was observed prior to the Salt Lake City event during the time period studied. However, a cluster of 4 preshocks within 80-100m of each other, possibly representing the failure of a critical asperity, was observed 5 km NW of the Richfield event during a four-hour period ten months before the mainshock.

The aftershocks studied in both regions during the first 15 days after the mainshock occupy areas smaller than the rupture areas estimated for the mainshocks using the method of Frankel and Kanamori (1983). Both aftershock sequences showed a spatial migration of the initial events that could only be discerned from the waveform data. One possible explanation for this migration could be propagating stress changes caused by either the occurrence of the aftershocks themselves or else by some other process. Stress drop estimates of 1-2 bars and 2-6 bars were calculated for the Salt Lake City and Richfield mainshocks, respectively.

3. Strain rates assessed from brittle deformation associated with earthquakes have been compared to estimates of total brittle-ductile deformation for the intraplate Great Basin of the western United States. Strain and deformation rates were determined by the seismic moment tensor method using historic seismicity and fault plane solutions. By subdividing the Great Basin into areas of homogeneous strain it was possible to examine regional variations in the strain field. Contemporary deformation of the Great Basin occurs principally along the active seismic zones: the southern Intermountain Seismic Belt -- 4.7 mm/yr maximum deformation rate, the Sierra Nevada front -- 28.0 mm/yr maximum deformation rate (including a large contribution from the 1872, M8.3 Owens Valley earthquake), and the west-central Nevada seismic belt -- 7.5 mm/yr maximum deformation rate. The earthquake-related strain shows that the Great Basin is characterized by regional E-W extension of 8.4 mm/yr in the north that diminishes to NW-SE extension of 3.5 mm/yr in the south (excluding the Owens Valley earthquake zone). These rates compare very well with the Great Basin opening rate of <9 mm/yr estimated by Jordan et al. (1985) from satellite geodesy and plate motion models. This result implies that most of the extension takes place by brittle fracture during earthquakes.

4. A geotomographic inversion method was used to derive the three-dimensional P-wave velocity distribution of the 1983, M_s 7.3 Borah Peak, Idaho, earthquake aftershock zone from local earthquake data. A data set

of 3,963 P-wave travel-times from 260 earthquakes recorded by 72 stations with more than 6 recordings per station have been selected from the approximately 400 aftershocks. The velocity inversion used 220 discretized blocks in a seven layer-block configuration.

The results (Figure 2) suggest the presence of low P-velocity material west of the main surface break. A low velocity body with reductions of P-velocity up to 0.3 km/s, compared to a one-dimensional layered model, has a map projection which is elongated and parallel to the surface fault. The zone is 4-8 km wide and extends from near-surface to about 10 km--roughly centered on the main fault plane that ruptured during the mainshock (rupture nucleation was at 16 km depth). The low velocity body extends well below the sedimentary layer and may represent a highly deformed volume or it may represent a dilatant body developed in response to deformation associated with large pre-historic events. Because of the small magnitude of the velocity changes, however, these results must be considered preliminary pending further testing with different starting velocity models.

5. The Utah-Idaho border region north of the Great Salt Lake is one of the most seismically active areas of Utah. Large historic earthquakes in this region include the 1934, M_L 6.6 Hansel Valley earthquake (with 0.5 m of surface displacement) and the 1975 M_L 6.0 Pocatello Valley earthquake. Over 1600 earthquakes which occurred in this region during 1962-1963 were relocated by applying a master event technique to phase data from the University of Utah seismic network. Initial station delays were derived from a master event located by a dense 50-station temporary array (Cooperative Univ. of Utah-MIT special study, 1983). These delays were used to relocate five other nearby earthquakes that served as secondary master events.

The relocated epicenters show systematic shifts relative to the catalog epicenters of up to 5-10 km in some areas. However, the regional seismicity pattern is similar to the original pattern seen in the catalog data--an inverted "Y" pattern centered on the Utah-Idaho border. A concentration of earthquakes trending northward from the state border includes aftershocks of the 1975 Pocatello Valley earthquake. Zones of activity extending SW and SE from the border began to develop several months after the 1975 main shock. The SW-trending zone encompasses the historically active Hansel Valley fault at the northern end of the Great Salt Lake.

Reports and Publications

Doser, D.I., and R.B. Smith, Source parameters of the 28 October 1983 Borah Peak, Idaho, earthquake from body wave analysis, *Bull. Seismol. Soc. Am.*, *75*, 1041-1051, 1985.

Eddington, P.K., Kinematics of Great Basin intraplate extension, M.S. thesis, University of Utah, 1985.

Thorbjarnardottir, B.S., Relative earthquake locations by cross-correlation of waveforms: Application to preshock-mainshock-aftershock sequences in Utah, M.S. thesis, University of Utah, 1985.

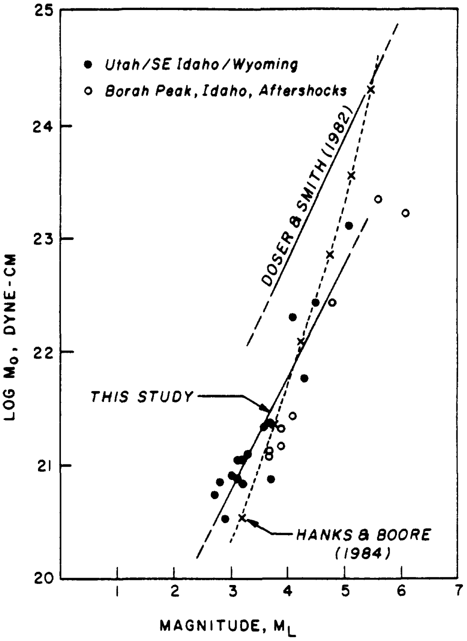

Figure 1. Moment-magnitude data for the southern Intermountain seismic belt. Solid circles represent data used to determine the relationship shown by the solid line (this study). Open circles represent Borah Peak aftershocks. The moment-magnitude relationships of Doser and Smith (1982) and Hanks and Boore (1984) are shown for reference.

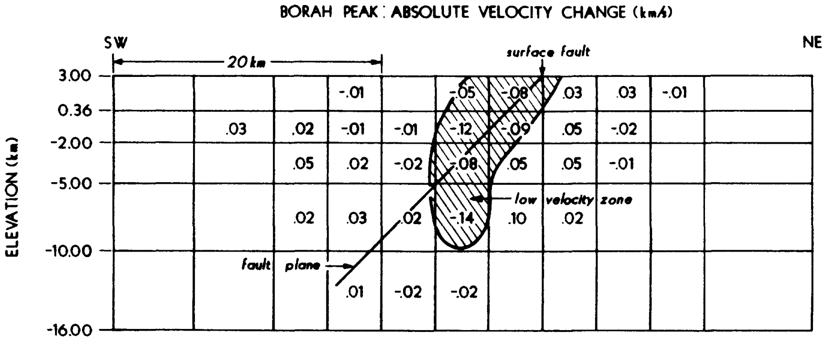

Figure 2. Cross section across the aftershock zone of the 1983 Borah Peak earthquake showing preliminary results of a geotomographic inversion of travel time data from aftershocks. Numbers show absolute velocity changes in km/sec relative to a horizontally-layered starting model. Numbers shown are average values from four grid elements extending 16 km along strike near the center of the surface break. Blank squares represent areas with no ray-path coverage.

Prediction of Ground Motion from the Goodnow, NY Earthquake of 7 October 1983.

Contract No. 14-08-0001-22047

George H. Sutton, Jerry A. Carter, Anne Suteau-Henson, and Noel L. Barstow
Rondout Associates, Incorporated, P.O. Box 224, Stone Ridge, New York 12484
(914) 687-9150

Investigations

1. Analyze waveforms of Goodnow New York Main Shock (M_b = 5.0) and any aftershocks recorded at RSNY (an RSTN station in New York, only 69 km from epicenter).

2. Generate full waveform synthetic seismograms showing frequency range 0-5 Hz for the Goodnow, NY earthquakes.

3. Choose a simple, small aftershock (similar to the main shock) to use as a "Green's function" to produce by superposition, the main earthquake.

Data Analysis: The short period P-waves for the Goodnow earthquake and 3 aftershocks recorded at RSNY were analyzed for polarized P-type motion. For each event, a 10 sec. long window was selected immediately before the S arrivals. The data were polarization-state filtered using a detector for rectilinear motion at an azimuth of -32° and an apparent angle of incidence of 60°. Adaptive polarization analysis was then performed on the state filtered data assuming a reference back azimuth of 148°. Azimuths between -30° and -34° and angles of incidence between 54° and 61° are found for the first arrivals. The determined back azimuth is considerably different from the theoretical back azimuth for this event (162°). This difference is attributed to an unknown amount of error in the orientation of the seismometers. The resulting seismograms were then low-pass filtered at 5 Hz, which is the bandwidth for which the synthetics were computed. Figure 1 illustrates the result of applying this procedure to data from the main shock recorded at the RSNY station of the Regional Seismic Test Network at a distance of 69 km.

Synthetics: Full-waveform synthetic seismograms were calculated using the "locked mode" procedure of Harvey, 1981, between 0 and 5 Hz for the Goodnow earthquake: distance 69 km; azimuth 162°; strike 173°; dip 60°; rake of 17°. The Grenville structure (from Aggarwal in Schnerk et al, 1976) was chosen, with an appropriate attenuation law (Table I). The RSNY instrument response was included for comparison with the data. Synthetics were calculated at source depths of 5, 7, 8, 10, 12, 13, 15 and 28 km.

Table I
Grenville Velocity (Schnerk et al, 1976) and Q Structure Used for Synthetics

H (km)	Vp (km/s)	Vs (km/s)	ρ (g/cm^3)	
4	6.1	3.52	2.80	
31	6.6	3.81	2.85	Qp = 1,100 + 150f
	8.1	4.68	3.30	Qs = 5/9 Qp

Results: Figure 2 shows a 10 sec window of the P-waveforms for the Main Shock, 2 aftershocks (A and B) within an hour of the main shock, and one aftershock (C), 5 days following the main shock. As mentioned above, these three-component data were first filtered to enhance rectilinear motion arriving at RSNY from the epicentral azimuth (162°) and then the horizontal components were adaptively polarized to radial and transverse motion. Interestingly, the waveforms do not all match one another. The first aftershock (trace A) occurred 20 minutes after the main shock and does show similar arrival times for P-wave type motion, particularly the second arrival (approximately 2 1/2 seconds after the P-wave onset). The second aftershock (trace B), looks different, yet it occurred only 20 minutes after the first. And finally the third aftershock (trace C) that was large enough (mag = 2.5) to be recorded at RSNY occurred five days later and looks somewhat like trace B, insofar as P-wave energy is arriving approximately 5 seconds after the initial P-wave on both traces.

In addition, the first motions for the main shock and aftershock A are compressional, whereas the first motions for shocks B and C are dilatational (First motions were impulsive and unambiguous on the unfiltered traces. The filters used for these figures are zero phase and do not preserve first motion.)

Given the density of portable stations recording at the time of the 10/12 aftershock, (trace C), there is enough first motion data to determine a fault plane solution. Indeed, the aftershock's mechanism differs slightly from the main shock and station RSNY is at an appropriate azimuth and distance to sense the difference in source mechanism. Thus, to model the main shock at station RSNY by superposition of aftershocks, we will need to select only shocks that are the same as the main. The first aftershock recorded is a good candidate. Seeber, 1984, (Seeber, L., 1984 USGS proposal unpublished MS) noted that about 20% of the aftershocks produced first motions in conflict with the fault plane solution of the main shock and suggested that different geometries of faulting occurred in different parts of the aftershock zone.

Preliminary results from the P-wave portion of the synthetic seismograms are shown in Figure 3 for a series of input source depths ranging from 5 to 15 km. Depth phases, if properly identified, provide precise focal depth information. The main shock and first aftershock vertical and radial, filtered waveforms match the waveforms calculated for input depths of 7 and 8 km fairly well. The fact that nearly all the well-recorded aftershocks of the Goodnow earthquake are located at hypocentral depths between 6 and 8 km (Seeber et al, in prep.) lends support to the interpretation of a 7-8 km depth for these two events. However, earlier interpretation of depth phases from more distant RSTN stations and from hypocentral solutions using near station data indicate a greater depth for the main shock.

The similarity of the synthetics to the recorded seismograms gives us some confidence in the relatively high-frequency synthetics. Ongoing work, includes tests of the sensitivity of computed seismograms (0-5 Hz) to input focal mechanism, velocity model, and attenuation. If we are not swamped by complexities and problems of non-uniqueness, we will be able to resolve details of the faulting processes.

References

Harvey, D., 1981, Seismogram Synthesis Using Normal Mode Superposition: The Locked Mode Approximation Method, Geophys. J. Roy. Astron. Soc., 66, 37-69.

Schnerk, R., Aggarwal, Y. P., Golisono, M., and England, F., 1976, Reg. Seism. Bull. of the Lamont-Doherty Network, Lamont-Doherty Geological Observatory, Palisades, NY.

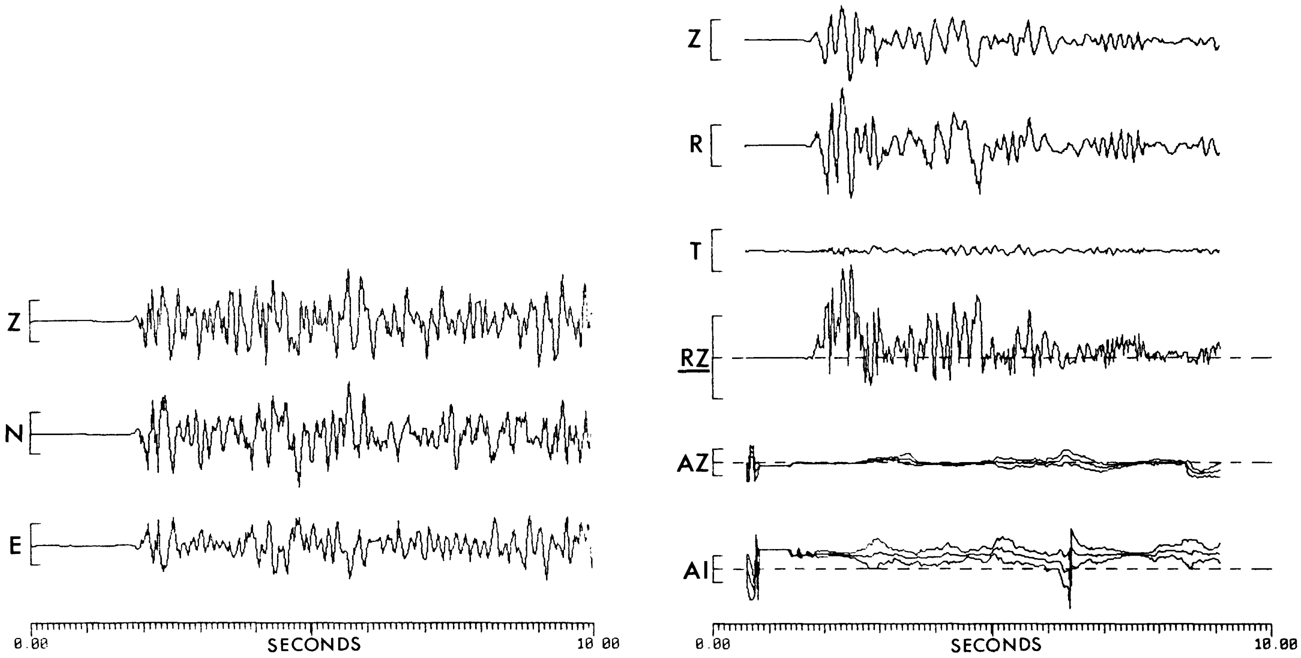

Figure 1. Goodnow, NY earthquake of 10/7/83, M_b = 5.0, P wavetrain at RSNY: left-raw data; right-adaptive polarization analysis of data after polarization state filtering for rectilinear motion at -32° azimuth and 60° apparent angle of incidence.

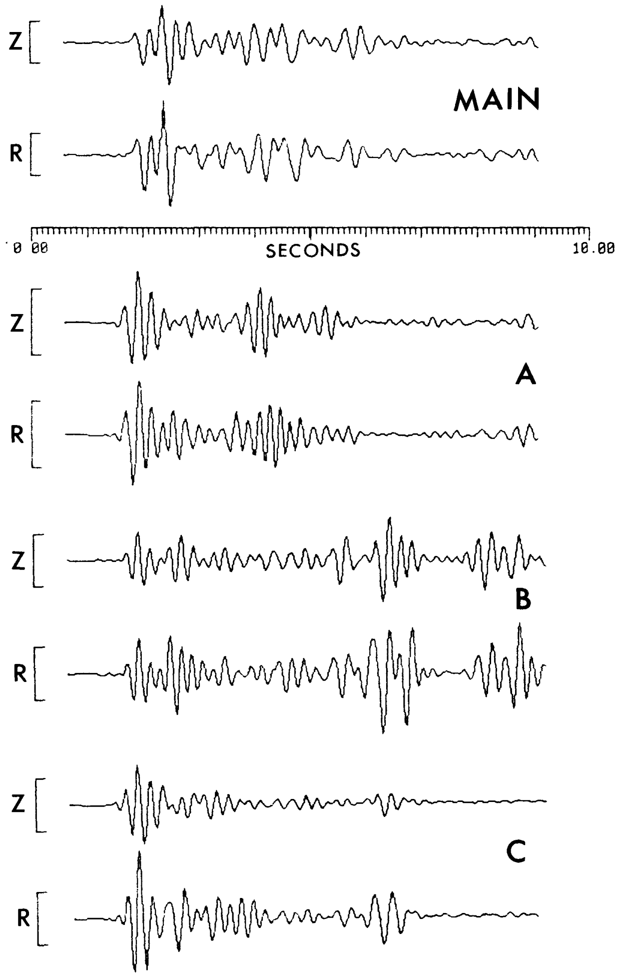

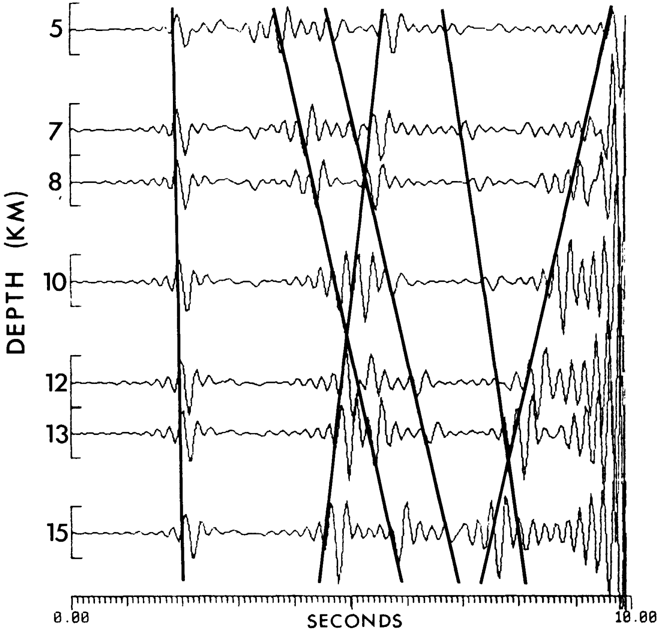

Figure 2 (Left). Polarization state filtered P waves from main Goodnow, NY earthquake and three aftershocks A, B, and C. Low pass filtered at 5 Hz.

Figure 3 (Above). Vertical component synthetic seismograms, 0-5 Hz, for different focal depths. Δ = 69 km, Az = 162°, Strike = 173°, dip = 60°, rake = 17°. Velocity/attenuation structure from Table I. Lines trending down to the right follow depth phases.

Central California Deep Crustal Study

9540-02191

Carl M. Wentworth
Branch of Western Regional Geology
U.S. Geological Survey
345 Middlefield Road, MS 975
Menlo Park, California 94025
(415) 323-8111 ext. 2474

Investigations

Seismic reflection profiling, in concert with other geophysics and geology, is being used to examine crustal structure between the California Coast Ranges and the Sierran foothills (see map, p. 149, USGS Open-File Report 85-22 for location of profiles; line CC-2 extends a further 30 km into the Sierra Nevada than shown).

1. Processing of line CC-2 across the east half of the San Joaquin Valley and into the Sierran foothills has proceeded well, due in part to the contractor experience gained by work on CC-1 and on similar data from Maine. The reconstruction line for CC-1 has been revised in accord with the results of that experience and reprocessing is underway.

2. An integrated interpretation for the 1983 Coalinga earthquake was developed using structure founded on reflection data, together with surface and subsurface geology, the refraction work of A. Walter and analysis of earthquakes by Eaton and by Eberhart-Phillips and Reasenberg. Dislocation modeling in the context of the coseismic surface uplift reported by Stein was carried out to test the conclusions.

3. Preliminary discussions have begun concerning interpretation of line CC-2, which extends across the east half of the San Joaquin Valley, the Foothills metamorphic belt, and into the Sierran batholith.

Results

1. Reflection lines CC-1 and CC-2 constitute a west-east transect in central California that extends in two overlapping segments from the core of the Diablo Range in the Coast Ranges 140 km eastward across the San Joaquin Valley into the Sierran batholith. The western segment of the transect (fig. 1) begins in exposed Franciscan rock, proceeds across a steeply east-dipping section of Great Valley sequence, and then crosses the San Joaquin Valley to Merced. Discontinuous subhorizontal reflections beneath the exposed Franciscan extend to the base of the crust, but decrease in prominence at 5 s (15 km), where refraction studies place a boundary between 5.8 and 6.9 km/s. This probably represents the base of Franciscan rock. The subhorizontal reflections from the Franciscan may represent stratiform rock common in the Diablo Range. The east-dipping reflections in the upper crust (EUR) may represent a young fault, which projects up-dip to the west approximately to the Calaveras fault. The similar reflections in the lower crust (ELR) may be related to a low velocity zone

inferred from refraction studies.

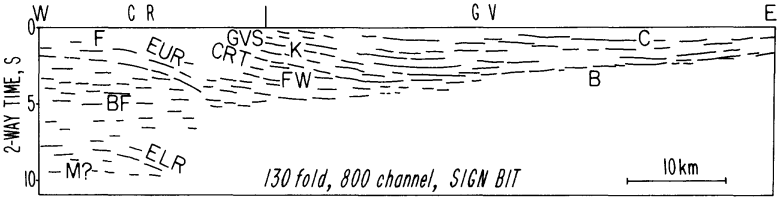

Figure 1.-- Line drawing of unmigrated seismic reflection profile CC-1. CR- Coast Ranges; GV- Great Valley; F- Franciscan assemblage; GVS- Great Valley sequence; K- Cretaceous strata equivalent to upper GVS; C- Cenozoic strata; FW- Franciscan wedge; B- Surface of crystalline basement; BF- base of Franciscan rock; M- Moho.

The steeply east-dipping Great Valley sequence (GVS) between the exposed Franciscan and the range front yields no reflections, although reflections do occur beneath it at 3-4 s. Beneath the range front the strata flatten abruptly, probably in a kink fold, and dip gently eastward in a section 4 km thick (K), only half the 8-km thickness of the steeply dipping section. Beyond the structural trough in the valley, the section rises and thins gradually eastward above a smooth basement. West of the trough, the 4-km thick section, which has interval velocities of 3.0-4.5 km, is discordantly underlain by an eastward thinning wedge (FW) of subhorizontally layered rock having interval velocities of 5.3-6.0 km/s. We infer this wedge to be Franciscan rock thrust eastward between the Great Valley sequence and its basement. Reflection details suggest thrust shortening in K as well. The top of the Franciscan wedge is the Coast Range thrust (CRT), which terminates down dip at the basement surface. Truncation of the lower 4 km of the steeply east-dipping Great Valley sequence by the Coast Range thrust can be explained by eastward ramping of the thrust wedge, probably controlled by abrupt shallowing of the basement beneath the Great Valley sequence.

2. The eastern, overlapping segment of the seismic reflection transect (fig. 2) extends eastward from the center of the San Joaquin Valley, crosses the Foothills metamorphic belt (FMB) and ends in the Sierra Nevada batholith (SNB) about 15 km northeast of the town of Raymond. The gently west-dipping base of the sedimentary section extends to a depth of about 3.5 km (2.3 s) at the west end of the record. Two very strong, west-dipping bands of reflections occur beneath the east side of the valley and the Foothill metamorphic belt, one in the middle crust (WMR) and one in the lower crust (WLR). Together, they define a zone about 9 km thick that dips westward at about 30°. These reflections extend down dip nearly to the base of the crust. Up dip, these reflections seems to coalesce with subhorizontal reflections beneath the batholith at a depth of 6-7 km (2 s). Another set of strong, west-dipping reflections occurs at the east end of the profile (WBR) at midcrustal depth beneath the batholith, below which subhorizontal reflections are evident.

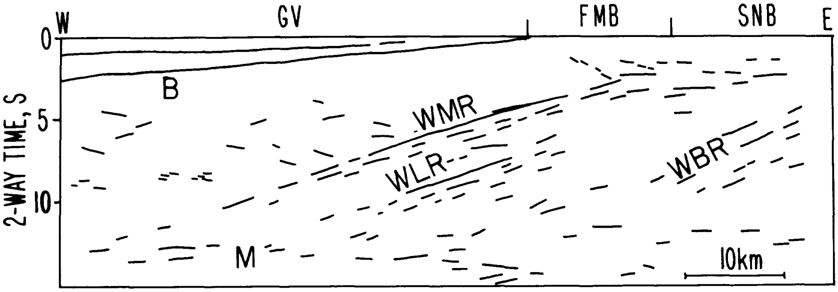

Figure 2.-- Line drawing of unmigrated seismic reflection profile CC-2. GV- Great Valley; FMB- Foothills metamorphic belt; SNB- Sierra Nevada batholith; B- surface of crystalline basement; M- Moho.

Identification of the geologic sources of these various elements of the reflection record from the record alone is difficult. Conservative use of the geologic context suggests that the strong west-dipping reflections in the center of the record (WMR and WLR) may represent structures associated with eastward obduction of Foothill belt rocks during the Nevadan orogeny or a west-facing subduction zone above which the volcanic rocks were generated before being emplaced as the Foothills metamorphic belt. The subhorizontal reflection at 2 s beneath exposed batholithic rocks may mark the base of granitic plutons or compositional layering within them.

3. The 1983 Coalinga earthquake occurred at the east margin of the Coast Ranges beneath Coalinga anticline, which forms the northwest segment in a 100-km-long zone of young anticlines located about 35 km northeast of the San Andreas fault. Northeast-directed thrusts (named Coalinga thrusts) terminate beneath the anticline at a depth of about 10 km in a series of upward-splaying reverse faults, above which the anticline has grown in the past 2 m.y. (fig. 3). A distinct flattening near the center of the northeast limb of the fold separates an upper and lower fold tier, each of which can be related to separate reverse-fault splays below.

The Coalinga mainshock, we conclude, occurred at the base of a reverse fault splay beneath the upper fold tier, producing a focal mechanism (Eaton, 1984) having a gently southwest-dipping focal plane that strikes northwestward, parallel to the fold axis. Dislocation modeling (fig. 4) that closely fits the observed surface uplift across the anticline (Stein, 1984) indicates about 2 m of slip on a 4-km-wide thrust rupture dipping 10° southwest and about 1.2 m of slip on the reverse rupture, which dips 55° southwest and extends 7 km up dip to a depth of about 3.4 beneath the center of the east limb of the fold, which is much shallower than can be demonstrated from the reflection record. This model requires that rupture propagated bilaterally back down the thrust and up the reverse fault. Aftershocks, described by Eberhart-Phillips and Reasenberg (written commun., 1984) and Eaton (written commun., 1985) delineated both rupture zones as well as various other zones along which complex readjustment to the mainshock deformation occurred.

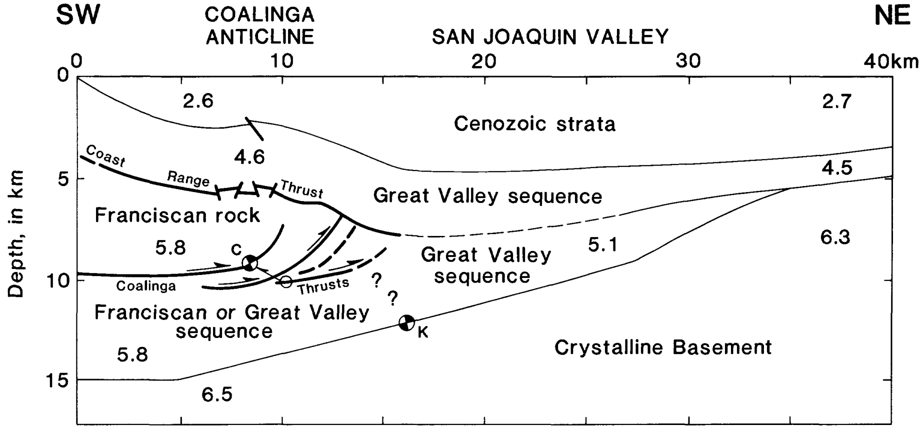

Figure 3.-- Cross section normal to Coalinga anticline and 7 km southeast of 1983 mainshock epicenter. Structure in upper 10 km of section based on seismic reflection profile SJ-19 and drill holes; surface of crystalline basement (6.3-6.5 km/s) from refraction work of Walter (1984). The western dip of the basement surface may be accomplished in part by throw on dip-slip faults, particularly in the steeper part near km 30. Seismic velocities from reflection and refraction interpretations. Location of the coseismic surface deformation above the westernmost reverse fault requires placing the mainshock hypocenter (Eaton, 1984) at the base of that fault, as shown (C), rather than at the projected location on the easternmost thrust. The approximate projected location of the 1985 north Kettleman Hills earthquake is also shown (K). Evidence concerning the identity of rock between the Coalinga thrusts and basement is conflicting: structural relations suggest lower Great Valley sequence, but the velocity is too high, equivalent to Franciscan rock, unless the GVS is metamorphosed.

Thrusting of the type responsible for the growth of Coalinga anticline probably extends the length of the Coalinga-Kettleman Hills-Lost Hills anticlinal trend with tear faults at the echelon steps in the trend. The earthquake occurred east of the north-trending Pleasant Valley-Joaquin Ridge structural boundary, a major tear structure against which Coalinga anticline and other folds terminate. Aftershocks with strike-slip mechanisms alined with the boundary indicate right-lateral movement, which is consistent with the large right-lateral step in the front of the Diablo Range that occurs there. The mainshock rupture planes probably terminated northwestward at this boundary, but aftershock mechanisms (Eaton, written commun., 1985) suggest that related thrusts extend northwestward beyond the structural boundary and under Joaquin Ridge in the southern Diablo Range. Such thrusting may be characteristic of the east margin of the Coast Ranges.

The M 5.5 north Kettleman Hills earthquake of August 1985 (Eaton, written commun.), located about 17 km southeast of the 1983 Coalinga earthquake, seems to have resulted from northwestward thrusting at the basement surface beneath the northeast margin of the anticline (K, fig. 3). This earthquake is fully consistent with the structure and tectonic style shown in figure 3 and implies active northeastward thrusting at the valley margin of the entire rock section above the west-dipping basement surface.

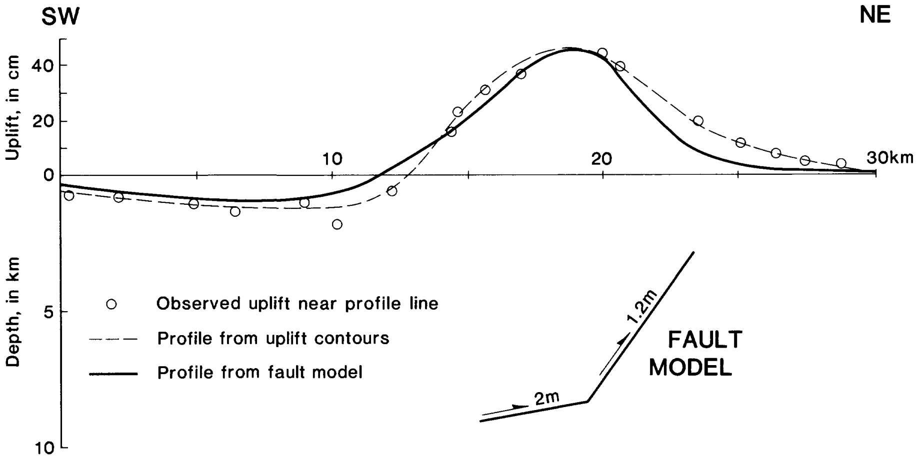

Figure 4.-- Comparison of observed coseismic surface uplift at Coalinga anticline (Stein, 1984) with uplift predicted from a fault model based on figure 3. The profile extends northeastward from the city of Coalinga along the greatest span of resurveyed benchmarks and passes through the observed uplift maximum. This span of uplift control happens to coincide northeast of the crest with a northeastward bulge in the plan pattern of uplift, which can account for the misfit in the curves there. Farther southeast, where the uplift pattern is more two-dimensional, the fit of modelled and observed uplift is much better northeast of the crest, but benchmark control southwest of the crest is largely lacking.

Reports

Wentworth, C.M., and Zoback, M.D., 1985, Central California seismic reflection transect: I-The eastern Coast Ranges and western Great Valley (abs.): submitted for Fall 1985 AGU meeting.

Zoback, M.D., Wentworth, C.M., and Moore, J.G., 1985, Central California seismic reflection transect: II-The eastern Great Valley and western Sierra Nevada (abs.): submitted for Fall 1985 AGU meeting.

Physical Constraints on Source of Ground Motion

9910-01915

D. J. Andrews
Branch of Engineering Seismology and Geology
U.S. Geological Survey
345 Middlefield Road, MS 977
Menlo Park, California 94025
(415) 323-8111, ext. 2752

Investigations

Separation of site effects from spectra of recorded ground motion.

An objective method to determine earthquake source parameters.

Effect of detection threshold and high-frequency attenuation on distribution of observed earthquake source parameters.

Results

The omega-squared spectral model with two independent parameters (stress drop, moment) provides a simple parameterization of ground motion spectra for statistical analysis. Accurate determination of source parameters of small earthquakes requires accounting for distortion of the source spectrum by each site response spectrum. I have inverted record spectra to find separate station and event spectra. Source parameters are found by an automated objective method using integrals of each event spectrum. Quantitative estimates of error are carried through the entire analysis. These methods are applied to digital records of aftershocks of the 1980 Mammoth Lakes, California earthquake sequence. Spectral shape, as measured by the ratio of dynamic to static stress drop, is remarkably constant and independent of source radius. Stress drop is found to be independent of source radius for the 90 events with best-determined source parameters. Stress drops have a log-normal distribution with the standard deviation being a factor of 2. Events with smaller stress drop are less likely to be detected, so it is possible that the true distribution of stress drops is an inverse power law with a gradual transition to a cutoff at the total shear strength.

Reports

Andrews, D. J., 1985, Objective determination of source parameters and similarity of earthquakes of different size, Fifth Ewing Symposium.

SURFACE FAULTING STUDIES

9910-02677

M. G. Bonilla
Branch of Engineering Seismology and Geology
U.S. Geological Survey
345 Middlefield Road, MS 977
Menlo Park, CA 94025
(415) 323-8111, Ext. 2245

Investigations

1. Appearance of active faults in exploratory trenches.
2. Field investigations of surface faulting.

Results

The compilation and analysis of data from various trench exposures was completed, and the first draft of a report on these studies was prepared. In addition to the conclusions given in the preceding "Summaries of Technical Reports" (U.S.G.S. Open-File Report 85-464) regarding visibility of fault strands in trenches, other characteristics of the faults were analyzed. Nearly all the faults have had Holocene displacements and nearly all the materials exposed in the trenches are unconsolidated.

The widths of strike-slip faults exposed in the trenches are less than for dip slip faults. The median width of the principal strands is 0.4 m for strike-slip faults and 1.2 m for dip-slip faults. The median width of the principal and subsidiary strands together is 5.5 m for strike-slip faults and 12.5 m for dip-slip faults. These widths were measured at right angles to the fault strike, but horizontally and therefore the given widths for the inclined dip-slip faults are larger, by perhaps 15 percent, than the width perpendicular to the fault surface. The correlation of fault width and fault displacement ranges from moderate to very poor.

Other phenomena revealed in the trenches were quantified. These are, in decreasing order of frequency, pebble rotation, fissures, gouge, slickensides, mixing, fault rubble and fault breccia, crushing, tectonic polish of clasts, and water barriers.

Reports

Crone, A.J., Machette, M.N., Bonillla, M.G., Lienkaemper, J.J., Pierce, K.L., Scott, W.E., and Bucknam, R.C., 1985, Characteristics of surface faulting accompanying the Borah Peak earthquake, central Idaho, in Stein, R.S., and Bucknam, R.C., eds., Proceedings of workshop 28, on the Borah Peak, Idaho, Earthquake: *U.S. Geological Survey Open-File Report 85-290, p. 43-58.*

SOIL DEVELOPMENT AND DISPLACEMENT ALONG THE HAYWARD FAULT

14-08-0001-21929

Glenn Borchardt
California Department of Conservation
Division of Mines and Geology
380 Civic Drive
Pleasant Hill, CA 94523-1997

(415) 671-4926

Investigations

Its high rate of activity (>5 mm/yr) and urban location make the Hayward fault potentially the most destructive in the San Francisco Bay Area (Steinbrugge and others, 1985). It has been at least 149 years since the last major earthquake occurred on the northern segment of the fault. The objective of this work is to use soils and sediments to determine the recurrence interval and the amount of displacement to be expected for major earthquakes on the Hayward fault.

This phase of the investigation concentrated on the Point Pinole study site along the northern segment. In an effort to locate the fault precisely and to measure its creep rate through the Regional Park, both the Southern Pacific railroad tracks and an old sewer line were surveyed. Four Quaternary sections were described and sampled on either side of the fault. A 10-cm thick peat layer discovered in the tidal marsh adjacent to the fault was investigated for continuity and extent.

Results

1. On June 4, 1985, the westbound track of the Southern Pacific Railroad had a right lateral deflection of approximately 25 mm through a distance of 90 m. To the northwest, an abandoned sewer line suffered no more than 142 mm of deflection through a distance of 120 m since its construction across the fault trace more than 46 years ago. This is less than 3 mm/yr--much less than the long-term creep rate at the U.S.G.S. alinement array at Parchester Village about 2 km to the southeast.

2. Soils were described and sampled in a small hand-dug excavation in the creep zone 3 m northwest of the alinement array at Parchester Village. An A/Bw/BC/C soil-horizon sequence overlies both sides of the fault to a depth of 140 cm. The only indications of fault movement in the 6-m long exposure were a few thin soil-filled fissures.

3. Quaternary soil sections from either side of the fault provide information useful for determining the amount of vertical crustal movement that has occurred at Point Pinole during the late Pleistocene. West of the fault, soil borings revealed that a Holocene alluvial fan deposited at current base level (mid-fan elevation of 2.3 m) has a Bw horizon (a B horizon with soil structure, but lacking clay films) overlying a zone of manganese oxide accumulation. East of the fault, an extensive bay cliff exposure revealed a late Pleistocene fan occurring at a mid-fan elevation of about 4.3 m. In addition to the Holocene Bw horizon and manganese oxide accumulation, this section has an underlying paleosol with extensive Bt horizon development. Clay films extending to depths over 3 m indicate that the paleosol formed under a climate with nearly three times the present rainfall. The paleosol may be up to 125,000 years old, with its alluvial parent material having been deposited during isotope stage 5a when sea level may have been at least 2 meters higher than at present. Vertical movement along the fault thus appears confined to less than 2 m during the last 125,000 years.

4. Cores taken from the tidal marsh adjacent to the fault at Point Pinole reveal a 10-cm thick peat layer at depths between 30 and 70 cm. Cores from a 30-m transect across an area thought to be in the shear zone showed no obvious offset of this layer. The layer is noticeably absent in tidal marsh exposures on the northeast side of the Point and thus appears related to local rather than regional subsidence.

Related Publications

Borchardt, Glenn, 1986, Smectites, in J. B. Dixon and S. B. Weed, eds., Minerals in soil environments (2nd edition): Soil Science Society of America, Madison, WI, in press.

Borchardt, Glenn, and Hill, R. L., 1985, Smectitic pedogenesis and late Holocene tectonism along the Raymond fault, San Marino, California, in D. L. Weide, ed., Soils and Quaternary geology of the southwestern United States: Geological Society of America Special Paper 203.

Steinbrugge, K. V., Davis, J. F., Lagorio, H. J., Bennett, J. H., Borchardt, Glenn, and Toppozada, T. R., 1985, Earthquake planning scenario for a magnitude 7.5 earthquake on the Hayward fault in the San Francisco Bay area, California Division of Mines and Geology Special Publication 78, in press.

Northern San Andreas Fault System

9910-03831

Robert D. Brown
Branch of Engineering Seismology and Geology
U.S. Geological Survey
345 Middlefield Road, MS 977
Menlo Park, California 94025
(415) 323-8111, ext. 2461

Investigations

Research activities in this reporting period were directed chiefly towards evaluating geologic and geophysical evidence regarding the continuity, recent activity, and the dip of the coastal fault zone that includes the Hosgri, San Simeon, Sur, and San Gregorio faults, and the relationship of these faults to onshore faults and folds that merge with the coastal zone between Monterey Bay and Point Buchon. Using reconnaisance geologic methods and existing mapping, I evaluated evidence for the amount and continuity of fault displacement at several key areas betwen Point Reyes in Marin County and Point Buchon in San Luis Obispo County. I also began an analysis of geomorphic and geologic evidence for recent faulting, using high altitude stereo photos of the coastal region in central California and, with Bob Jachens and Andy Griscom of the Branch of Geophysics, planned and started a modeling study of magnetic anomalies to evaluate continuity of faulting and fault geometry at depth. Through an agreement with Bill Ellsworth of the Branch of Seismology some project resources were allocated to improving seismic network capabilities in the transition region between the Transverse Range thrust province and the northern California strike-slip province.

Other activities included: 1) field and office conferences--in San Luis Obispo County, Ca.; Menlo Park, Ca.; Bethesda, Md.; and Washington, D.C.--with Nuclear Regulatory Commission staff and consultants and Pacific Gas and Electric Co. staff and consultants on matters related to the earthquake safety of the Diablo Canyon Power Plant, and 2) monthly meetings of the Policy Advisory Board for the Bay Area Regional Earthquake Preparedness Project.

Results

As is evident from published geologic, geophysical, and seismological data, several alternative interpretations are possible for the coastal zone of faulting. It may be simple and continuous or complex and overlapping, it may be dominated by strike slip motion or (at least in its southern part) by northeastward dipping thrust faults, and its current activity may be either distinct from--or associated with--a set of branching faults (such as the Nacimiento) that verge obliquely landward (southeasterly) from the coastal zone. Results are as yet inconclusive to resolve such questions, but field geologic relations, magnetic anomaly patterns, and seismicity suggest a zone of faulting that north of Point Sur is relatively well-defined, steeply dipping, and characterized by right-lateral strike slip and to the south becomes more diffuse, more complex, and with both thrust and strike slip components.

Reports

Brown, Robert D., Jr., and Kockelman, William J., 1985, Geology for decisionmakers: Protecting life, property, and resources: *Public Affairs Report, Bulletin of the Institute of Governmental Studies*, University of California, Berkeley, v. 26 no 1, 11 p.

——, and Kockelman, William J., in press, Editorial—Geologic principles for prudent land use: A decisionmaker's responsibility?: *Environmental Geology*, 2 ms. p. (Director's approval August 13, 1985).

Lienkaemper, J.J., and Brown, R.D., 1985, Map of faulting accompanying the 1966 Parkfield, California earthquake: *U.S. Geological Survey Open-File Report* 85-661.

LATE QUATERNARY SLIP RATES ON ACTIVE FAULTS OF CALIFORNIA

9910-03554

Malcolm M. Clark

Branch of Engineering Seismology and Geology
U.S. Geological Survey
345 Middlefield Road, Ms 977
Menlo Park, CA 94025
(415) 323-8111, ext. 2591

Investigations

1. Late Quaternary history of Owens Valley fault zone, eastern California (S. Beanland, M.M. Clark, S.K. Pezzopane, K.K. Harms).
2. Continue investigation of active faults in epicentral area of 1980 Mammoth Lakes earthquakes (Clark, Pezzopane, Loomis).
3. Faults near Coalinga (M.J. Rymer, J.J. Lienkaemper, Pezzopane).
4. Geologic studies of Quaternary faults in Gansu Province, north-central China (Rymer).
5. Historic slip rates along active faults of California (Lienkaemper).

Results

1. Field investigations show that right-lateral slip dominates along most of the Owens Valley fault zone. East of the Alabama Hills the zone has a distinct, but subordinate vertical component, east side down, with elongate grabens between the main fault trace and discontinuous traces 1-2 km to the west near the base of the Alabama Hills. Northward from Alabama Hills the narrow fault zone follows a straight course marked by sag ponds and low scarps in late Quaternary alluvium and lake beds. In this region the minor vertical component varies in both amount and sense of offset along strike. The zone displays sandblows and horizontally offset channels and meander scars.

2. Ground check of aerial photo lineaments and a fault in the headwaters of McGee Creek along and near south-to southeastward projections of Laurel-Convict fault trends show no evidence of either 1980 displacement or significant Holocene displacement. These features are in the epicentral region of some of the 1980 Mammoth Lakes earthquakes. One set of lineaments lies 1-2 km NNW of Big McGee Lake and appears unrelated to faulting. The fault is 2-3 km W and NW of Grass Lake. Although lacking evidence of Holocene movement, it may record earlier Quaternary displacement. The Laurel-Convict fault lies closer to the 1980 epicenters than does the nearby Hilton Creek fault, but shows none of the surface continuity and clear evidence for large Holocene displacement that characterize the Hilton Creek fault.

3. In August we (with R.V. Sharp) checked for surface rupture in the epicentral and aftershock areas of the 1985 Kettleman Hills earthquake sequence. The Kettleman Hills earthquakes were located southeast of the Coalinga earthquake sequence and, like the main shock of the Coalinga sequence, they produced no noticeable faulting-related surface rupture. After the Kettleman Hills earthquakes leveling measurements were made across the Nunez fault, northwest of Coalinga, to check for possible triggered slip. Leveling results indicated not only minor elevation changes, which are probably the result of continued postseismic slip from the July 22, 1983 M=6.0 earthquake on the Nunez fault and not triggered slip.

4. In September Rymer accompanied A.J. Crone and M.N. Machette to Gansu Province, Peoples Republic of China to study Quaternary faults. Reconnaissance work along the Yumu Shan fault, a south-dipping right-reverse fault, clearly indicated no late Holocene deposits were faulted, and early to middle Holocene deposits also might not be faulted. Along the Shitan Gou fault the last demonstrable movement was late Pleistocene in age. At several locations along the Shitan Gou fault zone alluvial fan deposits are displaced on moderately to steeply dipping reverse faults. At other locations, late Pleistocene deposits were primarily deformed into broad monoclinal warps with narrow, shallowly dipping subsidiary shear zones.

   Reconnaissance of easternmost fault scarps formed during the 1932 Changma earthquake (M=7.25) indicates displacement was dominantly left-lateral slip with a subordinate amount of normal slip on a fault dipping 50-70° to the south (mountainward). At a site where the composite late Quaternary scarp was easily measured, we determined a ratio between lateral and vertical slip of about 3:1.

5. In compiling historic rates of slip in California, two areas were identified as highest priority in re-evaluating the amount of and uncertainty in total historic slip on the oldest offset cultural features: 1) the 1966 Parkfield rupture along the San Andreas fault, and 2) the Hayward fault.

   Several features were surveyed and results have lead to useful conclusions regarding the spatial distribution of slip in characteristic Parkfield earthquakes and the recurrence interval and spatial distribution of slip in great earthquakes in this section of the San Andreas fault.

   The main fault trace in the 1966 Parkfield rupture has three principal segments: the southern segment trends N34W for 12 km, the central one N42W for 20 km, and the northern, N47W for 4 km. The "southwest fracture zone" broke discontinuously for 8 km parallel to and SW of the center of the central segment. Two features were surveyed on the southern segment, and one each for the other segments.

Parkfield earthquakes recur on average every 21 years and are apparently the same size, based on seismograms of the 1921, 1934 and 1966 earthquakes. The great earthquake of 1857 ruptured at least as far north as the southern Parkfield segment, possibly through all three Parkfield segments. Using the assumption that all post-1857 earthquakes are identical in displacement and that slip rate between earthquakes has been constant, the values of total displacement obtained from our 1985 surveys have been combined with other available data on slip starting in 1966 to deduce slip per event and interseismic slip for 5 localities.

On the southern segment, a total of 22.6 +/- 0.7 cm slip occurred at the Highway 46 fence (built in 1959). Event slip of 13 +/- 0.2 cm following the 1966 earthquake indicates an interseismic slip rate of 0.37 +/- 0.03 cm/yr. North of the highway 3 km, a total of 69 +/- 3 cm slip occurred at Water Tank fence since 1908. Average slip for the 1922, 1934, and 1966 earthquakes is 15 +/- 3 cm for each event. Slip at a 0.3 +/- 0.1 cm/yr rate between events is established by best fit of several strands of corroborative slip data.

On the central segment, Parkfield bridge indicates 126 +/- 2 cm total slip since 1932. Adjacent electronic distance measurements across the fault from 1974 to 1985 give an interseismic slip rate of 0.78 +/- 0.06 cm/yr, indicating an average slip for the 1934 and 1966 earthquakes of 42 +/- 2 cm per event. A fence on the southwest fracture zone at Ranchita Canyon Road shows only 8 +/- 4 cm of slip, a value similar to two independent measurements in 1966.

On the northern segment, Claassen Ranch fence slipped a total of 106 +/- 3 cm since 1946: 17 +/- 1.4 cm associated with the 1966 earthquake and 2.26 +/- 0.04 cm/yr interseismically.

A slip deficit exists at each of these localities, accrued since the great 1857 earthquake, if one assumes a 3.3 cm/yr long-term slip rate is expected at each. In the southern segment 3.0 +/- 0.1 and 2.9 +/- 0.2 meters have accrued at Highway 46 and Water Tank respectively. The central segment localities, Parkfield bridge and Ranchita Cyn. Rd. fence, taken together show 0.18 +/- 0.31 meter deficit in the last 128 years. The Claassen Ranch fence in the northern segment indicates a deficit of 0.29 +/- 0.17 meter.

To interpret the slip deficits in light of the conclusion by Sieh (1978) that channel offsets in 1857 from Cholame southward to Bitterwater Valley were 3 to 4 meters, J. D. Sims and I investigated those sites indicated by Sieh to be "good" or "excellent" in quality. We concluded that some of these offsets may be of nontectonic origin and yield equivocal estimates of slip. Materials into which these channels are cut are highly erodable and lithologically monotonous; the channels are very sinuous at the fault and elsewhere. Further investigations of these sites are needed. The only historic documentation of slip in this area is the 1905 field notebook of U.S.G.S. geologist H. R. Johnson who traced the 1857 rupture northward to the vicinity of Cholame where he sketched a 100 by 150 foot rectangular corral right-laterally offset. Scaling the offsets and the lengths of the corral sides from the sketch gives 7 +/- 2.5 meters offset, attributing error to all available discrepancies in Johnson's sketch. I interpret the location of the corral to be near the present position of Highway 46. Although the amount of offset at the corral remains highly speculative, because we do not have a directly measured value of lateral slip, in my judgment it is our only dated evidence for amount of slip in this section of the fault in 1857.

The Hayward fault investigations have not advanced as far as Parkfield. The foundations of the Gallegos Winery, built in 1880, are the oldest historically offset feature at high angle to the fault strike. The foundation structures have been disturbed since the original offset observations were made in 1970 by R.D. Nason. S. A. Mathieson and I prepared a detailed site map, and slip rate uncertainties are still being assessed in cooperation with R.D. Nason.

In the effort to locate the 1966 Parkfield rupture more precisely, a 1:12,000-scale map of the surface rupture was produced from the original field-annotated 1:6,000 airphotos and 1:24,000 topographic maps.

Reports

Lienkaemper, J.J., and Brown, R.D., 1985, Map of faulting accompanying the 1966 Parkfield, California, earthquake: U.S. Geological Survey Open-File Report 85-661.

Lienkaemper, J.J., Prescott, W.H., Sims, J.D., and Higgins, C.D., 1985, Parkfield Slip history: AGU Abstracts, San Francisco meeting.

Lubetkin, L., and Clark, M.M., 1986, Late Quaternary fault scarp at Lone Pine, California, in M.L. Hill, ed., Geological Society of America Centennial Field Guide, v. 1, Cordilleran Section, in press.

Sharp, R.V., Rymer, M.J., and Lienkaemper, J.J., in press, Surface displacement on the Imperial and Superstition Hills faults triggered by the Westmorland, California, earthquake of 26 April 1981: Bulletin Seismological Society of America.

AGE OF LATE QUATERNARY SURFACE RUPTURES ALONG THE THOUSAND SPRINGS-MACKAY SEGMENT OF THE LOST RIVER RANGE FAULT SYSTEM

14-08-0001-21992

B.D. Cochran
Department of Geology
University of Idaho
Moscow, Idaho 83843
(208) 885-6192

INVESTIGATIONS

The objectives of this investigation are: (1) to establish a chronology of faulting and surface rupture by locating primary and redeposited tephra in off-set and non off-set colluvium and alluvium; and (2) to establish a refined airfall distribution map and chronology of late Quaternary volcanic ashes originating from Cascade Range volcanoes in Washington and Oregon.

Preliminary Results

Objective One

The excavation of two 20.0 meter long trenches through a thick sedimentary sequence along the fault scarp at Willow Creek (locality WCS-T1; Figs. 1 and 2) and North Spring (locality NS-T1; Figs. 1 and 3) and the excavation of sediments deposited in an older "graben" at Rock Creek (locality RC-T1; Figs. 1 and 4) suggest that at least three episodes of faulting accompanied by surface rupture occurred within approximately the last 40,000 years. The stratigraphic relationships of the older (Qfo) clastic wedge at WCS-T1 (Fig. 2) to the oxidized and non-oxidized clay units (Qbc and Qyc) indicates that at least one episode of faulting occurred prior to the deposition of the late Pinedale alluvium (Qpa). A lower limiting age of this faulting episode has yet to be determined. The stratigraphic evidence suggests a pre-late Pinedale age.

Although the thin, nearly vertical clastic wedges (between 2.0W and 6.0W, Fig. 2) do not crosscut the late Pinedale gravels (Qpa), stratigraphic relationships of the thin clastic wedges to the younger fan gravels (QFy1 and QFy2) suggest that a younger episode of faulting occurred after the deposition of the late Pinedale alluvium (Qpa) but before the October 1983 event.

Redeposited volcanic glasses, which are attributed to the Mount Mazama Layer O tephra, dated to ca. 6,700 years B.P., are found in the younger deposit (Qfy2). The conspicuous absence of primary layer O deposits in sediments at trenches WCS-T1, NS-T1, and RC-T1 combined with the presence of redeposited layer O volcanic glasses may provide a maximum limiting age of 6,700 years B.P. for the pre-1983 post-late Pinedale faulting event. A minimum limiting age has not been determined.

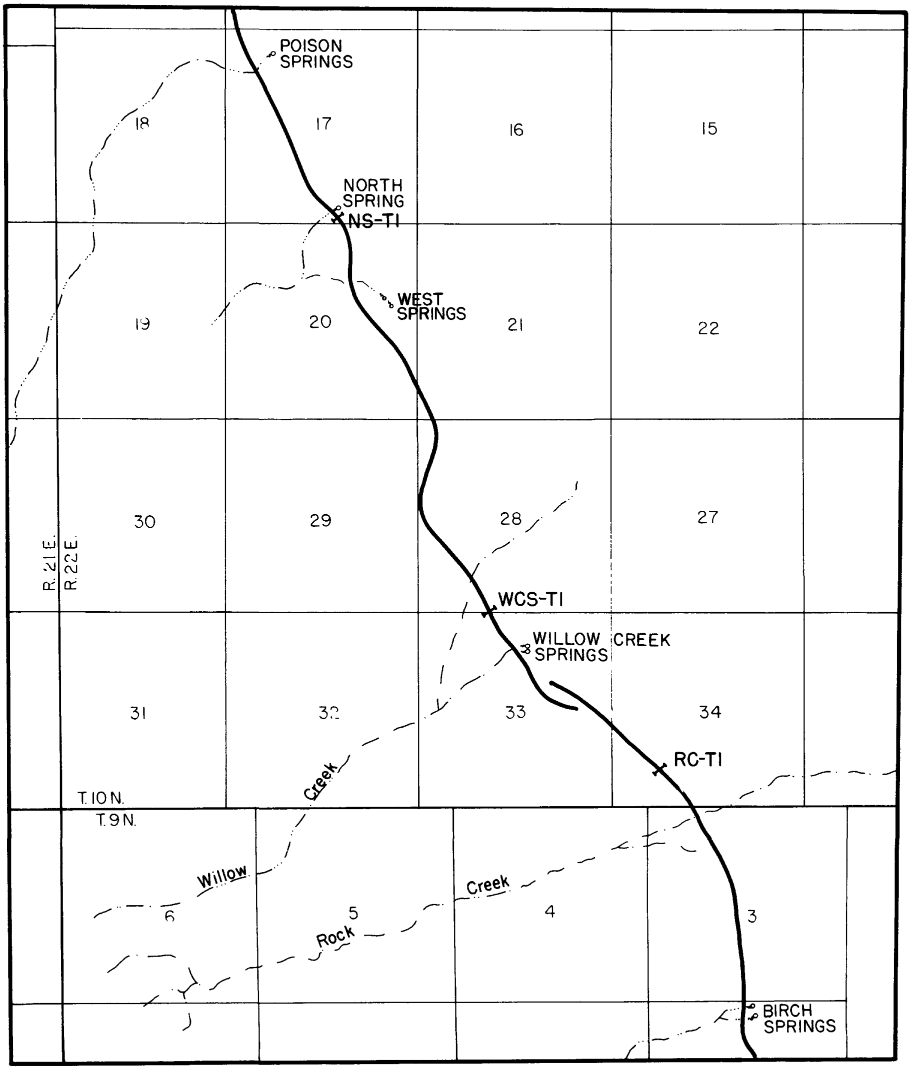

Figure 1. Location map of trenches excavated perpendicular to the October 1983 fault scarp along the Thousand Springs - MacKay segment of the Lost River Range Fault System.

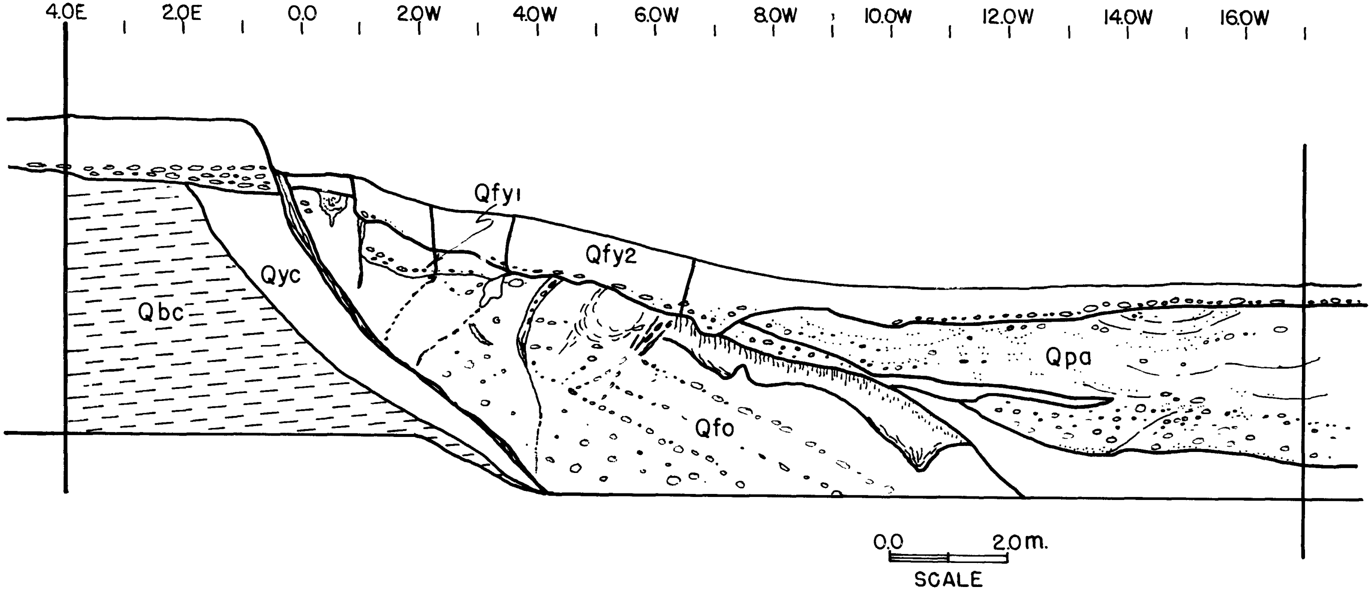

Figure 2. Cross-sectional diagram of trench WCS-T1 at Willow Creek. Symbol explanation: Qbc (early Quaternary), finely laminated blue clay; Qbc, oxidized yellow clay mixed with angular cobble gravel; Qfo (middle Pinedale), poorly sorted, angular to subrounded, stratified cobble gravels; Qpa (late Pinedale), moderately to poorly sorted, sub-rounded to rounded, stratified cobble-granule-pebble gravels; Qfy1, poorly sorted, non-stratified, angular to rounded, cobble-granule gravels; Qfy2, poorly sorted, angular to rounded, cobble-granule gravel grading vertically to massive silt.

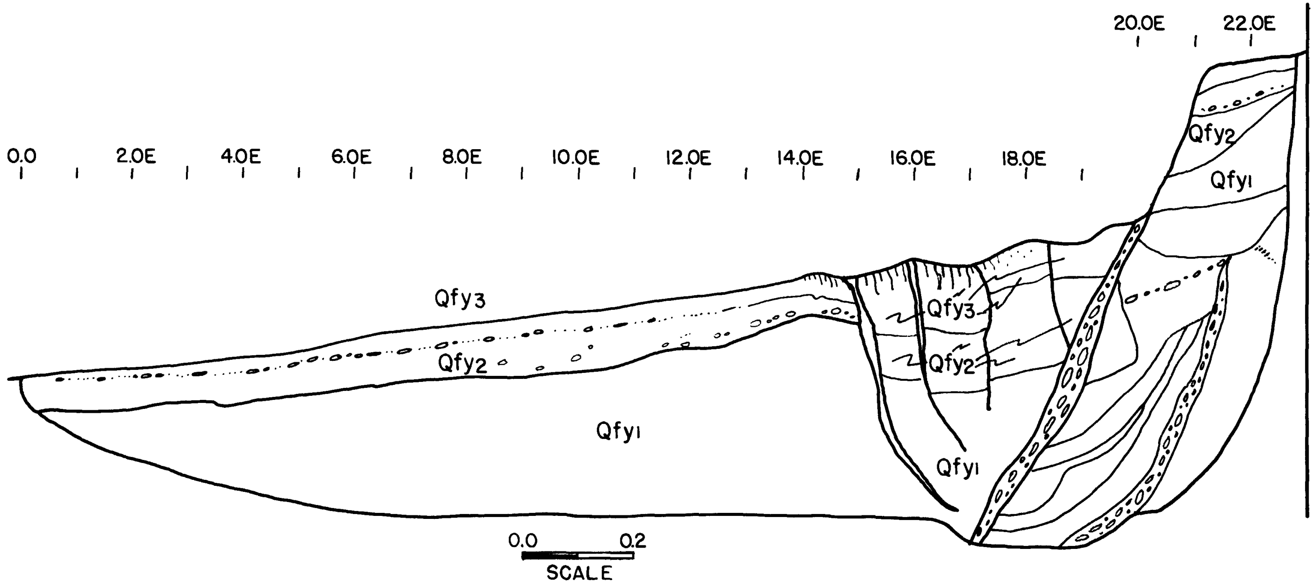

Figure 3. Cross-sectional diagram of trench NS-T1 at North Spring. Symbol explanation: Qfy1 (early Holocene?), poorly sorted, poorly stratified, very angular, clast supported, cobble-granule gravel; Qfy2 (middle Holocene), poorly sorted, poorly stratified, very angular, cobble-granule gravel, matrix supported in the upper part; Qfy3 (late Holocene), poorly sorted, non-stratified, angular, cobble-granule gravel grading vertically to massive silt. Qfy1 through Qfy3 conspicuously lack carbonate rinds thicker than 0.4mm.

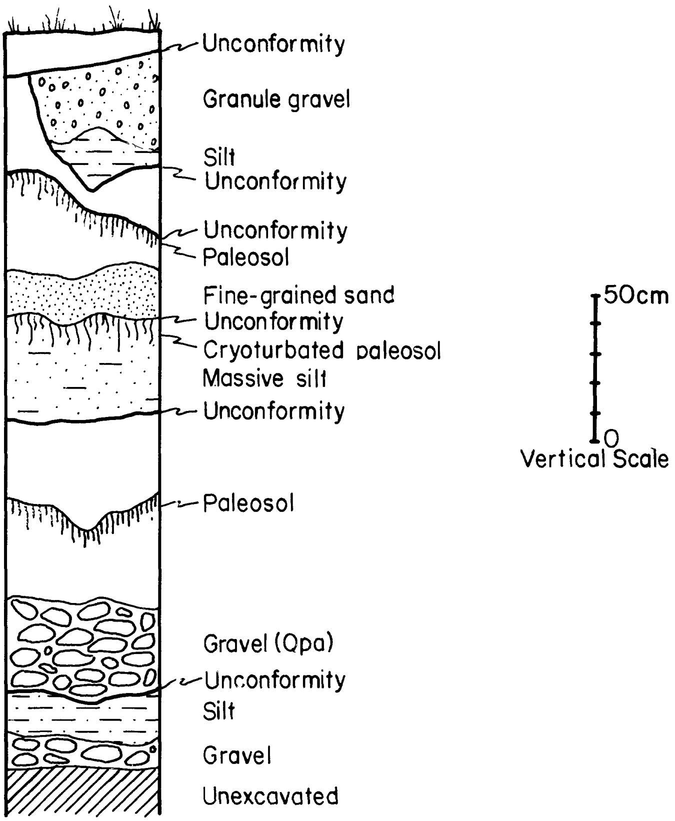

Figure 4. Stratigraphic diagram of trench RC-T1 at Rock Creek Explanation of key symbols: Qpa (late Pinedale), poorly sorted, subrounded to rounded cobble gravels.

At least three faulting events are recorded in the sedimentary sequences from trench NS-T1 (Fig. 3). Preliminary correlations of the deposits from NS-T1 to the sediments exposed in WCS-T1 suggest that the latest two faulting episodes (the October 1983 and post-late Pinedale faulting events) may be coeval at these localities. However, additional stratigraphic study and age relations are requisite before a definitive statement on correlation can be made.

The exploratory trench at RC-T1 (Fig. 4) was excavated in an older graben in order to locate primary tephra beds. If the graben formed prior to the Mazama, Tephra O, ash fall, ca. 6,700 B.P. then it would provide an excellent depositional basin in to which primary deposits of volcanic ashes would accumulate.

Correlation of the late Pinedale alluvium (Qpa) at WCS-T1 and RC-T1 are tentative; however, the calcium carbonate rind thicknesses of both units appear to be similar. The sedimentary sequence at the Rock Creek locality suggests that the graben formed after the deposition of late Pinedale alluvium (Qpa). The major unconformities (Fig. 4) suggest that several periods of erosion (and/or non-deposition) may have removed primary volcanic ash deposits.

Objective Two

Three primary tephra beds have been found in late Quaternary deposits in and adjacent to the study area (Fig. 1). The oldest tephra is attributed to Glacier Peak volcano in north-central Washington. At Little Redfish Lake, near Stanley, Idaho, organic rich sediment from beneath the tephra has been radiocarbon dated to 11,360 ± 190 years B.P. (WSU-3248).

Primary deposits of Glacier Peak tephra have been found in alluvium and colluvium in the Imnaha and Powder River drainages of northeastern Oregon. Other deposits of Glacier Peak tephra have been found at Riggens, Idaho and Lewiston, Idaho. Occurrences of Glacier Peak tephra at the localities mentioned above and at other localities throughout the Pacific Northwest indicate that the Glacier Peak tephra has a more extensive airfall distribution than previously reported (Fig. 5).

Primary deposits of Mazama Layer O tephra have been found in a variety of localities within the study area including a 60 centimeter thick deposit at West Spring (Fig. 1) and a 30 centimeter thick deposit in a kettle at Double Springs Pass. Layer O tephra, which has been found in lacustrine sediment at Little Redfish Lake has been radiocarbon dated at 6,800 ± 110 years B.P. (WSU-3247). Because Mazama tephra layer O has a wide-spread distribution (Fig. 6), it is an excellent chrono-stratigraphic marker horizon.

The youngest tephra is attributed to Mount St. Helen's set Ye. At Little Redfish Lake set Ye tephra has been "bracket" radiocarbon dated between 3,850 ± 85 years B.P. (WSU 3236) and 3,610 ± 80 years B.P. (WSU-3219). Primary deposits of set Ye tephra, found in alluvium and

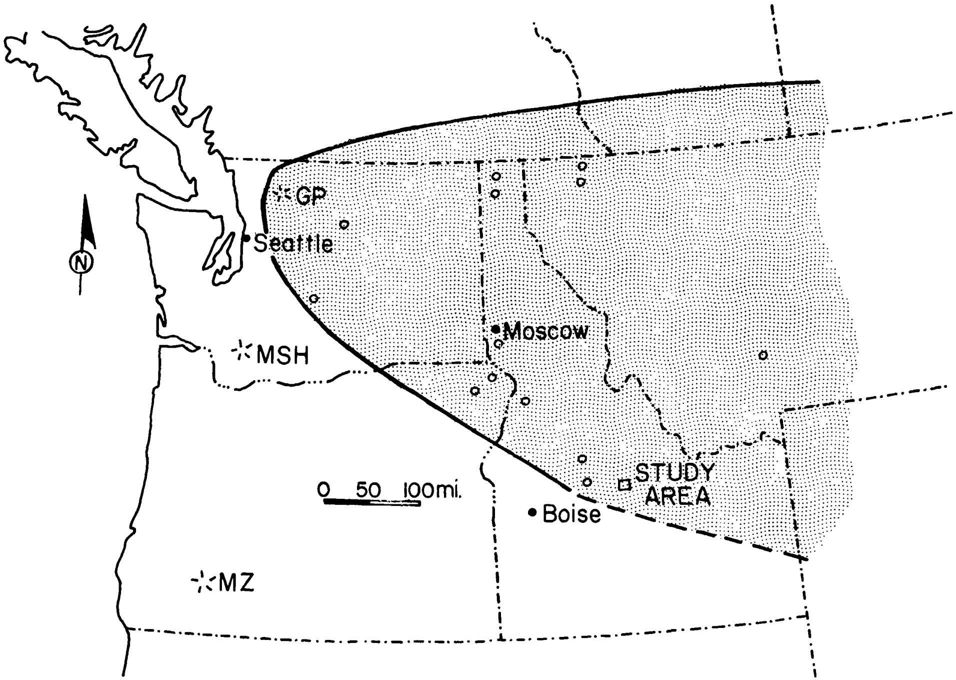

Figure 5. Airfall distribution of Glacier Peak tephra ejected ca. 11,300 years B.P. Open circles designate localities where primary deposits of Glacier Peak tephra have been found. GP, Glacier Peak; MSH, Mount St. Helens; MZ, Mount Mazama.

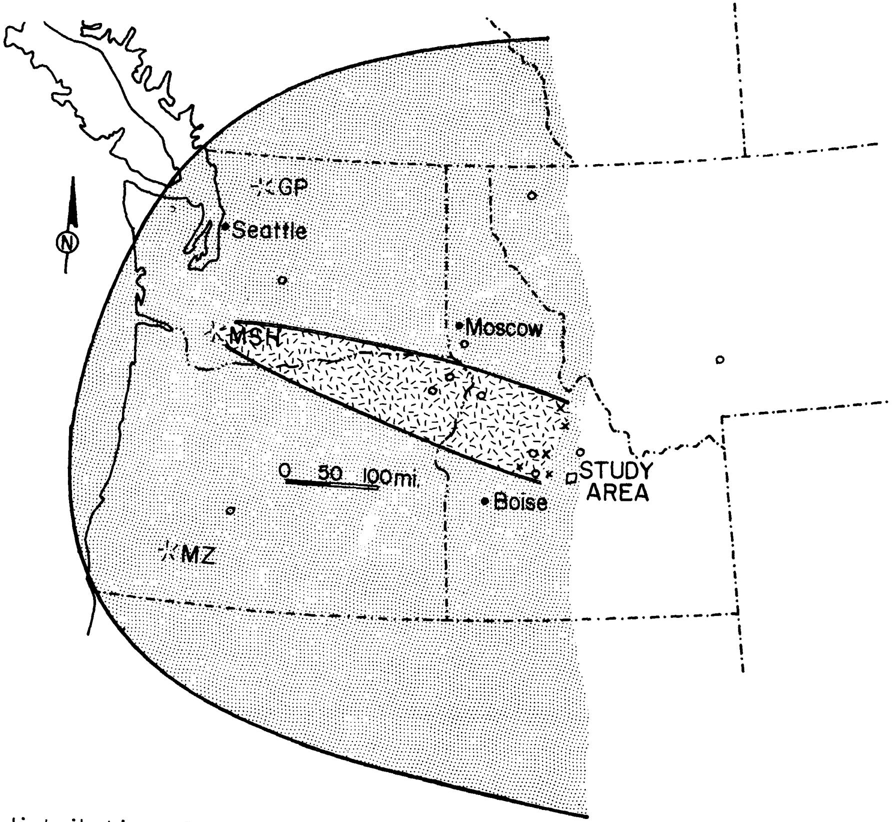

Figure 6. Airfall distribution of Mount Mazama tephra layer O (fine stipple) and Mount St. Helens tephra set Ye (dashed lines). Open circles designate localities where deposits of layer O crop out; lower case x represents localities of set Ye tephra. GP, Glacier Peak; MSH, Mount St. Helens; MZ, Mount Mazama.

colluvium in the Lone Pine Creek drainage (30 km northwest of the study area), Little Redfish and Jimmy Smith Lakes (60 km and 30 km, respectively, west of the study area) and at Challis, Idaho extends the airfall distribution further to the south and east than previously reported (Fig. 6).

ARTICLES

COCHRAN, B.D., 1985 (in preparation), Radiocarbon age, airfall distribution and petro-chemical characteristics of tephra ejected from Glacier Peak Volcano, North-Central Washington.

COCHRAN, B.D., 1985 (in preparation), Airfall distribution and radiocarbon ages of wide-spread tephra deposits originating from the Cascade Range Volcanoes of Oregon and Washington.

COCHRAN, B.D., 1985 (in preparation), Correlation and age of faulting along the Thousand Springs-MacKay segment of the Lost River Range Fault System.

EARTHQUAKE RESEARCH IN THE WESTERN GREAT BASIN

Contract 14-08-0001-21986

E.J. Corbett, W.A. Peppin, and U.R. Vetter
Seismological Laboratory
University of Nevada
Reno, NV 89557
(702) 784-4975

Investigations

This program supports continued studies with research focused on: (1) seismicity in the White Mountains Gap; (2) magmatic processes in Long Valley Caldera; (3) the UNR experimental digital network; (4) systematic variations in focal mechanisms with depth; (5) attenuation changes in earthquake regions connected with volcanism; (6) relocations of Mammoth Lakes earthquakes; (7) improved depth control on Mammoth Lakes earthquakes; (8) analysis of digital waveforms; and (9) digitization of field tapes for a more detailed analysis of the 1978 Wheeler Crest earthquakes. Progress in selected areas of this program is described below.

Results

A. *Seismicity in the White Mountains seismic gap*

Major earthquakes during the historic period have occurred in a northerly-trending belt from the southern Owens Valley in southeastern California to Winnemucca in north-central Nevada. Wallace (1978) pointed out that three "gaps" within this belt are likely candidates for future large earthquakes. Two of these are the Stillwater gap between the 1954 and 1915 ruptures, and the White Mountains gap between the 1872 and 1932 zones. The "White Mountains seismic gap" has been identified as an area in which the next major earthquake in the western Great Basin has a high likelihood of occurring, and increased seismicity in and around the White Mountains gap may be precursory to such an event (Ryall and Ryall, 1983).

The marked concentration of activity in the Bishop-Mono Lake-Mina region, including a major earthquake swarm and associated magmatic activity in and around Long Valley caldera from 1978 to the present, could presage the onset of a new episode of major faulting along the Sierran front. Synchronous with the Long Valley sequence a flurry of moderate (M_L around 5) earthquakes affected the entire Sierran boundary zone, from Doyle in the northwest to Inyokern at the south end of the Owens Valley -- suggesting that fluctuations in seismicity reported before large earthquakes in other regions may have reflected regional, rather than local stress changes. If so, such changes may indicate favorable conditions for large shocks to occur anywhere within a sizable region, rather than in the immediate vicinity of one or another cluster of small events (Ryall and Ryall, 1981).

In the region around the White Mountains gap since October 1978 more than 50 earthquakes with M_L 4.0-5.4 have occurred in the following zones: a NE-trending zone between Mono Lake, California and Luning, Nevada; at the north end and east side of the White Mountains; and in the northern Owens Valley. In addition, more than 200 shocks with M_L 4.0-6.3 have occurred in the Mammoth Lakes area. In comparison only 18 events with M_L 4.0 or greater were observed in this entire region (including the Mammoth Lakes area) during the previous nine-year period. Thus, the level of moderate seismicity since 1978 is about six times higher than the previous decade if the Mammoth Lakes sequence is excluded, and almost twenty times higher if it is included. The similarity between this pattern and that observed by Mogi (1969) before large earthquakes in Japan leads Ryall and Ryall (1983) to conclude that the potential for a major earthquake in the White Mountains gap is substantially higher now than it has been for at least the last two decades.

It is noteworthy that there is a "seismicity gap" that occurs between the heavy concentration of activity at Mammoth and the moderate activity east of Mono Lake along the California border (see figure). This zone of quiescence has persisted at least since 1978 and is centered directly on the northern terminus of the White Mountains fault zone. Observations of recent seismicity patterns indicate that this gap may be tightening. The upper half of the figure shows regional seismicity for the period prior to the Round Valley earthquake, clearly depicting the 30-km wide quiescent zone between the activity at Long Valley and the active zone east of Mono Lake. Beginning with the Round Valley earthquake, seismic events began to creep into this quiet zone from the south. Throughout 1985 (lower half of figure) seismic activity has continued to creep north in Long Valley as well a creep south from the Mono Lake area. In addition, the "rim" of this quiescent zone has become more continuous with events spreading west into Mono Lake and earthquakes becoming more numerous south and east of Dyer, Nevada. We will continue to monitor this area, and keep the USGS informed of new developments.

B. *Analysis of Wideband Digital Data.*

Some 4,500 wideband (0.1-50 Hz) digital displacement seismograms have been recorded for half a dozen earthquake sequences in the western Great Bassin, including the 1980 Mammoth Lakes events (Peppin, 1984a). These data have formed the basis for two abstracts presented at recent meetings of the AGU and SSA (Peppin, 1984b, 1985). Because of the discrepancy in results obtained from these excellent records as compared with work done by personnel from the USGS (Archuleta *et al.*, 1982), we found it necessary to present the results of this analysis in December 1984 and April 1985, the latter after completely redoing the analysis of spectral parameters. Based on consultation with attendees at these meetings, we have now satisfied ourselves that our analysis methods are valid, and are writing up the results for publication. Two results of importance have emerged. *First*, spectral corner frequencies published by Archuleta *et al.* are likely to be estimates of processes other than the source because of strong local (factor of 2.5) site effects. *Second*, again because of site effects and because the data used by Archuleta *et al.* sampled "non-hardrock" sites, the seismic moments inferred may be substantially overestimated by use of Brune's (1970) theory (factor of 4 or 5 when compared with a "hardrock" site.) Similar strong site effects have recently been observed at Mammoth (Archuleta *et al.*, 1985) and predicted theoretically (Barker, 1985.)

C. *1978 Wheeler Crest Aftershocks.*

The first significant earthquake generally associated with the Mammoth Lakes sequence occurred on October 4, 1978 under the Wheeler Crest segment of the Sierra Nevada. The University of Nevada recorded aftershocks of this event for 10 days following the event on seven radio-telemetered and 2 three-component wideband digital seismographs. We have completed hardware and software needed to convert the data to digital format so that the University of Washington interactive timing software can be used to analyze the events.

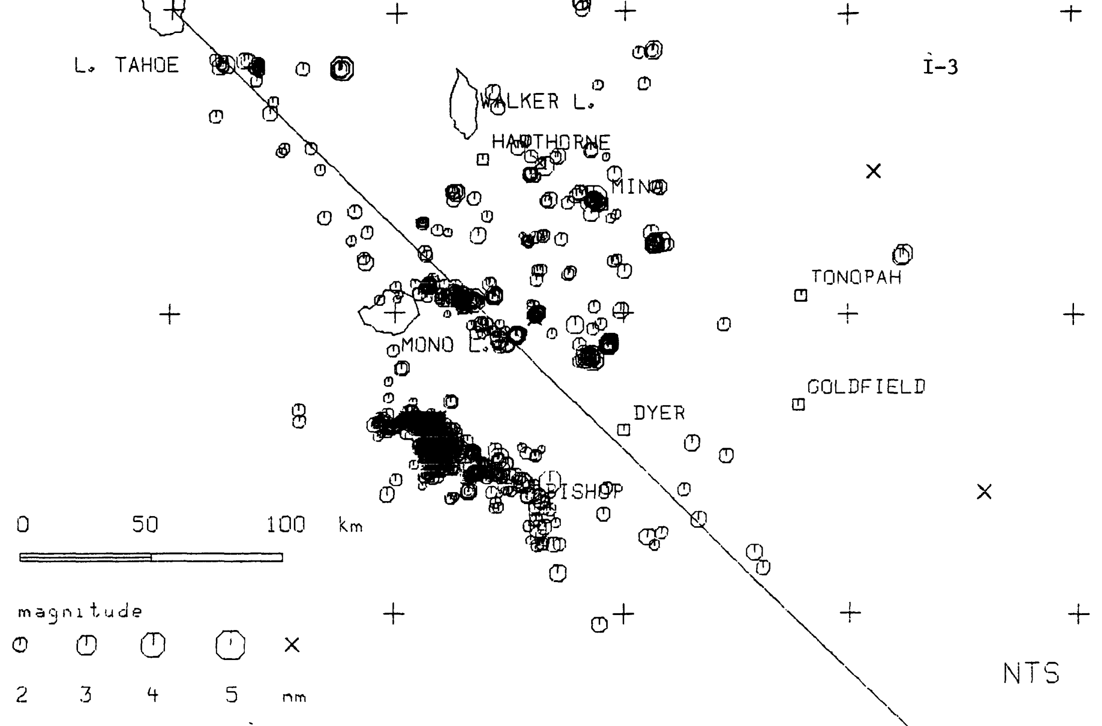

Nevada Seismicity -- 5/10 - 11/22/84

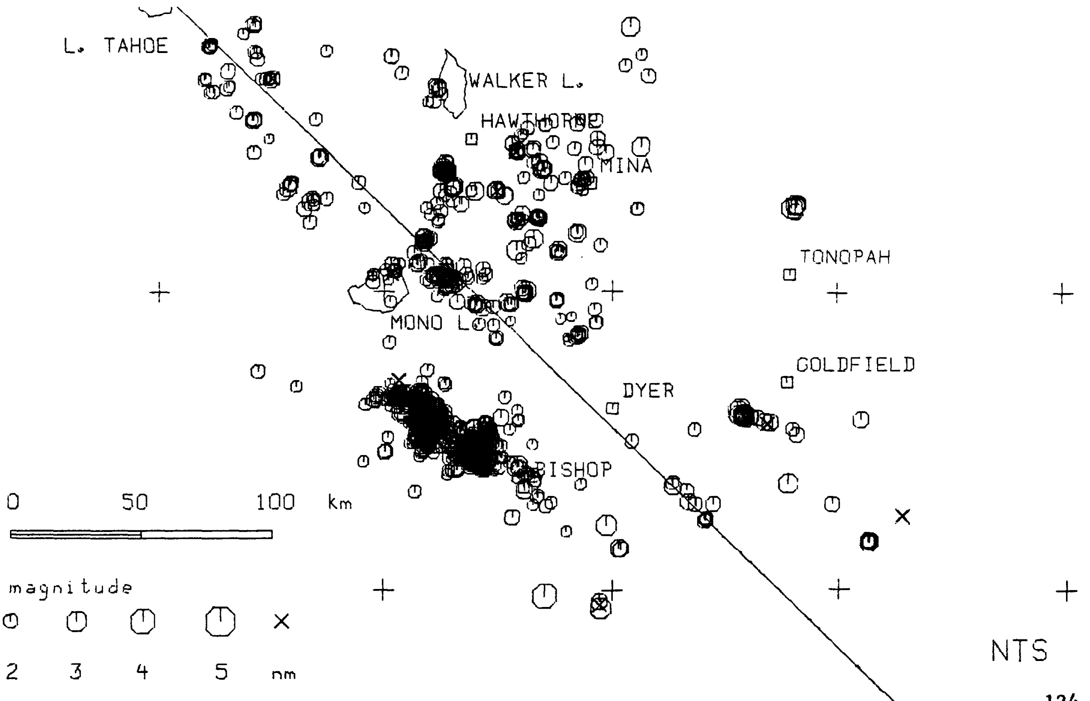

W. Nevada Seismicity -- Jan -Sep 1985

Several tens of aftershocks had been dumped to disc before the November 1984 earthquake forced us to set this project aside. Work on this project has been recently resumed by graduate student Bill Honjas who is currently merging and timing the data.

D. *The Round Valley earthquake and its aftershocks.*

At 10:08 am PST on November 23, 1984, an earthquake of magnitude 6.2 M_L (Pasadena) was felt widely throughout eastern California and western Nevada. The epicenter was located 22 km northwest of Bishop, California, under a broad circular depression known as Round Valley, that is located between the 2-km high escarpment of the Wheeler Crest on the west, and the less elevated depositional surface of the Bishop Tuff (referred to locally as the Sherwin Grade) on the east. The location of this earthquake was not unexpected because it occurred proximate to a major Sierra Nevada range-front fault, the Round Valley fault, which shows well-documented evidence of normal faulting up through the Holocene (Bryant, 1984). However, the evidence gathered from the mainshock and the thousands of aftershocks appears to indicate that the Round Valley earthquake most probably occurred on a fault quite different than the one expressed at the surface.

Initial work presented by Ryall and Hill (1984) and Corbett (1985) showed that the mainshock itself was most probably the result of rupture on a single well-defined fault plane, as indicated by the first 3 hours of aftershock activity. These data suggest that the initial rupture was on a vertical plane trending N 30° E that was 6 kilometers long and extended from 6 to 12 km depth. The location of the mainshock epicenter relative to these aftershocks further suggests that the rupture initiated in the upper northeast corner of this plane and then propogated unilaterally to the southwest and downward. A 3 by 3 km zone of no aftershocks in the vicinity of the mainshock has been interpreted as a possible asperity by Corbett *et al.* (1985). Focal mechanisms for aftershocks during the first 3 hours indicate strike-slip motion, with planes trending N 30° E that would correspond to left-lateral movement (Smith *et al.*, 1985). A first-motion fault plane solution was not obtainable for the mainshock due to a foreshock preceding it by 4.5 seconds. However, Barker and Wallace (in press) have performed an inversion on the teleseismic body waves for this event which also indicates left-lateral faulting on a NE-trending plane.

After these first few hours of activity, aftershocks began to occur frequently off of this main trend and at shallower depths, so that this simple zone quickly grew more complex. After three weeks the aftershock zone was a 12-km sided triangle with the initial NE trend still apparent as the main structure. Cross-sections of these data show that most of the off-trend activity is shallower than 6 km and tends to get progressively shallower to the NW. There is also a somewhat weaker suggestion of a planar structure that dips 80° to the NE and trends NW from the south end of the original fault rupture. Fault mechanisms for these shallower events show that these are predominately vertical-slip or oblique-normal events. Both of these types of mechanisms contain NE-trending planes, but they would correspond to down-to-the-west movement, which is at odds with the Quaternary tectonics that is observed at the surface. Due to the NW-trending line-up of some of the shallow normal events, one has the option of choosing down-to-the-northeast movement on NW-trending planes, but this trend is nearly perpendicular to the range-front fault at this point. In short, the many aftershocks that occurred off of the principal strike-slip trend suggest a complicated process of tectonic stress release that is quite different from the initial mainshock rupture as well the Holocene surface faulting. A possible explanation is suggested by Corbett *et al.* (1985), who note that the aftershock seismicity propagates westward and upward as a function of time. They suggest that this phenomenon is the result of pervasive fracturing of the shallow crust in response to the temporal migration of stresses and/or fluids. Although the presence of magmatic fluids is well documented under the Long Valley caldera, it is surprising that they may be located this far to the south, especially in light of the lack of extrusive rocks younger than the Bishop Tuff and the absence of geothermal activity in this area. Thus, one of the goals of our research is to try to understand this aftershock activity, and see how it may be related to possible presence of magma. Results of these studies will be presented at the Fall AGU meeting in San Francisco.

The aftershock zone is directly astraddle the Round Valley fault zone which has recognized down-to-the-east normal-fault movement as young as Holocene. Despite the proximity of this major Quaternary range-front fault, none of the aftershock trends and none of the focal mechanisms show evidence for motion on this fault. The temporal development of the aftershock zone is similar to the pattern of simple NNE trends developing into pervasive seismicity that was observed for the 1980 Mammoth Lakes sequence (Lide and Ryall, 1985).

References

Archuleta, R.J., E. Cranswick, C. Mueller, and P. Spudich (1982). Source parameters of the 1980 Mammoth Lakes, California earthquake sequence, *J. Geophys. Res.* **87**, 4595-4608.

Archuleta, R.J., J. Gibbs, E. Etheridge, J. Sena, R. Warrick, and R. Borcherdt (1985). Downhole measurements of strong ground motion, *Earthquake Notes,* **56 no. 1**, 5.

Barker, J.S. (1985). Modeling local structure using aftershocks of the May 1980 Mammoth Lakes earthquakes, *Earthquake Notes,* **56, no. 1**, 31.

Barker, J.S. and T.C. Wallace (in press). A note on the teleseismic body waves from the November 23, 1984, Round Valley, California earthquake, *Bull. Seis. Soc. Amer.*, submitted.

Brune, J.N. (1970). Tectonic stress and the spectra of seismic shear waves from earthquakes, *J. Geophys. Res.* **75**, 4997-5009. (Correction (1971), *J. Geophys. Res.* **76**, 5002.)

Bryant, W.A. (1984). Round Valley Fault Zone, Inyo and Mono Counties, *California Division of Mines and Geology, Fault Evaluation Report FER-158*, 8p.

Corbett, E.J. (1985). The Round Valley, California earthquake of November 23, 1984. *Earthquake Notes,* **56, no.1**, 30.

Corbett, E.J., D.M. Martinelli, and K.D. Smith (1985). Aftershock locations of the November 23, 1984 Round Valley, California earthquakes, *E⊕S, Trans. Amer. Geophys. Union,* submitted.

Lide, C.S. and A.S. Ryall (1985). Relationship between aftershock locations and mechanisms of the May, 1980 Mammoth Lakes earthquakes, *J. Geophys. Res.*, submitted.

Mogi, K. (1969). Some features of recent seismic activity in and near Japan, (2) Activity before and after great earthquakes, *Bull. Earthquake Res. Inst.* **47**, 395-417.

Peppin, W.A. (1984a). The University of Nevada, Reno, portable digital event recording seismograph system, *Seismological Laboratory rpt.*, Univ. Nevada, 115p.

Peppin, W.A. (1984b). Seismic moment of Mammoth Lakes earthquakes from close-in displacement seismograms, *E⊕S, Trans. Am. Geophys. Union,* **65**, 1117.

Peppin, W.A. (1985). What do spectral corner frequencies mean anyway? *Earthquake Notes,* **56, no.1,** 14.

Smith, K.D., D.M. Martinelli, and E.J. Corbett (1985). Focal mechanisms of the November 23, 1984 Round Valley, California earthquakes, *E⊕S, Trans. Amer. Geophys. Union,* submitted.

Ryall, A.S. and D.P. Hill (1984). The Round Valley earthquake sequence, unscheduled presentation at the Fall American Geophysical Union meeting, December 7, 1984, San Francisco, Ca.

Ryall, A. and F. Ryall (1981). Spatial-temporal variations in seismicity preceding the May 1980, Mammoth Lakes, California, earthquakes, *Bull. Seism. Soc. Am.* **71**, 747-760.

Ryall, A. and F. Ryall (1983). Increased potential for a major earthquake in the White Mountains seismic gap, California and Nevada, *Univ. Nevada Rpt.*, 23p.

Wallace, R.E. (1977). Profiles and ages of young fault scarps, north-central Nevada, *Geol. Soc. Amer. Bull.* **88**, 1267-1281.

DETAILED GEOMORPHIC STUDIES TO DEFINE LATE QUATERNARY FAULT BEHAVIOR AND SEISMIC HAZARD, CENTRAL NEVADA SEISMIC BELT

Contract #21970

Julia Fonseca, Philip Pearthree, William B. Bull,
Suzanne Hecker, and Oliver Chadwick
Department of Geosciences
University of Arizona
Tucson, AZ 85721
(602)621-6024

Investigations

1. Detailed analyses of faulting have been completed in the northern portion of the central Nevada seismic belt (CNSB), from the northern end of the 1954 Dixie Valley surface rupture, through the Stillwater seismic gap, and the southern and central portions of the 1915 Pleasant Valley surface rupture. Studies have focused on 1) age analysis of Holocene fault scarps, using solutions to the diffusion equation to estimate scarp ages and soil profile description and analysis to estimate surface ages; 2) tectonic landform analysis to assess Quaternary-long rates of uplift along mountain fronts; and 3) detailed analysis of the Sou Hills area, a transverse bedrock feature between Pleasant and Dixie valleys, to assess whether it consistently acts as a barrier to propagation of surface-rupturing earthquakes.

2. Soils and geomorphic data have been collected along other faults within the CNSB, including the 1954 Fairview Peak and 1932 Cedar Mountain surface ruptures, and along the Wassuk Range adjacent to Walker Lake. Field data from these reconnaissance studies are being analyzed to 1) assess temporal and spatial patterns of surface rupture during the Holocene in and adjacent to the CNSB; 2) evaluate longer-term patterns and rates of faulting in the CNSB; and 3) compare latest Pleistocene shoreline deformation with adjacent post-highstand surface displacement measurable from fault scarps.

Results

1. Detailed studies of Holocene faulting provide evidence with which to evaluate whether the area between the northern end of the 1954 Dixie Valley earthquake and the southern end of the 1915 Pleasant Valley earthquake is a seismic gap (the Stillwater seismic gap (SSG) of Wallace, 1978; Wallace and Whitney, 1984). Our objective is to assess whether essentially continuous surface-rupturing has occurred in the CNSB previously during the Holocene, and thus provide a context in which to consider whether major gaps between historic surface ruptures in the CNSB are likely to be filled in the near future.

   Soil profile development was the primary tool used to correlate surfaces across fault scarps and to estimate surface ages. Soil profile development was quantified using indices proposed by Harden (1982); we found the maximum horizon index (MHI) to be the most consistent indicator of relative soil age. Latest Pleistocene highstand shorelines in Dixie Valley and tephra explosed in Dixie and Pleasant valleys provide some absolute dates with which to calibrate the MHI in this area. In general, soils with MHI values <0.3 are mid- to late Holocene, 0.3-0.4 are early

Holocene or latest Pleistocene, and >0.4 are late Pleistocene or older. Most mid- to late Holocene soils have MHI values <0.2, but soils dominated by sodium develop argillic horizons (natrargids) quite rapidly, resulting in somewhat higher MHI values.

Topographic profile data were collected from alluvial fault scarps and analyzed using solutions to the diffusion equation. The primary method used to obtain values for kt (diffusivity·scarp age) was the finite initial slope method of Hanks et al (1984), where the initial scarp morphology is modeled as a ramp at the angle of repose of the scarp-forming material. The value of k was considered to be ∿1 m^2/ka for scarps formed in alluvial fan deposits in this area, the value obtained for Lahontan and Bonneville shoreline scarps (Hanks et al, 1984; Hanks and Wallace, 1985; Hecker and Fonseca, unpubl. data).

Age estimates of Holocene surface ruptures in the Dixie Valley-Pleasant Valley portion of the CNSB imply that the historic pattern does not duplicate earlier Holocene patterns. Studies in central Dixie Valley, along the central and northern portions of the 1954 surface rupture, restrict prior Holcoene faulting to the interval between deposition of the Mazama and Turupah Flat ashes (6.9-1.5 ka) (Chadwick et al, 1984; Bell and Katzer, in press). Hecker (in review) estimated that the most recent prehistoric surface rupture in central Dixie Valley occurred at ∿3 ka along the northern portion of the 1954 Dixie Valley earthquake and in the southern portion of the SSG, with no definitive evidence of earlier Holocene surface ruptures. Recently completed studies indicate that surface rupture at ∿3 ka extended along at least 20 km, and possibly the entire 40 km of the SSG, although morphologic fault scarp age estimates from the northern part of the SSG are generally slightly older.

Earlier Holocene surface rupture is suggested by relations observed at two localities in the SSG. Latest Pleistocene shoreline features along Stillwater Range were determined to be vertically displaced 9 m by faulting (Thompson and Burke, 1973). Since this is about 1.5 times greater than the maximum displacement across Holocene fault scarps in the same area, it may be evidence of an earliest Holocene surface rupture. Farther north in the SSG, a fan surface estimated to be early Holocene or latest Pleistocene in age is displaced about twice as much as a mid-Holocene inset terrace surface.

The most recent prehistoric surface rupture in Pleasant Valley and the eastern Sou Hills area, along the trace of the Pearce and Tobin segments of the 1915 surface rupture, apparently occurred during the early Holocene. Morphologic analysis of composite fault scarps, after removal of 1915 scarps, suggests an age of 3-15 ka for the prior event. However, a terrace deposit incorporating Mazama ash along the Tobin segment has been displaced only by the 1915 event (Wallace, 1984). A fan surface at the northern end of the Pearce segment, interpreted to be 7-11 ka, was displaced prior to 1915 by an amount similar to the 1915 displacement (0.5 m). The southernmost major segment of the 1915 event, located along the west side of the Sou Hills, apparently did not rupture in the early Holocene. Surfaces in this area interpreted to be of early Holocene-latest Pleistocene age were not faulted prior to 1915.

The SSG remains a candidate for a large earthquake in the near future. Possible synchroneity of displacement in the SSG and farther south along the 1954 surface rupture at ∿3 ka may indicate that fault displacements in these two areas are linked. Lack of mid- to late Holocene displacement in Pleasant Valley indicates that faulting in this area is not linked on a one-to-one basis with faulting in Dixie Valley. However, possible early Holocene displacement in the SSG could have been synchronous with the most recent prehistoric movement in Pleasant Valley. The evidence gathered to date suggests that if activation of faults in N-S-trending belts is characteristic of extensional deformation in central Nevada, different combinations of faults are involved during separate intervals of activity.

2. Investigation of late Quaternary and late Cenozoic normal faulting patterns in and around the Sou Hills strongly suggest that this area has acted as a persistent barrier to fault rupture propagation. The southern termination of the 1915 Pleasant Valley earthquake is along the west side of the Sou Hills (excluding a short scarp within the Stillwater Range which may have been active in 1915 and 1954; Wallace, 1984). As discussed above, the timing of most-recent prehistoric movement is diachronous in the major basins to the north and south of the Sou Hills; age estimates for fault scarps are generally consistent with a southward termination of an early Holocene surface rupture in Pleasant Valley in the eastern Sou Hills and a northward termination of a mid- to late Holocene surface rupture in Dixie Valley along the southwestern Sou Hills.

   Vertical displacements during individual surface ruptures appear to decrease in the Sou Hills relative to areas to the north and south, and spatial patterns of fault rupture become quite complex and discontinuous. Vertical displacement of late Cenozoic, pre-extension basalts, and thicknesses of basin fill deposits, also decrease toward the Sou Hills. The sense of primary Quaternary fault displacement changes from down-to-the-west to down-to-the-east at the southern end of the Sou Hills. Analysis of mountain front landforms that reflect relative rates of uplift over the last 10^5-10^6 years indicate that uplift rates decrease along the Stillwater and Tobin Ranges where they enter the Sou Hills area. Lower long-term displacement rates, combined with evidence that individual surface ruptures have died out in the Sou Hills, suggests that this area is a barrier to propagation of fault rupture which may limit the size of individual earthquakes in this region.

References

Bell, J.W., Katzer, T.L. (in press). Surficial geology and Quaternary tectonic history of the IXL Canyon quadrangle, Nevada Bureau of Mines and Geology Map.

Chadwick, O.A., Hecker, S., Fonseca, J. (1984). A soils chronosequence at Terrace Creek: Studies of late Quaternary tectonism in Dixie Valley, Nevada, U.S. Geol. Surv., Open-File Rept. 84-90, 29 p.

Hanks, T.C., Bucknam, R.C., Lajoie, K.R., Wallace, R.E. (1984). Modification of wave-cut and faulting-controlled landforms, J. Geophys. Res. **89**, 5771-5790.

Hanks, T.C., Wallace, R.E. (1985). Morphological analysis of Lake Lahontan shoreline and beachfront fault scarps, Pershing County, Nevada, Bull. Seis. Soc. Am. **75**, 835-846.

Harden, J.W. (1982). A quantitative index of soil development from field descriptions: Examples from a chronosequence in central California, Geoderma **28**, 1-28.

Hecker, Suzanne (in review). Timing of Holocene faulting in part of a seismic belt, west-central Nevada, Bull. Seis. Soc. Am.

Thompson, G.A., Burke, D.B. (1973). Rate and direction of spreading in Dixie Valley, Basin and Range province, Nevada, Geol. Soc. Am. Bull. **84**, 627-632.

Wallace, R.E. (1978). Patterns of faulting and seismic gaps in the Great Basin Province, in Proceedings of Conference VI, Methodology for identifying seismic gaps and soon-to-break gaps, U.S. Geol. Surv., Open-File Rept. 78-943, 857-868.

Wallace, R.E. (1984). Fault scarps formed during the earthquakes of October 15, 1915, Pleasant Valley, Nevada and some tectonic implications, U.S. Geol. Surv. Prof. Paper 1274-A.

Wallace, R.E., Whitney, R.A. (1984). Late Quaternary history of the Stillwater seismic gap, Nevada, Bull. Seis. Soc. Am. **74**, 301-314.

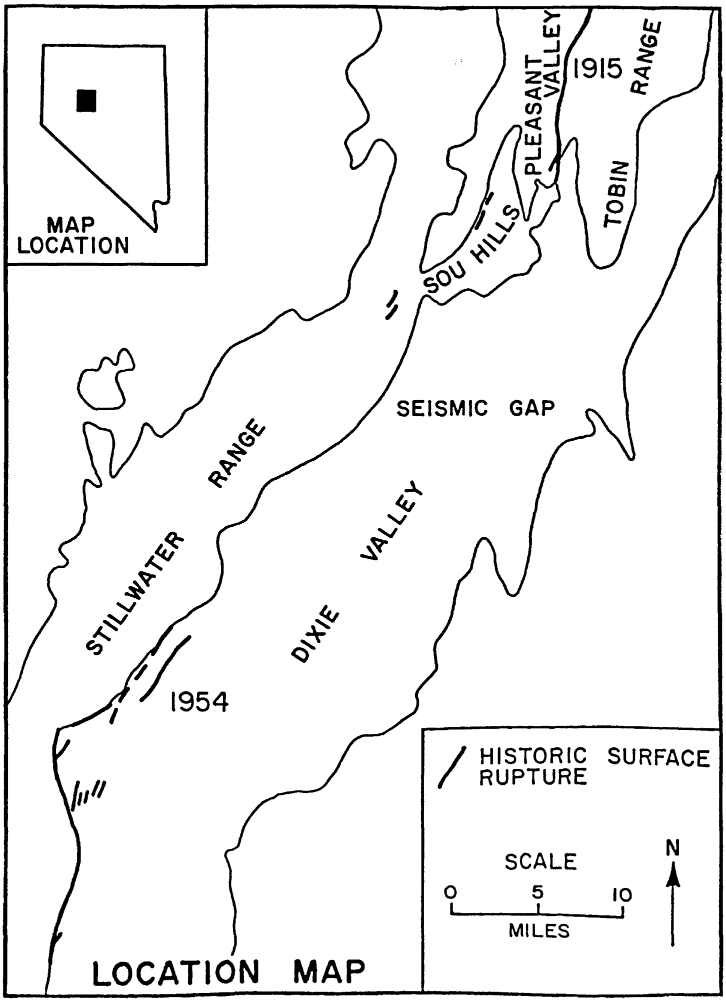

ADDITIONAL WORK TO DATE PROBABLE EARTHQUAKE DEFORMED BEDS IN KERN COUNTY, CALIFORNIA

Contract 14-08-0001-22018

D. L. Lamar and P. M. Merifield
Lamar-Merifield Geologists, Inc.
1318 Second Street, Suite 25
Santa Monica, CA 90401
Telephone: (213) 395-4528

W. E. Reed
Department of Earth and Space Sciences
University of California
Los Angeles, CA 90024

and
T. K. Rockwell
Geology Department
San Diego State University
San Diego, CA 92182

Investigations

Previous research (Lamar *et al*, 1979ab) revealed probable earthquake deformed sediments in Kern Lake, Kern County, California. To determine the times of the earthquakes samples of organic materal have been collected and submitted for carbon 14 dating under the current contract.

Results

No new results will be available until dating of the carbon 14 samples is obtained.

References

Lamar, D. L., S. G. Muir, P. M. Merifield and W. E. Reed (1979a), Possible earthquake deformed sediments in Kern Lake, Kern County, California: Geol. Soc. of Amer., Abstracts with Programs, Vol. 11, No.3, p. 88.

Lamar, D. L., S. G. Muir, P. M. Merifield and W. E. Reed (1979b), Description of earthquake deformed sediments in Kern Lake, Kern County, California: Lamar-Merifield Tech. Report 79-1, Final Tech. Report for U.S. Geol. Survey Contract 14-08-0001-16791.

COASTAL TECTONICS, WESTERN U.S.

9910-01623

Kenneth R. Lajoie

Branch of Engineering Seismology and Geology
U.S. Geological Survey
345 Middlefield Road, MS 977
Menlo Park, CA 94025
(415) 323-8111, ext. 2642

Investigations

1. Uplift and deformation of Pleistocene marine strandlines and deposits in the San Pedro area, Los Angeles County, California.

2. Holocene strandlines as recorders of paleoseismicity.

Results

1. Amino-acid analyses of fossil shells from bore-holes and surface outcrops in the Palos Verdes area indicate that marine sedimentation in the southwestern part of the Los Angeles Basin was continuous prior to about 300 ka B.P.; faunal data indicate sub-littoral deposition during this period of time. After 300 ka B.P. marine sedimentation was episodic (controlled by eustatic fluctuations); faunal data indicate littoral depositional conditions during these episodic incursions. These data indicate that this part of the basin shallowed due to sedimentation and tectonic uplift over at least the last 300 ka.

   Marine deposits younger than 200-300 ka B.P. do not appear east of the Newport-Inglewood fault zone. Existing data indicate that the 120 ka sea-level highstand did not extend across the fault nor east of the Palos Verdes Peninsula as previously believed. Consequently, the youngest identifiable Pleistocene marker across the fault is the 200-300 ka marine shell bed. Maximum vertical displacement of this marker is at least 75 m at Signal Hill.

2. Emergent Holocene strandlines are conspicuous records of paleoseismicity along many rapidly uplifting coastlines of the world. Generally, coseismic strandlines are produced and preserved only where uplift rates are sufficiently large (>1-2 m/ka) to offset the destructive effects of subsequent wave erosion. Along the West Coast of the United States these conditions are met only in three areas, all in compressional tectonic environments and two on local anticlines. As many as nine (9) emergent Holocene strandlines occur on the southern limb of the Ventura Avenue anticline in southern California where the independently derived uplift rate is about 10 m/ka. Between Shelter Cove and Cape Mendocino, uplift

rates range from 2-4 m/ka, and one (1) to nineteen (19) late Holocene strandlines occur along much of the coastline; rapid uplift in this area is related to convergence south of the Mendocino triple junction. The major difficulty in extracting histories of paleoseismicity from both of these records is that many of the strandlines are depositional and may be of storm origin. Also, only a few strandlines in each sequence are independently dated. Consequently, the uplift patterns (displacement or time predictable) cannot be determined. Data from Pleistocene strandlines along the Oregon and Washington coasts yield uplift rates from 0.0-0.3 m/ka. However, at Cape Blanco a 40-60 ka marine platform yields an uplift rate of at least 2 m/ka on an anticlinal crest. At Cape Blanco, an undated strandline at 2-4 m above sea level may represent coseismic uplift.

Reports

None.

QUATERNARY FAULT HISTORY AND EARTHQUAKE POTENTIAL OF THE HANSEL VALLEY AREA, NORTH-CENTRAL UTAH

14-08-001-21899

James McCalpin
Department of Geology
Utah State University
Logan, Utah 84322
(801) 750-1220

Investigations

Work has concentrated on detailed logging of arroyo walls along strike of the fault scarp of the 1934 M6.6 earthquake, the only historic event to cause surface rupture within the Bonneville Basin.

Results

1. Twelve faults occur in an 80-m wide deformation zone exposed in a 10-m deep gully which transects the fault. Nine stratigraphic units are exposed in the gully walls, and display increasing tectonic deformation with age (Table 1). Little Valley deposits (approx. 140-115?ka) are extensively fractured and faulted, but lack of marker beds and colluvial wedges precludes estimates of displacement or number of events. Overlying "Alpine" deposits (units 2 and 3, Table 1) are not pervasively fractured, but are offset by at least one major fault. Bonneville-cycle deposits (units 4 through 9, Table 1) are offset approximately 1.3-m by at least one, and possibly two, events.

2. Shell material for absolute dating was found only in unit 6, so "traditional" age control for faulting was poor. Therefore, bulk samples of silt-rich lacustrine sediments from units 1,2,3,6 and 8 were submitted for thermoluminescence (TL) dating to Alpha Analytic Inc. Two soup cans were augered into the arroyo walls in each unit and then sealed from moisture and light. Resulting ages were in correct stratigraphic order, and four of five matched the original age estimates based on sedimentology and ostracod faunas (Table 1). The date for unit 6 does not match traditional 14C and amino acid dates, for reasons not known. It appears that TL dating of inorganic silts can work for lacustrine sediments if the silt fraction is "zeroed" by sunlight prior to deposition, and allows dating of sediments beyond the reach of radiocarbon. Hopefully, dating may also work for other silty surficial deposits with a loessial component, such as colluvial wedges associated with fault scarps.

3. The recurrence history based on all dates appears thus: multiple events of unknown displacement from 140 ka to 66 ka, no events from 66 ka to 26 ka, one event between 26 ka and 12 ka, one event at about 12 ka, and one event in 1934 AD. Recurrence intervals vary from 40 ka to less than 12 ka, and suggest temporal clustering in the latest lake cycle.

Reports

McCalpin, James, 1985, Quaternary fault history and earthquake potential of Hansel Valley, north-central Utah: Summaries of Technical Reports, Vol. XIX, U.S. Geological Survey Open-File Report 85-22, p. 126-129.

Robison, R.M. and McCalpin, James, 1985, Evidence for recurrent Quaternary normal faulting along the trace of the 1934 Hansel Valley fault scarp, north-central Utah: Geological Society of America, Abstracts with Programs, Vol. 17, no. 4, p. 262.

McCalpin, James, 1985 Quaternary fault history and earthquake potential of Hansel Valley, north-central Utah: Summaries of Technical Reports, Vol. XX, U.S. Geological Survey Open-File Report 85-464, p. 105-108.

STRATIGRAPHY DISRUPTED BY TRACES OF THE 1934
HANSEL VALLEY FAULT SCARP AND BY OLDER PRE-HISTORIC EVENTS

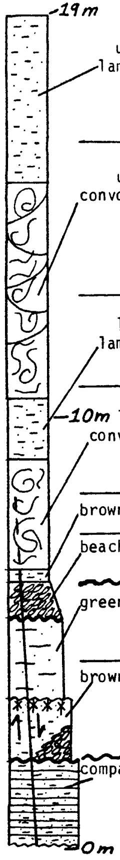

STRATIGRAPHIC UNITS	SEDIMENTOLOGY & Deformation	OSTRACODS (by Rick Forester) Species	OSTRACODS (by Rick Forester) Inferred Environment	ABSOLUTE AGES ^{14}C	ABSOLUTE AGES amino acids	ABSOLUTE AGES TL	LAKE BONNEVILLE CHRONOLOGY	Oxygen Isotope Stage
upper laminated silt 9	well laminated silt & clay	mixture of species	mixed alkaline poor & alkaline rich waters; lake regressing				Bonneville cycle-regression from Provo shoreline	1
upper convoluted silt 8	intact, rotated blocks of well laminated silt & clay, similar to unit above					*11,700± 1100 (not fully zeroed) Too old	-drop to Provo shoreline? -Bonneville flood?	2
lower laminated silt 7	alternating silt & clay laminae with 5 cm thick, rippled med-cse sand beds	"profundal assemblege"	alkaline rich water-deep lake				Bonneville cycle highstand ↑	2
lower convoluted silt 6	intensely convoluted mixture of clay, silt, sand, & floating pebbles; roll structures common			*15,450 + 650 (min.date)	*21,000 prelim	(not fully zeroed) Too old *40,100± 3200	deepening water ↑	2
brown lam. silt 5	well laminated silt		alkaline poor water, low-stand lake lake level rising					2
beach gravel 4	cross-bedded, well sorted medium pebble gravel						Bonneville cycle transgression	2
MAJOR UNCONFORMITY								
green silt 3	green silt with some clay, poorly laminated		alkaline poor water, low-stand lake			*67,000 ± 3800 (best date)	"Alpine" ↑ (early Wisconsin) cycle	4
brown silt 2	brown massive silt, gypsum crystals at top, laminations better defined toward bottom; locally overlies lacustrine bar gravels	Heterocypris n.sp. C. rawsonii Listaplini I. bradyii	alkaline poor water marginal lacustrine groundwater environment			(some trap saturation) *65,900 ± 4200	↓	4
MAJOR UNCONFORMITY								
compact silt	well laminated silt & clay, very compact; intensely fractured w/ steeply dipping small displacement joints	C.Sp. caudata type L. Sappaersis L. ceriotuberosa L. staplini C. beacorensis	alkaline rich water, deep lake			*115,200 ± 17,500	Little Valley Cycle	6?

STUDY OF SEISMIC ACTIVITY BY SELECTIVE TRENCHING ALONG THE SAN JACINTO FAULT ZONE, SOUTHERN CALIFORNIA

Contract 14-08-0001-22033

P. M. Merifield,
D. L. Lamar
Lamar-Merifield Geologists, Inc.
1318 Second Street, Suite 25
Santa Monica, CA 90401
Telephone: (213) 395-4528

and

T. K. Rockwell
Geology Department
San Diego State University
San Diego, CA 92182

Investigations

Mapping of Quaternary deposits along a 10-km segment of the fault zone between Hog Lake and Highway 371 north of Anza has been initiated. Soil chronologic studies by a graduate student at San Diego State University are also underway. These studies will provide a framework for selecting sites for trenching.

Results

A radiocarbon date has been obtained from offset blocked drainage deposits. The sample was dated by the University of Arizona (U. of A. sample No. A-4231); the sample yielded a radiocarbon age before present, carbon-13 corrected but not dendrochronologically corrected, of 9,470 ± 120. The deposits are apparently offset a minimum of 85-90 m, yielding a minimum Holocene slip rate of about 9 mm/yr.

Late Quaternary Tectonic Rates
Agua Blanca and Borderland Faults

Contract No. 14-08-0001-22012

Thomas Rockwell
Department of Geological Sciences
San Diego State University
San Diego, California 92182

Investigations

Detailed mapping of active fault traces and Quaternary deposits coupled with trenching studies at selected ponded drainages and sags to provide information on the slip rates, recurrence intervals, and characteristic earthquakes for the principal strands of the Agua Blanca fault.

Results

Studies have focused on four sections of the Agua Blanca fault: 1) the eastern end in Trinidad and San Matias valleys and its interaction with the San Pedro Martir fault; 2) Agua Blanca Valley where the fault is well expressed and displays a relatively simple geometry; 3) along Punta Banda ridge inland from the coast where the northern trace is well expressed; and 4) on Punta Banda itself where datable marine terraces are deformed.

The eastern end of the fault is structurally complex in its interaction with the San Pedro Martir fault: both the Agua Blanca and San Pedro Martir faults die out in activity near their common intersection near San Matias Pass and slip is apparently transferred via extensional oblique faulting in San Matias and Trinidad valleys which owe their origin to this slip transfer. Consequently, the rate of slip on the Agua Blanca fault, based on relatively minor offsets of late Quaternary deposits, is very low in eastern San Matias Valley (<< 1 mm/yr) but increases in rate in western San Matias Valley and Trinidad Valley to no more than 1 or 2 mm/yr (soil stratigraphic and radiocarbon age assessments pending).

In Agua Blanca Valley, the slip rate is constrained by offset latest Pleistocene alluvial fans (age estimate based on the strength of soil development) to no more than a few mm/yr. This estimate is preliminary but appears to preclude a large late Quaternary slip rate on this fault. Ongoing trenching studies indicate Holocene activity along this section of the fault but have not yet yielded the timing of the last event.

Similarly, at Punta Banda ridge southeast of Maneadero, the fault offsets alluvial fans and stream terraces of late Pleistocene and Holocene age (based on soil age determinations). Trenching has exposed the fault in Holocene deposits but again, the work is ongoing.

On Punta Banda itself, marine terraces are well exposed and four of the platforms are fossiliferous. The terraces have been surveyed with respect to elevation and indicate that: 1) Punta Banda is being tilted southward; 2) there are several active faults which appear to be synthetic to the main Agua Blanca fault and which displace the lowest terrace on the north side with up to 8 m of vertical separation (strike separation presently unknown); and 3) the Maximinos strand south of Punta Banda dies out as it comes onshore. The fossiliferous terraces have been collected and the fossils are being indentified and dated (coral was identified on two of the terraces and will hopefully provide absolute age control). Study of the activity of the Maximinos strand south of Punta Banda at the coast indicates, along with the deformation at Punta Banda itself, that some slip is being transfered across Punta Banda from the northern strand to the Maximinos strand. Punta Banda, then, appears to be, in part, a large pressure ridge between the Main and Maximinos strands of the fault which trend north to become the San Diego Trough and Coronado Banks fault zones offshore of San Diego.

Geochronology-^{14}C

9570-00374

Meyer Rubin
U.S. Geological Survey, National Center, MS 971
Reston, VA 22092
(703) 860-6114
8+928-6114

Investigations

The Radiocarbon Laboratory has been actively investigating the Yakataga Seismic Gap of Alaska with personnel of the Alaskan Branch (George Plafker). Dating of carbon samples from marine terraces in this very critical area reveal a rather short recurrence interval and a deficit in uplift compared to past earthquake positive disruptions. The fact that the fault controlling this area's tectonics has been relieved on both sides in the recent past emphasizes the possibility that a very large earthquake can occur in this area before the end of the century. Attendant tsunamis can devastate coastal cities in California, Mexico, and Alaska. Of course, this possibility needs further investigation before definite predictions can be made.

Results

Publications on this study are being prepared (Middleton Island Uplift History; Yakataga - Icy Cape Terrace Study).

The Charleston Earthquake Study continues to occupy a considerable percentage of the laboratory's effort, both in field work collecting samples and in dating them. Papers dealing with past earthquakes in the region have been published and others are in preparation. Recurrence intervals for disruptive earthquakes have been computed and predictions conservatively estimated. It is assumed that the coming report period will involve many more samples from the Charleston area.

Reports

Obermeier, Stephen, F., Gohn, Gregory S., Weems, Robert E., Gelinas, Robert L., and Rubin, Meyer, 1985, Geologic Evidence for Recurrent Moderate to Large Earthquakes Near Charleston, South Carolina: Science, vol. 227, pp. 408-411, 25 January 1985.

Weems, Robert E., Obermeier, Stephen F., Pavich, Milan J., Gohn, Gregory S., Rubin, Meyer, and Phipps, Richard L., 1986, Evidence for Prehistoric Holocene Earthquakes in the Charleston Region, South Carolina, Including an Earthquake at about 800 A.D.: _in_ Third U.S. National Conference on Earthquake Engineering, August 24-28, 1985, Charleston, South Carolina.

In addition, the laboratory is, in effect, on retainer to measure earthquake related samples immediately upon receipt.

Geochronology--Menlo Park

9570-00388

Robert Fleck
U.S. Geological Survey, MS 937
345 Middlefield Road
Menlo Park, CA 94025
(415) 323-2232
8+467-2232

Investigations

The Geochronology (Menlo Park) Project maintains and operates potassium-argon and rubidium-strontium laboratories that are used by guest scientists as well as by the Branch of Isotope Geology. Maintenance and operating supplies are funded by the project for all users of the laboratories. The project also produces age determinations of samples for Survey projects whose isotopic needs do not warrant collaborative involvement of Isotope Branch personnel or guest use of the facilities. During FY85, in addition to maintaining the above-mentioned capacity, funding from the Earthquake Hazards program supported age determinations of basalts for Dave Harwood.

Active Tectonics of the San Andreas Fault System in Southern California

Contract # 14-08-0001-22011

Kerry E. Sieh
Caltech 170-25
Pasadena, CA 91125
(818) 356-6115

During the past six months progress on this contract has proceeded along several fronts.

Carol Prentice is just completing her first summer's field work along the northern segment of the San Andreas fault, which last ruptured in 1906. She is attempting to determine long-term slip rates as well as the dates and characteristics of prehistoric large earthquakes northwest of San Francisco. In the Point Arena area wave-cut platforms and shoreline angles are offset, but not in any immediately obvious fashion. However, Carol is making progress in her mapping of the late Quaternary marine and fluvial deposits in this region. She has recovered detrital wood that may well enable her to date a thick series of fluvial gravels overlying the lowest wave-cut platform. She may also be able to determine the lateral offset of this wave-cut platform and associated seacliff.

At Fort Ross, farther southeast along the 1906 rupture, she has discovered one of the fences offset during the 1906 earthquake. Resurveying of this fence, which was surveyed shortly after the earthquake, will show whether or not afterslip has occurred along this part of the 1906 rupture. Our initial impression is that it has not. Nearby, Carol has recognized the toe of a landslide separated several hundred meters from its source. We recently collected charcoal from within the toe of this landslide. Hopefully this will be within the range of radiocarbon dating, and she will be able to determine a long-term slip rate for this segment of the San Andreas fault.

In addition, Carol is now engaged in assessing the potential of one site near Manchester for trenching studies. We are hopeful that she has found a site where dating and characterization of the one or more earthquakes prior to 1906 can be carried out.

Frank Webb has continued to analyze data he has collected during the spring and winter months in the Imperial Valley. He has found evidence for at least one and one-half meters of vertical deformation of the most recent (300 year old) shoreline of Lake Cahuilla, which filled large parts of the Coachella, Imperial, and Mexicali Valleys. He is currently investigating the possibility that the deformation is an isostatic response to the drying up of Lake Cahuilla rather than a product of seismotectonic deformation.

I have not collected any more data from the Indio site since my report of June.

Marcus Bursik has just completed his first summer of field work in the Mono Basin-Long Valley area, with partial support under this contract. He is investigating the relationship between tectonic faulting along the Sierra Nevada rangefront and volcanic events of the past several thousand years. The faulting pattern in the area is almost surely telling us something about the subsurface geometry of magma bodies in that area.

Steve Salyards continues his investigations into the possibility of using paleomagnetic secular variations to date otherwise undatable sediments in southern California. His analyses of several fine-grained beds at Pallett Creek give tight statistical clusters, but the orientations are far from the expected position on the secular variation curve derived from sites in Arizona. He has sampled and analyzed samples from liquefied beds at Tom Rockwell's Elsinore fault site, with the hope that various liquefaction layers will be datable by this technique and will fit on the secular variation curve. He has sampled fine sands from my Indio site, and these samples appear to fall about where they ought on the secular variation curve. In an attempt to better refine the secular variation curve for southern California, Steve has collected samples from pyroclastic flow and airfall beds of the latest large eruption in the Mono Lake area. This eruption is well constrained to dates between 1325 and 1365 A.D.

Pat Williams has continued office work related to his studies along the southern San Andreas fault. He recently received radiocarbon analyses which indicated that faulted foreset and bottomset beds in the Salt Creek drainage are only about 1,000 years old. These are encouraging results, because they indicate that the Salt Creek, near the southern end of San Andreas fault, has sediments comparable in age to those at the Indio site. Hence we may be able to compare seismic events at two sites along the southern San Andreas fault.

Very Precise Dating of Earthquakes at Pallett Creek and Their Interpretations

Contract # 14-08-0001-22026

Kerry E. Sieh
Caltech 170-25
Pasadena, CA 91125
(818) 356-6115

Analysis is nearly complete on the first suite of samples collected from Pallett Creek for very precise radiocarbon dating in the laboratory of Minze Stuiver at the University of Washington. These samples were collected in February 1985. In September 1985, the second suite of samples was collected from Pallett Creek; these are now in Stuiver's lab for processing and analysis. Once the very precise dates from these first samples are available, we can construct a plan for sample collection during the second year of the contract.

We remain hopeful that very precise dating of these samples will yield earthquake dates with uncertainties of only a couple of decades rather than a century. If we can achieve an increase of this magnitude in the precision of the dates, we will probably be able to recognize any patterns of recurrence in the past ten large earthquakes recorded at Pallett Creek.

Recognition of Individual Earthquakes on Thrust Faults (New Zealand)

14-08-0001-21984

Robert S. Yeats
Department of Geology
Oregon State University
Corvallis, Oregon 97331-5506
(503) 754-2484

Kelvin R. Berryman
Earth Deformation Section
New Zealand Geological Survey, D.S.I.R.
P.O. Box 30368
Lower Hutt, New Zealand
(644) 699-059

Investigations

1. Field work on the Dunstan Fault in central Otago by Ian Madin (OSU) and Sarah Beanland (NZGS) was completed in May, 1985, concentrating on the interference zone between NE-trending faults and NW-trending faults at the north end of the Manuherikia Basin.

2. A new tectonic map of central Otago with a Landsat base was prepared by R. S. Yeats and is now being reviewed in New Zealand and the U.S.A. (Fig. 2 of this report).

3. Sarah A. Barrow-Hurlbert (OSU) determined that there have been at least five faulting events on the Nevis reverse fault at Drummond Creek since about 23,000 years ago; this locality is described briefly below.

4. Barrow-Hurlbert also conducted a scarp-degradation study in the upper Nevis basin, central Otago; one of the first applications of this technique in New Zealand. This will be discussed in the next report summary after internal review at OSU is completed.

Results

1. Our interpretation that the NE-trending faults of central Otago (Figs. 1 and 2) were active more recently than the NW-trending faults came apart when Ian Madin discovered very fresh scarps on the NNW-trending Blue Lake fault adjacent to The Big Flat Basin (Fig. 2). The interference zone between NE- and NW-trending faults is relatively complicated, and additional NW-trending faults are found SW of the Blue Lake fault in the Dunstan Uplift and Manuherikia Basin.

2. As reported by Barrow-Hurlbert, the Upper Nevis Basin (located on Fig. 1) is covered in part by coalescing alluvial fans (Qf_5) deposited by streams flowing from ranges on both sides of the basin and now found 2-3 m above the present-day floodplain of the Nevis River at their distal edges and up to 7.5 m above floodplain deposits away from the Nevis River. On the basis of its degree of degradation, the Qf_5 surface is correlated to the Hawea glacial advance, which is older than a soil with a radiocarbon date of 20,500 years (S. Beanland, pers. comm., 1984). An age of 22,000-23,000 years is adopted here. This age is in general agreement with the ages of terrace scarps separating the older surfaces (Qf_3, Qf_4) from the Qf_5 surface as based on scarp degradation estimates by Barrow-Hurlbert (1985). At the north end of the Nevis Basin, a peat bed with a radiocarbon date of 9670 ± 130 years is buried 2.35 m beneath gravels redeposited from an overlying terrace. The peat is 80 cm above the floodplain of a tributary stream that grades to the Nevis River, indicating that the modern floodplain surface is younger than the peat.

On the south bank of Drummond Creek, the Qf_5 surface has been incised 1-3 m, and three degradational terraces are preserved (Highest, Middle, and Lowest Degraded Qf_5 surfaces in Figures 3 and 4). The Qf_5 surface and all three degradational surfaces are cut by the Nevis reverse fault, but the modern floodplain of Drummond Creek is not cut by the fault. A bulldozer trench (DC5) cuts the Highest Degraded Qf_5 surface and the main Qf_5 surface.

In the trench, the base of the Qf_5 fan deposits is offset 2.5 m, which is 0.9 m more than the offset of the Qf_5 surface itself. This is interpreted to represent at least one faulting event during the time of Qf_5 fan deposition, prior to faulting event 1 as shown on Fig. 4. Faulting event 1 uplifted the northwest side of the Qf_5 surface such that intrafan Stream A cut into this surface while seeking grade with the new fan slope (Panels 1 and 2, Figure 4). Another faulting event uplifted the Qf_5 and Highest Degraded Qf_5 surfaces (Panel 3, Figure 4), followed by a period of downcutting (Stream B) to form the Middle Degraded Qf_5 surface (Panel 4, Figure 4). Still another movement on the fault (Panel 5, Fig. 4) uplifted all of the surfaces and caused another period of downcutting by Stream C (ancestral Drummond Creek) that produced the Lowest Degraded Qf_5 surface and left only a remnant of the Highest Degraded Qf_5 surfacs on the upthrown side of the fault (Panel 6, Fig. 4). The most recent faulting event cut the Lowest Degraded Qf_5 surface and all older surfaces (Panel 7, Fig. 4). Subsequently, Drummond Creek has cut downward below the Lowest Degraded Surface.

In summary, five events are identified at the DC-5 locality since the beginning of deposition of the Qf_5 fan about

23,000 years ago. Each event had an average of 0.3 to 0.5 m of vertical offset, as based on (1) 0.3 m offset of the Lowest Degraded Qf_5 surface and (2) 2.5 m offset of the base of the Qf_5 fan deposit as measured in trench DC-5, assuming that one event occurred during the deposition of the fan and four events occurred after the fan was deposited.

Report

Barrow-Hurlbert, S. A., 1985, Geology and neotectonics of the Upper Nevis Basin, South Island, New Zealand: Oregon State University MS thesis, 161 p.

Yeats, R. S., 1985, Flexural-slip faulting in Grey-Inangahua Depression, South Island: Field guide to Giles Creek and Blackball scarps: New Zealand Geological Survey Report EDS 99, 19 p.

Yeats, R. S., in review, Tectonic map of central Otago based in Landsat: To be submitted to New Zealand Journal of Geology and Geophysics.

Yeats, R. S. and Berryman, K. R., in review, Northern South Island, New Zealand and Transverse Ranges, California - A tectonic comparison: To be submitted to Tectonics.

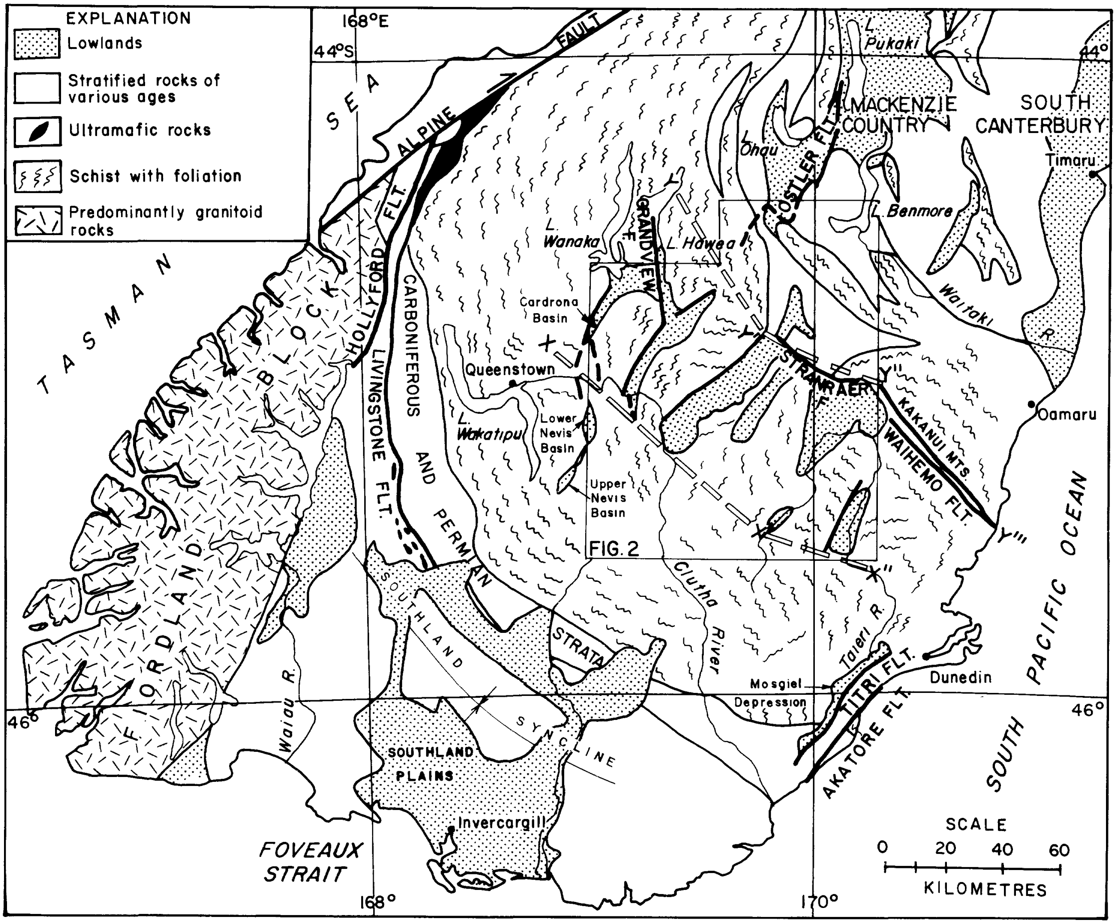

Figure 1. Tectonic map of southern South Island, from Yeats (in review). Lines XX'X", YY'Y"Y''', and the Waitaki River are boundaries of structural subprovinces 40 to 60 km wide, whereas individual ranges and basins in central Otago are 5 to 20 km wide.

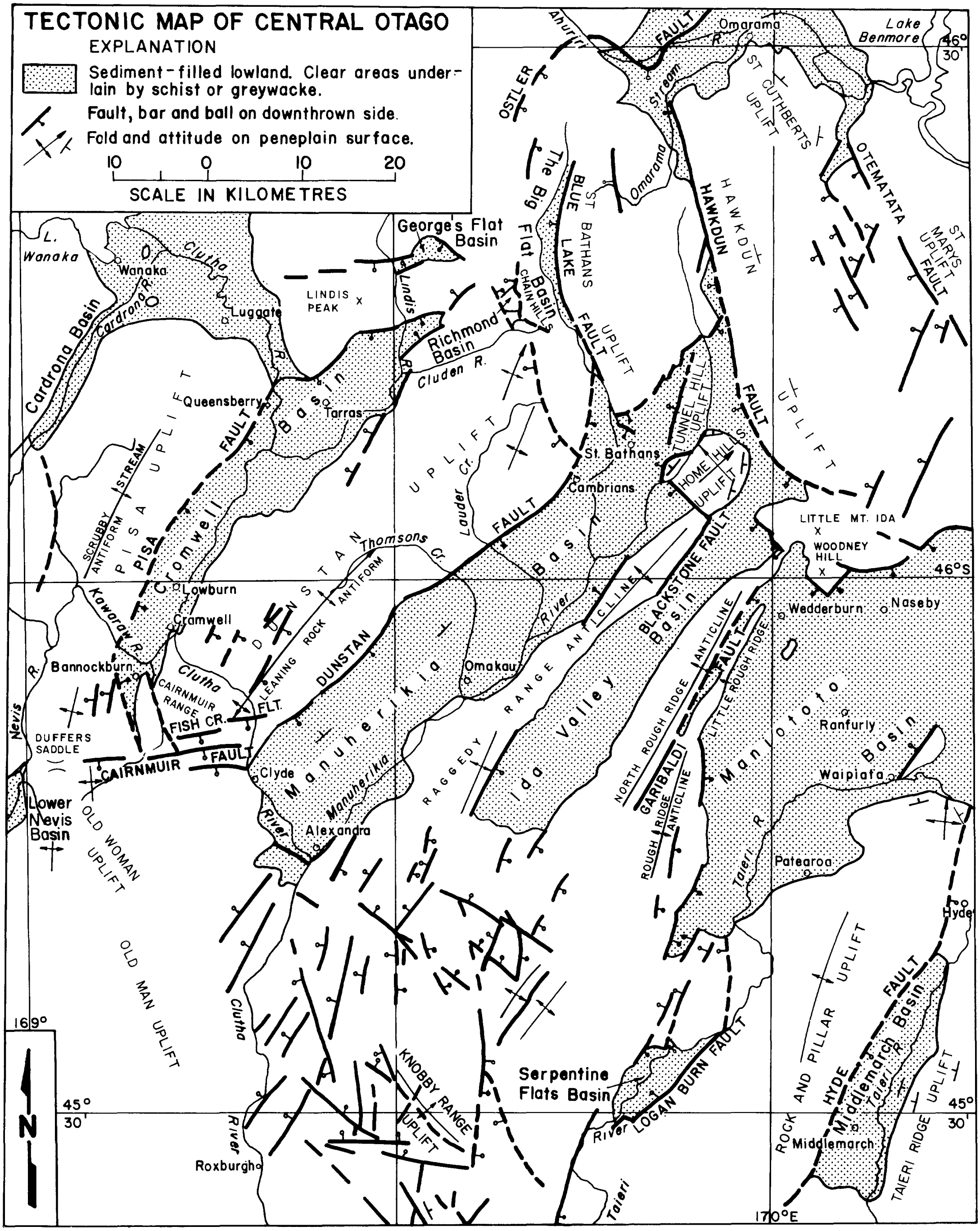

Figure 2. Tectonic map of Central Otago based on Landsat, from Yeats (in review). For location, see Figure 1.

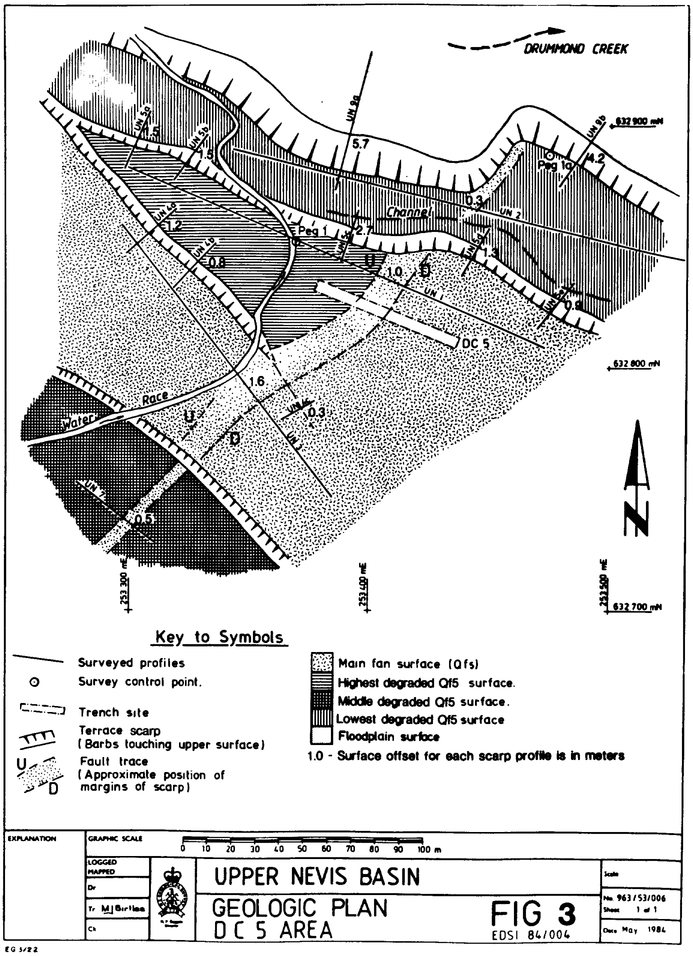

Figure 3. Map of Nevis fault in vicinity of Drummond Creek and Trench DC5, from Barrow-Hurlbert (1985).

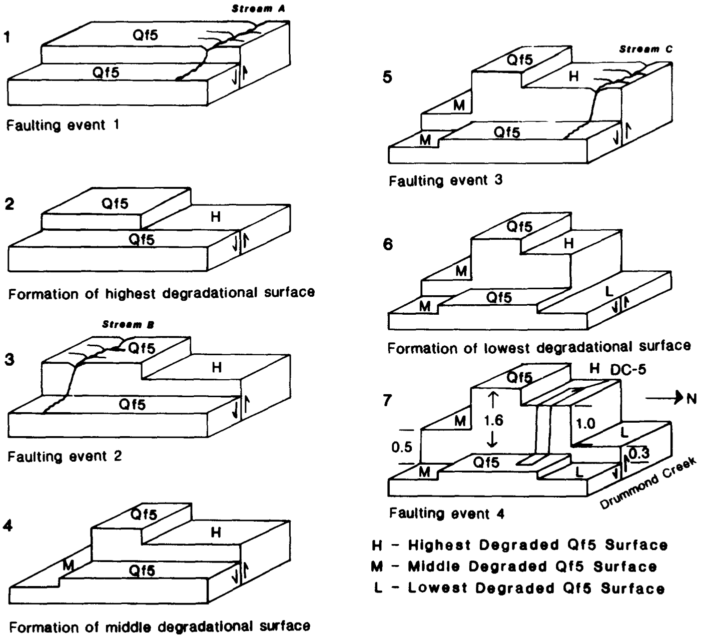

Faulting event 1

Formation of highest degradational surface

Faulting event 2

Formation of middle degradational surface

Faulting event 3

Formation of lowest degradational surface

Faulting event 4

Figure 4. Block diagrams showing sequence of faulting and degradational events on the Nevis fault producing landforms observed at Drummond Creek and Trench DC-5, from Barrow-Hurlbert (1985).

EVALUATION OF ACTIVITY OF THE SAN GABRIEL FAULT ZONE, LOS ANGELES AND VENTURA COUNTIES, CALIFORNIA

14-08-0001-21928

F.H. Weber, Jr.
Department of Conservation
Division of Mines and Geology
107 South Broadway, Room 1065
Los Angeles, CA 90012
(213) 620-3560

Investigations

This project was planned originally to consist of evaluation of the latest Quaternary activity of the San Gabriel fault principally by trenching and possibly other types of mechanical excavation (such as bulldozing). A modified plan additionally included emphasis on detailed site evaluation of several localities northwest of Saugus by very detailed field geologic mapping (Figure 1, Areas 1 and 2). The modified plan also included reconnaissance mapping of geomorphic features of the eastern portion of the San Gabriel fault and detailed investigation of the fault where it splits into northern and southern branches north of Pasadena (with Michael Wood) (Figure 1, Areas 3 and 4, respectively). Because of problems involving technical adminstrative procedures of the state, we have so far been unable to do the trenching.

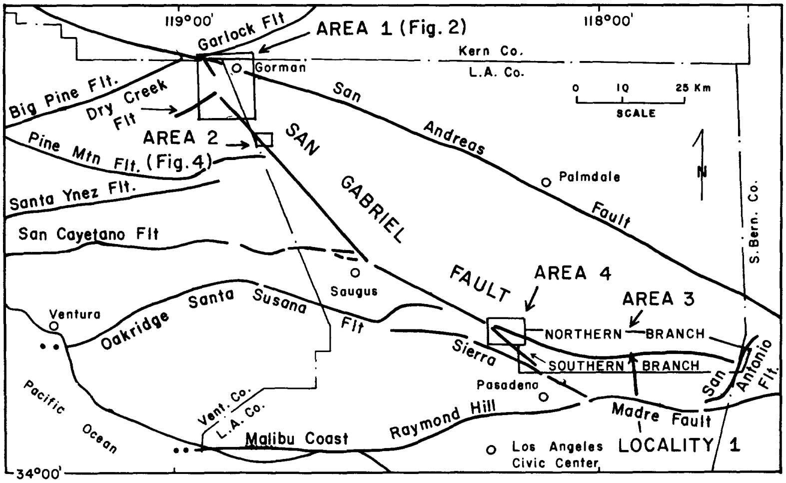

Figure 1. Fault map of a part of southern California showing the San Gabriel fault and areas along it discussed in this report. Area 1, northwestern terminus of the fault and vicinity; Area 2, Beartrap Canyon; Area 3, eastern portion of the fault; and Area 4, north of Pasadena where the fault splits into northern and southern branches.

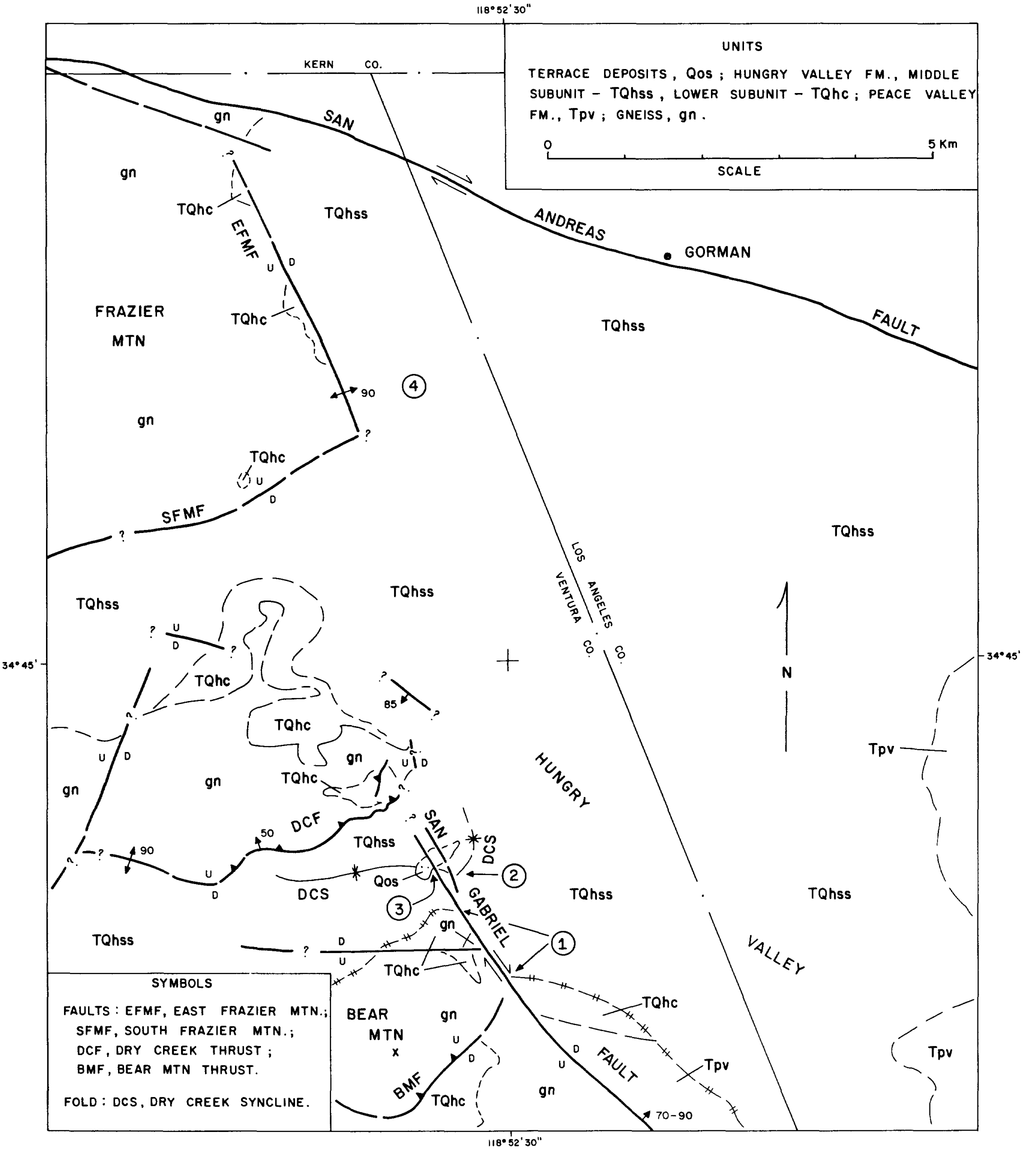

Figure 2. Geologic outline map of the Gorman-Hungry Valley-Bear Mountain area, California, showing the northwestern terminus of the San Gabriel fault and related structural elements. Map is highly simplified from major parts of Plates 1A and 2A of Weber (1985). Localities shown are discussed herein.

Results

1. Detailed mapping of the area that includes the northwestern terminus of the San Gabriel fault shows that the very steeply dipping fault is not overlapped by the Pliocene Hungry Valley Formation as depicted in previous studies (Crowell et al, 1982; other reports). The mapping shows, instead (Figure 2), that gently north-dipping beds of stratigraphically successive subunits TQhc and TQhss of the nonmarine Hungry Valley Formation are separated right laterally along the fault nearly 1.2 km (Figure 2, Locality 1). The older subunit, TQhc, is much darker than the commonly white TQhss, and each subunit is characterized by a distinctive assemblage of clasts. If the vertical component of displacement of the contact between the two subunits is about 100 m (downward on the east), then about 500 m of the nearly 1.2 km of separation consists of right slip. In addition, the mapping shows that the axial trace of the Pleistocene Dry Creek syncline, developed within beds of TQhc and TQhss, is offset right laterally 125-250 m (350m if the effects of drag are discounted) (Figure 2, Locality 2). Further, the base of very latest Pleistocene terrace deposits, about 0.5 km south of the apparent terminus of the fault, is offset 1 m downward relatively on the east, as seen in a small excavation made by hand (Figure 2, Locality 3; Figure 3). Evidence has not been found during the mapping that the San Gabriel fault once extended to the San Andreas fault, as hypothesized by Crowell (1982; other reports), unless the very steeply dipping east Frazier Mountain fault (Figure 2, EFMF, Locality 4) can be determined to have been connected to the San Gabriel fault prior to deposition of the Hungry Valley Formation. At the present, the northwesternmost segment of the San Gabriel fault appears to be part of an ongoing dynamic tectonic environment in the Frazier Park - Gorman region that is dominated by the San Andreas fault.

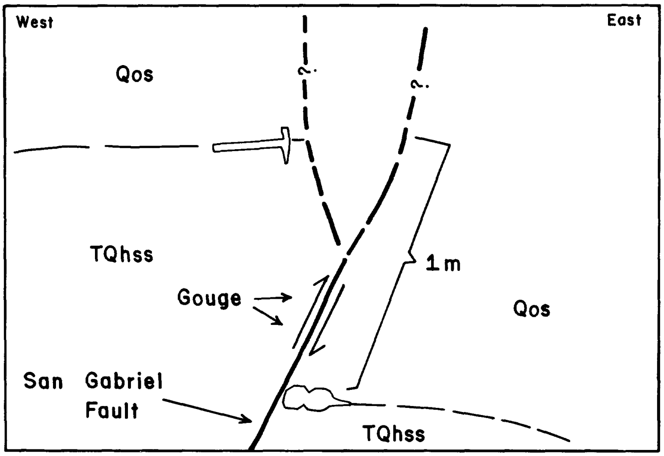

Figure 3. Photo overlay showing terrace deposits (Qos) offset downward 1m relatively on the east side of the principal trace of the San Gabriel fault just south of its apparent northwestern terminus (Figure 2, Locality 3). (Additional unit, TQhss, middle subunit of Hungry Valley Formation; outline of hammer and Brunton compass are for scale.)

2. A second place where upper Pleistocene deposits can be shown to be displaced along the northwestern portion of the San Gabriel fault zone is in Beartrap Canyon, about 13 km southeast of the northwestern terminus of the fault (Figure 4). There, a large landslide of probable late Pleistocene age, derived from granitic rocks and gneiss, extends eastward into an apparent graben formed between faults of the zone that is well-expressed in a bedrock wall about 8 km to the northwest, just northwest of Hardluck campground. The base of the landslide can be observed on the north side of Beartrap Canyon to overlie alluvium about 7-8 m above the bottom of the canyon (Figure 4, Locality 1). Possible scarp-like features on the surface of the landslide suggest that the graben may have continued to develop after occurrence of the landslide (Figure 4, Locality 2). The principal fault segment of the San Gabriel fault zone is exposed in the south wall of Beartrap Canyon (Figure 4, Locality 3). There, the fault separates very coarse landslide breccia on the east from finer breccia on the west. The locality is marked by heavy vegetation growing in the canyon bottom. The other, lesser fault (Figure 4, Locality 4) is also exposed on the south wall of the canyon. There is no evidence in the exposures in the canyon of strike slip occurring along these faults. Beartrap Canyon, however, appears to be deflected across the San Gabriel fault zone in such a way so as to suggest right slip along the zone during late Pleistocene time.

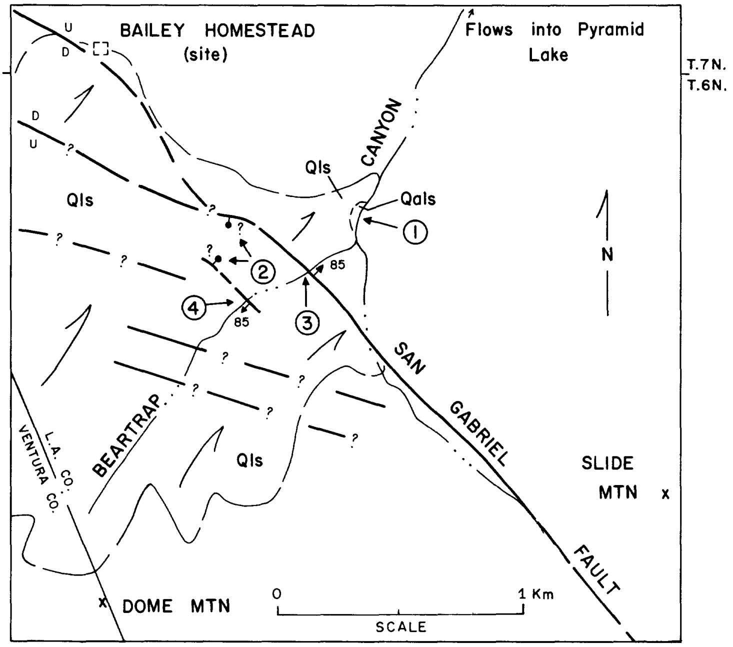

Figure 4. Geologic outline map along the San Gabriel fault zone in the Beartrap Canyon area, west of Pyramid Lake, California. Simplified from a part of Plate 3 of Weber (1985). Geologic units shown: Qls, landslide breccia, arrows show direction of slide; Qals, alluvium underlying landslide breccia. Localities shown are discussed herein.

3. Study of color aerial photographs discloses apparently youthful, north-facing scarps along the eastern part of the San Gabriel fault zone in the vicinity of Cogswell Dam, of the Los Angeles County Flood Control District, in the West Fork of San Gabriel Canyon (Figure 1, Area 3, Locality 1). These features have not yet been checked on the ground. (The photographs are part of the coverage of the Angeles National Forest taken for the United States Forest Service in 1969.)

References Cited

Crowell, J.C., 1982, The tectonics of Ridge Basin, southern California, in Crowell, J.C., and Link, M.H., eds., 1982, Geologic history of Ridge Basin, Southern California: Pacific Section, Society of Economic Paleontologists and Mineralogists, Los Angeles, California, p. 25-41.

Crowell, J. C., et al, 1982, Geologic map of Ridge Basin, southern California, in Crowell, J.C., and Link, M.H., eds., 1982, Geologic history of Ridge Basin: Pacific Section, Society of Economic Paleontologists and Mineralogists, Los Angeles, California.

Weber, F.H., Jr., 1985 (in press), Geology of selected areas along the San Gabriel fault from Saugus northwest to the San Andreas fault, and reinterpretation of slip history, Los Angeles, Kern, and Ventura counties, California: California Division of Mines and Geology Open-File Report.

Reports

Findings of the study have been utilized in preparation of the following reports:

Weber, F.H., Jr., 1985 (in press), Geology of selected areas along the San Gabriel fault from Saugus northwest to the San Andreas fault, and reinterpretation of slip history, Los Angeles, Kern, and Ventura counties, California: California Division of Mines and Geology Open-File Report.

Weber, F.H., Jr., 1985 (in press), New interpretation of geologic relationships involving the northwesternmost San Gabriel fault and the San Andreas fault, Kern, Los Angeles, and Ventura counties, California: California Geology.

The writer wishes to thank William A. Fraser, of the California Department of Water Resources, for arranging a trip by boat over Pyamid Lake in order to investigate faults exposed in Beartrap Canyon. Illustrations were drafted by Robin I. Weber. Word processing was done by Venice Huffman. The report was reviewed by Cliffton H. Gray, Jr. and Allan G. Barrows, co-principal investigator.

Analysis of Central California Network Data for Earthquake Prediction

U.S.G.S Contract 14-08-0001-A0036

Principal Investigator: Keiiti Aki 213-743-3510

Dept of Geological Sciences
University of Southern California
Los Angeles, CA 90089-0741

The goal of this study is to evaluate the validity of coda Q precursor using the USGS earthquake data archiving and processing system.

The decay rate of local earthquake coda has been shown to be characteristic to the area in which the epicenter and station are located (Aki (1969), Aki and Chouet (1975) and Rautian and Khaluturin (1978)), and was interpreted in terms of the attenuation property of S waves in the lithosphere under the area (Aki (1980)). The Q of S waves inferred from coda waves is called "coda Q".

Recently, several published and unpublished papers reported temporal changes in coda Q prior to the occurrence of an earthquake or volcanic eruption. In all these cases, the coda Q was anomalously low before the occurrence of earthquake or volcanic eruption.

In order to evaluate the validity of the coda Q precursor for California earthquakes, we initiated a systematic and comprehensive study of coda Q using the USGS Earthquake Data Archiving system developed by W.H.K. Lee et al (1983).

Figure 1 shows a schematic diagram of data processing for estimating coda Q. The left half of the diagram shows the data acquisition of digital waveforms and associated data from an online system operated at the U.S. Geological Survey, Menlo Park. It is part of the CUSP system originally developed by Carl Johnson and later modified for use at Menlo Park (Johnson and Stewart, 1985). A similar online system is used at the University of Nevada, Reno. After selecting events from the data tapes, we carried out further processing at the Stanford Linear Accelerator Center using an IBM 3081-K mainframe computer. As shown in the right-hand side of Figure 1, coda Q estimates are obtained from a step-by-step computational procedure following the concept of file-oriented processing. Each processing step creates documented output file(s) which are in turn used as input file(s) in the next step. We adopted this scheme of modular data processing because of the ease of implementation on computers.

We chose the Long Valley region as the first site for our coda Q study because of the Round Valley earthquake (M-5.7) of November 23, 1984. The seismic stations operated by the University of Nevada and the U.S. Geological Survey in the Long Valley region are shown in Figure 2. To study the spatial-temporal behavior of coda Q prior to the Round Valley earthquake, we selected 2 sub-areas for comparison as shown in Figure 2. Box A is a rectangular area (about 20 km by 25 km) which includes the aftershock area of the Round Valley earthquake. Because of a lack of magnitude 2 earthquakes in the aftershock area during the 2 months preceeding the Round Valley earthquake, Box A was chosen to include several earthquakes which occurred nearby during that period. Box B is a rectangular area of size similar to Box A, but is located to the northwest of the aftershock area and just south of the Long Valley caldera.

The temporal behavior of coda Q for earthquakes in the aftershock area (Box A of Figure 2) is shown in the left-hand side of Figure 3. The average value and standard error of coda Q^{-1} obtained for each earthquake is plotted against the time of occurrence of the earthquake. The horizontal lines represent the mean of the coda Q^{-1} averages for the entire period and the dashed lines represent one standard deviation about the mean. The upper and lower plots in Figure 3 correspond to the sampling of the coda waves over two different time windows (measured from the earthquake origin time) of 20 to 45 sec, and 30 to 60 sec, respectively.

We note that the coda Q^{-1} for the Box A (aftershock area) showed an anomalously high value about 150 days before the main shock and also a greater scatter than the coda Q^{-1} for the Box B. This result is consistent with the idea that the source region of the Round Valley earthquake is more fractured and thus attenuate and scatter coda waves more effectively.

During a recent visit to China and Japan, the P.I. was told about new cases of precursory coda Q^{-1} change for the Misasa earthquake, the western Nagano earthquake, and the Luquan earthquake. The reality of change was convincing, but the pattern was varied. Further work is needed to understand and validate this promising precursor.

References

Aki, K., Analysis of the seismic coda of local earthquakes as scattered waves, J. Geophys. Res., 74, 615-631, 1969.

Aki, K., Scattering and attenuation of shear waves in the lithosphere, J. Geophys. Res., 85, 6496-6504, 1980.

Aki, K., and B. Chouet, Origin of coda waves: source, attenuation and scattering effects, J. Geophys. Res., 80, 3322-3342, 1975.

Johnson, P., and W.S. Stewart, Caltech-USGS Seismic Processing System (CUSP): use documentation, U.S. Geol. Surv. Open-file Report, in preparation, 1985.

Lee, W.H.K., D.L. Scharre, and G.R. Crane, A computer-based system for organizing earthquake related date, U.S. Geol. Survey Open-file Report 83-518, 28 pp, 1983.

Rautian, T.G., and V.I. Khalturin, The use of the coda for determination of the earthquake source spectrum, Bull. Seism. Soc., Am., 68, 923-948, 1978.

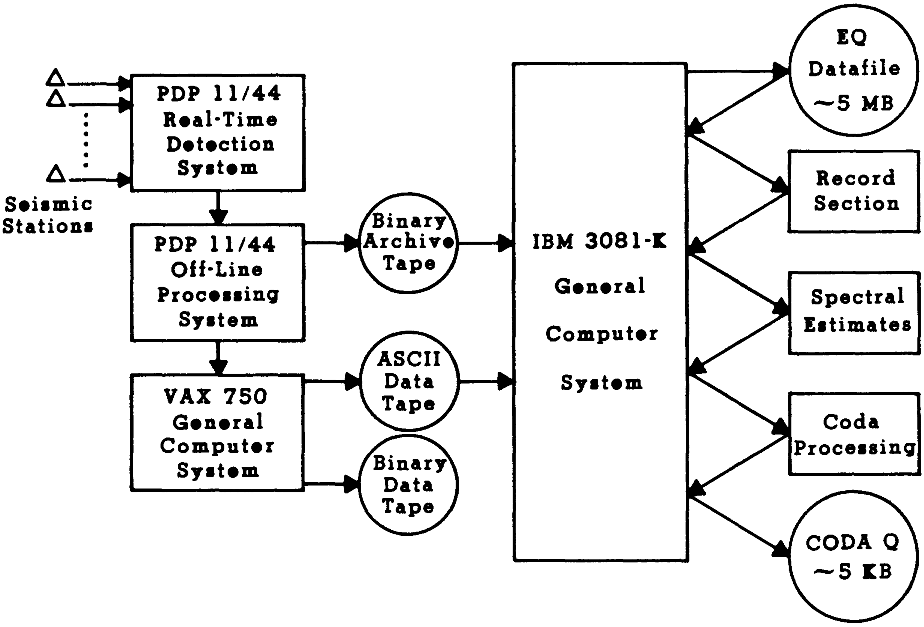

Figure 1. Schematic diagram of data processing for estimating coda Q.

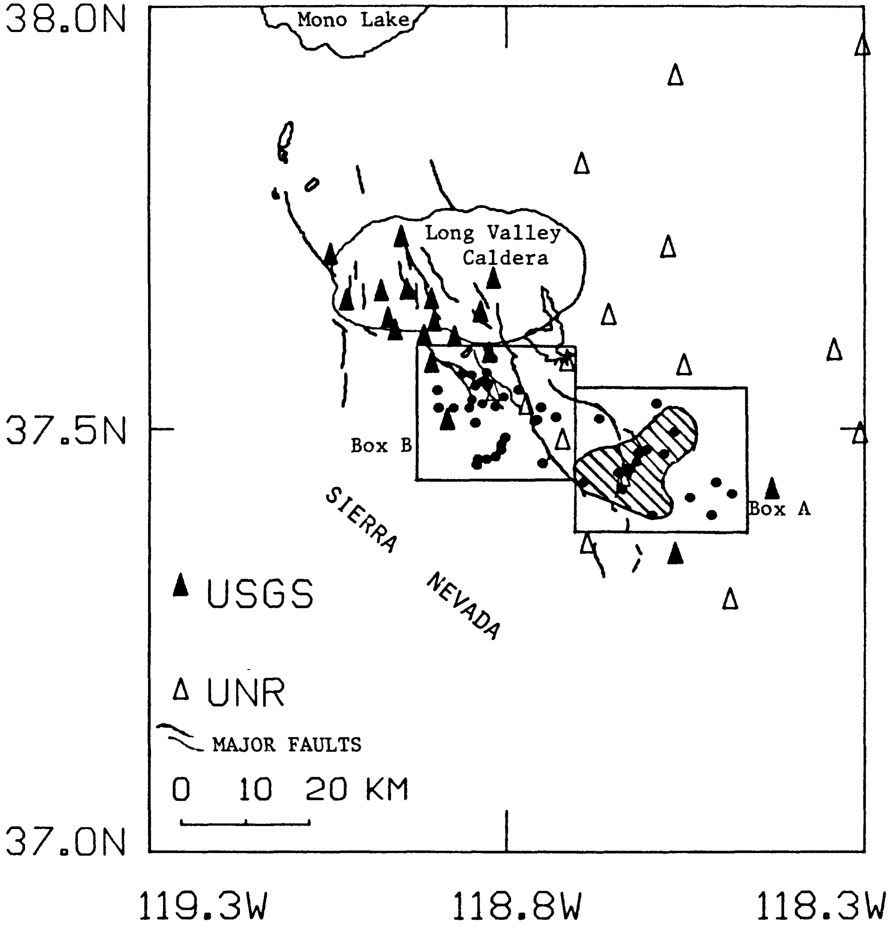

Figure 2. Map showing seismic stations operated by the University of Nevada (UNR), and the U. S. Geological Survey (USGS) in the Long Valley region. The shaded area is the aftershock zone of the Round Valley earthqauke of Nov. 23, 1984. The small dots are epicenters of earthquakes used for the coda Q study.

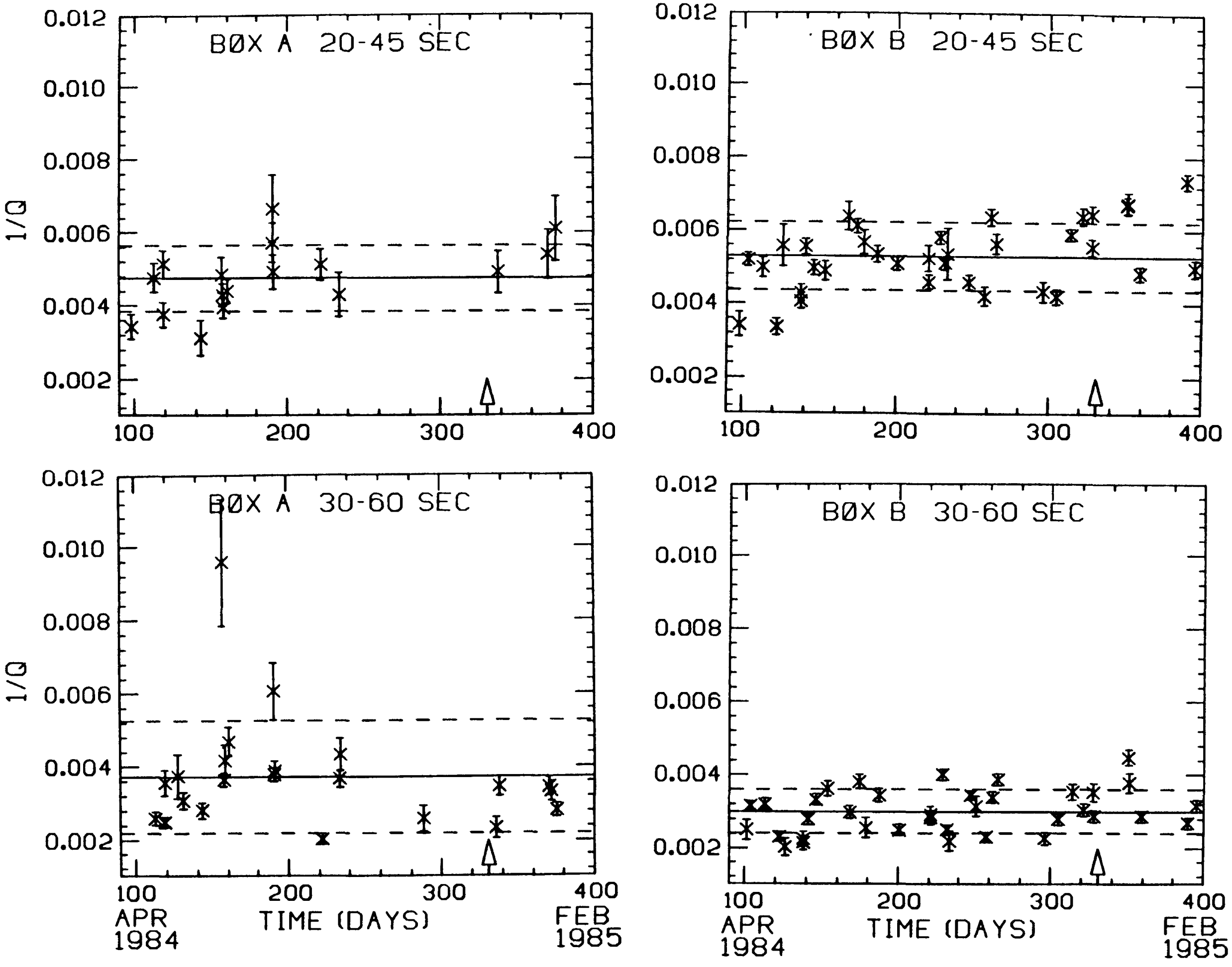

Figure 3. Temporal variation of coda Q^{-1} at 3 Hz for earthquakes in Box A (left), and in Box B (right). The arrow on the time axis indicates the occurrence of the main shock. See text for details.

THEORY AND STRATEGY OF EARTHQUAKE PREDICTIONS

Contract No. 14-08-0001-G-990
Principal Investigator: Keiiti Aki
University of Southern California
Department of Geological Sciences
Los Angeles, CA 90089-0741
(213) 743-3510

In the previous report we introduced our new numerical modeling in which a laboratory inferred friction law, the rate and state dependent friction law was applied to a one-dimensional mass-spring model. We found that this model predicts a recurrence process without suffering a smoothing effect. The smoothing effect happened in many numerical modelings in which the stress drop and slip along the fault became smoother and smoother when the simulation time goes on and the observed magnitude-frequency relation was violated. We also found that strong patches on a fault are necessary for having large earthquakes. After these studies, we have a practical model to be applied to some real cases about fault movement.

We are now ready to study are the recurrence time and stress drop for a recurrence process which has been studied and applied for the purpose of earthquake prediction. Because the healing process is included in the rate and state dependent friction law, we also can study the effect of long-term tectonic loading rate on stress drop.

Recent observation by Kanamori and Allen (1985) about earthquake recurrence time and average stress drop revealed a very interesting relation that the earthquakes with longer recurrence times have higher average stress drops. They attributed the difference in stress drop to the difference in long-term slip rate. In order to interpret their result in terms of the healing effect, we simulated earthquake recurrence using the one-dimensional mass-spring model incorporating the rate and state dependent friction law for different loading rates and heterogeneous strength distributions. We first calculated the stress drop and recurrence time as functions of loading rate for a homogeneous fault model. We found that the stress drop increases up to 30% when the loading rate decreases from 10 cm/yr to 0.01 mm/yr. This is roughly in agreement with the observation if we replot Kanamori and Allen's data in the form of stress drop vs. long-term slip rate (Figure 1). Thus, the observed great variability of stress drop from a few to a few hundred bars may not be attributed to the healing effect alone. Our numerical simulation shows that the variability may be due primarily to the spatial heterogeneity of strength on the fault.

Our simulation also suggests that of the two empirical laws which were inferred from the same laboratory friction data, namely the power law and logarithmic law, as discussed by Shimamoto and Logan (1984), the former can explain the observed stress drop vs. slip rate relation better than the latter which is an earlier version of the rate and state dependent friction law.

References

Kanamori, H., and C. R. Allen, Earthquake repeat time and average stress drop, manuscript for the 5th Ewing Symposium on Earthquake Source Mechanics, 1985.

Shimamoto, T., and J. M. Logan, Tectonophysics, 109, 165-175, 1984.

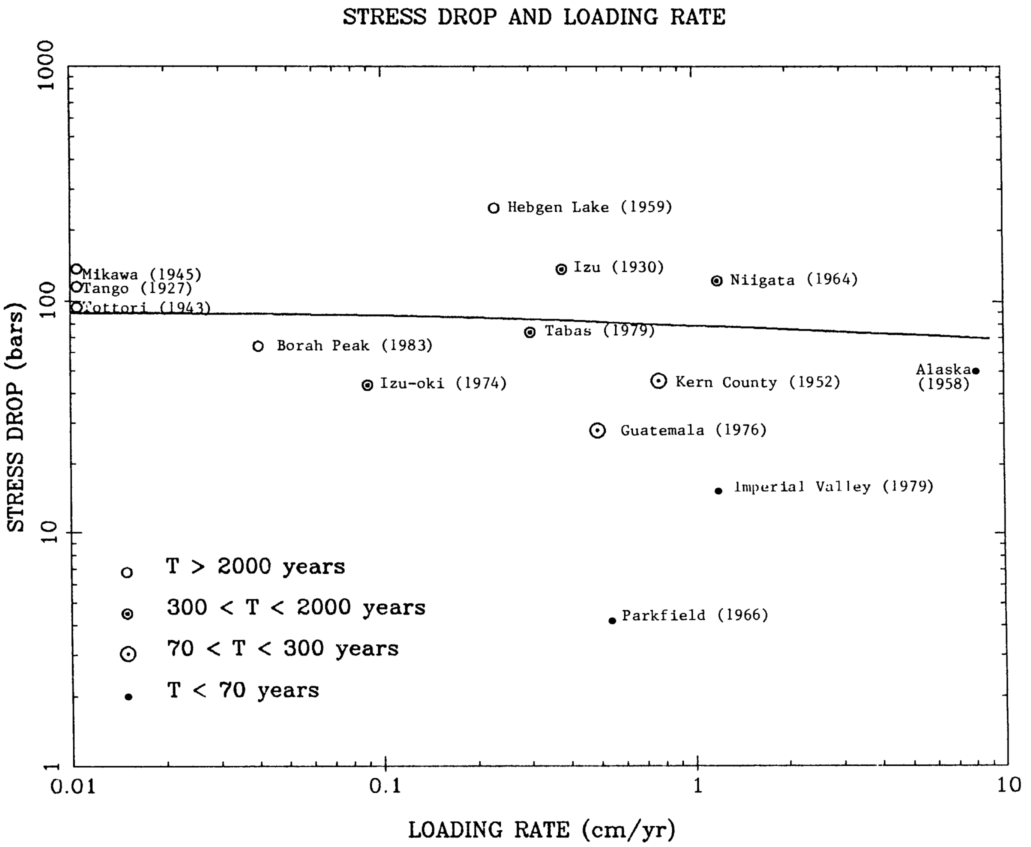

Figure 1. The stress drop vs. long-term slip rate relation. The slip rates are calculated from the seismic moments and recurrence times compiled by Kanamori and Allen (1985). The stress drops are also from Kanamori and Allen's paper. The curve is obtained for a homogeneous fault model using the rate and state dependent friction law with $A_3 - A_2 = 0.00007$.

Digital Signal Processing of Seismic Data

9930-02101

W. H. Bakun
Branch of Seismology
U.S. Geological Survey
345 Middlefield Road, MS-977
Menlo Park, California 94025
(415) 323-8111, Ext. 2777

INVESTIGATIONS

Continuation of studies of seismic activity at Parkfield, California and on the Calaveras fault east of San Jose, California.

RESULTS

The 1969-1984 history of seismic slip on the Calaveras fault in central California illustrates that slip histories can be used to help identify fault sections where significant future seismic slip is most likely. The rupture zones of the M_L=5.8 Coyote Lake earthquake of 6 August 1979 and the M_L=6.2 Morgan Hill earthquake of 23 April 1984 were relatively deficient in seismic slip in the decade before the earthquakes.

The next magnitude 6 earthquake on the Parkfield section of the San Andreas fault is due and should occur before 1993. The Parkfield prediction experiment is designed to monitor the details of the final stages of the earthquake preparation process.

Reports

Bakun, W. H., and A. G. Lindh, 1985, The Parkfield, California earthquake prediction experiment, Science, v. 229, no 4714, pp. 619-624.

Bakun, W. H., G. C. P. King, and R. S. Cockerham, 1985, Seismic slip on the Calaveras fault, California, Fifth Ewing Symposium on Earthquake Mechanics, submitted.

Bakun, W. H., and A. G. Lindh, 1985, Potential for future damaging shocks on the Calaveras fault, California, U.S. Geol. Survey Open-File Rept., in press.

Bakun, W. H., A. G. Lindh, and P. Segall, 1985, Overview of Parkfield, California earthquake prediction experiments (abs.), in press.

Li, Y. -Z, Y. F. Jin, W. H. Bakun, and F. G. Fischer, 1985, A cooperative (abs.) seismic network in western Yunnan province, Peoples Republic of China, in press.

Crustal Deformation Measurement in the Shumagin Seismic Gap, Alaska

14-08-0001-G944

John Beavan and Roger Bilham
Lamont-Doherty Geological Observatory of Columbia University
Palisades, New York 10964
(914) 359-2900

Investigations

1. Nine short (~ 1 km) level lines (Fig. 1) are measured approximately annually within the Shumagin seismic gap, Alaska. Surface tilt data are interpreted in terms of tectonic deformation at the Pacific - North American plate boundary.

2. Five absolute-pressure sea-level gauges are operated in the Shumagins (Fig. 2) in an attempt to measure vertical deformation associated with the Aleutian subduction zone. A two-component short-baseline tiltmeter is operated at one site.

3. Data from the sea-level and tilt sensors are transmitted to Lamont by satellite in near-real-time, and are examined for possible tectonic signals. Studies of noise level as a function of frequency are used to determine the relative usefulness of different types of measurement, and to evaluate the minimum size of tectonic signal that will be visible above the noise. Our data are compared with other crustal deformation data from the Shumagin gap.

Results

The leveling results are shown in Fig. 3, and the inferred tilt rates are listed in Table 1. The data show steady ground tilt down towards the trench, with a pronounced period of reverse tilt in 1978-80. The reverse tilt has been interpreted as resulting from a ~1m aseismic reverse slip episode on the Benioff zone at depths between ~25km and ~80km (Beavan et al 1983, 1984). The 1972-78 and 1980-85 data have been assumed to represent the normal strain accumulation in the area. We have modeled the reverse slip as a dislocation in an elastic half space; the duration of the tilt reversal is < 2 years implying that viscoelastic effects are unimportant. Figure 4a shows surface uplift, tilt and linear strain in the direction of plate motion for the dislocation model that best fits the data. Various model results are compared with observations in Table 2; the uplift observation in the Inner Shumagins is taken from the sea level data at SDP which shows < 100mm change between 1978 and 1980.

Savage (1983) proposed a simple elastic rebound model for strain accumulation in subduction zones. The main thrust zone is assumed to remain locked while the remainder of the plate interface slips steadily and aseismically. Strain therefore accumulates in precisely the reverse of the pattern in which it is released in the eventual earthquake. The surface displacements during the strain accumulation phase can be calculated by applying a dislocation model with virtual slip at the plate convergence rate on the main thrust zone. Thus Figure 4 can be used to model strain accumulation by changing the sign and multiplying the vertical scales by 0.075 (to match the 75mm/yr plate convergence rate). Table 3 summarizes our observations, Savage et al's (1985) strain observations and various model predictions. The uplift observations are taken from our sea level measurements, and are based on < 100mm change in sea level over the 1981-1985 period. None of the models in which the main thrust zone extends to the trench fit the observed data. The best fit is obtained with the upper end of the zone at 25-30km and the lower end at 50-80km (Fig 4b). This is not inconsistent with the available seismic evidence and implies that much of the shallow dipping (< 25km) part of the plate boundary is slipping aseismically. However, the model also implies that strain is accumulating in at least the 30-50 km depth range, and hence that great-earthquake potential exists despite the low observed surface strain rates. This is consistent with the historical evidence for great earthquakes (Davies et al 1981), though our 1978-80 data suggest that strain in this depth range can also be released aseismically. An alternative explanation of these discrepancies may be that the model is inadequate due to its assumptions of elastic rebound, half-space geometry, and neglect of viscoelastic effects.

Sea-level data analysis consists of removing predictable signals (e.g. tides) from the data, then differencing the residual signals to give relative vertical tectonic motion between sites (Fig. 5). The procedure is limited by the stability of the pressure gauge and its associated electronics, and by variations in oceanographic signals from site to site. The latter appear to be reducible to less than 20 mm rms for frequencies lower than 5 c/day. We are presently limited by much worse instabilities in the gauges, though these are being eliminated by replacement of the original Setra gauge/VCO combination with Paros pressure gauges (Fig. 6). No vertical motion above 100 mm has occurred at any site between 1981-85.

After initial settling, the tiltmeter shows rates of < 3 μrad/yr (Fig. 7). This is still substantially above expected tectonic rates; it may represent a thermoelastic signal. The tilt signal is quieter than tilt derived from sea-level differences at periods less than ~ 1 month; at longer periods sea-level becomes quieter.

References

Beavan, J., E. Hauksson, S.R. McNutt, K. Jacob & R. Bilham, 1983. Tilt and seismicity changes in the Shumagin seismic gap, *Science*, **222**, *322-325*

Beavan, J., R. Bilham & K. Hurst, 1984. Coherent tilt signals observed in the Shumagin seismic gap; detection of time dependent signals at depth?, *J. geophys. Res.*, **89**, *4478-4492.*

Davies, J.N., L. Sykes, L. House & K. Jacob, 1981. Shumagin seismic gap, Alaska peninsula: History of great earthquakes, tectonic setting, and evidence for high seismic potential, *J. geophys. Res.*, **86**, *3821-3955.*

Savage, J.C., 1983. A dislocation model of strain accumulation and release at a subduction zone, *J. geophys. Res.*, **88**, *4984-4996.*

Savage, J.C., M. Lisowski & W.H. Prescott, 1985. Strain accumulation in the Shumagin and Yakataga seismic gaps, Alaska, *submitted to Science.*

Reports

Beavan, J., K. Hurst, R. Bilham & L. Shengold, 1985. A densely-spaced array of sea-level monitors for the detection of vertical crustal deformation in the Shumagin seismic gap, Alaska, *J. geophys. Res., in press.*

Bilham, R., J. Beavan, K. Hurst & K. Evans, 1985. Crustal deformation metrology at Lamont-Doherty Geological Observatory, *J. geod. Soc. Japan, in press.*

Table 1

SHUMAGIN TILT RATES

	TIME PERIOD	RATE* µrad a^{-1}	AZIMUTH* degrees	CONFIDENCE LEVEL
INNER SHUMAGINS	1972-78	-1.0±0.3	NW†	95%
	1978-80	2.7±0.5	-27±21	99%
	1980-85	-0.4±0.2	-58±38	90%
OUTER SHUMAGINS	1978-80	0.7±0.6	NW†	---
	1980-85	-0.3±0.2	-65±37	---

* Positive rates indicate that the tilt is downwards towards the given azimuth.

† Level line only measured in one azimuth, so tilt azimuth is indeterminate.

Table 2

1978-80 1 m SLIP EPISODE IN SHUMAGINS

	OBSERVED	DISLOCATION MODEL for fault depth:			
		a 30-50 km	b 25-50 km	c 30-80 km	d 25-80 km
INNER SHUMAGINS					
TILT µrad	+5.4±1.0	-0.6	-1.0	+4.3	+3.8
UPLIFT mm	-100<u<100	-35	-45	+46	+36
OUTER SHUMAGINS					
TILT µrad	+1.4±1.2	+0.6	+5.1	-7.4	+1.4
UPLIFT mm	---	+249	+150	+370	+272

Table 3

STRAIN ACCUMULATION IN SHUMAGINS

		ELASTIC REBOUND MODEL for locked zone in depth range:				
	OBSERVED 1980-85	a 30-50 km	b 25-50 km	c 30-80 km	d 25-80 km	e 0-30 km
INNER SHUMAGINS						
TILT µrad/yr	-0.4±0.2	+0.05	+0.07	-0.32	-0.29	+0.04
STRAIN µstrain/yr	+0.01±0.03*	+0.02	-0.05	+0.03	-0.04	-0.15
UPLIFT mm/yr	-25<u<25	+2.6	+3.4	-3.5	-2.7	+1.0
OUTER SHUMAGINS						
TILT µrad/yr	-0.3±0.2	-0.04	-0.38	+0.56	-0.11	-0.05
STRAIN µstrain/yr	-0.03±0.05*	-0.04	-0.01	-0.13	-0.10	-0.23
UPLIFT mm/yr	-25<u<25	-18.7	-11.2	-27.7	-20.4	+13.6

* from Savage et al. [1985], assuming zero strain along strike of arc.

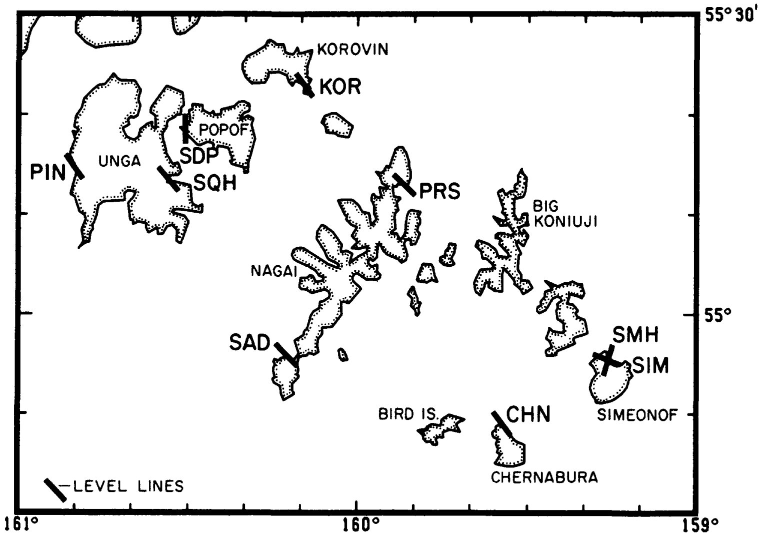

Figure 1. The Shumagin Islands, showing the locations and directions of first-order level lines, whose lengths vary between 600m and 1200m. The resultant of the data from lines SDP and SQH is used to estimate the tilt direction in the Inner Shumagins. The resultant of SIM and SMH is used for the Outer Shumagins.

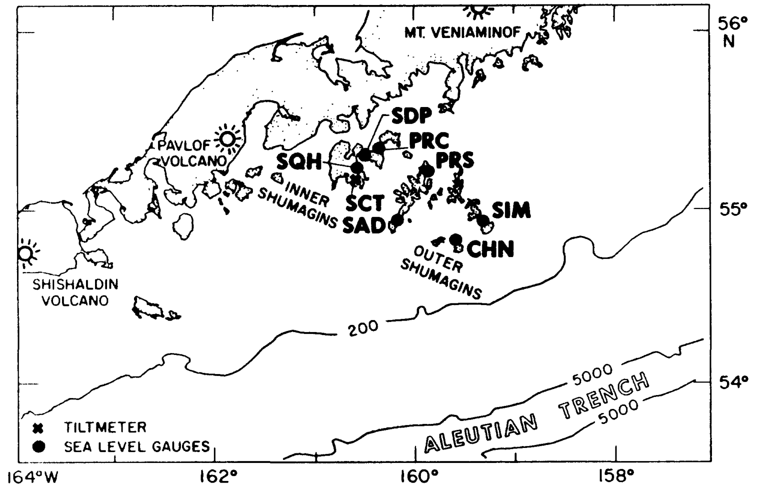

Figure 2. Location of the Shumagin Islands with respect to the trench and the volcanic arc. Depth contours are in metres. Note the locations of Pavlof Volcano and the Inner and Outer Shumagins. Also shown are the sites of sea-level gauges operated by Lamont-Doherty and by the National Ocean Survey (SDP), and the site of a short-baseline tiltmeter (SCT). Station SAD is no longer operative because of storm damage. Station CHN is not operating this year.

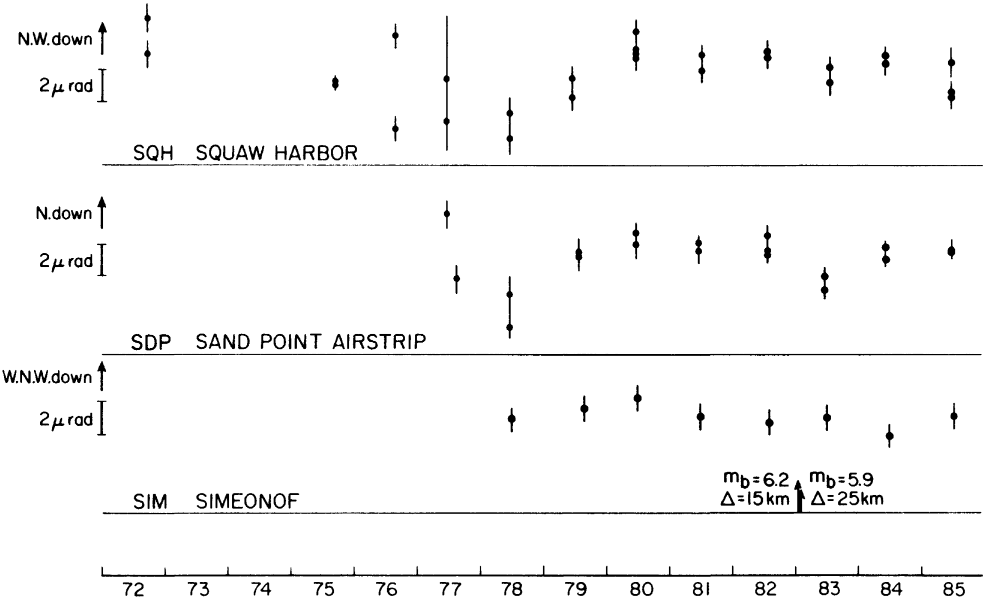

Figure 3a. See also Fig. 3b. All data (1972-1985) from level lines in the Shumagin Islands. All lines except SMH are oriented approximately in the direction of relative plate motion. The two data points each year represent the forward and backward runs of leveling. The error bars are $\pm 1\sigma$, based on variations in multiple readings of each stadia rod from each tripod position. The height differences between the ends of the lines have been converted to slope by dividing by the line length; changes in slope from year to year are due to ground tilt. Several benchmarks are set at each end of each line to guard against benchmark instability. Lines SIM and SAD have only one data point plotted for each year; this is because they have benchmarks between almost every tripod position and the overall tilt is estimated by averaging tilts between adjacent benchmarks.

Note particularly the 1.0 ± 0.3 μrad/yr tilt down toward the trench between 1972 and 1978 on line SQH. The resultant of lines SQH and SDP shows a reversal of tilt (2.7 ± 0.5 μrad/yr down away from the trench) between 1978 and 1980, and a return to tilt down towards the trench (0.4 ± 0.2 μrad/yr) between 1980 and 1985. The line at SIM in the Outer Shumagins may also show a tilt reversal in 1980, though not at high confidence level.

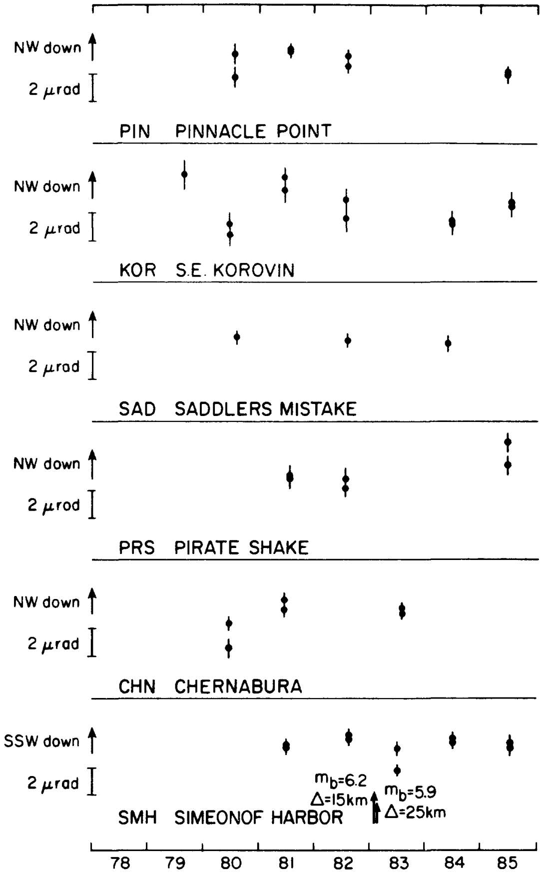

Figure 3b. See Figure 3a. Most of the NW-SE oriented lines show coherent behavior since 1980, with slow tilting down towards the trench. Clusters of microseismicity at shallow depths below KOR in 1978 through 1980 may contribute to its noisy behavior. The 1980 measurement on CHN was made immediately after setting the benchmarks, so there may be some settling error due to hardening of the concrete.

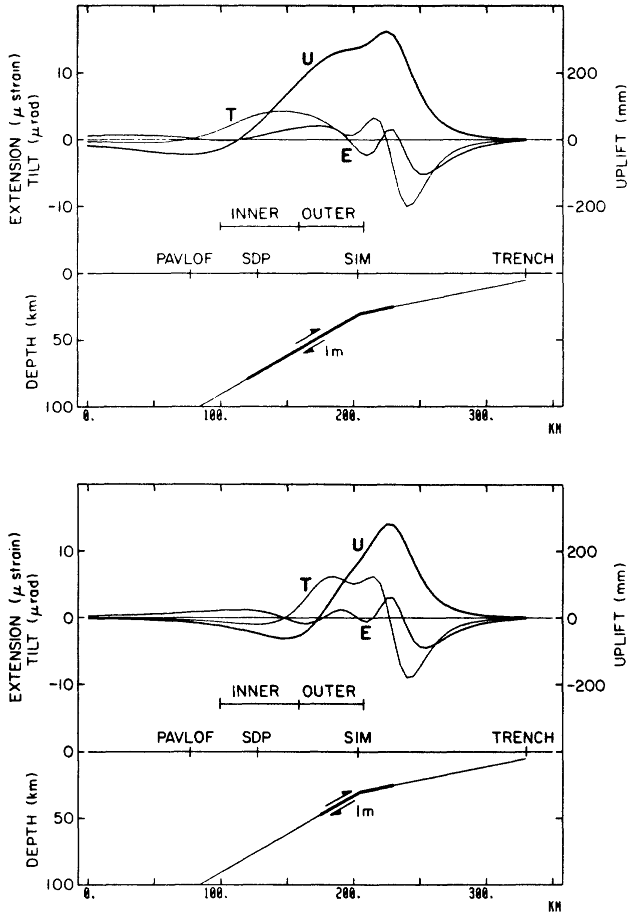

Figure 4 (a,b). Dislocation models showing surface uplift (U), tilt in the plate convergence direction (T), and horizontal linear strain in the plate convergence direction (E), for 1m reverse slip on the fault plane shown. Table 2 gives uplift and tilt at the positions of SDP and SIM, and compares various dislocation models with the 1978-80 observed data. Fig. 4a most closely matches the observations.

The figures can also be used to show strain accumulation using Savage's (1983) model. The polarity of uplift, tilt and strain should be changed, and the vertical scales multiplied by 0.075 to give annual deformation rates assuming a 75 mm/yr plate convergence rate. Table 3 gives uplift and tilt at SDP and SIM, and average strain over the intervals marked as the "inner" and "outer" islands. It also compares 1981-85 observations with various models. Figs. 4a and 4b both reproduce features of the observed data.

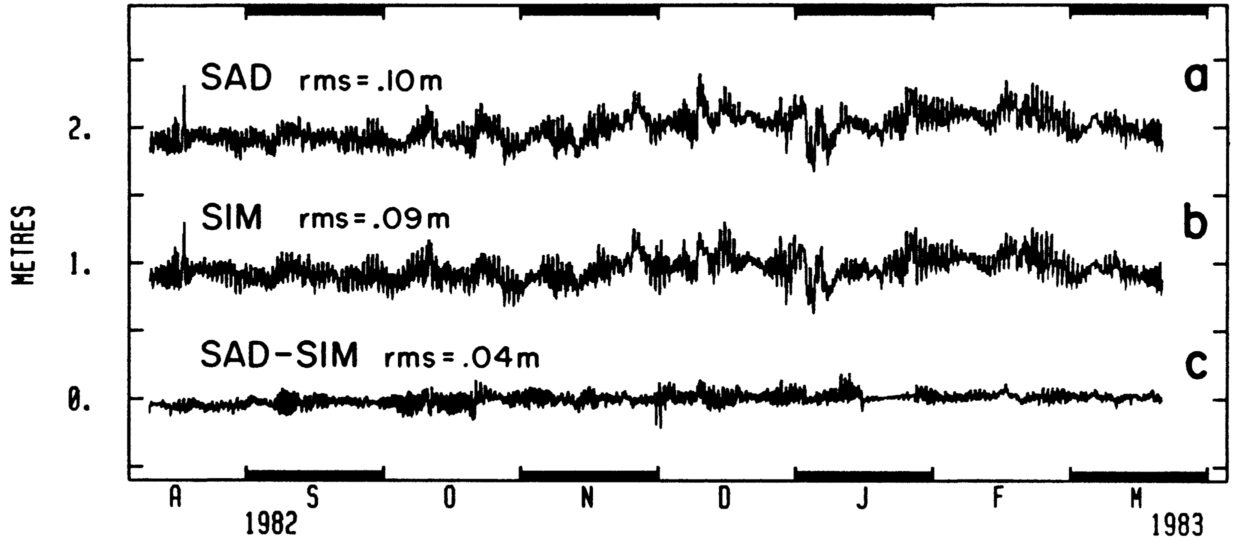

Figure 5. (a,b) Residual signals on two sea-level gauges after removing ~3 m tides. The rms amplitudes of these traces are .10 and .09 m, respectively. (c) The rms amplitude of the difference is .04 m; the differencing removes a certain amount of residual non-tidal coherence between the two series. The difference contains any tectonic signal that may be present. The traces are offset vertically for clarity.

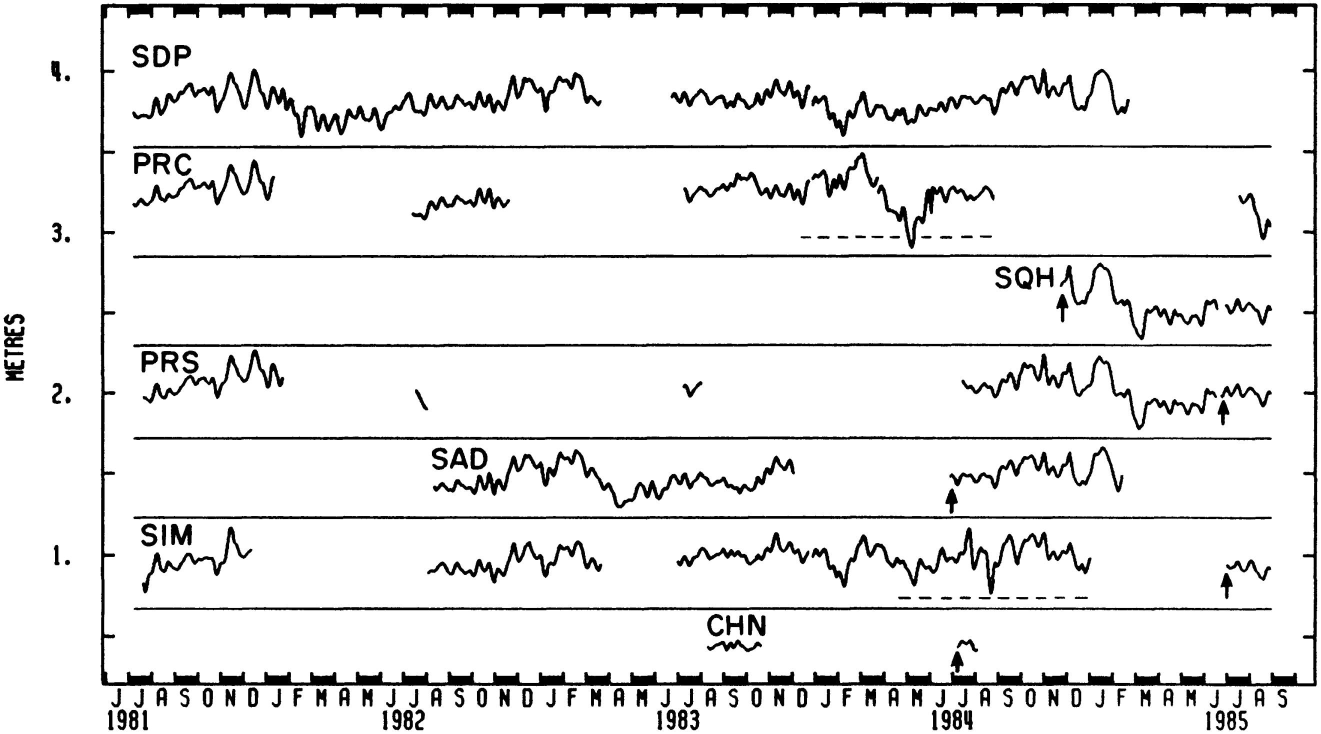

Figure 6. Data are processed to the stage represented by Fig. 5a or 5b, then are low-pass filtered with a 10-day cut-off. The resulting data are shown here, offset vertically for clarity. The top trace is the data from the NOS float-type gauge at SDP. This has been corrected for atmospheric pressure variations using air pressure recorded at the Lamont sites - the gaps in the data are due to gaps in the air pressure record. The dashed lines show data contaminated by severe pressure gauge drift that has been approximately corrected. The arrows show the times at which highly stable Paros gauges were installed at the sites. Long-period coherent signals are evident on several of the gauges. Differencing eliminates these and shows that no relative vertical uplift greater than 100 mm has occurred during 1981-1985. We expect substantially greater accuracy from the Paros gauges.

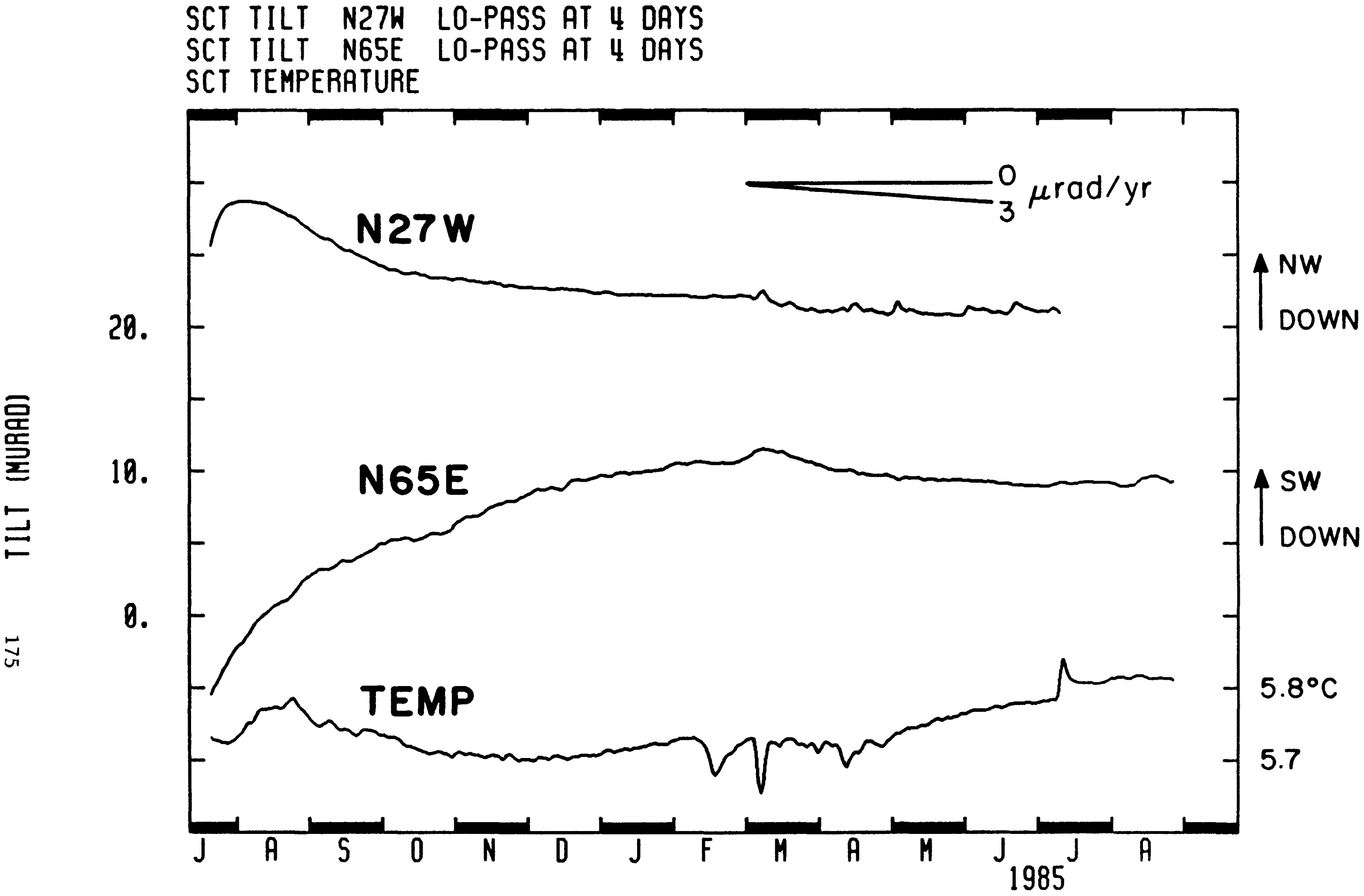

Figure 7. Low-pass filtered tilt and temperature records from the tiltmeter installation. The tiltmeters use mercury to define an equipotential, and capacitance transducers to measure tilt. They have a base-length of 600mm and are mounted on steel girders concreted to bedrock in a disused mine approximately 40m below ground level. The temperature spike in July 1985 was caused by a visit.

Crustal Deformation Observatory Part F

USGS 14-08-001-21989

Roger Bilham and John Beavan
Lamont Doherty Geological Observatory
Palisades, New York, 10964
(914) 359 2900

Investigations

1. The LDGO tiltmeter at Piñon Flat Observatory continues to be maintained in an investigation of coherence between data from various forms of long-baseline tiltmeter.

2. In September 1984 UCLA colleagues attempted a ten day experiment to read the micrometers from the long baseline tiltmeters at Piñon Flat four times a day. (Jackson and Rogers p. 369, U. S. Geological Survey Open File Report 85-464, July 1985). We investigated alleged inconsistencies in the resulting data.

3. A second micrometer reading system was added to the west end of the tiltmeter and the design of the existing micrometer sensors was improved substantially. Water level data and tilt data from the micrometer sensors for the last two years were edited.

4. Improved forms of LED image follower transducer have been investigated in a search for a reliable water level sensor suited to unattended remote operation.

Results

1. The water level sensors of the LDGO tiltmeter have operated with much improved reliability since the introduction of hard sealed plasma tubes and *in-situ* X-Y oscilloscopes to adjust the phase quadrature signal from the interferometer water level sensors. Loss of digital count occurs when interferometer illumination is instantaneously lost and in the past this has been typically at times of power failure. Recently, however, a family of spiders has taken to building a nest near the exit window of the laser at the West end, resulting in occasional fringe jumps. The nest is periodically removed while we seek a permanent remedy.

2. The cause of the poor correlation between the micrometer and laser interferometer outputs from the LDGO tiltmeter reported by Jackson and Rogers was found to be due to a combination of reading blunders, poor cleanliness of the water surface in the micrometer sensors, and physical disturbance to the measurement vaults by the investigators. Contrary to an assertion in their report no algae were present in the east end measurement system. The lack of correlation early in the first five days of the experiment appears entirely due to micrometer setting and reading errors. In Figure1 an analysis of a small portion of the experiment is shown in which no reading

blunders or fringe jumps occurred. The instrument is evidently functioning correctly. However, the apparent repeatability of setting the micrometer point to meet its subsurface reflection during most of the experiment was substantially worse than that typically obtained (± 1 µm) with a clean water surface and experienced observers. To attain optimum operating conditions the micrometer reservoirs are designed to be removed for cleaning without disturbance to the micrometer datum.

3. Fixed microscopes and fixed sources of back illumination have been added to the LDGO tiltmeter micrometer sensors. A source of ambiguity in setting the micrometer tip to touch the water surface has been identified and corrected. The micrometer tip is of finite radius and the silhouette of its approach to the water surface is observed with a microscope with a large objective lens. In its unmodified form the microscope's view of the micrometer tip is confused by parallax caused by the finite dimensions of the objective lens. To avoid this problem we mask the objective lens to form a narrow horizontal slit across a diameter, and to improve set-point accuracy we arrange the micrometer to be supported at a small angle of incidence to the water surface.

A second micrometer/microscope combination was installed at the west end of the tiltmeter. The correlation between this sensor (W2) and the existing sensor (W1) is shown in Figure 2 and the difference in water level indicated by the two sensors is shown in Figure 3.

4. Data from the micrometer sensors since their installation in March 1983 are presented in Figure 3. The long term trend evident in the upper trace labelled "tilt" compares favourably with data from the IGPP tiltmeter (Wyatt and Agnew, p. 353, U.S. Geological Survey Open File Report 85-464, July 1985). A least squares fit to the micrometer data, which have not been adjusted for vertical motions of the end mounts or temperature variations, yields a long term trend of less than 0.1 µradian per year. An annual term with an amplitude resulting in a maximum tilt rate of 1 µrad/a correlates with known (10°C) seasonal changes in vault temperature.

The two lower curves in Figure 3 show changes in water level at each end of the tiltmeter. The 2 mm decrease in water level in two years is caused by leakage and by draining of the end reservoirs during cleaning operations. In August 1984 flash flooding at Piñon Flat resulted in a 0.5 mm increase in water level in less than 2 hours due to direct leakage into the system through inspection risers along the path of the pipe. The leak rate from the 532 m long Polyvinyl Chloride pipe and end fittings is estimated to be less than 8 cm^3/day (1 µm per day).

5. Figure 3 illustrates data from a prototype LED image follower transducer. In this system a reduced image of an LED is formed after total internal reflection from the surface of the water in a glass walled reservoir. Vertical motion of the water surface,

h, displaces the LED image on a silicon bicell by a distance of 2h. The resulting amplified imbalance of the electrical outputs from the two halves of the bicell is used to drive the position of the bicell to an electrical null position. The position of the bicell is monitored by an LVDT displacement transducer. A revised form of this transducer is under test that operates by reflecting the LED image from the upper surface of the water. Although image intensity is much reduced the system is more compact and is immune to variations in water opacity and refractive index changes with temperature. With the introduction of a horizontal reflector close to the water surface, e.g. a semireflecting base to the measurement reservoir, it is possible to measure water *depth* in addition to monitoring changes of water *level.* This is of importance in the development of systems that must operate accurately over periods of many decades and its application to the indexing of the fringe count from the interferometer water level sensors to an absolute measurement scale is clearly of immense practical value.

Reports

Bilham R. Transducers in Michelson Tiltmeters, *China-United States Symposium on Crustal Deformation and Earthquakes,* Wuhan, PRC October 1985.

Figure 1 A subset of water level data from the east end of the LDGO tiltmeter obtained during the September 1984 UCLA experiment. The predicted 0.95 µm/fringe relationship between micrometer observations and laser interferometer output is clearly evident.

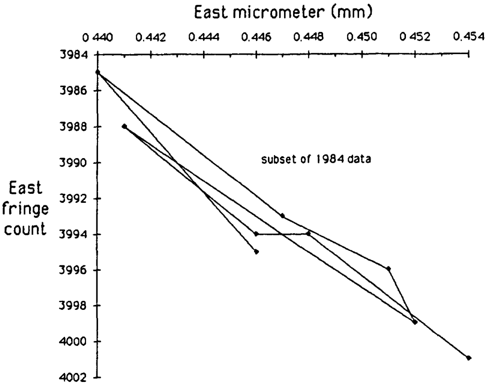

Figure 2 Water level observations from two micrometer sensors at the west end of the LDGO tiltmeter for a period of 200 days in 1985. Initial 0.2 mm settlement of an independent mount for W2 within the west end vault in March 1984 accounts for the discrepancy between the two data series before May 1985.

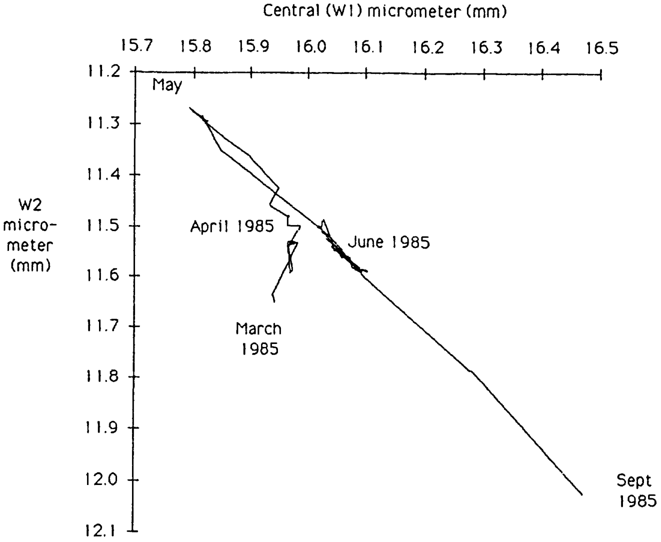

Figure 3 Micrometer data from the LDGO tiltmeter between March 1983 and September 1985. Superimposed on a net tilting of the Earth's surface at Piñon Flat of less than 0.09 µrad/a is a seasonal signal principally attributable to direct temperature effects on the instrument. The short curve (W1-W2) represents the difference in water level monitored by two micrometer sensors in the west end vault (see Figure 2). The lower two curves show changes of water level monitored at each end of the 532-m-long tiltmeter from which the tilt data are derived.

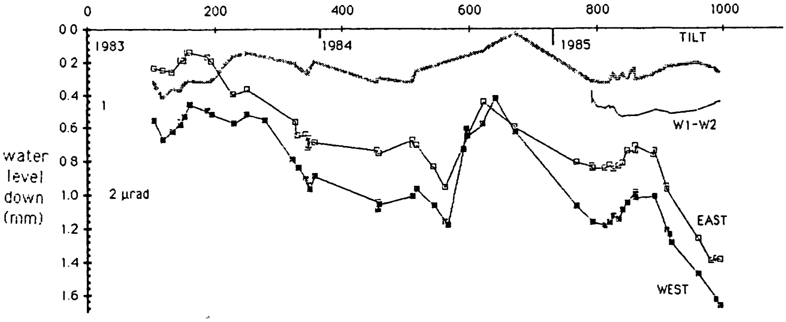

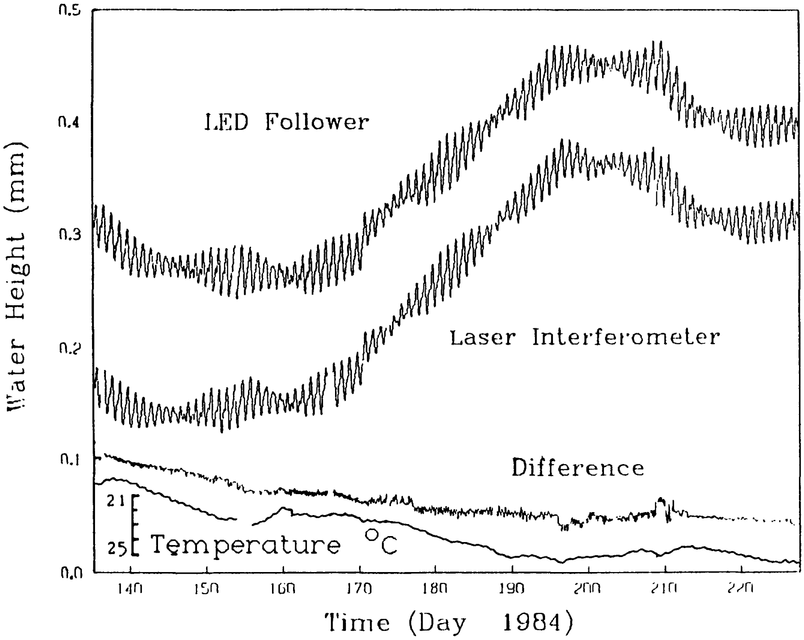

Figure 4 Data from a prototype LED image follower transducer. The discrepancy between the output of the laser interferometer and the LED follower is believed to be caused by a translucent algae that was discovered in the reservoir at the end of the experiment. Figure courtesy of Frank Wyatt.

Holocene and Quaternary Geologic Studies

9540-03787

Robert O. Castle
Branch of Western Regional Geology
345 Middlefield Road MS 975
Menlo Park, CA 94025
(415) 323-8111, ext. 2353

Investigations

1. Continued detailed investigations and analyses and report preparation on regionally developed historic vertical surface deformation in the Salton Trough and adjacent parts of southeastern California.

2. Continued preparation of reports on the magnitude and predictability of the so-called unequal-refraction error in geodetic leveling and interpretation of oscillatory vertical displacements athwart the San Andreas fault in the central Transverse Ranges.

Results

1. No new results to report on studies of the Salton Trough (see v. 20).

2. Anaylses of historical data indicate that procedures in force since the 19th century have effectively suppressed the unequal-refraction error in geodetic leveling. Although theoretical considerations argue that large refraction errors should accumulate where levelings traverse gentle slopes permitting long sight lengths, extensive examination of routinely developed results lend little support to this theory.

Reports

Castle, R.O., Gilmore, T.D., Mark, R.K., and Shaw, R.H., 1985, Empirical estimates of cumulative refraction errors associated with procedurally constrained levelings based on the Gaithersburg-Tuscon refraction tests of the National Geodetic Survey: Geophysical Research Letters, v. 12, no. 5, p. 239-242

Gilmore, T.D., and Elliott, M.R., 1985, Sequentially and alternatively developed heights for two representative bench marks: near Palmdale, California and along the Bill Williams River, Arizona: U.S. Geological Survey Open-File Report 85-399, 50 p.

Gilmore, T.D., Episodic regional uplift in southeastern California preceding major historic earthquakes in the Imperial Valley [abs]: Approved by Director.

Mark, R.K., Gilmore, T.D., and Castle, R.O., Evidence of the suppression of the unequal-refraction error in geodetic leveling [abs]: Approved by Director.

Remote Monitoring of Source Parameters for Seismic Precursors

9920-02383

George L. Choy
Branch of Global Seismology and Geomagnetism
U.S. Geological Survey
Denver Federal Center
Box 25046, Mail Stop 967
Denver, Colorado 80225
(303) 236-1506

Investigations

1. Rupture process of moderate-sized earthquakes. We are using digitally recorded broadband waveforms to characterize the rupture process of selected moderate-sized earthquakes. Currently under study is the Yemen earthquake of December 13, 1982. Also, a qualitative analysis is being pursued for all of the Selected Events chosen for special study by the Commission on Practice at the 1985 IASPEI General Assembly in Tokyo.

2. Teleseismic analysis of large earthquakes. We are developing methods with which to use digitally recorded broadband waveforms to detail the rupture process of large, complex earthquakes. In addition, we are participating in an IASPEI study to evaluate the current potential of the global seismograph stations to record very great earthquakes ($M>7.5$).

3. Teleseismic estimates of radiated energy. We have developed a method for computing radiated energy from direct measurements of broadband teleseismically recorded body waves.

Results

1. The broadband body waves have sufficient frequency content to resolve complexities of rupture. The Yemen earthquake of 1982 was found to consist of two events that occurred 3 sec apart on a steeply dipping normal fault that trended NNW. The analysis of the Selected IAPSEI Events showed that, in data containing a broad and continuous range of frequencies, depth phases and source-time functions can be easily and quickly read directly from the records.

2. Currently under study are a series of events near Copiapo, Chile, and the $M_S7.8$ earthquake that occurred off the coast of Chile on March 3, 1985. A report on the current worldwide capability to record on-scale records from very great earthquakes has been completed.

3. We have applied our algorithm for the computation of radiated energy using broadband data to two recent earthquakes, the Coalinga earthquake of May 1983, and the Borah Peak earthquake of October 1983. Our results indicate that indirect estimates of energy (for example, those depending on simplistic relations with seismic moment) may overestimate energy if the rupture process involves a sizeable component of aseismic slip.

Reports

Boatwright, J., and Choy, G. L., 1984, Teleseismic estimates of the energy radiated by shallow earthquakes: Journal of Geophysicial Research, in press.

Boore, D. M., Bolt, B. A., Choy, G. L., Kolesnikov, Y., Osawa, Y., and Seidl, D., 1985, Worldwide seismograph recording of great earthquakes, in preparation.

Seismic Analysis of Large Earthquakes and Special Sequences in Northern California

9930-03972

Robert S. Cockerham, Jerry P. Eaton
and A. M. Pitt
Branch of Seismology
U.S. Geological Survey
345 Middlefield Road, MS-977
Menlo Park, California 94025
(415) 323-8111, ext. 2963

INVESTIGATIONS

1. Development of regional velocity models and appropriate station corrections to improve hypocenter locations in northern and central California.
2. Acquisition of data necessary to produce California state seismicity maps ($M \geq 1.5$) for 1981-1984.
3. Preliminary analysis of 4 August 1985 Kettleman Hills earthquake sequence.
4. Completion of timing of earthquakes in the Yellowstone National Park-Hebgen Lake Region from 1973 to 1981 accompanied by development of a new velocity model for the region.
5. Continued monitoring and analysis of the seismicity in the Long Valley area.

RESULTS

1. Regional 1-dimensional velocity models and appropriate station travel-time corrections are being collected or calculated for northern and central California. Areas for which specific models have been obtained are 1) Coalinga-Kettleman Hills, 2) Parkfield, 3) Morgan Hill-Coyote Lake, 4) east San Francisco Bay, 5) San Francisco Peninsula-Santa Cruz Mountain area to northern end of creeping section of the San Andreas Fault, 6) Geysers geothermal area, 7) Mt. Shasta - Mt. Lassen area, and 5) Mono Lake - Long Valley caldera - Bishop area.
2. Hypocentral data from USGS northern and southern California seismic networks, U.C. Berkeley and U. Nevada at Reno seismic networks have been collected towards production of California State seismicity maps for 1981 through 1984 of $M \geq 1.5$ earthquakes.
3. On 4 August 1985 a M 5.5 earthquake occurred beneath the western edge of the Great Valley about 17 km east of Coalinga (Fig. 1), near the northeast end of the Kettleman Hills anticline. The aftershock zone of this sequence abuts the southeastern end of the Coalinga aftershock zone, but the two do not overlap (Fig. 1). The number of aftershocks recorded during the first week was about 220 for Kettleman versus about 2600 for Coalinga this difference is in accord with the difference between the main shocks magnitude, M 6.7 - Coalinga and M 5.5 - Kettleman Hills. However,

the lengths of the aftershock zones are comparable: about 20 km for Kettleman and 30 km for Coalinga. Thus, the Kettleman Hills aftershock zone is disproportionately large compared to that of the Coalinga aftershock zone. The main shock was preceeded by five foreshocks within a few kilometers of its hypocenter during the 24 hours before the main shock (starting with a M 3.4 22 hours before the main shock and ending with a M 4.5 25 minutes before the main shock). P-wave first motion data suggests thrust faulting along a plane striking N 52°W and dipping 12°SW for the main shock. The underlying cause of the Kettleman Hills earthquake appears to be the same as that of the Coalinga earthquake, thrusting of the eastern edge of the Coast Ranges eastwards over the stiff, resistive basement underlying the Great Valley.

4. The timing of earthquakes in the Yellowstone National Park-Hebgen Lake region from 1973 to 1981 was completed. The data set of approximately 6000 earthquakes was rerun with a new, improved 1-D velocity model and station travel-time corrections. The model and station corrections were determined by E. Kissling from a full inversion of P-wave travel-times using a subset of Yellowstone earthquake and explosion data. The quality of hypocenter solution was improved and epicentral scatter was reduced (Fig. 2). A 3-D inversion of all 6000 events to study crustal structure of the Yellowstone region is underway. A catalog of the hypocentral data is in preparation.

5. The level of seismic activity within Long Valley caldera has continued to decline from 2 to 3 quakes per day ($M \geq 1.0$) in 1984 to an average of about 0.5 quakes per day (Fig. 3a) in 1985. However, the seismicity rate within the Sierran block to the south of the caldera (Fig. 3b) has continued at a level of about 5 events per day ($M \geq 1$); due mainly to aftershocks of the 23 Nov. 1984 Round Valley earthquake (Fig. 4). The overall epicentral pattern for this area has remained the same (Fig. 4).

REPORTS

Eaton, J.P., D.H. Richter, and H.L. Krivoy, Cycling of magma between the summit reservoir and Kilauea Iki Lake during the 1959 eruption of Kilauea Volcano, Hawaii, in USGS Prof. Paper 1350, in press.

Eaton, J.P., The north Kettleman Hills earthquake of August 4, 1985 and its first week of aftershocks-a preliminary report, U.S. Geol. Survey internal report, 29 p., 1985.

Hill, D.P., and R.S. Cockerham, Seismicity in Long Valley caldera, California EOS, v. 66, (Abst.), 1985.

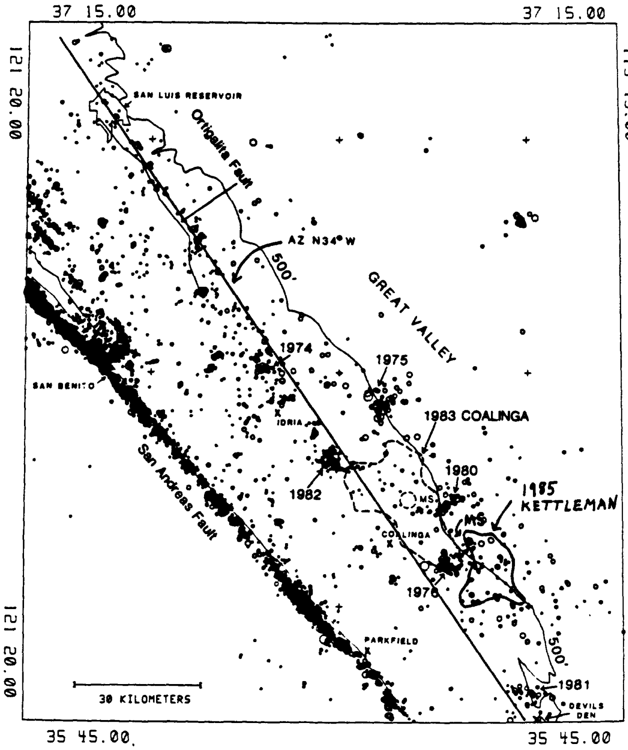

FIGURE 1. Epicentral map of central Coast Ranges of California. The aftershock regions of the 1983 Coalinga and 1985 Kettleman Hills earthquakes are outlined; the epicenters of the main shocks are labeled "MS".

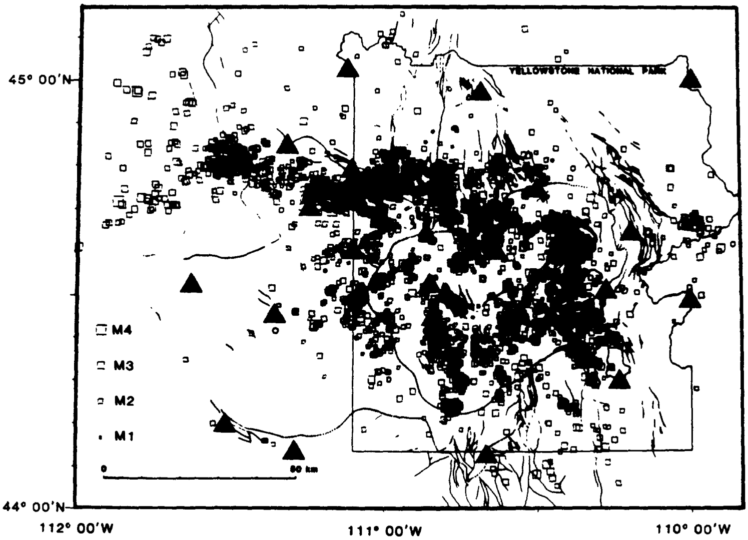

Figure 2. Earthquake epicenters in the Yellowstone Region, 1973-1981. Yellowstone phase 1 and 3 calderas are indicated by heavy dotted lines, faults with evidence of Quaternary movement by light solid and dotted lines. Triangles indicate seismograph stations (not all in operation at the same time).

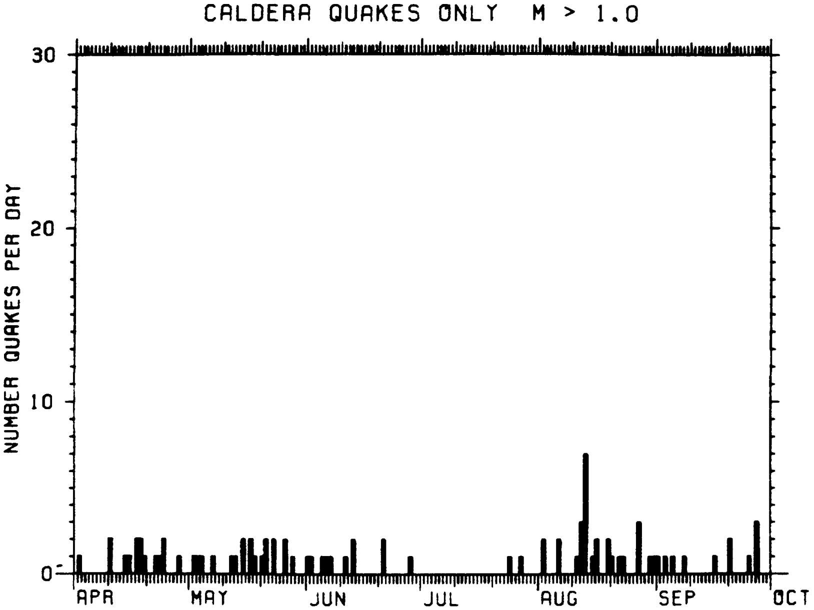
CALDERA QUAKES ONLY M > 1.0

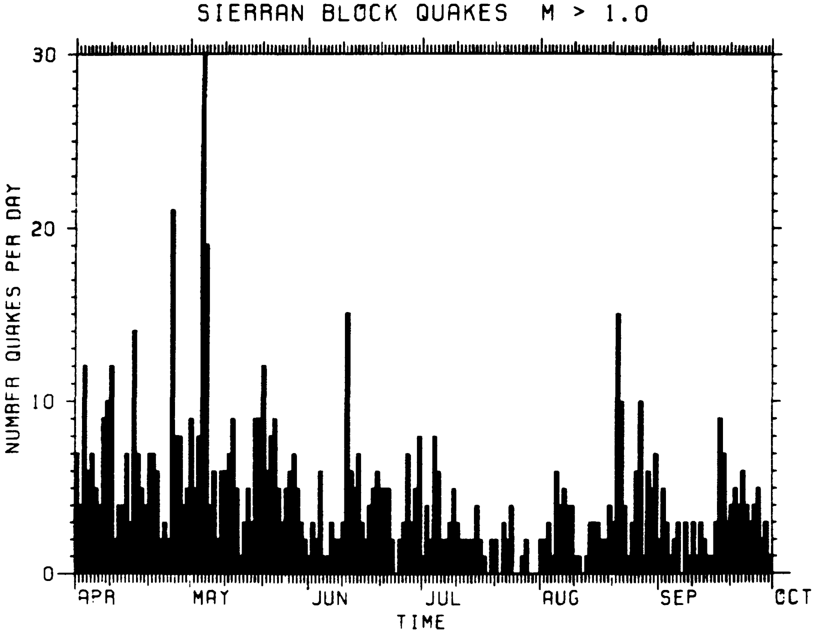
SIERRAN BLOCK QUAKES M > 1.0

FIGURE 3. Histograms of number of earthquakes per day for inside Long Valley caldera (A) and the Sierran block (B) to the south of the caldera.

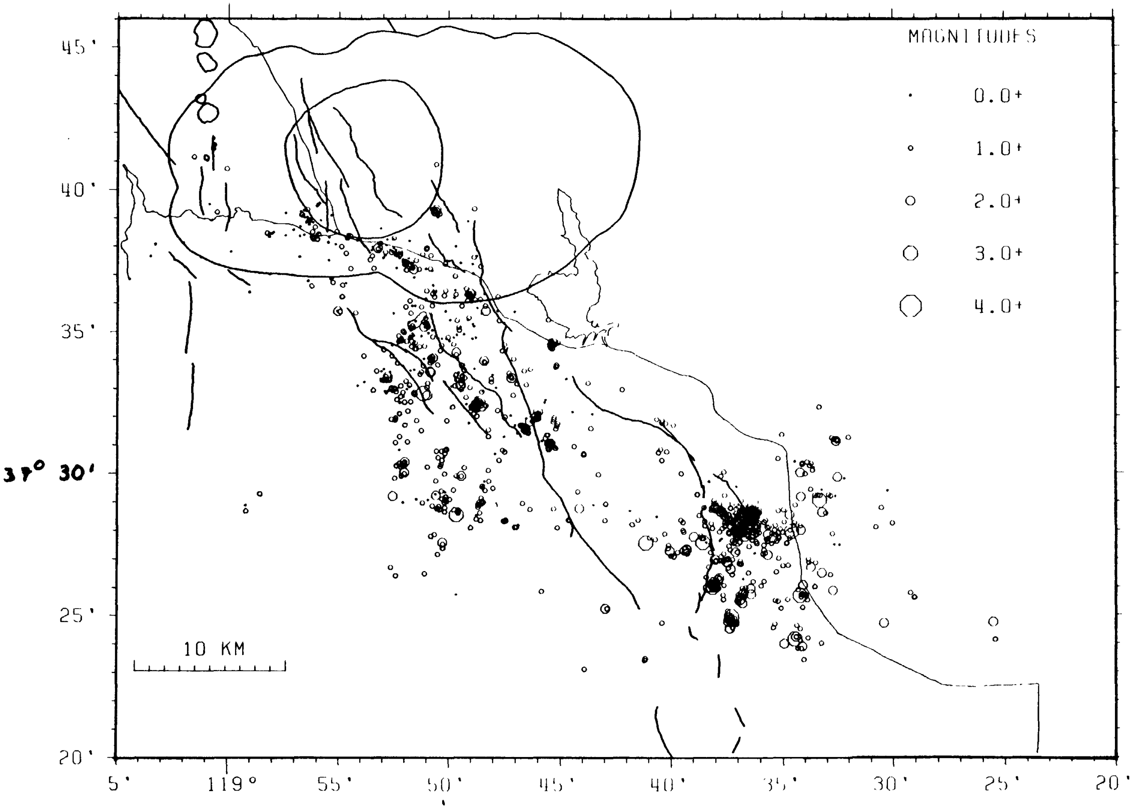

FIGURE 4. Epicentral map of hte Long Valley caldera area from 1 April through 30 September, 1985 of M ≥ 1.0.

SEARCH FOR ELECTROMAGNETIC PRECURSORS TO EARTHQUAKES
(66730)

William Daily
Lawrence Livermore National Laboratory
P.O. Box 808, L-156
Livermore, California 94550
(415) 422-8623

Observations of electromagnetic (EM) precursors have been reported for large earthquakes in Japan, Iran, Chile, and the Soviet Union (e.g., by Gokhberg, et al., 1980). In addition, recent observations of very low frequency (VLF) precursors measured by GEOS satellites have been reported by Parrot and Lefeuvre (1984). Mechanisms and semiquantitative models advanced to explain the observations have been discussed by Gokhberg, Gufeld and Dobrovolsky (1979) and Warwick, Stoker, and Mezer (1982). Laboratory demonstration of radio frequency emission from cracking rocks has also been reported (Nitsan, 1977; Vorobev, 1977). Reported herein are the results of a study to search for EM earthquake precursors along the San Andreas Fault system in California, using ground based, broadband electromagnetic monitors.

Several very low frequency radio receivers have been built to monitor broadband EM noise near a fault zone. These receivers have been placed into operation near the San Andreas Fault in 1983 and 1984. It is unlikely that one such monitoring station will be capable of monitoring events along more than a few hundred kilometers of the fault. Therefore, we have emplaced receivers along the San Andreas Fault. The exact location of each site was determined by: 1) the estimated probability of an earthquake of Richter magnitude greater than about 5 (precursors are typically seen only with larger magnitude events); 2) accessibility of site to facilitate deployment and periodic equipment checks; 3) isolation from cultural sources of wide band EM noise; 4) availability of power source and reasonable security. To allow some discrimination of source location, monitoring stations were spaced far enough apart that signals from an event will not be seen equally well by all sensors. If the source region for these signals is deep (a few kilometers), signals at the surface should be confined near the epicenter--attenuation will be high due to propagation long distances through high loss crust from the source. If the source region is near the surface, signals will be measurable at larger distances. From these considerations and published measurements of precursors, we estimate that the locations monitored should be a few hundred kilometers apart, but also chosen for their high potential as an epicenter for a large earthquake. The five locations chosen for placement of monitors are: 1) Coyote Lake, near Morgan Hill; 2) Bear Valley, near Hollister; 3) Turkey Flat, near Parkfield; 4) Adobe Mountain, near Palmdale; and 5) Pinon Flat U.S.G.S. observatory near Palm Springs.

Cultural noise, both narrow band and broadband is the main source of low frequency signal. Narrow band signals are mostly from marine related VLF transmissions above about 20 kHz. In addition, there are harmonics of 60 Hz from the electric power grid. Broadband signals result from several sources, but especially from automobile ignition systems. Of course, there is a continual lightning-induced low frequency background. Any EM emission associated with a seismically active area will most likely be broadband.

Laboratory measurements from cracking rocks are of broadband EM emission. All proposed mechanisms for EM earthquake precursors would result in broadband emissions. Finally, all reported EM precursors were presumed to be broadband emissions. Therefore, for maximum signal to noise ratio, we designed the receivers to be broadband with three bands recorded: 1) 200 Hz to 1 kHz, 2) 1 kHz to 10 kHz, 3) 10 kHz to 100 kHz. Each system uses a three-meter-long vertical monopole antenna referenced to a ground plane. Data is recorded continuously on a strip chart recorder and each station is battery powered.

The broadband capability helps to reduce variation in cultural noise, especially the narrow band (radio station) sources. Reported measurements of events indicate that a high sensitivity system is not required. Each channel has a 60 dB dynamic range (logarithmic amplifiers) recorded on the strip chart recorder. This is used because of its effectiveness, simplicity, reliability, and low cost.

The signal received by each station is very site specific. At some sites, the signal in all frequency bands is continuously highly variable on a time scale of a few hours. At other sites, the measured signal levels are nearly constant for periods of weeks at a time. The reason for this difference is unknown, but some sites may have high levels of cultural noise which would be variable in amplitude.

The largest earthquake on the San Andreas since deployment of our stations had an epicenter near Morgan Hill and occurred on April 24, 1984. Only the station at Coyote Lake was fully operational at the time of and immediately prior to this event. About six days prior to this event a prominent signal minimum which lasts about 28 hours was observed on the station at Coyote Lake. This minimum was recorded in the bands 200 Hz to 1 kHz and 1 kHz to 10 kHz, but the gain was improperly adjusted for the band 10 kHz to 100 kHz so that no data was collected in that frequency interval. The partial data available from the Adobe Mountain (Palmdale) site and the Turkey Flat (Parkfield) site do not show a signal strength reduction comparable to that seen at Coyote Lake (Morgan Hill). However, April 20, 1984, a decrease in ambient EM power similar to that seen at Morgan Hill was reported by Mr. Joe Tate at Sausalito, California, 120 km to the northwest of Morgan Hill (private communication, 1984).

It is tempting to make a connection between the anomalous EM signals seen at Morgan Hill and Sausalito and the earthquake a few days later at Morgan Hill. It is likely premature to make such a connection. On the other hand, the data are encouraging enough to warrant continued monitoring of EM power along the San Andreas until a more complete data set is collected.

Bibliography

Gokhberg, M. B., V. A. Morgounov, T. Yoshino, and I. Tomizawa, "Experimental Measurement of Electromagnetic Emissions Possibly Related to Earthquakes in Japan," J. Geophys. Res., 87, 7824, 1982.

Gokhberg, M. B., I. L. Gufeld, I. P. Dobrovolsky, and G. I. Shevtsov, "Studies of Mechanoelectric Effects under Laboratory Conditions," Preprint N 9, Acad. of Sci. of the U.S.S.R., Moscow, 1980.

Gokhberg, M. B., I. L. Gufeld, and I. P. Dobrovolsky, "On the Sources of Electromagnetic Earthquake Precursors," Preprint N 10, Acad. of Sci. of the U.S.S.R., Moscow, 1980.

Gokhberg, M. B., V. A. Morgounov, and T. Yoshino, "The Experimental Results of Appearance of Electromagnetic Emissions Related with Earthquake at Sugadaira Observatory in Japan," University of Electro-Communications, I - 5 - I.

Nitsan, U., "Electromagnetic Emission Accompanying Fracture of Quartz-Bearing Rocks," Geophys. Res. Letters, 4, 333, 1977.

Parrot, M. and F. Lefeuvre, "Study of VLF Emissions Apparently Associated with Earthquakes from Ground-Based and GEOS Satellite Data, Results of the ARCAD 3 Project and of the Recent Programmers in Magnetospheric and Ionospheric Physics," 2-25 Mai 1984, Toulouse, France, 1984.

Vorob'ev, A. A., "Electromagnetic Radiation in the Process of Crack Formation in Dielectrics," Difektoskopiya, No. 3, 128, 1977.

PIEZOMAGNETIC MONITORING IN THE SOUTH PACIFIC REGION

14-08-0001-22021

Michael T. Gladwin
Department of Physics
University of Queensland
St. Lucia
Australia 4067.

1. INVESTIGATIONS. An array of 25 remote magnetometer stations spaced on average 100km apart has previously been established during 1980-82 and operated successfully in the tectonically active South Pacific Islands of Vanuatu, the Solomons and Papua New Guinea (U.S.G.S Contract 14-08-00001-17771). Each station consists of a high stability (0.25nT) proton precession magnetometer sampled synchronously with the other stations every 5 minutes by a microprocessor controller. Along with diagnostics on the station performance (magnetometer signal strength and oscillator frequency, temperature, battery and solar and reserve power status, and controller diagnostics and printer status), this data is collected every three hours by a GOES satellite link, and also printed at each site on a backup printer (with 13 month capacity).

Owing to termination of funding for the maintenance of this array and processing of the data during 1983-84, the present period has been taken up with recovery and maintenance of the field stations, and recovery of station data. Typical recovered data from the 1983 period is shown in Figure 1.

A number of Vanuatu sites were dismantled, and the equipment installed at three additional sites in the Rabaul Harbour area, as part of the volcano monitoring network there. The city of Rabaul was placed on stage 2 alert for evacuation during 1984. Figure 2 shows the resulting data set from the Rabaul area. Stations RAB,MAT,BLU and TAV are within five kilometers of each other in the Rabaul Harbour area. The differences of the data sets from these stations show clear evidence of changes in the magnetic field of order of 2 - 5 nT localised to the RAB site. Noise on the MAT station differences is accounted for by cultural activity in the immediate vicinity.

LIST OF PUBLICATIONS

GLADWIN M.T.(1983) Piezomagnetic Monitoring in the South Pacific Region. I.U.G.G., XVIII General Assembly, Hamburg, August 1983, p. 143.

GLADWIN M.T.(1985) Piezomagnetic Monitoring in the South Pacific Region. Pageoph. (In Press)

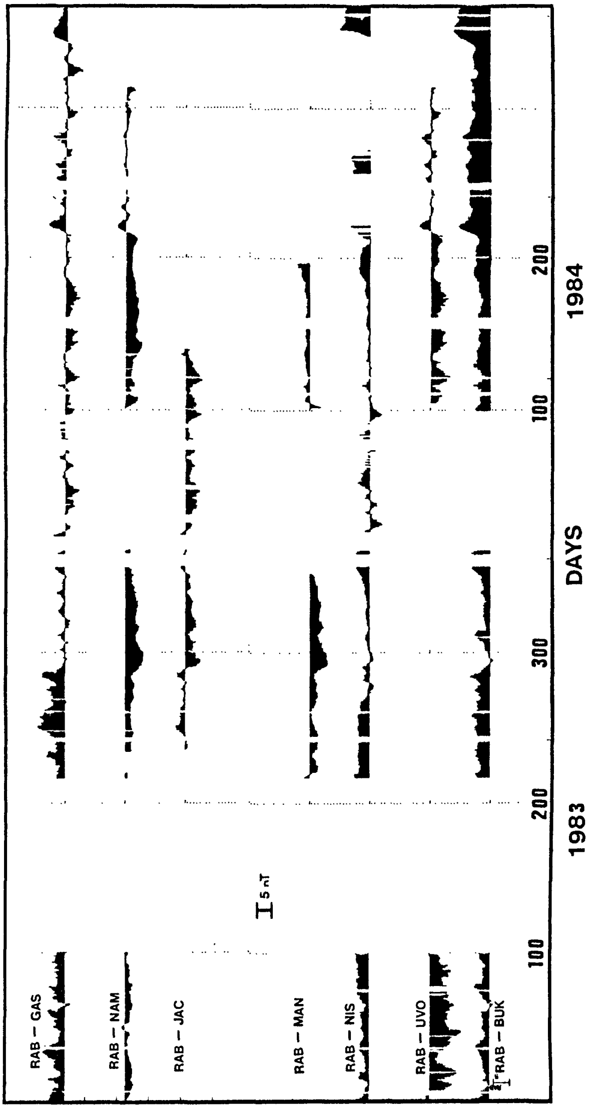

FIGURE 1. Typical station differences for the N.G./ Solomon Is. network during 1983-84. These are derived from a 5 day running average of data. Recovery of this data has not yet been completed. Changes in the RAB magnetic field on day 290,1983 and day 210,1984 will be examined in further reports.

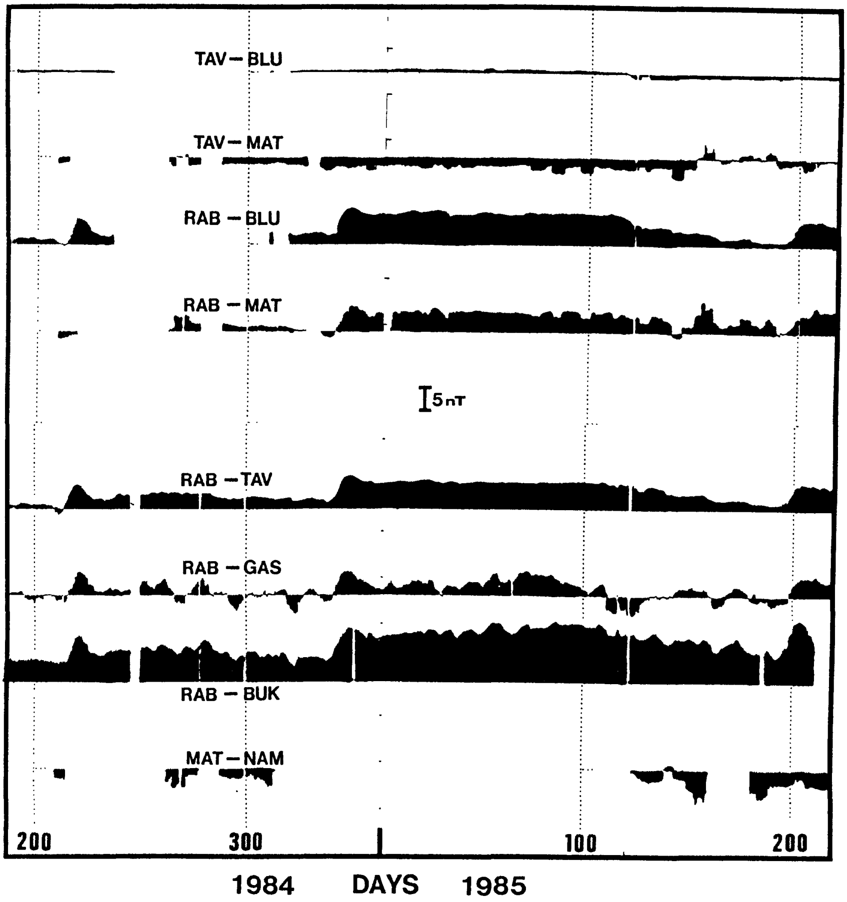

FIGURE 2. Station differences for the Rabaul network (stations RAB,MAT,TAV,BLU, all within 5 km of each other) and also the lower two plots show differences with stations UVO (200 km distant) and MAN (100 km distant). Significant changes in magnetic field at RAB and TAV are well determined and are probably stress related.

Quantitative Determination of the Detection History of the California Seismicity Catalog

14-08-0001-G-992

R. E. Habermann
School of Geophysical Sciences
Georgia Institute of Technology
Atlanta, Georgia 30332
(404) 894-2860

Many people have proposed that changes in seismicity rates can occur as part of the process of preparation for large earthquakes. Numerous rate changes can be observed in any seismicity data set. Most of these changes are not followed by large earthquakes and, therefore, are not precursors. If these changes are to be used as part of an earthquake prediction program, one must be able to distinguish between those that are possible precursors and those that are not. We have found that a great deal of information about seismicity changes can be obtained by examining the distribution of such changes in the magnitude domain. Plots which show this distribution are termed magnitude signatures. They are particularly useful for recognizing man-made changes in seismicity data.

Man-made changes in seismicity data can be broadly classed into two groups: detection changes and magnitude shifts. Both types of changes naturally divide seismicity data into groups of smaller and larger events. A detection change involves increases or decreases in the number of small events reported without much change in the number of larger events. A magnitude shift, a change in the magnitude assigned to a given event, causes changes with different signs in different magnitude bands. For instance, if the magnitudes of events decrease, magnitude bands with a lower cutoff will show rate decreases and magnitude bands with an upper cutoff will show rate increases. In order to recognize such changes, therefore, one must examine seismicity changes as a function of magnitude band. We use plots termed magnitude signatures for this purpose.

The different characteristics of the types of changes described above affect the appearance of magnitude signatures. These characteristics are summarized graphically in Figure 1 and described here.

DETECTION INCREASES

A schematic magnitude signature for this type of change is shown in Figure 1A. Detection increases are characterized by the following features:

- Increases (negative z-values) in the data sets which contain smaller events (on the left side of the plots).
- Lack of change (z-values near 0) in the data sets which contain larger events (on the right side of the plot).
- Negative z-values throughout the magnitude signature.
- A plateau of negative z-values in the data sets which contain the

larger small events (as you approach the center of the plot from the left).

DETECTION DECREASES

A schematic magnitude signature for this type of change is shown in Figure 1B. Detection decreases are characterized by the following features:

* Decreases (positive z-values) in the data sets which contain smaller events (on the left side of the plots).
* Lack of change (z-values near 0) in the data sets which contain larger events (on the right side of the plot).
* Positive z-values throughout the magnitude signature.
* A plateau of positive z-values in the data sets which contain the larger small events (as you approach the center of the plot from the left).

MAGNITUDE SHIFTS

A schematic magnitude signature for this type of change is shown in Figure 1C. A magnitude increase has the same characteristic appearance, but the signs of all the z-values are the opposite. The principle characteristic which identify magnitude shifts are:

* The occurrence of z-values of different signs in the magnitude signature.
* The occurrence of waves or other aberrations of the shape of normal detection related magnitude signatures.

The effects of detection changes can be taken care of by using a magnitude cutoff which eliminates the smaller events affected by the change. The magnitude cutoffs which would be appropriate are illustrated in Figure 1A and B. Magnitude shifts can be corrected for by using magnitude corrections, simply reversing the magnitude change.

MAN-MADE CHANGES AT PARKFIELD

The seismicity catalog for the Parkfield segment of the San Andreas Fault shows a rather simple detection history, probably because of it's remote location. A strong decrease in reported activity occurs at Parkfield during January 1978. This change is suspected to be related to the network operation because this time is the boundary between final and preliminary data. We have examined final data for the first six months of 1979 but that period of time is too short to make reasonable decisions about rate changes in larger events (which are necessary for assessing the reality of an observed change).

A second interesting change at Parkfield occurs during September 1980. The magnitudes of events reported near Parkfield at that time appear to decrease systematically by 0.15 units. This decrease is apparently related to two factors. First, a special study done by Lindh during the last several months of 1980 and second, the introduction of RTP coda measurements into the system between November 1980 and early 1981.

A number of real seismicity rate changes have been documented at

Parkfield. Several appear to be related to the sequence of large events there during 1975. Others are temporally related to the nearby Coalinga event.

MAN-MADE CHANGES IN THE CALAVERAS FAULT REGION

The seismicity catalog for the Calaveras region shows an extremely complex detection history. This may be due to the fact that this region is close to the center of the network and is therefore affected by almost any change in the network operation. The changes we have observed are listed in Table 1. The Table includes the amount of magnitude shift and the magnitude band affected, the repeat factor for the given range (<1 = detection decrease, >1 = detection increase) for each change.

Table 1. Observed Changes in the Calaveras Region.

	Shift		Repeat	
Date	Range	Amount	Range	Factor
29-Oct-69	0.0-1.40	-0.15	0.0-2.00	1.25
20-May-70	0.0-2.19	0.20	0.0-0.69	0.50
09-Sep-70	1.3-2.19	-0.20	0.0-1.19	0.50
12-Jan-72	0.8-2.19	-0.10	0.0-0.79	3.00
29-Nov-72	0.7-1.90	-0.15		
21-Mar-73	0.0-1.40	-0.20	0.0-2.00	2.00
12-Dec-73	No Synthetic Generated			
15-May-74	0.9-1.59	-0.10	0.0-1.10	0.50
21-Aug-74	0.0-1.29	0.10	ALL	2.50
11-Dec-74	1.6+	-0.30	0.0-1.39	0.50
30-Apr-75	1.1-1.79	-0.20		
11-Feb-76	1.0-2.50	0.20		
14-Apr-76	0.0-2.39	-0.20	0.0-1.29	0.50
15-Aug-79	No Synthetic Generated			
30-Jul-80	No Synthetic Generated			
26-Nov-80	2.0-2.49	-0.10	0.0-1.29	2.00
09-Sep-81	0.0-0.99	-0.30	0.0-1.59	0.50
04-May-83	0.9-1.79	-0.10	0.0-0.69	0.20
25-Jan-84	1.4-1.89	-0.10	0.0-1.10	2.00
11-Apr-84	No Synthetic Generated			

REPORTS

The Detection History of the Calaveras Fault: A Preliminary Assessment

The Detection History of the Parkfield Segment of the San Andreas Fault: A Preliminary Assessment

Man-Made Seismicity Changes

Construction of Synthetic Magnitude Signatures

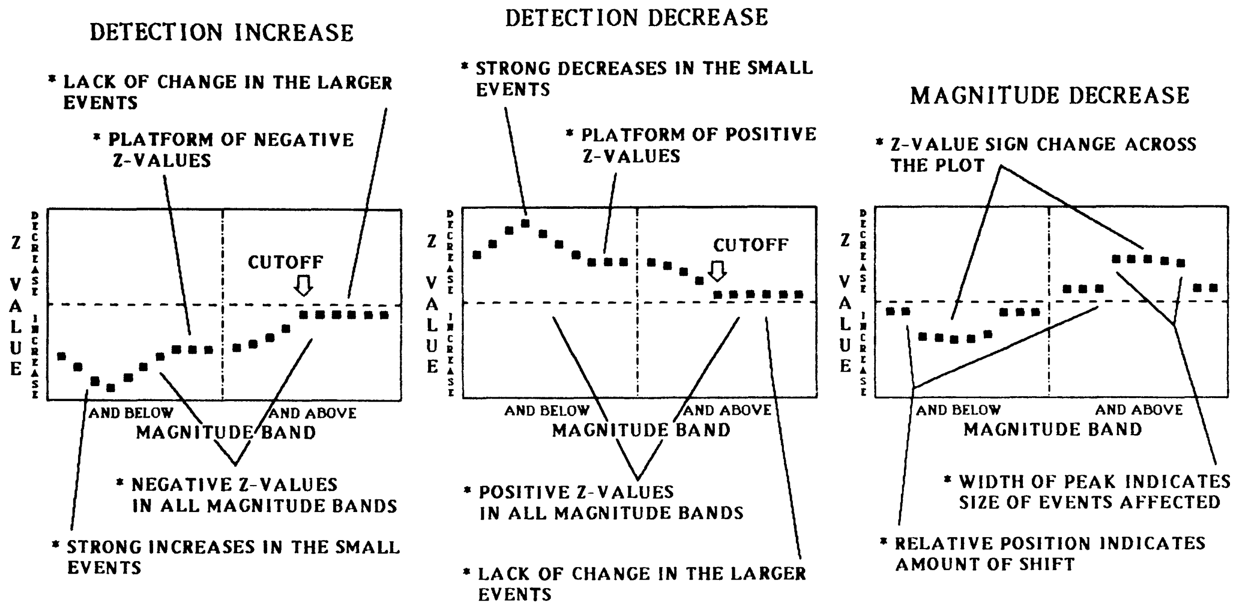

Figure 1. Magnitude signatures show the z-value which results from comparing rates during two time periods in various magnitude bands. Positive z-values indicate that the rate during the second period is lower than that during the first, rate decreases. Negative z-values indicate rate increases. The magnitude bands are arranged so that those on the left side of the plot are bounded by the upper limit given on the horizontal scale. For instance, the point above 2.0 on the left side of the plot gives the z-value for the magnitude band $M < 2.0$. The magnitude bands on the right side of the plot are bounded by the lower limit given on the horizontal scale. For instance, the point above 2.0 on the right side of the plot gives the z-value for the magnitude band $M \geq 2.0$. This division divides each magnitude signature into four quadrants. The three major types of man-made seismicity changes have different characteristic appearances in magnitude signatures as shown in this Figure.

Analysis of Earthquake Data from the Greater Los Angeles Basin and Adjacent Offshore Area, Southern California

#14-08-0001-G-983

Egill Hauksson
Ta-liang Teng
Geoffrey Saldivar
Center for Earth Sciences
University of Southern California
Los Angeles, CA 90089-0741
(213) 743-7007

INVESTIGATIONS

We are analyzing earthquake data recorded by the USC and CIT/USGS networks during the last 11 years in the Los Angeles basin. Below we present some of the preliminary results of seismotectonic analysis of recent earthquakes along the Newport-Inglewood fault zone which cuts across the eastern half of the Los Angeles basin. We also present some results from our analysis of the 1979 New Year's Day, Malibu earthquake (M_L=5.0) and its aftershocks.

RESULTS

The main results of this study consist of improved earthquake locations that can be used to infer the tectonic structure and the mode of strain release along faults in the Los Angeles basin. Further, the set of fault plane solutions provides new insight about the state of stress around the major faults and forms the basis for a seismotectonic interpretation.

Newport-Inglewood fault. The recalculated hypocenters are shown in Figure 1. Earthquakes of magnitude between 3.0 and 4.0 are shown as large symbols. The epicenters are scattered in space mainly to the east of the southern section of the Newport-Inglewood fault. Along the northern end of the fault most of the seismicity falls within the width of the fault zone. The Newport-Inglewood fault is considered to be locked and the occurrence of small earthquakes off the fault reflects accumulation of elastic strain around the fault that leads to brittle failure on favorably oriented small scale faults.

The majority of the fault plane solutions determined for earthquakes along the Newport-Inglewood fault show reverse faulting on steeping dipping planes. A few solutions show right lateral strike-slip motion.

Fault plane solutions determined for the southern section of the NIF are shown in Figure 1. These are lower hemisphere equal area mechanisms. The black quadrants indicate regions of tension (the position of the tension or T-axis is indicated by an open small circle) and the white quadrants represent regions of compression (the position of the maximum compression or P-axis is similarly indicated by a filled small circle).

The strike-slip solutions that are located near the surface trace of the NIF itself are shown in the center lower section of Figure 1 (e.g. solutions number 4,8,15,17 and 20). Toward the right and above in Figure 1, we show reverse mechanisms, which in most cases have steeply dipping planes. Most of these earthquakes have magnitudes in the range 2.9-3.7 and the variability in the orientation of the nodal planes may reflect real variations in the fault structure as well as the accuracy with which we can determine these solutions. No obvious depth dependence on the type of faulting was found. Locally, in some cases, we appear to have similar solutions (e.g. solutions number 23,24 and 26) and (e.g. 2 and 28).

The numerous earthquake focal mechanisms of events located on small subsidiary faults several kilometers away from the NIF itself remain mostly unexplained so far. Clusters of events in the Baldwin Hills, south of Newport Beach and the northeast of Long Beach show both strike-slip and reverse faulting occurring within a spatially limited area. These focal mechanisms could be indicative of block rotations or heterogeneous material properties that permit faulting along an ensemble of planes of weaknesses with different strike and slip.

The Malibu earthquake (M=5.0) that occurred near the western offshore extension of the Santa Monica fault was located at 33°N 57.8' and 118°W 41.1 and at a depth of 9 km. The fault plane solution of the mainshock as determined from first motions recorded by short period high-gain seismic stations in southern California shows a thrusting mechanism with one plane dipping 55-60° to the north striking 285-290° or west-northwest, and the second plane dipping 30-36° to the south and striking 90-100 ° or east-west (Figure 2). More than 400 aftershocks were recorded during 1979. Fault plane solutions for most of the 21 aftershocks of $M>3.0$ show a similar thrusting mechanism as the mainshock (Figure 2). The mainshock and the aftershocks were relocated using a velocity model by Corbett (1984) and a set of station delays. The aftershocks of $M>2.5$ form a diffuse zone of scattered activity between depths of 3-10 km with a lateral extent of 6 km (Figure 2). The spatial scatter of the aftershocks may result from the sparse station distribution in this coastal region.

REPORTS

Hauksson, E. and G. Saldivar, Recent seismicity (1970-1984) along the Newport-Inglewood fault, Los Angeles Basin, southern California, EOS, vol. 65, no. 45, p. 996, 1984.

Hauksson, E., T. L. Teng, T. L. Henyey, J. K. McRaney, L. Hsu and G. Saldivar, Earthquake Hazard Research in the Los Angeles Basin and its Offshore Area, U.S.C. Geophysics Laboratory Technical Report #8501, 1985.

Hauksson, E., T. L. Teng and J. McRaney, The Santa Barbara Channel Easter Swarm of April 1984, USGS Semi-Annual Data Review Meeting in Santa Barbara, California, September, 1984.

Saldivar, G., E. Hauksson and T. L. Teng, The Malibu Earthquake (M=5.0) and Its Aftershock Sequence, Southern California, January, 1979, submitted to AGU Fall Meeting, 1985.

Hauksson, E., Constraints on the Velocity Structure of the Crust in the Los Angeles Basin and the Central Transverse Ranges, Southern California, submitted to AGU Fall Meeting, 1985.

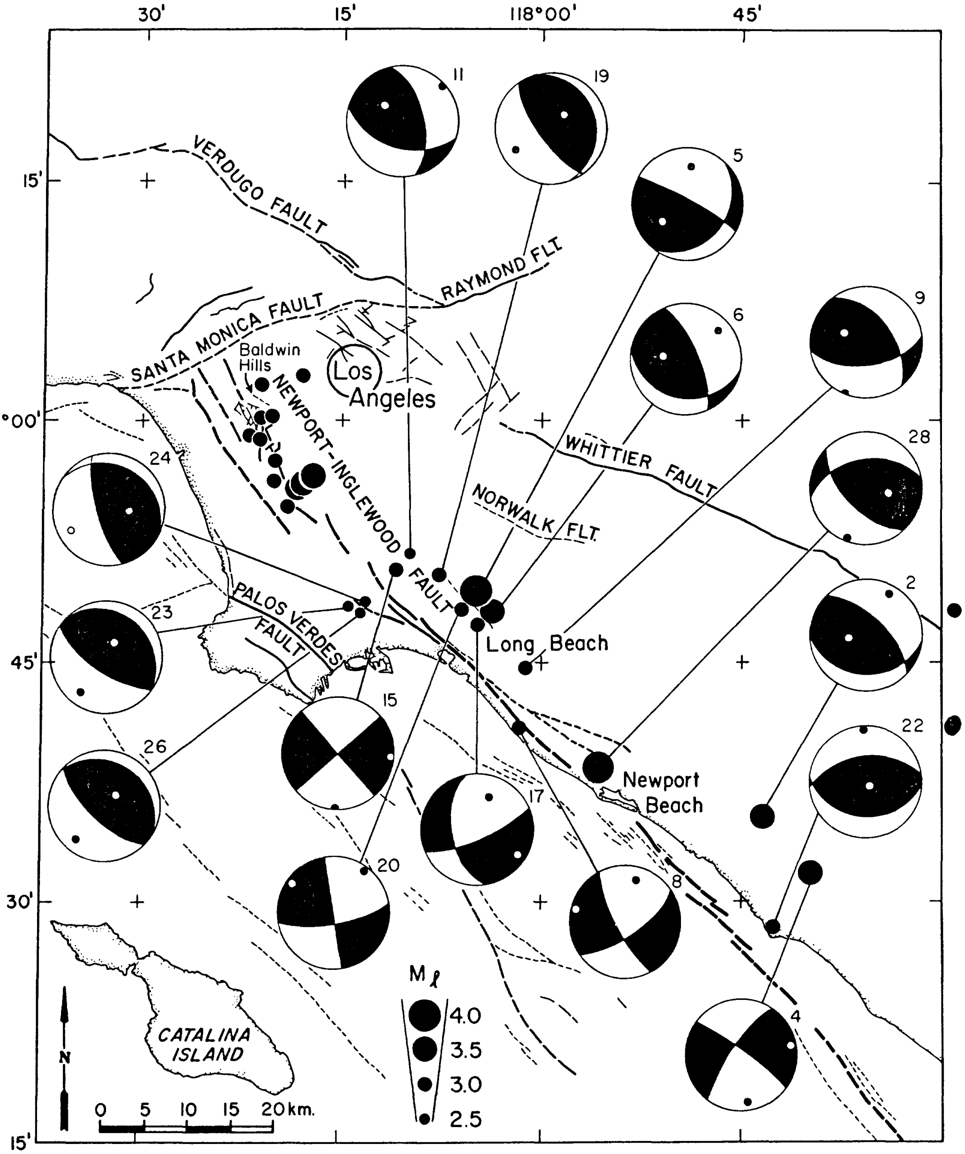

Figure 1. Single event lower hemisphere fault plane solutions for earthquakes along the southern section of the Newport-Inglewood fault.

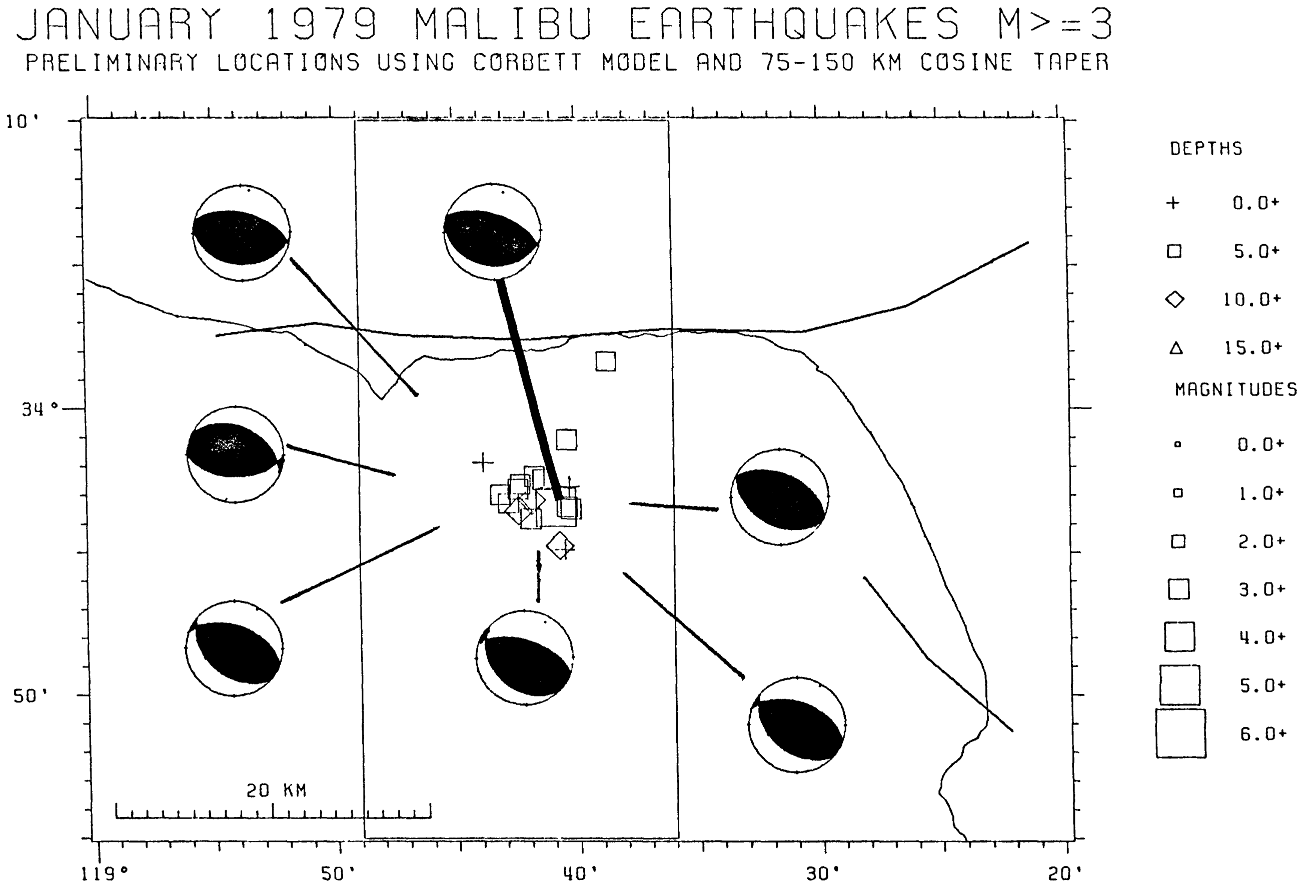

Figure 2. Epicenters and fault plane solutions for the January 1979 Malibu earthquake (M=5.0) and its aftershocks.

SEARCH FOR PRECURSORS TO EARTHQUAKES IN THE VANUATU ISLAND ARC BY MONITORING TILT AND SEISMICITY

14-08-0001-18350

Bryan L. Isacks
Department of Geological Sciences
Cornell University
Ithaca, NY 14853
(607)256-2307

Investigations

This report covers the period April 1, 1985 to September 31, 1985 for the operation and analysis of data from the Vanuatu (New Hebrides) seismograph and tilt networks. The networks include twenty stations distributed along 500 km of the arc, seven bubble level tiltmeter stations, two periodically releveled arrays of benchmarks (1 km aperature), and a 100 m two-component water tube tiltmeter.

Results

1. The most important earthquakes caught by the local network have occurred in a series of complex but spatially coherent sequences located in the interplate boundary west and northwest Efate island. The sequences included one magnitude (Ms) 7.1 earthquakeon July 15, 1981, the largest event caught so far, and 10 moderately large events (Ms = 5.8-6.4). The locations of these events and the associated aftershock zones and clusters of small events strongly concentrate in several specific areas that may be the sites of the controlling asperities in this part of the interplate boundary. The most concentrated and persistently active areas are located in the structurally complex zone of transition between the Southern New Hebrides island arc and the complex central New Hebrides region. Sequences in 1978-1979 and 1981 formed a coherent space-time pattern that we can interpret as the progressive partial rupture of two asperities. Sequences in 1983 expanded the area activated during the previous sequences, but also reactivated the two main asperities.

After a nearly two year period of relative quiescence the region northwest of Efate was again activated during the the past six months. On July 3, 1985 a magnitude (Ms) 6.4 earthquake occurred near the epicenterof the large earthquake of July 15, 1981, at a location about 20 km arc-ward (and probably down-dip) of the 1981 hypocenter. This position is coincident with the northern edge of the zone of the very intense concentration of seismicity located northeast of Efate island. The aftershock zone of this event defined by the local network occurred up-dip of the epicenter and reactivated the asperities defined by the previous 1978-1981 sequences.

The picture that is emerging from the now seven year sample of seismicity is a highly heterogeneous spatial distribution of seismicity characterized by repeated activation of very specific areas of the interplate boundary and of adjacent interplate regions. Work is underway to define better the spatial extent and structure of the zones of these discrete zones to determine if exactly the same area is activated of if there is a very fine scaled progressive development of seismicity that can be resolved by careful re-analysis of the arrival time data.

An interesting pattern is developing in the seismicity farther north of the 1978-1985 sequences, near southern Malekula and Epi islands. This is the region of the interplate boundary "between" the rupture zones of the 1965 central New Hebrides sequence and the July, 1981 earthquake. An outstanding question in our project is whether this region is a "capable" seismic gap. In contrast to the Efate region this area has been remarkably quiet during the past seven years. The region now appears to have been clearly activated by the July, 1981 earthquake. Late aftershocks occurring during several months following the shock define several clusters beneath southern Malekula and two linear zones located south of Malekula. These zones are near the northern end of the aftershock zone of the July, 1981 earthquake.Both zones have a strike nearly perpendicular to the arc. A third linear zone with a strike also perpendicular to the arc was defined by a cluster in 1984, while in May, 1985 the second linear zone was reactivated in an aftershock sequence of a magnitude (mb) 4.6 earthquake.

The linear trends are sub-parallel to the southern end of the westwardly protruding Santo-Malekula block of the central New Hebrides island arc. Study of the locations is underway to determine the tectonic significance of these zones. The depths of a number of earthquakes in the western or "trenchward" parts of these zones are calculated to be in the range of 50-80 km, which would place the events in the lower part of the lithosphere of the sub-oceanic plate. However, a detailed study of these events done in cooperation with S. Roecker (MIT) shows that locations in this particular region are characterized by a double minimum in the variation of RMS residual as a function of depth, one shallow and one deep. This demonstrates a weakness of the network in controlling depth for the western parts of the zones.

2. The seismic and tilt networks continued operation through the period without major problems. The Cromemco Z-80 based tape recording system was completed at Cornell during June and July. Additional software was developed to make this system operate with the event-recording system already in operation. The tape recording system will operate in parallel with the analog recording system and will thus offer a additional level of redundancy. Both systems record the analog signal sent across the telemetry network. A staff member from ORSTOM visited Cornell for the final assembly and testing, and the system started operation in late September.

Reports

Marthelot, J.-M., J.-L. Chatelain, B. L. Isacks, R. K. Cardwell, E. Coudert, 1985, Seismicity and Attenuation in the Central Vanuatu (New Hebrides) Islands: A New Interpretation of the Effect of Subducting the D'Entrecasteaux Fracture Zone, J. Geophys. Res., 90, (in press).

Chatelain, J.-L., B.L. Isacks, R.K. Cardwell, R. Prevot, and M. Bevis, 1985, Patterns of seismicity associated with a magnitude 7 earthquake in the central New Hebrides island arc, submitted to J. of Geophysical Research.

Chatelain, J.-L., B.L. Isacks, R. Prevot, 1985, Detailed study of a moderate size earthquake episode in the central New Hebrides island arc, (Abstr.), EOS, 66, 298.

Instrument Development and Quality Control

9930-01726

E. Gray Jensen
Branch of Seismology
U.S. Geological Survey
345 Middlefield Road - Mail Stop 977
Menlo Park, California 94025
(415) 323-8111, Ext. 2050

Investigations

This project supports other projects in the Office of Earthquake, Volcanoes and Engineering by designing and developing new instrumentation and be evaluating and improving existing equipment in order to maintain high quality in the data acquired by the Office.

Results

Expansion of the CALNET microwave is continuing. During this time a microwave repair station was completed in Menlo Park. Development also proceeded on improved discriminators with higher dynamic range and sharp cutoff digital filters. Samples of the new J502 VCO and V02L VCO were installed in Yellowstone.

New computer programs were received and slightly modified to aid schematic drawing and printed circuit board layout.

Ongoing projects included maintenance and calibration of VCO's, radios and seismometers for use in Continental US, Alaska and the USSR. Additional parts for the maintenance of PDR-2 recorders were sent to the P.R.C. (China).

SOUTHERN CALIFORNIA COOPERATIVE SEISMIC NETWORK

9930-01174

Carl E. Johnson
Branch of Seismology
U.S. Geological Survey
Seismological Laboratory 252-21
Pasadena, California 91125

INVESTIGATIONS

1. Southern California Network Operations
Operations and maintenance of the southern California seismic network continued through the reporting period without significant failure. At present 248 predominantly short-period, vertical instruments are telemetered to Caltech for analysis.

2. Routine Network Analysis
Routine processing using stations of the southern California cooperative seismic network was continued for the period April 1985 through September 1985. Routine analysis in cooperation with Caltech personnel includes the interactive timing of phases, event location, magnitude calculation, and final catalog production using the CUSP analysis system. At present 2000 events detected each month are being analyzed in this manner with a regional magnitude threshold approaching 1.2.

3. HVO CUSP
Full off-line analysis capability was added to the real-time component running on the dual VAX 11/750 CUSP installation being operated by the Hawaiian Volcano Observatory. This system now provides automatic P-picking and preliminary locations following event detection. Real-time detection and event capture processing requires less than 6% of the available CPU time on the VAX 11/750, leaving the remainder for background and interactive analysis. Background processing running on the on-line computer includes automatic coda analysis, demultiplexing, trace winnowing, magnitude calculation, record archiving, and procedures for managing and accessing the event, phase, and trace relational data base. The usual interactive graphical tools are also available. During the evaluation period which is now in progress, CUSP has been detecting and processing in excess of 50 events per day with a false trigger rate of less than 10%, largely due to the density of the island network. A substantially higher detection rate is possible, but is currently suppressed by network sensitivity parameters. This compares to roughly 5 events being processed each day using traditional methods.

4. Locations and Lateral Heterogeneity
In order to educe the effect of basins and troughs on earthquake location methods, a program has been developed that permits the calculation of exact travel-times for events in a particular class of laterally heterogeneous crustal models. In particular, travel-times can be determined for layered spheres and layered cylinders embedded to

arbitrary depths in a layered half space. Such models are good analogs for deep basins and structural troughs. The results are being used to evaluate common earthquake locations methodologies as generally applied to structurally complex situations.

5. Focal Mechanisms and the State of Stress on the Southern San Andreas Fault

The state of stress on the southern San Andreas fault is being analyzed from focal mechanisms of small earthquakes with epicenters within 10 km of the active trace of the fault from Parkfield to the Salton Sea. Particular attention is being paid to the Cajon Pass region where the San Jacinto fault intersects the San Andreas. Relocations of all $M \geq 2.6$ earthquakes between 1978 and 1985 along the fault, are being calculated for a more accurate depth determination and focal mechanisms are being determined for all of these events. The focal mechanisms are being compared to local seismogenic structures and analyzed for information about the state of stress using the techniques of Angelier.

6. Foreshocks in Southern California

Analysis of the characteristics of immediate foreshocks those that occur within hours or days of their mainshocks in southern California is continuing. The probability as a funtion of magnitude that an earthquake will be a foreshock has been determined and the variation in that probability as multiple events occur is now being analyzed. Site-specific probabilities are also examined, especially for the Parkfield region. The results are applied to time dependent earthquake hazard assessment.

RESULTS

1. Focal Mechanisms and the State of Stress on the Southern San Andreas Fault

Preliminary results show that three distinct stress regimes can be recognized on the southern San Andreas - the Carrizo Plains, Mojave and San Gorgonio sections. The Carrizo Plains section, from Parkfield to Fort Tejon, has very few earthquakes and focal mechanisms that consistently show right lateral strike-slip parallel to the plate motion vector (N40°W). The Mojave section, from Fort Tejon to Cajon Pass, has a slightly higher rate of seismic activity and mechanisms that predominately show oblique thrusting subparallel to the local strike of the San Andreas (N60°W). The San Gorgonio section, from Cajon Pass to the Salton Sea, has the highest rate of seismicity and right lateral strike-slip and oblique normal faulting both parallel to the plate motion vector but not parallel to the local strike of the San Andreas (N60°W). Inverting the focal mechanism data for the stress tensor using the method of Angelier (1984) shows that all three regions have a horizontal, north-south striking, maximum principal stress, a vertical intermediate principal stress and a horizontal, east-west striking minimum principal stress.

2. Foreshocks in Southern California

The probability that a $M \geq 5.0$ earthquake near Middle Mountain on the

San Andreas fault will be followed within 5 days by a characteristic Parkfield earthquake is estimated to be 80% ± 40%. The probability that the Parkfield earthquake will occur within 1 hour of the possible foreshock is approximately 20% and decays as time$^{-0.9}$ with elapsed time after the possible foreshock. The probabilities that the Parkfield earthquake will occur within 5 days after a M = 2.0, M = 3.0, or M = 4.0 earthquake at Middle Mountain are estimated to be 5%, 18%, and 40%, respectively. These numbers are based on a statistical study of the earthquakes recorded in the Parkfield area since 1932.

Reports

1. Jones, L.M., Seismotectonics of the Cajon Pass region of the southern San Andres fault, *Trans. Amer. Geophys. U.*, *66*, p. 383, 1985.
2. Jones, L.M., Focal mechanisms and the state of stress in the San Andreas fault in southern California, *Trans. Amer. Geophys. U.*, in press, 1985.

Seismic Study on Rupture Mode of Seismic Gaps

Contract No. 14-08-0001-G-979

Hiroo Kanamori
Seismological Laboratory, California Institute of Technology
Pasadena, California 91125 (818-356-6914)

Investigations

1) The mechanism of the March 3, 1985, Valparaiso, Chile, earthquake

2) Earthquake Sequences in the Southeastern Solomon Islands

Results

1) The mechanism of the March 3, 1985, Valparaiso, Chile, earthquake

We determined the mechanism of the 1985 Valparaiso, Chile, earthquake using the long-period Rayleigh waves recorded by the IDA stations. Eight stations (HAL, ALE, ESK, GUA, KIP, SUR, PFO, CMO) and 16 Rayleigh phases are used. The spectral data at a period of 256 sec are inverted using the method described by Kanamori and Given(1981) to obtain the source parameters. We corrected the phase data for the phase delay due to the lateral heterogeneity of the earth. For this correction, we used the earth model M84C obtained by Woodhouse and Dziewonski (1984). First, we inverted the data with a constant source process time of 40 sec. The result of this inversion showed a systematic azimuthal variation of phase indicating an overall rupture propagation to the south. A unilateral rupture model with a rupture length of 170 to 250 km and the corresponding rupture velocity of 2 to 3 km/sec adequately explain this azimuthal variation. The inclusion of lateral heterogeneity and the unilateral rupture propagation reduced the variance of inversion by 46% with respect to the case with a laterally homogeneous model and the constant source delay. However, since there is some trade off between the rupture velocity and the lateral heterogeneity, the rupture length determined above is subject to some uncertainty.

Since the dip angle cannot be determined well in this type of inversion, we constrained it to be 20 degrees. The result is summarized in Table 1. Figure 1 shows a schematic diagram of the rupture zone and the mechanism diagram. The seismic moment is 1.2×10^{28} dyne-cm ($M_w=8.0$). If the dip angle differs from 20 degrees, the above value of the seismic moment should be multiplied by $\sin(20^\circ)/\sin\delta$, where δ is the dip angle.

We are planning to perform a more detailed analysis as more data become available to us.

2) Earthquake Sequences in the Southeastern Solomon Islands
(Wesnousky, Astiz, Kanamori)

The 350-km stretch of the Solomons Islands Trench that lies adjacent to the islands of Gaudalcanal and San Cristobal has been the site of 10 large shallow earthquakes since 1966: an earthquake doublet (June 15, 1966, Ms=7.5,7.3), a quadruplet (May 20,21, 1977, Ms=6.7,7.5,7.5,7.5), a doublet (November 4,5, 1979, Ms=6.9,7.1), and two single events (October 23, 1979, Ms=7.1 and February 7,1984, Ms=7.7). The depth distribution and source complexity of these events are examined by modeling WWSSN long-period P-waveforms. The close temporal association and large size of earthquakes precludes collection of P-waveforms for the latter of the two 1966 earthquakes and the 2nd and 3rd events of the 1977 sequence. Waveforms recovered for the remaining events are consistent with thrust mechanisms and generally show smooth traces that can be modeled with simple trapezoidal source-time functions, with the exceptions of the November 4, 1978 event (preceded by a small subevent several seconds prior to the main shock) and the P-waveforms of the February 7, 1984 event which exhibit relatively higher frequency energy. Earthquake depths range from 15 to 45 km. The depths of the June 15, 1966 and February 7, 1984 earthquakes are 38 km and 25 km, respectively. Each event in the 1978 doublet is located at 15 km depth. In contrast, the final shocks in each of the 1977 and 1979 sequences occur at greater depths (45 km and 25 km, respectively) than the corresponding initial events (each 15 km). Combination of the P-waveforms with IDA Rayleigh wave data available for the 1978, 1979, and 1984 sequences further indicates that northward thrusting of the Indian plate beneath this portion of the Solomon Islands is also accompanied by a significant component of left-lateral motion.

Table 1 March 3, 1983, Valparaiso
Depth (assumed) = 16 km

Seismic Moment	Nodal Plane 1			Nodal Plane 2		
	dip	slip	strike	dip	slip	strike
1. 2 x 10^{28} dyne-cm	70°	90°	177°	20°	90°	-3°

Rupture Length	170 to 250 km
Rupture Velocity	2 to 3 km/sec

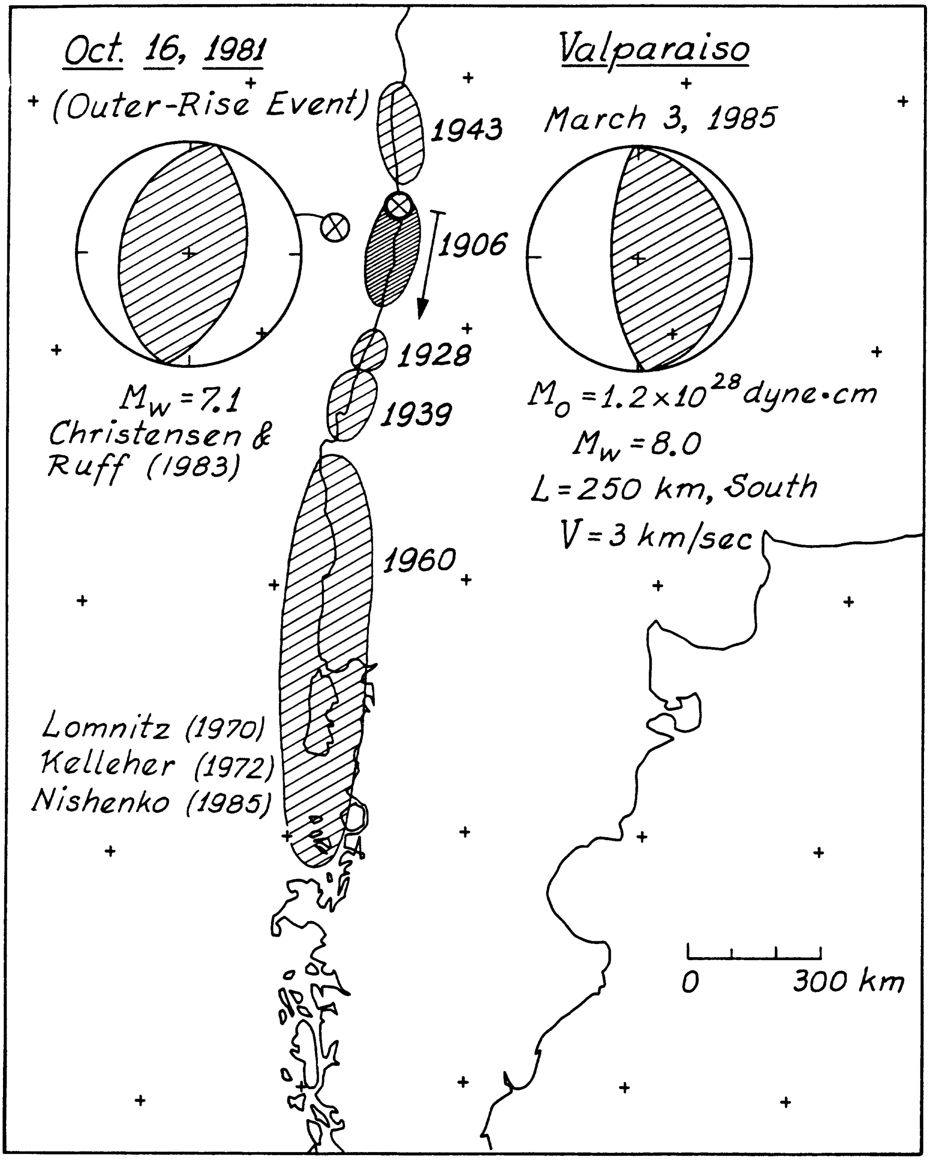

Figure 1.

The mechanism of the 1985 Valparaiso, Chile, earthquake and the rupture zones of large earthquakes along the Chilean coast. The mechanism of a compressional outer-rise event is also shown.

FAULT MECHANICS AND CHEMISTRY

9960-01485

C.-Y. King
Branch of Tectonophysics
U.S. Geological Survey
345 Middlefield Road, MS/977
Menlo Park, California 94025
(415) 323-8111, ext. 2706

Investigations

1. Water temperature and radon content were continuously monitored at three water wells in San Juan Bautista and Parkfield, California.

2. Water level was continuously recorded at six other wells.

3. Water samples were periodically taken from most of these wells for chemical analyses.

4. Radon content of ground gas was continuously monitored at two sites (Limekiln A and Cienega Winery) along the San Andreas fault in the Bear Valley area, California, and at a site in Nevada Test Site.

5. Slip events generated along a laboratory fault were studied.

6. Most of this period was used to edit three special collections of papers.

Results

A special collection of 32 papers on "Earthquake Hydrology and Chemistry" has been published in Pure and Applied Geophysics, volume 122, 1984/85, and as a book.

Reports

King, C.-Y., 1985, Radon monitoring for earthquake prediction in China: Earthquake Prediction Research, v. 3, p. 47-68.

King, C.-Y., 1984/85, Earthquake hydrology and chemistry, editor's note: Pure and Applied Geophysics, v. 122, p. 141-142.

King, C.-Y., 1984/85, Impulsive radon emanation on a creeping segment of the San Andreas fault, California: Pure and Applied Geophysics, v. 122, p. 340-352.

Prediction Methodology for Subduction Zone Earthquakes
Central Aleutian Islands

Grant Number 14-08-0001-G-881

Carl Kisslinger and Selena Billington
Cooperative Institute for Research in Environmental Sciences
Campus Box 449, University of Colorado
Boulder, Colorado 80309
(303) 492-8028

The research during April - September, 1985 was focused on 1) temporal variations in the seismicity rates in subregions of the Adak seismic zone, as shown by both the teleseismic and local earthquake catalogues; 2) systematic survey of stress regime in the zone from spectral analysis of microearthquakes, and 3) a search for temporal variations in focal mechanisms in the vicinity of the identified asperity on the main thrust zone on the basis of the patterns of first P-motion polarities.

Temporal Variations in Seismicity Rates

The pronounced reduction in the rate of occurrence of earthquakes located with the Central Aleutians Seismic Network that began in September, 1982, has been compared to the rates revealed by the events reported in the NEIC PDE file. Both the Adak catalogue and the PDE hypocener file were purged of aftershocks and swarms by a simple algorithm, lower magnitude cuts of M_D 2.3 and m_b 4.5 were applied to the two lists, respectively, and depth cutoffs of 75 km and 100 km imposed. The location bias in the teleseismic catalogue caused by the well-known effects of the downgoing, high-velocity subducting slab was approximately removed by shifting the PDE epicenters by the mean longitude bias known from previous studies (0.18° to the east), and assuming that any event shallower than 100 km in a given longitude range has occurred on the main thrust zone. The zone from 175° W to 178.5° W was divided into five strips on the basis of bathymetric features and recognized differences in seismicity patterns, Fig. 1. These were labeled: West, Adak Canyon, SW2, Central, and East. The West region, which lies mostly in the Delarof Island block, was analyzed, but eliminated from further consideration now because the teleseismic data show that it is not involved in the current quiescence.

The activation in subregion SW2, previously discussed in detail, is clearly shown in the teleseismic data, Fig. 2. The mean rate of occurrence of independent events above m_b 4.5 in the thrust zone has been 0.4/quarter for the 91 quarters from the beginning of 1963 through the third quarter of 1985. During 1976 through the second quarter of 1980, the rate was 0.28/quarter, and SW2 had been identified as not very active. From July, 1980 through September, 1985, the rate has been 0.52/quarter. The local data, on the other hand, show a modest but distinct decrease in activity beginning in September, 1982. The conclusion is that the already low b-value in SW2 (0.7), has dropped to an even lower value.

If the SW2 data are excluded, the most of the zone shows, in the PDE data, the quiescence noted in the local data. For example, in the Central region, 175.38° W - 176.50° W, the most active of these subregions, the rate for the 91 quarters, 1963-1985.3, was 0.79 ± 1.00 per quarter. In the third quarter of 1982, the rate changed from 1.18 ± 1.14 during the preceding 22 quarters to 0.42 ± 0.67 per quarter for the following 12 quarters. This rate change is significant at better than the 95% confidence level by the standard t-test. The onset of this change agrees in time very well with the beginning of quiescence in the local data set. When all of the subregions exclusive of SW2 are combined, the quiescence is not so obvious because of the differences in starting time at different places. The increase in teleseisms in the Adak Canyon region, figure 2, is all in the eastern part of that region and is probably part of the activation of SW2.

The principal conclusions of the study so far are: (1) the quiescence in the Adak zone first identified in the fall of 1982 is a real and persistent geological phenomenon; (2) teleseismic catalogues can be used for high-resolution studies of seismicity patterns, but there are problems with mislocation biases and statistical evaluation, because of the small number of total evens for a small geographical region; (3) the temporal variations in earthquakes rates detected in the Adak zone are not uniform across the whole zone, but begin and end at different times that apparently related to differences in the very localized tectonic regime; and (4) the hypothesis that a strong earthquake, magnitude 7 or greater, is likely to occur in Adak Canyon before the end of October, 1985, is sufficiently supported by the totality of the data that it must be fully tested and the results evaluated, whatever they might be.

There has not been a single teleseismically locatable earthquake (m_b greater than about 4) within the defined quiescent zone since May 27, 1985. This behavior can be compared with the average rate of 8.3 ± 4.1 per year for the same region for the preceding 22.75 years.

Systematic Monitoring of the Stress Regime

In a published study of SW2 we demonstrated the value of spectral analysis of the local network seismograms for monitoring the stress state at selected places within the seismic zone. Our long-term goal is to evaluate the space-time patterns of stress drops, or apparent stresses, for the whole zone as time passes. We have started on the analysis of the East subregion since 1981, and will eventually have documentation for all of the thrust zone monitored by the Adak network.

The data for the East subregion so far analyzed have not shown any clustering in time or space of high or low stresses that would be interesting in terms of fault processes.

First Motion Pattern Studies

During the first years of the analysis of data from the Adak seismographic network, the region was partitioned into small subregions, primarily to allow the use of station corrections in the routine location of hypocenters. In light of the recent interest in the subregion SW2 as the site of a recently activated asperity (Bowman and Kisslinger, 1985) and as the possible site for the triggering of a major earthquake sometime soon (Kisslinger *et al.*, 1985), P-wave first-motion data in the subregions immediately around and including SW2, as recorded by the Adak network, have been examined to try to characterize the focal mechanisms of small earthquakes there.

A description of the method used to generate composite focal mechanism information has been published by us previously. The method is based on a comparison of all available P-wave first-motion data from a group of earthquakes in a small geographic region with all possible patterns of first motion observable with a network of stations.

(For a network of 13 stations, for example, each of which could record either a dilatational or compressional first motion, there are 2^{13} possible patterns of first motion.) The patterns of first motion which match the largest number of available first-motion data are then examined for compatibility with a double couple solution, for representative take-off angles and azimuths of rays on a focal sphere for the small region.

Ten years of local-network data were examined in each of the subregions around SW2. In each of the subregions, two patterns of first motion stood out in the analysis -- one (pattern I) which corresponds to dilatations recorded at each local station (a thrust mechanism) and a second one which was unique to each subregion (collectively called pattern II). The second patterns differ one from another, but when examined on focal spheres they turn out to apparently represent the same focal mechanism. Only one nodal plane is defined in each case, and in each case it is the same nodal plane, that of a thrust plane dipping northwest. The distributions in space and time of events which had data fitting each of the selected patterns were examined. In one of the subregions (SW1) there was a change in predominant focal mechanism from I to II in July, 1983. In the other subregions there are not enough first-motion data to distinguish between events fitting pattern I and those fitting pattern II so as to establish a temporal change.

Recent Publications Based on the Research

Bowman, J.R. and C. Kisslinger, Seismicity associated with a cluster of earthquakes of $m_b \geqslant 4.5$ near Adak, Alaska: Evidence for an asperity?, *Bull. Seism. Soc. Amer.*, *75*, 223-236, 1985.

Engdahl, E. R., and S. Billington, Focal depth determination of central Aleutian earthquakes, in press, *Bull. Seism. Soc. Amer.*, 1986.

Kisslinger, C., C. McDonald and J. R. Bowman, Precursory time-space patterns of seismicity and their relation to fault processes in the central Aleutian Islands, *Programme and Abstracts of IUGG, XXIII General Assembly*, 1985.

Silliman, A. H., and S. Billington, Seismicity associated with a recent earthquake of m_b 5.8 beneath Adak Canyon, central Aleutian Islands, in press, *Bull. Seism. Soc. Amer.*, 1985.

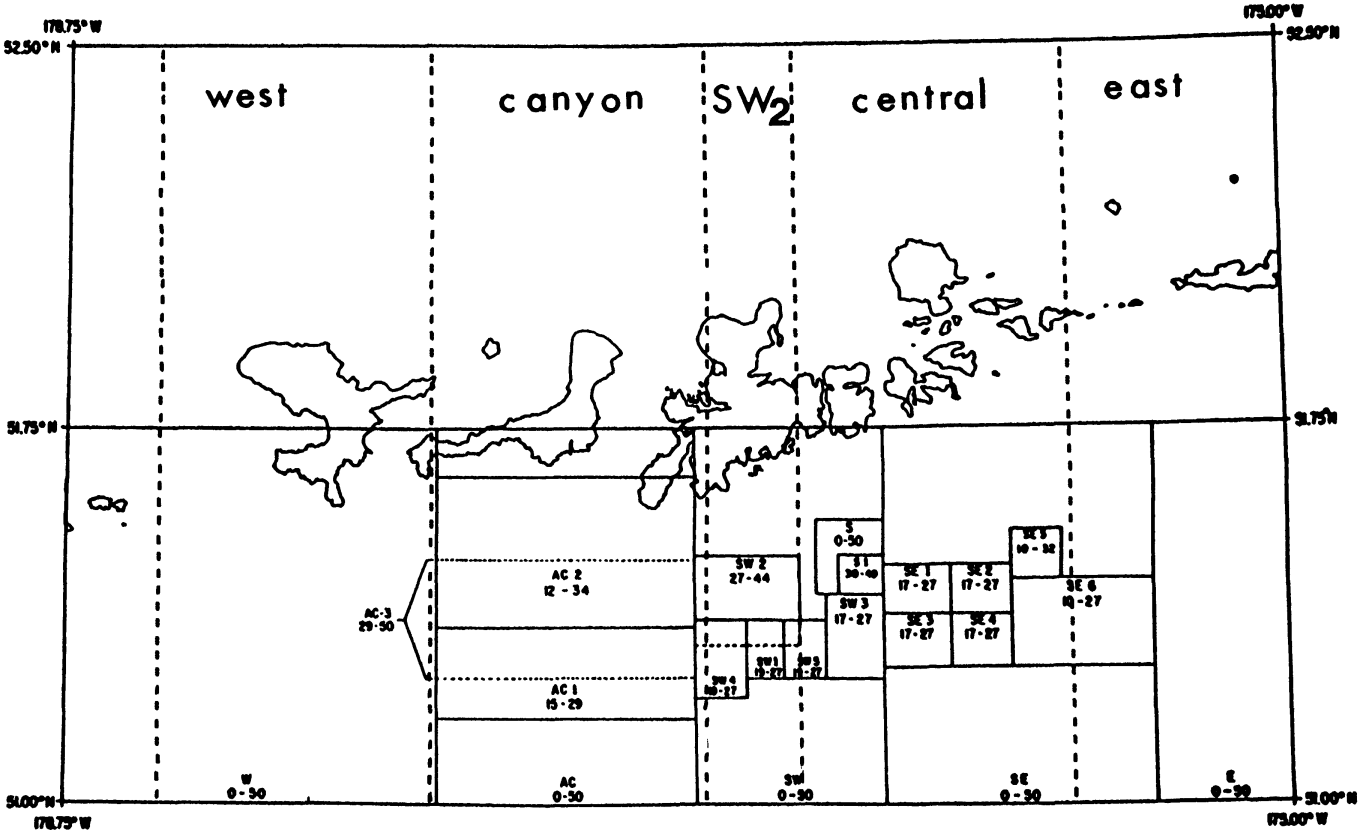

Figure 1. Regionalization adopted for comparing teleseismic and local occurrence rates. The five strips labelled with large letters are used for the PDE-listed events; the small rectangles are the subregions used for routine local network location determinations. PDE epicenters are shifted 0.18° to the east to correct approximately for teleseismic location bias. The West subregion does not exhibit quiescence in the PDE data.

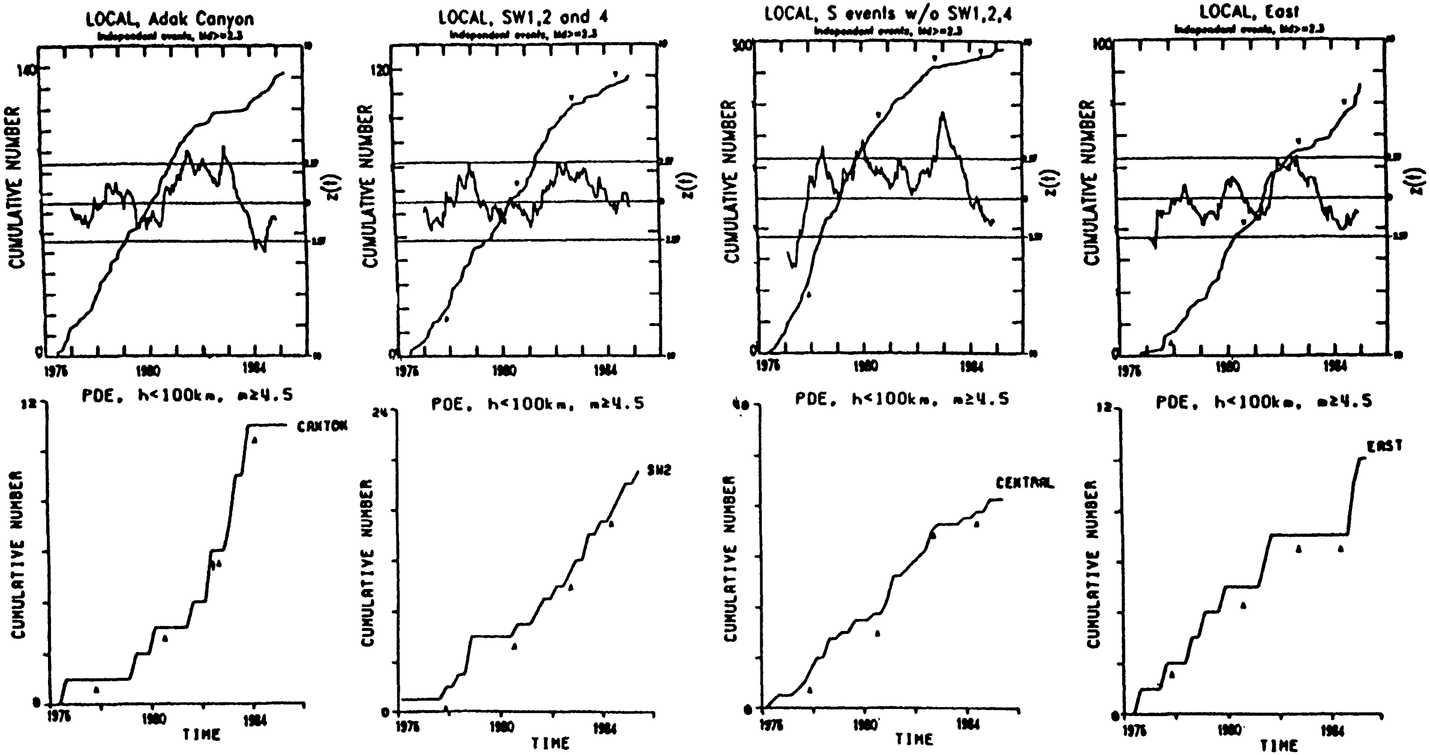

Figure 2. Comparison of local (top) and PDE (bottom) occurrence rates, May, 1976 - June, 1985, by major subregions. Independent events in the main thrust zone above the chosen magnitude cutoff are included. The arrowheads mark: Nov., 1977, M6.7 in Central region; July, 1980, beginning of activation in SW2; Sept., 1982, beginning of local data quiescence; May, 1984, m_b 5.8 in SW2. Z(t) in top figures is the z-test for significance of differences of successive 12 month running means of number of events. Peaks and troughs exceeding the two parallel lines mark rate decreases and increases, respectively, significant at greater than the 99% confidence level.

Microearthquake Data Analysis

9930-01173

W. H. K. Lee
U. S. Geological Survey
Branch of Seismology
345 Middlefield Road, Mail Stop 977
Menlo Park, California 94025
(415) 323-8111, Ext. 2630

Investigations

The primary focus of this project is the development of state-of-the-art computation methods for analysis of data from microearthquake networks. For the past six monthis I have been involved mainly in studying coda decay of local earthquakes. Because we would like to process and analyze large amounts of data (of the order of 10 billion bytes), we need to optimize our computer code for the coda decay research. The current code consists of FORTRAN modules interfaced by drivers written in a new high-level language called REXX. We have completed the first level of optimization by improving input/output and data access. The current code executes about twice as fast as that described in the previous Semi-Annual Report. However, additional optimization is underway before we finalize the computer code.

Results

We completed a paper on a preliminary study of coda Q in California and Nevada. In addition, Bob Crosson of the University of Washington is applying our current computer code on his Washington local earthquake data.

Although I was not able to attend the 23rd General Assembly of the International Association of Seismology and Physics of the Earth's Interior in Tokyo, Japan, due to health reasons, I was the co-convenor for the Symposium of Historical Seismograms and Earthquakes. I was responsible for preparing a preliminary proceedings volume which was distributed one month before the Symposium. I am now editing the final Symposium proceedings for publication by Academic Press, New York.

Reports

Lee, W. H. K., Aki, K., Chouet, B., Johnson, P., Marks, S., Newberry, J. T., Ryall, A. S., Stewart, S. W., and Tottingham, D. M., A preliminary study of coda Q in California and Nevada, submitted to Bull. Seism. Soc. Am.

Lee, W. H. K., Meyers, H., and Shimazaki, K., Introduction to the Symposium on Historical Seismograms and Earthquakes, (abstract), 23rd General Assembly of the International Association of Seismology and Physics of the Earth's Interior, Tokyo, Japan, August, 1985.

Taggart, J. N., Lee, W. H. K., and Meagher, K. L., The U.S. Geological Survey's database of seismic events, (abstract), 23rd General Assembly of the International Association of Seismology and Physics of the Earth's Interior, Tokyo, Japan, August, 1985.

CONSTRUCTION OF AN ELECTROMAGNETIC DISTANCE-MEASURING SYSTEM

66701

Judah Levine

Time and Frequency Division
National Bureau of Standards
Boulder, Colorado 80303
(303) 497-3903

Investigations

We have continued our testing and evaluation of a three- wavelength system for measuring baselines up to 50 km long with fractional uncertainties of about 0.02 ppm. The instrument is designed to measure the refractivity of the atmosphere by measuring the path differences between three signals: two optical and one microwave. The optical wavelengths used are 632 nm (He-Ne red) and 441.6 nm (He-Cd blue); the microwave frequency is 8.1 GHz.

Results

During this reporting period, we concluded that the source of the problems discussed in our previous reports was due to unexpectedly large phase shifts in the input optical system. We designed and constructed a totally new system using a steerable refracting telescope of our own design in place of the commercial reflecting telescopes used previously. These components were recently installed in our system, and we have been conducting field tests for the last few weeks. The results of the field tests are most gratifying. We can detect no sign of our previous systematic errors, and we are confident that we have corrected the problem completely or at least reduced it to an insignificant level.

Our initial tests use a baseline of about 900 m long. We have conducted many experiments to test the coherence between the refractivity determined by the optical system and the value that is deduced from end-point measurements of the pressure and temperature. We find very good agreement between the two over a wide range of temperatures and pressures. The measurements have been performed every day (except during the two recent snow storms) for the last two weeks and the measurements span many different atmospheric conditions. The two refractivity determinations always agree. In particular, our previous systematic error in which the apparent refractivity depended on wind velocity is no longer with us. We were able to verify this very quickly, since on the afternoon of the second day of testing the winds reached velocities of 70 km/hr with gusts that were considerably faster.

We feel that mesurements over a baseline of this length are important, since it is reasonable to insist on good agreement between end-point and baseline-averaged values of atmospheric properties. This will be less true for longer baselines and unambiguous tests of the instrument will therefore be more difficult once we go to the longer baselines.

We are not yet ready to use the full system to make distance measurements and we are limited to refractivity measurements for the time being. As we have discussed previously, the refractivity measurement is the hardest part of the job since the effects are differential between the colors.

Our current plans are to continue these measurements for another few days and then to begin measurements over our longer 25 km baseline. We are also planning a series of joint measurements using our instrument and a commerical distance-mesuring system within the next few weeks.

We plan to present our results at the Fall AGU meeting.

MAGNETIC FIELD OBSERVATIONS

9960-03814

R. J. Mueller
Branch of Tectonophysics
U.S. Geological Survey
345 Middlefield Road, MS/977
Menlo Park, CA 94025
(415) 323-8111 ext. 2533

INVESTIGATIONS

1) Investigation of total field magnetic intensity measurements and their relation to seismicity and strain observations along active faults in central and southern California.

2) Recording and processing of synchronous 10 minute magnetic field data and maintenance of the 25 station telemetered magnetometer network and its receive telemetry system for central and southern California.

3) Processing and analysis of on-site recorded data from portable magnetometer networks in California.

RESULTS

1) The installation of three new telemetered magnetometers in the Parkfield region of central California was completed in June, 1985. These magnetometers are located at Varian Ranch (VRR), Hog Canyon (HGC), and at Turkey Flat (TFL), see Figure 1. These stations greatly increase the capability of the network to uniquely resolve tectonically generated local magnetic fields. The new magnetometer stations use the new low-frequency satellite telemetry system to return the data in real-time (ten minute interval) to Menlo Park.

2) The Hot Creek (HCRM) magnetometer station, located in the Long Valley caldera, was moved and converted to Sutron type satellite telemetry. The sample interval was changed from 15 minutes to 10 minutes.

3) New digital electronic systems, to measure the frequency outputs from electronic pressure transducers and transfer the measurement to Sutron satellite data collection platforms, were designed and bench tested. The systems are to be used in a lake level monitoring experiment at Crowley Lake in the Long Valley caldera.

4) A visit to the People's Republic of China was made between September 1 and September 30, 1985 as part of the Protocol for Scientific and Technical Cooperation in earthquake studies, signed by the U.S. Geological Survey, the National Science Foundation, and the State Seismological Bureau of the People's Republic of China. The purpose of this trip was to provide five on-site recording magnetometer systems and one geodetic measuring system to the Chinese and instruct them in the usage of these equipment. The five magnetometer systems were provided to the Beijing State Seismological Bureau and the geodetic equipment to the Yunnan State Seismological Bureau. In addition to providing the equipment, the magnetic and geodetic networks established in 1980 and 1982 were resurveyed.

REPORTS

Johnston, M. J. S., Silverman, S., Mueller, R. J., and Breckenridge, K. S., Secular Variation, Crustal Sources, and Tectonic Activity in California, 1976-1984 , _J. Geophys. Res._, v. 90, no. B10, pp. 8707-8717, 1985.

Johnston, M. J. S., Chen Zhong-Yi, and Mueller, R. J., Strain and Magnetic Field Changes on the Red River Fault System Near Dengchaun and Liante, Yunnan, China: 1980-1985, Trans. A.G.U. (in press), 1985.

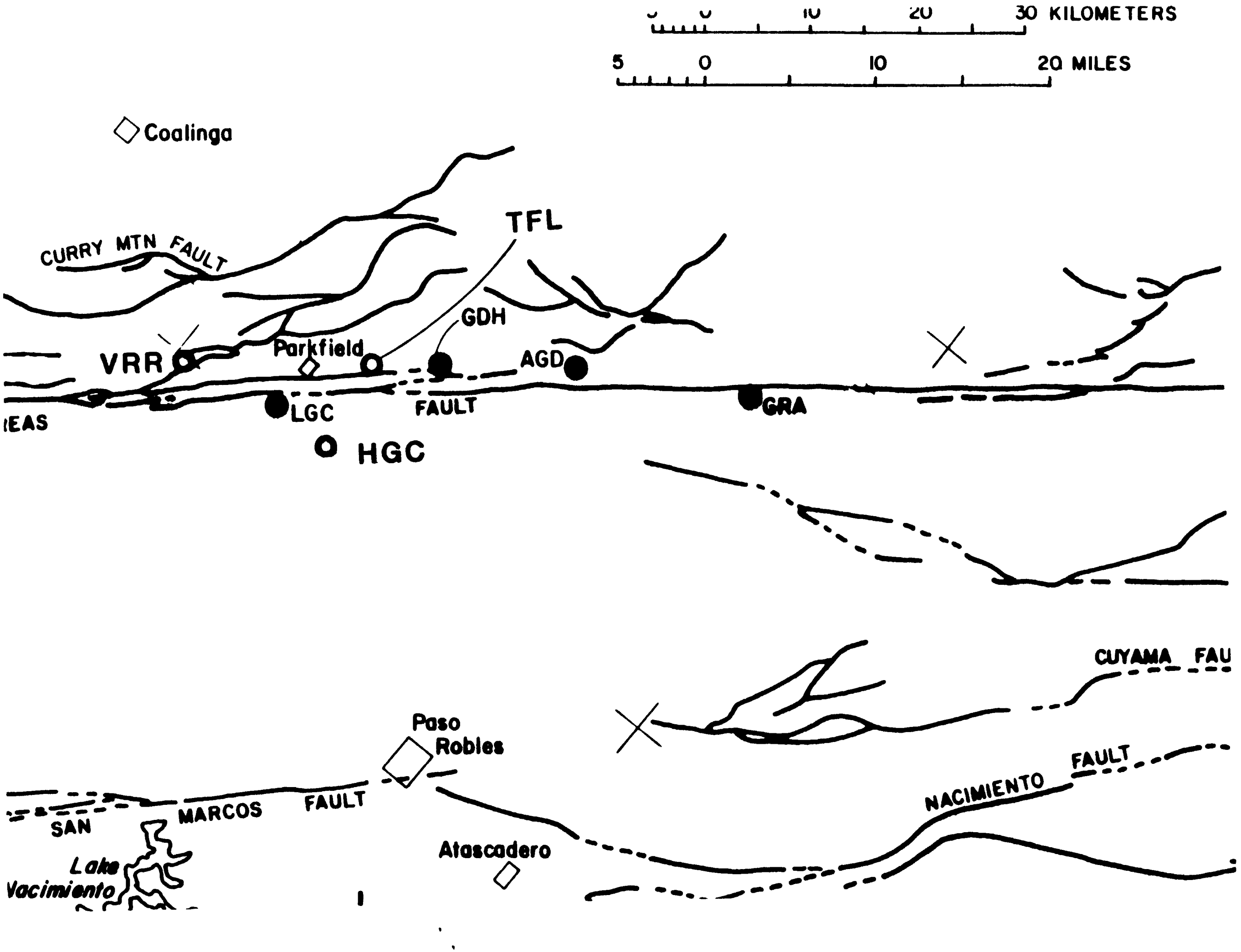

FIGURE 1

Locations of the three new magnetometer stations installed in the Parkfield region of central California.

Stable Isotope Analyses

9750-00383

J.R. O'Neil
Branch of Isotope Geology (MS 937)
U.S. Geological Survey
345 Middlefield Road
(415) 323-8111, ext. 2598

Investigations

1. Analyses of D and ^{18}O are made of ground waters collected bimonthly at several sites along active fault systems in California with the aim of tracing changes in local hydrological regimes that precede or accompany earthquakes.

2. In a search for geochemical precursor phenomena, soil gases at several sites along the San Andreas fault are analyzed for amount and isotopic compositions of CO_2 and H_2.

3. The stable and radiogenic isotopic compositions and water contents of fault gouge, mylonites, and related materials are analyzed with the aim of learning the physical chemical conditions of formation, the porosity, and source rocks of such material.

Results

1. The role of groundwater in active fault zones is poorly understood and yet is clearly of major importance for interpreting a number of the geophysical and geochemical characteristics of fault zone materials. Fortunately, water has built-in natural tracers, D and ^{18}O. By measuring the variations in the concentrations of these isotopes in natural waters and in the rocks with which they have interacted, it is possible to (a) identify recharge areas and trace the movement of waters in complicated hydrological systems, (b) identify the origins of waters, (c) estimate water-rock ratios, and (d) estimate temperatures of water-rock interactions.

   With some of these possibilities in mind, stable isotope analyses were made of rocks and entrapped aqueous fluids in samples of fault gouge collected by Marc Zoback at depths to 400m in an active part of the San Andreas fault system in California. The most important finding is that the fault gouge is an open system permeable to fluid flow. Such permeability has important implications concerning heat flow along the fault zone.

General conclusions of this study are:

(a) The permeability of the gouge is high enough to allow meteoric waters to descend and mix with a brine (formation water) that is entering the system from below or laterally.

(b) The porosity of about 10% does not change significantly with depth.

(c) Clay minerals constitute only about 42% of this gouge, previously considered to be composed dominantly of clay.

(d) The bulk of the clays grew at a former time when climate or topography were different from those prevailing at the present location of the Gabilan Range.

2. After almost five years of measurements of stable isotope ratios of perennial spring waters from seismically active regions of California, we are able to identify what appear to be "sensitive" waters. The most interesting spring to date is one from Chabot College located on the Hayward fault. Periodically the aquifer feeding this spring is effectively sealed-off and another aquifer containing meteoric water (that by its isotopic composition most likely is of Pleistocene age!) becomes the source of water exiting the spring. The onset of the phenomenon is sudden but recovery times are of the period of months. The oxygen isotope data for this spring are shown in the figure. Local seismic activity of low magnitude is only weakly correlated with the phenomenon.

   It is to be emphasized in this report that such an effect has not hitherto been recognized. Whatever the origin of this phenomenon, it must involve a significant set of forces in the crust. Whether seismic activity is related to setting them in motion remains to be seen.

Reports

O'Neil, James R. (1985) Water-rock interactions in fault gouge, PAGEOPH vol. 122, P. 440-446.

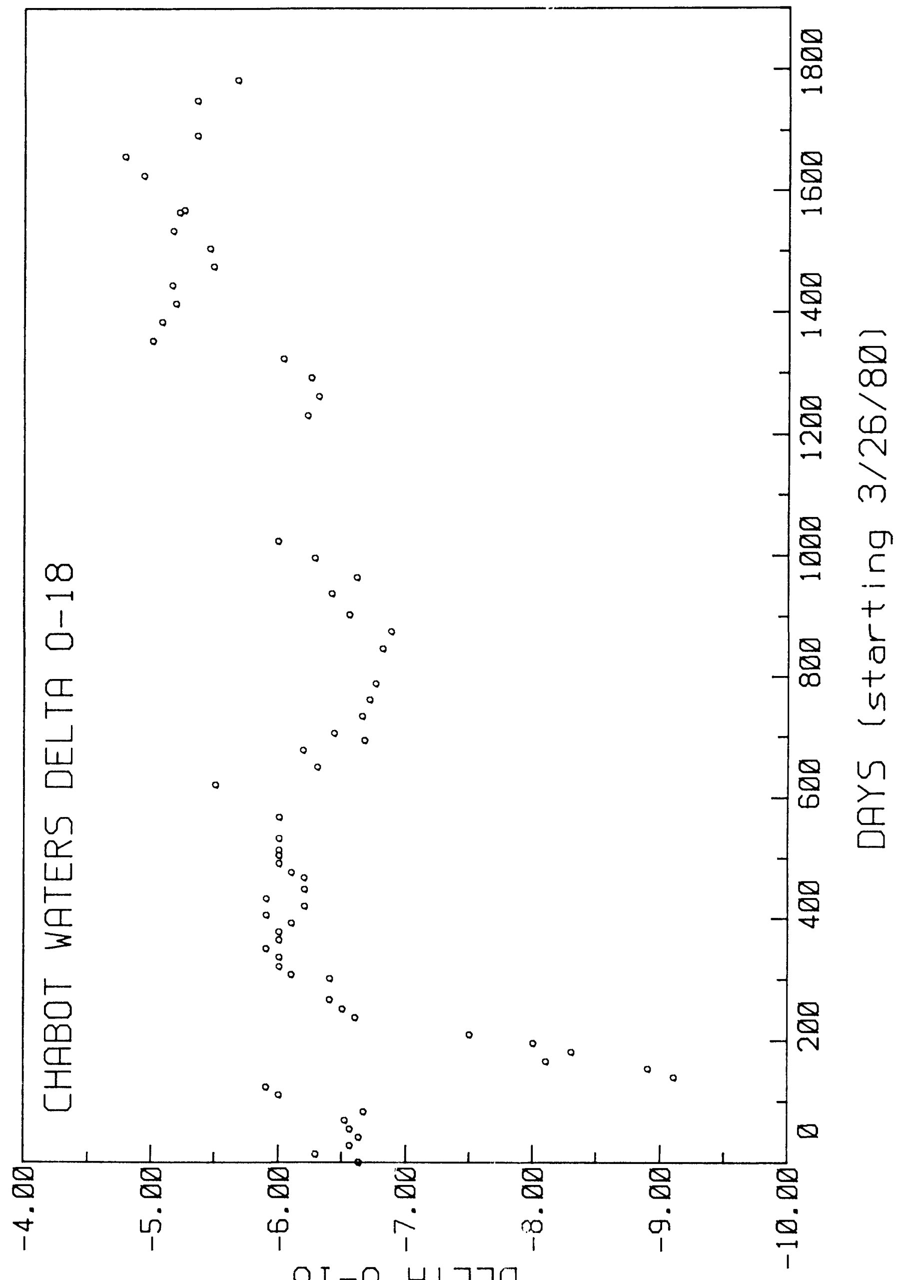
CHABOT WATERS DELTA O-18
DAYS (starting 3/26/80)
DELTA O-18
0
200
400
600
800
1000
1200
1400
1600
1800
-4.00
-5.00
-6.00
-7.00
-8.00
-9.00
-10.00

CRUSTAL STRAIN

9960-01187

W.H. Prescott, J.C. Savage, M. Lisowski, N. King
Branch of Tectonophysics
U.S. Geological Survey
345 Middlefield Road, MS/977
Menlo Park, California 94025
(415) 323-8111, ext. 2701

Investigations

The principal subject of investigation was the analysis of deformation in a number of tectonically active areas in the United States.

1. Strain Accumulation in Southern California, 1973-1984

Repeated surveys of selected lines from five trilateration networks along the San Andreas fault in southern California have been used to deduce the 1973-1984 strain accumulation records at five localities. The secular rate of engineering shear strain accumulation is about 0.3 μrad/a with the plane of maximum shear parallel to the local strike of the San Andreas fault. The secular rate of accumulation of areal dilatation is negligible. The data were examined to detect evidence for fluctuations in the rate of strain accumulation. For this examination 19 lines were removed from the data set: four because they exhibited an obvious coseismic offset and 15 others because they contained at least one very anomalous measurement that could reasonably be attributed to a survey blunder. (The incidence of such blunders appears to be one in every 75 measurements.) The remaining data consist of 104 lines with an average of 10 measurements each. Although the strain accumulation plots for the five networks may exhibit marginally significant temporal fluctuations, we are not convinced that those fluctuations are greater than could be attributed to survey error. In particular, we are unable to demonstrate that the 1973-1979 southern California strain anomaly reported by Savage et al. [1981] is real. Given the uncertainty in the random and systematic errors in measurement, the strain measurements in southern California are probably consistent with linear-in-time strain accumulation. The strain accumulation plots for the Salton network clearly established that, unlike the deformation reported after the 1940 Imperial Valley earthquake, no acceleration in the shear strain rate has yet been observed following the 1979 Imperial Valley earthquake.

2. Strain Accumulation in the Shumagin Seismic Gap, Alaska, 1980-1985

Strain accumulation in the Shumagin seismic gap was estimated from repeated trilateration surveys made between 1980 and 1985. The measured rate of shear strain accumulation (0.02 ± 0.03 μrad/a) was an order of magnitude less than the rate (0.18 μrad/a) predicted for seismic subduction. The absence of measurable shear-strain accumulation in the Shumagin Islands suggests that the main thrust zone there may not be locked but rather may slip stably. If this is indeed the case, the probability of a great, shallow thrust earthquake in the Shumagin gap is greatly diminished.

3. The Shumagin Islands Earthquake of October 9, 1985

A M_s=6.4 earthquake occurred just seaward of the outermost Shumagin Islands on October 9, 1985. The Shumagin trilateration network had been surveyed just 4 months earlier as well as in 1981 and 1983. The 1985 measurements do not appear to exhibit any significant anomalies. Thus, we conclude no significant precursors were apparent 4 months before the earthquake although the epicenter was perhaps only 10 km from the edge of the trilateration network.

4. Strain Accumulation Across the Totschunda Fault, Eastern Alaska, 1909-1985

The Totschunda fault is a major right-lateral fault in eastern Alaska near the Yukon border. At its north end the Totschunda fault merges with the Denali fault near Mentasta Pass whereas on the south the fault is lost in the ice fields of the St Elias Mountains. Because the Totschunda fault is colinear with the Fairweather fault farther south, a connection between the two has been postulated. In the summer of 1985 an International Boundary Commission triangulation arc established in 1909 across the Totschunda fault near Chitistone Pass was resurveyed. The rate of shear strain accumulation in the 1909-1985 interval was only $\dot{\gamma}$ = 0.10 ± 0.06 μrad/a, far below the rate $\dot{\gamma}$ = 1.6 ± 0.2 μrad/a recently measured on the Fairweather fault for the interval 1967-1983.

5. Strain Accumulation in Central Vancouver Island, British Columbia

A 1982 trilateration network and a 1947 triangulation network located in central Vancouver Island were studied to determine measurement precision and horizontal strain accumulation. The 1982 trilateration network was comprised of 23 distance measurements (average length 24 km), which covered a 30 km by 50 km area near the town of Gold River, east of Nootka Sound. The 1982 survey was performed by the Geodetic Survey of Canada using techniques similar to those employed by the USGS. Atmospheric refractivity corrections to the measured distances were derived from aircraft-flown, temperature-humidity profiles and end-point air pressures. The standard error in a distance L (m) was estimated to be $\sigma = (a^2+b^2L^2)^{1/2}$, where a = 0.0067 m and b = 0.26×10^{-6}. There were 54 angle measurements common to the 1947 and 1982 networks. The standard error in a 1947 angle measurement was 2.3", and the estimated standard error in a 1947 to 1982 angle change was 2.4". Assuming uniform strain, the average rate of shear strain accumulation between 1947 to 1982 was 0.23 ± 0.12 μrad/yr with the axis of maximum contaction bearing N56°E±12°. The accumulation of strain in the Gold River area was found to be similar to that observed in northwestern Washington. The northeast compression found in the geodetic networks could be reproduced with a two-dimensional, elastic dislocation model of the Cascadia subduction zone by locking the shallow interface between the Juan de Fuca and North American plates to a depth of about 20 km. The model could not account for some details of the vertical deformation and it was not consistent with the north-south compressive stress indicated by shallow earthquake focal mechanisms. Although the possibility of a large, shallow, thrust earthquake is inferred from the strain data, the uncertainty in the strain accumulation and the tectonic complexity of the area make such a conclusion speculative.

6. Horizontal Deformation Across the Eastern Garlock Fault, California

A geodetic measurement of horizontal strain accumulation across the eastern 150 km of the Garlock fault shows maximum left-lateral shear across a vertical plane that is about 15° from the average east-northeastward trend of this section of the fault. The average principal strain rates calculated from the changes in Geodolite measured distances during the period from 1972 to 1984 are $\dot{\varepsilon}_1 = 0.07 \pm 0.01$ μstrain/yr and $\dot{\varepsilon}_2 = -0.11 \pm 0.02$ μstrain/yr (extension reckoned positive) with the axis of maximum extension (ε_1) oriented N76°W ± 2°. The maximum shear strain rate is 0.18 ± 0.01 μstrain/yr (engineering shear) across a vertical plane oriented N59°E ± 2° for left-lateral shear or N31°W for right-lateral shear. The strain accumulation appears to be uniform across the network, even though the trend of the Garlock fault changes from N75°E to due east. The plane of maximum left-lateral shear is more closely aligned with the strike of the Garlock fault outside of the area covered by the network (N63°E) and the Owl Lake fault

(N57°E) within the network. Maximum right-lateral shear is approximately parallel to the eastern California seismic belt, which passes along the eastern front of the Sierra Nevada Mountains and through the Mojave Desert.

7. Geodetic Measurements near Parkfield, California, 1959-1984

Trilateration measurements have been made by various agencies since 1959 near Parkfield, California, in the transition zone between the central creeping section and the southern locked section of the San Andreas fault. Within the transition zone there are now several creepmeters and alinement arrays, four small-aperture trilateration networks, and a broad trilateration network extending to the Pacific coast. Line-length changes observed after the 1966 $M_L = 5.6$ Parkfield earthquake indicate a geodetic moment of $4.5 \pm 1.0 \times 10^{25}$ dyne-cm. The data are consistent with 91 ± 8 cm slip on a rupture zone 30 km long and 3 to 8 km deep or 59 ± 5 cm on a 30 km long zone 2 to 10 km deep. This moment estimate includes some postseismic slip, and is a factor of two to four greater than the moment determined from surface waves. The post 1966 data set is well suited to discriminate between the effects of surface and deep slip. Surface slip rates determined by creepmeters, alinement arrays, and small-aperture trilateration networks decrease from 25 mm/yr at Slack Canyon to zero south of Highway 46; a gradient of roughly of -0.48 ± 0.01 mm/yr/km. Deformation of the broad trilateration network is consistent with shallow slip of 2.9 ± 1.2 mm/yr from the surface to a depth of 16 km and 34.4 ± 5.5 mm/yr below 16 km. The trilateration data alone do not uniquely constrain both the transition depth from shallow to deep slip and the deep slip rate. A transition depth near 16 km is preferred because it provides the best fit to the data and the predicted slip rate is consistent with the slip rate in the creeping zone northwest of Parkfield as well as the late Holocene slip rate southeast of Parkfield. Significant along-strike variations in the observed deformation are not fit by this simple two-dimensional model.

8. The Distribution of Relative Plate Motion Along the San Andreas Fault System from Hollister, California to the Mendocino Triple Junction

Recent work on the distribution of the relative motion between the Pacific and North American plates suggests that a fundamental change in the nature of the fault system occurs at Hollister, California. South of Hollister the relative plate motion rate is about 33 mm/yr and all of it occurs as aseismic slip at the main trace of the San Andreas fault. North of Hollister the total relative motion appears to be about 25-35 mm/yr, consistent with that to the south. However, the plate motion is not concentrated on the San Andreas fault, either seismically or aseismically. Rather the San Andreas is accommodating only about one-third of the plate motion, while the rest is distributed over a broad zone to the east of the fault. There is no evidence of any relative motion to the west of the San Andreas fault. East of the San Andreas fault, the observations are consistent with either of two scenarios: the motion may be accommodated elastically on one or several of the parallel faults located there; or the motion may be distributed anelastically over the entire region. The observations suggest that the San Gregorio fault is not contributing significantly to the relative plate motion at present. The slip rate at depth on the San Andreas fault between Hollister and Point Reyes, California is inferred to be about 10-15 mm/yr. Although this rate is much slower than usually accepted values, it is consistent with the limited geologic evidence for rates over the past few thousand and hundred thousand years.

9. Global Positioning System: A Status Report

We are in the process of implementing a capability of measuring three-dimensional position differences using the Department of Defense's Global Positioning System navigation satellites. Two TI-4100 receivers were delivered in early October and a third is expected within a few weeks. Nearly all of the hardware and software required to process the data are on hand, but a substantial amount of work remains before we will be able to routinely produce differences. Until delivery of the third receiver, the first two are measuring the relative positions of stations Allison and Loma Prieta on a weekly basis. These stations are part of a network of frequently measured geodolite lines. The horizontal component of the position difference is well known from the geodolite observations.

Reports

Savage, J. C., 1985, A plate flexure approximation to postseismic and interseismic deformation, J. Geophys. Res., 90, 8570-8580.

Yu, Shui-Beih and William H. Prescott, 1984, Horizontal strain accumulation in the northern San Francisco Bay Region, California, Bull. of the Inst. of Earth Sciences, Academia Sinica, v. 4, pp. 117-129.

Seismic Studies of Fault Mechanics

9930-02103

Paul A. Reasenberg
U.S. Geological Survey
345 Middlefield Road, Mail Stop 977
Menlo Park, California 94025
(415) 323-8111, ext. 2049

Investigations

1. Development of a computer algorithm to obtain double-couple fault-plane solutions from earthquake first-motion polarity data.

2. Investigation of seismicity clustering.

Results

1. Algorithms for computing and displaying double-couple earthquake fault-plane solutions from first motion polarities were implemented and tested. The inversion is accomplished through a two-stage grid-search procedure that finds the source model minimizing (one-norm) a normalized, weighted sum of first-motion polarity discrepancies. Two weighting factors are incorporated in the minimization: one reflecting the estimated variance of the data, and one based on the absolute value of the theoretical P wave radiation amplitude. The latter weighting factor gives greater (lesser) weight to observations near radiation lobes (nodal planes). Recent enhancements include reporting of multiple fault plane solutions for a given earthquake, corresponding to relative minima in the misfit function. Uncertainty of the resulting fault-plane solution is obtained from the estimated uncertainty in the data used in that solution, and is reported in terms of a confidence interval for each parameter (strike, dip, rake) of the solution. An Open-file report describing the inversion and listing the source code (and companion code for displaying the fault plane solutions) is in the review process and should be completed shortly.

2. In a previous Semi-annual report, and in Reasenberg (1985), an algorithm was described for identifying space-time clusters in a seismicity catalog. Initial application of the algorithm was toward the goal of removing dependent events from the catalog. Now we turn to another problem, that of studying the composition and structure of the identified clusters. A comparative study of the characteristics of clusters in the seismicity of three regions - central California, southern California and the Tokai-Kanto region of Japan - was started.

References

Reasenberg, P., 1985, The second-order moment of central California seismicity, 1969-1982, J. Geophys. Res., 90, 5479-5495.

COUPLED DEFORMATION - PORE FLUID DIFFUSION EFFECTS IN FAULT RUPTURE

14-08-0001-G-978

J.W. Rudnicki
Department of Civil Engineering
Northwestern University
Evanston, Illinois 60201
(312)491-3411

Investigations

1) Dilatant hardening effects due to uplift and near-fault microcracking accompanying fault slip.

2) Coupled deformation - diffusion effects accompanying slip on an impermeable fault.

3) Induced pore fluid pressures in dilatant jog zones.

Results

1) We are investigating the effects of coupling between pore fluid diffusion and dilatancy accompanying slip on the postpeak deformation of a layer loaded by a combination of shear displacement and normal stess. A fault or frictional surface is assumed to have formed at peak stress and the subsequent deformation is due to a combination of slip on the frictional surface and elastic unloading in the surrounding material. The shear stress on the fault is related to the slip and decreases from a peak value τ_p to a residual value τ_r as the slip increases from zero to δ_o. Dilatancy due to uplift and near-fault microcracking is associated with slip, but saturates when the shear stress reaches τ_r. Calculations are simplified by assuming that the flux of pore fluid into the layer is proportional to the difference between the pore fluid pressure on the fault and that in an exterior reservoir.

Extremely small amounts of dilatancy (4% of the slip) consistent with observations in experiments [Barton, 1976; Tenfel, 1981] and confined to the slip surface can stabilize failure. The results are, however, very sensitive to the parameter $h(\tau_p - \tau_r)/G\delta_o$ where h is the width of the layer and G is the elastic unloading modulus. In some cases, failure is completely prevented because stabilization persists until the shear stress on the sliding surface has been reduced to the residual value. This stabilization is, however, accompanied by a sharp drop in pore pressure on the slip surface. If the magnitude of this drop approaches the initial ambient level of the pressure, then the resulting decrease in the pore fluid bulk modulus terminates the stabilizing effects. Thus, stability depends on the ambient value of pore pressure, as observed by Martin [1980], because this value limits the magnitude of pressure drop that can occur.

Changes in normal stress intended to simulate those that occur in the axisymmetric compression test have been included in the calculation. These, as expected, are destabilizing. For slip weakening data inferred for Westerly granite by Wong [1982], and other prameters representative of Martin's experiments, the critical value of pressure at which undersaturation and instability occur is consistent with values observed by Martin for transition from stable to unstable behavior. Our calculations also suggest an increase in the value of this critical pressure with strain-rate consistent with Martin's experiments. The dependence of the critical pressure on effective stress observed by Martin is not predicted. This appears to result, not from a pore pressure effect, but from the dependence of the difference $\tau_p - \tau_r$ on effective normal stress which has been neglected in the calculations. Data on other rock types [Wong, 1986] suggest, however, that this difference can either increase or decrease with effective confining stress and, consequently, the trends observed by Martin [1980] may be specific to Westerly granite.

2) We have also continued application of our solution for sudden slip on an impermeable fault plane. As described in publication 4 listed below, the differences between this solution and that for a permeable fault [Booker, 1974; Rice and Cleary, 1976] could be significant in assessing the role of pore fluid effects on variety fault processes. In particular, the shear stress induced on the fault plane does not decrease monotonically from its short time undrained value to its long-time value, but first rises to a peak about 20% in excess of the difference between its drained and undrained values. We have recently obtained expressions for the time-dependent stress changes off the fault plane and are investigating the possibility that these changes along with the pore pressure changes can trigger aftershocks.

3) Following suggestions of Sibson [1985] that pore fluid effects may play a role in arresting ruptures at dilational fault jogs, we have made some estimates of the magnitude of these effects. In particular, we have estimated the magnitude of the suctions induced by opening a tensile crack with a uniform circular opening and a ramp time function. For an opening of about 0.1 m and a 1 - 10s rise time, values suggested by Sibson [1986], and plausible values of the diffusivity and material parameters the suction of the center of the patch is on the order of the 10% of the shear modulus. This is, of course, likely to be an upper estimate for several reasons: the average pore pressure over the patch will be smaller, the dilatant deformation may be distributed more broadly through the structure rather than localized on discrete cracks and the decrease of the pore fluid will present pore pressure drops from exceeding the ambient level. Nevertheless, it does suggest that large suctions can be induced dynamically.

References

Barton, N. Int. J. Rock Mech. Min. Sci. & Geomech. Abstr. 13, 255-279, 1976.

Booker, J.R. J. Geophys. Res., 79, 2037-2044, 1974.

Martin, R.J., Geophys. Res. Letters, 7, 404-406, 1980.

Rice, J.R. and M.P. Cleary, Rev. Geophys. Space Phys., 14, 227-241, 1976.

Sibson, R.H., Stopping of earthquake ruptures at dilatational fault jogs, Nature, to appear, 1985.

Teufel, L., in Mechanical Behavior of Crustal Rocks, Geophysical Monograph 24 (The Handin Volume), American Geophysical Union, 135-145, 1981.

Wong, T.F., J. Geophys. Res., 87, 990-1000, 1982.

Wong, T.F., On the normal stress dependence of the shear fracture energy, submitted for Proceedings of 5th Maurice Ewing Symposium on Earthquake Source Mechanics, 1986.

Publications

1. Rudnicki, J.W., Effect of pore fluid diffusion on deformation and failure of rock, in Mechanics of Geomaterials, (edited by Z.P. Bazant), Proceedings of the IUTAM William Prager Symposium on Mechanics of Geomaterials: Rocks, Concrete, Soils, September 11-15, 1983, Northwestern University, Evanston, Illinois. John Wiley & Sons, Ltd., 315-347, 1985.

2. Roeloffs, E. and J.W. Rudnicki, Coupled deformation-diffusion effects on water level changes due to propagating creep events, Pure and Applied Geophysics, Special Issue on Earthquake Hydrology and Chemistry (ed. by C.-Y. King) 122, 560-582, 1984/85.

3. Rudnicki, J.W., Stabilization of failure by dilatant hardening accompanying fault slip (Astract), EOS. Trans. Am. Geophys. Union, 66, 382, 1985.

4. Rudnicki, J.W., Slip on an impermeable fault in a fluid-saturated rock mass, submitted for Proceedings of 5th Maurice Ewing Symposium on Earthquake Source Mechanics, May 20-24, 1985. Arden House, Harriman, New York.

Hydrogen Monitoring

Motoaki Sato and Susan Russell-Robinson
Branch of Igneous and Geothermal Processes
U.S. Geological Survey, MS 959, Reston, VA 22092

Investigations

Hydrogen (H_2) concentrations in soil along the San Andreas and Calaveras faults are continuously monitored at seven sites by using fuel-cell sensors and telemetered to Menlo Park, CA. Efforts are directed toward the accumulation of valid field data, possible correlations with seismic data, understanding of mechanisms for H_2 emissions along active faults and their genetic links with tectonic processes that trigger damaging earthquakes, and improvement of the monitoring method.

Results

Shore Road (H2SH) has been uneventful since April '85 except for two minor and brief events on June 23 and July 19 (Fig. 1).

Wright Road (H2WR) showed discontinuous shifts probably caused by telemetry noise. When the noise was removed, two abrupt inexplicable changes remained. The changes occurred on June 18 and July 24 (Fig. 2). The pattern of these events are unusual and could have been caused by electrical disturbances in the ground, but a tectonic cause cannot be ruled out.

When the earlier record of 1985 (Feb. - May) were carefully examined, we found that minor H_2 events at this site were coincident with the oscillatory slip events at Shore Road (SHR1) which is 8.6 km away (Fig. 3a-c). The coincidence is significant because it means that the oscillatory slip has a wider influence on the H_2 emission than the unidirectional lateral slip event of March 18, suggesting a completely different tectonic nature of the "oscillatory slip".

Cienega Winery (H2CW) was uneventful as usual until Sept. 5, when a cluster of peaks of several hundred ppm started appearing for 4 days (Fig. 4). What this event means in terms of tectonic processes is under investigation.

Melendy Ranch (H2MR) appears to have a power supply problem because it started showing flat-topped diurnals. Because the flat tops correspond to the zero voltage in the telemetry system and because this happens at night, malfunctioning of the solar panel or the storage battery is suspected. Larger solar panels have been ordered for replacement. In spite of this problem we recognized two small H_2 events on May 25 and 26 (Fig. 5).

Slack Canyon (H2SC) has been plagued by noise of unknown origin (possibly the sensor). The noise is so severe that we have not been able to extract a useful information out of the data yet.

Middle Mountain (H2MM, H2M2) has been without isolation amplifiers because rain flooded the instrument vault through a conduit hole and destroyed the electronics. The data obtained are strange and show definite ground-loop problem. The restored record of H2M2 after removal of identifiable cross talks with the creepmeter is shown in Fig. 6. The record indicate that the amplititude of diurnal variation increased during June and July, perhaps precursory to the M 5.5 Kettleman Hills earthquake of August 4, 1985.

Parkfield (H2PK) continues to produce valid data. A comparison of the H_2 data obtained since May '84 with the creepmeter record (Fig. 7) does not show a clear-cut relation, although there is a possibility that an increase in H_2 precedes a reversal in slow continuous creep from left-lateral to right-lateral. If a right-lateral continuous creep is interpreted to be an increasing extensional strain normal to the fault plane, the above relation may make a sense.

Gold Hill (H2GH) is similar to Melendy Ranch in having the flat-top diurnals. The solar panel will be replaced as soon as shipment arrives. In spite of the problem, we found a peak on June 7 (Fig. 8).

H_2 Emissions along the San Andreas Fault and the 1983 Coalinga Earthquake

By going over the H_2 record of 1982 and 83 and the seismic data we found correlations between H_2 peaks observed at Parkfield and Slack Canyon (and possibly at Cienega Winery) and larger earthquakes that occurred around Coalinga during the period as shown in Fig. 9. To explain why the earthquakes on different faults were genetically related to the anomalous H_2 emissions along the San Andreas fault, we propose the following scenario illustrated in Fig. 10:

The San Andreas fault zone is underlain by ophiolitic rocks of the Pacific plate at depth (perhaps 10 km +). The top of the plate is serpentinized by ground water and thus ductile. The compression of the North American plate and the Pacific plate at the boundary region causes visco-plastic movement of the serpentinites which pushes the brittle upper crust upward along the boundary. This causes tensional stress normal to the San Andreas fault and adjacent faults dilatating the fault zone. The H_2, generated during the serpentinization, starts escaping rapidly toward the surface due to its high buoyancy and mobility. When serpentinites are finally squeezed into fault planes near the base of the brittle crust in the maximum stress area, the compressive stress in the ductile crust is relieved and the H_2 emission starts declining as the fault zones contract. At the same time, damaging earthquakes are triggered in the area where the fault is wedged and lubricated by serpentinites.

Reports

Sato, M., A. J. Sutton, and K. A. McGee (1985) Anomalous hydrogen emissions from the San Andreas fault observed at the Cienega Winery, central California, Pure & Appl. Geophys., 122, 376-391.

Sato, M., A. J. Sutton, K. A. McGee, S. Russell-Robinson (in press) Intense H_2 anomalies along the San Andreas fault near Coalinga and their possible genetic links with the 1983 Coalinga earthquake. EOS, AGU Fall mtg. abst.

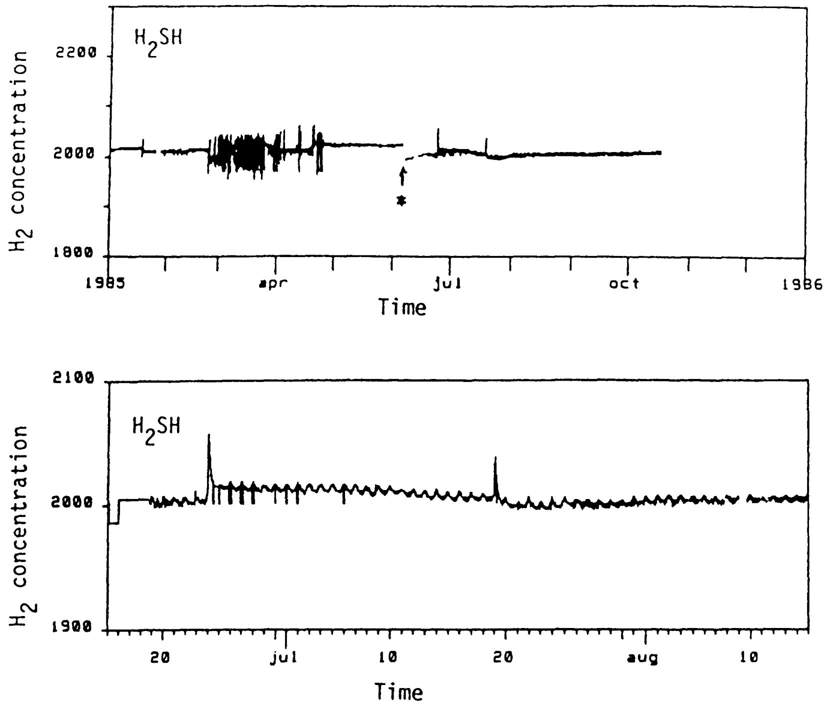

(Fig. 1) The H_2 concentration in soil observed at the Shore Road site (H2SH) in 1985 (top) and between June 15 and August 15, 1985 (bottom). H_2 concentration is shown in System counts where zero ppm is biased to about 1950 counts and 100 counts correspond to abount 350 ppm. The mark (*) denotes service and battery change.

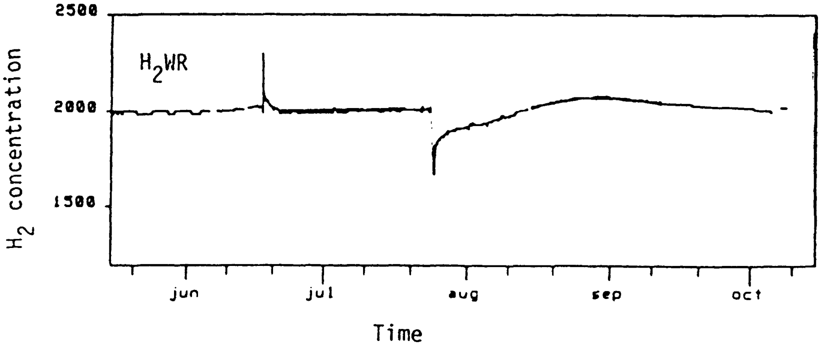

(Fig. 2) The H_2 record obtained at the Wright Road site (H2WR) between May 15 and October 15, 1985. Telemetry noise has been removed as much as justifiable, but still two unexpalained events remain.

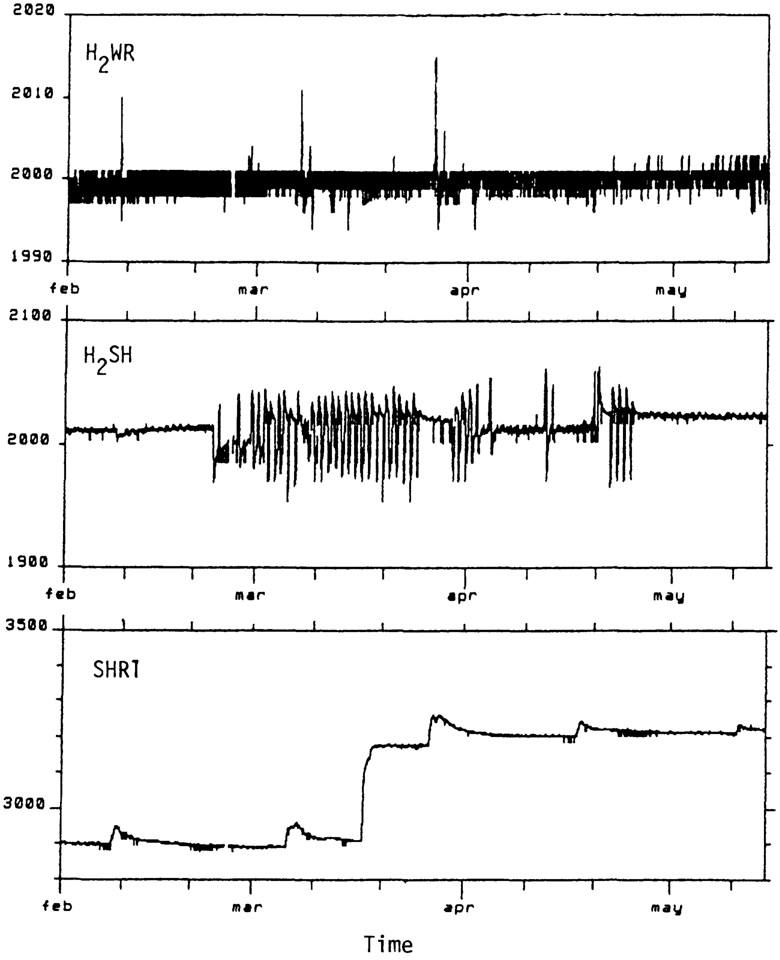

(Fig. 3a) Time-coincidence between minor hydrogen events observed at Wright Road (H2WR) and oscillatory slip events observed at Shore Road (SHR1), and that between increased amplititudes of H_2 diurnals at Shore Road (H2SH) and a unidirectional slip at SHR1.

Fig. 3b

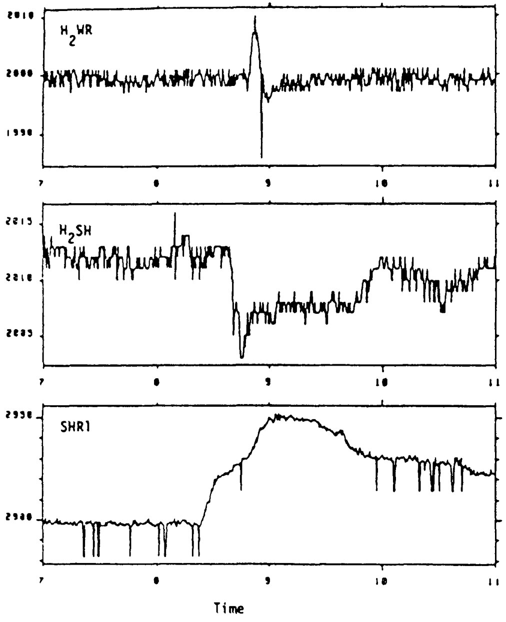

Fig. 3c

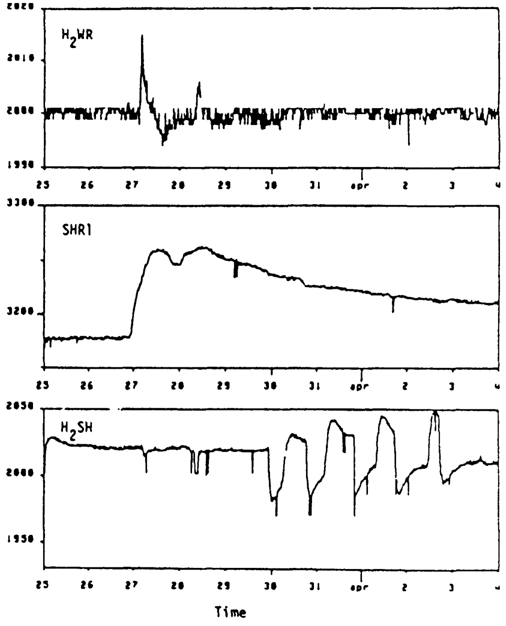

(Fig. 3b) Coincidence of a positive peak at Wright Road (H2WR), a negative peak at Shore Road (H2SH), and an oscillatory peak at Shore Road (SHR1) on February 8, 1985 (GMT).

(Fig. 3c) Coincidence of 2 positive peaks at Wright Road (H2WR), 2 negative peaks at Shore Road (H2SH), and a twin oscillatory slips at Shore Road (SHR1), observed in March 1985. Time scale is in GMT.

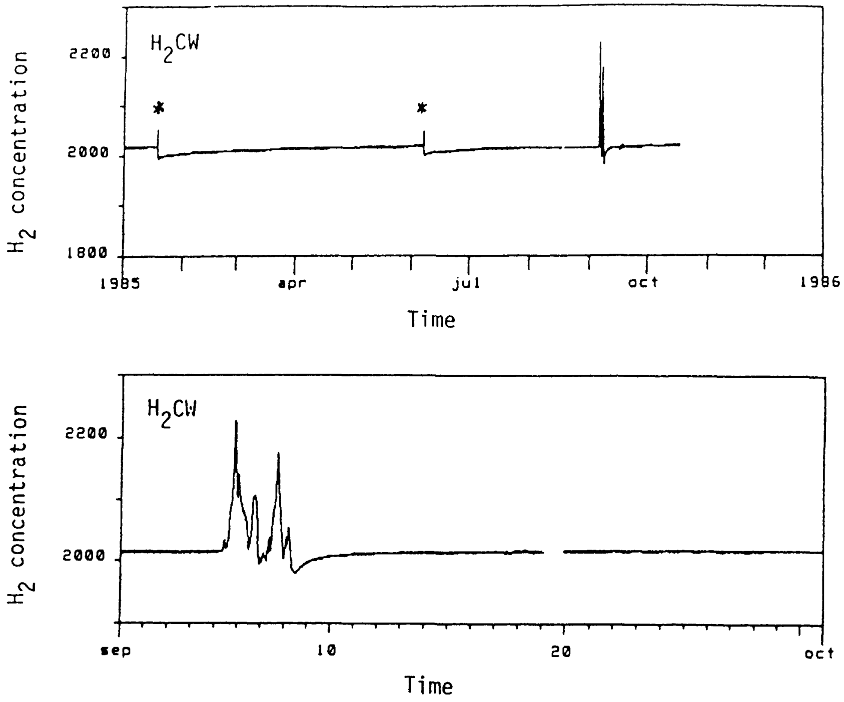

(Fig. 4) A cluster of peaks observed at the Cienega Winery site (H2CW) in September, 1985. The time is in GMT.

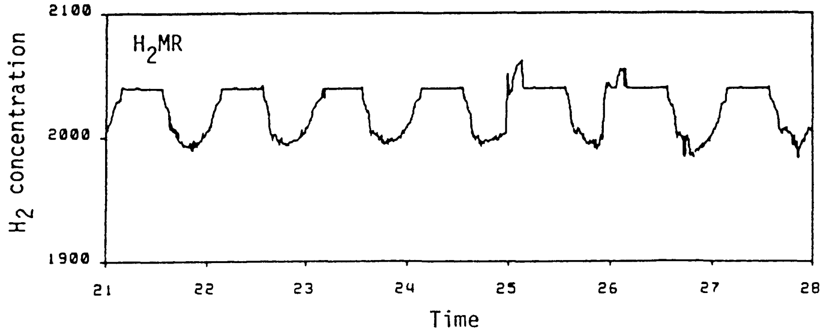

(Fig. 5) Two minor peaks recognized at the Melendy Ranch site in May 1985. Time is in GMT. The flat-topped diurnals were probably caused by solar panel problems.

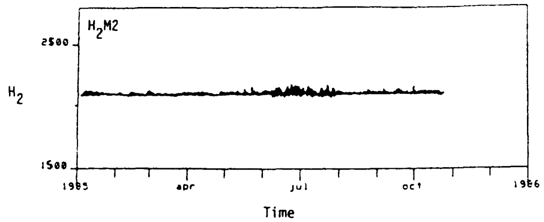

(Fig. 6) H_2 record obtained at the Middle Mountain site (H2M2) in 1985. Note increased diurnals in June and July. The values should be multiplied by ten times to be comparable with other site data.

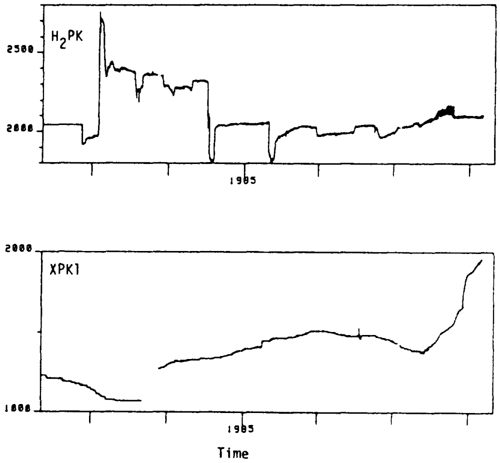

(Fig. 7) Comparison of H_2 record (H2PK) and creepmeter record (XPK1, courtesy of the creep project) obtained at the Parkfield site to obtain an insight into the H_2 degassing mechanism.

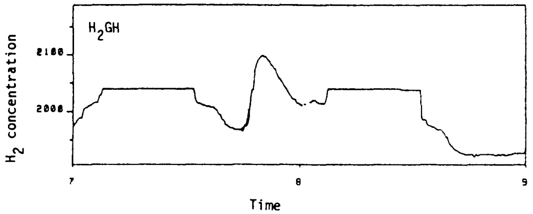

(Fig. 8) An H_2 peak observed at the Gold Hill site (H2GH) on June 7, 1985. The flat-topped diurnals were probably caused by power supply failure.

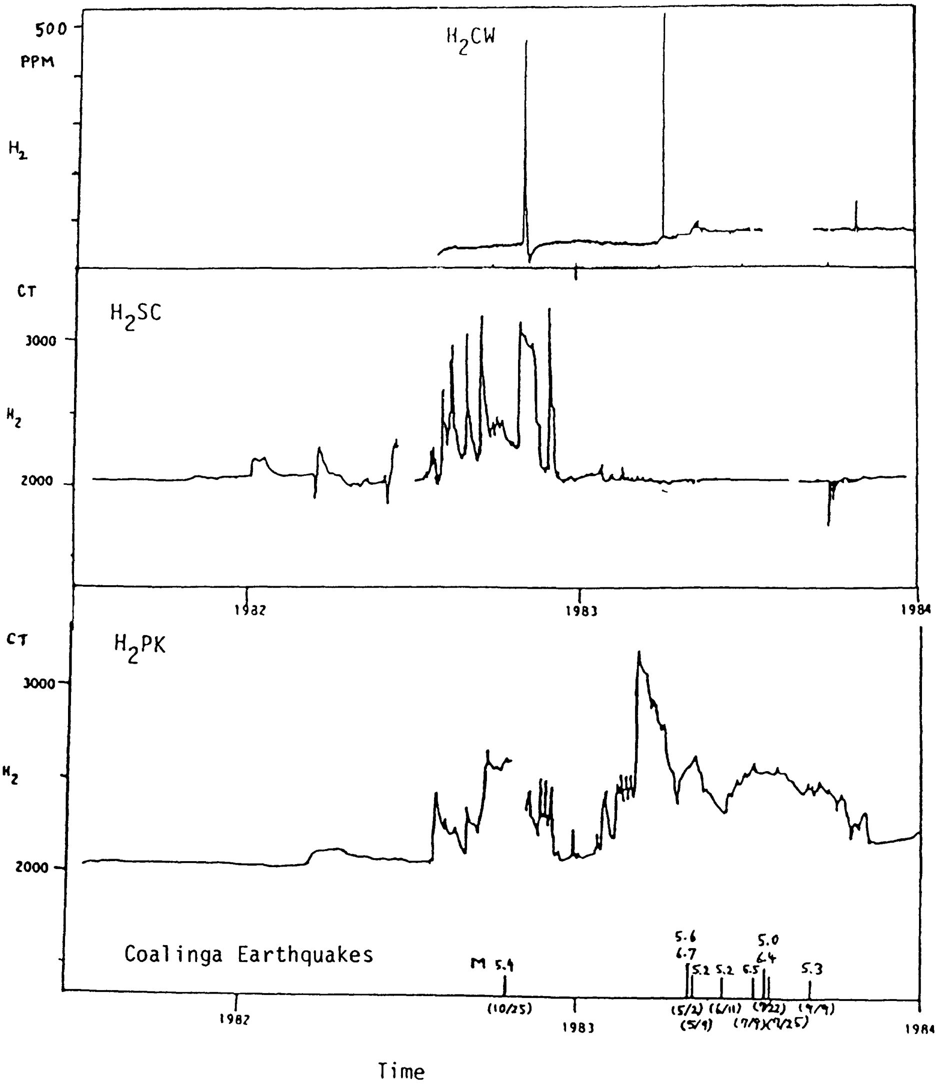

(Fig. 9) Correlations of H_2 peaks observed at Parkfield (H2PK), Slack canyon (H2SC), and Cienega Winery (H2CW) and the earthquakes that occurred near Coalinga in 1982 and 1983. The H_2 scale for H2PK and H2SC is same as in Fig. 1.

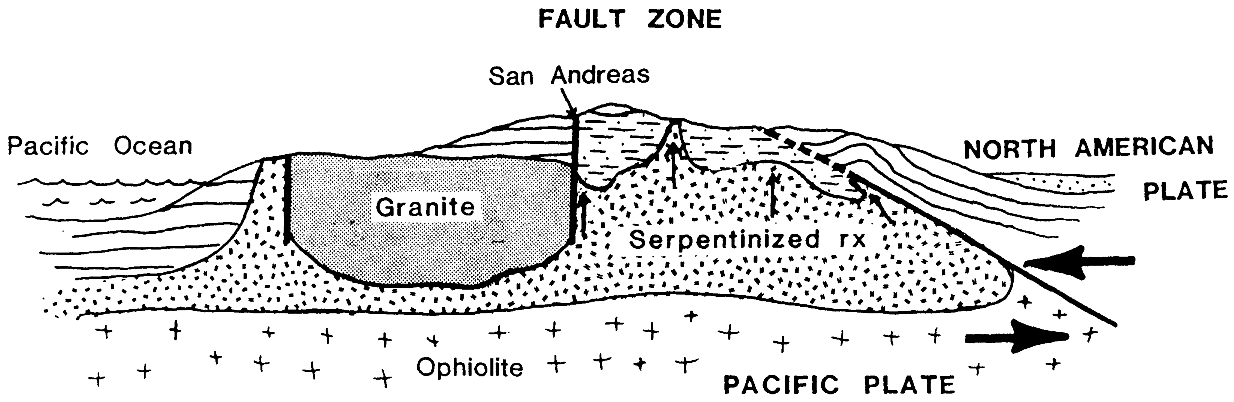

(Fig. 10) A cartoon illustrating a poosible link between intense H_2 peaks observed along the San Andreas fault and earthquakes that occurred near Coalinga in 1982 - 83. The serpentinized top of the ophiolitic middle crust probably acted as a ductile medium for transmission of compressive stress, lubricating agent, and source of hydrogen gas.

GREAT EARTHQUAKES AND GREAT ASPERITIES, SOUTHERN CALIFORNIA: A PROGRAM OF DATA ANALYSIS

Lyyn R. Sykes and Leonardo Seeber
Lamont-Doherty Geological Observatory of Columbia University
Palisades, New York 10964
(914) 359-2900

14-08-0001-G-948

Investigations

During 1985 we have utilized earthquake data from the CIT-USGS catalog, paleomagnetic determinations, paleoseismicity and historical accounts of seismicity to examine the southern San Andreas fault system.

Results

1. Block rotation along the southern San Jacinto fault zone. The 100 km long portion of the San Jacinto fault zone from the Anza Plateau to the Imperial Valley is characterized by a series of northeast cross faults which span the 3 to 7 km wide zone. Although major earthquakes are associated with right-lateral ruptures on the northwest strands, aftershocks and background seismicity occupy the entire fault zone and are often associated with left-lateral cross faults. A system of faults and blocks across the Coyote Ridge at the northwestern end of this zone could transfer right-lateral shear between two overlapping strands by rapid clockwise rotation. Southeast of Coyote Ridge, the San Jacinto fault zone occupies a broad valley characterized by deformed Plio-Quaternary terrestrial clastics. Several cross faults are recognized in this young structural domain. Paleomagnetic data from poorly lithified sediments of the Ocotillo formation in the Borrego Badlands and straddling the Inspiration Point cross-fault, yield normal and reversed characteristic magnetizations that deviate from geomagnetic north and south by 20° to 30° clockwise. This rotation has occurred in the last 0.7 to 1.0 my, since the sediment is younger than 1 my and the sampled reversal is older than 0.7 my. The minimum rate of rotation is then 0.3-0.7 μrad/y, corresponding to a minimum overall displacement rate of 0.2-0.5 cm/y for the San Jacinto fault zone. Offset channels and a cluster of 1968 aftershocks associated with the Inspiration Point fault suggest ongoing left slip and clockwise rotation. The triangular Clark Basin between the Borrego Badlands and Coyote Mtn. may reflect pull-apart fanning between rotating and translating portions of the San Jacinto fault zone. A detailed resolution of block kinematics within fault zones such as the San Jacinto fault zone at both the geologic and geodetic time scale may help to understand the pattern of deformation leading to a major rupture.

2. Quiescence of the southern San Andreas fault and adjacent secondary seismicity. The southern San Andreas fault in the area from the Pinto Mountains to Bombay Beach (Salton Sea) is nearly quiescent at the microearthquake level. The closest seismicity is located 3-5 km NE of the fault. The most active region is about 20 km wide and extends from as far north as the Pinto Mountain fault to as far south as the Mecca

hills. Relocation of earthquakes using only stations NE of the San Andreas fault and proximal to the activity does not seriously affect epicentral locations, suggesting that the observed offset of epicenters from the San Andreas fault is not an artifact of velocity inhomogeneity. Many of the earthquakes that occur within this region can be ascribed to structures strikeing NE and conjugate to the San Andreas fault. Focal mechanisms of earthquakes between 1976 and 1985 were examined. Events with essentially common focal mechanisms were found to define linear trends parallel to nodal planes. Structures thus defined are consistent with a NNE axis of maximum compression, in contrast to generally N-S P axes determined in the southern Salton Trough and central Transverse Ranges. Three large blocks are bounded by the Pinto Mountain, Blue Cut, Chiriaco and San Andreas faults. The western portions of these blocks are currently active in response to accumulating elastic strain across a locked San Andreas fault. None of the major E-W striking surface faults are seismically active, however, microearthquakes define E-W en echelon structures in the northern block. A $M_L \approx 4$ event in a previously quiescent locality NE of the 1947 Morongo Valley earthquake occurred in January 1985. This is the largest event to occur in the study area in the period from 1976 to 1985. A second set of 5 events with $3<M_L<4$ occurred 14 km to the SE during January. These events fall on a NE striking lineament defined by earlier earthquakes. The asymmetric concentration of activity in the north portion of the study area suggests that this area has localized higher stress. Alternatively, the closely spaced active structures are uniquely sensitive to the level of stress on the San Andreas fault.

3. Seismicity and fault kinematics along the Brawley seismic zone and adjacent regions. The Brawley seismic zone is the most active section of the San Andreas fault system in southern California. It is defined by a broad band of earthquakes that trends just west of north and connects the southern San Andreas to the Imperial fault. The high rate of microearthquake activity, combined with the shallow nature of the seismicity, the high areal heat flow, the lack of known large (M>6) earthquakes, and the orientation of the fault zone relative to the plate motion vector suggest that the Brawley seismic zone should be dominated by extensional tectonics. Detailed analysis of the microearthquake data from the CIT-USGS catalog reveals, however, that north of the surface rupture involved in the 1979 Imperial Valley earthquake, the Brawley seismic zone is not a single simple fault, but is composed of a complicated series of nearly-orthogonal en echelon northeast striking left-lateral faults that intersect other fault segments striking north or north-west. Very few of the earthquake focal mechanisms examined could be interpreted as pure normal fault solutions. Instead the predominate syle of seismic deformation is strike-slip or oblique strike-slip. Some earthquakes even exhibit focal mechanisms with a large component of reverse faulting. These events are generally located at block corners where faults intersect and could be the result of rotations induced by regional shear. Other earthquake hypocenters define a nearly-vertical northeast-striking planar feature that parallels the southern end of the Salton Sea and connects the Superstition Hills fault zone with the Brawley seismic zone. Motion along this tranverse structure is also left-lateral and may be accomodating relative slip between the two major

fault zones as they converge at the head of Imperial Valley. Such secondary structures may control the distribution of slip between major wrench faults in California, as demonstrated by the occurrence of triggered slip on the Superstition Hills fault after the 1979 event and the occurrence of a large (M_L=5.5) earthquake on the Brawley seismic zone 10 hours after the 1942 Superstition Hills earthquake (M_L=6.5).

Publications

Nicholson et al., Seismicity and fault kinematics through the eastern Transverse ranges, California: Block rotation, strike-slip faulting and shallow-angle thrusts, submitted to Journal of Geophysical Research

Nicholson et al., Seismic deformation along the Southern San Andreas fault: Implications for conjugate slip and rotational block tectonics, to be submitted to Tectonics.

Nicholson et al., Seismicity and fault kinematics along the Brawley seismic zone and adjacent regions (abstract), EOS, Trans. AGU, 1985.

Seeber, L. and Nicholson, C., Block rotation along the San Andreas fault system in California: Long-term structural signature and short-term effects in the earthquake cycle, preprint.

Seeber, L., and N. L. Bogen, Block rotation along the southern San Jacinto fault zone (abstract), EOS, Trans. AGU, 1985.

Williams et al., Quiescence of the southern San Andreas fault and adjacent secondary seismicity (abstract), EOS, Trans. AGU, 1985.

Williams et al., Seismotectonics of the easternmost Transverse Ranges, California: Patterns of activity on secondary structures, in preparation.

Analysis of Seismic Data from the Shumagin Seismic Gap, Alaska

USGS 14-08-0001-G-946

John Taber and Klaus H. Jacob
Lamont-Doherty Geological Observatory of Columbia University
Palisades, New York 10964
(914) 359-2900

Investigations

Digitally recorded seismic data from the Shumagin seismic gap in eastern Aleutian arc, Alaska, are analyzed for detecting space-time variations in the seismicity, focal mechanisms, and dynamic faulting parameters that could be precursory to a major earthquake expected in this seismic gap. The seismic results obtained from the network data are being integrated with crustal deformation data that are independently collected, with volcanicity data of nearby Aleutian volcanoes, and with teleseismic information to identify basic tectonic processes which may be precursory to a great earthquake.

Results

Recent results of related investigations have created some new questions regarding the seismotectonic process in the Shumagin region. New probability estimates for the Alaska-Aleutian arc (Nishenko and Jacob, 1985) suggest that the Shumagin seismic gap is in the center of a 700 km long region of high conditional probability for great earthquakes. This means that a great earthquake might begin outside the Shumagins and our local instrumentation might miss any precursors.

Savage et al (1985) show that there has been no significant strain accumulation in the Shumagins during the period 1980-1985, as measured by trilateration surveys. This result must be reconciled with leveling data that show continuous tilting toward the trench during the same time period (Beavan et al, 1985). Locking the plate interface at depths below 25 km and with a sharp bend at about 40 km will fit both tilt and trilateration observations (Beavan et al, 1985). But this deep locked zone corresponds to a region that has been modeled as moving previously (1978-1980) in an aseismic slip event (Beavan et al, 1983, 1984). This implies that some unknown portion of the movement on the plate boundary beneath the Shumagins may occur aseismically. This conclusion can be reconciled with the historic record of great earthquakes (Davies et al, 1981) if, for instance, any aseismic slip is limited to only an 80 km wide section of arc directly beneath the Shumagins, or if it represents only a moderate percentage of the total long-term plate motion.

There is some seismologic evidence to suggest that a perhaps aseismically slipping portion of the Shumagin gap is in some way different from adjacent regions. Figures 1 and 2 show that a double Benioff zone exists to the west of the Shumagins but not beneath it. The double zone also exists to the east of the Shumagins. If the presence or absence of a double zone is related to the stress within the slab, then the stresses must vary between the regions. A variation in stresses at depth may correspond to a variation in the state of stress along the main thrust zone. Such a variation could mark the difference between sections that break only in major earthquakes and those sections where slip occurs primarily or partially aseismically.

A significant decrease in the rate of occurrence of events greater than Mb=5.5 was noted by Hauksson et al (1985) for the period since 1979 in the Shumagin gap region. An event with Ms=6.4 occurred within the Shumagins on 10/09/85, just before the submission of this report. A significant decrease in rate for moderate earthquakes still exists, but only to the west of the Shumagins. The recent event does not necessarily represent an immediate precursor to a gap-filling earthquake, although in conjunction with the aseismic slip postulated in one interpretation it may represent some preparational stage prior to a larger event. However the most recent event was located too shallow in the subduction zone to dynamically grow into a larger rupture, as were two events that occurred in 1983 (Taber et al, 1984).

References

Beavan, J., R. Bilham, and K.Hurst, Coherent tilt signals observed in the Shumagin seismic gap: Detection of time-dependent subduction at depth?, **J. Geophys. Res., 89,** 4478-4492, 1984.

Beavan, J. E. Hauksson, S.R. McNutt, R. Bilham, and K.H. Jacob, Tilt and seismicity changes in the Shumagin seismic gap, **Science, 222,** 322-325, 1983.

Beavan, J., K. Hurst, and R. Bilham, Results from 13 years crustal deformation measurements in the Shumagin Islands seismic gap, Proceedings of NEPEC meeting, September, 1985.

Davies, J., L. Sykes, L. House, and K. Jacob, Shumagin seismic gap, Alaska Peninsula; History of great earthquakes, tectonic setting and evidence for high seismic potential, **J. Geophy. Res., 86,** 3821-3856, 1981.

Hauksson, E., J. Armbruster, and S. Dobbs, Seismicity patterns (1963-1983) as stress indicators in the Shumagin Seismic Gap, Alaska, **Bull. Seismol. Soc. Am., 74,** 2541-2558, 1984.

Nishenko, S.P. and K. Jacob, Hazards evaluation for large and great earthquakes along the Queen Charlotte-Alaska-Aleutian seismic zone: 1985-2005, Proceedings of NEPEC meeting, September, 1985.

Savage, J.C., M. Lisowski and W.H. Prescott, Strain accumulation in the Shumagin and Yakataga seismic gaps, Alaska, submitted to **Science**, 1985.

Taber, J.J., J. Mori, and J. Beavan, February 14, 1983 earthquake sequence in the Shumagin seismic gap, Alaska (abstract), **EOS, 16,** 241, 1984.

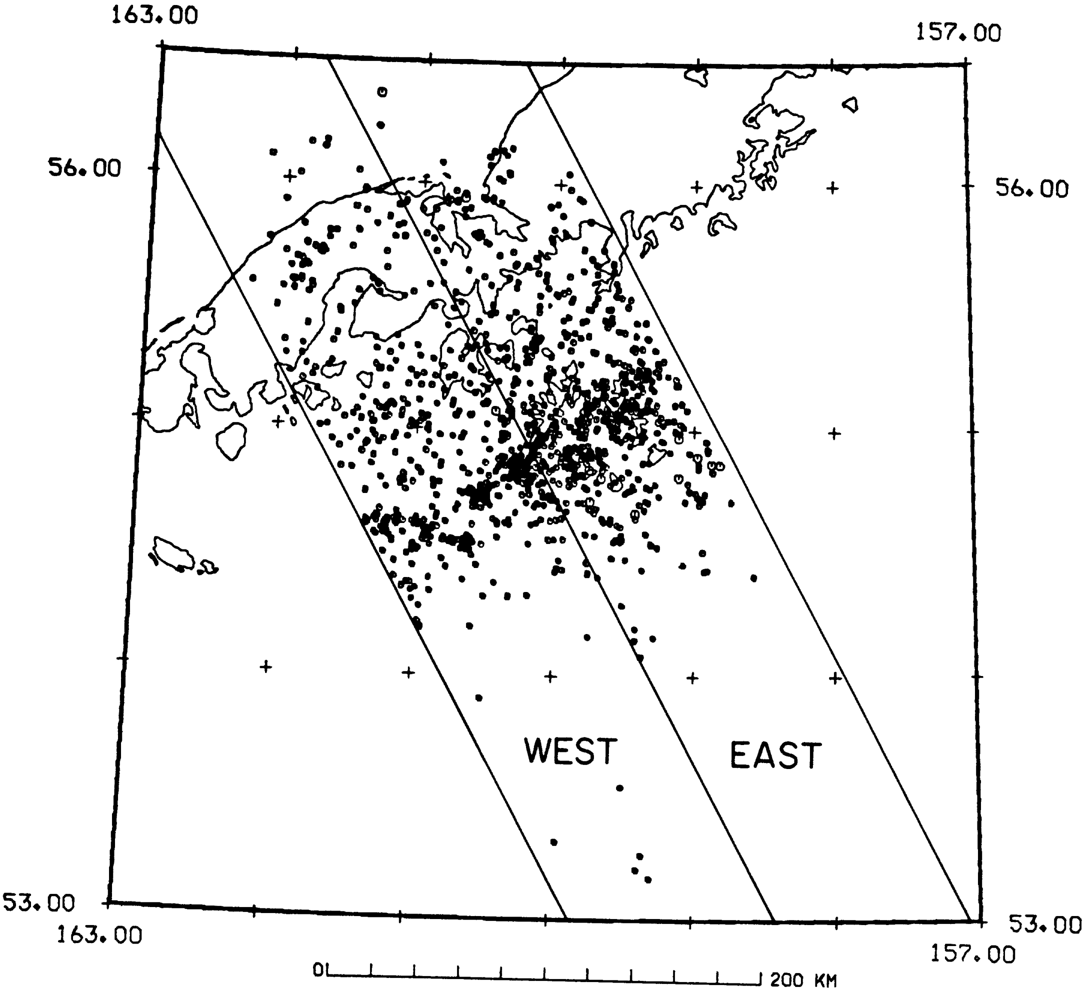

Figure 1. Seismicity in the center of the Shumagin network from 1979-1984, divided into eastern and western sections.

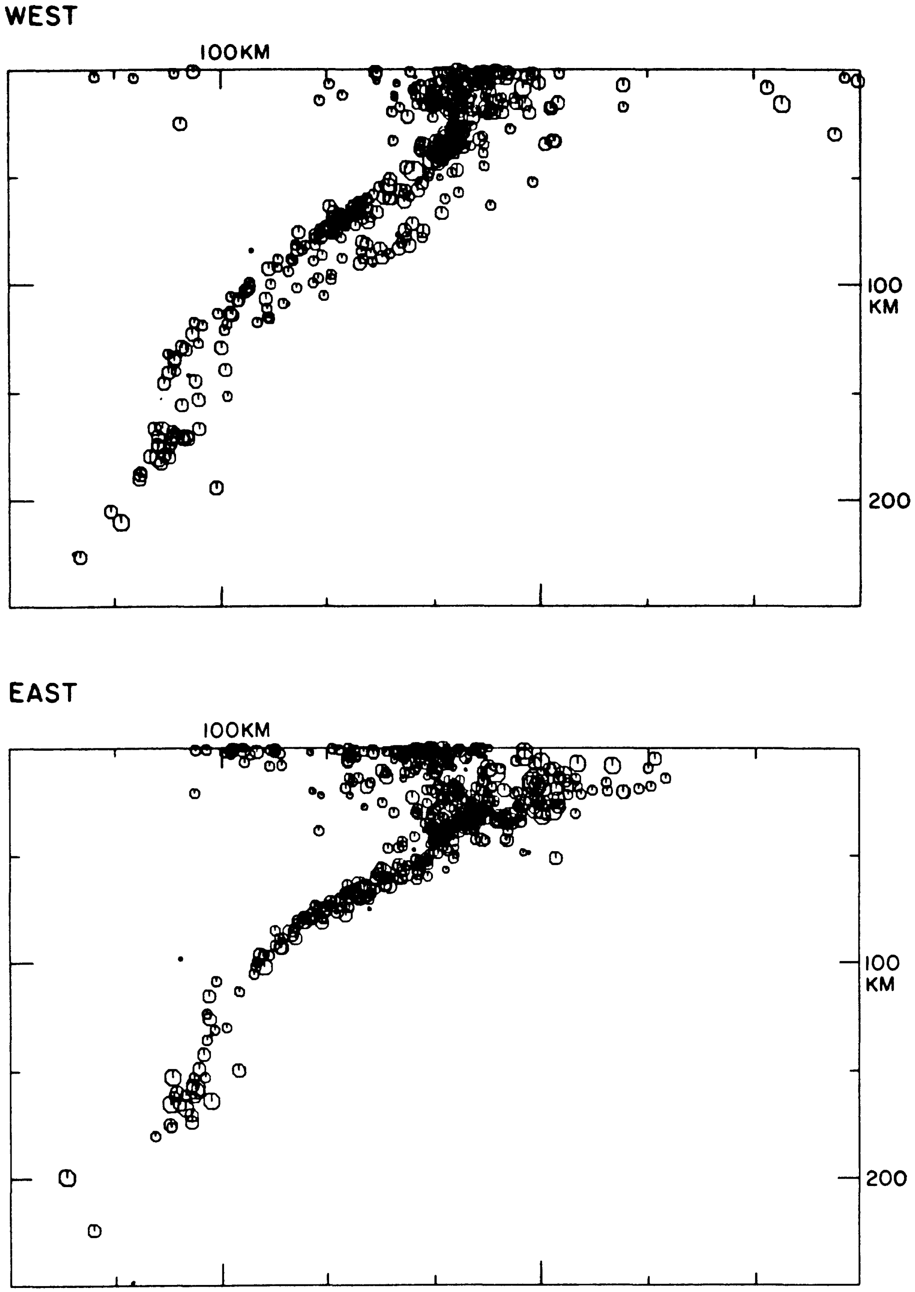

Figure 2. Cross sections of the two regions outlined in figure 1. Note the lack of a double Benioff zone in the eastern section.

Earthquake Process

9930-03483

Robert L. Wesson
Branch of Seismology
U.S. Geological Survey
922 National Center
Reston, Virginia 22092
(703) 860-7481

INVESTIGATIONS

1. Analysis of theoretical and numerical models of the processes active in fault zones leading to large earthquakes.

2. Analysis of seismological and other geophysical data pertinent to understanding of the processes leading to large earthquakes.

RESULTS

The problem of creep and afterslip has been considered as a problem of quasi-static equilibrium following Stuart and others (1985). At any point on the fault surface the external stress plus the dislocation stress less the resistance to shear must sum to zero. For a single rectangular dislocation the equilibrium condition can be considered at the center of the rectangle and the dislocation stress can be calculated from available expressions. For viscous and quasi-plastic characterizations of the rheology of the fault zone, analytic solutions have been obtained for the resulting differential equations. For a step function in external stress of amplitude T, applied to a halfspace containing a rectangular dislocation extending from the surface downward to a depth D, the displacement asymptotically approaches T*D/(mu*alpha), where mu is the rigidity and alpha is a constant depending on the geometry. The result is relatively insensitive to the geometry as alpha decreases monotonically from 0.61 for a square dislocation to 0.42 for a infinite strip. For the viscous case, creep curves have the form (1. - exp(-at)), where a = mu*alphs*w/(eta*D), where w is the width of the fault zone and eta is the viscosity of the fault zone material. For the quasi-plastic case, solutions have the form empirically deduced by Crough and Burford (1977). More complicated dislocation distributions can be simulated by considering the sum of contributions from a dislocation surface divided into rectangular elements. The dislocation stresses can then be calculated through a matrix formulation. The elements of this "stress influence matrix" can be calculated for several pertinent geometries in an elastic halfspace and in an infinite elastic plate. In general, the resulting system of nonlinear, ordinary differential equations must be solved numerically, but an analytic solution is straightforward for the viscous case. The solution for this case is the sum of decaying exponentials, the decay rates of which correspond to the eigen values of the stress influence matrix. Comparison between simulations and observations of creep and afterslip allow the determination of rheological properties of fault zone materials. For example, creep event 13 studied by Crough and Burford (1977) seems to have been initiated by a shear stress change of about 0.5 bar. Fault zone material at this location can be characterized by quasi-plastic relation of the form strain rate equals 2.7e-3 times shear stress raised to the power 1.6.

REFERENCES

Crough, S. T., and R. O. Burford, Empirical law for fault creep events, Tectonophysics, 42, 53-59, 1977.

Stuart, W. D., R J. Archuleta and A. G. Lindh, Forecast model for moderate earthquakes near Parkfield, California, J. Geophy, Res., 90, 592-604, 1985.

REPORTS

Wesson, R. L., A model for aftershocks and afterslip in California, The 23rd General Assembly of the International Association of Seismology and Physics of the Earth's Interior, Tokyo, Japan, Abstracts, 413, 1985.

Central American Seismic Studies

9930-01163

Randall A. White, David H. Harlow
Branch of Seismology
U.S. Geological Survey
345 Middlefield Road, MS/977
Menlo Park, California 94025
(415) 323-8111, ext. 2570

Investigations

We are continuing to examine the tectonic origin and the seismic characteristics of shallow ($Z < 15$ km), destructive earthquakes along the volcanic chain in Central America. We are focusing on these earthquakes because the historical record indicates that these earthquakes produce a greater impact on the populations of Central America than subduction zone earthquakes, which are typically smaller (magnitude 7.5 to 8.0) than those of other circum-Pacific thrust zones. These shallow earthquakes are more frequent and occur at much smaller hypocentral distances from the major population centers which are concentrated along the volcanic chain.

Significant results of studies on recent earthquakes

Figure 1-3 show 28 shallow earthquakes of $Ms \geq 6.0$ that have occurred since 1904 within the volcanic arc or back-arc region of Central America. Isoseismal intensity maps were prepared from newspapers and other documents for 18 earthquakes for which no intensity maps have previously been published. For all earthquakes within a few kilometers of the active volcanic chain, the areas of intensity VII or greater are found to be of similar size though some have the long axis parallel to, and others perpendicular to the volcanic chain.

Magnitudes (Ms) for the earthquakes since 1963 were taken from the NOAA catalog. We established magnitudes for most of the earthquakes prior to 1963 from the maximum amplitude of horizontal surface waves at DBN (De Bilt, Netherlands using the magnitude formula given in the station bulletin. For four events we estimated magnitudes based upon the extent of damage. We find that the largest earthquakes at 19 different sites along the active volcanic chain all have magnitudes between about Ms 6.0 and 6.5. Focal mechanisms for earthquakes along the volcanic chain show three types of mechanisms: dextral strike-slip motion parallel to the volcanic chain, sinestral strike-slip motion perpendicular to the volcanic chain, and normal motion along north and northeast trending faults. Behind the volcanic chain, especially along the Caribbean-North American plate boundary in Guatemala, damaging earthquakes occur much less frequently but have magnitudes ranging up to 7.5.

We have obtained seismograms recorded at Guatemala City for the earthquakes after 1930 and are able to distinguish direct P and Pn phases in some cases, and small S-P times in others to confirm the shallow origin of these earth-quakes.

Significant results of micro-seismicity studies: Figure 4 shows the epicenters of recent shallow micro-earthquakes located during cooperative projects between the USGS and Nicaragua from 1975 to 1978, Guatemala during 1982, and El Salvador during 1984. Notice that over 90 percent of the epicenters lie along the chain of active volcanoes, at the same locations as most of the recent damaging earthquakes in the region, shown in Figure 1. Along the chain of active volcanoes we have recognized at least four different types of earthquakes, all of which may produce damage:

1) The first type, *tectonic* earthquakes, occur at the offsets in the volcanic chain and are characterized by a mainshock followed by aftershocks whose numbers decrease exponentially with time, and b-values of 0.6 to 1.2.
2) The second type, *volcanic* earthquakes, occur just beneath active volcanoes and usually are accompanied by volcanic eruptions. These earthquakes occur in swarms characterized by a slow growth of seismic energy and later, volcanic activity, with the largest earthquakes near the middle of the period of seismic activity, preceeding or accompanying the initial eruption. B-values are probably about 2.0 or greater.
3) The third and most common type we call *tectono-volcanic* earthquakes. These earthquakes are midway between tectonic and volcanic type earthquakes in both energy release vs. time and b-values. They occur between the volcanoes as frequent swarms of usually low level seismic energy. Occasionally a swarm will grow large enough to produce damaging earthquakes. The largest event is usually preceeded by a period of increasing seismicity and followed by a longer period seismicity. These swarms have b-values of 1.4-1.8 and are probably related to the subsurface movement of magma beneath these volcanoes but are never accompanied by eruptions.
4) The fourth type we call *collapse* earthquakes because the events are probably caused by the collapse or slumping of part of the volcano or caldera. In the only good example we found, seismic activity increased for about a week and ended with the largest event of the series. The series had a b-value of 1.4.

It appears that many of the damaging earthquakes of types 2, 3 and 4 may be forecast a few days in advance because of the periods of growing precursory seismicity that usually precede the main shock. The persistent reports of foreshocks and the nature of recently recorded microearthquake swarms at the volcanoes lead to the intriguing suggestion that, at a minimum, many of these earthquakes could be forecast within a socially useful timeframe. We plan to carefully evaluate these reports and to examine closely the possibility that the style of tectonic deformation along the volcanic chain creates a rupture process that is characterized by foreshock activity.

Little is known about the tectonic origin of these shallow volcanic chain earthquakes. We propose a new model in which shallow earthquakes are caused by right-lateral slip along the volcanic chain due to a subduction vector 5° to 20° oblique to the dip of the Benioff zone. The model is consistent with both seismic focal mechanisms and geologic surface features in El Salvador and Nicaragua. In Guatemala and at the Costa Rica-Panama border, the data are more complex due to interactions of other tectonic features but are not inconsistent with the proposed model.

REPORTS

White, Randall H., 1985. The Guatemala earthquake of 1816 on Chixy-Polochic fault: Bull. Seismol. Soc. Am., 75, pp. 455-473.

Harlow, David H., and R. A. White, 1985. Shallow earthquakes along the volcanic chain in Central America: Evidence for oblique subduction. Earthquake Notes, 55, p. 28.

White, R. A. and D. H. Harlow, 1985. Catalog of significant earthquakes of Central American volcanic arc and back-arc since 1904, Proceedings of the IASPEI symposium on historical seismograms and earthquakes, August 27-28, 1985, Tokyo, Japan.

FIGURE CAPTIONS

Figure 1-3: ISOSEISMAL MAPS OF SIGNIFICANT EARTHQUAKES OF THE CENTRAL AMERICAN VOLCANIC ARC AND BACK-ARC. Triangles denote volcanoes of the Quaternary volcanic chain. Squares denote important cities and towns. Lightly shaded areas denote ares of MM VII damage. Heavier shading denotes areas of MM VII damage. White areas within shaded areas denote areas of MM IX. Dashed concentric circles denote epicenters of other significant events.

Figure 4: RECENT MICROSEISMICITY OF THE CENTRAL AMERICAN VOLCANIC ARC AND BACK-ARC. Events were located using local networks operated during cooperative projects between the USGS and Nicaragua (1975 -1978), Guatemala (1982-1985), and El Salvador 1984-1985).

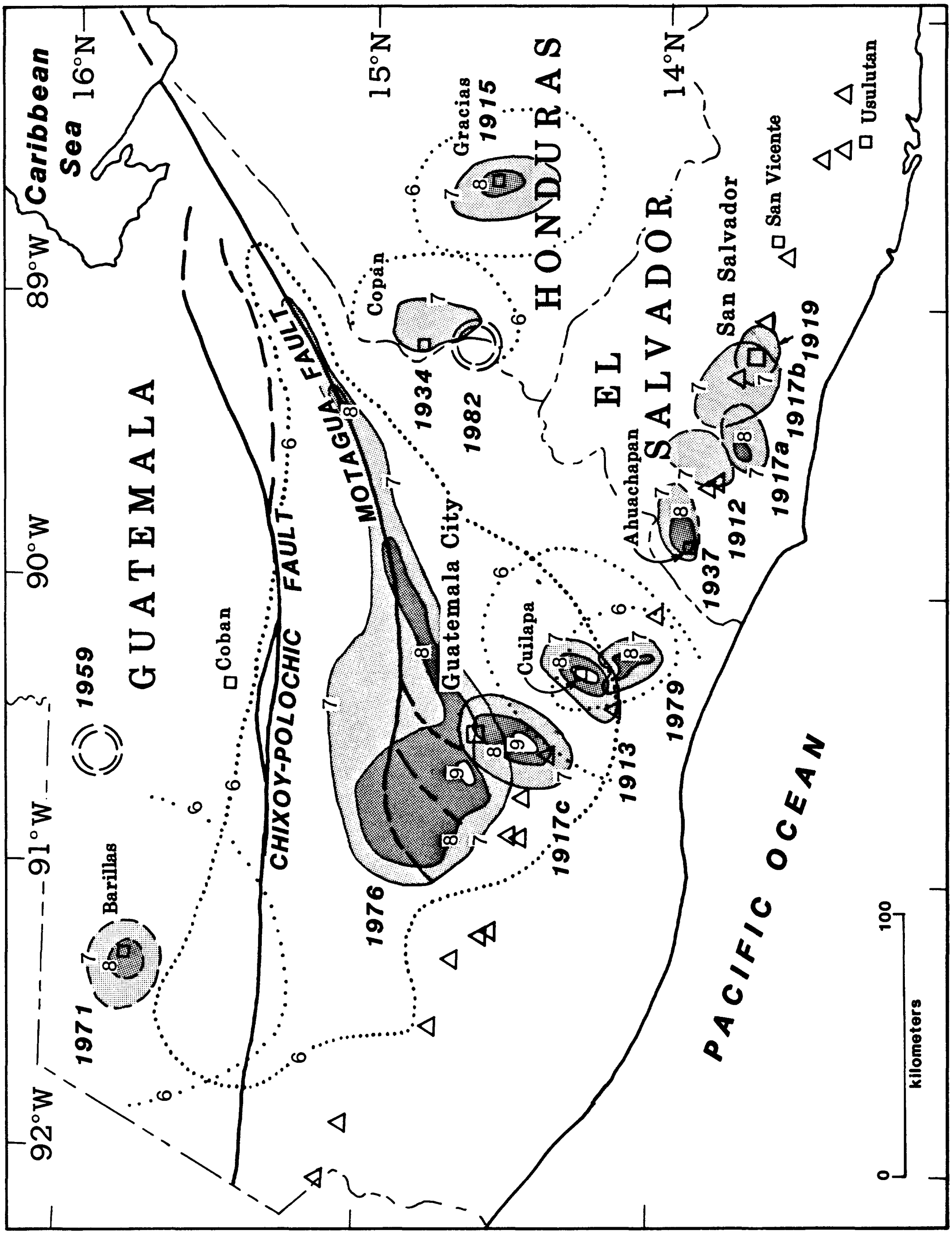
Caribbean Sea
16°N
15°N
14°N
89°W
90°W
91°W
92°W
HONDURAS
GUATEMALA
EL SALVADOR
PACIFIC OCEAN
CHIXOY-POLOCHIC FAULT
MOTAGUA FAULT
Gracias
1915
Copán
1934
1982
San Salvador
San Vicente
Usulutan
Ahuachapan
1937
1912
1917a
1917b
1919
Guatemala City
Cuilapa
1913
1979
1917c
1976
Coban
1959
Barillas
1971
6
7
8
9
0
100
kilometers

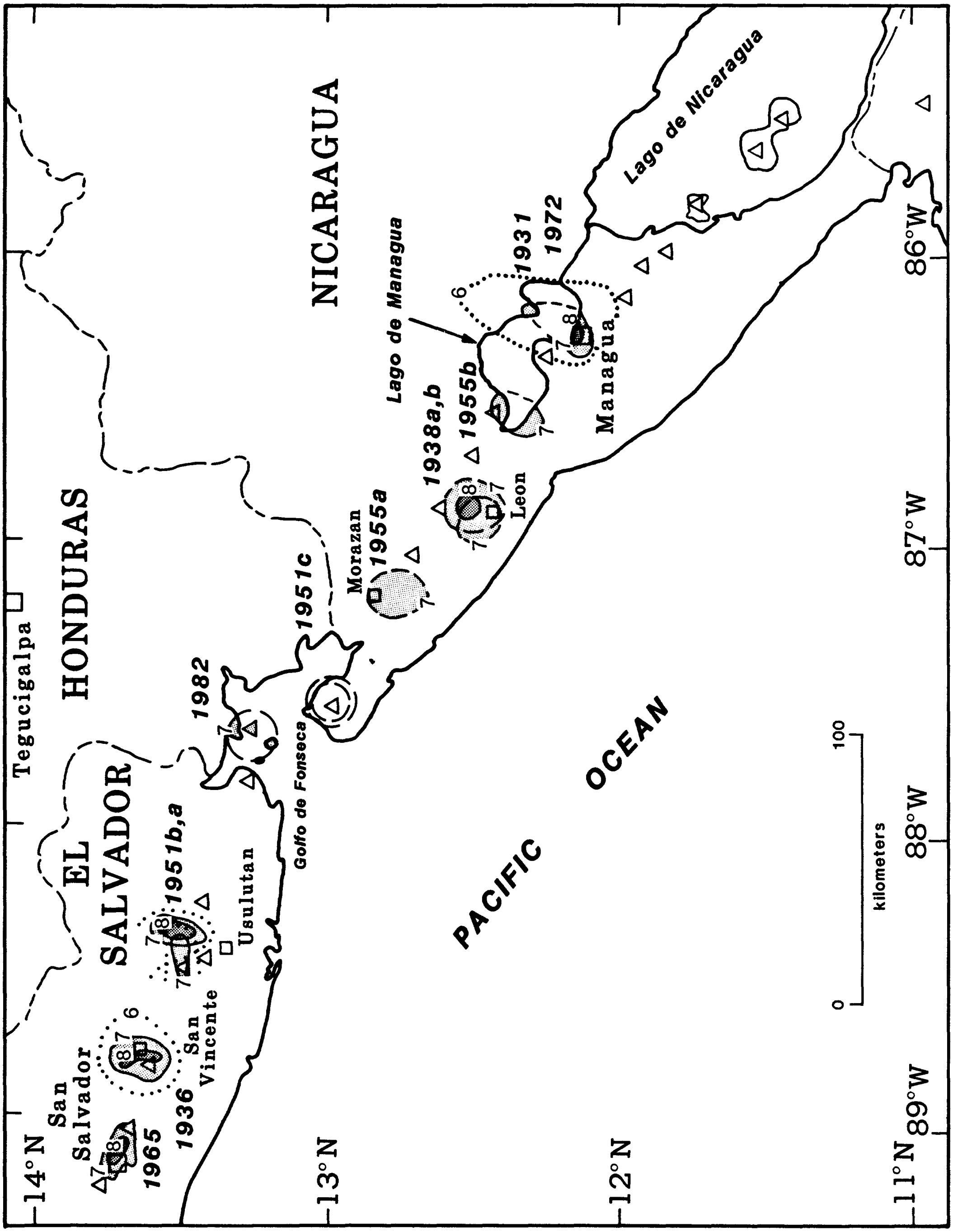
HONDURAS
Tegucigalpa
NICARAGUA
EL SALVADOR
San Salvador
San Vincente
Usulutan
Golfo de Fonseca
Morazan
Leon
Managua
Lago de Managua
Lago de Nicaragua
PACIFIC OCEAN
1965
1936
1951b,a
1982
1951c
1955a
1938a,b
1955b
1931
1972
6
7
8
0
100
kilometers
14°N
13°N
12°N
11°N
89°W
88°W
87°W
86°W

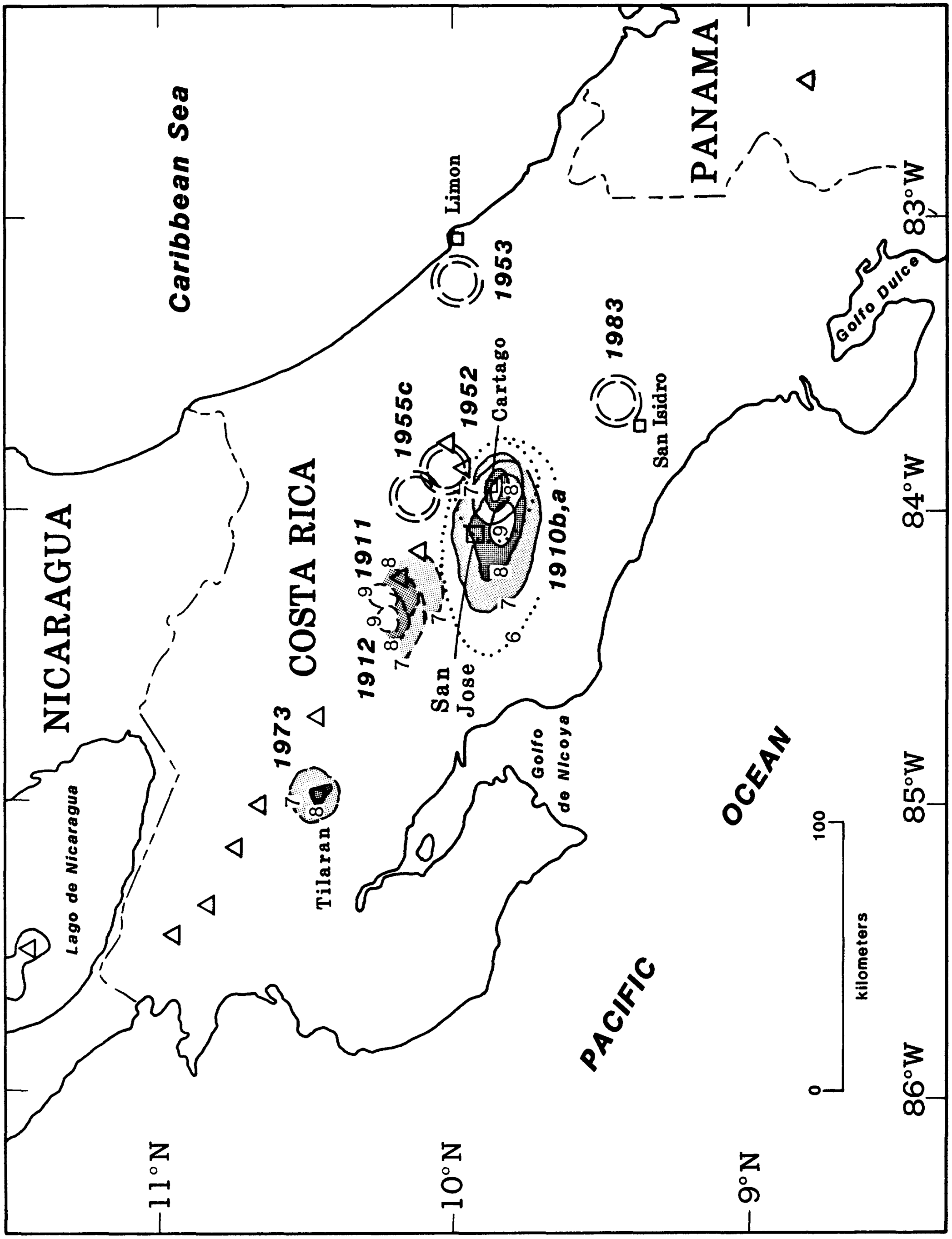
NICARAGUA
COSTA RICA
PANAMA
Caribbean Sea
PACIFIC
OCEAN
Lago de Nicaragua
Golfo de Nicoya
Golfo Dulce
Limon
Cartago
San Jose
San Isidro
Tilaran
1953
1983
1952
1955c
1911
1912
1910b,a
1973
6
7
8
9
11°N
10°N
9°N
83°W
84°W
85°W
86°W
0
100
kilometers

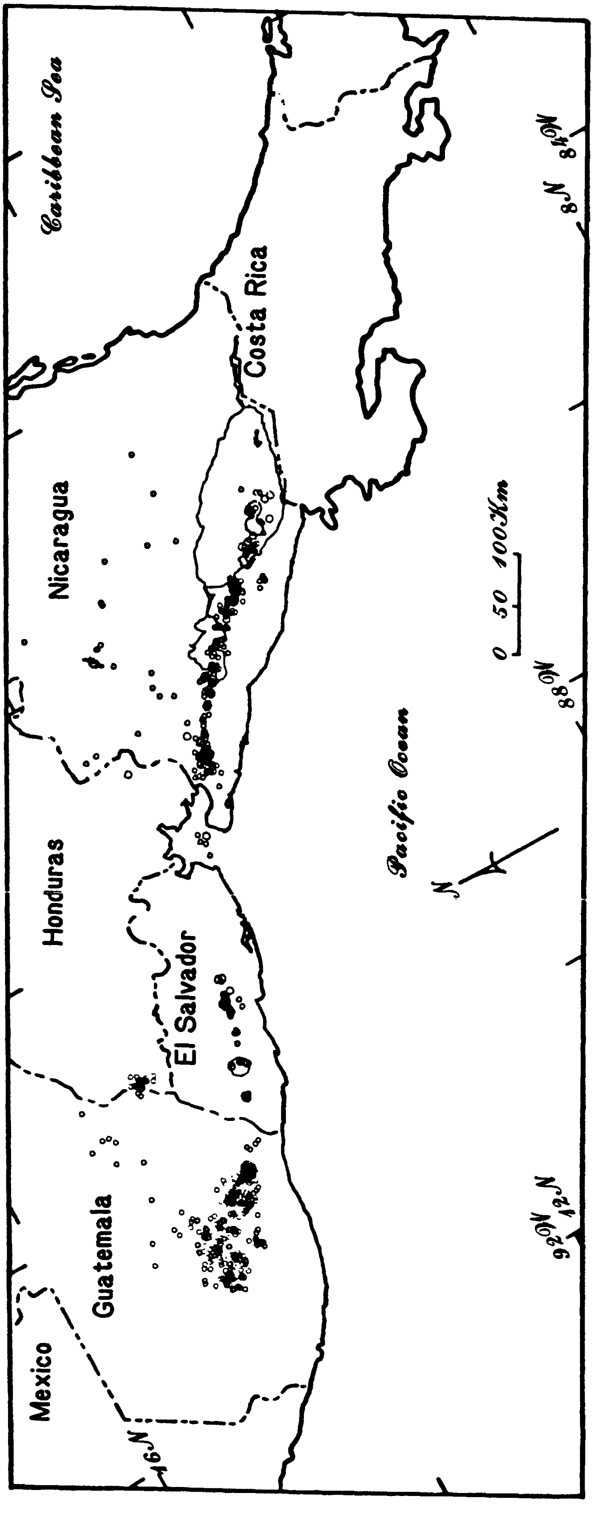
Caribbean Sea
Costa Rica
Nicaragua
Honduras
El Salvador
Guatemala
Mexico
Pacific Ocean
0 50 100 Km
N
84°W
8°N
88°W
92°W
12°N
16°N

Absolute Gravity Measurements in the Long Valley Caldera

14-08-0001-22005

Mark A. Zumberge
Glenn Sasagawa
Mary Kappus
Institute of Geophysics and Planetary Physics
University of California, San Diego
La Jolla, California 92093
(619) 452-3533

The 1980 earthquake swarm in the Long Valley region was associated with uplift reaching 40 cm over several years. This uplift, observed with periodic levelings, is indicative of subsurface magma movements (Castle, Estrem, Savage, 1984). The amount of gravity change accompanying the uplift may be useful in constraining models of possible mechanisms.

Since a gravity measurement is not tied to a series of points, vertical uplift could be mapped in an inexpensive and timely manner. We hope to complement measurements made in Long Valley with relative gravity meters (Jachens and Roberts, 1985) by making absolute gravity measurements at selected locations.

In the IGPP gravity meter the trajectory of a free falling retroreflector is measured with a Michelson interferometer and accurately timed with an atomic clock. The position of the falling mass x(t) in a uniform gravitational field is

$$x(t) = x_0 + v_0 t + 1/2\ gt^2.$$

We obtain g by least squares fitting a quadratic to the position versus time data collected.

The absolute gravity meter uses atomic length and time standards and we believe it is not subject to drift. Two operators can measure one site per day, with an accuracy of 10 microgals. This implies that an uplift on the order of 3 cm could be detected. The instrument has been deployed in the field since June 1984 and we have obtained a number of measurements in Nevada and California, including the Long Valley Caldera.

A site at the Mammoth Lakes Forest Service Vistor´s Center has been measured in July 1984, February 1985 and July 1985. No significant change in gravity was observed during this period. In July 1985 we established a site at the former Mammoth Elementary School. Table 1 presents the data from these sites. Figure 1 plots gravity versus time at the Mammoth Lakes Forest Service Visitor´s Center.

Some of the data in Table 1 include a -7 microgal correction due to the finite bandwidth of a photomultiplier which introduces a systematic error into the measurement. The correction was determined by comparing photomultiplier gravity data with data accquired using a fast avalanche photodiode. We are still evaluating this correction term.

We intend to continue measurements in the Long Valley area and to expand the number of sites. The instrument has completed over a year of field operations with no major problems. In addition to making gravity measurements in the field, we will continue to investigate possible sources of systematic error in the gravity meter and develop new ways to increase the accuracy of the device.

References

Castle, R.O., J.E. Estrem, J.C. Savage (1984). Uplift across Long Valley Caldera, California, J. Geophys. Res., 89, 11507-11516.

Jachens, R.C., C.W. Roberts (1985). Temporal and areal gravity investigations at Long Valley, California, J. Geophys. Res. (in press).

Table 1

Mammoth Lakes Forest Service Visitor's Center
37.65°N 118.95°W

Date	Mean g (m/s^2)	σ (μgal)	Number of Drops	Uncertainty (μgal)
1984:191	9.79 232 585	203	1100	12
1985:051	9.79 232 578	115	1000	10
1985:198	9.79 232 587	114	700	11

Mammoth Lakes Elementary School (abandoned)
37.64°N 118.85°W

1985:199	9.79 269 662	62	1000	9

Values are transferred to the floor level from the 109 cm instument height with a relative gravity meter.

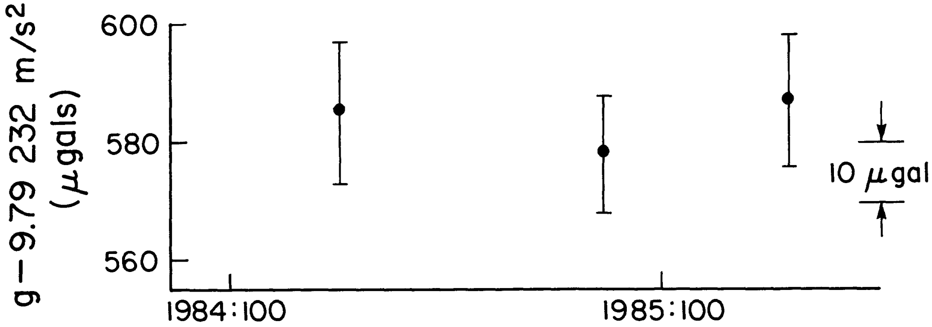

Figure 1. Gravity measurements at the Mammoth Lakes Forest Service Visitor's Center between July 1984 and July 1985.

Creep and Strain Studies in Southern California

Contract No. 14-08-0001-21979

Clarence R. Allen and Kerry E. Sieh
Seismological Laboratory, California Institute of Technology
Pasadena, California 91125 (818-356-6904)

Investigations

This semi-annual Technical Report Summary covers the six-month period from 1 April 1985 to 30 September 1985. The contract's purpose is to monitor creepmeters, displacement meters, and alignment arrays across active faults in the southern California region. Primary emphasis focuses on faults in the Coachella and Imperial Valleys.

Results

During the reporting period, alignment arrays were resurveyed across the San Jacinto fault at COLTON (twice), across the San Andreas fault at UNA LAKE, PALLETT CREEK, CAJON, WATERMAN CANYON, SANTA ANA WASH, and DILLON ROAD, across the Coyote Creek fault at BAILEYS WELL, across the Superstition Hills fault at SUPERSTITION HILLS, across the Imperial fault at HIGHWAY 80, and across the Garlock fault at CAMERON. In addition, creepmeters and displacement meters were serviced where they straddle the San Andreas fault at LOST LAKE, and MECCA BEACH (twice), the Brawley fault at HARRIS ROAD, the Superstition fault at SUPERSTITION HILLS, and the Imperial fault at HEBER ROAD, ROSS ROAD, and TUTTLE RANCH. All of these localities are described in Louie *et al*. (1985).

No significant creep events were detected, nor any significant changes with respect to the overall situation recently described in Louie *et al*. (1985).

Gradual progress is being made in conversion of telemetry of the continuous recording creepmeters at MECCA BEACH, ROSS ROAD, HEBER ROAD, and TUTTLE RANCH from telephone lines to the satellite-based SMS/GOES system. Because potential vandalism will prohibit such telemetry from the current station at MECCA BEACH, a new creepmeter installation is underway at SALT CREEK, about 7 km farther southeast along the San Andreas fault. A new installation will also be necessary at ROSS ROAD, where we will have to move the creepmeter across the street in order to have available a suitable antenna site.

Publication

Louie, J. N., Allen, C. R., Johnson, D. C., Haase, P. C., and Cohn, S. N., 1985, Fault slip in southern California: Seismol. Soc. America Bull., v. 75, p. 811-833.

On-Line Seismic Processing

9930-02940

Rex Allen
Branch of Seismology
U.S. Geological Survey
345 Middlefield Road, MS 77
Menlo Park, California 94025
(415) 323-8111 ext 2240

Investigations and Results

The #2 Real-Time Processor (RTP) at Menlo Park has been expanded to handle 152 stations. With the 256 stations in the #1 system we will now be able to put over 400 stations on line.

The Mark II version of the RTP is now running in the prototype system. This is a Motorola VME/10 using a 68010 processor and standard off-the-shelf peripherals (A/D, etc.). The picker routine proper as well as the associator programs are now coded in FORTRAN. Except for system interface (interrupt service intitialization, etc) only the input filters are in assembly language. The prototype mimics the Mark I RTP in that it produces phase-cards only, with no saving of the digital record. It has allowed us to make estimates of what can be expected of later versions using the 68010 or 68020 processor in a more efficient hardware configuration.

The currently operating setup can handle 12 analog lines, and the same 68010 processor operating with no wait states will handle about 24 . The target system, a multiprocessor using a dozen or so 68020 elements will be able to deal with something over 32 stations per processor.

The project effort at this point is directed toward implementation of the operating RTP software in the more efficient hardware, and also in modifying the software to better serve current branch requirements. Performance enhancements we expect to provide include the following items.

a) Location of earthquakes using a full iterative location routine instead of the fast trial locator as in the Mark I. This will give better online locations, and also may provide another method of detecting noise glitches and other such spurious events.

b) Detection of teleseisms by at least a selected subset of the CALNET stations.

c) More rapid identification, location, and magnitude estimates for earthquakes. The current RTP provides a preliminary location and phase list at about 200 seconds after the first p-phase arrival. We expect to cut this to 10 seconds or less.

d) Optional saving of the digital seismic record. The Mark I RTP is unable to save a copy of the digital record for later offline analysis. I expect the Mark II to be able to do this if required, since it would be useful at some sites.

Jim Ellis has completed the software and digital hardware for running John Evans' teleseism detection algorithm in a low power microprocessor and has tested it using artificially generated input signals. The analog front end has some problems which must be corrected before testing with real seismic signals.

An open file report on Ellis' high speed interface for Tektronix Graphics Terminals is almost complete. This report will allow anyone who wants one to build it themselves so we can get out of the business of supplying interfaces to others.

Tectonic Tilt Measurement: Salton Sea

14-08-0001-21918

John Beavan and Roger Bilham

Lamont-Doherty Geological Observatory of Columbia University
Palisades, New York 10964
(914) 359-2900

Investigations

Water level measurements have been made at two or three sites on the Salton Sea since 1950. Two of the data sets consist of weekly to monthly tide staff readings with 3 cm resolution, the other is a continuous paper-chart recording of a float-type gauge with approximately 3 mm resolution. We have brought up to date an earlier analysis of these data (Wilson and Wood, 1980) that showed significant tectonic tilting. We are attempting to reduce the noise level of the data by improved processing techniques, including use of weather records to identify particularly noisy data. We have started installation of our own pressure-sensor based water level gauges in order to provide continuous recording and much higher accuracy than the existing gauges. Our ultimate aim is to identify tectonic or earthquake-related signals in the data.

We are also investigating the detailed geometry and topography of the San Andreas fault in the vicinity of the Salton Sea, to see how these relate to the local tectonics (Bilham and Williams, 1985).

Results

The gauge locations and the results of Wilson and Wood (1980) are shown in Fig. 1. Our processing through the end of 1983 is shown in Fig. 2, where the data have a 1-year low-pass filter applied. The processing includes several improvements over Wilson and Wood's: (1) The three data-sets do not represent a single gauge at a single location - each gauge has been moved (<0.5 km) on several occasions. We have checked the leveling data used to tie the sites together and have identified a 10 cm datum error in the SSSP data when the gauge was moved in Jan 1980; (2) Two gauges were run independently at FTJS between 1951 and 1970. Differencing their data (Fig. 3) gives an indication of the long-term stability of the tide-staff readings. This is good (< 1 cm) except for a rather sharp change in the Coachella readings shortly before the site was abandoned in favor of the SSSP site; (3) The data samples from the three sites are not taken simultaneousy - sometimes the closest observations are two weeks apart. We have approached this problem by fitting smoothing splines to the data, then differencing these (Fig. 4) - however, there may still be significant aliasing errors in the data.

Our data show that the increase of noise level apparent in the post-1972 Wilson and Wood data can be resolved into clear signals between 1972 and 1975. These signals are not associated with rainfall (Fig. 2); we are presently investigating wind, atmospheric pressure and gauge malfunction as possible explanations.

Our results agree with those of Wilson and Wood up to 1978 where their analysis ended. Since 1979 the NW-SE tilt rate has been virtually zero, and since 1978 significant uplift of ~2 cm (~1.4 μrad tilt) has occurred at the east site (SSSP) relative to the west (FTJS), particularly between 1978-1981. Sharp (1983) also observes E-W tilt changes in 1981 on a short fault-crossing level line near SSSP; these changes were in the same sense but as much as an order of magnitude larger. These observations may represent regional tilting, but are more likely a localised uplift associated with aseismic deformation of the Durmid anticline (Bilham and Williams, 1985).

Analyses of sea-level data obtained during the Brawley zone earthquake swarm of January 1974, and at the time of the M=5.6 Westmorland quake of April 1981, show no evidence for seismicity-related crustal deformation above the noise level.

Data from our first pressure-gauge instrument (at SSSP) are shown in Fig. 5. The 36-40 kHz output of the Paroscientific pressure sensor is counted for 12 min and recorded digitally with resolution < 1 mm. The system has worked well to date, with the exception of data gaps caused by the combination of frequent power failures and a re-booting problem in the data-collection computer. This will be fixed shortly when an additional gauge is installed at a second site. Also shown in Fig. 5 are data from the float gauge at SB. These were digitized from the paper charts on an x-y table, and are subject to amplitude errors of < 1% and timing errors of several minutes.

Principal noise sources in these data are (1) a common-mode sea-level change due to rainfall and evaporation that is easily removed by differencing; (2) seiching with a fundamental period of ~3 hr. The seiching is excited by wind storms and can reach 150 mm peak-peak amplitude. The time-constant for damping the seiche is 2-3 days; hence tide-staff readings can be in error by ~ ±40 mm even several days after a storm. The seiche amplitude is > 20 mm during 10% of the data collected to date, implying that approximately this percentage of the 1951-85 tide-staff data could have aliasing errors greater than the tide-staff resolution. We are presently investigating whether the noise in the 1951-85 data can be reduced by omitting data collected during the several days following high winds.

Fig. 6 shows spectra of the sea level data, and the coherence and phase between SSSP and SB. The fundamental and higher-mode seiches are obvious as bands of high coherence; the phase relation between the sites is either ~0° or ~160° depending on the spatial behavior of the mode. Differencing the SSSP and SB data-sets removes the long-term signal (Fig. 5a), but not the seiching because of the site dependence of the seiche amplitude and phase. Seiching that is coherent between sites may be removed by Wiener filtering; we have been able to remove 50% - 75% of the seiche energy by this means (Fig. 5a). (This result may be improved when data from a second pressure gauge are available, since they will have better timing and higher resolution than the paper-chart records.) If we are only interested in signals much longer than 3 hr duration, then the seiching can be removed by low-pass filtering (Fig. 5b). No vertical tectonic motion > 5 mm (0.1 μrad tilt) has occurred during May - August 1985.

References

Bilham, R.G. & P.L. Williams, 1985. Saw-tooth segmentation and deformation processes on the southern San Andreas Fault, *Geophys. Res. Lett.*, **12**, *557-560.*

Sharp, R.V., 1983. Salton Trough tectonics and Quaternary faulting, *U.S. Geol. Surv. Open File Rept.*, **83-918**, *130-133.*

Wilson, M.E. & S.H. Wood, 1980. Tectonic tilt rates derived from lake-level measurements, Salton Sea, California, *Science*, **207**, *183-186.*

Reports

Bilham, R.G., 1985. Transpression and earthquake prediction on the southern San Andreas Fault in the Coachella Valley, California, *NEPEC meeting, Pasadena, Ca, 29 May 1985, U.S. Geol. Surv. Open File Rept., in press.*

Bilham, R.G. & P.L. Williams, 1985. Saw-tooth segmentation and deformation processes on the southern San Andreas Fault, *Geophys. Res. Lett.*, **12**, *557-560.*

Hudnut, K., J. Beavan & R. Bilham, 1985. Salton Sea-Level data - active transpression on the southern San Andreas Fault (abstract), *EOS*, **66**, *383.*

IT-2

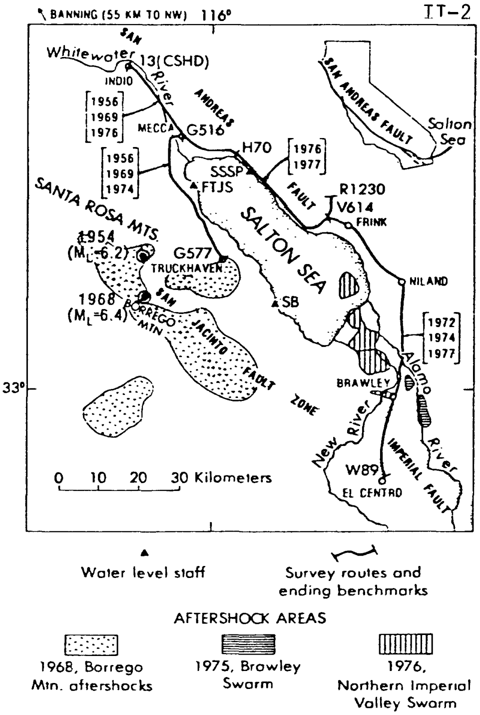

Fig. 1 Map of the Salton Sea area, southern California, showing routes of repeated first-order leveling and locations of terminal benchmarks [13(CSHD), G516, H70, R1230, V614, W89, and G577]. Years in brackets indicate the dates of leveling. The water-level staffs are located at Fig Tree John Springs (*FTJS*), Salton Sea State Park (*SSSP*), and Sandy Beach (*SB*). Locations of the aftershock areas of the 1968 Borrego Mountain earthquake are adapted from Hamilton (*9*). Locations of the 1975 Brawley swarm area are from Johnson and Hadley (*10*), and locations of the 1976 Northern Imperial Valley swarm are from Schnapp and Fuis (*11*): $M_L = 6.2$ and $M_L = 6.4$ are Richter magnitudes for moderate-size earthquakes during the years indicated.

0036-8075/80/0111-0183$00.50/0 Copyr

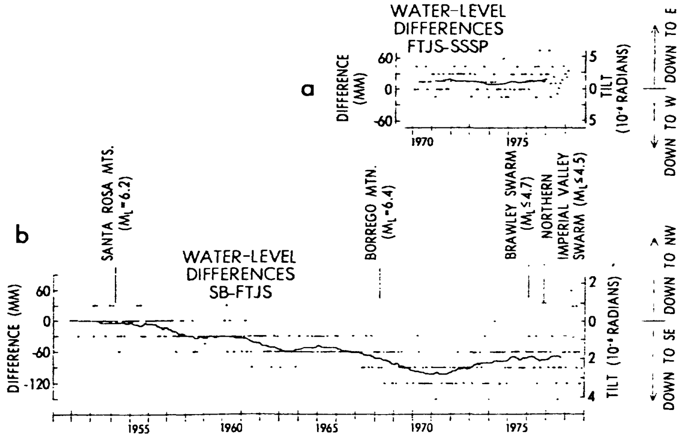

Fig. 2. History of water-level differences between pairs of stations on the Salton Sea. The continuous line is a 27-point running average; (a) water-level differences for the *FTJS-SSSP* pair; (b) water-level differences between *SB* and *FTJS*. Original data are shown as points.

Figure 1. Index map and results from Wilson & Wood (1980).

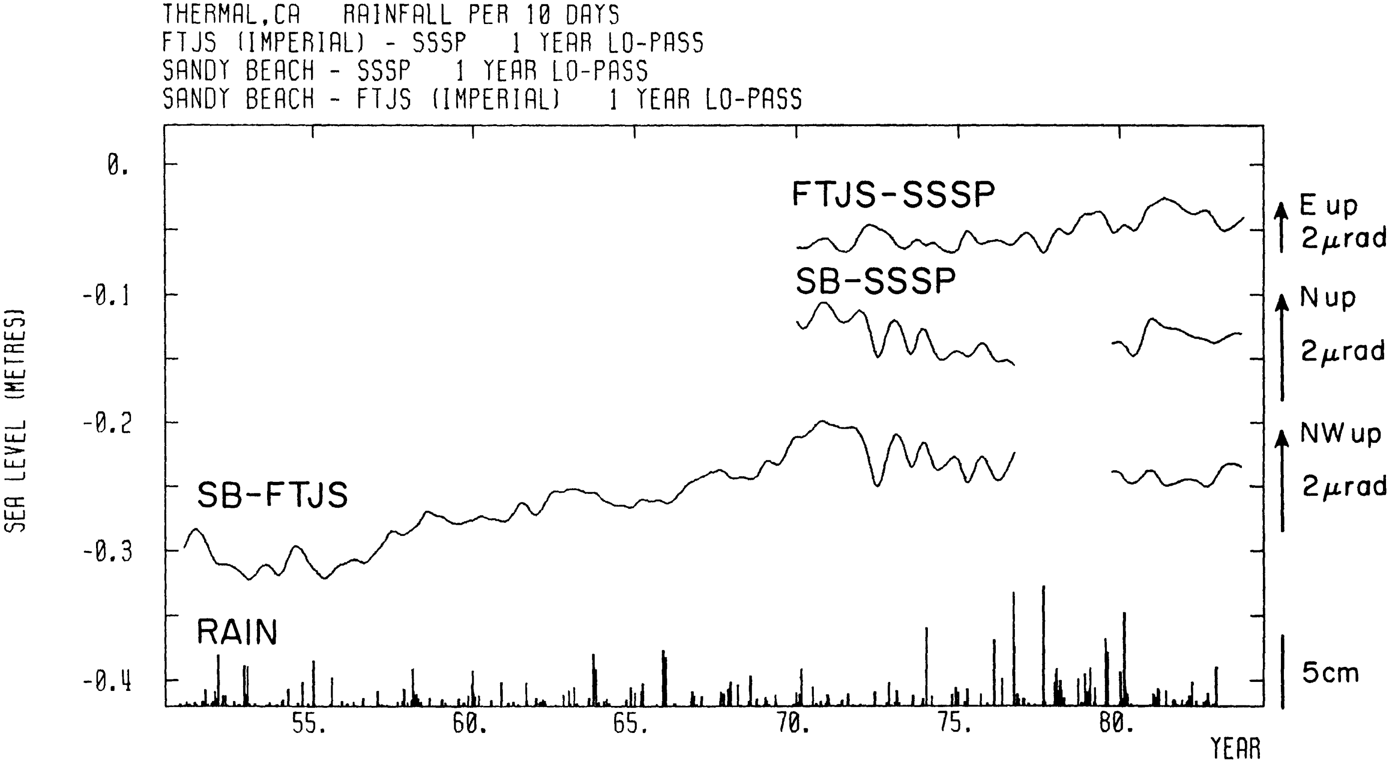

Figure 2. Differences between sea-level records, using data sampled at 10-day intervals (see Fig. 4). After differencing, a 1-year low-pass filter has been applied. We reproduce the results of Wilson & Wood (1980) up to 1978. Since 1979, the NW-SE tilt has been zero, and there was ~2 cm uplift of SSSP relative to FTJS between 1978-1981 in the E-W direction. The data show some evidence of recovery since then.

The gap represents a period when the SB gauge was inoperative following hurricane damage. Tick marks on the time axis are at the start of the labelled year. The curves are offset vertically for clarity.

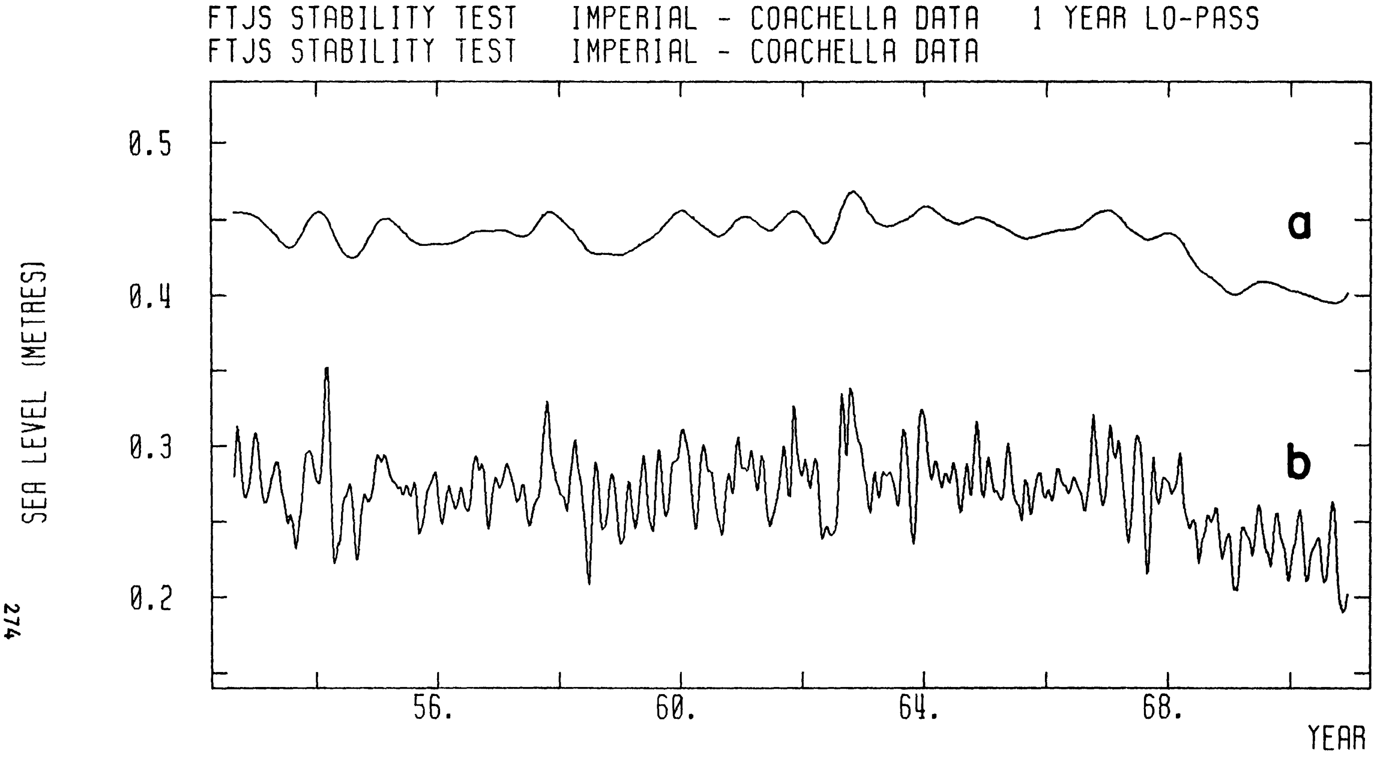

Figure 3. Stability attainable by the tide-staff gauges. Two nearby (~ 0.5 km) gauges (reading accuracy 3 cm) track within a maximum excursion of 13 cm at 10-day periods (b), and 4 cm at annual periods (a), with the exception of the last two years data before the one gauge was discontinued. The long-term offset is < 1 cm (excluding the last two years). The curves have been offset vertically for clarity.

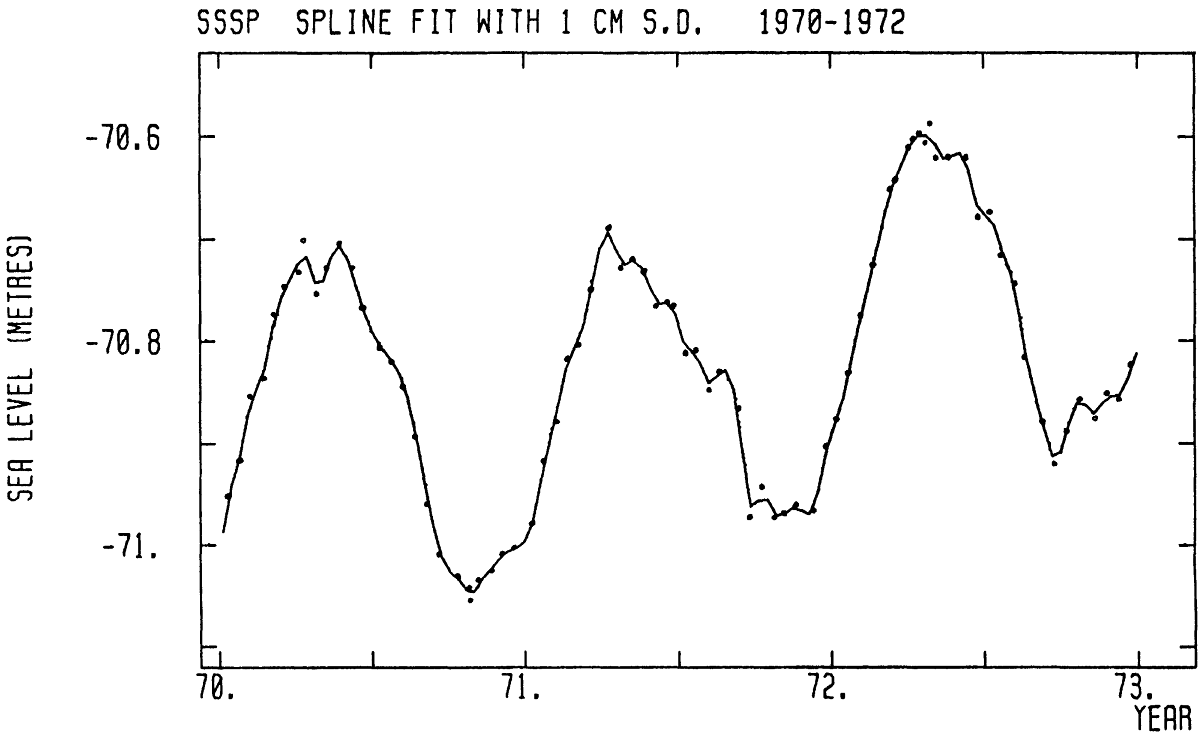

Figure 4. Fitting of smoothing spline fuction to the sea-level data. The dots are observed data that are read to ± 1.5 cm. The continuous line is the spline fit, which is sampled at 10 day intervals for further analysis. Tick marks on the time axis are at the start of the labelled year.

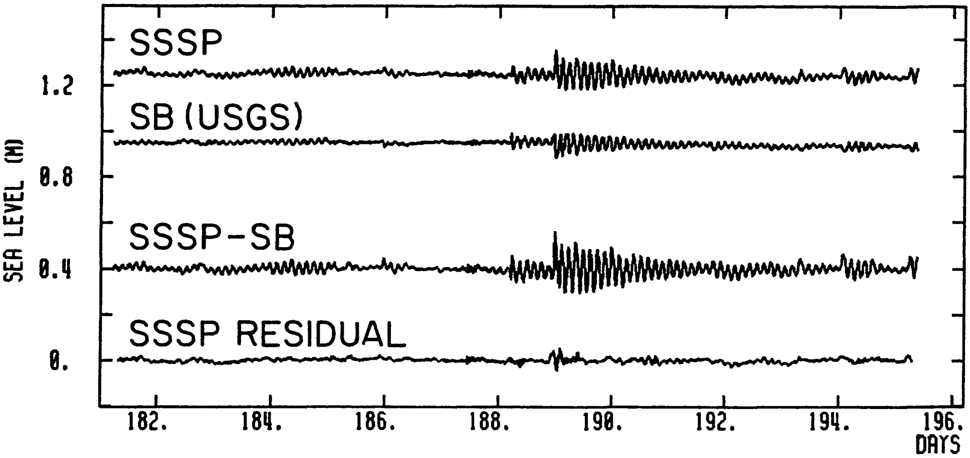

Figure 5a. Two weeks digital data from pressure sensor gauge at SSSP, and from USGS float-type gauge at SB (digitized from paper chart). Differencing the data (SSSP-SB) removes any long-term sea-level change, but not the seiche signal. The amplitude and phase relation between the seiche at any two sites is fairly constant; hence it can be removed in part by Wiener filtering. The lower trace shows the effect of a 5 hour filter.

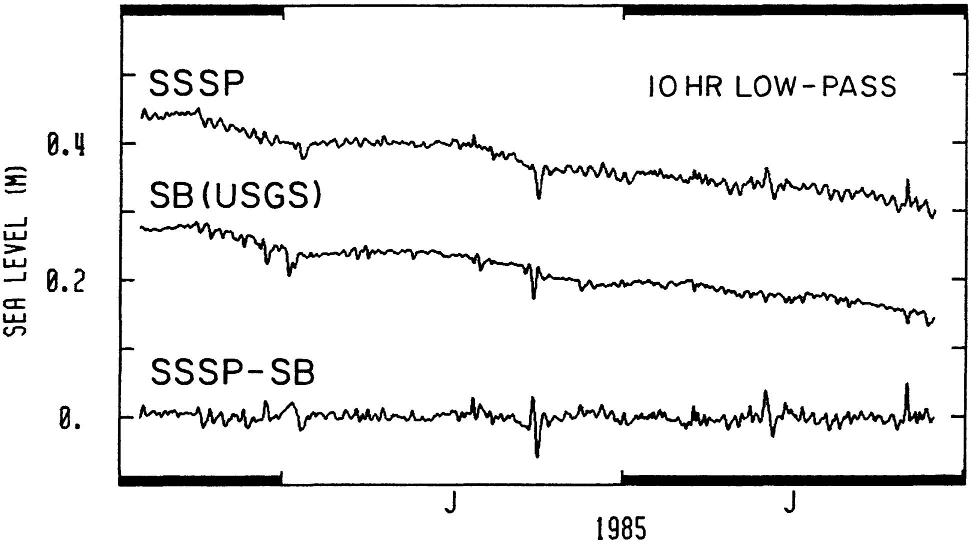

Figure 5b. The first ten weeks data from the pressure sensor gauge at SSSP. The data have been low-pass filtered at 0.1 c/hr. Also shown are data digitized from the paper-chart recordings of the USGS float-type gauge at SB. Differencing the data (SSSP-SB) gives an estimate of relative vertical tectonic motion, assuming that variations of air pressure, water temperature and salinity between sites have been allowed for. No motion > 5 mm (~ 0.1 μrad tilt) has occurred during May - August 1985.

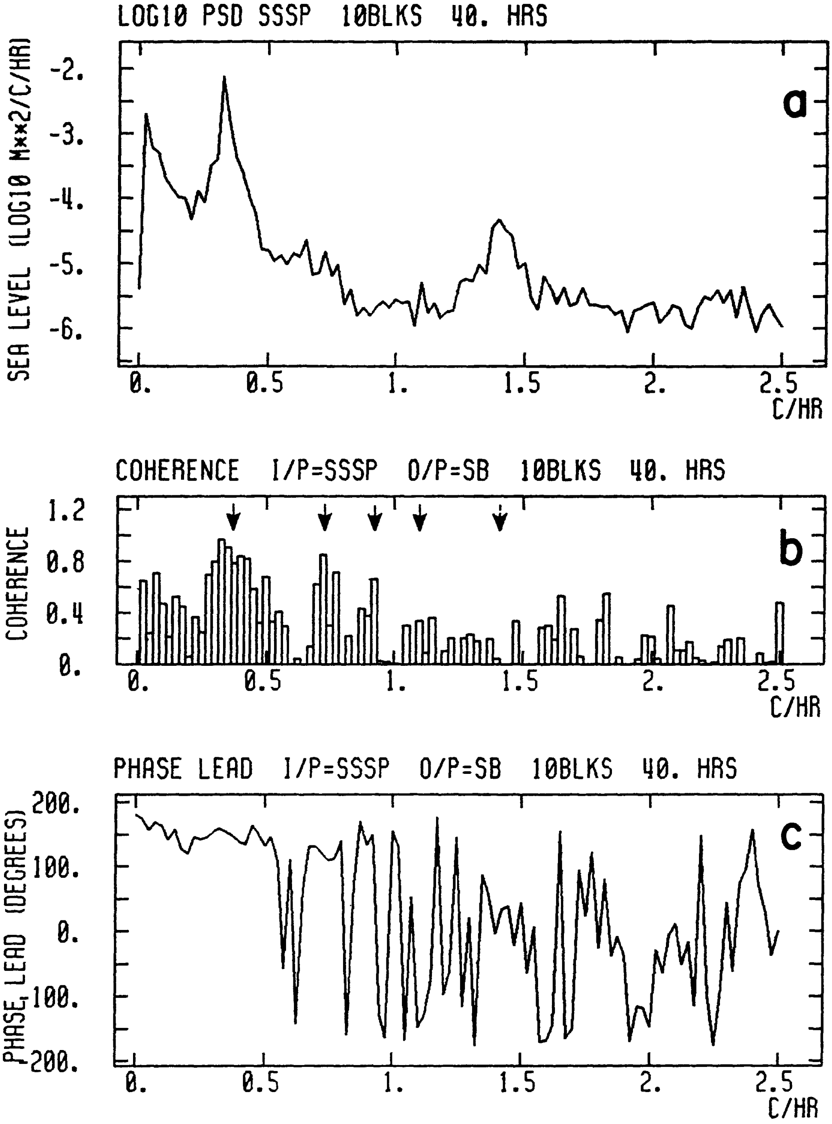

Figure 6. (a) Power spectral density of SSSP data. The principal seiche modes at ~ 0.3 c/hr and ~ 1.5 c/hr are clearly seen. (b) Coherence between SSSP and SB. The bands of higher coherence (arrows) indicate the fundamental and higher-order seiche modes. The phase relation (c) between these sites is ~ 180 ° for the first few modes. The ~ 1.5 c/hr mode may have ~ 0 ° phase difference, but the coherence is low at these frequencies because of insufficient time and amplitude resolution on the paper-chart records.

PARKFIELD TWO-COLOR LASER STRAIN MEASUREMENTS

9960-02943

Robert Burford
Branch of Tectonophysics
U.S. Geological Survey
345 Middlefield Road, MS/977
Menlo Park, California 94025
(415) 323-8111, ext. 2574

and

Larry Slater
CIRES
University of Colorado
Boulder, Colorado 80309
(303) 492-8028

Investigations

The CIRES two-color laser ranging system has been operated at the Parkfield CAR HILL site to obtain frequent distance readings to reflector sites designated in Figure 1. Additional measurements were made occasionally to sites without permanent reflectors as well as to reference marks at the permanent sites.

Results

Data are currently handled as in the past (see previous report), but some progress has been made in an effort to convert to on-site automated data entry.

Plots of length changes obtained since late June, 1984 are shown in Figure 2. Details of these changes since April 1, 1985 are shown in Figure 3. The record for station MID (Figure 2) is composed of 2 separate parts owing to loss of the original reflector during late December 1984, with resulting loss of zero. The reflector pier at PITT has shown continuing instability and the line has been dropped. A new station will be established as a replacement (station POMO, Figure 1).

Results of a model, consisting of shallow slip plus uniform strain, indicate that dextral shear (tensor) accumulated at a rate of 1.3 ± 0.3 ppm/yr through March 1985, followed by a period of near-zero strain (-0.3 ± 0.2 ppm/yr) until late July, when shear-strain accumulation resumed at a rate of 2.8 ± 0.9 ppm/yr (Figure 4). Inferred displacement across the San Andreas fault indicates shallow slip (upper 2 km) during two episodes: August-September 1984 (34.3 ± 5.3 ppm/yr) and April-August 1985 (35.2 ± 2.2 mm/yr). The model also indicates significant fluctuations in areal dilatation within the network. However, the dilatational component is subject to systematic error due to possible drift in instrument scale. Occasional comparisons between the observatory instrument and a portable 2-color geodimeter indicate that drift between the two instruments is about +0.4 ± 0.1 ppm/yr (observatory-portable). Assuming that the observatory instrument alone has been drifting linearly with time, residual dilatational trends were +0.9 ± 0.4 ppm/yr until about mid-February, 1985, -4.5 ± 1.2 ppm/yr from mid-February until early May, and +5.2 ± 1.3 ppm/yr from early May through August, 1985. The areal expansion during the latter period is partially accounted for by strain release associated with the North Kettleman Hills earthquake main shock (M_L=5.5, August 4, 1985, 26 km NE).

PARKFIELD 2-COLOR NETWORK

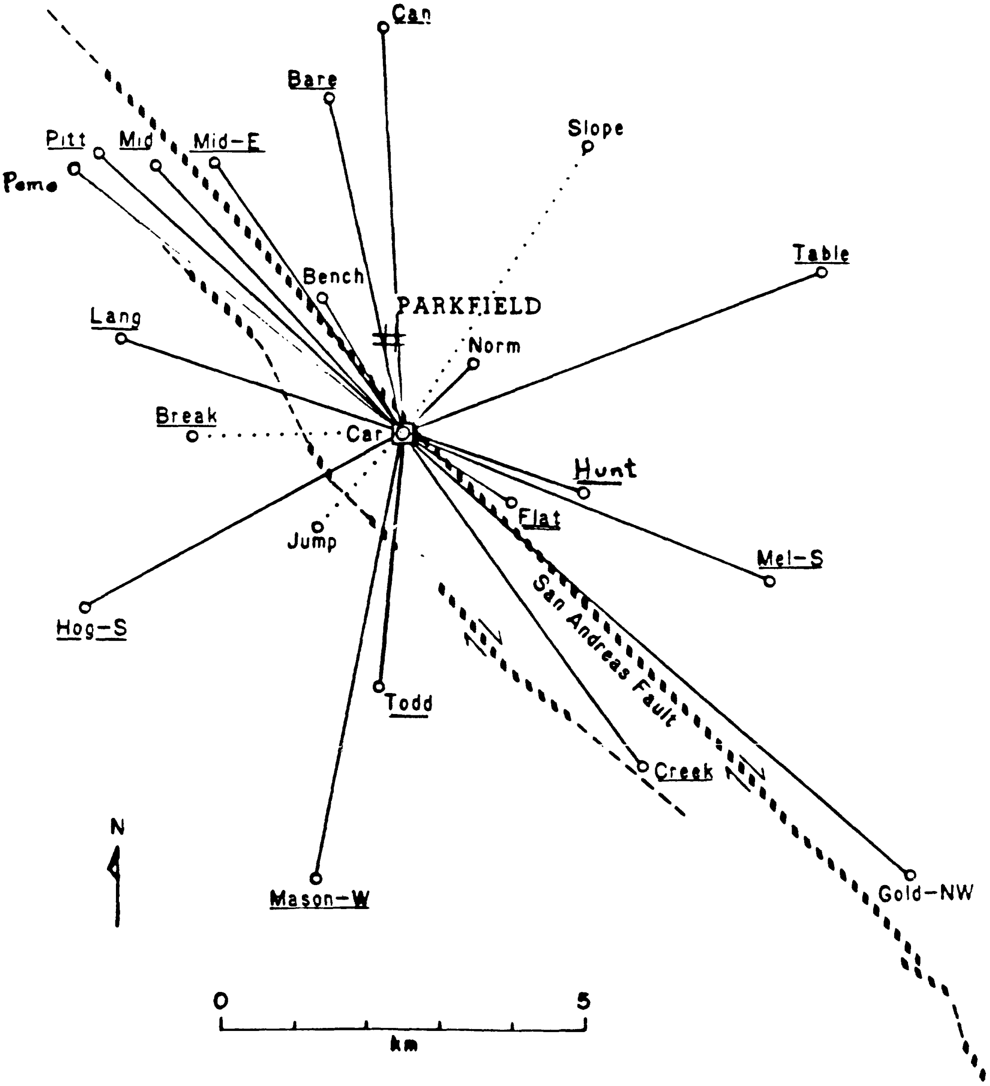

Figure 1

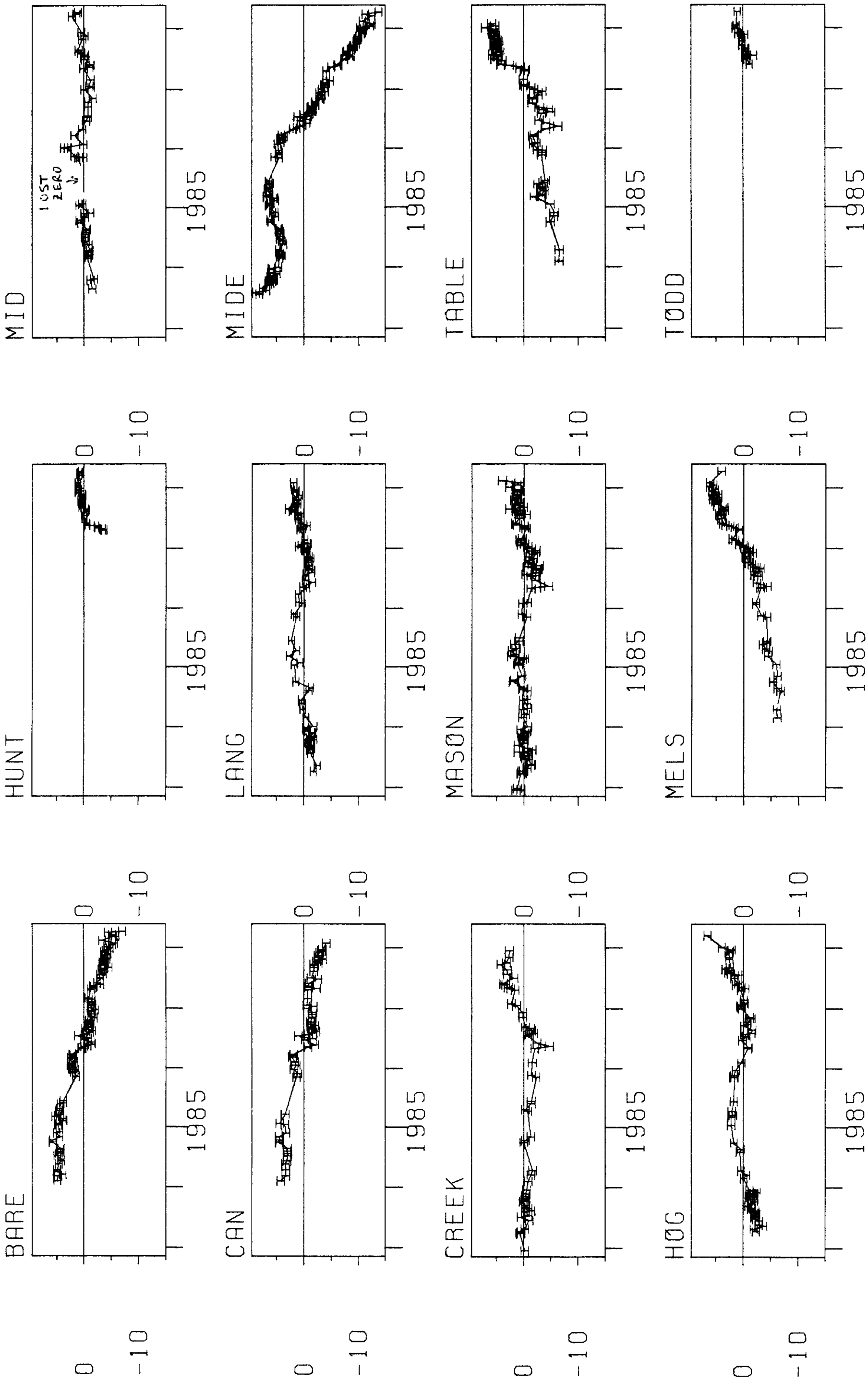
BARE
CAN
CREEK
HOG
HUNT
LANG
MASON
MELS
MID
MIDE
TABLE
TODD
1985
0
-10
LOST ZERO

Figure 2

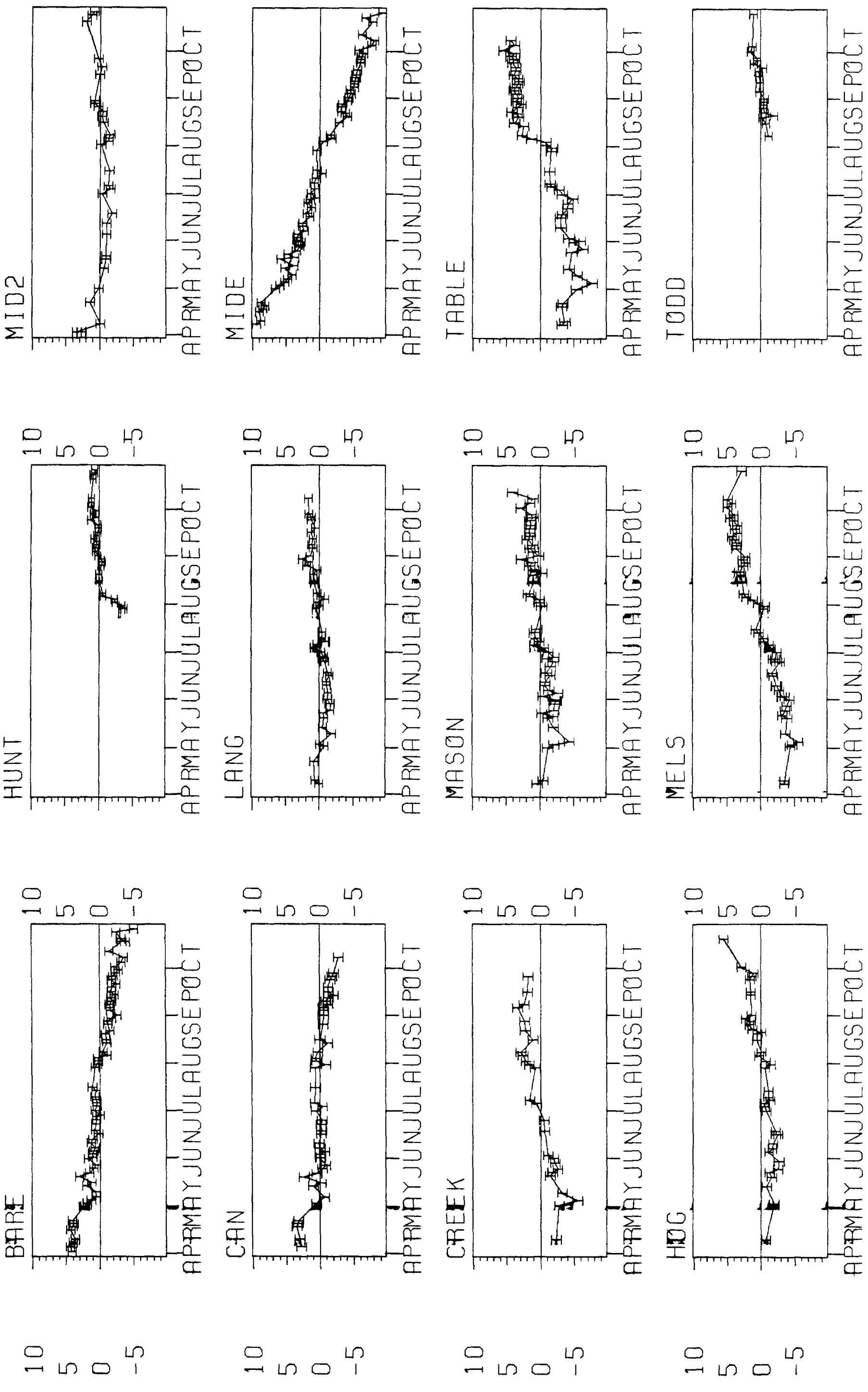
BARE
CAN
CREEK
HOG
HUNT
LANG
MASON
MELS
MID2
MIDE
TABLE
TODD
10
5
0
-5
APRMAYJUNJULAUGSEPOCT

Figure 3

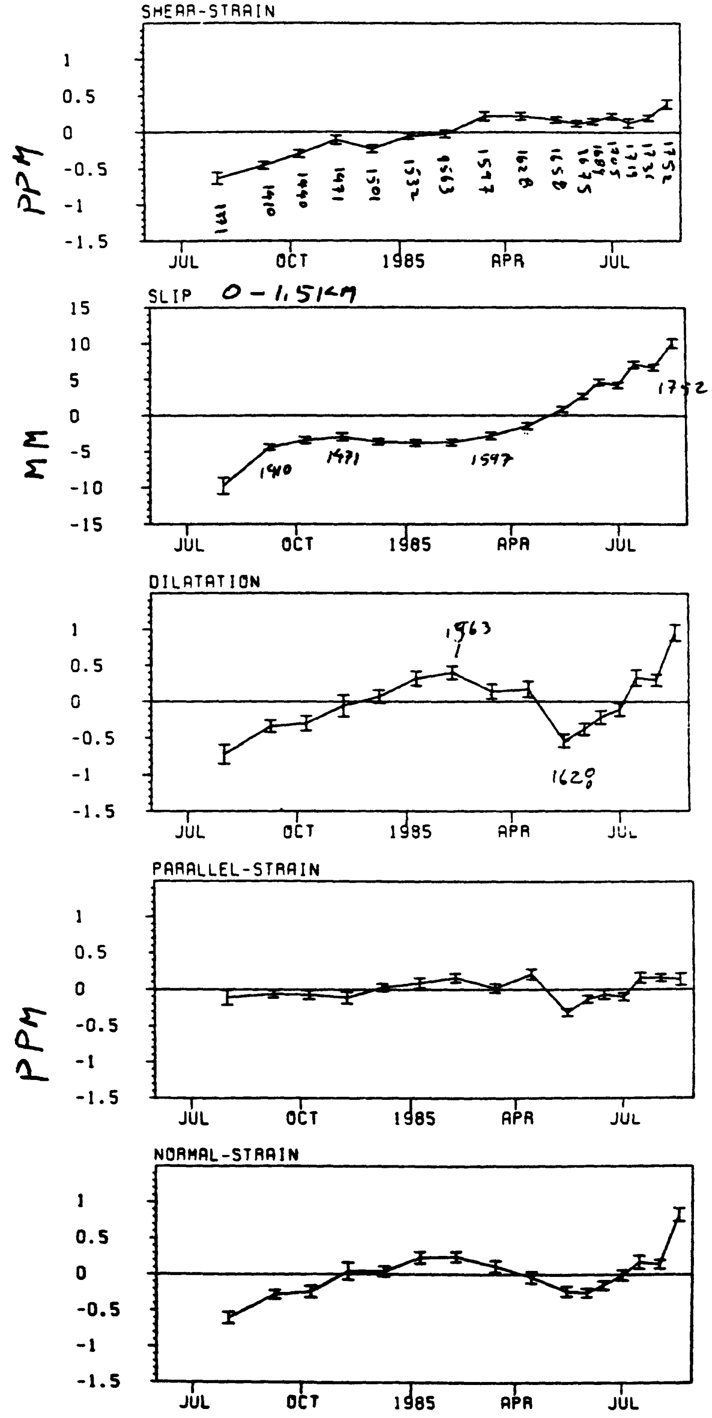
SHEAR-STRAIN
PPM
1
0.5
0
-0.5
-1
-1.5
1381
1410
1440
1471
1501
1532
1563
1597
1628
1658
1675
1689
1705
1719
1731
1752
JUL
OCT
1985
APR
JUL
SLIP 0 - 1,5KM
MM
15
10
5
0
-5
-10
-15
1410
1471
1597
1752
JUL
OCT
1985
APR
JUL
DILATATION
1
0.5
0
-0.5
-1
-1.5
1563
1628
JUL
OCT
1985
APR
JUL
PARALLEL-STRAIN
PPM
1
0.5
0
-0.5
-1
-1.5
JUL
OCT
1985
APR
JUL
NORMAL-STRAIN
1
0.5
0
-0.5
-1
-1.5
JUL
OCT
1985
APR
JUL

Figure 4

Investigation of Radon and Helium as Possible Fluid-phase Precursors to Earthquakes

14-08-0001-2203

Y. Chung
Scripps Institution of Oceanography
University of California, San Diego
La Jolla, California 92093
(619) 452-6621

Investigations:

1. Monitoring radon, helium, and other geochemical parameters in a network of thermal springs and wells along the San Andreas, San Jacinto, and Elsinore faults in southern California for possible precursory effects associated with earthquakes.

2. A general study of the relationships between these components and variations which may be due to changes in ambient conditions, seasonal effects and meteorological factors.

3. Continuous radon monitoring at network sites with field-installed Continuous Radon Monitors (CRM's) for possible short-term anomalies that may be precursory to earthquakes.

4. Comparison study of long-term variations between the CRM and the discrete Rn data. Partition of radon between the gas and water phases.

5. Joint U.S.-Chinese geochemical studies with scientists at the Institute of Geology, State Seismological Bureau (SSB) for earthquake prediction in both countries.

Results:

1. Discrete sampling for radon and helium measurements at our southern California network sites was conducted at monthly intervals during the past six months. No major earthquakes occurred in the network region during this period. Data observed at the Arrowhead site along the San Andreas fault near San Bernardino showed a sharp peak (100% above baseline) in April 1985, and have since returned to the baseline level. However, the helium peak is less impressive. This appears to have concluded the large-amplitude fluctuations which began in mid-1983.

2. Three of our network sites are being monitored for radon variations with the USC Continuous Radon Monitors (CRM's). At Arrowhead, the radon level observed between December 1984 and April 1985 was fairly constant at a much higher level due to the deployment of another CRM unit which has higher counting efficiency. After April, this unit was replaced by another unit which gives radon levels quite comparable to that of 1983 and 1984. Although Teng at USC reported a 100% radon change at his Arrowhead site before the August 4 Kettleman Hills earthquake (M=5.6), our Arrowhead data showed no significant changes. It is not clear why such a difference in CRM observations exists within a small area. This suggests that the radon source and its transport mechanism are highly localized. At Murrieta along the Elsinore fault, the

1985 data indicated a decrease toward a minimum in March and increased but with large fluctuations due to extensive plumbing activities. The discrete Rn and He data are also highly variable. At Hot Mineral Well near Bombay Beach by the Salton Sea, the main well has been used for both CRM monitoring and discrete sampling since January 1985. The CRM was initially set up for monitoring both the gas-phase and dissolved radon by circulating air through the stripping system. Large variations were observed. Since abundant gas bubbles were observed, the flushing probe was removed in March and replaced by a glass funnel to collect only the gas-phase radon for monitoring. The radon level has been more stable than that observed earlier using a stripping probe. The discrete Rn and He data obtained from the main well showed large variations due to variation in gas bubbles collected in the sampler.

3. All the CRM monitoring data are obtained on the gas-phase radon while all the discrete measurements are on dissolved radon. Radon concentration in the gas-phase as determined from the CRM data is about 20 to 25 times that in the water-phase. The variation of this partition ratio is comparable to the discrete radon variation. A general linear correlation exists between these two parameters.

4. Our joint U.S.-Chinese program is being supported by NSF. The areas designated for joint studies include part of our southern California network and Long Valley in the U.S., and Peking and S.W. Yunnan in China. Our field work in the designated areas in China was carried out during May and June 1985. Samples were collected from Peking and S.W. Yunnan along the Red River Valley for dissolved gases and He isotope measurements. Preliminary results indicate that helium at both areas is crustal with $^{3}He/^{4}He$ ratio less than atmospheric. The results will be reported at the 1985 AGU Fall Meeting in San Francisco.

Reports:

Y. Chung, Radon variations at Arrowhead and Murrieta Springs: Continuous and discrete measurements, PAGEOPH, 122, 294-308 (1984/85).

Analysis of Natural Seismicity at Anza

9910–03982

Jon B. Fletcher
A. McGarr

Branch of Engineering Seismology and Geology
U.S. Geological Survey
345 Middlefield Road, MS 977
Menlo Park, California 94025
(415) 323-8111, Ext. 2384, 2708

Investigations

1. The digital seismic array centered on the Anza seismic gap of the San Jacinto fault has now been operational for about three years. Moment, source radius, stress drop, and energy for both *P*- and *S*-waves are routinely calculated for nearly all events with $M \gtrsim 2$. The source parameter catalogue now includes almost 400 events. Time series, displacement and acceleration spectra, and the catalogue have been used in a wide variety of investigations such as the rates of high-frequency decay in displacement spectra, the scaling of earthquake source parameters, and the relationship of seismic stress drops to the state-of-stress in seismogenic fault zones.

2. As the Anza stations are surface placements, both attenuation and scattering which are presumed to be severe in the shallow low velocity layers commonly found near the earth's surface, may be cutting out the high frequencies ($f > 10 - 20$ Hz) resulting in unusually low values of stress drop. In order to investigate these phenomena a dense array of seismometers was set up at Pinyon Flat to study the coherence of body waves and coda. If energy within a particular window is coherent then we would infer it is arriving from the source and not generated locally under each site. Beamforming techniques may also illuminate whether coda is made of arrivals from some small number of identifiable reflectors or whether scattering on a smaller scale (larger number of scatterers and more uniform distribution) generates a cumulative effect.

3. The rupture characteristics of $M_L \sim 3$ earthquakes in the Anza area were studied with a technique using *P*- and *S*-waveforms and empirical Green's functions. This study seeks to determine the variation in stress drop of earthquakes in the region and to identify complexity and directivity in the rupture process of these events. The waveforms of adjacent small earthquakes (M_L 1.5) were used as empirical Green's functions and were deconvolved from the waveforms of the $M_L \sim 3$ events to yield the displacement pulses of the $M_L \sim 3$ events corrected for all propagation effects.

Results

1. The catalogue of Anza events now comprises 393 events from Oct. 1982 to July 1985: locations are shown in Fig. 1. Earthquakes continue to occur in clusters, which have been identified using early Anza data and include the two clusters at the ends of the Hot Springs and Coyote Creek faults, the Cahuilla swarm, the cluster under the town of Anza, and the more disperse seismicity near the Buck Ridge fault. A cross-cutting trend that includes the cluster at the end of the Coyote Creek fault and Buck Ridge seismicity is clearly defined. Seeber (personal communication) has pointed out that the cross-cutting trend (NE–SW direction) appears to be made up of short lineaments with northward trend. Similarly the northwest trend near station KNW appears to be made up of smaller groups with an east-west trend. Although not always consistent between clusters, within a cluster both conjugate fracture planes may be activated.

   The largest earthquake had a moment of 5.6×10^{22} dyne-cm and the smallest, 1.5×10^{17} dyne-cm. Stress drops calculated using the Brune source model vary from 0.1 bar or less to about 100 bars: generally the largest events have the largest stress drops. A peak in distribution of hypocenters with depth at about 15 km coincides with the depth of the largest stress drop obtained for an Anza event of 420 bars (Feb. 25, 1980, data are strong motion recordings). This depth which may mark the upper boundary of a brittle-ductile transition (Sibson, 1982) is deeper than the 10- to 12-km usually found for the rest of the San Andreas fault. The higher peak stress drop and the increase in depth may be related to the lithology of the Southern Californian Batholith.

2. Figure 2 shows an event recorded on 8 of the 9 stations installed at the dense array at Pinyon Flat Observatory. The recording instruments are Sprengnether DR–100's with 3-component 2 Hz geophones each digitized at 200 samples/sec. Common timing was achieved by driving each unit from a common 1 megahertz oscillator and synchronizing each unit in succession to better than 0.1 milliseconds with a master clock. While the *P*-waves look alike (are relatively coherent), the seismograms diverge significantly immediately after the direct *P*-wave arrival which is comprised of just a cycle or less: apparently a high percentage of the individual peaks in these traces are generated locally. Stations AZA, AZB and AZC are distributed around a circle with a radius of 50 m; AZD, AZE, and AZF on a circle of 100 m; and AZG, AZH, and AZI on a circle of 300 m. Slowness is calculated for a 0.6 second window on a portion of the coda in Fig. 3. The double-lobbed (the peak at 105° azimuth is not as significant as the other two) pattern is very similar to that for the *P*-wave suggesting that the scattering must be near the source.

   Coherence is near 1 out to 30 Hz and higher for most, but not all master-slave pairs using a window around the *P*-wave. On the other hand *S*-waves are rarely coherent beyond 10 Hz. These results suggest that short spectral windows around the *P*-wave may yield source spectra more reliably than *S*-wave spectra.

3. An analysis of the path-corrected displacement waveforms for several $M \sim 3$ events in the Cahuilla area reveals striking differences in stress drop and rupture complexity.

Variations in static stress drop of a factor of four are found for events within 200 m of each other and eleven minutes apart in time. Differences are also apparent in the impulsiveness of the path-corrected velocity pulses, indicating that the dynamic stress drop also varies between these events.

For some of the events studied, the deconvolved displacement pulses indicate that rupture occurred as two distinct sub-events separated in time by several hundredths of a second. Two events are characterized by unilateral rupture growth, as evidenced by the azimuthal variation in the widths and amplitudes of the displacement pulses. One event that clearly shows such directivity has a M_L of 2.4.

The inverse radon transform was applied to the displacement pulses of some of the earthquakes, in an attempt to image the slip velocity on each fault as a function of time and position. In this inversion, the fault was assumed to be one-dimensional and to rupture in a horizontal direction. The inversion for one M 2.4 event indicates that its rupture velocity was about equal to the shear wave velocity. The largest Cahuilla event recorded by the network (M_L 3.7; 5/14/85) appears to consist of two sub-events, with the second sub-event located about 200 m south of the first one.

Reports

Fletcher, J. B., L. C. Haar, F. L. Vernon, J. W. Brune, T. C. Hanks, and J. Berger, 1985, The effects of attenuation on the scaling of source parameters for earthquakes at Anza, California, to be published in the *Proceedings of the Fifth Ewing Symposium, AGU Monograph.*

Fletcher, J. B., L. C. Haar, T. C. Hanks, L. M. Baker, F. L. Vernon, J. Berger, and J. N. Brune, The digital array at Anza, CA, processing and initial interpretations of source parameters, to be submitted to *AGU.*

Brune, J. W., J. B. Fletcher, F. L. Vernon, L. C. Haar, T. C. Hanks, and J. Berger, Low stress drop earthquakes in light of new data from the Anza, California telemetered digital array, *Proceedings of the Fifth Ewing Symposium, AGU Monograph.*

Frankel, A., Fletcher, J., Vernon, F., Haar, L., Hanks, T., Brune, J. and Berger, J., Observations of stress drop variation and rupture complexity for $M_L \sim 3$ earthquakes near Anza, California, *Abstract for the 1985 Fall Meeting of the AGU.*

References

Sibson, R. H., 1982, Fault zone models, heat flow, and the depth distribution of earthquakes in the continental crust of the United States, *Bull. Seismol. Soc. Am.* **72**, 151-163.

Figure Captions

1. Epicenter map for Oct. 1982 to July 1985 for the Anza section of the San Jacinto fault. Locations are calculated using both P- and S-wave arrival times at the local digital array. The size of the circle is proportional to seismic moment. Triangles denote the site of the digital telemetered stations.

2. Vertical component seismograms from the dense array at the Pinyon Flat Observatory for an event that was located near the Buck Ridge fault. Note the similarity of the initial P-wave and the dissimilarity of the rest of the seismograms.
3. Slowness calculated for a 0.6 second window starting just after the P-wave. This plot was calculated by F. L. Vernon of the University of California, San Diego using a computer program developed by T. Bostwick and P. Spudich of the U.S. Geological Survey, Menlo Park, CA.

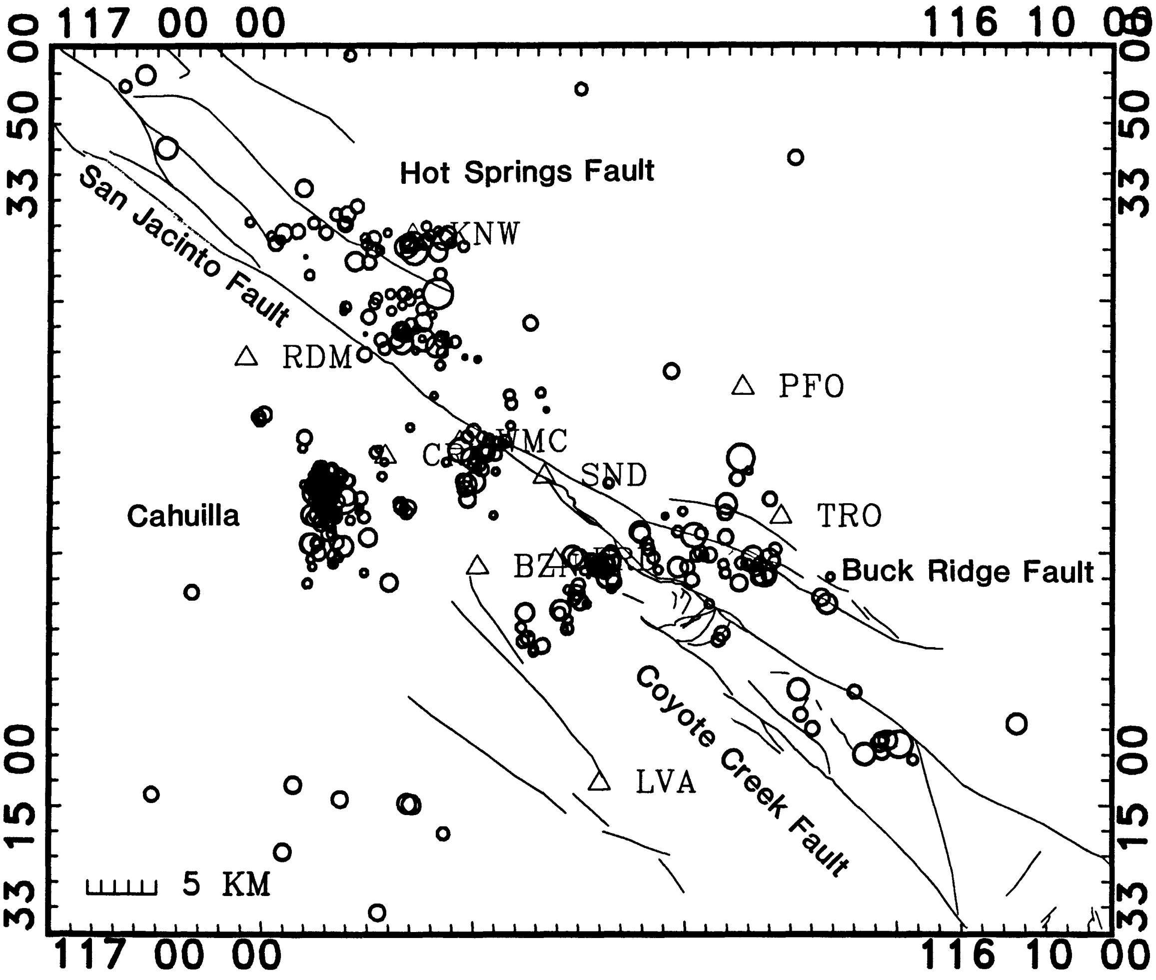
117 00 00
116 10 00
33 50 00
33 15 00
Hot Springs Fault
San Jacinto Fault
Buck Ridge Fault
Coyote Creek Fault
Cahuilla
KNW
RDM
PFO
WMC
CR
SND
TRO
BZN
LVA
5 KM

Fig.1

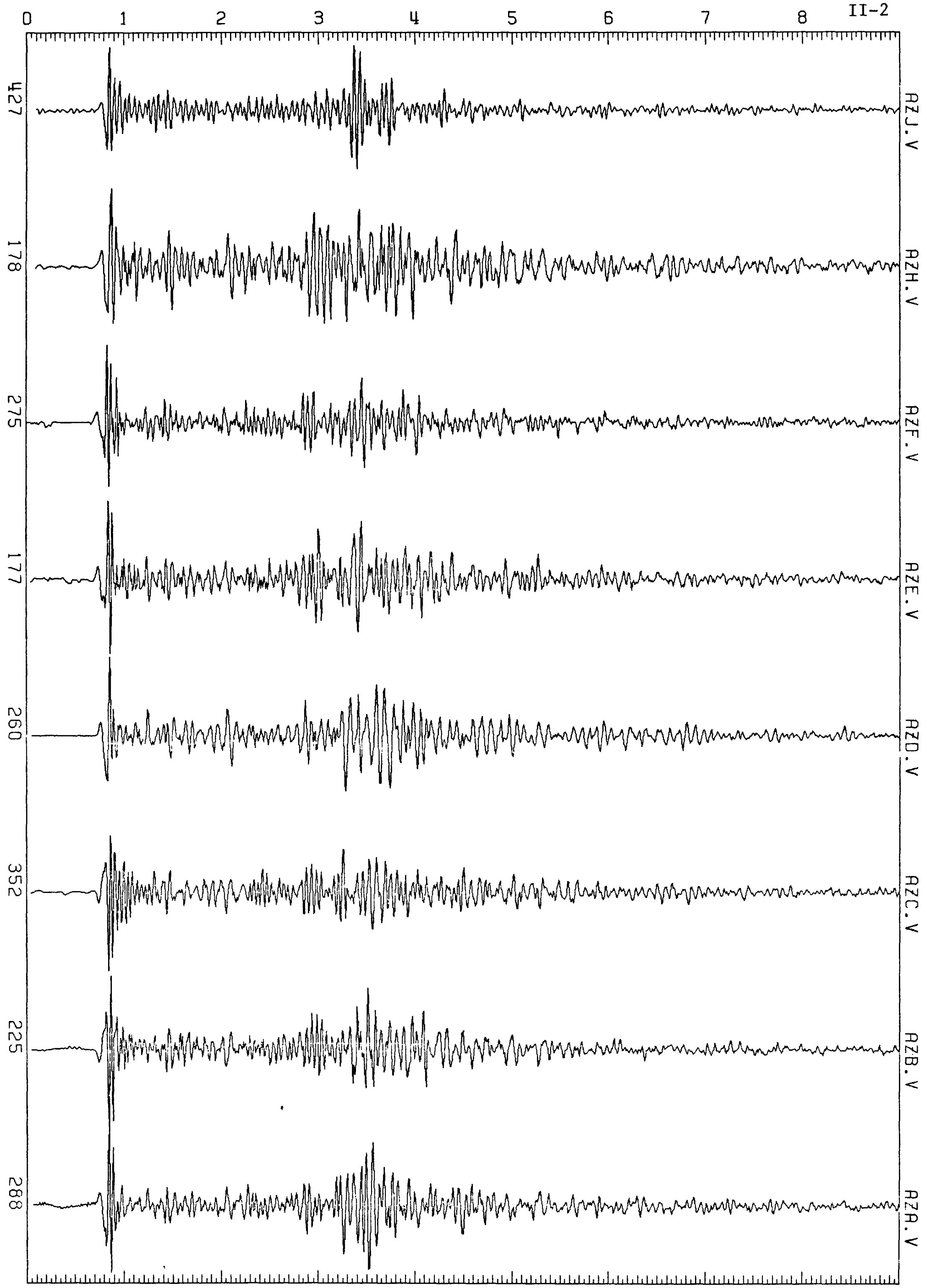
0
1
2
3
4
5
6
7
8
427
AZJ.V
178
AZH.V
275
AZF.V
177
AZE.V
260
AZD.V
352
AZC.V
225
AZB.V
288
AZA.V

Fig.2

* P+CODA ON VERTICALS DAY 180 *
STACKED S-PLANES
WINDOW = 1.20-1.80 SECONDS
SAMPLING INTERVAL = 0.025 (SEC/KM)
FREQUENCY = 3.000-45.001 HZ
AT 1.560 HZ INTERVALS
S = 0.182 AZIMUTH = 105.945
S = 0.103 AZIMUTH = 255.964
S = 0.152 AZIMUTH = 189.462

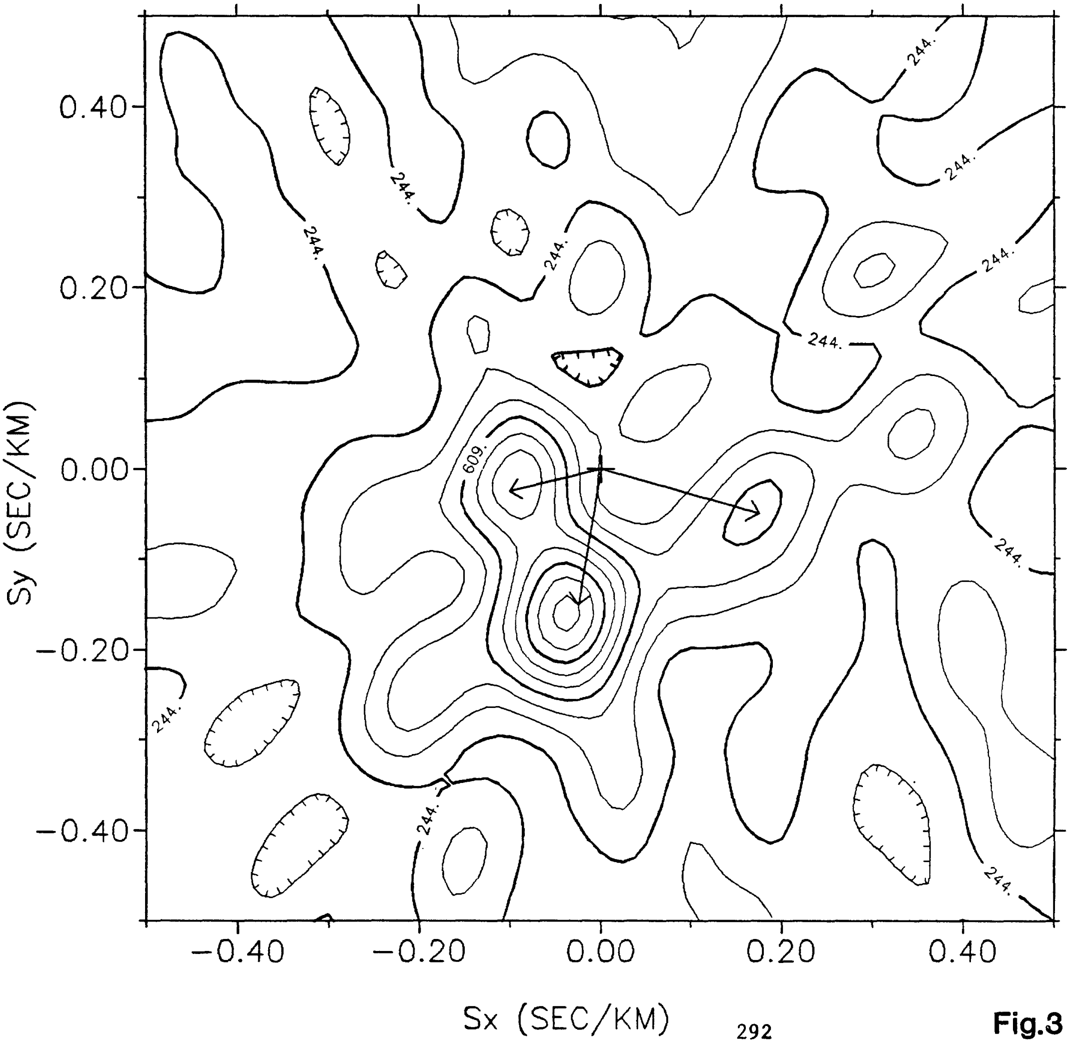

Fig.3

Theodolite Measurements of Creep Rates on San Francisco Bay Region Faults

Contract No. 14-08-0001-21988

Jon S. Galehouse
San Francisco State University
San Francisco, CA 94132
(415) 469-1204

We began measuring creep rates on San Francisco Bay region faults in September 1979. Amount of slip is determined by noting changes in angles between sets of measurements taken across a fault at different times. This triangulation method uses a theodolite set up over a fixed point used as an instrument station on one side of a fault, a traverse target set up over another fixed point used as an orientation station on the same side of the fault as the theodolite, and a second traverse target set up over a fixed point on the opposite side of the fault. The theodolite is used to measure the angle formed by the three fixed points to the nearest tenth of a second. Each day that a measurement set is done, the angle is measured 12 times and the average determined. The amount of slip between measurements can be calculated trigonometrically using the change in average angle.

We presently have theodolite measurement sites at 20 localities on faults in the Bay region. Most of the distances between our fixed points on opposite sides of the various faults range from 75-215 meters; consequently, we can monitor a much wider slip zone than can be done using standard creepmeters. The precision of our measurement method is such that we can detect with confidence any movement more than a millimeter or two between successive measurement days. We remeasure most of our sites about once every two months.

The following is a brief summary of our results thus far:

Seal Cove-San Gregorio fault - We began our measurements on the Seal Cove fault (Site 7) in Princeton, San Mateo County, in November 1979. For the next 5.7 years, the Seal Cove fault showed net movement at a rate of 1.2 millimeters per year in a right-lateral sense. However, details regarding the tectonic slip are difficult to ascertain because of seasonal effects, often involving apparent left-lateral slip that tends to occur toward the end of a calendar year.

Various logistic problems have occurred at our Site 8 across the San Gregorio fault near Pescadero in San Mateo County. The width of fault zone we are monitoring (452 meters) is the widest of all our 20 sites and measuring it is difficult. We have had considerable variations in the amounts and directions of movement from one measurement day to another. The presently-calculated average is 2.8 millimeters per year of right-lateral slip for the past 3.2 years.

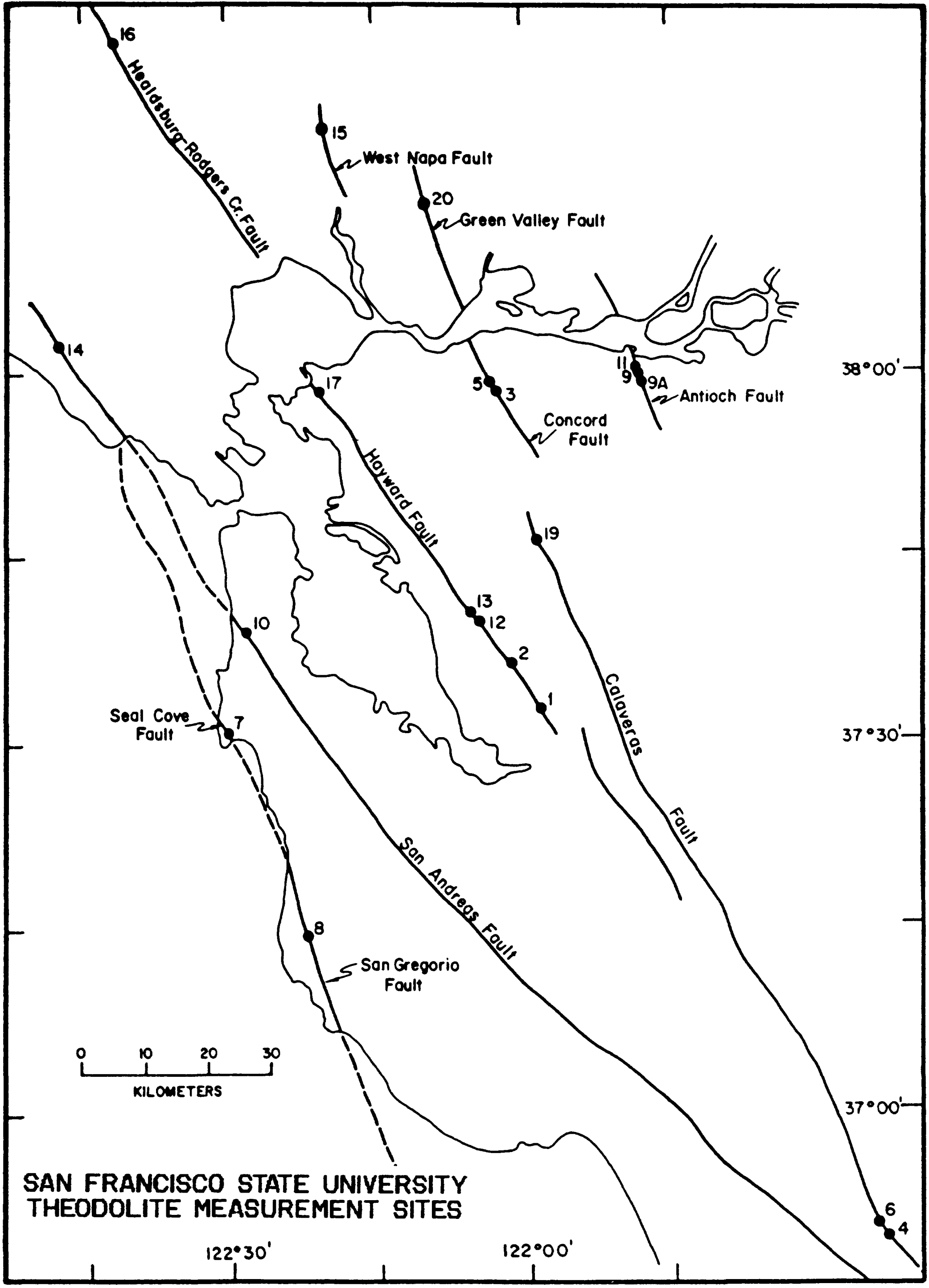

SAN FRANCISCO STATE UNIVERSITY
THEODOLITE MEASUREMENT SITES

San Andreas fault - In the 5.6 years since March 1980 when we began our measurements across the San Andreas fault in South San Francisco (Site 10), virtually no net slip has occurred. This indicates that the San Andreas fault is locked in the San Francisco area. We recently (February 1985) reestablished our Site 14 in Marin County, this time at the Point Reyes National Seashore Headquarters. Preliminary results during the next six months indicate no net slip. Our Site 18 (not shown on the location map) in the Point Arena area has averaged about one millimeter per year of right-lateral slip in the four years from January 1981 to January 1985.

Rodgers Creek fault - In the five years since August 1980, our Site 16 on the Rodgers Creek fault in Santa Rosa has had an average of 1.5 millimeters per year of right-lateral slip. However, our results show large variations in the amounts and directions of movement from one measurement day to another. These are probably due to seasonal and/or gravity-controlled mass movement effects, not tectonic slip.

West Napa fault - In the five years since July 1980, our Site 15 on the West Napa fault in the City of Napa has shown an average of about one millimeter per year of right-lateral slip. Similarly to our results for the Rodgers Creek fault, however, large variations up to nearly a centimeter have occurred in both a right-lateral and a left-lateral sense between measurement days. The magnitude of these nontectonic effects is obscuring the small amount of any tectonic slip that may be occurring.

Green Valley fault - Last year (mid-June 1984) we established a new site (Site 20) on the Green Valley fault north of Suisun Bay. We measured nearly a centimeter of right-lateral slip during the next 1.2 years. We need to monitor this fault for a longer period of time before we know if it is really moving this rapidly.

Hayward fault - We began our measurements on the Hayward fault in late September 1979 in Fremont (Site 1) and Union City (Site 2). During the next six years, the average rate of right-lateral slip has been about 4.6 millimeters per year in Fremont and about 4.7 millimeters per year in Union City.

We began measuring two sites within the City of Hayward in June 1980. In the 5.2 years since then, the average rate of right-lateral movement has been about 4.9 (Site 12) and about 4.2 (Site 13) millimeters per year.

We began measurements in San Pablo (Site 17) near the northwestern end of the Hayward fault in August 1980. For the past five years, the average rate of movement has been about 4.4 millimeters per year in a right-lateral sense. However, superposed on this overall slip rate are changes between some measurement days of up to nearly a centimeter in either a right-lateral or a left-lateral sense. Right-lateral slip tends to be measured during the first half of a calendar year and left-lateral during the second half.

Our theodolite triangulation results for the Hayward fault are quite comparable to those determined by U.S.G.S. creepmeters. The Hayward fault appears to be creeping at a rate of about four and one-half millimeters per year.

Calaveras fault - We have three measurement sites across the Calaveras fault and the nature and amount of movement are different at all three. We began monitoring our Site 4 within the City of Hollister in September 1979. Slip along this segment of the Calaveras fault is quite episodic, with times of relatively rapid right-lateral movement alternating with times of little net movement. For the past six years, the fault moved at a rate of 7.5 millimeters per year in a right -lateral sense.

At our Site 6 across the Calaveras fault on Wright Road just 2.3 kilometers northwest of our site within the City of Hollister, the slip is much more steady than episodic. In the six years since October 1979, the Calaveras fault at this site has been moving at a rate of 14.6 millimeters per year in a right-lateral sense, the fastest rate of movement of any of our sites in the San Francisco Bay region.

U.S.G.S. creepmeter results in the Hollister area are quite similar to our theodolite results. Creepmeters also show a faster rate of movement at sites on the Calaveras fault just north of Hollister than at sites within the City of Hollister itself.

The rate of movement is much lower at our Site 19 in San Ramon, near the northwesterly terminus of the Calaveras fault. Only about one millimeter per year of right-lateral slip has occurred during the past five years.

The epicenter of the 24 April 1984 Morgan Hill earthquake occurred on the Calaveras fault between our Hollister area sites which are southeast of the epicenter and our San Ramon site which is northwest of it. Four papers that we published regarding our theodolite measurements and observations of surface displacement related to the earthquake are listed at the end of this summary. No unusual movement appears to have occurred prior to the Morgan Hill earthquake.

Concord fault - We began our measurements at Site 3 and Site 5 on the Concord fault in the City of Concord in September 1979. Both sites showed about a centimeter of right-lateral slip during October and November 1979, perhaps the greatest amount of movement in a short period of time on this fault in the past two decades. Following this rapid phase of movement by about two months were the late January 1980 Livermore area moderate earthquakes on the nearby Grenville fault.

After the relatively rapid slip on the Concord fault in late 1979, both sites showed relatively slow slip for the next four and one-half years at a rate of about one millimeter per year right-lateral.

However, in late Spring-early Summer 1984, both sites again moved relatively rapidly, slipping about seven millimeters in a right-lateral sense in a few months. The rate has again slowed since late August 1984 (through early October 1985).

The overall rate of movement on the Concord fault (combining the two periods of relatively rapid movement with those of slower movement) is about 4.3 millimeters per year (Site 3) and 3.2 millimeters per year (Site 5) of right-lateral slip in the past six years.

Antioch fault - We began our measurements at the more southeasterly of two original sites on the Antioch fault (Site 9) in the City of Antioch in January 1980. During the next 27 months, we measured a net right-lateral displacement of nearly two centimeters. However, large changes in both a right-lateral and a left-lateral sense occurred between measurement days. Three times left-lateral displacement occurred toward the end of one calendar year and/or beginning of the next. We abandoned this site in April 1982 because of logistic problems and relocated it (Site 9A) just southeast of the City of Antioch in November 1982. In the 2.7 years until August 1985, the fault at this new site has had net movement in a right-lateral sense at a rate of 1.7 millimeters per year.

The more northwesterly of our original sites on the Antioch fault (Site 11) is located where the fault zone appears to be less specifically delineated. In the 5.3 years from May 1980 to August 1985, we have measured an average of 1.7 millimeters per year of left-lateral slip. Much subsidence and mass movement creep appear to be occurring both inside and outside the Antioch fault zone and it is probable that these nontectonic movements have influenced our theodolite results. However, a recent (1984) trench across the Antioch fault within the City of Antioch showed soil horizons also offset in an apparent left-lateral sense.

Reports and Publications

Galehouse, J.S., 1984, Theodolite measurements following the 24 April 1984 Morgan Hill earthquake, in U.S. Geol Survey Open-File Report 84-498, pp. 72-75.

Galehouse, J.S., and Brown, B.D., 1984, Southeastern limit of surface displacement on the Calaveras fault associated with the 24 April 1984 Morgan Hill earthquake, in U.S. Geol. Survey Open-File Report 84-498, pp. 85-91.

Galehouse, J.S., 1985, Theodolite Measurements: in Geodetic Observations section of "The Morgan Hill, California Earthquake of April 24, 1984"; U.S. Geol. Survey Bull. 1639, in press.

Galehouse, J.S. and Brown, B.D., 1985, Surface Displacement Near Hollister: in Geological Observations section of "The Morgan Hill, California Earthquake of April 24, 1984"; U.S. Geol. Survey Bull. 1639, in press.

DEEP BOREHOLE PLANE STRAIN MONITORING

14-08-0001-22025

Michael T. Gladwin
Department of Physics
University of Queensland
St. Lucia
Australia 4067.

FIELD STUDIES

Two Borehole Capacitance Strain Monitors (BCSM) have been deployed and operational in California since 1983, in 150 meter deep boreholes at San Juan Bautista and at Pinon Flat. These instruments are capable of resolving vector plane strain to 0.2 nanostrain. A third instrument to be deployed in early 1986 will have significantly improved noise figures. Four types of data are available from the present instruments.

1. Continuous low frequency plane-strain data for real time regional deformation mapping.
2. In-situ static shear field estimates when the instrument is implanted immediately after drilling.
3. Far field static offsets (elastic and plastic) related to the strain relief of nearby earthquakes and the stress redistributions which result.
4. High resolution shear strain seismology of the earthquake rupture process.

Current investigations have concentrated on the first three types of measurements.

RESULTS

Resolution of the 1984-85 data into hydrostatic (P) and maximum shear (S) strains is shown in Figure 1. The calibration used for these calculations was an estimate of the hydrostatic and shear response factors for each site (following Gladwin and Hart, 1985). It is clear from this figure that environmental effects such as atmospheric pressure, precipation, and thermal effects which do affect the hydrostatic strain are not evident on the shear strain plots for either site. The strain step at San Juan Bautista due to the Morgan Hill earthquake on 24 April, 1984 can be seen on both shear and hydrostatic data. Figure 2 shows the shear strain at San Juan in greater detail for this event. Shear at Pinon Flat is also shown in the figure for comparison. Both records continue on pre-established trends, and performance remains excellent.

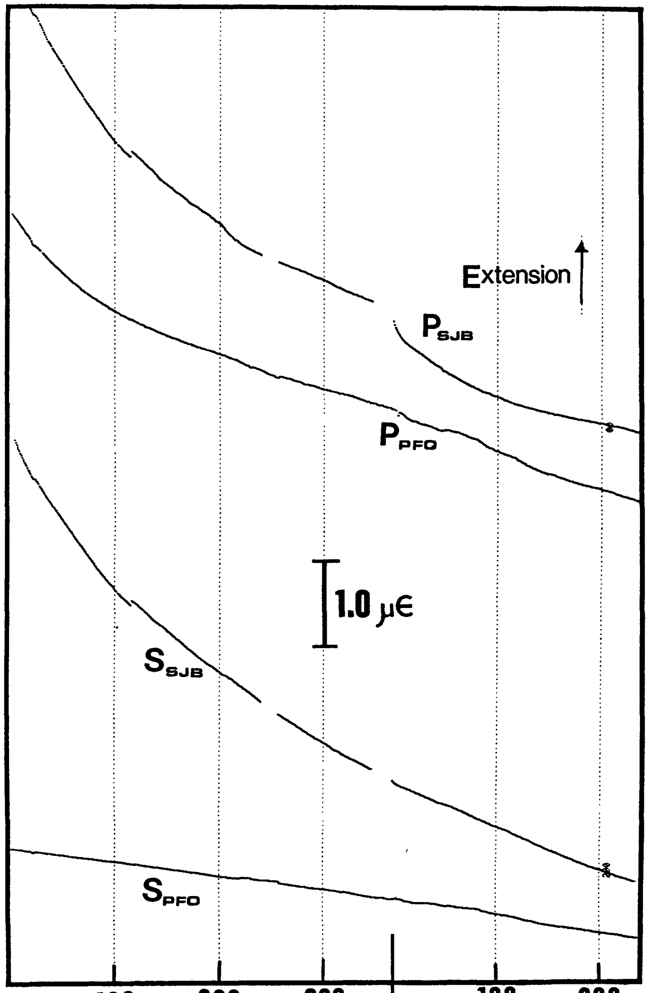

FIGURE 1. Strain measurements at Pinon Flat (PFO) and at San Juan Bautista (SJB) during 1984 and 1985. The upper two curves (hydrostatic strain P) show normal environmental effects which are not present in the lower curves (maximum shear strain S). The strain steps at SJB on day 115,1984 are associated with the Morgan Hill earthquake. The instruments were disturbed at the end of 1984 for testing of a high frequency version of the instrument.

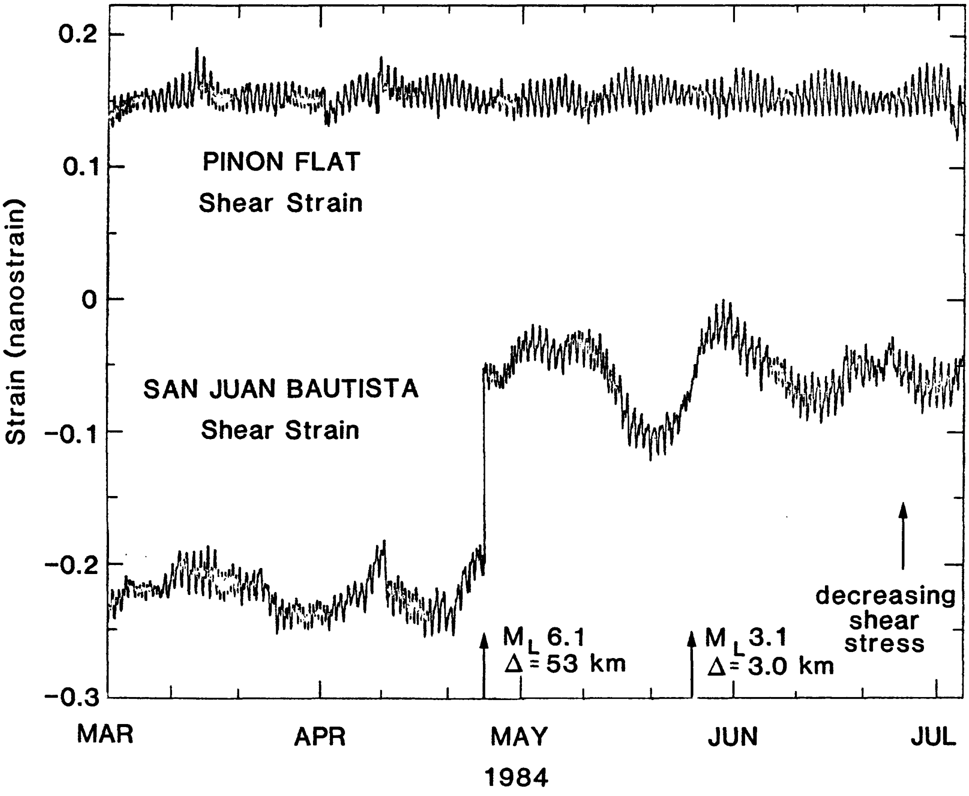

FIGURE 2. Shear strain plot (detrended) for SJB and PFO during the period of the Morgan Hill event. The PFO data are presented in the top trace to illustrate normal shear strain data. The strain relief of the Morgan Hill event was followed in mid-May by a major strain accumulation event probably associated with the second earthquake shown in the figure.

Development of a reliable in-situ calibration procedure for these instruments has been the major task for this report period. Such a calibration procedure is not trivial because individual components of borehole instruments experience deformations which are not simple multiples of surrounding rock strain in the corresponding direction. Observed deformations depend on shear and hydrostatic response factors of the instrument inclusion which are functions of the effective instrument, grout and rock moduli, and the thickness of the grout. Thus direct comparison of the tidal signal for each gauge with the equivalent theoretical tide, using the major spectral component M_2, is not an adequate procedure. Amplitude calibration using simple spectral analysis applied separately to hydrostatic and shear tidal components is also not adequate because of varying response factors for each gauge.

The present method involves least squares fitting to theoretical ocean-loaded earth tides for each vector component with proper allowance for the different response of the instrument to hydrostatic and shear applied strain fields. An example of the results of this procedure is shown in Figure 3.

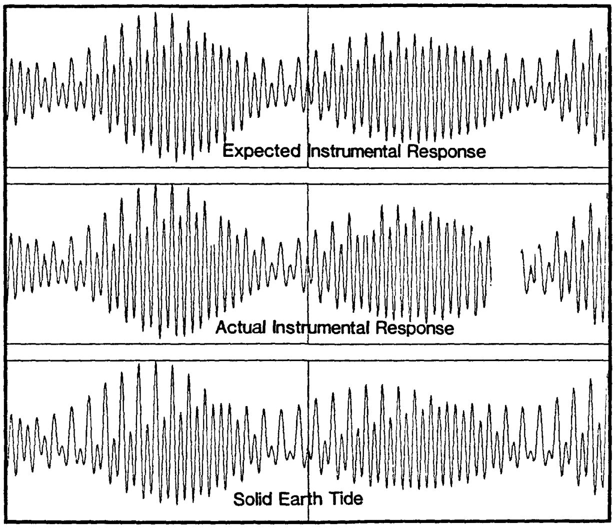

COMPARISON OF TIDES .PFO (at 5 E of N)

FIGURE 3. Comparison of observed instrument response with the response calulated using shear and hydrostatic response factors derived from the least-squares fitting technique. Note that this signal is much closer to the actual signal than the ocean-loaded solid earth tide in this direction. The figure covers a time interval of 37.5 days commencing February 7, 1984.

The lower plot in Figure 3 shows the theoretical ocean-loaded solid earth tide (at 5 degrees East of North) at Pinon Flat. The middle plot shows the observed instrument response at this angle, while the top plot shows a calculated instrument response using shear and hydrostatic response factors derived by the least square procedure described in Gladwin et.al.,1985. Results of the new calibration procedure applied to the observed strain step previously reported for the Morgan Hill earthquake, 24 April,1984, will be reported at the Fall meeting of the A.G.U.

Data from the San Juan instrument was used, together with other strainmeter data from the Morgan Hill earthquake, to indicate that while observed co-seismic offsets are generally in good agreement with expectations from elastic dislocation theory, and while post-seismic deformation continued following the main event with a moment comparable to that of the main shock, pre-seismic strain or tilt perturbations from days to minutes before the main shock are not apparent above the present resolution. Precursory slip for these events, if any occured, must have had a moment less than 1% of that of the main event. This strong constraint on the size and amount of slip triggering major ruptures makes prediction of the onset times and final magnitudes of the rupture zones, for events such as these, a difficult task. These data are most easily explained by an inhomogeneous faulting model for which various areas of the fault plane have different stress-slip constitutive laws.

With the good data base now obtained from these instruments, analysis of the diagnostic data also obtained from them is now being carried out. Correction of the strain record for uphole temperature fluctuation and other spurious effects seem to be limited to less than 2% of the observed deformations in either site to this time. Definition of noise limits of the present system will be attempted in the next period.

LIST OF PUBLICATIONS

GLADWIN, M.T. (1984) High Precision Multi-Component Borehole Deformation Monitoring. Rev. Scientific Instruments. Vol 55, No 12, pp 2011-2016.

GLADWIN M.T. and GWYTHER R.L. (1985) Borehole Vector Strain Measurements in California. (in press)

GLADWIN,M.T.,GWYTHER.R.L. and HART.R. (1985) Tidal Calibration of Borehole Vector Strain Instruments. EOS Transactions (in press).

GLADWIN, M.T. and HART, R. (1984) Design Parameters for Borehole Strain Instrumentation. Pure and Applied Geophysics (in press).

GLADWIN M.T. and JOHNSTON M.J.S. (1984) Strain Episodes on the San Andreas Fault following the April 24 Morgan Hill, California Earthquake. EOS Trans., Vol 65, No 45, p 852.

GLADWIN M.T. and JOHNSTON M.J.S. (1986) Borehole Earth Strain Associated with the April 24,1984 California Earthquake (Submitted for Publication).

JOHNSTON M.J.S.,GLADWIN M.T., and LINDE A.T.(1985) Pre-seismic Failure and Moderate Earthquakes in California. 23rd General Assembly of IASPEI, Abstracts.

LOW FREQUENCY DATA NETWORK

9960-01189

J. Herriot, K. Breckenridge, S. Silverman
U.S. Geological Survey
Branch of Tectonophysics
345 Middlefield Road, MS/977
Menlo Park, California 94025
415-323-8111, ext. 2932

Investigations

1. Real-time monitoring, analysis, and interpretation of tilt, strain, creep, magnetic, and other data within the San Andreas fault system and other areas for the purpose of understanding and anticipating crustal deformation and failure.

2. Compilation and maintenance of long-term data sets free of telemetry-induced errors for each of the low frequency instruments in the network.

3. Development and implementation of graphical display systems for the purpose of monitoring seismic and surface deformation activity in real-time.

4. Installation of satellite-based telemetry system for reliable real-time reporting and archiving of crustal deformation data.

Results

1. Data from low frequency instruments in southern and central California have been collected and archived using the Low Frequency Data System. In the six months three million measurements from 125 channels have been received and subsequently transmitted on the Low Frequency 11/44 UNIX computer for archival and analysis.

2. One effort of the project has been to provide real-time monitoring of designated suites of instruments in particular geographical areas. Terminals are dedicated to real-time color graphics displays of seismic data plotted in map view or low frequency data plotted as a time series. During periods of high seismicity these displays are particularly helpful in watching seismic trends. The system is used in an ongoing basis to monitor seismicity and crustal deformation in the Mammoth Lakes and Parkfield

regions. This monitoring capability also available in Reston, VA.

3. The project continues to operate a configuration of one PDP 11/44 computer running the UNIX operating system and two PDP 11/03 running real-time data collection software. This 11/44 has been operational as our analysis machine with less than 1% down-time. The two 11/03 machines operate redundantly for robustness. The data from the Network have been made available to investigators in real-time. Data only minutes old can be plotted. Events such as creep events can be monitored while they are still in progress. The prediction working group has made extensive use of the timely plots produced routinely by Kate Breckenridge.

4. Two AT&T PC 7300 computers have been procured to collect satellite telemetry data. Software developed on the 11/44 to control and collect data from the satellite ground station is being refined for use on the AT&T computers.

5. The project continues to use a 5-meter satellite receiver dish installed in Menlo Park for retrieval of real-time surface deformation data from Alaska, California, and the South Pacific islands. The GOES-6 (GOES-4, etc.) geostationary satellite together with transmit and receive stations makes possible a greatly improved telemetry system. Stan Silverman and Kate Breckenridge attended the GOES DCS Technical Group Meeting in Seattle, WA, reporting on the progress of our satellite ground station.

6. The project continues to develop color graphics and color hardcopy capabilities for use in real-time seismic displays. Using the advanced graphics software with color graphics devices we have demonstrated our real-time seismic and low frequency data monitoring ability to visiting government officials, scientific investigators, and public interest groups.

7. The project is taking an active part in the Parkfield Prediction Working group. Stan Silverman has automated daily monitoring of strain in that region, and is the alternate monitor for Parkfield strain events. Kate Breckenridge is the alternate monitor for Parkfield creep events, which includes contact via paging system during periods of increased activity. Jim Herriot participated in a Parkfield data-center working group, whose recommendations are currently under consideration.

Reports

Breckenridge, K., Johnston, M. J. S., 1985, Catalog of Locations Low Frequency Instrumentation in California, 1985; U.S. Department of the Interior, U.S. Geol. Surv. Open-File Report 85-212.

Johnston, M. J. S., Silverman, S. A., Mueller, R. J., and Breckenridge, K., 1985, Secular Variation, Crustal Contributions, and Tectonic Activity in California, 1976-1984, Journal of Geophysical Research, v. 90, p. 8707-8717.

Repeat Gravity Studies

9380-03074

Robert C. Jachens and Carter W. Roberts
Branch of Geophysics
U.S. Geological Survey, MS 989
Menlo Park, CA 94025
(415) 323-8111, x 4248

Investigations

1) Remeasured southern California precision gravity base station network during May, 1985, including measurement of a station at the Holcomb Ridge 2-color geodimeter site.

2) Conducted ground gravity and magnetic surveys near Parkfield, CA, and examined limited aeromagnetic data in order to define subsurface configuration of gabbroic body exposed at Gold Hill and to map detailed structure of the San Andreas fault zone.

3) Remeasured precision gravity network in the vicinity of Long Valley Caldera, California.

4) Expanded gravity survey of Long Valley to examine detailed subsurface structure beneath the south and east moats.

Results

1) The latest temporal gravity surveys in southern California show that most stations continue to experience a pattern of low amplitude, short period gravity fluctuations. Stations at Glendale and Tejon Pass, which showed large gravity changes of +39 microgals and +28 microgals, respectively, between the May, 1984 and January, 1985 surveys, yielded values during the most recent survey that are more typical of their respective long-term values.

   Nearly nine years of data from the 12 stations scattered along the San Andreas fault and into the Mojave Desert shows little or no indication of secular gravity variations. Linear regression analyses of the gravity changes with time yield low annual rates of change such as +0.35 μGal/a at Tejon Pass, +0.23 μGal/a at Palmdale, +1.43 μGal/a at Cajon Pass, -0.62 μGal/a at Glendale, and -0.95 μGal/a at El Mirage.

2) Gravity and magnetic data near Parkfield, CA, indicate that the gabbroic body exposed at Gold Hill does not extend laterally in the subsurface much beyond the limits of the outcrop. It is bounded on the northeast by a near vertical contact that extends to a depth of at least 0.5 km. A new aeromagnetic survey in progress should permit better definition of the depth extent of this body. The combined gravity and magnetic data suggest

that the dense and magnetic Gold Hill body is embedded in a much larger dense, non-magnetic body, possibly composed of metamorphosed Franciscan rocks.

3) Gravity data from the Long Valley surveys currently are being reduced.

TILT, STRAIN, AND MAGNETIC MEASUREMENTS

9960-02114

M.J.S. Johnston, R. Mueller, D. Myren, A. Jones,
C. Mortensen, and V. Keller
Branch of Tectonophysics
U.S. Geological Survey
345 Middlefield Road, MS/977
Menlo Park, California 94025
(415) 323-8111, ext. 2132

Investigations

1. To investigate the mechanics of failure of crustal materials using deep borehole vector and dilational strainmeters data and data from surface strainmeters, tiltmeters, and arrays of absolute magnetometers.

2. To develop physical models of incipient failure of the earths crust by analysis of real-time records of these and other fault zone data.

Results

1. The high sensitivity, wide dynamic range and bandwidth of deep borehole three-component and dilational strainmeters at the shorter periods (0.1 seconds to 10,000 seconds) has not been fully utilized at instrumented sites in California. To remedy this a programmable 16-bit digital seismic event recorder with on-site recording (G.E.O.S.) has been used to record pre-event and event data at more than six sites in California during seismic events, nuclear explosions and in strain noise studies. Power spectral density estimates show general consistency from site to site and, except for about 10 dB of 6 second microseismic noise, decrease with increasing frequency from about -170 dB at about 10 dB per decade of frequency. Peak power in strain seismograms of local earthquakes and nuclear explosions occurs between 0.1 and 1 Hz. Detection of pre-rupture strains at the 10^{-10} strain level appear possible in this period range from these data.

2. Measurements of dilational Earth strain in the frequency band 25 to 10^{-5} Hz have been made on a deep borehole strainmeter installed near the San Andreas fault. These data are used to determine seismic radiation fields during nuclear explosions, teleseisms, and local earthquakes, and ground noise during seismically quiet times. Strains of less than 10^{-10} can be clearly resolved at short periods

(<10 sec) using wide dynamic range digital recorders (GEOS), permitting measurement of the static and dynamic strain variations in the near field of local earthquakes. Noise spectra for Earth strain referenced to 1 ε^2/Hz show that strain resolution decreases at about 10 dB per decade of frequency from -150 dB to 10^{-4} Hz to -223 dB at 10 Hz. The first near-field recordings from an earthquake as small as M_L 3.2,, obtained on May 26, 1984, near the San Andreas fault at San Juan Bautista, California, indicate no precursive strain release at the 10^{-11} level. Coseismic strain release of 1.86 nanostrain observed at a distance of 3.2 km is consistent with that calculated from a simple dislocation model of the event. Ground displacement spectra, determined for this event from strain data and instrument corrected seismic velocity data from colocated surface seismometers, indicate a significant lower corner frequency in the strain data and, by implication, different source parameters for the event. For more distant events, ground spectra are generally similar.

3. Arrays of differential magnetometers and intermediate-baseline geodetic nets have been installed and surveyed since 1980 at the northern end of the Red River fault in Yunnan Province. On the basis of seismic recurrence and other evidence a moderate to large earthquake is expected within the next few years. Simple uniform strain models have been fit to the strain data from arrays at Liante and Dengchaun on the northwest extension of the Red River fault. At Liante the primary feature of the data is a uniform well determined negative dilation of 1.9 μstrain/a. Negative dilation of 1.2 μstrain is evident also in the Dengchaun data with a marginally significant shear in a direction N60W. Test line data indicate repeatibility in distance measurements during this time to better than 3 mm on a 734 m line. In contrast, the net line length changes are between 10 and 100 mm on lines typically between 4 and 7 km in length. Magnetic measurements in the region of high magnetization on the west side of the fault at Dengchaun show an increase in local magnetic field of up to 1.5 nT/a over sites on the east side of the fault. In contrast, no significant magnetic changes have occurred in the Liante array. This result is in accordance with tectonomagnetic theory since the absence of regional magnetic anomalies indicate remanent and induced rock magnetization of less than 0.001 A/m.

4. A system for differential lake tilt at four sites around Crowley Lake in Long Valley, California, was designed and the installation organized for late fall. At each of these stills water level will be measured to better than 1 mm to provide six independent lake tilt measurements radial and

tangential to the resurgent dome. New digital electronic systems, to measure the frequency outputs from electronic pressure transducers and transfer the measurement to Sutron satellite data collection platforms, were also designed and bench tested.

5. A visit to the People's Republic of China was made between September 1 and September 30, 1985 as part of the Protocol for Scientific and Technical Cooperation in earthquake studies, signed by the U.S. Geological Survey, the National Science Foundation, and the State Seismological Bureau of the People's Republic of China. The purpose of this trip was to provide five on-site recording magnetometer systems and one geodetic measuring system to the Chinese and instruct them in the usage of these equipment. The five magnetometer systems were provided to the Beijing State Seismological Bureau and the geodetic equipment to the Yunnan State Seismological Bureau. In addition to providing the equipment, the magnetic and geodetic networks established in 1980 and 1982 was resurveyed.

Reports

Johnston, M. J. S., Review of Tectonomagnetic and Tectonic Activity in California, 1974-1985, Abs. I.A.S.P.E.I., Tokyo, Japan, August 19-30, 1985.

Johnston, M. J. S., Borcherdt, R. D., and Linde, A. T., Measurements of Short Period Strain (0.1-10^5 s) in the near field of an Earthquake (M_L 3.2) near San Juan Bautisa, California, Trans. A.G.U. (in press), 1985.

Johnston, M. J. S., Chen Zhong-Yi, and Mueller, R. J., Strain and Magnetic Field Changes on the Red River Fault System Near Dengchaun and Liante, Yunnan, China: 1980-1985, Trans. A.G.U. (in press), 1985.

Johnston, M. J. S., Gladwin, M. T., and Linde, A. T., Preseismic Failure and Moderate Earthquakes in California, Abs. I.A.S.P.E.I., Tokyo, Japan, August 19-30, 1985.

Johnston, M. J. S., Silverman, S. A., Mueller, R. J., and Breckenridge, K. S., Secular Variation, Crustal Sources, and Tectonic Activity in California, 1976-1984, *J. Geophys. Res.*, v. 90, no. B10, pp. 8707-8717, 1985.

Maxwell, G. L., Borcherdt, R. D., Johnston, M. J. S., Malin, P. E., Sacks, I. S., Myren, D., Renaker, E., and Glassmoyer, G., On Extending Bandwidth and Resolution for Near-Souce Seismic Observations near Parkfield, CA, Trans. A.G.U. (in press), 1985.

Mortensen, C. E. and M. J. S. Johnston, Review of Instrumentation for Crustal Deformation Measurements Meeting on Crustal Deformation, Wuhan, China, October, 1985.

Myren, G. D., Johnston, M. J. S., and Linde, A. T., Borehole Dilatometer Strain During the August 4, 1985, Kettleman Hills Earthquake, Trans. A.G.U. (in press), 1985.

Earthquake and Seismicity Research Using SCARLET and CEDAR

Contract No. 14-08-0001-21981

Hiroo Kanamori, Clarence R. Allen, Robert W. Clayton
Seismological Laboratory, California Institute of Technology
Pasadena, California 91125 (818-356-6914)

Investigations

1) Seismicity in the Imperial Valley Region.

2) Lateral velocity variations in Southern California.

Results

1) Seismicity in the Imperial Valley Region.
(Diane I. Doser and Hiroo Kanamori)

Focal depths from over 1000 earthquakes occuring between 1977 and 1983 in the Imperial Valley-southern Peninsular Ranges are used to study relationships between the depth of seismicity, heat flow, and crustal structure. This study used relocated A- and B-quality events from the Caltech catalog that were carefully selected to insure focal depth precision of ± 2 km. Regional variations in focal depth, especially in the central Imperial Valley, may be related to crustal structure. These variations are studied by rheologic modeling. A comparison of focal depths of earthquakes occuring before and after the October 15, 1979 ($M=6.6$) earthquake indicates that aftershocks during the first two months of the sequence were 2 to 3 km deeper than earthquakes occurring in other time periods. The deepest earthquakes in Imperial Valley are spatially associated with a subbasement dome near the northern end of the Imperial fault. This dome coincides with the region where the Imperial fault undergoes a transition from stick-slip behavior to aseismic fault creep. Models of slip during the 1979 mainshock are also compared with pre- and post-mainshock seismicity. A relocation of the 1940 ($M=7.1$) mainshock suggests that this sequence began by rupturing the same portion of the fault that experienced slip during the 1979 mainshock.

2) Lateral Velocity Variations in Southern California
(Thomas M. Hearn and Robert W. Clayton)

The plate boundary and major crustal blocks in southern California are imaged by a tomographic backprojection of the Pg first arrivals recorded by the Southern California Array. The method, formulated specifically for local earthquake arrival times, is a fast iterative alternative to direct least-squares techniques. With it we solve the combined problem of determining refractor velocity perturbations and source and station delays. Resolution and variance are found empirically by using synthetic examples.

A map showing lateral velocity variations at a depth of approximately 10 km is obtained. The results show a strong correlation with surface tectonic features. Clear velocity contrasts exist across the San Andreas, the San Jacinto, and the Garlock faults. The Mojave region has the slowest velocities while the Peninsula Ranges have the highest. The San Jacinto block has velocities intermediate between Mojave and Peninsula Range velocities, and also has early station delays. This may indicate that the San Jacinto block has overridden Mojave material on a shallow detachment surface. No velocity variations are found associated with the Transverse Ranges; which we interpret to mean that the surface batholithic rocks in this area do not extend to Pg depths.

A tomographic inversion of the Pn arrivals in southern California yields new information about wave velocities and topography on the Moho discontinuity. We produced maps of Pn velocity and Pn station delays. The Pn velocities do not show the dramatic correlation with surface faults that is found for the shallower Pg arrivals (Hearn & Clayton, 1985). This implies that the lower crust and mantle are largely decoupled from the upper crust. Undoubtedly this is due to the different responses of the brittle uppercrust and the ductile lower crust to tectonic and isostatic stresses. Detachment faults must play an important role in separating the crust.

In general, velocities on the American plate are higher than on the Pacific plate, but no distinct transition is observed. The Colorado river region has extremely thin crust due to basin and range type extension. The Transverse ranges have a small root as seen in the station delays, and which also results in slightly lower Pn velocities there. The Peninsula ranges also have slow Pn velocities, but they do not have late station delays. Any root to the Peninsula ranges must be very narrow. Isostatic balance must be maintained primarily through lateral density contrasts.

References

Webb. Terry H. and Hiroo Kanamori, Earthquake focal mechanisms in the Eastern Transverse Ranges and San Emigdio Mountains, Southern California and evidence for a regional decollement, *Seismol. Soc. Am., Bull., 75* n. 3, 737-757, June 1985.

Doser, Diane I., and Hiroo Kanamori, Depth of seismicity in the Imperial Valley Region (1977-1983) and its relationship to heatflow, crustal structure, and the October 15, 1979 earthquake, *Jour. Geophys. Res.*, in press.

Hearn, Thomas M., and Robert W. Clayton, Lateral velocity variations in Southern California: 1. Results for the upper crust from Pg-waves. Submitted to the Bulletin of the Seismological Society of America, August, 1985.

Hearn, Thomas M., and Robert W. Clayton, Lateral velocity variations in Southern California: 2 Results for the lower crust from Pn-waves. Submitted to the Bulletin of the Seismological Society of America, August, 1985.

HYDROLOGICAL MONITORING ALONG SAN ANDREAS AND SAN JACINTO FAULTS, SOUTHERN CALIFORNIA, DURING SECOND HALF OF FISCAL YEAR 1985

Contract 14-08-0001-21982

D. L. Lamar and P. M. Merifield
Lamar-Merifield Geologists, Inc.
1318 Second St., #25
Santa Monica, CA 90401

Investigations

Water levels in twenty-two wells along the San Andreas and San Jacinto fault zones were monitored during the current reporting period. Water levels and barometric pressure at one well were monitored by an Envirolabs data logger, Model DL-120-MCP, which is linked by telephone to our IBM Personal Computer. Another nine wells were monitored continuously with Stevens Type F recorders, two being maintained by Linda Woolfenden of the Geological Survey. The remaining wells were probed monthly.

Long-term water-level changes are displayed on computer-generated hydrographs for each well. Daily rainfall is plotted on the graphs for direct comparison with water levels. Long-term hydrographs of wells along the San Andreas fault typically show seasonal response to rainfall. Most of the wells along the San Jacinto fault zone are in confined aquifers which are not affected by seasonal rainfall. Short-term fluctuations in water level seen on the Stevens recorder charts and Envirolabs plots are caused by barometric pressure changes related to weather fronts, earth tides and solar thermal tides.

Water levels are measured every 15 minutes on the well equipped with an Envirolabs data logger. The measurements are stored on magnetic tape and data are sent to the IBM Personal Computer in our office via telephone twice a week. The data logger has operated without malfunction. Hydrographs are generated by a Bausch and Lomb digital plotter connected to the IBM Personal Computer.

Results

Short-term water-level records of wells along the San Jacinto fault have shown anomalies interpreted to be strain events in the past (Merifield and Lamar, 1981, 1985); no such anomalous water-level changes have been observed during the past six months. No unusual long term water level changes were observed along either the San Andreas or San Jacinto faults. The program was not funded for FY 1986 and monitoring has been discontinued.

References

Merifield, P. M. and D. L. Lamar, 1981, Anomalous water-level changes and possible relation with earthquakes: Geophys. Res. Lett., v. 8, p. 437-440.

Merifield, P. M. and D. L. Lamar, 1985, Possible strain events reflected in water levels in wells along San Jacinto fault zone, southern California, Pure and Applied Geophysics, v. 122, p. 245-254.

GEODETIC STRAIN MONITORING

9960-02156

John Langbein
Branch of Tectonophysics
U.S. Geological Survey
345 Middlefield Road, MS/977
Menlo Park, California 94025
(415-323-8111, ext. 2038

Investigations

Two-color geodimeters are used to survey, repeatedly, geodetic networks within selected regions of California that are tectonically active. This distance measuring instrument has a precision of 0.1 to 0.2 ppm of the baseline length. Currently, the crustal deformation is being monitored within the south moat of the Long Valley Caldera in eastern, California, and near Pearblossom, California on a section of the San Andreas fault that is within its Big Bend section. Periodic comparisons with the proto-type, 2-color geodimeter are also conducted near Parkfield, California. These inter-comparison measurements serve as a calibration experiment to monitor the relative stabilities of the portable and proto-type geodimeters.

Results

1) Long Valley

We have expanded the two-color geodimeter network to 39 baselines which is shown in Figure 1. The majority of the expansion include the baselines using Whitmore and Lookout as a common station. Measurements will be made infrequently for these two subnetworks, but the data should provide information concerning displacement of the Hilton Creek fault and magma injection beneath the resurgent dome.

The line-length change data shown in Figure 2 involve frequent measurements using the station at Casa plus infrequent measurements using the station at Miner. The data indicate that the rate of extension has been steadily decreasing during the last 2-1/4 years. An extreme example is the baseline Casa-Lomike which extended at +7.9±0.8 ppm/a during summer 1983, then at +4.1±0.9 ppm/a during summer 1984, and at 0.1±0.9 ppm/a during summer 1985. A model composed of two point sources of inflation beneath the resurgent dome plus dextral slip on a shallow fault within the zone defined by the January 1983 earthquake zone is consistent with the spatial pattern of inhomogeneous extension. Furthermore, this model is also compatible with the line-length changes observed during the interval 1983.55-1984.61 by Savage and others in 1984 who used a single-color Geodolite to measure a network that sparsely spans the caldera and its immediate surroundings. The computed time dependence of these three sources of deformation indicate that both the rate of fault slip and the rate of inflation are steadily decreasing. The geometry of the two-color network allows an independent determination of fault slip, but the distribution between the deep, 14 km, and shallow, 6.5 km, inflation sources cannot be resolved.

2. Pearblossom

Due to the high rate of deformation and our limitation of only one operating two-color geodimeter that is currently reliable and portable, the frequency of observations at Pearblossom has been significantly reduced. This network was resurveyed in April and September 1985. The strain changes from these surveys are plotted in Figure 3 along with the results from the previous measurements since October 30, 1980. The data from the past 6 months is consistent with the previous observations.

3. Instrument Inter-Comparison

The data from 5 sets of measurements, from June 1984 through August, 1985, have been analyzed in terms of the relative change in instrument length scale between the portable and proto-type two-color geodimeters. The data consists of nearly simultaneous measurements of distances using both instruments at a common site and approximately 6 reference monuments located between 1.6 to 7.1 km from the central site at Parkfield, CA. From these observations, the difference in distances for each baseline using the 2 instruments is tabulated as a function of time. With this method, tectonic strain change is canceled and leaves the relative variation of instrument length scale as the dominant parameter. The data indicates that the two instrument have changed their length relative to each other. The heavy curve in Figure 4 shows the apparent drift of the prototype relative to the portable instrument in terms of parts per million of the total line-length and multiplied by 2 for comparison with areal dilatation.

With this experiment, it is not clear which instrument is drifting. It is interesting to note that the inferred dilatation from Parkfield (light, solid line) roughly correlates with the change in instrument scale of the prototype instrument. The dilatation from Pearblossom (dashed line) remains essentially unchanged during this interval. It is important to note that the Parkfield dilatation relies entirely on measurements by the prototype instrument and the Pearblossom data relies upon the portable instrument. Perhaps the apparent fluctuation in length scale of one instrument relative to the other is due to drift of the prototype, 2-color geodimeter.

Computation of dilatation from the Parkfield, two-color geodimeter relies upon modeling the deformation in terms of uniform strain plus surface slip on the San Andreas fault. For the period from July 1984 through August 1985, uniform strain plus uniform slip from the surface to roughly 1.5 km in depth appeared to satisfy the data from this network which is centered 2 km S.E. of the town of Parkfield. Along with the dramatic fluctuations in dilatation, the tensor shear strain for a plane parallel to the San Andreas fault accumulated at a rate of approximately 1 ppm/a from October 1984 through March 1985. The net accumulation of shear strain from April to August, 1985 is insignificant. One interpretation of the apparent high rate of shear is that the fault beneath 8 to 9 km slipped a total of 30 mm between October 1984 and March 1985. The shear strain accumulation would also be consistent with less slip which came to a shallower depth.

Reports

Linker, M.F., Langbein, J.O., and McGarr, A., 1986, Decreasing in deformation rate observed by two-color laser ranging in Long Valley Caldera, Eastern California, 1983-1984, Science, in press.

Langbein, J.O., Linker, M.F., and Tupper, D.L., 1985, Steady decrease in extension rate within the Long Valley Caldera, Eastern California 1983.48-1985.67 (abs.), EOS, in press.

Burford, R.O., Langbein, J.O., Linker, M.F., and Slater, L.E., 1985, Displacements within the Parkfield two-color Geodimeter network associated with the August 1985 Kettleman Hills Earthquake (abs.), EOS, in press.

Slater, L.E., Hamann, D., Burford, R.O., and Langbein, J.O., 1985, Two-color Geodimeter strain monitoring at Parkfield, California (abs.), EOS, in press.

Figure Captions

1. Map showing the locations of the baselines that comprise the 2-color geodimeter network within the Long Valley Caldera.

2. Line-length changes for 21 baselines of the two-color geodimeter network. The length changes have been normalized to the nominal length of each baseline. The error bars correspond to one standard deviation.

3. Extensional strain changes inferred from line-length measurements for an 12 baseline network near Pearblossom, California. The strain components are tensor quantities and have been rotated into a coordinate system that is normal and parallel to the local strike of the San Andreas fault.

4. Results on the intercomparison of instrument length scale between the prototype and portable two-color Geodimeters. The heavy, solid curve represents twice the change in ppm of the instrument length scale of the prototype relative to the portable instrument. Secular scale drift is 0.4±0.1 ppm/a. The light solid curve is the areal dilatation inferred from measurements using the prototype instrument at Parkfield. The dashed curve is the areal contraction (-1.0 x DIL) inferred from measurements using the portable instrument at Pearblossom.

LONG VALLEY NETWORK

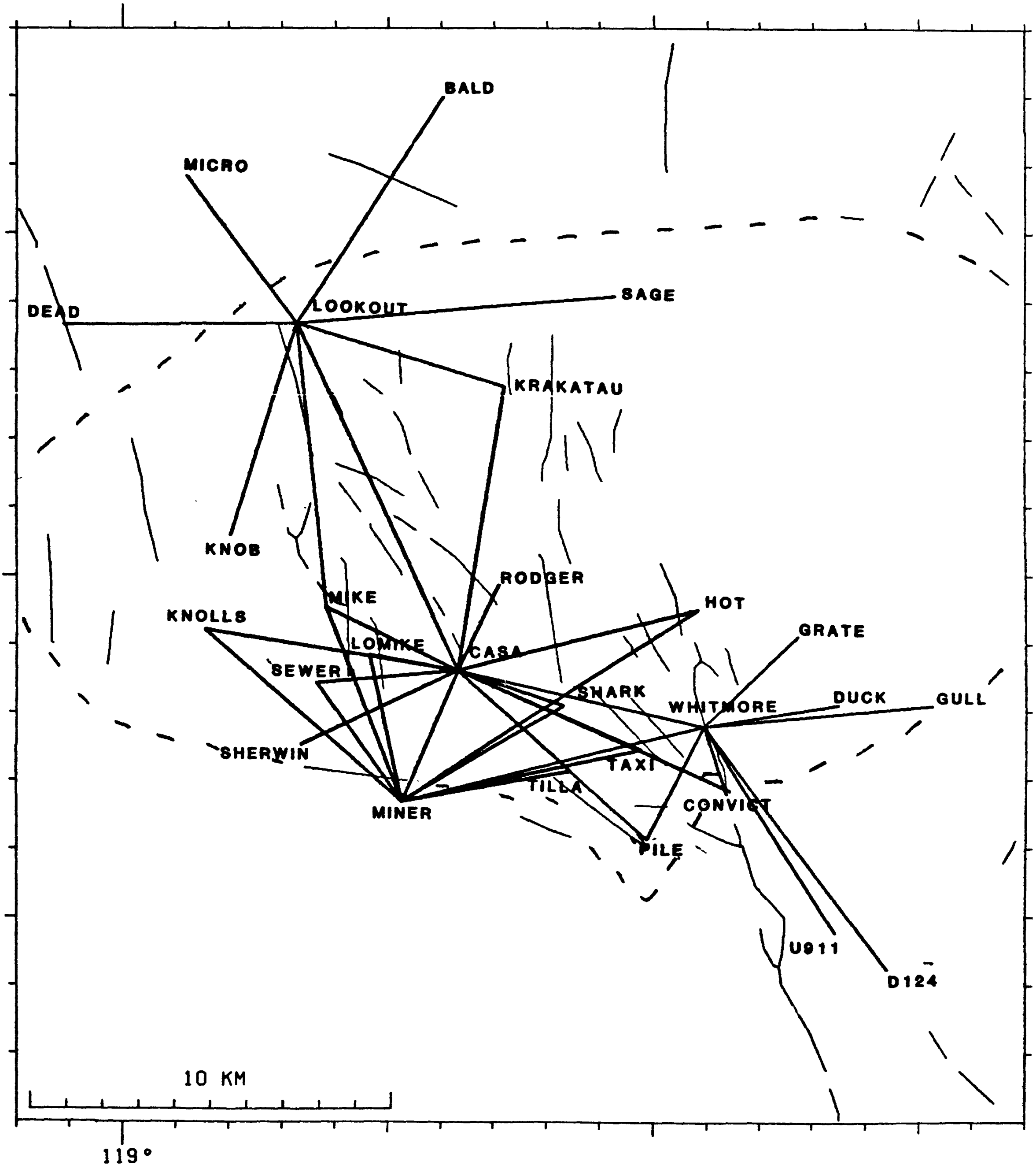

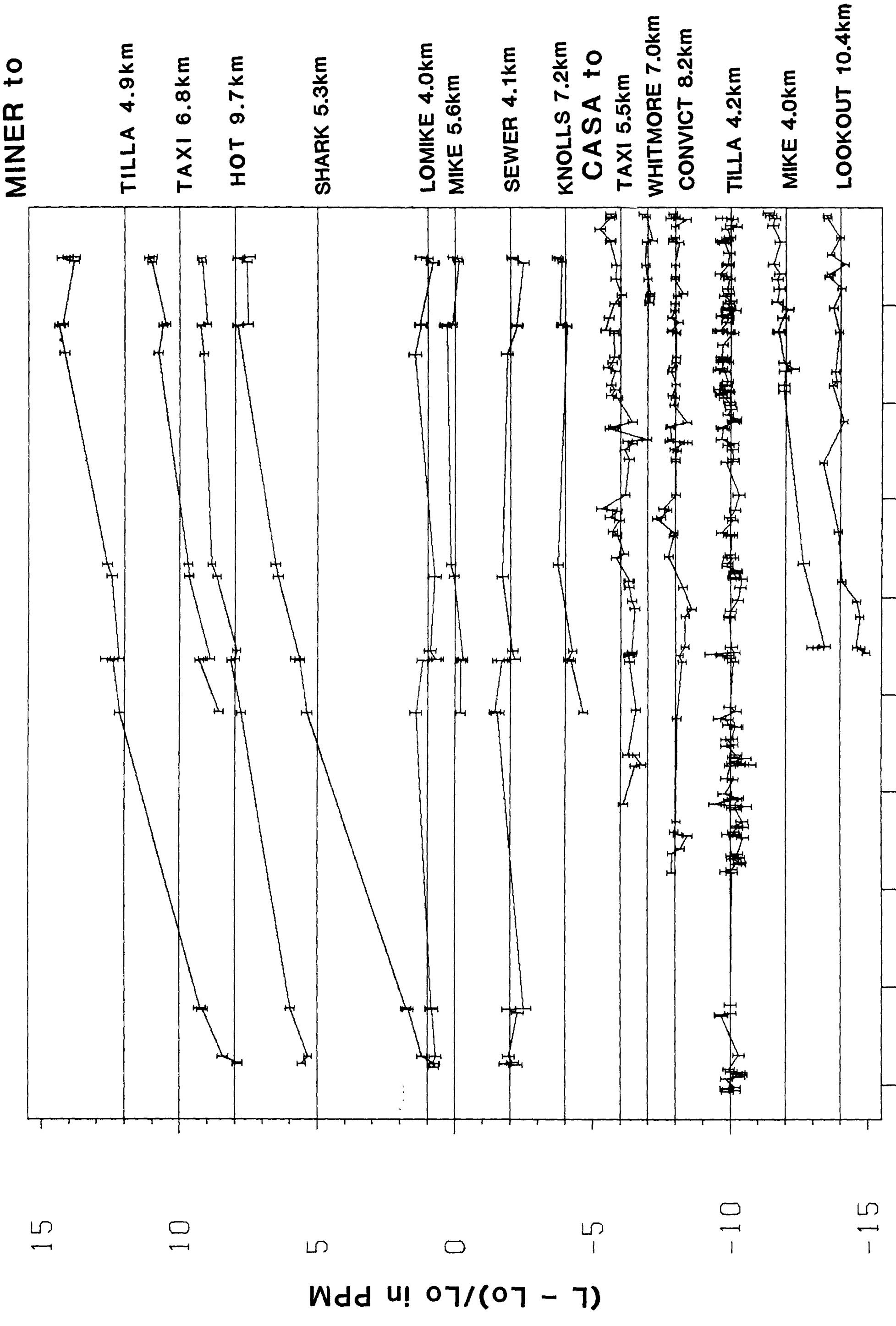
MINER to
TILLA 4.9km
TAXI 6.8km
HOT 9.7km
SHARK 5.3km
LOMIKE 4.0km
MIKE 5.6km
SEWER 4.1km
KNOLLS 7.2km
CASA to
TAXI 5.5km
WHITMORE 7.0km
CONVICT 8.2km
TILLA 4.2km
MIKE 4.0km
LOOKOUT 10.4km
1984
1985
15
10
5
0
-5
-10
-15
(L - Lo)/Lo in PPM

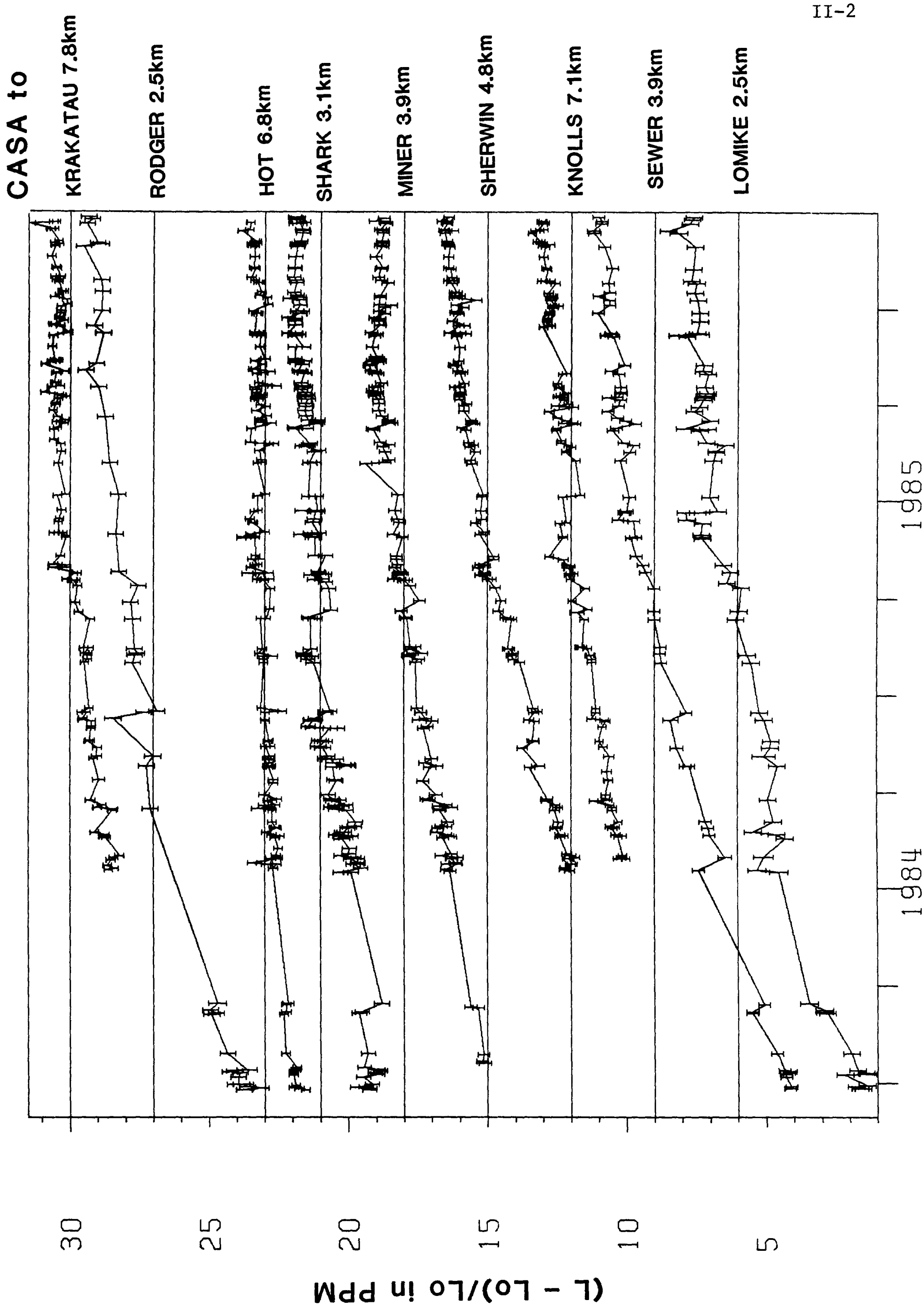
CASA to
KRAKATAU 7.8km
RODGER 2.5km
HOT 6.8km
SHARK 3.1km
MINER 3.9km
SHERWIN 4.8km
KNOLLS 7.1km
SEWER 3.9km
LOMIKE 2.5km
30
25
20
15
10
5
(L - Lo)/Lo in PPM
1984
1985

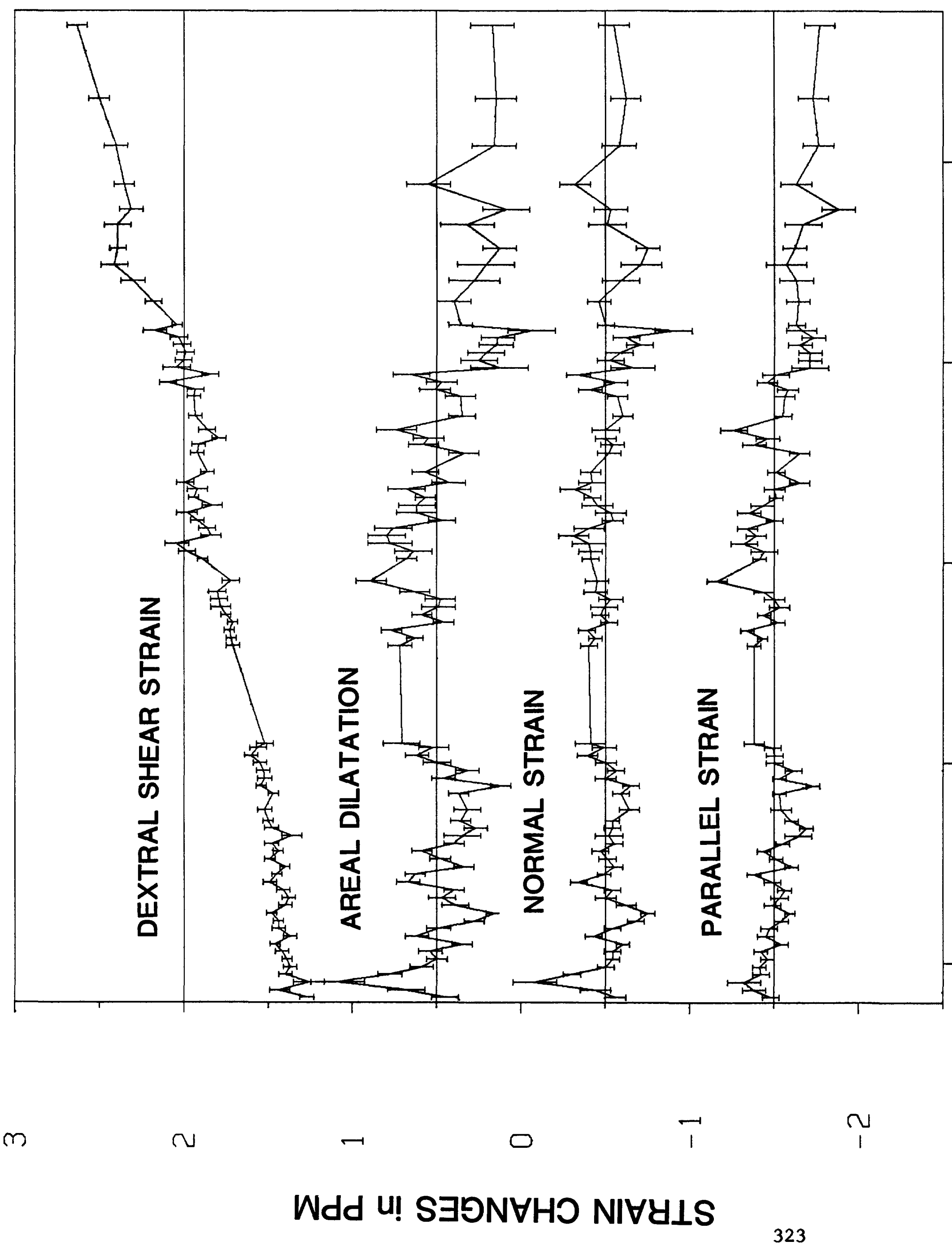
DEXTRAL SHEAR STRAIN
AREAL DILATATION
NORMAL STRAIN
PARALLEL STRAIN
1981
1982
1983
1984
1985
3
2
1
0
−1
−2
STRAIN CHANGES in PPM

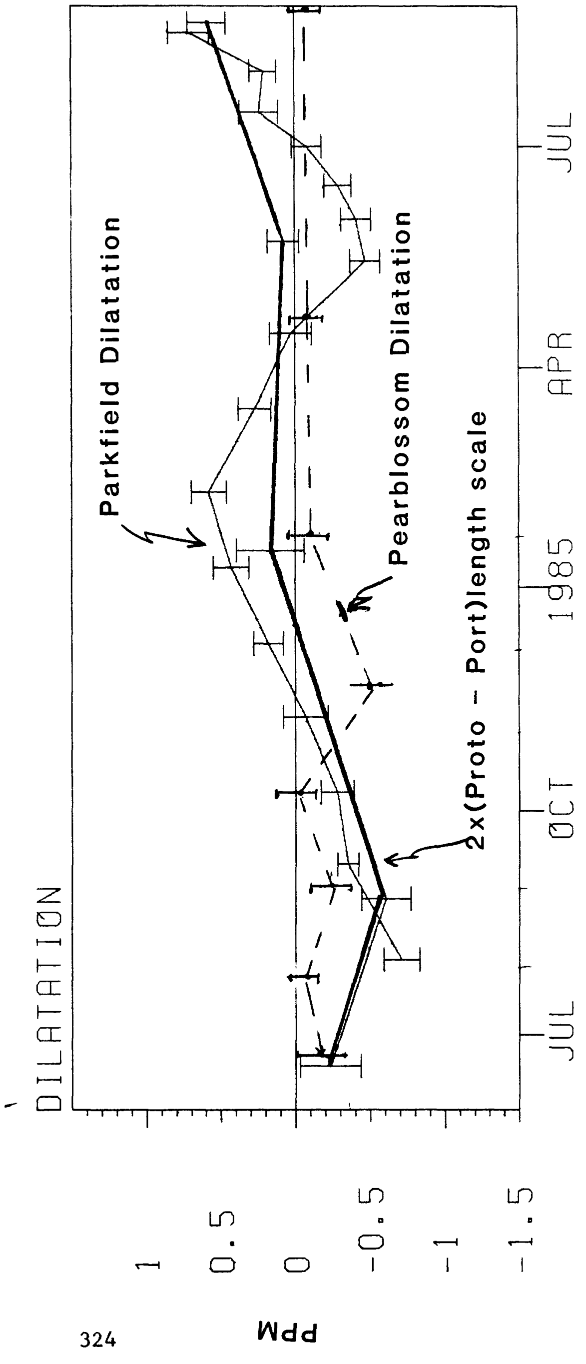
DILATATION
Parkfield Dilatation
Pearblossom Dilatation
2x(Proto - Port)length scale
JUL
OCT
1985
APR
JUL
1
0.5
0
-0.5
-1
-1.5
PPM

Parkfield Prediction Experiment

9930-02098

Allan G. Lindh, William Bakun, Catherine M. Poley
Branch of Seismology
U.S. Geological Survey
345 Middlefield Road, MS-977
Menlo Park, California 94025
(415) 323-8111, Ext. 2042

Investigations and Results:

SEISMICITY PATTERNS

Efforts to bring the 1966 hypocentral region into better focus continue. Our current best locations are shown in cross-section in Figure 2. In the blowup of the 1966 hypocentral region (Figure 2b), MM3 is the box we assume will contain the foreshocks to the next Characteristic Parkfield Earthquake (CharPEQ). The hypocentral depths of the 1966 foreshock and main event (small and large filled stars) have estimated standard errors of 1-2 km.

SEISMICITY RATES

The dominant features of the long-term seismicity are the increase in activity that accompanied the two M4.5-5 events in 1975 (open stars in Figure 1), and the apparent decrease in activity during 1984-5 in both the large Parkfield (Figure 2a) and the Middle Mountain (Figure 2b) boxes.

In light of the long-term prediction for a CharPEQ in 1988, the quiescence since 1984 might be interpreted as evidence for something like Mogi's "Stage 3" of the seismic cycle, and as such might tend to reinforce the expectation that the next CharPEQ will occur by 1992. However in light of the variations in length of reported "periods of quiescence", and the lack of any clear correlation with the magnitude of the earthquakes that sometimes appear to follow them, it is not clear that a "quiescence", if real, would significantly perturb the conditional probabilities based on the historical data alone. In addition one question clouds any interpretation of the apparent decrease in seismicity rates in Figure 2 as a "premonitory quiescence".

The complication is that the Coalinga earthquake (2 May 1983, M 6 3/4) had a profound effect on creep meters in the Parkfield area (Mavko et al., 1985), with two of the nearest sites ceasing right lateral motion altogether (Figure 2c). The Middle Mountain creepmeter (XMM1) resumed right lateral slip after about 14 months in July, 1984, but at a reduced rate. The seismicity in MM3 entirely ceased at the M1.5 level during this same time period (Figure 2c), strongly suggesting that the effects of the Coalinga earthquake at Parkfield were not confined to the near surface. Several of the creepmeters in the Parkfield area continue to report slip rates significantly below those observed prior to 1983; XPK1 still continues (as of July 85) to record no right-lateral slip (Figure 2d). The possibility that the apparent reduction in seismicity rate is due to continuing effects of the Coalinga earthquake cannot be discounted.

FORESHOCKS

The last two CharPEQs (1934 and 1966) were preceded by immediate foreshock sequences containing one or more M5 events of 72 and 4 hours duration, respectively. The two M5 foreshocks in 1934 were located within 5 km to the NW of the main event (Wilson, 1935; Bakun and McEvilly, 1981); the M5 foreshock in 1966 was located about 1.5 km to the NW of the main event at the same approximate depth (Figure 1). Thus the prospects seem good that the next Parkfield earthquake will be preceded by foreshock activity in the MM3 box, and if some means could be found to identify such foreshocks as they occur, they would provide a powerful short-term precursor.

Because of their potential for short-term prediction, some effort has been devoted to the question of foreshock identification, but to date no general applicable criteria have been established. Thus the only use of foreshocks which can be implemented at this time is statistical, in the sense that after the occurrence of a given earthquake which can be identified as a potential foreshock, the probability of occurrence of a larger earthquake might be enhanced for some time period. Lucy Jones has calculated such probabilities for earthquakes in southern California (Jones, 1985) and for Parkfield (Jones, oral communication, 1985) and finds that for any M5 event at Parkfield there is a 33 percent chance of it being followed by a larger event within five days. On the basis of the seismicity data presented here, we can attempt an independent estimate.

Since we have already assumed that the hypocenter of the next Parkfield earthquake will be near the hypocenter of the last event, we can confine our calculations to seismicity near that point; given the practical limitations on resolving earthquake locations, this is essentially equivalent to confining our attention to events within the MM3 box (Figures 1b and 2c).

Primarily on the basis of detection and location capabilities, we have chosen two threshold levels that define the onset of a potential foreshock sequence within MM3; they are one M1.5 event, or two M1 events within a 72 hour period. Since 1980 when detection capabilities achieved this level in the Parkfield region, these alarm levels have been reached an average of about 5 times per year (Figure 2c). However since the apparent overall decrease in activity in 1983, they have averaged only three alarms per year. These numbers allow us to make a very simple -- and very approximate -- estimate of the probability gain (Aki, 1981) associated with a potential foreshock sequence within MM3.

If we wish to estimate the empirical probability of a given event within MM3 being a foreshock, we need an estimate of the frequency of such events, and the probability that the next characteristic Parkfield event will be preceded by foreshocks. Since we know that at least two of the last four Parkfield events had foreshock sequences at the M 3-5 level, an estimate of 0.5 for the probability of the next event having some foreshock activity at the M1 level seems conservative. Thus it remains to estimate the frequency of potential foreshock sequences within MM3.

We have estimated that there is a 95 percent chance that the next CharPEQ will occur by 1993, this implies that approximately 25 potential foreshock alarms will occur during the time interval within which the earthquake is expected. Assuming a 50 percent chance the next event will have some sort of foreshock sequence within MM3, this implies a 2 percent chance that any given foreshock alarm will be followed by a M6 Parkfield earthquake.

ALARM IMPLEMENTATION

All the signals from the 400+ seismic components of the CALNET are telemetered in real time directly to U.S.G.S. Western headquarters in Menlo Park, California, where they are recorded on a variety of media, and also processed directly in real-time by computers which provide estimates of earthquake locations and magnitudes within 3-5 min. of their occurrence. These locations are used to trigger automatic alarm systems, which on the basis of hypocenter and magnitude activate paging systems and place phone calls to alert the seismologists responsible for surveillance. Alarms based on the foreshock scenarios in MM3 described above have been in operation since April 1985. The scientists responsible for surveillance have computer terminals in their homes, and thus when an alarm goes off, can quickly review the seismic data and contact those responsible for checking other kinds of data and/or making decisions.

FIGURE CAPTIONS

Figure 1. Cross sections of seismicity for 1975-June 1985. Symbol size is proportional to magnitude; the smallest symbol represents 2.3-2.99 in (a) and 1.5-2.29 in (b). a) Cross-section of the seismicity of $M \geq 2.3$ along the section A-A' (Figure 1). Relative focal depths are generally accurate to 1 km or less; depths of the shallow shocks to the northwest of the Middle Mt. box are less accurate, with an uncertainty of about 2 km. For reference, the hypocenters of the immediate M=5.1 foreshock and the main shock in 1966 are shown as small and large solid stars respectively; the other two stars are the 1975 M=4+ shocks. The lines at B and B' denote the boundaries of the Middle Mt. box. Creepmeter locations are given by 3 letter names along the top of the figure. b) Blow-up cross-section of the seismicity of $M \geq 1.5$ along the section B-B' (Figure 1). Hypocenter locations are based on a revised set of station corrections for master events within the Middle Mt. box (locations will differ slightly from those in 2a). The section is divided into 3 boxes - MM1, MM2, and MM3 - denoting 3 clusters of events.

Figure 2. Time histograms of seismicity $M \geq 1.6$, and cumulative creep near Middle Mt. (1979-June 1985). Times of New Idria and Coalinga main events are shown by vertical lines. a) MM1 seismicity (Figure 2b). Note spurt of activity in May 1983. b) MM2 seismicity (Figure 2b). Note spurt of activity in late 1983. c) MM3 (1966 hypocentral area) (Figure 2b). Also shown as short vertical bars are those times when the MM3 foreshock alarm now in use (since April 1985) would have been triggered (see text). d) Cumulative creep near MM for creepmeters XMM and XPK (Figure 2a). Note the correlation between the decrease in seismicity and the decrease in rate of creep following the Coalinga earthquake in May 1983.

Reports

Bakun, W. H., and A. G. Lindh, 1985, The Parkfield Califiornia, Earthquake Prediction Experiment, Science, vol. 229, no. 4714, p. 619-624.

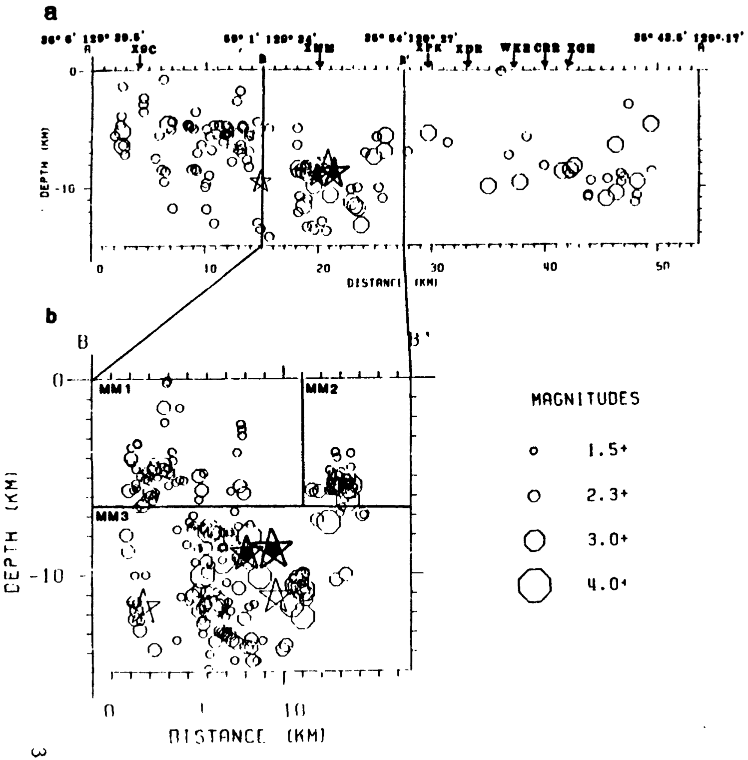

Figure 1

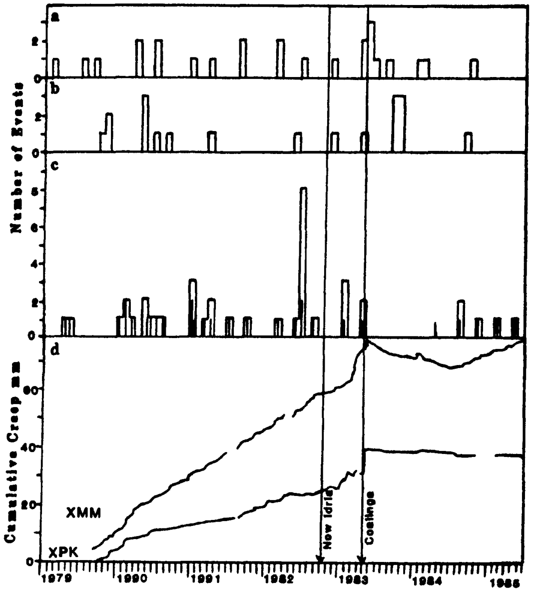

Figure 2

High Sensitivity Monitoring of Resistivity and Self-Potential Variations in the Hollister and Palmdale Areas for Earthquake Prediction Studies

U.S.G.S. Contract no. 14-08-0001-22029

P.I.: Theodore R. Madden
Department of Earth, Atmospheric and Planetary Sciences
Massachusetts Institute of Technology
Cambridge MA 02139
617/253-6384

There have been an unusually large number of breakdowns in telephone line connections and digital recording systems but the two arrays are back in proper working order. We are investigating new procedures for the data analysis in order to get at the signal related residuals in our dipole comparisons. Figure 1 shows a reanalysis of Hollister data at the time of the Morgan Hill event in which time shifts across the array, diurnal resistivity variations, and resistivity drifts are included in the analysis. The apparent day to day consistency of the results makes it appear that we are observing true resistivity variations, but we have been stung before by this criterea. Nevertheless these preliminary results are encouraging. We still need an analysis that can use the redundancy in the array data to identify non signal related noise so that this noise can be subtracted out rather than edited out as we are presently doing. There are hints, but no clear indications of changes associated with the Morgan Hill event. We believe the analysis can be further improved, however.

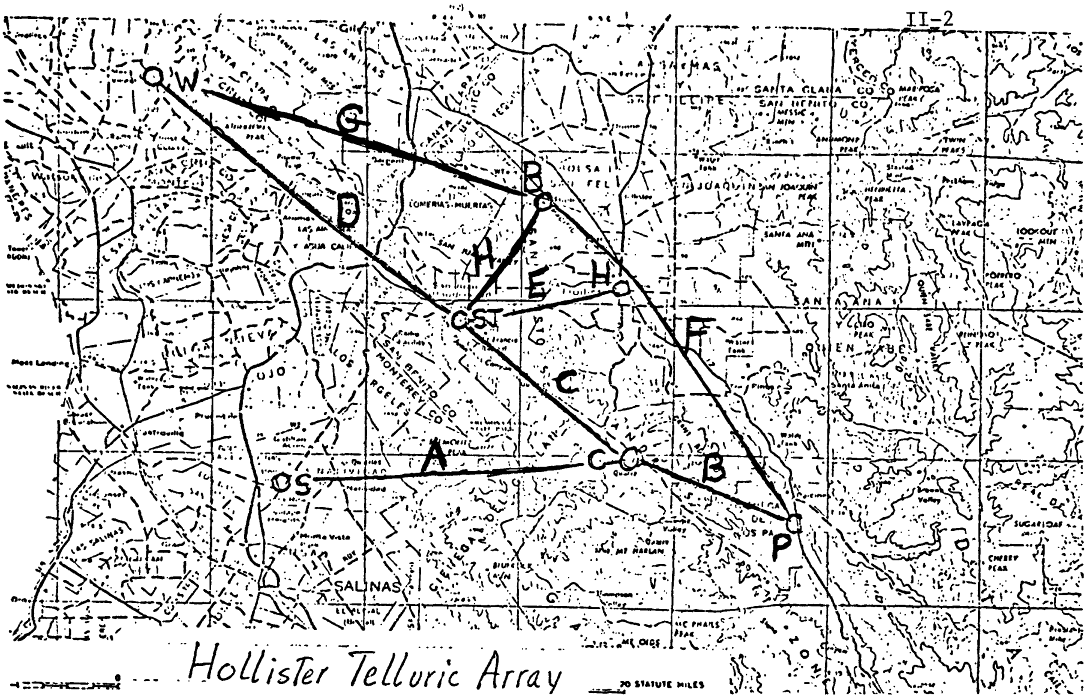

Hollister Telluric Array

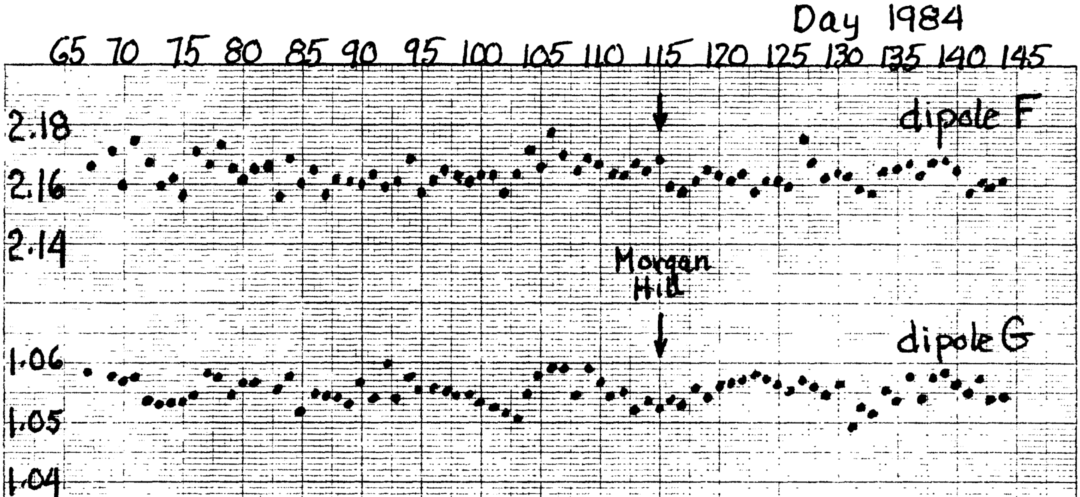

Fig1 Dipole Telluric Signal magnitudes relative to dipoles A+B
Hollister Array

SEISMIC WAVE MONITORING IN CENTRAL CALIFORNIA

USGS Contract 14-08-0001-21985

T.V.McEvilly and R. Clymer
Seismographic Station
University of California
Berkeley, California 94720
415/642-4494

Hollister Area P-Wave Travel-Time Monitoring

P-wave travel-time monitoring has continued in the Hollister area (Figure 1) with our aging (10-year old), single-channel real-time correlator and recording system, and a 1970-vintage P-wave vibrator.

The precision of the measurements is indicated by the results of stability tests consisting of repeated measurements of an 8-sec deep-crustal reflection on path T-Z in Bickmore Canyon west of Bear Valley (Figure 1). With the system in its present configuration, travel times on such tests scatter over about 1 msec and amplitude varies about 20%. Applying these results to our actual monitoring data indicates: 1) In Bear Valley, on path W-B, repeated measurements show a scatter of 5-10 msec, and 2) at the Winery and Stone Canyon areas, first-arrival travel times scatter over about 1 msec or somewhat less, depending on signal-to-noise ratio.

While precision appears to be quite good, accuracy is degraded considerably by seasonal variations of up to about 6 msec for first arrivals at the Winery and Stone Canyon areas. The cause is very-near-surface moisture variations. Our solution has been to monitor near-surface times with geophones below the water table at most source and receiver sites, and then to simply subtract the near-surface variations from the path data. The resulting corrected data are shown in Figures 2 and 3. The efficacy of the correction procedure is difficult to quantize, but we suspect that the 1-3 msec long-term variations cannot be considered meaningful. A travel-time change of 4-5 msec would probably indicate a real change occurring at depth.

We have chosed a different method of dealing with seasonal variations at Parkfield. All receivers are to be in boreholes at depths in excess of 100 m. With the vibrator fixed, data from several sites will be recorded simultaneously. Data for a path on which changes are not expected will be used as a reference to remove spurious changes at the source end from the other paths. This should produce a correction at least as accurate as the present procedure, with a considerable increase in field efficiency.

Shear-Wave Vibrator

In the summer of 1984, Amoco Production Company donated a shear-wave vibrator in excellent condition to the program, giving us the capacity of monitoring S-wave travel time and amplitude. In addition, we believe we can monitor S-wave velocity anisotropy by a simple procedure. Robertson and Corrigan (1983) have shown that an S-wave vibrator will radiate S_V or S_H waves toward the receiver depending on the orientation of the vibrator baseplate, and that this could be used to measure anisotropy in a near-surface shale. Results of a vertical seismic profile accomplished with our S-wave vibrator at the Geysers geothermal area in the fall of 1984 confirmed these results.

We think this new capability has exciting implications for earthquake prediction research at Parkfield, since S-wave amplitude and anisotropy may be more sensitive indicators of fault-zone properties that P-wave parameters.

New Recording System

To monitor S-wave and P-wave parameters at Parkfield will require 3-component receivers and recording of a considerably larger data set than that at Hollister. A data acquisition system is now on order that features 16-bit analog-to-digital conversion at several geophone sites with digital telemetry to a central computer-based recording system capable of considerable editing and processing. Storage will be on magnetic tape in SEG-Y format suitable for further processing with DISCO software at the Center for Computational Seismology at Lawrence Berkeley Laboratory. In addition to recording vibrator data, the system will be capable of operating in event-recording mode for recording earthquake data.

Parkfield Accomplishments

Figure 4 shows sites for 3-component borehole seismometer installations. Four of these were accomplished in the spring of 1985. At the two sites indicated by question marks, installation attempts failed. They may be attempted again in FY86, depending on funding. The Gold Hill package is clamped in at open hole. The installations are a cooperative effort of the USGS, UC Santa Barbara, and UC Berkeley.

One week of preliminary data gathering with the S-save vibrator and the single-channel recording system laboriously produced the following results.

1) A surprisingly high signal-to-noise ratio, even at a source-receiver offset of 10-11 km. Coherent, reproducible, source-generated signals were present to 12-15 sec travel time, with an indication of a coherent event at 20 sec.
2) Complex S-wave arrivals that change in character when the vibrator baseplate is rotated.

We plan to determine if further processing of these records will provide evidence of anisotropy. Regardless, we conclude that we can detect changes in the dissimilarity of the waveforms. Such changes, should they occur, would indicate variations in fault zone properties.

References

Clymer, R.W. and T.V. McEvilly (1981). Travel-time monitoring with VIBROSEIS, *Bull Seism Soc Am, 71,* 1903.

Peacock, Sheila and Stuart Crampin (1985). Shear-wave vibrator signals in transversely isotropic shale, *Geophysics, 50,* 1285.

Robertson, James D. and Dennis Corrigan (1983). Radiation patterns of a shear-wave vibrator in near-surface shale, *Geophysics, 48,* 19.

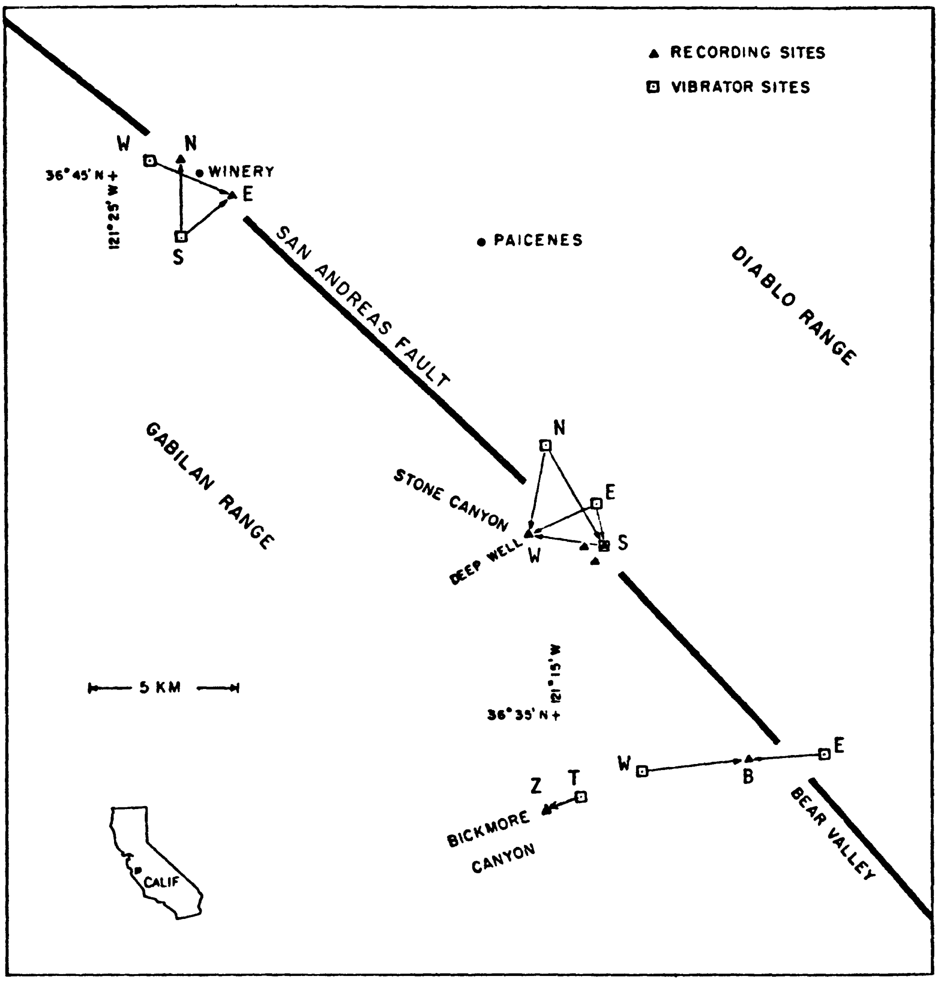

FIGURE 1. Source and receiver sites, Winery, Stone Canyon and Bickmore Canyon areas.

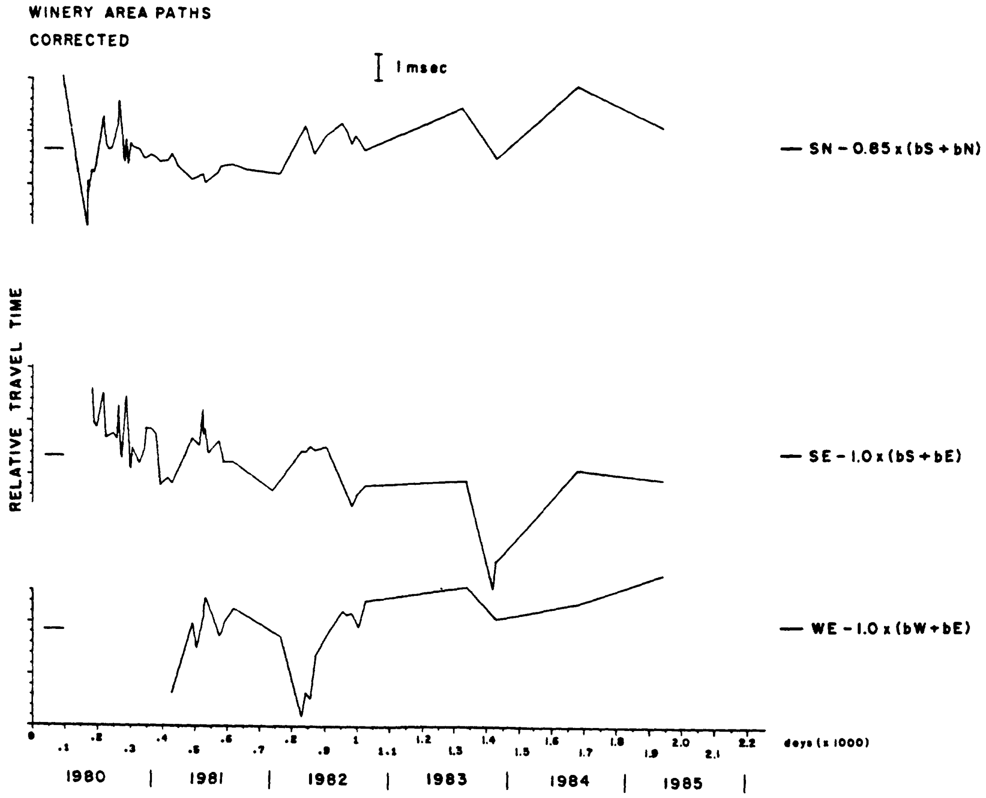

Figure 2 . Winery area first-arrival travel times with near-surface (seasonal) corrections. Upper-case letters refer to site designations shown in Figure 1. Two upper case letters together indicate the source and receiver ends of a path, respectively. A lower-case 'b' followed by an upper-case letter implies that a borehole data set at that site was used for near-surface corrections to the path data. The associated numbers are scale factors.

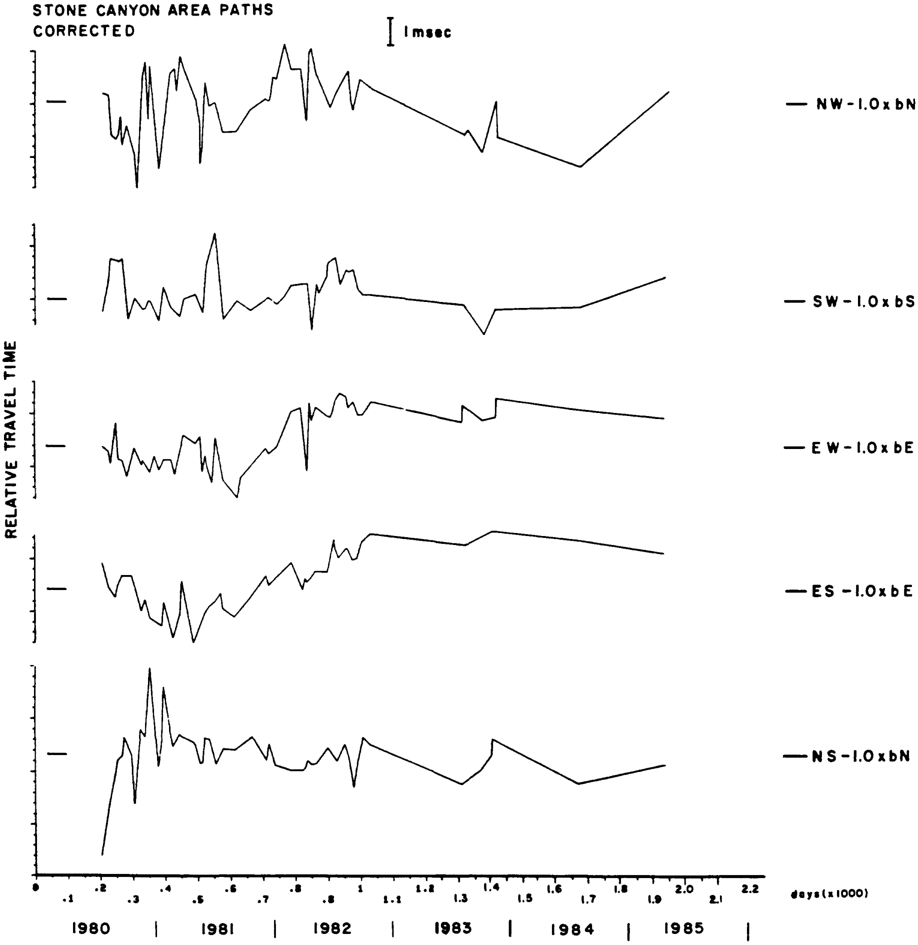

Figure 3. Stone Canyon area first-arrival travel times, with near-surface (seasonal) corrections. Site W has a surface geophone array and no borehole geophone for near-surface control. Thus paths NW, EW, and SW only have vibrator-end near-surface corrections applied. The receiver at site S is a borehole package, thus no receiver-end near-surface correction is necessary for paths NS and ES. Site designations as in Figure 6.

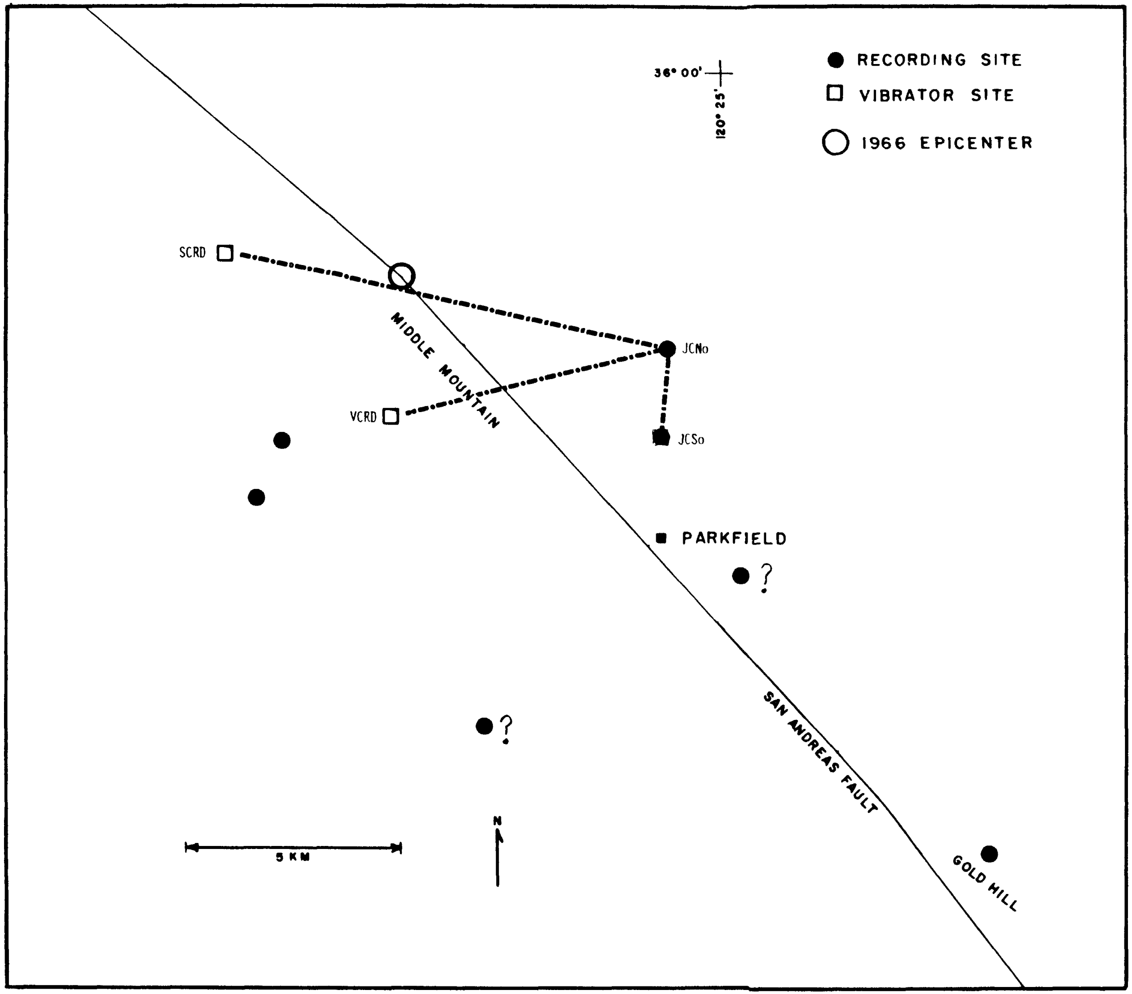

Figure 4 . Parkfield area location map. Filled circles indicate planned or established 3-component, borehole seismometer packages. Open squares show vibrator sites for preliminary recording in June, 1985, using the UC Santa Barbara borehole seismometer at site JCNo.

Active Seismology in Fault Zones

9930-02102

Walter D. Mooney
Gary S. Fuis
U.S. Geological Survey
Branch of Seismology
345 Middlefield Road, Mail Stop 977
Menlo Park, California 94025
(415) 323-8111, Ext. 2569

Investigations

1. Investigations of the seismic properties of fault zones, in relation to earthquake prediction, and to deep earth structure.

2. Continuation of analysis of seismic-refraction data in southern Alaska. This is part of the Trans-Alaska Crustal Transect (TACT) (Fuis, Ambos, Mooney, Page).

3. Continued analysis of the crustal structure of the Central Valley of California (Mooney, Walter, Whitman, Colburn).

4. Continued analysis of seismic refraction and reflection data from central California, including the region of the May 2, 1983, Coalinga earthquake (Walter); completion of a manuscript on tectonic wedging associated with emplacement of the Franciscan assemblage (Walter, C. Wentworth and others).

5. Continued analysis of seismic refraction data from the Columbia Plateau, eastern Washington State (Catchings and Mooney).

6. Initiation of analysis of seismic refraction data from Maine and Quebec (Luetgert, Klemperer, Mann).

7. Submission of manuscript to Science magazine on the deep crustal structure of Yunnan Province, PRC. Visit by Chinese scientist to USGS for several months (Mooney).

8. Analysis of aftershock refraction profiles near Coalinga, Calif. (Macgregor-Scott and Walter).

Results

1. The deformation of rocks due to faulting may be described in three increasing levels, corresponding to successively greater reduction of the seismic velocity of the rocks. The lowest level of deformation will lead to microcracking and limited microfracturing of the rocks, and will not have a significant effect on the velocity of the rocks, particularly if they are saturated, as is generally the case in situ. Densely fractured rocks, such as are found adjacent to major strike-slip fault zone, show greatly reduced Vp and Vs, and an increased Vp/Vs ratio. If the fractures are oriented due to a deviatoric stress field, velocity anisotropy will result, and can be determined with precise velocity measurements. High

levels of continuous deformation will produce fault gouge which is generally 30-40 percent lower in seismic velocity than the protolith at a given confiding pressure. Fault gouge therefore is easily detectable within the fault zone from seismic measurements.

Many seismic studies in central California have identified a pronounced low velocity zone (LVZ) extgending to seismogenic depths along the creeping segment of the San Andreas fault. This LVZ has been attributed to deep fault gouge, and Wu (1984) presents geologic and geochemical evidence that fault gouge is stable to depths of 10-12 km in the crust, thereby lending credance to this hypothesis.

The evidence indicates that the creeping segments of the San Andreas fault in central California contain thick LVZs, whereas the locked segments of the fault have either no or a very thin LVZ. Thus the slip behavior along segments of the fault appear to be related to the presence or absence of a LVZ along the fault.

Continental faults may locally be traced on seismic reflection sections to the Moho. According to Sibson's (1977) model for continental fault zones, deep faults consist of mylonitic rocks. Recent seismic reflection data and computer modelling of these data are all consistent with mylonitic rocks within deep faults.

Oceanic transform faults (fracture zones) have not been studies as intensely as continental faults, but the available evidence clearly indicates that they are underalin by abnormally thin crust which has lower P-wave velocity than normal oceanic crust. The low velocities in fracture zones has been attributed to intense fracturing and alteration of the crust, much like the fracturing and alteration that takes place in continental faults.

2. In 1984, the U.S. Geological Survey initiated the Trans-Alaska Crustal Transect (TACT) program--a coordinated geological and geophysical study of the structure, composition and evolution of the Alaskan crust along the Trans-Alaska oil pipeline corridor from Valdez to Prudhoe Bay and across the adjacent Pacific and Arctic continental margins. TACT is a major element of the multi-institutional Trans-Alaska Lithosphere Investigation (TALI). The TACT project was launced in southern Alaska; in succeeding years the investigations will shift northward with the goal of completing the transect by the end of the decade.

   Initial interpretation of geologic, seismic, gravity and magnetic data along the Trans-Alaska pipeline corridor in the northern Chugach Mountains and southern Cooper River Basin indicates that the accretionary Chugach Terrane (CGT) and the composite Peninsular/Wrangellia terrane (PET/WRT) are thin (<10 km) rootless sheets bounded on the south by north-dipping thrust faults that sole into a shallow, horizontal, low-velocity zone. The north margin of the CGT has been relatively underthrust at least 40 km beneath the PET/WRT along the north-dipping Border Ranges fault system (BRFS), the suture between the two terranes. Adjacent to the BRFS, uplift and erosion of 30-40 km since Jurassic time has exposed blueshist facies rocks in the CGT, and mafic and ultramafic cumulate rocks in the PET/WRT. Seismic refraction/wide-angle data reveal a sequence of at least four north-dipping, paired low- and high-velocity layers, extending beneath the northern CGT and southern PET/WRT, which we interpret as a stacked section of thin slices of subducted oceanic crust and upper mantle, the upper two pairs of which are now attached to the continental plate.

3. Application of synthetic seismogram modeling of seismic refraction data from the Great Valley, central California reveals a complex one dimensional structure. The first layer has a high velocity gradient which begins with a Vp = 1.6 km/sec and Vs = .2 km/sec which increases linearly to a depth of 2.93 km to velocities of 4.1 km/sec and 0.90 km/sec respectively. The Q structure appears to be simple with an average Q=100 for the first layer. Q for the remainder of the model was not studied.

   The second layer, a gradient with velocity of 4.25-4.40 km/sec is truncated by a low velocity zone which extends from a depth of 4.8 km to 6.20 km and has a velocity of 4.23 km/sec. Previous models ruled out phase E as a multiple or converted phase. Thus, it must be a primary reflection from the bottom of the low velocity zone.

   Layers 3 and 4 are simple gradients extending from 6.20-8.00 km and velocity of 5.70-5.95 km/sec, and 8.00-12.10 km, 5.95-6.3 km/sec respectively. The remainder of the crust and upper mantle can be modeled as either simple steps or complexly as alternating high and low velocity zones depending on the travel time interpretation. The simple model interprets two phases as primary reflections from the top of each layer. The complex model interprets these phases as delayed reflected branches from the bottom of low velocity zones. Despite the differences between the models in certain regions, both models are strikingly similar to the data and neither of them can be ruled out as a possible structure for the crust-moho transition zone. Future two-dimensional modeling will help to distinguish between the two models.

4. Interpretation of seismic refraction data collected along two profiles intersecting in the hypocentral region of the 1983 Coalinga earthquakes provides a velocity structure for the region. An 83-km long E-W profile extended from the San Joaquin Valley to the Diablo Range across Anticline Ridge, 1 km south of the M_L=6.7 main shock epicenter. A 102-km long NW-SE profile extended sub-parallel to the Diablo Range front along the syncline west of Anticline Ridge. Traveltime data from four shotpoints along the E-W profile and five shotpoints along the NW-SE profile have been modeled by 2-D ray-tracing techniques. In the San Joaquin Valley the velocity of the Cenozoic strata increases from 1.6 km/s near the surface to about 3.6 km/s at 3.6 km depth. Near the top of the Cretaceous Great Velley sequence (GVS), the velocity increases abruptly to 4.0-4.3 km/s. With increasing depth of burial the velocity of the GVS in the valley increases to over 5.0 km/s. On the western flank of the valley, velocity inversions within the GVS indicate high formation pore pressures.

   In the San Joaquin Valley, the GVS overlies a basement with a velocity of 6.3-6.4 km/s, indicative of a mafic composition. The dip of the basement increases westward of the valley axis from less than 5° to about 10°-12°. The basement plunges to an estimated 14-15 km depth at the front of the Diablo Range where an east-pointing wedge of 5.7-6.1 km/s Franciscan rocks lies between the GVS exposed at the surface and the mafic basement. Depth of the boundary separating the GVS and Franciscan wedge increases eastward to a junction with the mafic basement under the upturned western flank of the San Joaquin Valley. East of the Franciscan wedge the San Joaquin Valley is underlain by a basin containing several additional kilometers of sedimentary strata associated with the GVS. Unreversed refraction data support a deeper layer within the mafic basement with velocities exceeding 7 km/s and a Moho depth of 28-30 km near the front of the Diablo Range. Comparison of the refraction velocity models to the hypocentral locations of the 1983 earthquakes reveals that the source region for the M_L=6.7 main shock and larger aftershocks is within the Franciscan wedge and that the seismicity extends upward into the GVS.

5. In August 1984, the U.S.G.S., in conjunction with D.O.E./Rockwell Hanford Operations conducted a seismic-refraction survey over the Columbia Plateau of east-central Washington and northeast Oregon. The 260-km-long profile, centered on the Pasco Basin (within the Hanform Property), trended N 50° E from 30 km south of Wasco, OR., to 50 km northeast of Warden, WA. The survey consisted of 8 shots (900 to 2300 kg), 4 shotpoints, and 240 station locations (930-m spatial sampling interval between shots).

   Our interpretation suggests that the Columbia River Basalt Group (CRBG) (V_p = approx. 6 km/s) is variable in thickness but is generally less than 7 km deep and is interbedded with sediment at depth. Underlying the (CRBG) are thick sediment accumulations (as deep as 12 km) beneath some of the basins. Atypically high velocity basement rocks (V_p = 6.5 km/s) underlie the sediments within basins, but basement velocities outside the basins are more typical (V_p = 6.1 km/s). Normal faulting is observed near the basin edges. Low-velocity zones exist in the intermediate crust (about 25 km) and near the Moho (38 km). A thick high-velocity lower crust (V_p = 7.5 km/s), relief on the Moho, and a high-velocity upper mantle (possibly as high as V_p = 8.4 km/s), combined with the above observations, suggest that this area of Columbia Platea resulted from continental rifting.

6. In 1984 the U.S. Geological Survey collected 700 km of refraction data across the Appalachian orogen in Maine. A 100 km strike-line in coastal Maine, west of Penobscot Bay, is here interpreted on the basis of both refracted and reflected phases. Techniques of seismic reflection processing, including NMO (normal moveout) velocity corrections, and CMP (common mid-point) stacking, are applied to these conventionally-acquired refraction data in order to enhance the visibility of reflected phases. The geometry of the most laterally-continuous reflections is defined by these techniques and correlated with reflections seen on a crossing, near-vertical reflection profile. Conventional ray-tracing analysis of refracted and wide-angle reflected phases in the refraction data constrains the velocity structure to about 14 km depth, and provides evidence for high-velocity material (> 6.5 km/s) between 4 and 7 km depth, and for lower velocities (< 6.3 km/s) from 7 km to at least 14 km depth. The reflection velocity analysis, based on single-fold constant-velocity sections and study of common-midpoint stacked sections, confirms the existence of this zone of reduced velocity in the crust from 7 to 14 km. The combined refraction/reflection interpretation of this profile, in conjunction with data from crossing refraction and near-vertical reflection lines, provide a velocity and structural characterisation of a

part of the Maine coastal belt.

7. A manuscript was submitted to Science magazine which reported the first seismic refraction profiles in Yunnan Province, southwestern China, and define the crustal structure in an area of active tectonics on the southern end of the Himalaya-Burma Arc. The crust ranges in thickness from 38-46 km, and is described seismologically by three layers. Seismicity is confined generally to the upper layer, whose base appears to constitute the brittle-ductile transition. The mean crustal velocity is less than 6.4 km/s, allowing for a crustal composition compatible with normal continental crust and consisting mainly of meta-sedimentary and silicic intrusive rocks, with little mafic or ultra-mafic rocks. This suggests a crustal evolution involving sedimentary processes on the flank of the Yangtze Platform and possibly the accretion of oceanic plateaus, rather than the accretion of oceanic island arcs, as previously proposed. An anomalously low upper mantle velocity (7.7 km/s) is observed on one profile but not another at right angles to it. This may be indicative of active tectonic processes in the mantle, or of seismic anisotropy.

8. Aftershocks of the May 2, 1983, $M_L = 6.7$ (BERK) earthquake near Coalinga were recorded using 120 portable vertical-component seismographs deployed along a profile striking sub-parallel to the regional structure and extending from the epicentral region to a point about 100 km southeast. An explosion profile, recorded along roughly the same line as the earthquake profile, constrained the velocity structure to a depth of about 16 km. The traveltimes of earthquake arrivals have not been used to constrain the lower crustal velocities and the crustal thickness.

   Seven aftershocks ($M_L < 2.6$) were located using the P-wave arrival times at selected stations along the refraction profiles as well as at local earthquake-network stations. Most of the hypocenters are located at depths between 7 and 10 km. These earthquakes occurred in intermediate-velocity rocks (5.6-6.0 km/s) lying above a mafic basement (6.5+ km/s at 15-km depth). Both the earthquake and explosion record sections show evidence for a velocity inversion above the top of the mafic basement. The aftershock seismograms recorded at ranges greater than 60 km show secondary arrivals interpreted to be PmP reflections. The arrival times and amplitudes of these PmP arrivals, modeled using two-dimensional ray tracing, suggest that the Moho is not a step discontinuity in velocity but rather a transitional zone located at a depth of 28 ± 2 km.

Reports

Fuis, G. S., Ambos, E. L., Mooney, W. D., and Page, R. A., Velocity structure of accreted terranes of southern Alaska (abs): EOS Transactions American Geophysical Union (December 1985 Meeting).

Fuis, G. S., Ambos, E. L., Mooney, W. D., and Page, R. A., 1985, Crustal structure of southern Alaska--preliminary results of the TACT 1984 seismic refraction experiment (abs): Seismological Society of America, Earthquake Notes, Eastern Section, v. 55, p. 23.

Plafker, G., Nokleberg, W. J., Fuis, G. S., Mooney, W. D., Page, R. A., and Ambos, E. L., 1985, 1984 results of the Trans-Alaska Crustal Transect in the Chugach Mountains and Copper River Basin, Alaska (abs): Geological Society America Abstracts with Programs (Vancouver, B. C., 1985 meeting).

Ambos, E. L., Fuis, G. S., Mooney, W. D., Page, R. A., Plafker, G., Nokleberg, W. J., and Campbell, D. L., 1985, Lithospheric structure in southern Alaska from 1984 TACT seismic refraction data (abs): EOS Transactions American Geophysical Union, v. 66, p. 301.

Page, R. A., Plafker, G., Fuis, G. S., Noklebert, W. J., Ambos, E. L., Mooney, W. D., Accretion and subduction tectonics in the Chugach Mountains and Copper River Basin, Alaska: initial results of TACT: (submitted to Geology).

Fuis, G. S., Ambos, E. L., Mooney, W. D., Page, R. A., and Campbell, D. L., 1984, Preliminary results of TACT 1984 seismic-refraction survey of southern Alaska in The United States Geological Survey in Alaska-- Accomplishments during 1984: (in press).

Fuis, G. S., Ambos, E. L., Mooney, W. D., Page, R. A., Plafker, G., Nokleberg, W. J., and Campbell, D. L., Lithospheric structure of southern Alaska from Seismic Refraction Data: The TACT Program. (abst), 23rd General Assembly of IASPEI, Tokyo, Japan, page 727.

Klemperer, S. L., and Luetgert, J. H., Seismic reflection NMO and CDP processing applied to conventional refraction data from coastal Maine, to be submitted to B.S.S.A.

Walter, A. W., Velocity Structure near Coalinga, California in Rymer, M. J., and Ellsworth, W. L., eds., Mechanics of the May 2, 1983 Coalinga, California, earthquake: U.S. Geological Survey Prof. Paper. (in press).

Wentworth, C. M., Blake, M. C., Jones, D. L., Walter, A. W., and Zoback, M. D., 1984, Tectonic wedging associated with emplacement of the Franciscan assemblage, California Coast Ranges, in Blake, M. C., ed., Franciscan Geology of No. CA. Soc. of Economic Paleontologists and Mineralogists, Pacific Section, pp. 163-174.

Mooney, W. D., and Ginzburg, A., Seismic expression and internal properties of continental fault zones. Submitted to PAGEOPH.

Kan, Rong-Ju, Hu Hong-Xiang, Zeng Rong-Sheng, Mooney, W. D., and McEvilly T. V., Crustal structure and evolution of Yunnan Province, PRC, from seismic refraction profiles.

Kohler, W. M., and Fuis, g. S., Travel-time, time-term, and basement depth maps for the Imperial Valley region, California, from explosions: in review for Bulletin Seismological Society of America.

Catchings, R., and Mooney, W. D., 1985, Crustal structure of the Columbia Plateau, Earthquake Notes, v. 55, no. 1, p. 22.

Macgregor-Scott, N. and Walter, A. W., 1985, Data report for two-Earthquake-Source Refraction Profiles Crossing the Epicentral Region of the 1983 Coalinga, California, Earthquakes, U.S. Geol. Survey Open-File Report 85-435, 64 p.

Macgregor-Scott, N. and Walter, A., 1985, Constraints on Crustal thickness near Coalinga, California, from Earthquake Refraction Profiles, Earthquake Notes, v. 55, no. 1, p. 30.

Crustal Deformation Observatory, Part (i): Shallow Borehole Tiltmeters

14-08-0001-21939

Sean-Thomas Morrissey
Saint Louis University
Department of Earth and Atmospheric Sciences
P.O. Box 8099 - Laclede Station
St. Louis, MO 63156
(314) 658-3129

Objective: To apply the latest innovations and technology of instrumentation and installation methods to the shallow borehole tiltmeters at Pinon Flat such that their performance, particularly with regard to longterm stability, will compare more favorably with the data from the long baseline tiltmeters.

Accomplishments: Three tiltmeters were reinstalled at Pinon Flat in May of 1985. The first phase of our study involved removing the existing tiltmeter and "factory" electronics, removing the bubble sensor and attaching it to the new tapered pipe, connecting the new low thermal noise electronics, and reinstalling the sensor in the same borehole in the bottom of a 4 meter access pit. Plans were made for four tiltmeters, so five electronics systems were assembled and tested. Unfortunately, one of the sensors at CDO had failed, so only three were available for the experiment. The objective was to determine whether the secular drift was actually noise in the ground that was spatially incoherent even over short (10 meter) distances, or whether it involved the sensor and/or its installation, and whether the latter noise was a linear function of the sensor temperature that could be removed from the data.

Two of the sensors are labeled Alpha and Beta, and are 10 meters apart in 4 meter open access pits with 1 meter boreholes in the bottom. The third, the Delta unit, is about 3/4 km to the southeast. The Alpha and Beta units were reinstalled first. No unusual problems were encountered. The bubble sensors were remounted to the new cast stainless pipe, fitted with direct burial signal cable, and installed in the small borehole with the usual bonded sand. The lower half of the 10-meter borehole installation tool was used for handling and aligning the sensors. Both units stabilized very rapidly, establishing a baseline at earth tide (10^{-7}) sensitivity within 24 hours. When remounting the bubble sensor to the tapered pipe for the Delta unit, a problem occurred in that the threads seized in the mounting, preventing the bubble shell from mating properly to the seating plane of the pipe. No reasonable effort would either undo or further tighten the bubble. It was reinstalled anyhow, with the expectation that the highly stressed connection would cause unprecendented drift and render the data useless. There was some thought of turning it off, but the unit leveled out after about a month and has been "behaving well" since.

The data are recorded by the Pinon Flat Observatory digital data system, under the auspices of Frank Wyatt of UCSD. There was some problem with our temperature data for a couple of months after the reinstallation, so it is not complete throughout the time period. The CDO digital data is compiled and sent to investigators at 6 month intervals, so the attached data (Segment 23) only runs from 16 May through 8 August 1985 of the reinstallation study, and only a few weeks of thermal data is available.

The central question of this first phase of the effort is whether the long term drift of the data is from the instruments or in the ground. The fact that Alpha and Beta, though only 10 meters apart in competent rock, have recorded significantly different data both before and after the reinstallation makes one suspect that the instrument system and/or the installation method is the source. In our redesign of the instrument electronics, we have been able to reduce direct electronics thermal effects to about 0.5 nano-radians per degree C. We have not attempted to do anything about the bubble sensor, although we have seen that it has thermal sensitivities of as much as several micro-radians per degree C, depending on the mechanical parameters of the bubble mount. (The pressure spring and washers can move laterally more than 1 mm.) The data usually show a linear relationship to the bubble temperature, of either polarity.

This behavior is shown in Figure 1, where a segment of the CDO data is plotted against the longest available borehole temperature segment (of the Beta unit). The bottom trace is the temperature data, ranging from $13.04^{\circ}C$ to $13.97^{\circ}C$, or slightly less than $1.0^{\circ}C$, during which the average thermal tilt was about 2.5 PPM(microradians). It must be pointed out that the data of four of the channels was inverted for this plot; i.e. they have negative rather than positive thermal coefficients. Such a linear error for temperature is not uncommon for high resolution instruments, such as gravimeters and surveying instruments. That the data is continuous in time readily allows removal of this first order temperature component from any segment of the data, as has been demonstrated with the Adak data in previous reports. There is also a small rainfall event that is more likely a surface strain disturbance. Note that it does not show identically on the three instruments. However, the linear temperature relationship means that the secular thermal drift can readily be removed by least-squares fitting. With the Adak (Aleutians) data, we have seen that the fitting coefficients remain very stable for many years as long as the bubble sensor is not disturbed.

Figures 2, 3 and 4 show the raw data before and after the reinstallation. With the typical rapid stabilization of the bonded sand installation technique, we would reasonably expect the secular trend of the pre-installation data to continue if it is a function of the ground noise. This, in fact, is generally true of the Alpha data after about 20 days. However, the NS data of the Beta unit has taken a different tack, and both components of Delta have changed slope, even though the ground thermal temperature is a positive ramp for this part of the year. This makes the bubble and/or electronics suspect for the change of thermal behavior. Even though care was taken not to jar the bubble sensor, it may have shifted in the Beta unit, and most probably did when we were dealing with the seized threads of the Delta unit. It may be coincidental that the Alpha data did not change character or slope; complimentary noise sources may have been providentially cancelling out. This was common with the old "factory" electronics. Further evaluation of this effort awaits more data.

Further Plans: The holes for the second and third phases of the effort, the 10 meter and 20 meter installations, are being drilled in October 1985, and the 10 meter depth sensors will be installed in November. The pneumatic tamping system needed for the 20 meter depth is not yet complete, but should be ready for use in the installations in the 20 meter holes by February.

The USGS did not fund a proposal in response to RFP 1586 to continue this work. Since the initial funding was delayed by 9 months, the second year of effort began July 1, 1985, so success in the 10 meter installations and a successful proposal in 1986 may be able to continue the effort in late 1986. The Palmdale tiltmeter effort was discontinued, so the instrument shelters from there will be used at Pinon Flat.

8 October 1985
Sean-Thomas Morrissey
Senior Research Scientist

Figure 1.

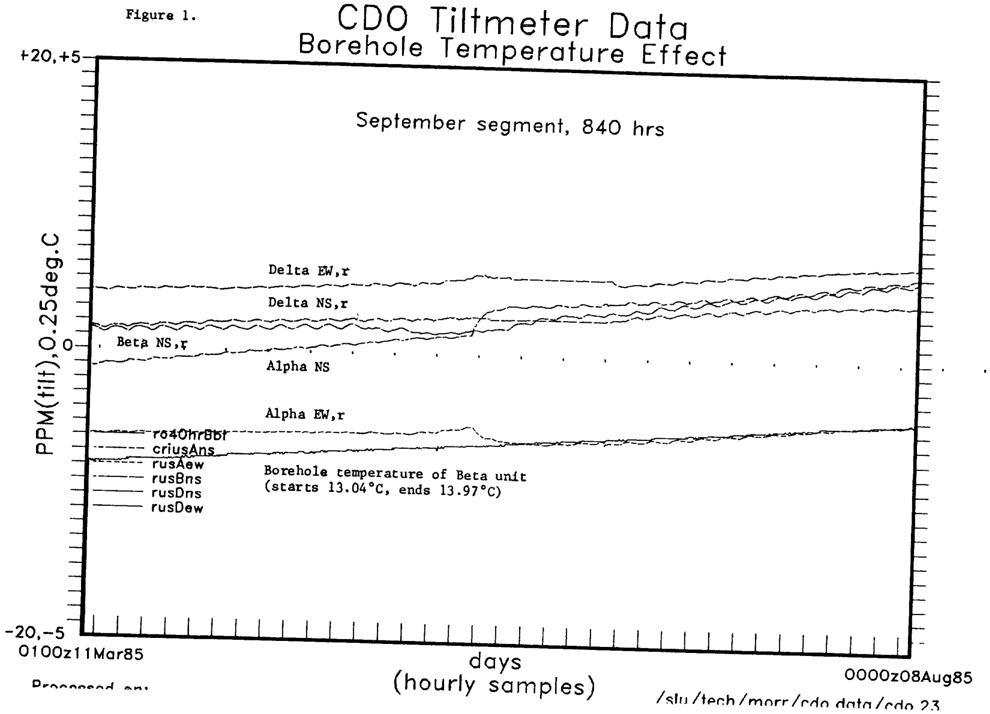

Figure 2.

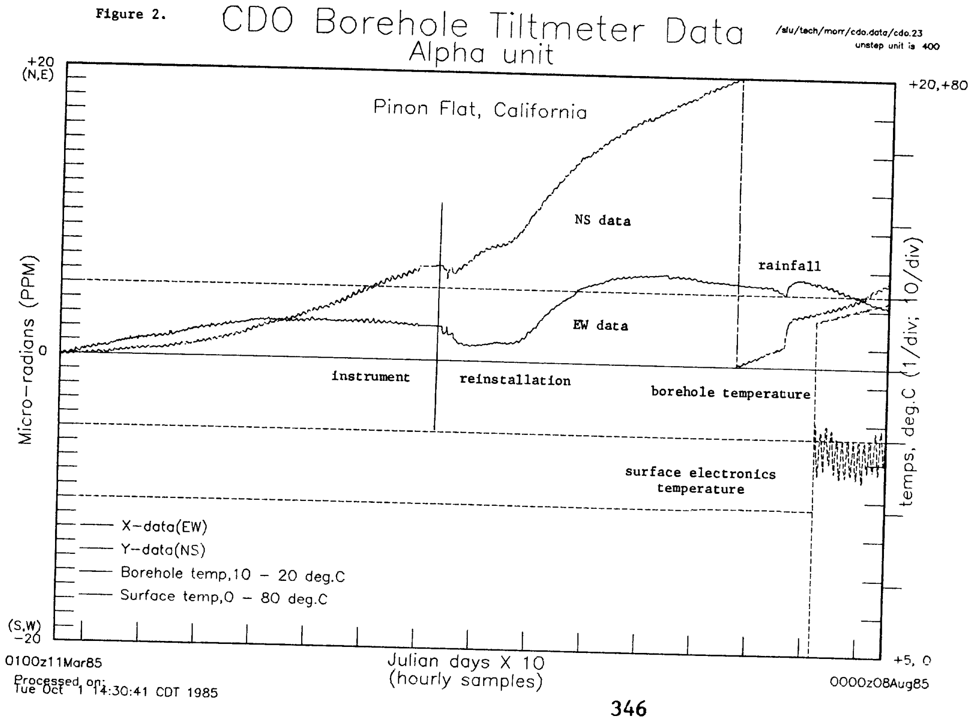

Figure 3. CDO Borehole Tiltmeter Data
Beta unit

/slu/tech/morr/cdo.data/cdo.23
unstep unit is .400

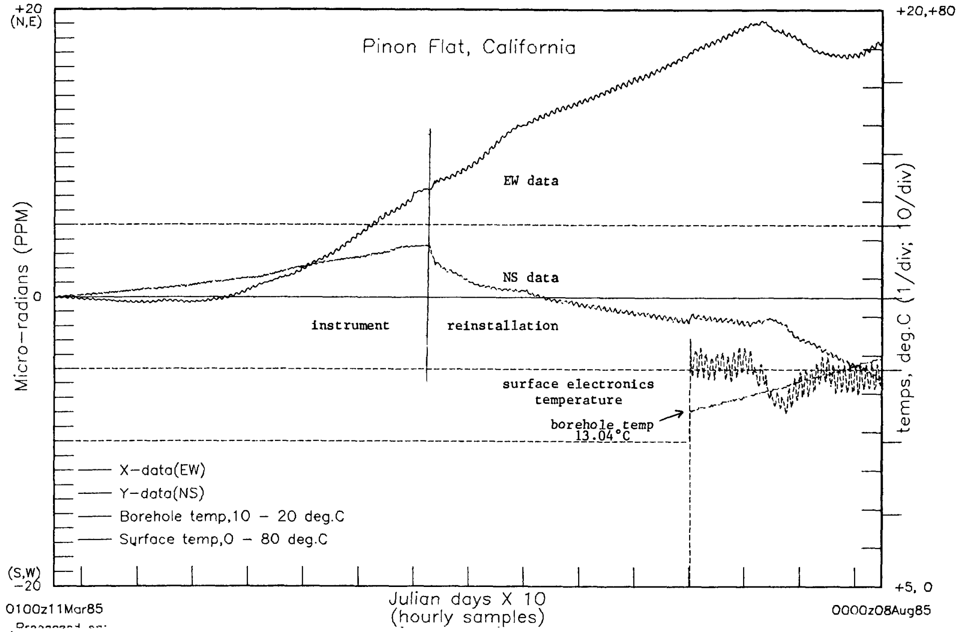

Figure 4. CDO Borehole Tiltmeter Data
Delta unit

/slu/tech/morr/cdo.data/cdo.23
unstep unit is .400

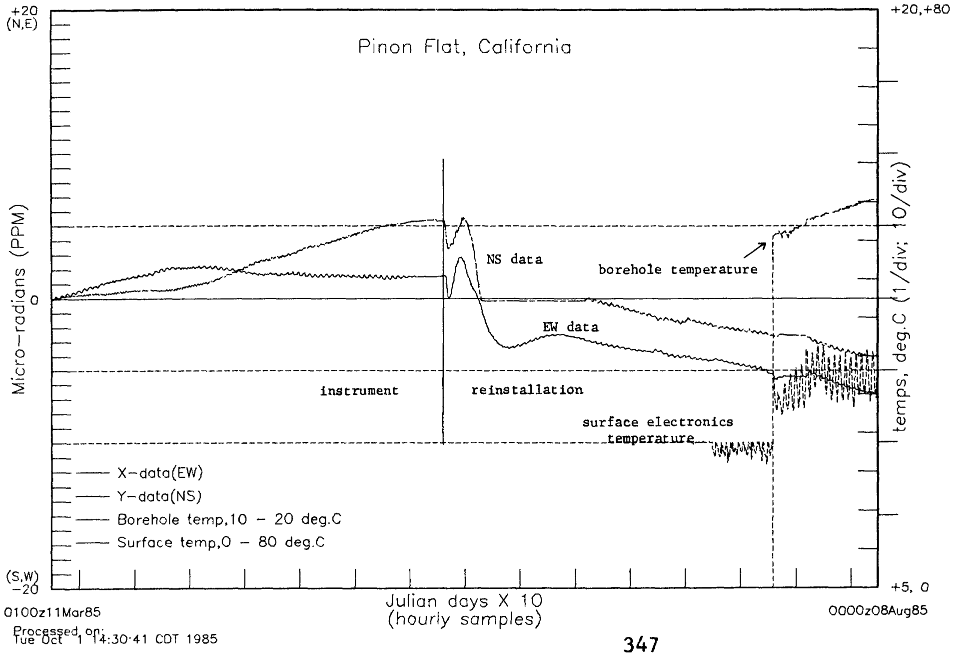

Cooperative Tiltmeter Program at Parkfield, California

14-08-0001-22017

Sean-Thomas Morrissey
Saint Louis University
P.O. Box 8099 - Laclede Station
St. Louis, MO 63156
(314) 658-3129

Objective: To apply the latest state-of-the-art technology to shallow borehole tiltmeter installations and data acquisition in the Parkfield area, which is forecast to be the locale of a moderate earthquake in the near (3-8 years) future. Considerations of the current failure model, based on known creep data and fault-constituitive models, allows locating the tiltmeters such that probability of acquiring large coherent signals during the precursory stages is enhanced. The cooperative aspect involves the assistance of the U.S. Geological Survey in site selection, preparation, maintenance, and data acquisition.

Accomplishments: Since the start of the program in January 1985, a concerted effort has been made to build the electronics and procure the hardware for the installation effort within the scope of the program manpower committments. A proposal in response to RFP 1586 for funds to instrument additional sites has been reported to be funded only at a level sufficient to maintain the current effort, pending the results. Efforts are underway to install six instruments at two sites, namely Gold Hill on the Jack Ranch and the Hefflenger Ranch off the Turkey Flat Road. These sites correspond to the regions of the most intense deformation anticipated by the model of Stuart et al. (JGR 90, 592-604). The attached figure shows the relationship of these sites, located at kilometers (from the 1966 epicenter) 11 and 19, to the theoretical uplift rates during the preparatory phases of the predicted earthquake. The potential tiltmeters are indicated as large black arrows pointing in the direction of downward tilt. The sites at Km 11 and Km 19 (the third and fourth arrows) are the locations of maximum expected deformation during the pre-failure process.

In May 1985 these sites, the Gold Hill and Turkey Flat sites, along with several others, were visited and evaluated with the assistance of Tom Burdette of the USGS. Shallow refraction equipment (Bison) was used to determine the depth of the overburden to competent rock, which was about 3 meters at Turkey Flat and 2 meters on the shallow rise near the Gold Hill dilatometer. We delayed beginning negotiations with the driller in the hope that funds for two other sites would be found. Currently, drilling is scheduled for October 1985, with the installations planned for November or December. We will use our digital data system (the former Palmdale equipment) to digitize on-site and transmit to a logging micro at the two-color geodimeter site. Either serial digital data or reconverted analogue output will be available for the USGS telemetry system, either via GOES or the Menlo Park microwave. The tiltmeters and tiltmeter electronics for five of the units are now available and have been tested for well over a year; this was the hardware waiting for installation in Palmdale, which has been discontinued. The new electronics being procured will provide for upgrading the oscillator system and the auto-zeroing systems (see the last Southern California report) of these units, as well as providing three more complete systems. The cast stainless housings have been completed (and heat treated) for all the planned tiltmeters.

Reports: The Principal Scientist presented a paper, "The Significance Expected of Near-Surface Tiltmeter Data from Parkfield, California," to the National Earthquake Prediction Evaluation Council (NEPEC) in a special meeting on Parkfield at Menlo Park on 26 July 1985. At the meeting it was brought out that recent data from the Parkfield area creepmeters and dilatometers have shown correlation between period "events" of weeks to months duration, regardless of the long-term "secular" trend of the data. It seems that these intermediate period events might have considerable significance with respect to fault instability studies, and may have in fact been precursory to the neighboring Coalinga, CA, earthquake, if it had not been raining heavily and the scientists were unsure whether the events on the creepmeters were rain noise or the real thing. It is expected that these events will also be seen on the tiltmeters.

Action Required by the USGS: We have not yet negotiated the "cooperative" details of the site preparation, installation of instrument pits, getting air cells, etc., with the USGS at Menlo Park, but no difficulties are expected. We have only verbal word from Reston that the program will be continued for another year. No written confirmation or contract negotiations have been received as of this date.

8 October 1985
Sean-Thomas Morrissey
Senior Research Scientist

Figure 1. Theoretical uplift rates at the ground surface at three phases of the pre-earthquake process at Parkfield, CA. (after Stuart et al: Parkfield Forcast Model, JGR,90,592-604)

(Uplift/subsidence rates in mm/bar, where 10 mm/bar = 1.1 mm/yr)
(Tiltmeter long term stability at 10m depth is 0.1ppm/yr, or 0.1mm/km/yr)

A) Maximum resistance of locked patch: shear stress = 0.10

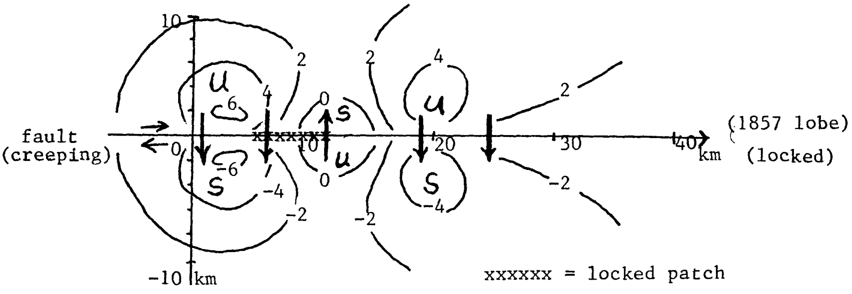

B) End of slow load stage: shear stress = 1.00

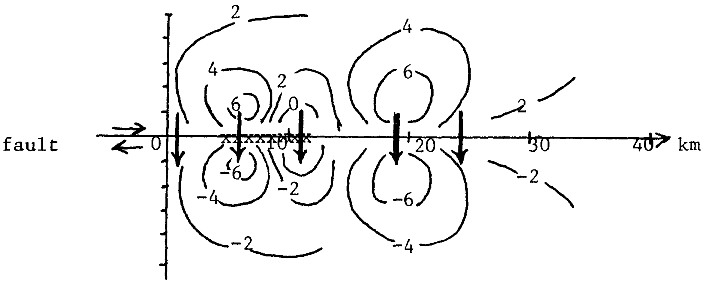

C) End of precursor stage: time of incipient failure: shear stress = 1.20

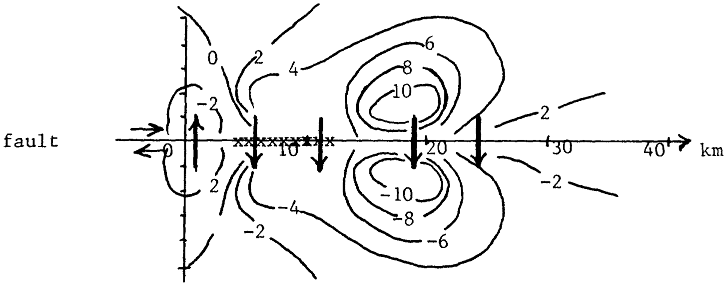

Tiltmeters are indicated as large arrows in the direction of subsidence. All the tiltmeters will be within 1 km of the fault; the unit at km 1 may not be installed because of the topography.

Tiltmeter and Earthquake Prediction Program in S. California and at Adak, AK

14-08-0001-21244

Sean-Thomas Morrissey
Saint Louis University
Department of Earth and Atmospheric Sciences
P.O. Box 8099 - Laclede Station
St. Louis, MO 63156
(314) 658-3129

I: Task 1: The Tiltmeter System

Objective: To continue to improve the performance of bubble sensor tiltmeter systems and to investigate other sensor systems for use in moderate depth boreholes, seeking relatively low-cost, readily deployed instrumentation.

Accomplishments: The crystal stabilized digitally generated sine excitation oscillator was improved further by using a LM356 voltage reference for better than 1 PPM amplitude control. These units were installed at CDO (Pinon Flat, CA) and Adak, AK. The zero control system reliability was improved by using the ETI motor driven potentiometer, and a complete new controller circuit card was designed for it. The motor runs on 9 ma at 9 v, and the controller runs it in approximately 1 PPM steps after a delay of 4 hours after an off-scale condition is detected. The microthermometer system was redesigned to use the LM35A intrinsically calibrated sensor. A compact circuit board supports four sensors with a single precision reference.

A pair of Frederics Company electrolytic bubble sensors was mounted to a plexiglass plate and calibrated on the tilt table at 5 PPM increments. The linearity was very good over a range of several hundred microradians. When operated with an unmodified electronics system for the Autonetics bubble (including the bridge circuit), the output is about 50 mv/PPM. We plan to mount the glass bubble sensors in a tapered housing for some long-term stability tests for possible use in large signal conditions. There was no time for further work on the new biaxial inductive transducer tiltmeter discussed in previous reports.

II: Task 2: The Installation Method

Objective: To improve the installation methods for borehole instruments with a goal of installing them as deep as 100 meters.

Accomplishments: Considerable work was done on a new concept in the design of an installation tool to allow tamped-sand installations in boreholes of any reasonable depth. We decided to use miniature air-pneumatic cylinders to carry out, under electrical control from the surface, the activities that are done by hand in open access pit installations. These include the dispensing of dry bonded sand and water, and the sand tamping itself. Lab constructed pneumatic sand valves allow the bonded sand supply to be lowered in reservoirs to the bottom of the hole on the utility and TV carrier system, and dispensed there without the previous problem of cement dust from the sand falling through a long hose. The downhole sand and water supplies are more than ample for the borehole installation. A four cylinder sand tamper was prototyped for testing; eight cylinders will eventually be needed. When the installation tool is complete, all the mechanical functions will be electrically controlled from the surface. The entire system, including the air compressor, runs off a 500 watt portable generator. It will be used in 20 meter deep installations at Pinon Flat in late winter.

A study of a figure in an unpublished paper by D.C. Agnew on the attenuation of cyclic thermal cycles with increasing depth lead us to the conclusion that the Adak borehole diurnal thermal variations were about two orders of magnitude greater than they should be. It became apparent that the approximately 1 meter of bagged vermiculite insulation did not have the thermal mass (i.e. specific heat) required to shield the sensor as if it was installed at the same depth in the legendary "homogeneous halfspace." An effort was made at Adak in the 1985 summer maintenance trip to improve the thermal barrier above and around the borehole pipes in the very shallow (2 meter) installation pits. This was accomplished by "dirt bagging," or the half-filling of 50 to 70 large heavy trash bags with soil and placing them in the pits in place of the vermiculite, around and above the plastic tube that protects the upper half of the borehole pipe. The vermiculite was replaced above the dirt bags. The results were dramatic, as shown in Figure 1, which is of several channels of borehole temperatures before and after the dirt-bagging effort.

This thermal barrier reduced the diurnal noise to less than 1% of the previous level. However, diurnal extremes (such as the very rare sunny Aleutian day) are still evident, and the more subtle temperature changes, mostly due to rainfall, are readily apparent, whereas before they were completely masked. Figure 2 shows a study of the residual of the tilt data after the earth tides are removed. We expected an obvious decrease in the residual noise, but it is not very obvious in this short segment. Even some periodic diurnal effects are still present, but these may be barometric, ocean load effects, solar heating of the hill, etc., that are not currently well analyzed or understood. Certainly the improved thermal stability will allow the use of less "pre-processed" thermal profiles for removing direct effects of temperature on the sensor.

III: Task 3: The Digital Data System

Objective: To continue to develop and operate a digital data acquisition system to acquire geodetic data and to thoroughly monitor the environment of the instrument installations.

Accomplishments: The Adak digital system continues to operate with impressive reliability and continuity. Since August 1980, 206 floppy disks have been logged, at 0.5 mbyte each, with 70 channels of data from five independent remote 14-channel digitizers. Less than 24 hours of data is missing from 61 months of recording. The new 16-bit, 1802-based micro replacement for the old 12-bit digitizer has been designed and programmed and circuit boards printed; three units are currently complete. It is much more reliable than the old unit, and will be used at Parkfield, CA. The new system exactly emulates the transmission format of the old.

IV: Task 4: The Data Interpretation

Objective: To process the digital data and make efforts to remove the environmental noise from the data, so as to establish the intrinsic long-term stability of the tiltmeters. Various analysis techniques are then utilized to present the data in meaningful formats such that any precursory tilt events would become evident.

Accomplishments: A fair criticism of the previous work in using least-squares fitting techniques to remove the thermal noise was that the inflections of the fitted thermal curves could induce an artificial coherence between data series. So the thermal profiles have been further smoothed using sequential cubic spline fits at 50 and 720 hours, triangularly averaged over a 100% window. The residual tilt series are now devoid of any resemblance of inflections of the thermal profiles. Using much less smoothed data would be preferable, because the smaller events might be fitted, especially the rainfall transients. However, the older thermal data has too much diurnal noise. With the new data after the "dirt-bagging," it may be possible to use much shorter period thermal data for the process.

This would be especially important in the light of recent data from the Parkfield area creepmeters and dilatometers, where intermediate period events of weeks to months have been correlated between the instruments, regardless of the long-term "secular" trend of the data. It seems that these intermediate period events might have considerable significance with respect to fault instability studies, and may have in fact been precursory to the Coalinga, CA, earthquake, if it had not been raining heavily and the scientists were unsure whether the events on the creepmeters were rain noise or the real thing. An effort was made to look at the last year of Adak data for intermediate term coherence at the west site . (The cumulative three year data set (since installing the new electronics) was not available because of disk storage problems on the USGS PDP 11/70 computer. The annual cycles are much more readily fitted and removed if there are several.) In Figures 3 and 4 the last year of Adak west site data is shown in first the raw form, automatically edited to remove the 1 PPM auto-zeroing steps, then in corrected form, where the well smoothed borehole and surface temperature profiles have been fitted and removed. Similar periodic events present in all three tiltmeters are seen in each component. Many of these are barometric loading changes and/or rainfall events expected at the shallow 2 meter instrument depth. They should be greatly diminished in holes of reasonable depth, 10 meters or more, as are being used at Parkfield and Pinon Flat.

Problems Encountered: A proposal in response to USGS RFP 1586 was not successful in continuing funds for this effort. Although the holes were drilled in April 1982, the instruments in the Palmdale area had not been installed because of a vagueness of purpose and lack of USGS committment to research related to the deflated Palmdale "bulge." However, the tiltmeter instrumentation, installation techniques, and data analysis techniques have shown continuous progress. The funds not used in the Palmdale installations (mostly travel and final site preparations) will be used to complete development of the electric-pneumatic installation system for use at Pinon Flat and Parkfield. The Adak tiltmeters might continue to operate as long as this researcher continues to operate the seismic network there for CIRES of the University of Colorado.

Future Plans: A proposal to continue the tiltmeter instrumentation, installation techniques, and data analysis studies will be submitted in 1986.

Reports: The Principal Scientist presented a paper, "The Significance Expected of Near-Surface Tiltmeter Data from Parkfield, CA," to the National Earthquake Prediction Evaluation Council (NEPEC) in a meeting at Menlo Park on 26 July 1985.

Sean-Thomas Morrissey
Senior Research Scientist
15 October 1985

Figure 1

Adak Tiltmeter Data
Improvement of Thermal Barrier

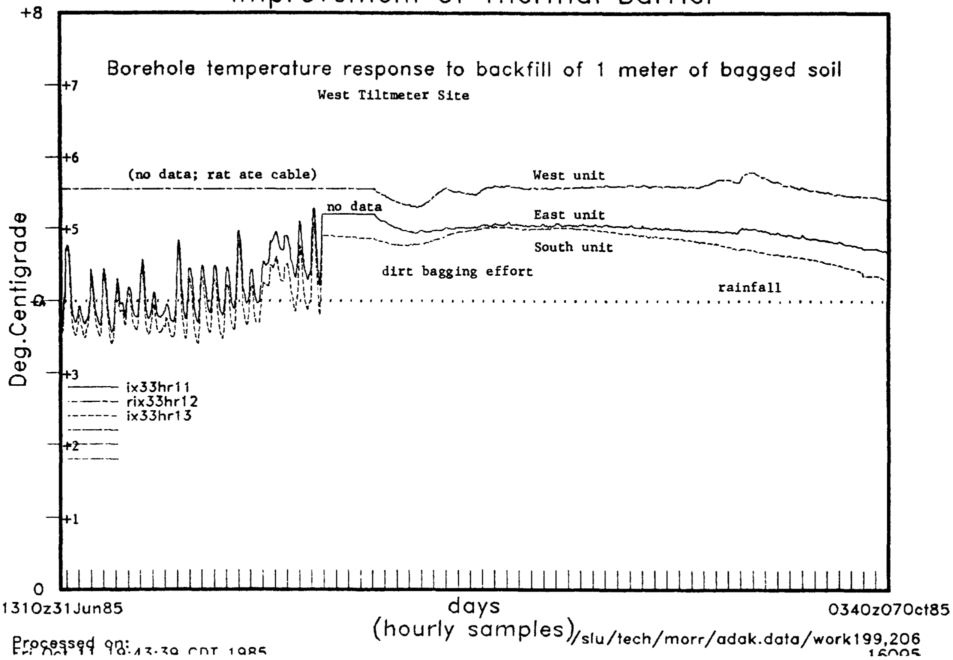

Figure 2

Study of Residual Tilt Noise
Adak West site, West unit, NS data

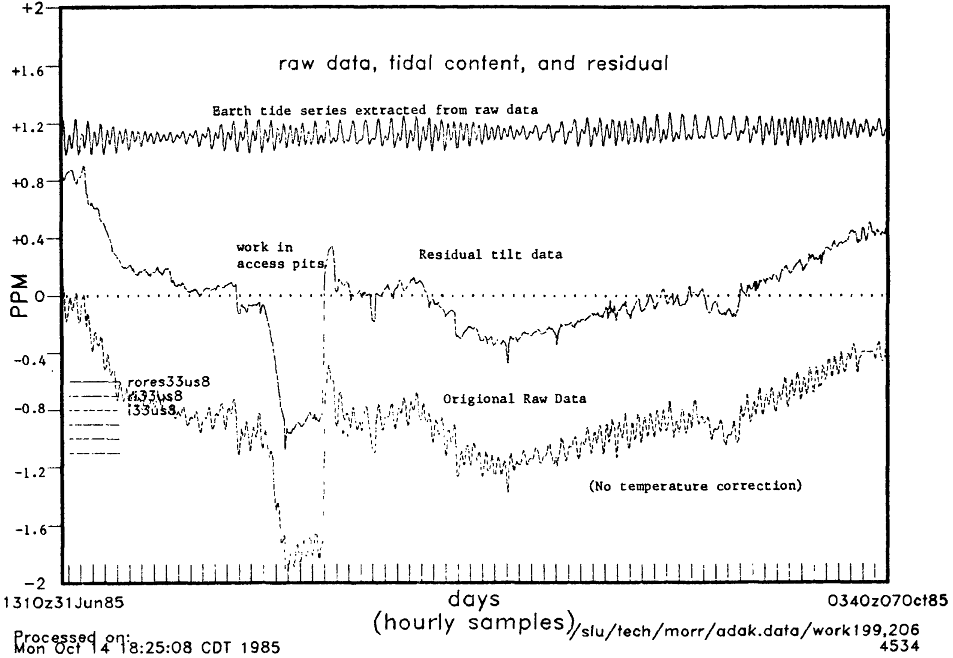

Figure 3

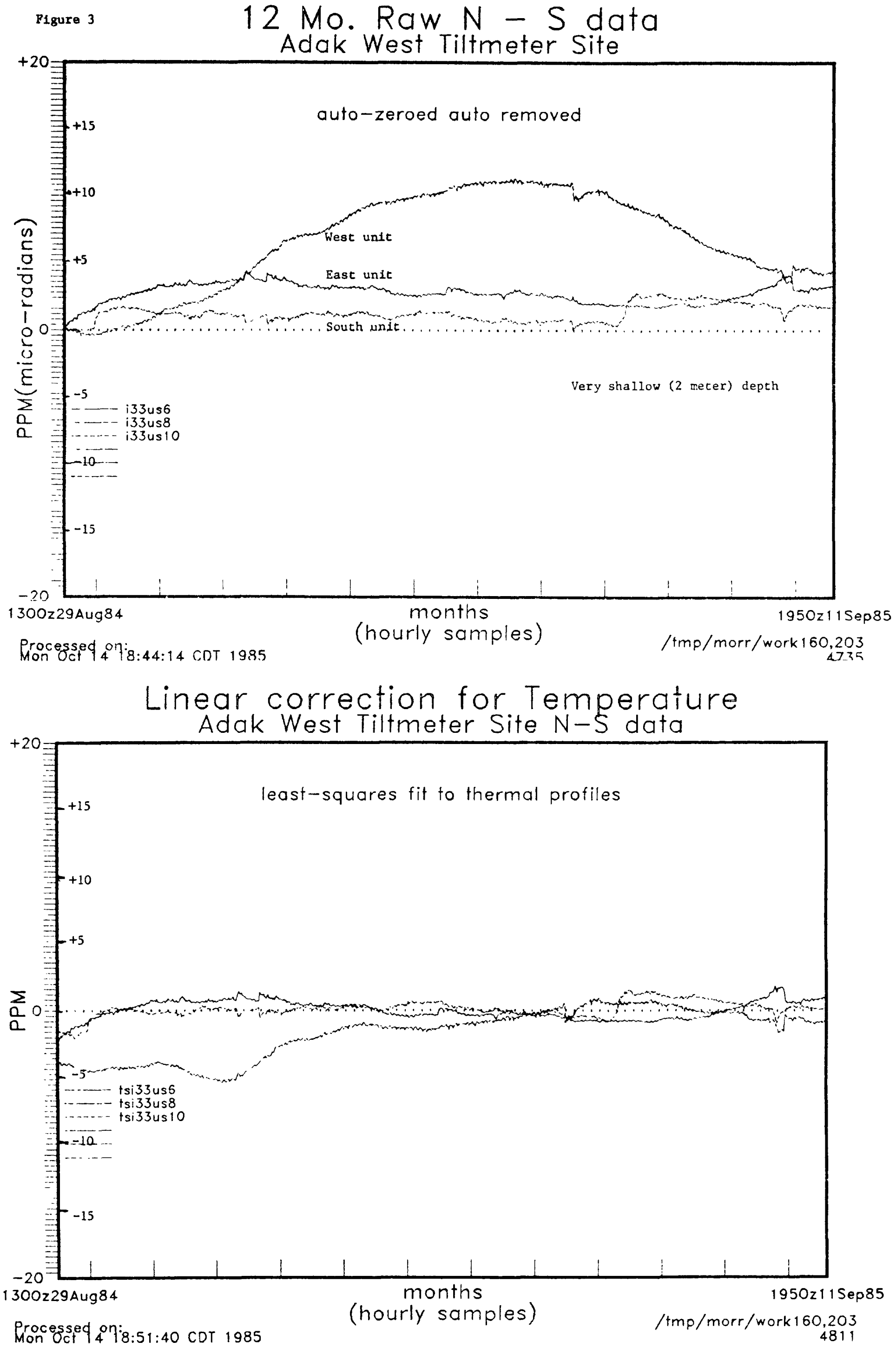
12 Mo. Raw N - S data
Adak West Tiltmeter Site
auto-zeroed auto removed
PPM(micro-radians)
+20
+15
+10
+5
0
-5
-10
-15
-20
West unit
East unit
South unit
Very shallow (2 meter) depth
i33us6
i33us8
i33us10
1300z29Aug84
months
(hourly samples)
1950z11Sep85
Processed on:
Mon Oct 14 18:44:14 CDT 1985
/tmp/morr/work160,203
4735
Linear correction for Temperature
Adak West Tiltmeter Site N-S data
least-squares fit to thermal profiles
PPM
+20
+15
+10
+5
0
-5
-10
-15
-20
tsi33us6
tsi33us8
tsi33us10
1300z29Aug84
months
(hourly samples)
1950z11Sep85
Processed on:
Mon Oct 14 18:51:40 CDT 1985
/tmp/morr/work160,203
4811

Figure 4

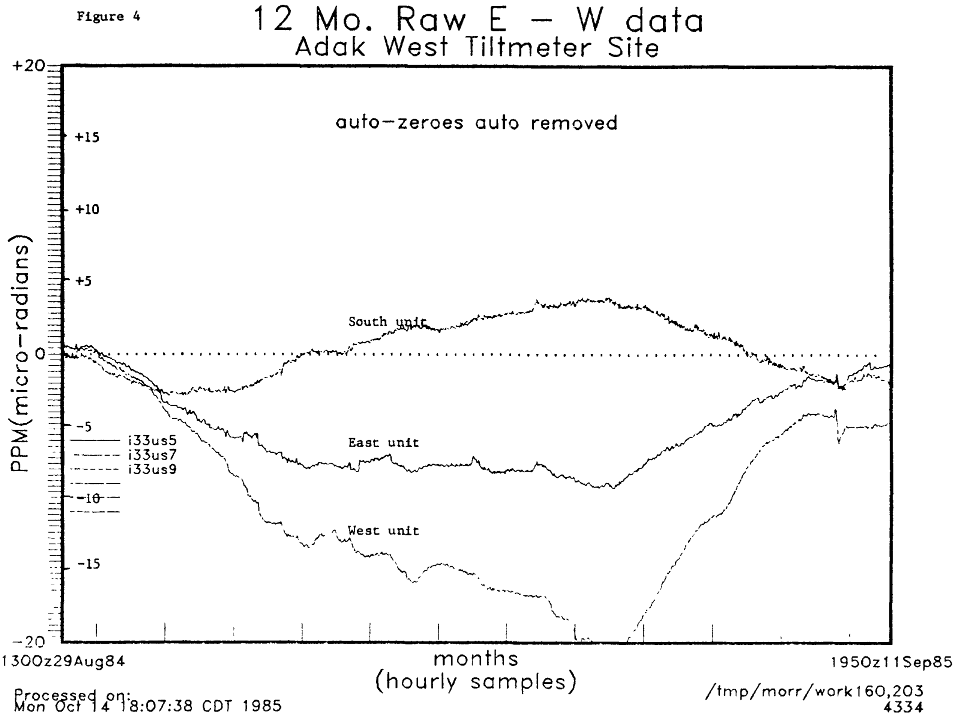
12 Mo. Raw E – W data
Adak West Tiltmeter Site
auto-zeroes auto removed
PPM(micro-radians)
+20
+15
+10
+5
0
-5
-10
-15
-20
South unit
East unit
West unit
i33us5
i33us7
i33us9
1300z29Aug84
months
(hourly samples)
1950z11Sep85
Processed on:
Mon Oct 14 18:07:38 CDT 1985
/tmp/morr/work160,203
4334

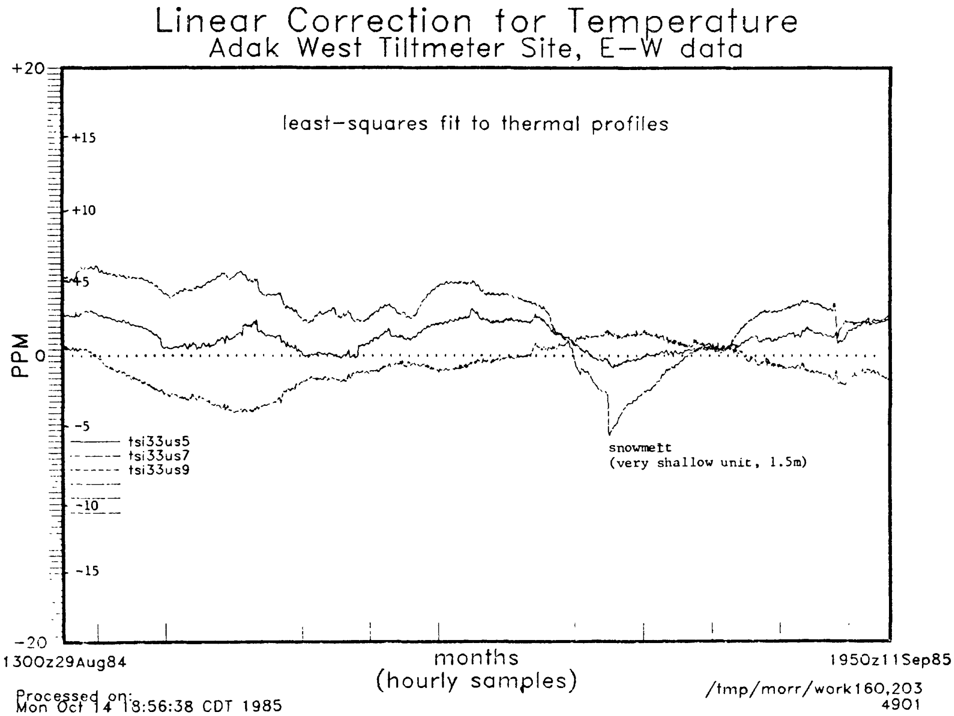
Linear Correction for Temperature
Adak West Tiltmeter Site, E–W data
least-squares fit to thermal profiles
PPM
+20
+15
+10
+5
0
-5
-10
-15
-20
tsi33us5
tsi33us7
tsi33us9
snowmelt
(very shallow unit, 1.5m)
1300z29Aug84
months
(hourly samples)
1950z11Sep85
Processed on:
Mon Oct 14 18:56:38 CDT 1985
/tmp/morr/work160,203
4901

EXPERIMENTAL TILT AND STRAIN INSTRUMENTATION

9960-01801

C.E. Mortensen
Branch of Tectonophysics
U.S. Geological Survey
345 Middlefield Road, MS/977
Menlo Park, California 94025
(415) 323-8111, ext. 2583

Investigations

1. The satellite telemetry system is completely operational in the Parkfield and Mammoth regions now. Most of the strainmeters, creepmeters, tiltmeters, magnetometers and hydrogen monitor stations in these areas are being telemetered via the GOES satellite to the Direct Readout Ground Station (DRGS) in Menlo Park. As of September, 27 Data Collection Platforms (DCPs) are returning data to the DRGS at 10-minute intervals. Of these, 13 DCPs are reporting data from 20 separate instruments in the Parkfield region; 7 DCPs are returning data from 15 instruments in the Mammoth region; 3 DCPs return data from as many instruments in southern California and 4 DCPs operate at sites in central California. At most of these sites the old digital telemetry system based on phonelines and radio links will be operated in parallel with the satellite system until the computers dedicated to operating the DRGS can be installed. This overlap period permits a comparison of the two systems. To date the satellite is proving to be much more reliable than the telephone-based system, principally due to the elimination of problems associated with the quality of phonelines. The DRGS is also more reliable now than the old telemetry receive system. For example, the satellite system recorded signals at the time of the Mexico City earthquake while the old system was broken. Difficult problems associated with full implementation and finalization of the satellite telemetry system now appear to be mostly administrative rather than technical in nature.

   In addition to the DCPs returning data at 10-minute intervals, 5 DCPs return data at 3-hour intervals from 4 sites in California and 1 site in Alaska. The DRGS also records data from 7 water wells that are monitored by John Bredehoeft of WRD, and 27 strainmeter, magnetometer, and tidegauge sites throughout the South Pacific, operated by M. Gladwin of Queensland University, both cooperative programs.

Stan Silverman has procurred 2 AT&T PC computers to serve as a dedicated operating system for the DRGS. He is installing these now.

2. Doug Hopkins travelled to Alaska in August and, with some help from John Rogers, resurrected the tiltmeter site at Cape Yakataga. He installed a new DCP at the site to return data to Menlo Park. He found that the tiltmeters registered 44 +/- 10 microradians tilt downward in a direction 241 +/- 14 degrees during the period 9/82 to 9/85.

3. Alan Jones has redesigned and rebuilt the creepmeter electronics. He has also designed and built electronics for a coarse resolution creepmeter having a large range of movement, which Sandy Schulz has adapted from water-level recorders. She has installed these "big creep" instruments at the sites of several existing creepmeters in the Parkfield region to record fault offset at the ground surface during earthquakes.

4. Networks of tiltmeters, creepmeters and shallow strainmeters have been maintained in various regions of interest in California. A network of 14 tiltmeters located at seven sites monitors crustal deformation within the Long Valley caldera. Other tiltmeters are located in the San Juan Bautista and Parkfield regions. Creepmeters are located along the Hayward, Calaveras and San Andreas faults from Berkeley to Parkfield, and shallow strainmeters are located in the Parkfield region. A tiltmeter station, consisting of a pair of biaxial instruments, is operated at Cape Yakataga, Alaska. Observatory type tiltmeters and strainmeters are located at the Presidio Vault in San Francisco and a tiltmeter is sited in the Byerley Seismographic Vault at Berkeley. Data from all these instruments are telemetered to Menlo Park via the GOES satellite, by phonelines and radio links, or both.

Results

With the announcement in April of an earthquake prediction for the Parkfield region, concentration on timely monitoring of the data from the instruments located there was intensified. On several occasions, such as the occurrence of the Kettleman Hills earthquake, and at times of local creep events, the reliability and near-real-time capability of the satellite telemetry system proved its worth as an aid to informed decision-making.

Reports

Mortensen, C. E., J. E. Estrem, R. P. Liechti and J. A. Westphal, 1985, Changes in ground tilt at the Casa Diablo geothermal field in the Long Valley caldera, California, EOS, EOS, v. 66, n. 18, p. 411.

Dilatometer Operations

9960-03815

G. Douglas Myren
Branch of Tectonophysics
U.S. Geological Survey
345 Middlefield Road, MS/977
Menlo Park, California 94025
415-323-8111, ext. 2705

Investigations and Results

This project is involved with the installation and maintenance of dilatometers (volumetric strainmeters).

Since April 1st of 1985 our effort has continued both in Parkfield, California and at other sites throughout the state.

Through May of this year we concentrated on the routine maintenance of the dilatometers; which included the ordering of AC power at the Mammoth Lakes, Devils Postpile instrument.

In June the instrument installed at Eades in the fall of 84 was hooked up to surface electronics, 12 bit satellite telemetry and 12 bit phoneline telemetry. On site barometric pressure was also installed.

In July we installed 12 bit satellite telemetry at Adobe Mtn., and Searle Rd., and reinstalled the radio shot-phone link at Adobe Mtn. Based upon previous experiments with the GEOS on site digital recording of dilatometer and seismic data, we have selected four dilatometer sites, Devils Postpile, Devils Punchbowl, Gold Hill 2, and Echo Valley, for GEOS recording. We began these installations in July. Conditioning of the dilatometer signal inputs is helping to keep the signal within range of the GEOS.

Late July we made an attempt at clearing the Frolich dilatometer hole. Sand dump cleaning did not bring us a cleared section of 905'. Tom Moses ordered a Gyro survey (inclinometer/orientation), this told us the hole kicked out at 905 (a dog leg) making it impossible to get our cement dump through this section. More on this story later.

In August the Devil's Postpile instrument was prepared for AC power by installing the necessary ac/dc converters for Strain and GEOS, battery chargers for backup batteries, heaters for the temperature sensitive GEOS, and shelves and benches for additional space.

September was spent improving the dilatometer electronics to GEOS signal.

Throughout the past 6 months we have worked to perfect an automatic system of opening the pressure relief valve down the hole. The circuit has been designed but needs improvement.

Helium Monitoring for Earthquake Prediction

9570-01376

G. M. Reimer
U. S. Geological Survey, MS 963
Denver Federal Center
Denver, CO 80225
(303) 236-7886

Investigations

The variations of helium in soil-gas from sample collecting stations along the San Andreas Fault near San Benito, California continue to be observed and related to nearby seismic activity. A system to monitor soil-moisture concentrations was emplaced during the summer of 1985. Soil-moisture is suspected as having a primary influence on the seasonal helium variations and it may be possible to compensate for this variable and reduce uncertainty in defining the helium decreases that precede seismic activity. Data will be collected for a year to evaluate this theory.

Results

Empirically, the observations show that helium decreases precede seismic activity. The criteria for defining a decrease and relating it to a seismic event are based on the following: Averaged soil-gas helium concentrations must show 2 consecutive decreases of at least 4 parts per billion; a time frame of 1.5 to 7.5 weeks is selected for which seismic activity could occur and be temporarily related to the start of the helium decrease; the earthquake must be $M \geq 4$ and occur in an elliptically-shaped area with axes of 160x80 km centered near San Benito. All earthquakes that occur spatially or temporarily within the empirically derived "windows" are considered one event (as to include obvious aftershocks).

Figure 1 shows the helium concentrations through September, 1985. During the last year, there has been only one episode that fit the criteria for a helium decrease. That event occurred February 25 and corresponded to a March 21 $M=3.0$ earthquake near San Juan Bautista. Magnitude 3 is below the defined threshold of our definition of an earthquake event to be preceded by a helium decrease but the epicenter of this event was within the area of our sample collecting stations. There may be a correlation with magnitude (or total energy release) and distance to our sample collection stations.

There have been no major earthquakes in the study area during the past year. This quiescence will significantly enhance our understanding of the helium data base to determine a frequency of decreases that are not related to subsequent seismic activity. The most recent data indicate a plateau for the helium soil-gas concentrations. Although this does not represent a decrease by definition, it does occur at a time when there should be a seasonal increase. This is an example of a condition that might be resolved by the soil-moisture readings.

Reports

Reimer, G. M., 1985, Prediction of central California earthquakes from soil-gas helium fluctuations: PAGEOPH, v. 122, p. 369-375.

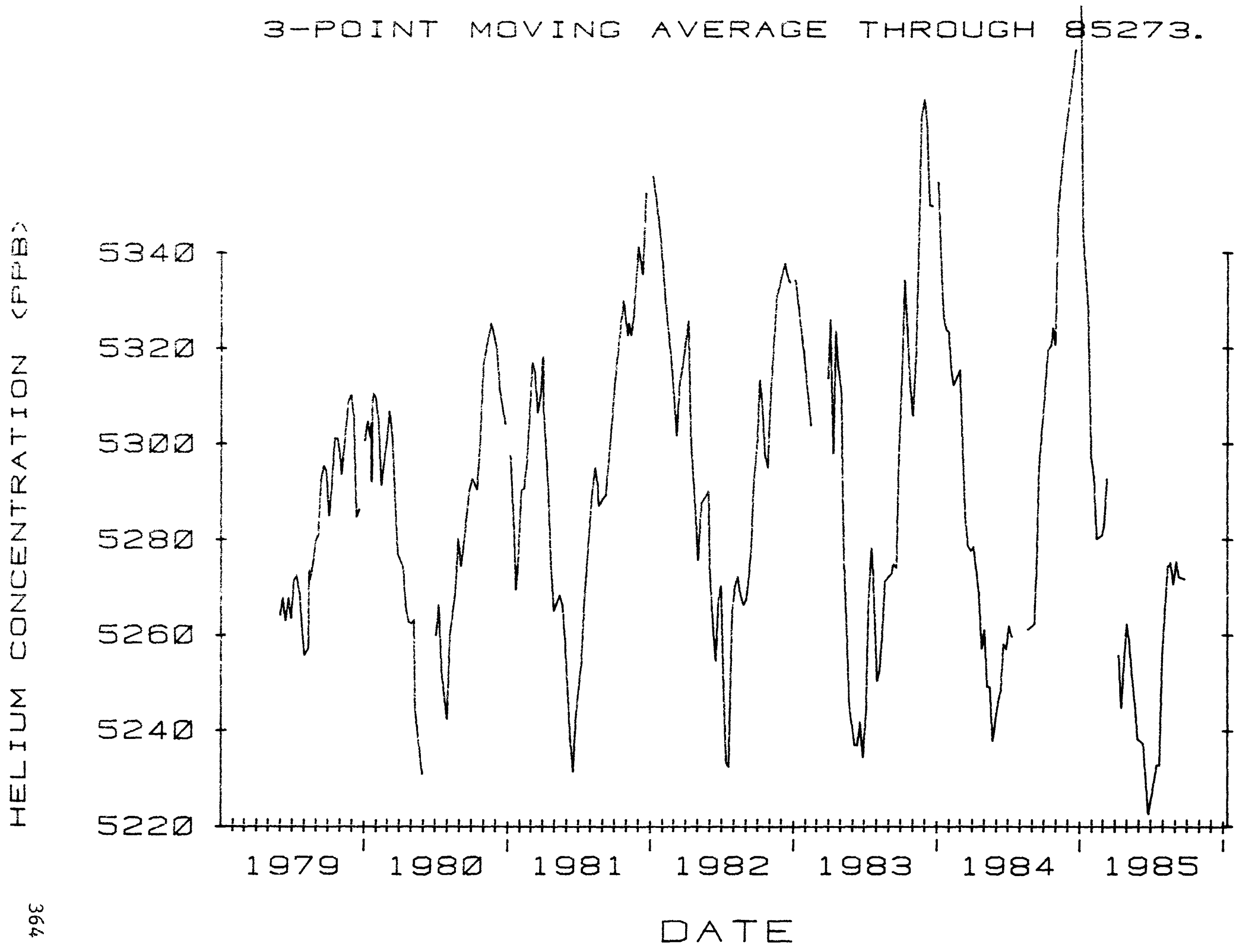

HELIUM SOIL-GAS CONCENTRATIONS NEAR HOLLISTER, CA.

3-POINT MOVING AVERAGE THROUGH 85273.

FAULT ZONE TECTONICS

9960-01188

Sandra S. Schulz, Beth D. Brown
Branch of Tectonophysics
U.S. Geological Survey
345 Middlefield Road, MS/977
Menlo Park, California 94025
(415) 323-8111 x 2763

Investigations

1. Directed maintenance of creepmeter network in California.
2. Updated archived creep data on PDP 11/44 computer.
3. Installed a new creepmeter near the 2-color laser observatory south of Parkfield, California.
4. Continued to establish and survey alinement array network on California faults.
5. Awarded contract to a private surveying firm to survey arrays in Imperial Valley and Parkfield.
6. Monitored creepmeter and alinement array data for retardations or other possible earthquake precursors.

Results

1. Currently 29 extension creepmeters operate; 21 of the 29 have on-site strip chart recorders, and 19 of the 21 are telemetered to Menlo Park. A computer program continues to check Parkfield telemetry data once each hour and alert Project personnel via 'beeper' whenever unusual fault movement occurs.

2. Fault creep data from all USGS creepmeter sites along the San Andreas, Hayward and Calaveras faults have been updated through July 1985, and stored in digital form (1 sample/day). Telemetry data covering the period between July 1985 and the present are stored in digital form (1 sample/hour), updated every 10 minutes, and merged with the daily-sample data files to produce complete plots when needed.

3. A new 30-meter-long creepmeter (XTA1) was installed across the San Andreas fault near the 2-color laser observatory

south of Parkfield (Figure 1). The creepmeter site was chosen using a fault zone slip pattern established by survey data from an alinement array emplaced one year ago. The surveys indicated a slip rate over the array's 198-meter length of approximately 11 mm/yr. The creepmeter signal is being recorded on-site and transmitted over both telephone and satellite telemetry to Menlo Park, where it has been added to the beeper alert system.

4. Currently 30 alinement arrays are surveyed across five (5) active faults in California (San Andreas, Hayward, Calaveras, Nunez, and Imperial). Alinement arrays are remeasured every 90-120 days and are used to guide emplacement of creepmeters, check creepmeter measurements, and monitor fault movement where creepmeters are logistically impractical. Figure 2 shows alinement array data for the Parkfield area for 1983 through June 1985. Figures 3a, b, c, and d show comparisons between array and creepmeter data, all plotted on the same scale. The reversal in creep from left to right lateral at Middle Mountain (Figure 3a) was apparent in array data in mid-June, two weeks before it appeared on the creepmeter (XMM1). Apparently the reversal was measureable over the 100-meter width of the array before it became obvious at the fault trace where the 30-meter creepmeter could respond to it. Also of interest on Figure 2 is left-lateral movement at the Highway 46 array (H464), near the southern extent of surface creep. It could represent actual left-lateral movement, as recorded by creepmeter TWR1 approximately 20 km farther south in the Palo Prieto Pass area, or may indicate the Highway 46 array crosses a subsidiary fault trace moving in response to movement on a nearby main trace.

5. Final award of contract was granted to a private firm to survey selected alinement arrays in Imperial Valley and Parkfield. Every three months, data from the surveys are being received, processed, and evaluated.

6. Following the Coalinga earthquake of May 1983, several Parkfield creepmeters recorded dramatic creep rate changes. Some stations showed sharp decreases, while one station (XMM1) showed reversal from right to left-lateral creep that persisted until July 1985. That month, coincident with small earthquakes beneath the station, right-lateral creep resumed at a rate approximately one-half the pre-Coalinga rate. In late September 1985, station XPK1 north of Parkfield began recording creep at a rate not seen there since before the Coalinga earthquake. Stations to the south of XDR1 (WKR1, CRR1, and XGH1) continue to record decreased creep rates.

Creep and Alinement : Parkfield , CA

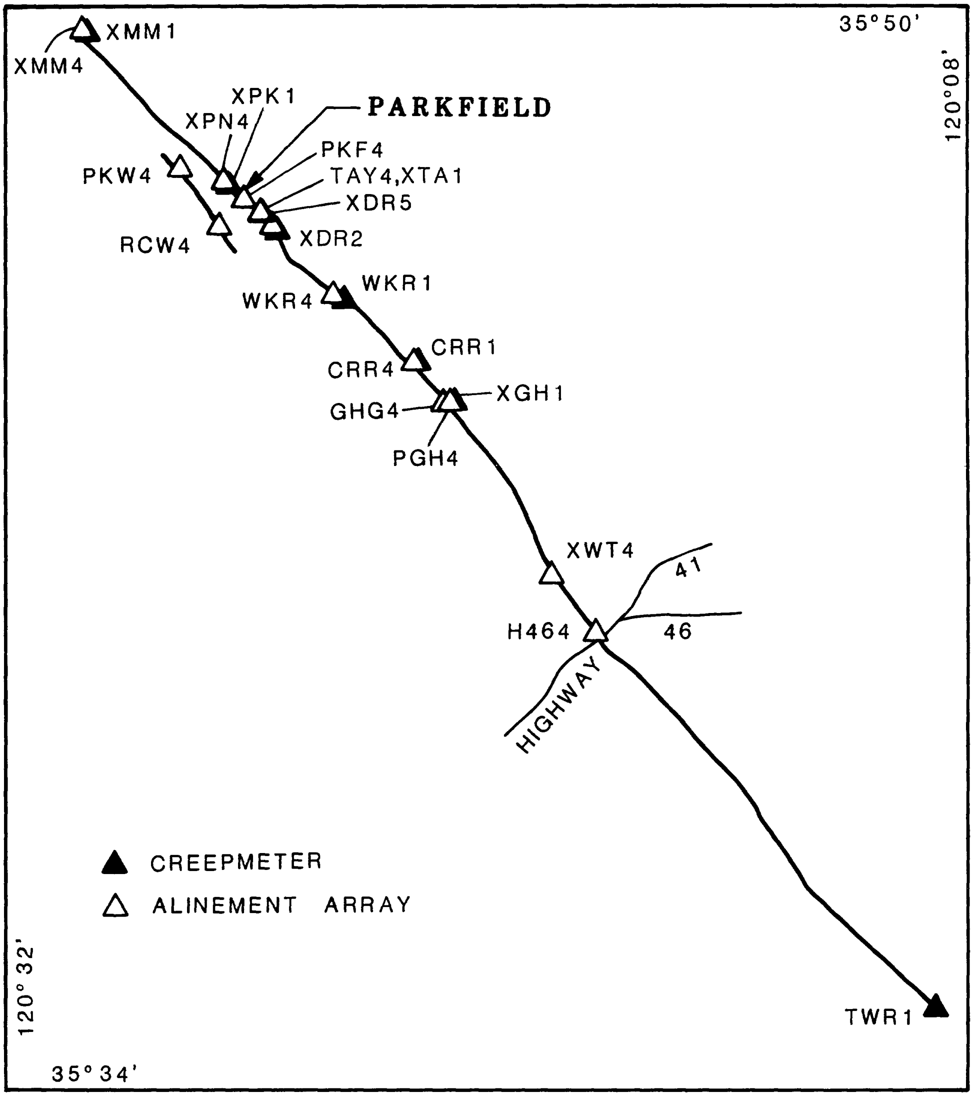

FIGURE 1

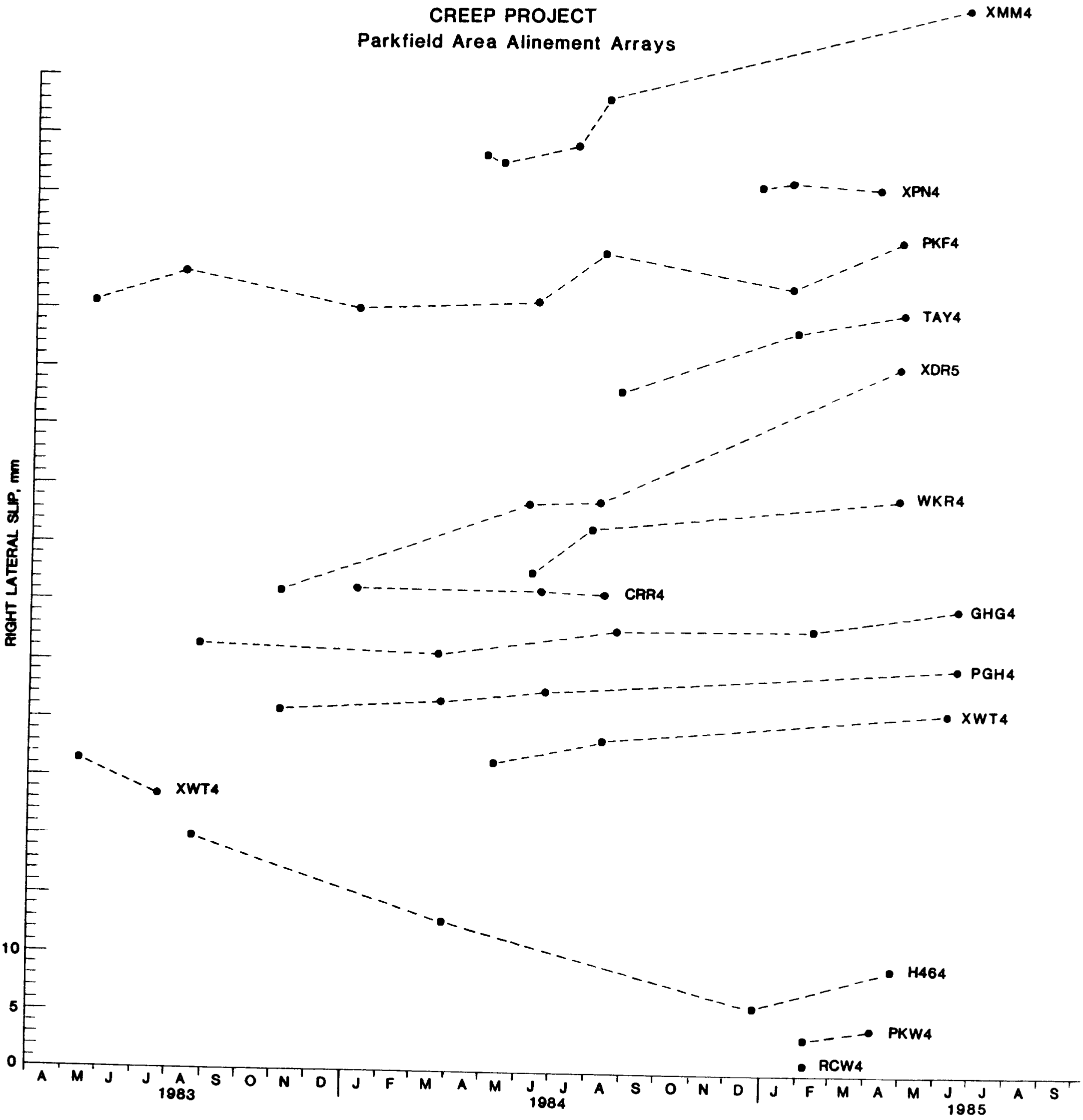
CREEP PROJECT
Parkfield Area Alinement Arrays
RIGHT LATERAL SLIP, mm
0
5
10
XMM4
XPN4
PKF4
TAY4
XDR5
WKR4
CRR4
GHG4
PGH4
XWT4
XWT4
H464
PKW4
RCW4
A
M
J
J
A
S
O
N
D
1983
J
F
M
A
M
J
J
A
S
O
N
D
1984
J
F
M
A
M
J
J
A
S
1985

FIGURE 2

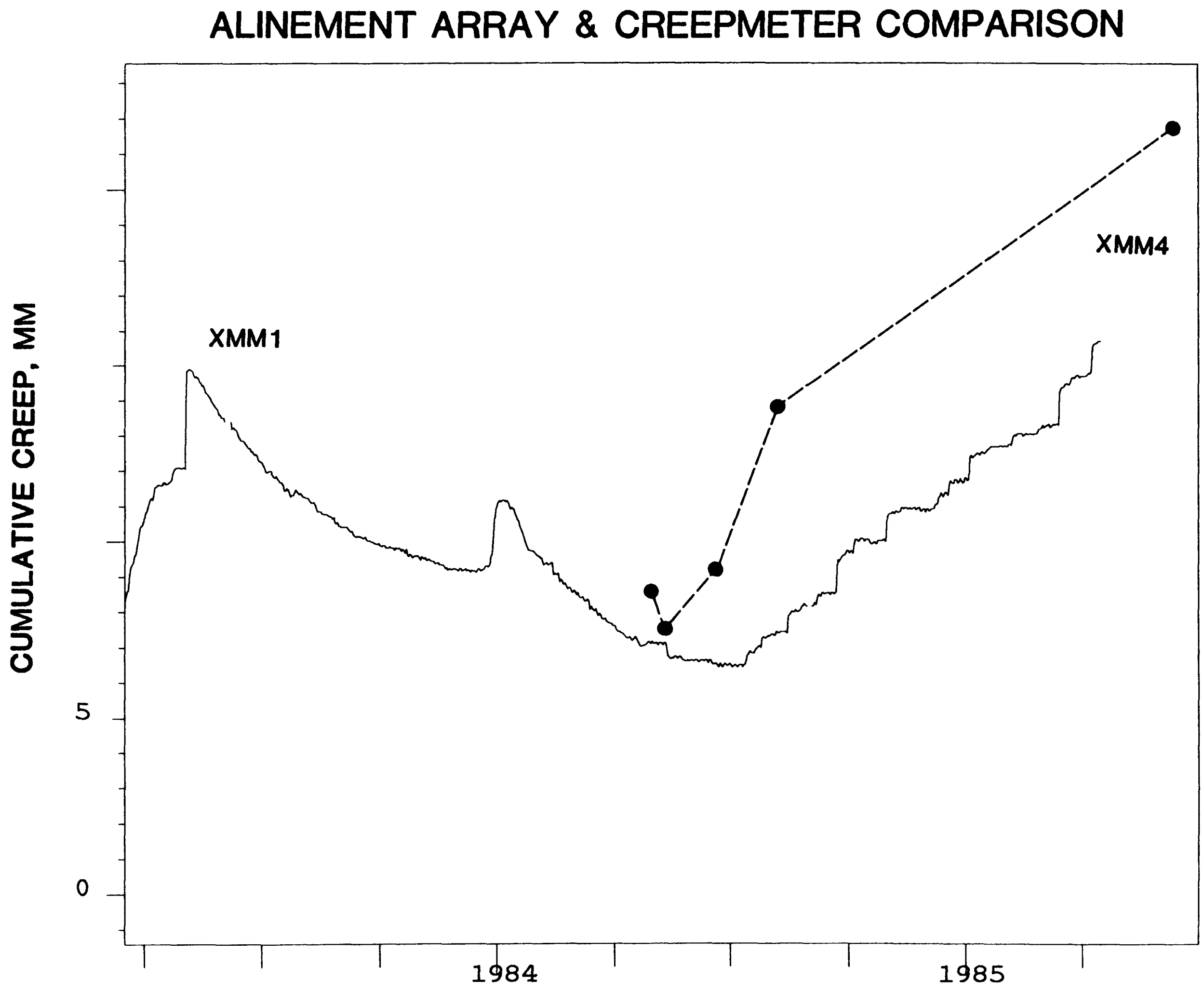
ALINEMENT ARRAY & CREEPMETER COMPARISON
XMM1
XMM4
CUMULATIVE CREEP, MM
5
0
1984
1985

FIGURE 3a

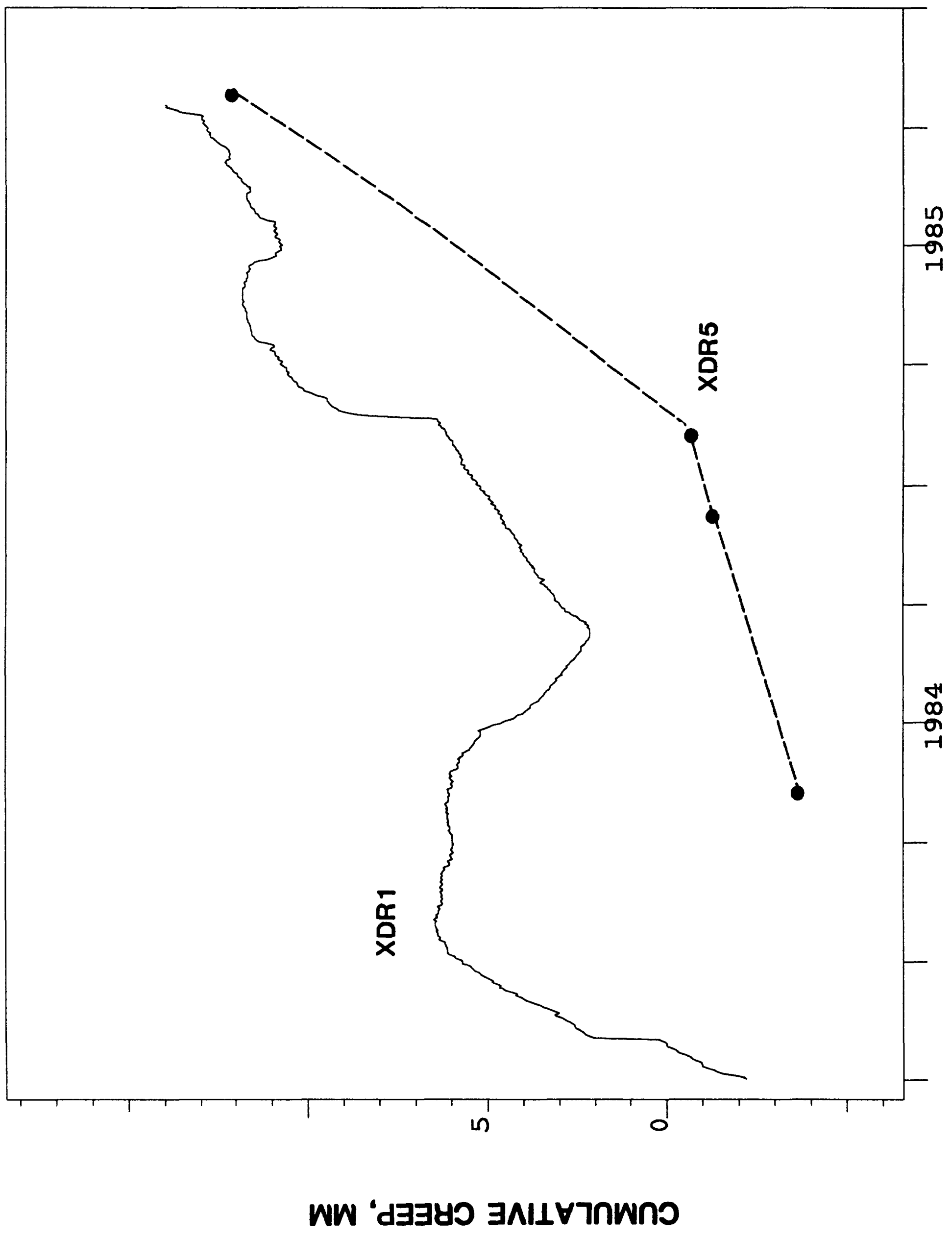

ALINEMENT ARRAY & CREEPMETER COMPARISON

FIGURE 3b

ALINEMENT ARRAY & CREEPMETER COMPARISON

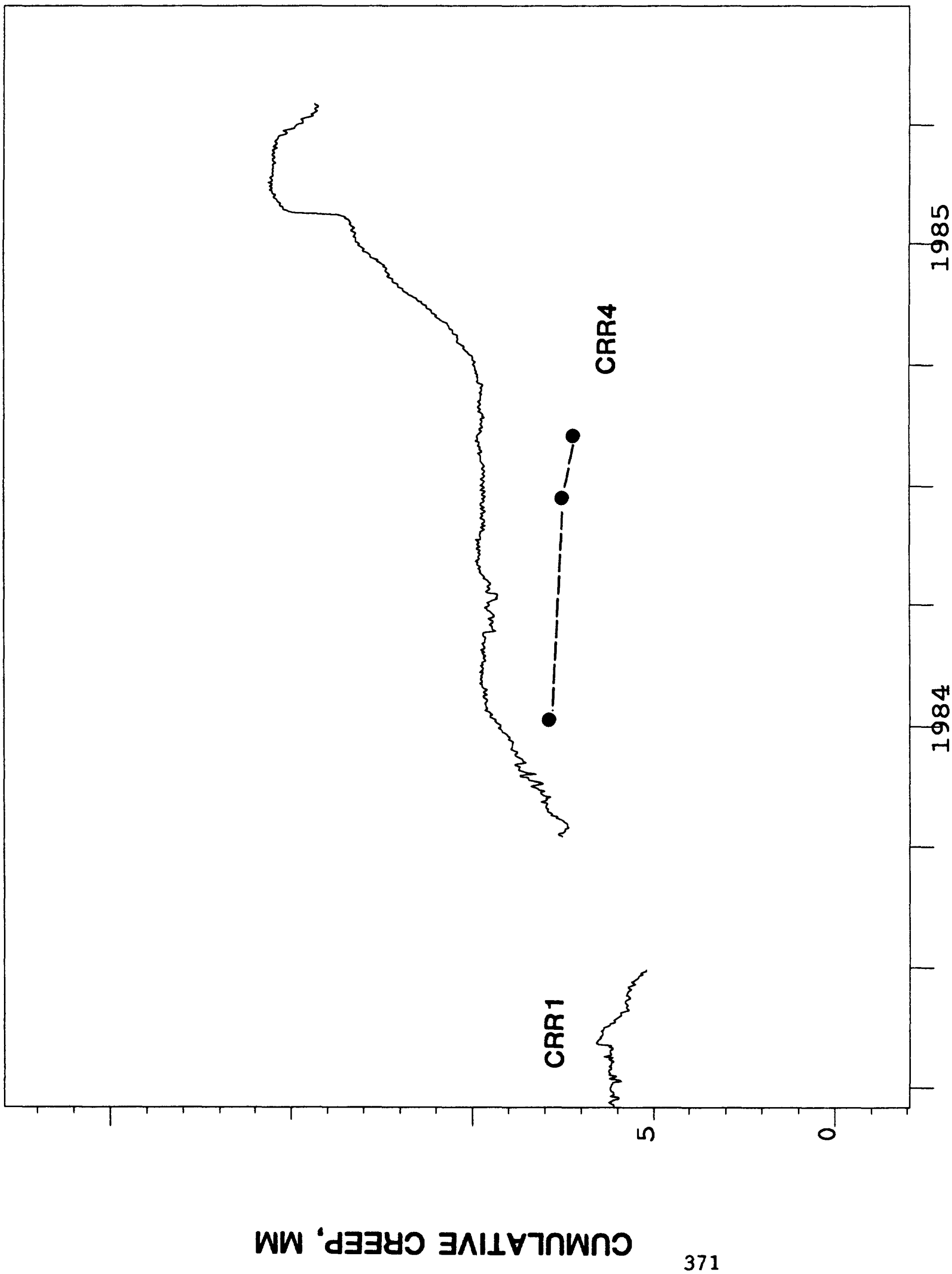

FIGURE 3c

ALINEMENT ARRAY & CREEPMETER COMPARISON

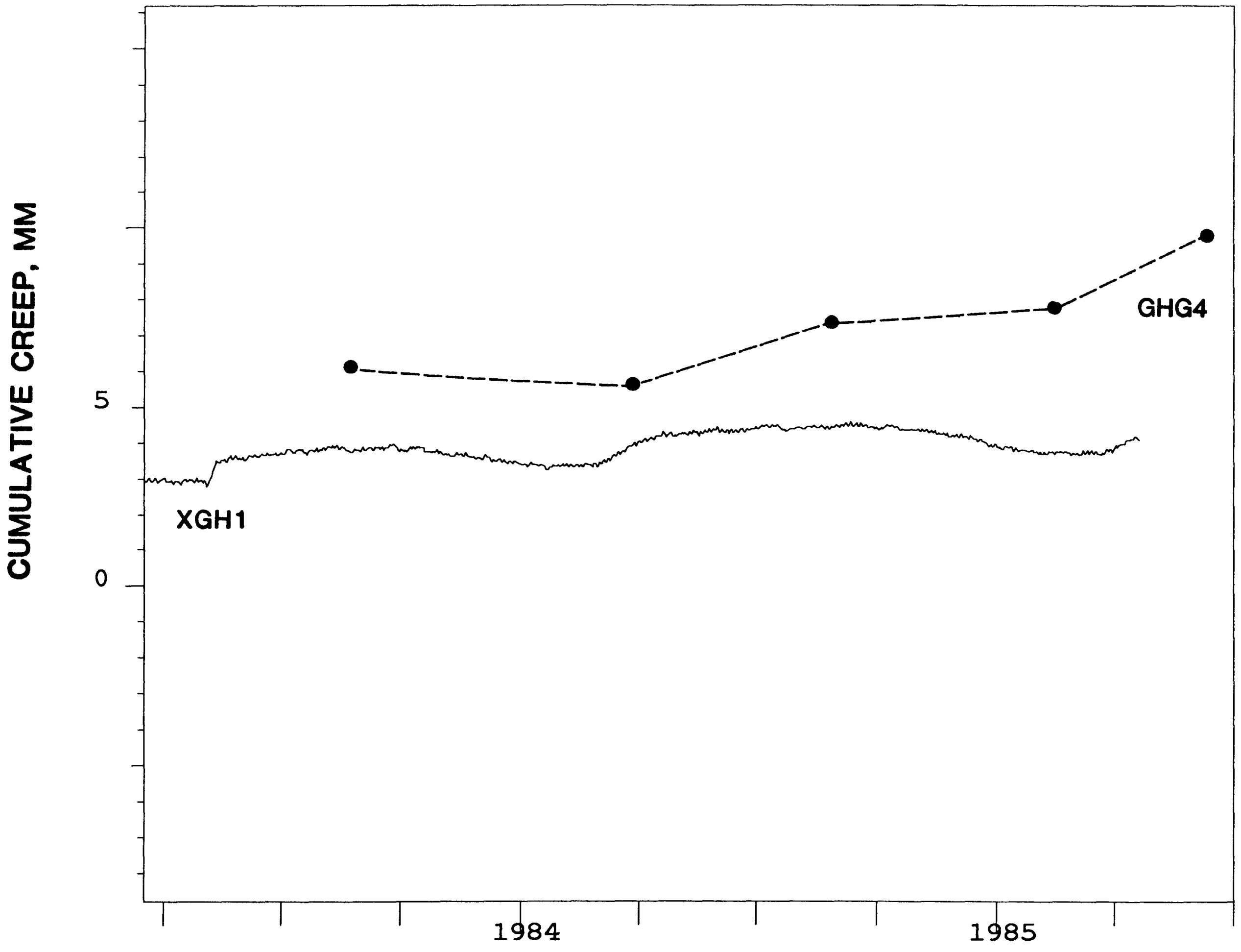

FIGURE 3d

THE EXTENSION AND OPERATION OF A COMPUTER-CONTROLLED MONITORING NETWORK FOR RADON AND OTHER GEOCHEMICAL PRECURSORS, AND LABORATORY STUDIES ON SEISMO-GEOCHEMICAL PRECURSORS

14-08-0001-21268

M.H. Shapiro, A. Rice, S. Stryker, and T.A. Tombrello
Div. of Physics, Mathematics, and Astronomy - Caltech
Pasadena, CA 91125
(818) 356-4277

INVESTIGATIONS

Funding limitations have required us to limit monitoring on the Caltech radon/geochemical monitoring network to four sites during the past six months. The other stations on the network have been shut down, and three of the remaining four stations will be terminated in mid-December of 1985. The monitoring station at the Kresge Seismological Laboratory in Pasadena will be continued without USGS support.

RESULTS

In mid-August a major radon excursion began at our Lytle Creek station. Since this station, in past years, has recorded radon excursions that could be traced to non-tectonic environmental influences, additional data from Lytle Creek were examined carefully. Owing to relatively dry conditions for the past two years, the water level at Lytle Creek fell relatively rapidly over the past several months.

At the onset of the rapid step increase in radon (Figure 1.), an inflection in the water level record was noted. Likewise, a change in the character of the CO-2 data from Lytle Creek was observed to start at the same time as the radon excursion. Unlike a previous episode of high radon at Lytle Creek, the CO-2 level decreased rather than increased. Thus, it appears unlikely that the radon fluctuations are being driven by carbon dioxide bubbling in the well (note that the sharp spikes in the CO-2 record are the result of an instrument problem). Nevertheless, the decline in carbon dioxide level probably indicates a change in the chemistry of the well water.

Approximately six weeks after the start of the radon anomaly a magnitude 5 earthquake occured on the San Jacinto Fault about 15 km from the monitor. This earthquake was felt widely in southern California. As can be seen from Figure 1, the radon level at Lytle Creek did not return to baseline either shortly before or just after this earthquake. Instead, the level has continued to rise. At this time we are uncertain about the interpretation of the anomaly; however, we feel that there is a fair probability that it is tectonically related.

Figure 3. shows plots of thoron and background from Lytle Creek. The thoron level has been relatively normal (generally fluctuations in thoron as well as radon have been seen during CO-2 driven radon excursions.) A small increase in the background level has accompanied

the major radon excursion; however, this increase is quite consistent with the increased level of radon daughters that would remain in the monitor vault at the start of the succeeding measuring cycle.

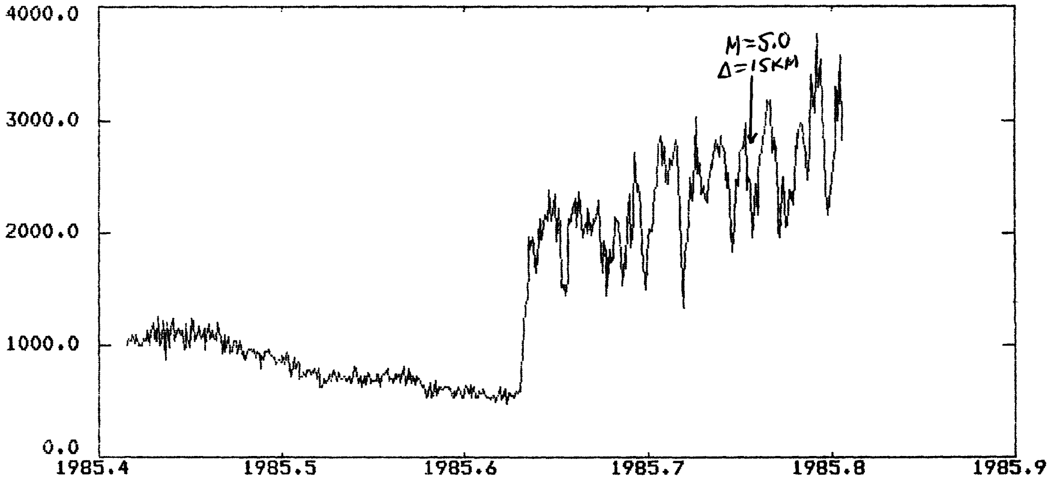

Recent Lytle Creek Radon

M=5.0
Δ=15KM

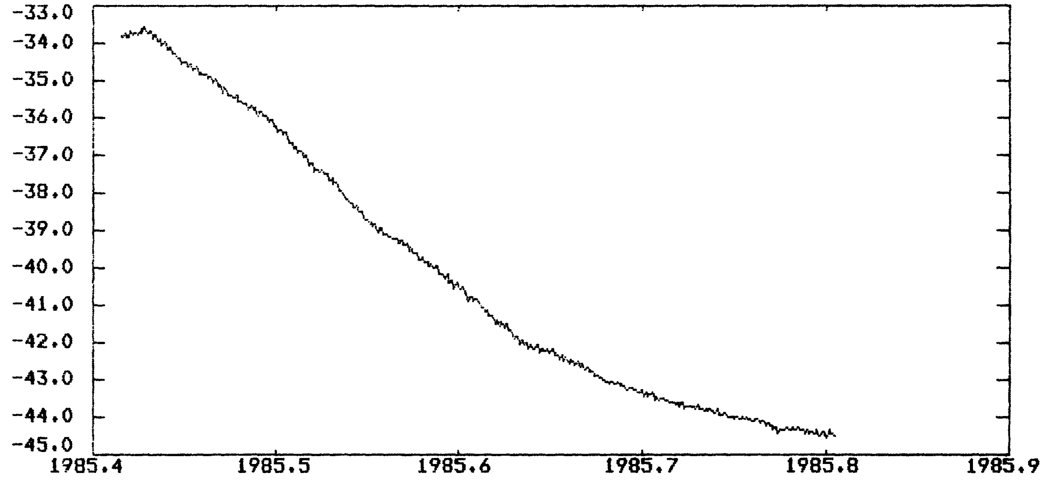

Lytle Creek Water Level

Figure 1

Lytle Creek CO-2

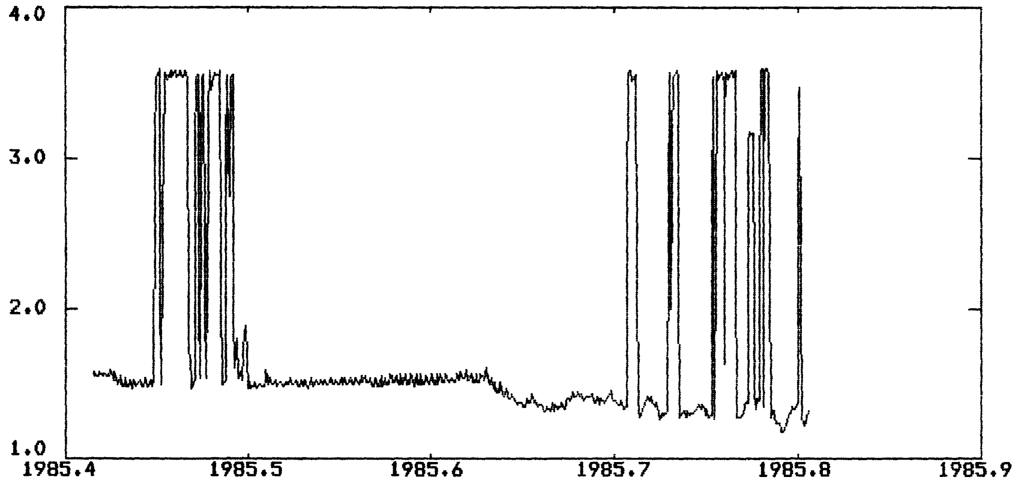

Lytle Creek Water Temperature

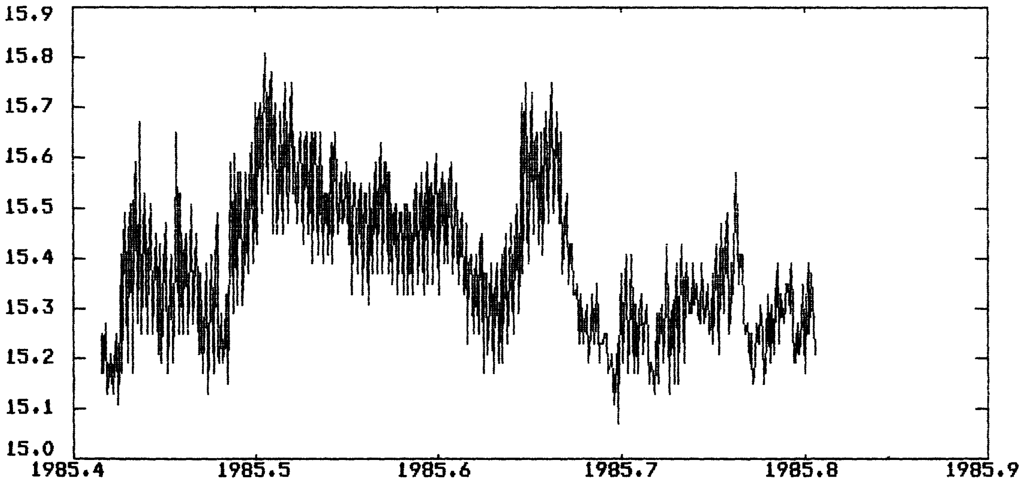

Figure 2

Lytle Creek Thoron

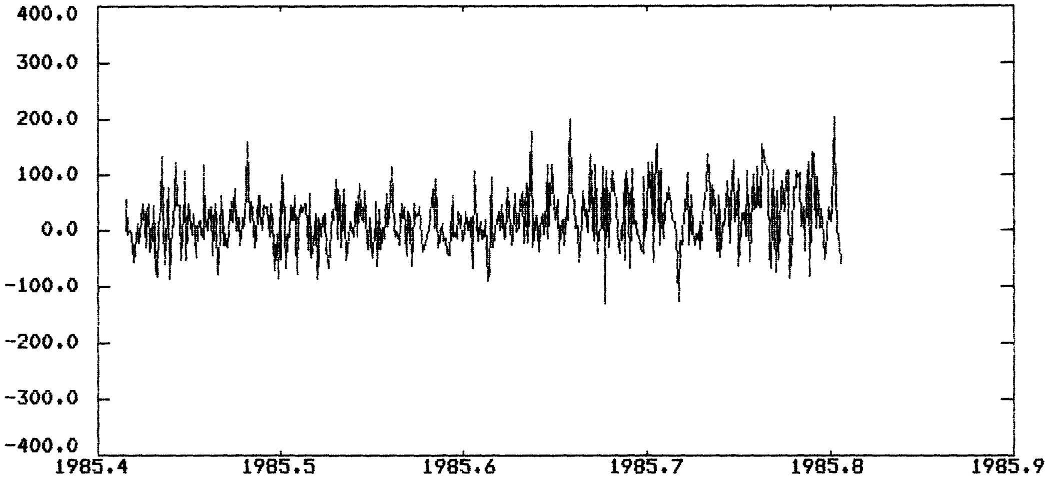

Lytle Creek Background

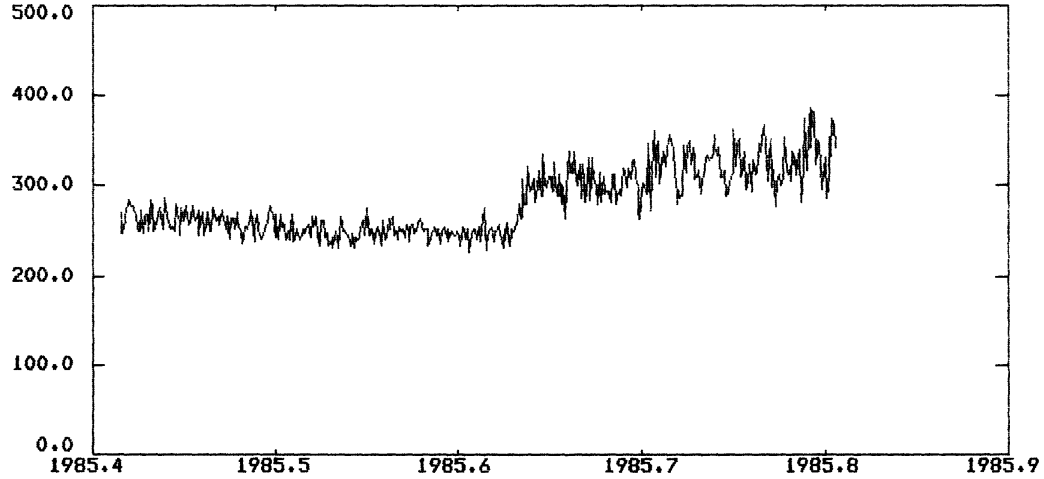

Figure 3

MODELING AND MONITORING CRUSTAL DEFORMATION

9960-01488

Ross S. Stein, Wayne Thatcher
Branch of Tectonophysics
U.S. Geological Survey
345 Middlefield Road, MS/977
Menlo Park, California 94025
(415) 323-8111, ext. 2120

Investigations

1. Investigation of the role of geodetic survey measurements in the study of active tectonic processes, earthquake repeat times, and the relation of these present-day measurements to geological indicators of recent deformation and the earthquake cycle.
2. Study of deformation accompanying and following dip-slip faulting in regions of compressional tectonics (1983 M_s 6.7 Coalinga, CA, earthquake), and in regions of extensional tectonics (1983 M_s 7.3 Borah Peak, ID, earthquake).
3. Analysis of a field test to study the accumulation of refraction error in historical leveling surveys, and correction of southern California data for refraction and rod error.

Results

1. Geodetic Measurement of Active Tectonic Processes

Repeated geodetic observations are sufficiently precise to detect the growth of mountains, the relative movements of the great lithospheric plates, and present-day rates of fault slip and earthquake strain accumulation. The cyclic buildup and release of strain across major faults can be monitored over the short-term (~years or less) using ultra-precise modern techniques, and longer term movements can frequently be determined by utilizing the historic record of measurements, which in many active regions extend back into the late 19th century. Since about 1970, annual laser ranging surveys in the western U.S. and southern Alaska have delineated the pattern and current rates of deformation in these seismically active regions and begun to provide accurate fault slip rates to compare with late Holocene geological estimates. The imperfect balance between interseismic strain buildup and coseismic strain release introduces a component of permanent deformation into the earthquake cycle that under favorable conditions can be estimated geodetically, providing another link between present-day movements and those preserved in the recent geologic record. Examples include tectonically elevated former shore-lines related to great interplate thrust earthquakes and deformed river terraces observed in intraplate reverse faulting environments. Despite the relative uniformity of longer term deformation rates, accumulating evidence indicates considerable short-term irregularity, at least in some regions. Perhaps the best-documented example comes from southern California, where rapid, correlated changes among gravity, elevation, and horizontal strain measurements have recently been observed. (Thatcher)

2. Postseismic Deformation Associated with Large Intraplate Earthquakes

Leveling surveys carried out following the 1983 Coalinga (M_s = 6.5) and 1983 Borah Peak (M_s = 7.2) earthquakes, supplemented by less complete results from other intraplate dip-slip shocks, are used to determine the pattern and mechanism of short-term (~1 year) postseismic intraplate deformation. Movements differ notably from those observed following large plate boundary thrust events. Although the postseismic deformation is discernible, it is small, averaging only ~5% of the coseismic movements and having nearly the same spatial pattern. Clearly, such motions are best explained by continued minor slip on the same fault that ruptured during the earthquake itself. In contrast, short-term movements following intraplate thrust events are large (~20% coseismic), differ markedly from coseismic deformation, and are conveniently explained by transient slip downdip of the coseismic rupture plane. However, limited evidence from intraplate shocks indicates a temporal broadening of the movement profile, suggesting a deepening of slip or ductile deformation. Resurveys at Coalinga and Borah Peak covering the first 2 years after the mainshock reveal modest deformation caused primarily by continued slip on the coseismic fault. The results in hand indicate significant differences between intraplate and plate boundary environments, both in the rheological properties beneath the seismogenic zone and consequently in the mechanics of strain accumulation and release in these regions. (Thatcher and Stein)

3. Saugus-Palmdale, CA, Field Test for Refraction Error in Historical Leveling Surveys

A field test was conducted in southern California during May-June 1981 to study the accumulation of unequal refraction error along a 50-km-long route rising 612 m between Saugus and Palmdale, California. The route has been leveled repeatedly since 1955, with observed elevation changes of 200 mm. The experiment was designed to compare leveling characteristic of the period before 1964 with contemporary leveling, to measure the parameters that control atmospheric refraction, and to remove the refraction error from the surveys. The observed temperature structure was well represented by a power law relation, $T = a + bz^c$, and depended on atmospheric conditions and the ground surface beneath the line of sight. The refraction-corrected leveling satisfies specifications and standards for First Order control surveys. Correction for refraction using Kukkamaki's balanced-sight equation effectively removed the observed 51 mm divergence between short- and long-sight leveling. Some simplified forms of the correction, where dT is approximated from T or the ground surface properties, perform equally well. The historical leveling surveys over the Saugus-Palmdale grade were corrected for refraction errors based on the results of the experiment, and also for rod scale errors considered in previous investigations. The corrected cumulative uplift near Palmdale reached 65 ± 16 mm with respect to Saugus during the period 1955-65. This is about one-third the value obtained before correction for refraction error. The corrected displacement profiles reveal previously unrecognized deformation in the epicentral region of the $M_L = 6.4$ 1971 San Fernando earthquake during the decade prèceeding the mainshock. (Stein, Whalen, Holdahl, Strange, and Thatcher)

Reports

Atwater, B. F., J. C. Tinsley, R. S. Stein, D. A. Trumm, A. B. Tucker, D. J. Donahue, A. J. T. Jull, L. A. Payden, 1985, Alluvial plains and earthquake recurrence at the Coalinga anticline: submitted to the U.S. Geol. Surv. Prof. Pap. on the 1983 Coalinga Earthquake, 45 pp.

Barrientos, S., S. N. Ward, J. R. Gonzalez-Ruiz, and R. S. Stein, 1985, Inversion for moment as a function of depth from geodetic observations and long period body waves of the 1983 Borah Peak, ID, earthquake, in Proceedings of Workshop XXVIII on the Borah Peak, Idaho, earthquake, U.S. Geol. Surv. Open-File Rep. 85-290, 485-518.

Stein, R. S., 1985, Evidence for surface folding and subsurface fault slip from geodetic elevation changes associated with the 1983 Coalinga, California, Earthquake, submitted to the *U.S.G.S. Professional Paper* on the Coalinga Earthquake, 45 pp.

Stein, R. S., 1985, Role of the North American Vertical Datum for earthquake research and prediction: An example from the Great Basin, *Proceed. 3rd Internat. Symp. on No. Amer. Vertical Datum*, D. B. Zilkoski, ed., p. 227-236.

Stein, R. S., and S. E. Barrientos, 1985, Planar high-angle normal-faulting in the Basin and Range: Geodetic analysis of the 1983 Borah Peak, Idaho, earthquake, *J. Geophys. Res.*, v. 90, in press.

Stein, R. S., and S. E. Barrientos, 1985, The 1983 Borah Peak, Idaho, earthquake: Geodetic evidence for deep rupture on a planar fault, in Proceedings of Workshop XXVIII on the Borah Peak, Idaho, earthquake, *U.S. Geol. Suv. Open-File Rep.* 85-290, 459-484.

Stein, R. S., and R. C. Bucknam, eds., 1985, Proceedings of Workshop XXVIII on the Borah Peak, Idaho, earthquake, *U.S. Geol. Surv. Open-File Rep.* 85-290A (Introduction and 40 research papers) and 85-290B (field guide and maps), 720 pp.

Stein, R. S., C. T. Whalen, S. R. Holdahl, W. E. Strange, and W. Thatcher, 1985, Saugus-Palmdale, California, field test for refraction error in historical leveling surveys, *Journ. of Geophys. Res.*, special issue on Vertical Crustal Motions, in press.

Stein, R. S., and R. C. Bucknam, 1985, Basin and Range viewed from Borah Peak (News article and cover), *EOS, Trans. Amer. Geophys. Un.*, *66*, 600-603.

Thatcher, W., and R. S. Stein, 1985, Postseismic deformation from intraplate earthquakes: Comparison with plate boundary events, submitted to the *AGU Monogrph on Proc. of 5th Ewing Symp.* on Earthquake Source Mechanics.

Thatcher, W., 1985, Geodetic measurement of active tectonic processes, in *Active Tectonics - Impact on Society*, National Research Council, Washington, D.C., in press.

Thatcher, W., 1985, Cyclic deformation related to great earthquakes at plate boundaries: Models and observations, *Proc. Int'l Symp. on Recent Crustal Movements*, Wellington, New Zealand, in press.

Abstracts

Atwater, B. F., J. C. Tinsley, R. S. Stein, D. A. Trumm, and A. B. Tucker, D. J. Donahue and A. J. T. Jull, 1985, Progress toward estimation of earthquake recurrence at Coalinga anticline, California, EOS, 66, in press.

Stein, R. S., C. T. Whalen, S. R. Holdahl, and W. E. Strange, 1985, Saugus-Palmdale, CA field test for refraction error in historical leveling surveys, EOS, 66, in press.

Thatcher, W., and R. S. Stein, 1985, Postseismic deformation from intraplate earthquakes: Comparison with plate boundary events, EOS, 66, in press.

NEARFIELD GEODETIC INVESTIGATIONS OF CRUSTAL MOVEMENTS, SOUTHERN CALIFORNIA

Contract No. USDI-USGS 14-08-0001-21997

Arthur G. Sylvester
Department of Geological Sciences, and
Marine Science Institute
University of California
Santa Barbara, CA 93107
(805) 961-3156

INVESTIGATIONS

Repeated surveys of 20 of 45 existing precise leveling arrays across active faults were done during the first six months of the contract period. Ten new arrays were established and surveyed, chiefly across the central and southern San Andreas fault, and across the San Jacinto fault. The leveling array at Pinyon Flat Geophysical Observatory was resurveyed twice, and the array at Dalton Canyon Geophysical Observatory was abandoned.

The purpose of these surveys is to search for and monitor the spatial and temporal nature of vertical displacement across active and potentially active faults. Thus, we document pre-, co-, and post-seismic displacement and creep, if any, especially where seismographic, paleoseismic and geomorphic data indicate current or recent fault activity. The investigations are intermediate in scale between the infrequent, regional geodetic surveys traditionally done by the National Geodetic Survey, and point measurements by continually recording instruments such as creepmeters, tiltmeters, and strainmeters. All surveying is done according to First Order, Second Class standards.

Locations of arrays are shown in Figure 1, and histories of surveys are given in Table 1.

RESULTS

New Arrays

Two new arrays were established across the actively creeping segment of the San Andreas fault at Lewis Creek and Mustang Grade in central California. Three arrays were established across the San Andreas fault in the "Coachella Valley seismic gap": one at Miracle Hill near Desert Hot Springs, one at North Shore adjacent to R. V. Sharp's earlier, now partly obliterated line, and one at Bat Caves Buttes. These three arrays complement our existing array at Painted Canyon in the Mecca Hills. A sixth new array across the San Andreas fault was established in Cajon Pass at Lost Lake.

Two arrays were established across the San Jacinto fault at San Bernardino Valley College and Massacre Canyon. These complement our array at Anza in the Anza seismic gap.

One array each was established across the Garlock fault at Cameron and across the range front fault along the western flank of the Pilot Range, Nevada. A 15 cm diameter pipe, which supplies water to the town of Mina, has broken periodically over the fault in the last several years, perhaps because of active vertical movement. If that is true, it would be one of only two places in the world where vertical creep is documented.

Resurveys

Pinyon Flat - Resurveys were done in March and August, 1985, to give us a total of 17 since the array was established in 1979. Motions continue to be about 0.4 ppm between long-base fluid tiltmeter bench marks, and range from 0.4 to 2 ppm for Class B rod marks as reported previously by Sylvester (1984).

McGee Creek - Following the 23 November 1984 earthquake (M 5.7) in Round Valley, a resurvey in December showed a height change of 2 mm across the Hilton Creek fault relative to a survey in July. Our resurvey in July 1985 showed a recovery of 1 mm, leading us to conclude that the 2 mm height change observed one month after the earthquake was a strain transient, similar to those we have observed following moderate earthquakes elsewhere in southern California. These include the Pleito thrust in 1982, and the San Jacinto fault in 1983.

Parkfield - Together with the U.S. Geológical Survey, we monitor two tilt arrays near the San Andreas fault and a leveling array across the San Andreas fault. After 5 surveys in 5 years, the tilt arrays begin to show valley-side-down tilt just barely above the noise level: 1 microradian/yr. Whether the mountain is actively rising or the valley is subsiding non-tectonically is not clear, although permissive arguments can be made for the former. The array across the San Andreas fault shows the NE side of the fault has risen nearly 15 mm relative to the SW side in 5 years. Surveys are not sufficiently frequent to determine whether the movement is aseismic creep or dynamically-triggered slip caused by nearby Coalinga earthquakes.

Pasadena - We established a 1600 m-long leveling array across the Sierra Madre fault in Arroyo Seco near where the fault was located in excavation for a bridge abutment at the Jet Propulsion Laboratory (Fig. 2). In 1984 the array was surveyed in July and August, and surprisingly, the mountain side (north) of the line rose 5 mm relative to the south side in the six week period between the two surveys. We resurveyed the line two more times in 1985, again in July and August, and found that the north side rose another 2 mm between August 1984 and July 1985, and still another millimeter between July and August 1985 (Fig. 3). A search of NGS data shows that bench mark B 172 rose 7 mm relative to 1306 from 1978 to 1984.

In Figure 3, we believe that the data spike at bench mark 19 is caused by minor vandalism of the bench mark between the first and second surveys.

It should be noted that the height changes are not absolute. The data can be equally interpreted that the valley side (south) has gone down, and thus, may be blamed on non-tectonic subsidence of the valley. Alternatively, however, strain may be propagating eastward from the San Fernando area along the frontal fault system of the San Gabriel Mountains, just as Thatcher (1975) postulated it would following the 1971 earthquake, and that the height changes we measure are a manifestation of that strain. In that earthquake, the mountains did rise more than 2 m relative to sea level. We do not measure a similar height change in our leveling array across the Sierra Madre fault in Santa Anita Canyon, 13 km farther eastward. Of all the arrays we monitor, this one bears continued monitoring the most closely over the next few years.

San Fernando - Two PK nails, one on each side of, and about 100 m from, the 1971 surface rupture of the San Fernando fault still survive from their emplacement on 13 February 1971, four days after the 1971 San Fernando earthquake. From 13 February 1971 to December 1976, they showed about 8 mm of height change (Sylvester and Pollard, 1975). We remeasured the height difference between the two PK nails in August 1985 and found nearly 4 mm more vertical movement has accumulated. It would be rank speculation to say when, between 1976 and 1985, the insignificant movement occurred.

Lompoc - Following a minor earthquake and ground rupture in a quarry in 1981 (Yerkes and others, 1983), we established a leveling array across the surface trace of the causative bedding plane fault. We have observed very little subsequent movement across the fault, even after a similar earthquake in April 1985 on the other side of the quarry. But we have documented 60 microradians of east-west tilt in 4 years. The tilt is downward and away from an area of intense quarrying, leading to the conclusion that the tilt is due to rebound of the quarry floor as it is progressively unloaded. That interpretation is consistent with the probable cause of the earthquakes (Yerkes and others, 1983).

Anza - We have performed two complete and one partial relevelings of the Anza array across the San Jacinto fault in 1985. This gives us a total of 24 surveys in four years with no significant changes to report either for the first half of 1985 or for the entire four years.

Koehn Lake - In August 1985 we resurveyed a leveling array established one year before across the Garlock fault near Saltdale on the north edge of Koehn Dry Lake. We documented about 4 mm of height change, lake-side (south) down across the fault which is consistent in direction with continuing subsidence of the valley due to well documented withdrawal of groundwater for irrigation (Holzer, 1984).

China Lake - Following a series of minor and moderate earthquakes in Indian Wells Valley in 1982, we established two

L-shaped leveling arrays across surface traces of fault ruptures in two fault zones on the floor of the valley. The seismic activity ceased when the arrays were first surveyed. Low level activity commenced again in spring 1985, but we found no differential height changes within the arrays or tilt of the arrays as a whole when the arrays were resurveyed in August 1985.

Remaining Arrays - Leveling arrays at San Juan Bautista and in the Santa Barbara, Death Valley areas and some in the Palmdale area have not been resurveyed in 1985. We contemplate a return soon to Death Valley where the easternmost bench mark in the array across the Artists Drive fault has shown steady uplift of about 0.5 mm/yr since it was established in 1970. The array should be lengthened, and some close attention needs to be paid to the condition and geologic setting of that bench mark.

REFERENCES CITED

Holzer, T. L., 1984. Ground failure induced by ground-water withdrawal from unconsolidated sediment. pp. 67-105 in Holzer, T. L., ed., Man-induced Land Subsidence. Reviews in Engineering Geology VI, Geological Society of America.

Sylvester, A. G., 1984. Leveling precision and bench mark motions, Pinon Flat Observatory, California. Journal of Geophysical Research 89 (B9), 7949-7956.

Sylvester, A. G., and D. D. Pollard, 1975. Afterslip on the Sylmar fault segment. Chap 18 in G. B. Oakeshott, ed., San Fernando, California, earthquake of 9 February 1971. California Division of Mines & Geology Bulletin 196, 227-233.

Yerkes, R. F., W. L. Ellsworth, and J. C. Tinsley, 1983. Triggered reverse fault and earthquake due to crustal unloading, northwest Transverse Ranges, California. Geology 11, 287-291.

TABLE I. UCSB LEVELING ARRAYS

LOCATION	LATITUDE	LONGITUDE	QUADRANGLE	INITIAL SURVEY	MOST RECENT SURVEY	TOTAL # SURVEYS
SANTA BARBARA						
Cook	34 25'10"	119 43'00"	Santa Barbara	8/70	8/82	11
Cabrillo	34 22'20"	119 41'25"	Santa Barbara	9/70	6/82	16
Lorinda	34 25'20"	119 43'25"	Santa Barbara	8/70	8/82	7
Castillo Connect	34 25'00"	119 43'25"	Santa Barbara	10/73	8/82	5
Portesuelo	34 25'20"	119 43'35"	Santa Barbara	8/70	6/84	9
Bath	34 24'10"	119 41'40"	Santa Barbara	4/71	8/82	8
Chapala	34 24'50"	119 41'30"	Santa Barbara	4/71	8/82	8
Natoma	34 24'50"	119 41'25"	Santa Barbara	8/70	6/82	8
Castillo	34 24'50"	119 41'35"	Santa Barbara	2/72	8/82	6
Yanonali	34 25'00"	119 41'10"	Santa Barbara	7/70	8/82	8
State	34 24'55"	119 41'55"	Santa Barbara	10/70	8/82	8
SAN ANDREAS FAULT ZONE						
San Juan Bautista	36 50'48"	121 32'00"	San Juan Bautista	9/75	8/83	16
Lewis Creek	36 17'42"	120 52'30"	Lonoak, Hepsedam	8/85	8/85	1
Mustang Grade	36 11'35"	120 46'12"	Monarch Peak	8/85	8/85	1
Flenge Flat	35 55'55"	120 31'18"	Stockdale Mtn.	4/82	7/85	4
Pitt Ranch	35 55'08"	120 28'56"	Parkfield	4/82	8/85	6
Parkfield	35 53'42"	120 26'02"	Parkfield	4/82	8/85	7
Wallace Creek	35 16'09"	119 49'27"	McKittrick Summit	7/83	6/84	2
Camp Dix	34 57'48"	119 26'41"	Ballinger Canyon	7/82	7/82	1
Caballo	34 52'97"	119 13'02"	Sawmill Mountain	8/82	6/85	4
Mesa Valley	34 48'46"	118 54'20"	Frazier Mtn.	2/77	6/85	19
Una Lake	34 33'00"	118 06'15"	Palmdale	8/79	8/84	5
47th St. East	34 31'03"	118 02'47"	Palmdale	12/76	9/83	12
Big Rock Springs	34 26'04"	117 50'00"	Valyermo	10/80	7/84	9
Pallett Creek	34 25'10"	117 54'00"	Juniper Hills	6/78	6/85	14
Llano	34 31'06"	117 47'53"	Lovejoy Buttes	3/81	7/84	4
Lost Lake	34 16'34"	117 28'00"	Cajon	8/85	8/85	2
Miracle Hill	33 56'03"	116 28'00"	Seven Palms Valley	9/85	9/85	1
North Shore	33 35'02"	115 55'57"	Mortmar	9/85	9/85	1
Painted Canyon	33 36'15"	116 01'20"	Mecca	9/83	9/85	3
Bat Caves	33 25'26"	115 49'04"	Durmid	9/85	9/85	1
DEATH VALLEY						
Triangle Spring	36 42'40"	117 07'20"	Stovepipe Wells	10/70	1/84	5
Sewage Treatment	36 30'20"	115 52'25"	Chloride Cliff	10/70	1/84	5
Artists Drive	36 25'00"	116 51'00"	Furnace Creek	4/70	1/84	9
Hanaupah	36 14'05"	116 53'00"	Bennett's Well	10/70	1/84	8
Fish Lake Valley	37 24'28"	117 51'47"	Soldier Pass	9/71	7/85	6
SAN JACINTO FAULT ZONE						
SBVCollege	34 05'08"	117 18'37"	San Bernardino S	7/85	8/85	2
Massacre Canyon	33 50'35"	116 59'45"	San Jacinto	8/85	8/85	1
Pinyon Flat	33 35'00"	116 26'00"	Palm Desert	10/79	8/85	17
Anza	34 35'00"	116 39'35"	Idyllwild	1/81	8/85	24
TRANSVERSE RANGES						
JM Quarry	34 36'30"	120 26'44"	Lompoc Hills	8/81	6/85	8
Juncal	34 29'00"	119 30'15"	Carpinteria	8/70	8/80	7
Grapevine	34 55'30"	118 55'30"	Grapevine	7/79	8/85	9
San Fernando	34 18'03"	118 25'35"	San Fernando	2/71	8/85	10
JPL	34 12'05"	118 09'52"	Pasadena	5/84	8/85	4
Santa Anita Canyon	34 10'05"	118 01'03"	Mt. Wilson	8/84	8/85	4
Dalton Canyon	34 10'09"	117 48'04"	Glendora	6/81	6/83	7
LONG VALLEY						
YMCA	37 37'34"	118 55'37"	Mt. Morrison	7/83	7/84	1
McGee Creek	37 33'39"	118 47'08"	Mt. Morrison	7/82	7/85	6
MOJAVE DESERT						
SNORT	35 44'52"	117 45'00"	Ridgecrest North	7/83	8/85	5
Airport	35 42'41"	117 43'16"	Ridgecrest North	7/83	8/85	5
Cameron	35 05'37"	118 18'16"	Monolith	8/85	8/85	1
Koehn Lake	35 22'16"	117 51'03"	Saltdale SE	8/84	8/85	2
Duravan	35 17'05"	117 53'25"	Cantil	9/74	9/83	13
NEVADA						
Mina	38 21'58"	118 03'08"	Sodaville	7/85	7/85	1

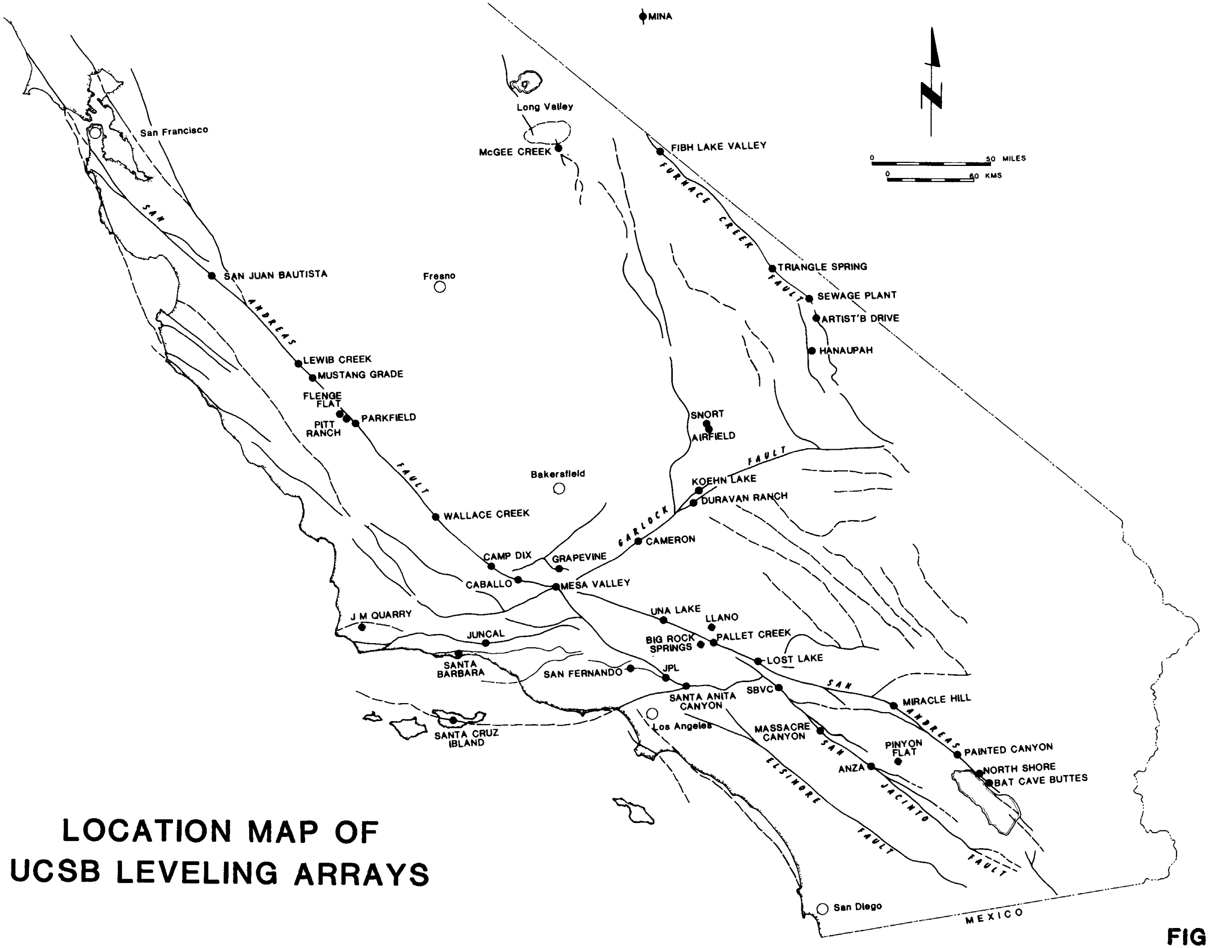

LOCATION MAP OF UCSB LEVELING ARRAYS

FIG. 1

SITE MAP OF JPL LEVELING ARRAY

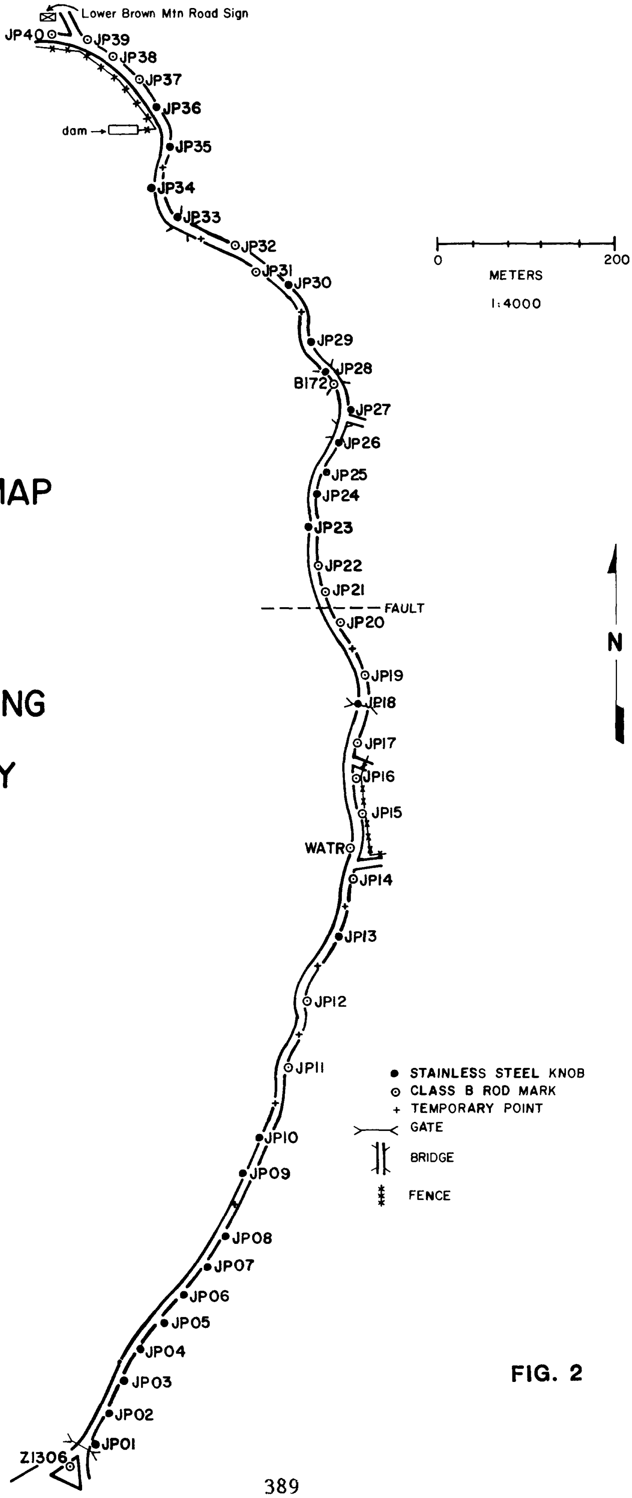

FIG. 2

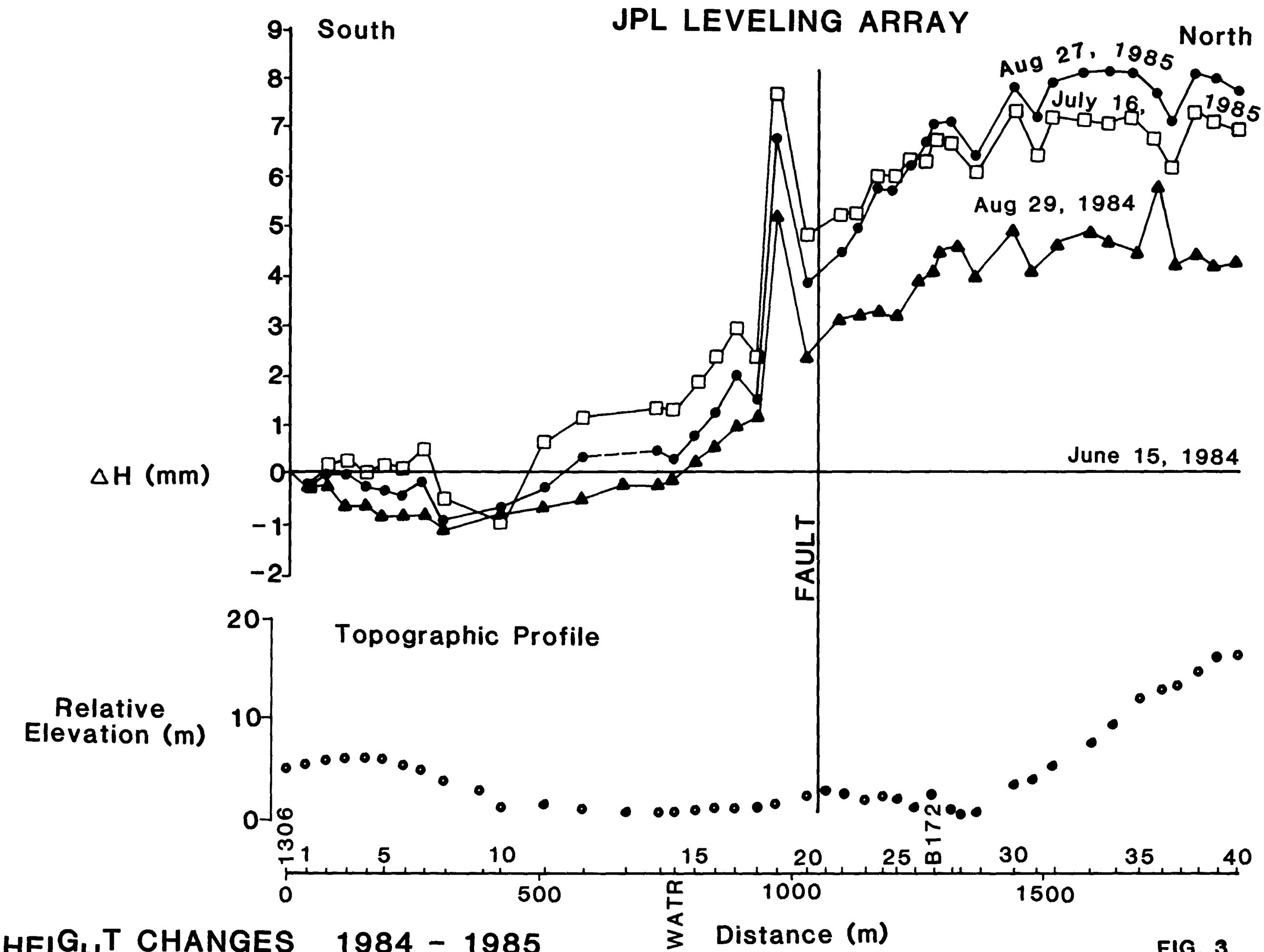

HEIGHT CHANGES 1984 - 1985

FIG. 3

Analysis and Interpretation of Releveling and Other Geodetic Observations in Seismically Active Areas in the Western U.S.: Implications for Earthquake Prediction

14-08-0001-21998

M.N. Toksöz and R.E. Reilinger
Earth Resources Laboratory
Massachusetts Institute of Technology
Cambridge, Massachusetts 02142
(617) 253-7852

INVESTIGATIONS

1. Contemporary deformation in the Imperial Valley, California.
2. Epeirogenic and intraplate movements - impact on society (a project under the auspices of the Geophysics Study Group, National Research Council, National Academy of Sciences).
3. Finite element models of surface deformation due to postseismic, viscoelastic relaxation.

RESULTS

1. Constraints on the Age of the Present Fault Configuration in the Imperial Valley, California. Recent analysis of heat flow in the Imperial Valley suggests that the seismic patterns, and hence the presently active faults defined by these seismic patterns, are ephemeral over the 4-5 m.y. time scale of the troughs formation (Lachenbruch *et al.*, 1985, JGR). We present independent evidence to support the relatively young age of the present fault configuration in the Imperial Valley. Specifically, the large majority of historic seismic activity in the Imperial Valley has occurred on the Imperial and Brawley faults. These right-stepping, enechelon faults are joined by the Mesquite basin, a region of presently active crustal extension and subsidence. Geodetic observations indicate that the Mesquite basin subsided approximately 15 cm coseismically and an additional 15 cm during the postseismic period for the 1940, M7.1 Imperial Valley earthquake. More recent geodetic monitoring shows that the basin subsided 10-15 cm between 1978 and 1980, presumably in association with the 1979, M6.5 Imperial Valley event. Seismic refraction studies indicate that the Mesquite basin is characterized by about 500 m of basement relief. Assuming a conservative (upper limit) estimate for the average recurrence time for major earthquakes on the Imperial-Brawley fault system of 100 years and estimating 15 cm of subsidence per earthquake for the Mesquite basin (this is a lower limit as it ignores any postseismic or interseismic subsidence), 500 m of basin relief would develop in about 300,000 years, considerably less than the 4-5 m.y. age of the Imperial Valley. Thus, our analysis provides independent support for the ephemeral nature of the present fault configuration in the Imperial Valley.

2. Epeirogenic and Intraplate Movements. Major deformations of the earth's surface are largely consistent with the tenets of plate tectonics, which predict that such activity should be focused at the various boundaries along which massive lithospheric plates collide, pull-apart, or slide past one another. Yet crustal deformations also occur well into the interior of these plates. Some may represent the "distributed" effects of distant plate boundaries, as for example the earthquakes of the intermontane western United States. Some, such as the geodetically observed uplift over a deep magma chamber in the Rio Grande rift of New Mexico, may correspond to incipient formation of a new plate boundary. Others, like the subtle, broad uplifts, and subsidences in the nominally "stable" cratonic interiors, are much more puzzling. Such motions often appear estranged, if not divorced, from accepted plate tectonic processes. Post-glacial rebound, a well-known phenomena in portions of North America and Europe, also appears to be an inadequate explanation for many observations.

Understanding contemporary motions of plate interiors is often hindered by the paucity and uncertain accuracy of relevant geophysical and geodetic observations. Yet intraplate tectonics constitute more than a scientific enigma. Even seemingly slow vertical motions may threaten river courses or seafront properties on socially relevant time scales, and the subtle strains accumulating elsewhere may portend future earthquakes or volcanos in the least predictable places.

3. Postseismic Viscoelastic Relaxation. We have recently installed a new finite element program (ADINA - Automatic Dynamic Incremental Nonlinear Analysis) for determining the static and dynamic displacement and stress analysis of very general and complex structures. This computer program is being used to investigate postseismic deformational processes associated with the 1959, M~7.5 Hebgen Lake, Montana earthquake (Reilinger, 1985) and the 1940, M~7.1, Imperial Valley, California earthquake (Sauber *et al.*, 1984).

PUBLICATIONS

Reilinger, R.E., A strain anomaly near the southern end of the San Andreas fault, Imperial Valley, California, *Geophys. Res. Lett.*, v. 12, 561-564, 1985.

Reilinger, R.E., and S. Larsen, Constraints on the age of the present fault configuration in the Imperial Valley, California, *EOS, Trans. Am. Geophys. Union*, in press, 1985.

Sauber, J., R. Reilinger, and M.N. Toksöz, Postseismic viscoelastic relaxation associated with the 1940 Imperial Valley earthquake, *EOS, Trans. Am. Geophys. Union*, v. 65, 190, 1984.

Reilinger, R.E., Postseismic viscoelastic relaxation following the 1959, M=7.5 Hebgen Lake, Montana earthquake, *EOS, Trans. Am. Geophys. Union*, v. 66, 383, 1985.

Reilinger, R.E., The earthquake deformation cycle: Implications for the North American vertical datum (NAVD), *Proceedings of the 1985 NAVD Symposium*, Rockville, MD, 251-260, 1985.

Brown, L.D., and R.E. Reilinger, Epeirogenic and intraplate movements (in) *Active Tectonics - Impact on Society*, ed. R.E. Wallace, National Academy of Sciences, in press, 1985.

Crustal Deformation Observatory Program and Related Studies at Piñon Flat Observatory

14-08-0001-21987

Frank Wyatt and Duncan Carr Agnew
Institute of Geophysics & Planetary Physics
Scripps Institution of Oceanography
University of California, San Diego
La Jolla, CA 92093
(619) 452-2019

This contract provides assistance for independent investigators working at Piñon Flat Observatory (PFO) under the sponsorship of the U.S. Geological Survey. This assistance includes: research coordination, instrument operation and testing, data recording, preliminary data reduction, and collaborative data analysis. This effort is part of a cooperative program to evaluate instrumentation for measuring long-period (days to years) ground deformation in a tectonically active area. The evaluation of these different techniques involves understanding and reducing sources of noise in the instruments as well as developing improved methods to describe the errors of the measurements.

The most recent activities at Piñon Flat Observatory have focused on the installation of a cluster of intermediate-depth borehole tiltmeters: an Askania tiltmeter at 25 m depth, in cooperation with Walter Zürn of Karlsruhe University; two 10 m-deep tiltmeters developed by Sean-Thomas Morrissey of St. Louis University; and two tiltmeters for operation at 25 m designed by Judah Levine and Charles Meertens of the University of Colorado. These five sensors are to be located within 100 m of one another and, together with the existing long baselength tiltmeters and other borehole sensors, should clarify the differences (and similarities) between the various techniques. Completion of this array is expected by the spring of 1986.

Discussions, by Dave Jackson (UCLA), with the Office of Charting and Geodetic Services has led to a plan for a closely-spaced class A rod mark "farm" at PFO. This too is scheduled for installation in early 1986. These monuments will be compared with the ultra-stable monuments (optical anchors) used in the long tiltmeters at the site in an effort to identify sources of noise. Monitoring of this experiment is to be conducted by the survey team from UCSB under the direction of Art Sylvester.

Other research projects currently underway at the site include those by: St. Louis University (evaluation of shallow-borehole tilt), Lamont-Doherty Geological Observatory (long baselength tilt and water-height measurement techniques), U.S. Geological Survey - Water Resources Division (well-water height), Air Force Geophysics Laboratory (borehole tilt and deep borehole alignment techniques), Carnegie Institution of Washington and U.S. Geological Survey (volumetric borehole strain), University of Queensland (linear borehole strain), and Sandia National Laboratory (seismic-strain monitoring).

Crustal Deformation Observatory Part J: Askania Borehole Tiltmeter

14-08-0001-21990

Frank Wyatt, Duncan Carr Agnew, Hadley Johnson
Institute of Geophysics & Planetary Physics
Scripps Institution of Oceanography
University of California, San Diego
La Jolla, CA 92093
(619) 452-2019

This contract supports the installation and operation of an Askania borehole tiltmeter at Piñon Flat Observatory (PFO) and analysis of data from it. This work is part of the Crustal Deformation Observatory (CDO) program, as a cooperative enterprise with Dr. Walter Zürn of Karlsruhe University (West Germany), who has provided the instrument on loan. The goals of this project are to: establish techniques and costs for installing a removable borehole tiltmeter at different depths, compare these borehole tilt measurements with those from other adjacent borehole installations and from nearby long-base surface tiltmeters, and use a commercially available transducer to attempt to accurately monitor tilt in a tectonically active area.

We received the tiltmeter from Dr. Zürn in February 1985, and conducted our preliminary trials in the basement seismic-vault of IGPP. At this near-shore site the tidal tilts are very large; the purpose of this setup was simply to familiarize ourselves with the operation of this instrument. Subsequently, we prepared a shallow vault (depth, 3 m) at Piñon Flat Observatory for testing in a quieter environment; the tiltmeter was installed there on 1985:233, and is working satisfactorily (though the drift rates in such a location are, of course, high). Finally, the signal and power wires have been laid out and connected for the borehole installation; drilling of the hole (a 20 cm hole drilled to 28 m, reamed to 30.5 cm, then widened to 35.6 cm over the upper 12 m for near-surface casing) was completed on 1985:268. The design of the casing and instrument-support housing has been completed; grouting of this, and installation of the instrument, is expected this fall.

Piñon Flat Observatory:
A Facility for Studies of Crustal Deformation

14-08-0001-21996

Frank Wyatt, Duncan Carr Agnew,
Mark A. Zumberge, Jonathan Berger
Institute of Geophysics & Planetary Physics
Scripps Institution of Oceanography
University of California, San Diego
La Jolla, CA 92093
(619) 452-2019

Introduction

This contract supports the ongoing program at Piñon Flat Observatory (PFO) by providing a common location with shared facilities for improving precision geophysical instruments. The work done there includes establishing the accuracy of various instruments in measuring different geophysical quantities (primarily tilt and strain) by comparing results from them with data from the best instruments available (the so-called reference standard instruments). This comparison also allows reliable monitoring of strain and tilt changes in the region near the observatory, between the San Jacinto and southern San Andreas faults. We describe recent work that promises to improve the data quality from the long-base laser strainmeters, and an experiment in testing for the presence of anomalous deformation signals.

Laser Strainmeter Observations and Corrections

The ongoing identification of noise sources has led to a number of refinements to the three laser strainmeters. The most recent records, shown in Figure 1, indicate the effects of these improvements. The least reliable instrument is the North-South strainmeter, whose southern end-monument is relatively unstable; both it and the East-West strainmeter show a clear correlation with the weather. The optical anchors installed on the Northwest-Southeast instrument (in late 1983) should have eliminated its sensitivity to near-surface conditions; however, the laser beam for this sensor passes through a small-angle steering prism at its center, and small vertical movements of this prism can cause relatively large apparent strains. This appears to be the cause of the residual weather-to-strain correlation on this instrument. We have also found a correlation of the corrected NW-SE strain with vault temperature; this problem has been reduced by installing better temperature-regulating equipment.

All three of the strainmeters are also susceptible to instability of the laser frequency-standard, in this case a quartz Fabry-Perot interferometer. Under sponsorship of NSF, and with equipment funds from DoD, we are monitoring the laser frequencies relative to an iodine-stabilized laser, a primary length standard, using a transportable Zeeman-stabilized laser built by us as a transfer-standard. The initial results are presented in Figure 1, shown slightly offset from the strain data. These point frequency-measurements (only two for the NS and EW, and four for the NW-SE strainmeter) indicate the strain change caused by frequency drift. For these admittedly sparse data, the agreement of this correction signal with the observations is quite good and encourages us to proceed in monitoring the frequencies much more often. The variance of all three records is reduced by applying this correction; for the EW and NW-SE strainmeter the final secular signal is nearly zero (EW: $-0.02\ \mu\varepsilon/a$; NW-SE: $+0.06\ \mu\varepsilon/a$). The data in Figure 1 are probably aliased, especially if variations in the PFO laser frequencies are occurring in episodic steps. If this is so then using these measurements to correct the strain record would introduce spurious changes into it. We are therefore installing at PFO a fiber-optics system to transmit light from all three strainmeter lasers to a central facility at which the frequency measurements can be made more routinely.

Testing for Anomalous Deformation Signals: An Example

While further instrument development is an important part of work on continuous crustal deformation measurement, it is also worth considering how such measurements would be used if one were looking for an anomalous signal. We have used data from the long-base instruments at PFO to limit the size of an event detected by the Caltech creepmeter on the San Andreas fault at Mecca Beach, just north of the Salton Sea and 54 km from PFO. Sometime between days 88 and 93 of 1984 (the exact time is uncertain because of poor timing on the recorder) a creep event occurred, with about 5.5 mm of creep in 10 hours and a total of 6.7 mm in over 20 hours; a second, smaller event occurred about six days later.

Any sizable slip in this short a time would produce detectable offsets on the instruments at PFO, but we must quantify the term "sizable." Figure 2 shows the strain and tilt data from some of the PFO instruments, after removing the tides (using harmonic analysis for the period 1984:40-135). While several of the long-base instruments do show unusual behavior, these events coincide with exceptional weather at Pinyon Flat: on day 87, clouds and very high winds, and on day 92, light clouds and rain. Because of its partial burial, the NW strainmeter is least affected by weather; though it should be most sensitive to strains from this creep event, it shows nothing obvious.

The steps in analyzing these data are first to process them to enhance the signal and reduce the noise, and then to use the processed result to answer some question about the source. We adopted a relatively simple method: each series was lowpassed and decimated to give hourly spacing. We then found the difference between values 10 hours apart as a function of time, converting a 10-hour offset (our presumed signal) into an isolated deflection away from zero. To proceed further we took a probabilistic approach, and attempted to answer the question, "Given that the slip-moment (the orientation being assumed) exceeds a specified amount, what is the probability that the data would be as observed?" Because of its low noise and high sensitivity to strike-slip motion on this part of the fault, the NW laser strainmeter is weighted the most heavily in this analysis. Over the 130-hour interval within which the event occurred, a moment-magnitude 3.3 creep event (5 mm of slip over an area 9 km on a side) is quite possible, or at least cannot be ruled out. A magnitude 3.9 is extremely improbable; we may confidently assume that something this large (5 mm over an area of 10 by 40 km) did not occur. Other creep measurements along the fault confine the event to a distance of at most 15 km, but of course give no evidence on its distribution with depth; if the lateral and vertical extent were limited to 15 by 5 km, the PFO data bound the slip to be less than 4 cm.

Piñon Flat Observatory 1983:240 to 1985:070

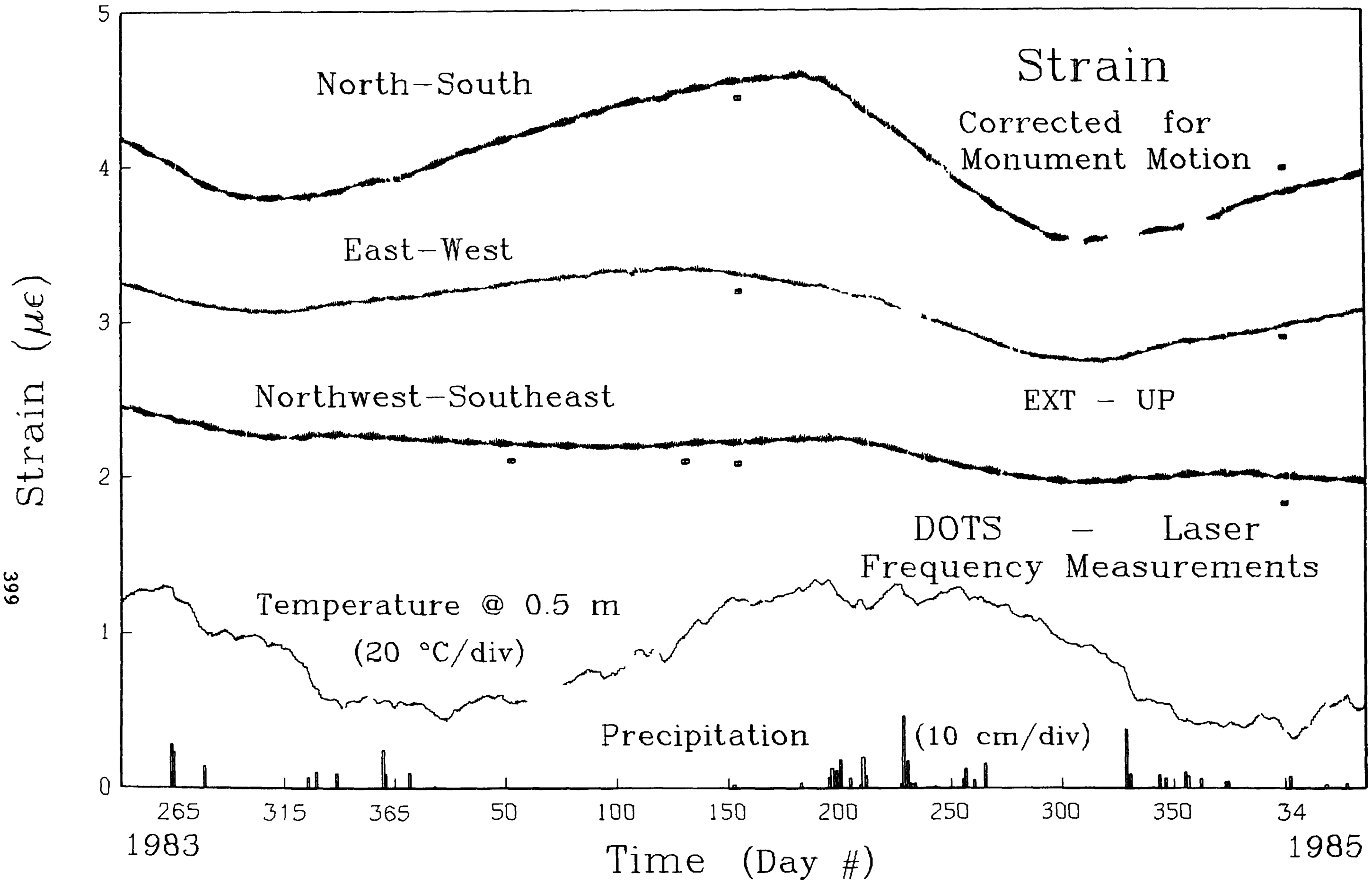

Mecca Beach Creep Event: Long-base Strain and Tilt Piñon Flat Observatory

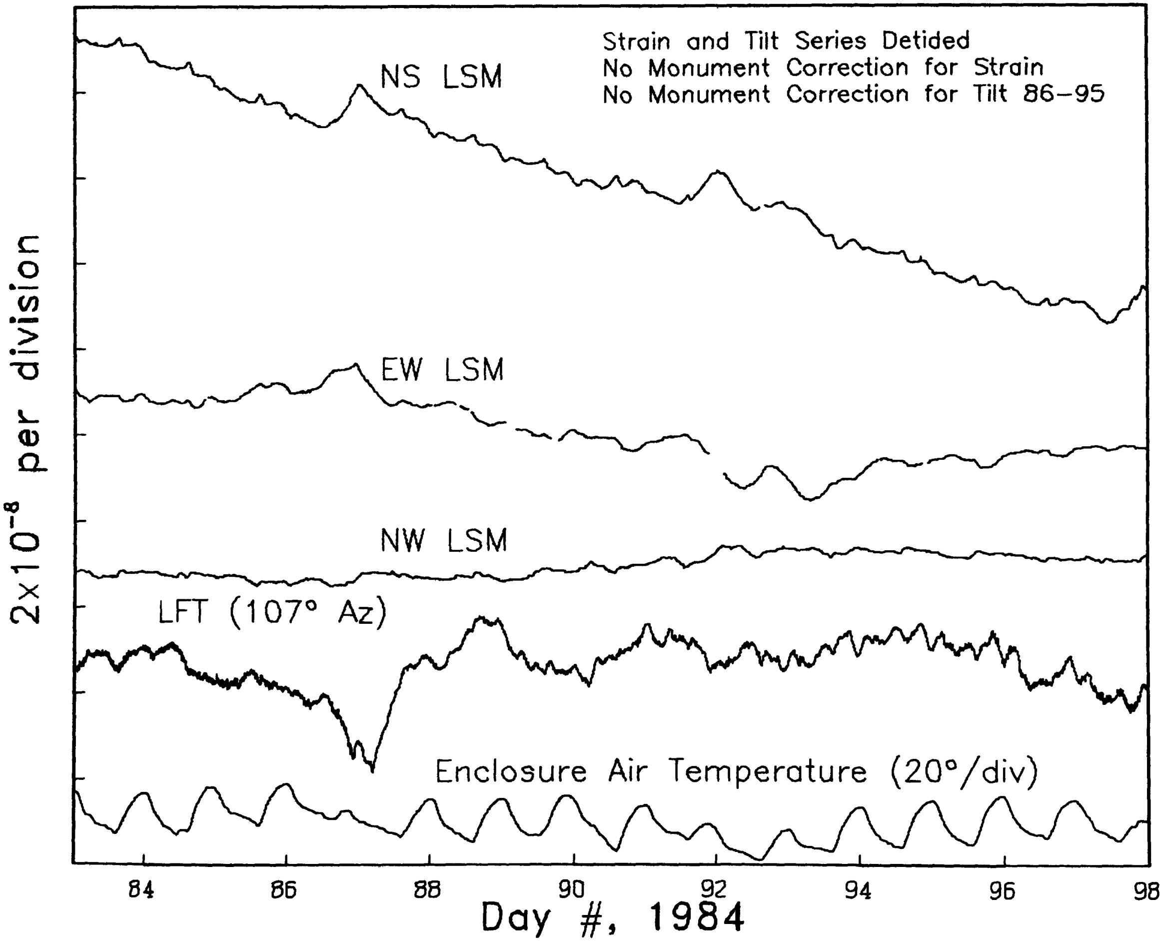

IMPERIAL COLLEGE OF SCIENCE AND TECHNOLOGY
GEOLOGY DEPARTMENT
LONDON SW7 2BP
BRITAIN

STRESS CORROSION AND MICROSEISMIC ACTIVITY DURING FAILURE OF ROCKS

CONTRACT: 14-08-0001-21287

PRINCIPAL INVESTIGATORS: B. K. Atkinson, N. J. Price

REPORT PREPARED BY: B. K. Atkinson, P. G. Meredith, Zheng Jie

Investigations

The aim of this project, to improve our understanding of the chemical effects of pore water in controlling the long term strength of rocks in the upper levels of the earth's crust, remains unchanged. In this report period we have been running experiments to study the subcritical crack growth of granite in different sized specimens, and to study the inhibition of crack growth by use of water repellant fluids. We have also studied the influence of subcritical crack growth and crack healing on the low cycle fatigue strength of rocks. Work has continued under the aspices of ISRM to develop reliable ways of testing the fracture toughness of rocks. In this regard, we have made some progress with a new apparatus to measure the fracture toughness of rock in shear loading. Finally, we have completed an analysis of the large experimental data base obtained by us on the chemical influence of water on the low strain rate sliding stress of faults in rock.

Results

1. We have finished, and updated to the time of writing, the most complete compilation of experimentally determined fracture mechanics parameters yet attempted for geological materials. This compilation includes data on tensile and shear linear elastic, as well as non linear elastic parameters. The compilation is computer based and will be updated periodically in the light of new work.

2. Further experiments and analysis of low cycle fatigue experiments on experimentally faulted basalt and granite have been made. The data for Westerly granite exhibit markedly different patterns of behaviour between wet and dry conditions. No significant fault strength recovery was observed for any granite specimen under nominally dry conditions over hold periods up to 35 days. In contrast, there were significant increases in the strength of fault zones in granite for every specimen tested under wet conditions for hold periods exceeding 100 hours. We conclude, therefore, that the presence of pressurized pore water

increases crack healing rates dramatically. Increases in sliding stress of over 20% were observed over 1000 hours. There appears to be a good correlation between strength recovery and time, but there does not seem to be any correlation with effective confining pressure. Data for basalt are less consistent. Some strength recovery was noted in some specimens over 100 hours, but others showed no change over 1000 hours.

3. Significant reduction in subcritical crack velocity can be obtained for a given stress intensity factor by treating Westerly granite with water repellant fluids. This varies from one order of magnitude in velocity for soaked specimens to three orders of magnitude in velocity for vacuum impregnated specimens. There is no obvious advantage to be gained by using one water repellant fluid rather than another. The subcritical crack growth index is not significantly alterred by treating the rock with water repellant fluid.

4. Subcritical crack growth data for Merrivale granite in air and water at 20°C have been obtained for a range of double torsion specimen sizes (specimen lengths from 14 to 61 cm). Provided that precations are taken to scale the other dimensions of the specimen, size does not seem to seriously influence the results. Tests in air are generally well described by single straight lines. Tests in water, however, often show a lowering of the slope as crack velocity decreases. Thus greater subcritical crack growth susceptibility is shown at the slower crack velocities. Acoustic emission event rates can be used to monitor subcritical crack growth, and they reinforce the above observations.

5. A new loading jig for both shear and tensile fracture toughness tests on rock has been developed. It is based on the double torsion specimen. Rotating torque arms or direct compression arms are used to apply the load. We have been through several prototypes of this apparatus, but have now found a rather satisfactory configuration. Using this apparatus we have successfully propagated mode III (shear) cracks in Black gabbro specimens. The shear fracture toughness is approximately 5.25 MPa. m½, which compares with a value for the tensile fracture toughness of about,3 MPa. m½. We are now about to use this apparatus for a wide range of fast and subcritical crack growth studies on rocks in shear.

6. We have analysed a large body of our experimental data on the chemical influence of water on the slow strain rate sliding of faults in rock. Rock types studied include: quartzite, sandstone, novaculite, granite, basalt and greywacke. Recent theoretical work by Lehner and Battaille holds the key to understanding the diverse weakening behaviour shown by these rock types under conditions simulating the upper 15 km of the earth's crust. The fault sliding rate is controlled by the fastest of: stress corrosion of fault plane asperities and their failure, interface reactions in solution processes, and fluid phase transport of rate controlling species in solution processes. For this scheme to apply

overall strain rates must be slow enough so that dry friction behaviour does not obtain, and temperatures must be low enough so that thermally activated plastic creep mechanisms do not operate in parallel. The observed response of test rocks varies because the rate of the three controlling mechanisms will vary from rock to rock, all other conditions being equal. A major barrier to applying this model to interpret natural fault zone behaviour in terms of laboratory experiments is a lack of hard data on the influence of hydrostatic pressure on the subcritical growth of cracks in rocks.

Reports

Atkinson, B. K. and Meredith, P.G. (1985) Fracture mechanics parameters for geological materials. In Rock Fracture Mechanics and Geophysical Applications (Atkinson, B. K. ed.) Academic Press (to be published).

Atkinson, B. K. and Meredith, P.G. (1985) Subcritical crack growth in minerals and rocks. In Rock Fracture Mechanics and Geophysical Applications (Atkinson, B. K. ed.) Academic Press (to be published).

Crampin, S. and Atkinson, B. K. (1985) Microcracks in the earth's crust. First Break. 3, 16-20.

Meredith, P.G. and Atkinson, B. K. (1985) Fracture toughness and subcritical crack growth during high temperature tensile deformation of Westerly granite and Black gabbro. Phys. Earth Planet. Int., 39, 33-51.

Ouchterlony, F. and Atkinson, B. K. (1985) Experimental methods in rock fracture mechanics. In Rock Fracture Mechanics and Geophysical Applications (Atkinson, B. K. ed.). Academic Press (to be published).

ROCK MECHANICS

9960-01179

James Byerlee
U.S. Geological Survey
Branch of Tectonophysics
345 Middlefield Road, MS/977
Menlo Park, California 94025
(415) 323-8111, ext. 2453

Investigations

Laboratory experiments are being carried out to study the physical properties of rocks at elevated confining pressure, pore pressure and temperature. The goal is to obtain data that will help us to determine what causes earthquakes and whether we can predict or control them.

Results

During the shearing of fault gouge, strength changes are often observed at faster strain rates. These changes are characterized by a transient stress peak before reaching a final equilibrium value. Conversely, a stress drop and a gradual rise to the equilibrium strength accompany changes to slower rates. To study the phenomena, frictional sliding experiments were performed on sawcut samples filled with a layer of Ottawa sand. Pore fluid volume and shear stress were measured as strain rate were alternated between 10^{-7}/sec and 10^{-5}/sec. Pore volume increased at the fast rate and decreased at the slower rate, verifying that gouge dilation is a function of strain rate. Pore volume changed until the critical void ratio of the granular material was reached for a particular rate of strain. Because of this, the degree of consolidation of the grains must also depend on rate. Soil mechanics studies have shown that over consolidated soils typically exhibit a peak in shear stress before reaching a lower steady-state value, while the strength of underconsolidated soils slowly rises to the final value, as we have also observed in these experiments. Therefore, the transient stress behavior can be explained simply by the overconsolidated nature of the gouge at the new rate when the strain rate is increased from 10^{-7}/sec to 10^{-5}/sec, and the underconsolidated state when the rate of strain is lowered. Natural fault gouges may exhibit similar behavior as they become overconsolidated and stronger with time.

Reports

C. Morrow, and J. Byerlee, 1985, Pore pressure and its effect on the mechanical behavior of materials in the seismogenic zone, Proc. Conf. Seis. Soc. Am.

D. Lockner and J. Byerlee, 1985, Complex resistivity measurements of confined rock, J. Geophys. Res., v. 90, No. B9, p. 7837-7847.

Summary of Final Technical Report
Contract No. 14-08-0001-19864

GPS Geodesy

Charles C. Counselman III

Dept. of Earth, Atmospheric, and Planetary Sciences
Massachusetts Institute of Technology
Cambridge, MA 02139
Tel. (617) 253-7902

A program of sufficiently precise and frequent measurements of geodetic "baseline" vectors between widely separated monuments set in the ground can reveal the spatial and temporal distribution of strain in the earth's crust. To improve the precision of such measurements was the goal of this contract.

One measurement technique was studied: radio interferometry using signals from the Global Positioning System (GPS) satellites. The chief problems were (1) to eliminate effects of the ionosphere on the propagation of the signals, and (2) to determine the orbits of the satellites more accurately.

Ionospheric effects were eliminated by combining observations of the signals in two frequency bands. New, dual-band, antennas and receivers were built for this purpose. This equipment was used to observe the satellites simultaneously from sites several thousand kilometers apart, in order to determine the satellite orbits.

As a result of our research under this contract and related Air Force contracts, and of a separate, proprietary, technological development which we were able to exploit, we are now (September 1985) able to determine a 30-kilometer baseline with sub-centimeter precisions in all three coordinate components.

Mechanics of Earthquake Faulting

9960-01182

James H. Dieterich
U.S. Geological Survey
Branch of Tectonophysics
345 Middlefield Road, MS/977
Menlo Park, California 94025
415-323-8111, ext. 2573

Investigations

Constitutive Properties of Faults - Variable Normal Stress

Work began on experimental measurement of fault constitutive properties under conditions in which normal stress is independently varied during slip. Earlier exploratory tests have indicated that variation in normal stress can result in displacement dependent changes in fault friction that mimic velocity dependent effects seen under constant normal stress conditions.

Nucleation and Triggering of Earthquake Slip

Analysis and modeling of the processes associated with the nucleation and triggering of earthquake slip was continued. Emphasis was given to investigating the characteristics of the fault patch where unstable slip nucleates, effect of earth tides or other periodic loads in controlling the timing of earthquakes and to the processes controlling the timing of foreshocks and aftershocks.

Deformation Mechanics of Active Volcanoes

Analysis continued of the 1975 Kalapana, Hawaii earthquake and of processes controlling the deformation and evolution of the south flank of Kilauea volcano.

Results

Constitutive Properties of Faults - Variable Normal Stress

No results to report. Most of the necessary equipment modifications have been completed. Systematic testing will begin in October of this year.

Nucleation and Triggering of Earthquake Slip

Application of a state-variable fault constitutive law to analysis of the nucleation of earthquake slip has yielded the following principal results: First, unstable fault slip may only begin if the slipping patch exceeds a critical radius, r_c. The critical radius is a function of normal stress, loading conditions and constitutive parameters which include D_c, the characteristic slip distance. Second, for a patch larger than the critical radius, at an initial stress, τ , above the steady state frictional strength, τ_s, slip accelerates to instability. The time delay from the application of τ to the time of instability varies from seconds to times on the order of elapsed time since the previous slip event on the fault patch depending on the magnitude of the stress step. Over a wide range of conditions the logarithm of the time to instability linearly decreases as the difference $\tau - \tau_s$ increases. It is proposed that this delayed instability following a stress step may be an important process in controlling the timing of a mainshock following a foreshock and in controlling aftershock sequences. The familiar 1/t decay in aftershock occurrence rate is satisfied by this assuming the initial stress, $\tau - \tau_s$, acting on the nucleation patches for the aftershocks has a uniform statistical distribution over the population of nucleation patches. Third, displacements during the accelerating slip that leads to instability are proportional to D_c. Unless D_c for earthquake faults is significantly greater than that observed on simulated faults in the laboratory, premonitory displacements in earthquake nucleation zones may be too small to detect using current strain instrumentation methods. Fourth, the velocity dependence of the fault constitutive law acts to inhibit the triggering of earthquakes by earth tides. Correlation of seismicity rates with tidal stress is directly proportional to the amplitude of tidal shear stresses and inversely proportional to the total shear stress acting across the fault and the velocity coefficient in the fault constitutive law. Using constitutive parameters characteristic of laboratory faults the model predicts significant correlation of earthquakes with the semi-diurnal component of the earth tides (seismicity rate enhancement of tidal maxima vs tidal minima of 0.05 or greater) only when the ratio of the tidal stress changes to total shear stress is greater than about 2×10^{-4}. Assuming an amplitude of tidal stress of 0.02 bars this result indicates that correlation of earthquakes with earth tides would be evident only under conditions where the total shear stress is less than 100 bars.

Deformation Mechanics of Active Volcanoes

Finite element analysis of the deformation associated with the 1975 Kalapana, Hawaii earthquake indicates fault slip occurred along a near horizontal surface at a depth near the original ocean floor beneath the volcano. Following previous studies the driving force for the earthquake is interpreted to be repeated injections of magma into the southwest and east rift zone of Kilauea volcano. A wedge-shaped block is inferred to comprise the south flank of Kilauea. The block is bounded on the bottom by a horizontal fault, presumed to be the ancient ocean floor and at the end by the dikes that make up the volcano rift zones. A stability analysis of this wedge shaped block suggests that fault friction controls the slope of the volcano flank and internal growth of the volcano. The solutions are sensitive to the density structure of the model. Assuming the pore pressure is normal hydrostatic, the coefficient friction of the basal fault appears to be in the range 0.25 to 0.50 depending upon the density structure. A structure consisting of high density dikes adjacent to the rifts and low density flows away from the rifts favors the high fault friction.

Reports

Dieterich, J.H., 1985, A Model for the Nucleation of Earthquake Slip, submitted to the proceedings volume Fifth Maurice Ewing Symposium on Earthquake Source Mechanics, 28 p.

Dieterich, J.H., 1985, Nucleation and Triggering of Earthquake Slip (abstract), The 23rd General Assembly of International Association of Seismology and Physics of the Earth's Interior (IASPEI), Tokyo, Japan, p. 389.

Okubo, P.G., Large-Scale Rock Friction Experiments: Stick-slip and Constitutive Friction Laws, The 23rd General Assembly of International Association of Seismology and Physics of the Earth's Interior (IASPEI), Tokyo, Japan, p. 390.

Okubo, P.G., and Dieterich, J.H., 1985, Constitutive Relations for Dynamic Fault Slip, submitted to the proceedings volume Fifth Maurice Ewing Symposium on Earthquake Source Mechanics, 23 p.

Thermal, Mechanical, and Chemical History of Wasatch Fault Cataclasite and Phyllonite, Traverse Mountains Area, Salt Lake City, Utah: Age and Uplift Rates from K/Ar and Fission Track Measurements

14-08-001-G-886

S. H. Evans, W. T. Parry, and R. L. Bruhn
Department of Geology and Geophysics
University of Utah
Salt Lake City, UT 84112
(801)581-6619

Introduction

The footwall of the Wasatch Fault in the Traverse Mountain locality is the Little Cottonwood stock, a porphyritic quartz monzonite. The age of the intrusion is 31.1 ±0.9 m. y. determined by potassium-argon dating of hornblende (Crittenden et al., 1973). Near the Wasatch Fault, footwall rock has been subjected to multiple alteration and deformation episodes with progressive displacement of the footwall. An early epidote, chlorite, sericite, magnetite alteration assemblage developed in phyllonite and cataclasite and a later laumontite, prehnite, hematite, clay alteration assemblage developed during cataclasis. Fluid inclusion characteristics record the history of fluid pressure, temperature, and composition as reported by Parry and Bruhn (1984,1985), Bruhn and Parry (1985), and Parry (1985). Fluid inclusions that record the transition temperature from quasi-plastic flow to frictional deformation are associated with hydrothermal alteration to chlorite, epidote, and sericite and were trapped at minimum temperatures of 223°C to 353°C and minimum fluid pressures of 1150 b to 2800 b. The fluids average 13 mole percent CO_2 and 8.2 weight percent NaCl. A radiometric age of hydrothermal sericite suggests that the age of the alteration is 17.6 ±0.7 m. y. If maximum fluid pressure is near lithostatic, the minimum depth of formation of the alteration was 11 km at 337°C consistent with a thermal gradient of 30°C/km.

We report here the results of fission-track measurements on apatite from the Little Cottonwood stock in the Traverse Mountains area that establish the uplift history of the footwall block of the Wasatch Fault. Uplift rates are determined from apatite data from samples in vertical sequence, a calculation that does not require knowledge of either the geothermal gradient or annealing temperature (Naeser et al., 1980). Uplift rates may also be calculated from single apatite measurements, the appropriate annealing temperature, and the geothermal gradient.

Analytical Techniques

Samples of the Little Cottonwood quartz monzonite were collected from the Traverse Mountain area at the southern end of the Salt Lake segment of the Wasatch fault at approximately 305 m intervals from near the summit of Lone Peak to the valley floor. Apatite was separated from approximately 13 kg of rock using standard magnetic and heavy liquid techniques.

Apatite separates were dated using techniques described by Naeser (1978). Samples were irradiated in the lazy susan of the TRIGA research reactor of the U. S. Geological Survey at Denver, Colorado. The population method was used in determining the age of apatites. The uncertainty for each fission track date was derived by the method given by Johnson et al. (1979). Results of fission-track dating are given in Table 1.

Results of Mineral Dating

Mineral dating of various samples of the Little Cottonwood stock shows the effects of tectonic uplift and hydrothermal alteration. The apatites studied range in age from 7.3 m.y. to 12.9 m.y. (Table 1). There is a general increase in age with elevation within the footwall block (Figure 1). The youngest sample (LP 84-8) has an age of 7.3 m.y. and comes from near the Wasatch Fault in Corner Creek where the Little Cottonwood stock hosts a hydrothermal mineral assemblage of laumontite, prehnite, clay, and hematite. Fluid inclusions from this area show a mean homogenization temperature of 100°C. The oldest sample (LP 84-1) has an age of 12.9 m.y. and comes from near the summit of Lone Peak at an elevation of 3,384 m. Three samples come from the 1,829 m elevation and range in age from 7.3 ± 1.5 m.y. to 9.6 ± 1.8 m. y. Crittenden et al. (1973) present an apatite fission-track date for a sample from the 1,829 m elevation of 8.5 ± 1.0 m.y. consistent with our data presented in Table 1.

Figure 1 shows a plot of the apparent apatite ages versus elevation. Error bars are also shown on the Figure. Low uranium contents, low induced track densities, and textures of the apatite that include abundant fluid inclusions and fractures leads to the large error bars.

Uplift History

The fission-track ages of apatites record the uplift history of the Little Cottonwood stock. The uplift rate indicated by the youngest samples at 1,529 m to 2,439 m elevation shown on Figure 1 is sufficiently high so that an apparent closing temperature of 105 ± 10°C may be used. Apparent uplift rates for the Little Cottonwood stock may be derived from the data plotted in Figure 1 assuming that the 105 ± 10°C isotherm is stationary as uplift proceeds and apatite ages thus record passage of the Little Cottonwood stock upward through this isotherm (Evans and Nielson, 1982). A distinct change in slope is apparent in Figure 1 indicating a change in uplift rate at about 10 m. y. An uplift rate calculated from a regression line through the data older than 10 m. y. is 0.17 mm/yr. The uplift then accelerated to 0.76 mm/yr starting at about 10 m.y.

Using the thermal gradient indicated by fluid inclusion studies (Parry and Bruhn, 1985) of 30°C/km, the uplift must have been at least 3 km during the last 8 m.y. in order to expose the apatite near the base of Lone Peak at the surface. Such uplift would require a rate of 0.38 mm/yr. Hydrothermal muscovite in the same sample formed from fluids at pressures of 2800 b, temperatures up to 350 °C, and K/Ar age of 17.7 ±0.7 m. y. must have been uplifted at a rate of 0.67 mm/yr (Parry and Bruhn, 1985). Displacement rates for the last 19,000 years reported by Swan et al. (1981) from trenching studies are 0.6 to 1.4 mm/yr.

The pattern of uplift in the Traverse Mountain area derived from fission-track measurements is similar to that described by Naeser, et al. (1980) for the Farmington Complex in the Ogden segment of the Wasatch Fault. They report a low rate of uplift of 0.012 mm/yr for the period from 90 m.y. to 10 m.y. and then accelerated uplift of 0.4 mm/yr from 10 m.y. to the present.

References

Bruhn, R. L. and Parry, W. T., 1985, Thermal, mechanical, and chemical history of Wasatch Fault cataclasite and phyllonite, Traverse Mountains area, Salt Lake City, Utah: in National Earthquake Hazards Reduction Program, Summaries of Technical Reports Volume XX, U. S. Geol. Surv. Open-File Report 85-464, p. 356-364.

Crittenden, M. D., Jr., Stuckless, J. S., Kistler, R. W., and Stern, T. W., 1973, Radiometric dating of intrusive rocks in the Cottonwood area, Utah: J. Res. U. S. Geol. Survey, v. 1, p. 173-178.

Evans, S. H.,Jr., and Nielson, D. L., 1982, Thermal and tectonic history of the Mineral Mountains intrusive complex: Geothermal Resources Council, Transactions, v. 6, p. 15-18.

Johnson, N. M., McGee, V. E., and Naeser, C. W., 1979, A practical method of estimating standard error of age in the fission-track dating method: Nuclear Tracks, v. 3, no. 3, p. 93-99.

Naeser, C. W., 1978, Fission-track dating: U. S. Geol. Survey Open-File Report 76-190 (revised 1978).

Naeser, C. W., 1979, Fission-track dating and geologic annealing of fission tracks, in Lectures in Isotope Geology, E. Jager and J. C. Hunziker, eds.: Springer-Verlag, p. 154-169.

Naeser, C. W., Bryant, B. R., Crittenden, M. D., Jr., and Sorensen, M. L., 1980, Fission-track dating in the Wasatch Mts., Utah: an uplift study:Proceedings of Conference S, Earthquake hazards along the Wasatch and Sierra Nevada Frontal Fault Zones, U. S. Geol. Surv. Open-File Rept. 80-801, p. 634-646.

Parry, W. T., 1985, Estimation of X_{CO2}, P, and fluid inclusion volume from fluid inclusion temperature measurements in the system $NaCl-CO_2-H_2O$: Econ. Geol., in press.

Parry, W. T., and Bruhn, R. L., 1984, Thermal, mechanical, and chemical history of faulting, Wasatch normal fault zone, Utah: EOS, v. 65, p. 1114 (abstract).

Parry, W. T., and Bruhn, R. L., 1985, Pore fluid and seismogenic characteristics of fault rock at depth on the Wasatch Fault, Utah: J. Geophys. Res., in press.

Table 1. Apatite fission track ages from the Little Cottonwood stock, Utah.

	ρ_s		ρ_I		Φ		Age	±S	No of grains	U	Elev.
Sample	Tracks/cm^2	Tracks	Tracks/cm^2	Tracks	Neutrons/cm^2	Tracks	m.y.	m.y.	counted	ppm	Meters
LP 84-1	9.11×10^4	41	2.33×10^5	105	5.51×10^{14}	1035	12.9	2.3	50/50	9	3,384
LP 84-2	9.33×10^4	42	2.51×10^5	113	5.50×10^{14}	1035	12.2	2.2	50/50	10	3,061
LP 84-3	8.89×10^4	40	2.98×10^5	134	5.49×10^{14}	1035	9.8	1.8	50/50	12	2,744
LP 84-4	8.22×10^4	37	2.98×10^5	135	5.48×10^{14}	1035	9.0	1.7	50/50	12	2,439
LP 84-6	8.44×10^4	38	2.87×10^5	129	5.46×10^{14}	1035	9.6	1.8	50/50	11	1,829
LP 84-8	6.66×10^4	30	2.96×10^5	133	5.44×10^{14}	1035	7.3	1.5	50/50	11	1,829
LP 84-9	7.33×10^4	33	2.91×10^5	131	5.43×10^{14}	1035	8.2	1.6	50/50	11	1,524
LP 84-10	8.00×10^4	36	2.87×10^5	129	5.42×10^{14}	1035	9.0	1.7	50/50	11	2,134
LP 84-11	8.89×10^4	40	3.07×10^5	138	5.41×10^{14}	1035	9.4	1.7	50/50	12	2,378
LP 84-12	7.11×10^4	32	3.07×10^5	138	5.40×10^{14}	1035	7.5	1.5	50/50	12	1,829

The decay constant for spontaneous fission of ^{238}U used is $\lambda_F = 7.03 \times 10^{-17}$ yr^{-1} (Naeser, 1979).

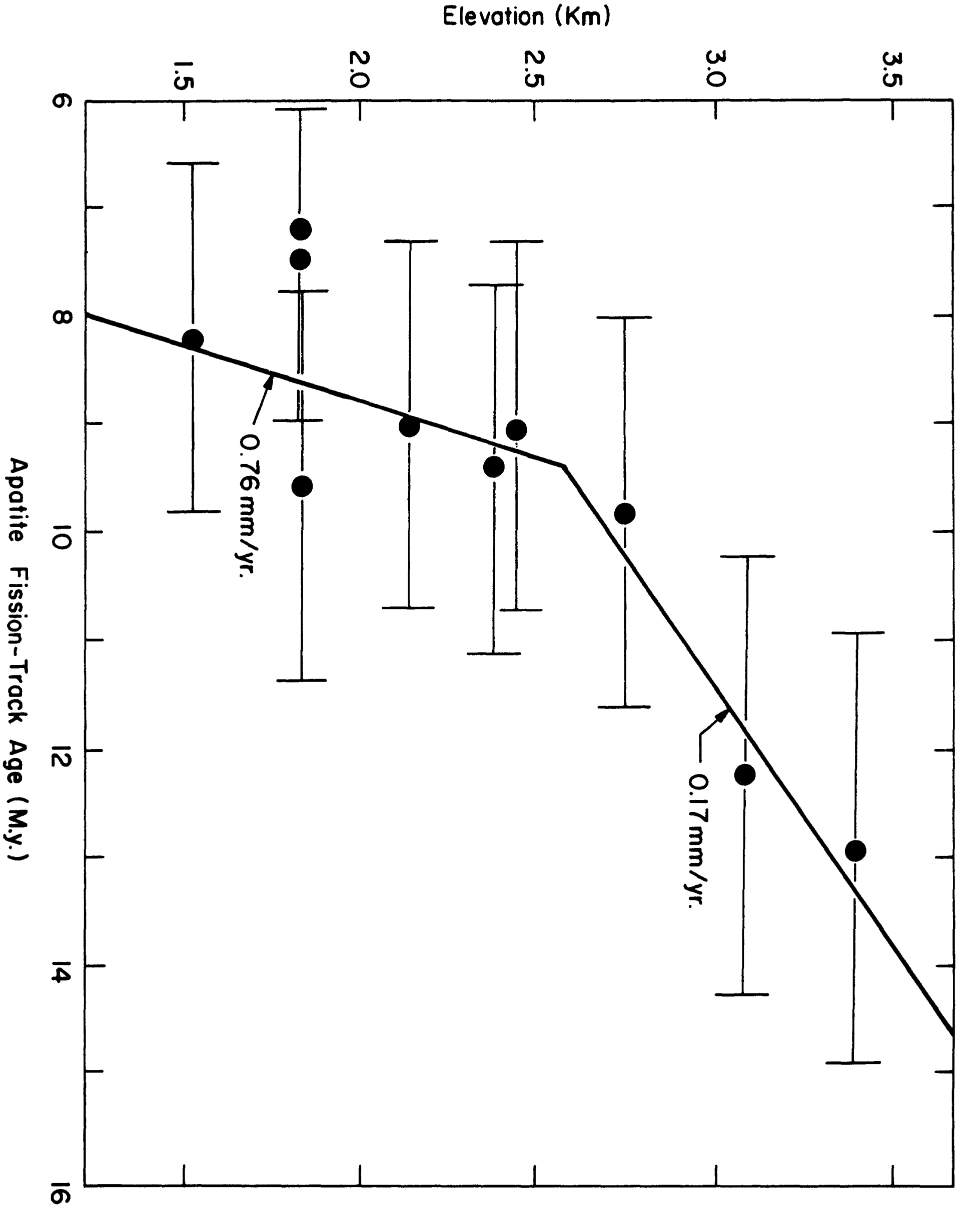

Figure 1. Plot of apparent apatite age versus elevation for samples from the Little Cottonwood stock in the Traverse Mountain area, Utah.

Earthquakes and the Statistics of Crustal Heterogeneity

9930-03008

Bruce R. Julian

Branch of Seismology
U.S. Geological Survey
345 Middlefield Road - MS77
Menlo Park, California 94025
(415) 323-8111 ext. 2931

Investigations

Both the initiation and the stopping of earthquake ruptures are controlled by spatial heterogeneity of the mechanical properties and stress within the earth. Ruptures begin at points where the stress exceeds the strength of the rocks, and propagate until an extended region ("asperity") where the strength exceeds the pre-stress is able to stop rupture growth. The rupture termination process has the greater potential for earthquake prediction, because it controls earthquake size and because it involves a larger, and thus more easily studied, volume within the earth. Knowledge of the distribution of mechanical properties and the stress orientation and magnitude may enable one to anticipate conditions favoring extended rupture propagation. For instance, changes in the slope of the earthquake frequency-magnitude curve ("b-slope"), which have been suggested to be earthquake precursors and which often occur at the time of large earthquakes, are probably caused by an interaction between the stress field and the distribution of heterogeneities within the earth.

The purpose of this project is to develop techniques for determining the small-scale distributions of stress and mechanical properties in the earth. The distributions of elastic moduli and density are the easiest things to determine, using scattered seismic waves. Earthquake mechanisms can be used to infer stress orientation, but with a larger degree of non-uniqueness. Some important questions to be answered are:

** How strong are the heterogeneities as functions of length scale?

** How do the length scales vary with direction?

** What statistical correlations exist between heterogeneities of different parameters?

** How do the heterogeneities vary with depth and from region to region?

Scattered seismic waves provide the best data bearing on these questions. They can be used to determine the three-dimensional spatial power spectra and cross-spectra of heterogeneities in elastic moduli and density in regions from which scattering can be observed. The observations must, however, be made with seismometer arrays to enable propagation direction to be determined. Three-component observations would also be helpful for identifying and separating different wave types and modes of propagation.

The stress within the crust is more difficult to study. Direct observations require deep boreholes and are much too expensive to be practical for mapping small-scale variations. Earthquake mechanisms, on the other hand, are easily studied and reflect the stress orientation and, less directly, its magnitude, but are often not uniquely determined by available data.

This investigation uses earthquake mechanisms and the scattering of seismic waves as tools for studying crustal heterogeneity.

Results

Stress field and tensile crack instability near a magma chamber

Work reported in an earlier semiannual report has shown that, contrary to what is often assumed, fluid-driven tensile cracks can, in some cases, propagate unstably and cause earthquakes. One of the most interesting cases is that of cracks emanating from a pressurized cylindrical or spherical cavity in a homogeneous infinite elastic medium subjected to uniform stresses at infinity, taken to be a model of a magma chamber. During the last six months, we have used published theoretical results of Mindlin for the stress field around a tunnel to compute the stress field around a horizontal cylindrical magma chamber near the surface of a gravitating half space. This analysis shows that the free surface and gravity produce large effects. Furthermore, stress computations based on line sources, which have been the basis of most previous analyses of magma chambers, though reasonably accurate near the surface, are quite inaccurate at depth. The qualitative nature of the stress field above the magma chamber is such as to make tensile cracks more unstable than in an infinite medium, so that larger earthquakes are possible. Work is continuing to analyze crack instability quantitatively and to include the effects of tectonic deformation.

Mechanism of volcanic tremor

Most recent studies of volcanic tremor have considered it to be caused by resonance of magma-filled channels excited by some disturbance such as unsteadily propagating cracks. We have developed an alternative model, which attributes tremor to flow-induced vibrations of the walls of cracks transporting magma. Exact analytic solution of the relevant non-linear differential equations is impractical, but numerical solution shows that such a model does predict tremor-like oscillations for realistic values of crack dimensions, magma properties and flow rates. We have succeeded in deriving the analytic stability criterion that predicts when flow will generate tremor and when it will not, as well as in predicting the frequency of incipient tremor. Work is continuing to derive an approximate analytic expression for the relation between tremor amplitude and frequency.

Modeling seismic-wave codas

Investigations are continuing into seismic-wave coda shapes predicted from a physical model of elastic-wave scattering that takes into account the earthquake source mechanism, the vector nature of elastic waves, and possible anisotropy in the statistical distribution of heterogeneities in the earth. All cases (P-to-P, P-to-S, S-to-P, S-to-S) can now be treated. S-to-S scattering is the strongest, and controls the predicted total coda envelope in most cases. To observe most scattering involving P waves, array observations, which can separate waves of different phase velocity, will be needed. Nevertheless, significant variations in coda shape are predicted, and coda shape alone may be useful in determining earthquake depths and focal mechanisms and the properties of the crust. In the future, we plan to collect data on coda shapes and to compare them with the theoretical predictions.

Long Valley caldera dilatometer

In order to gather data on the earthquake mechanisms at Long Valley caldera, the USGS has installed a Sacks-Evertson dilatometer near the Devil's Postpile, about 3 km southwest of the caldera. The instrument was cemented into the borehole in late 1983, and since September, 1984, both low- and high- frequency data have been telemetered to Menlo Park. About one years worth of low-frequency data have now been collected (Figure 1). The secular strain rate during this interval has been about 10 microstrain per year, which is significantly higher than the rates normally attributed to curing and expansion of cement around newly-installed dilatometers. Furthermore, the strain rate has not decreased with time, as do signals caused by cement curing. The signal therefore probably contains a large component of geophysical origin. Of particular interest is a period of very high strain rate (about 20 to 40 microstrain per year) from April to June, 1985, whose origin is not yet understood. This anomaly may possibly be related to hydrological phenomena, because it corresponds roughly to the time of the spring run-off. If so, similar anomalies can be expected to occur each spring.

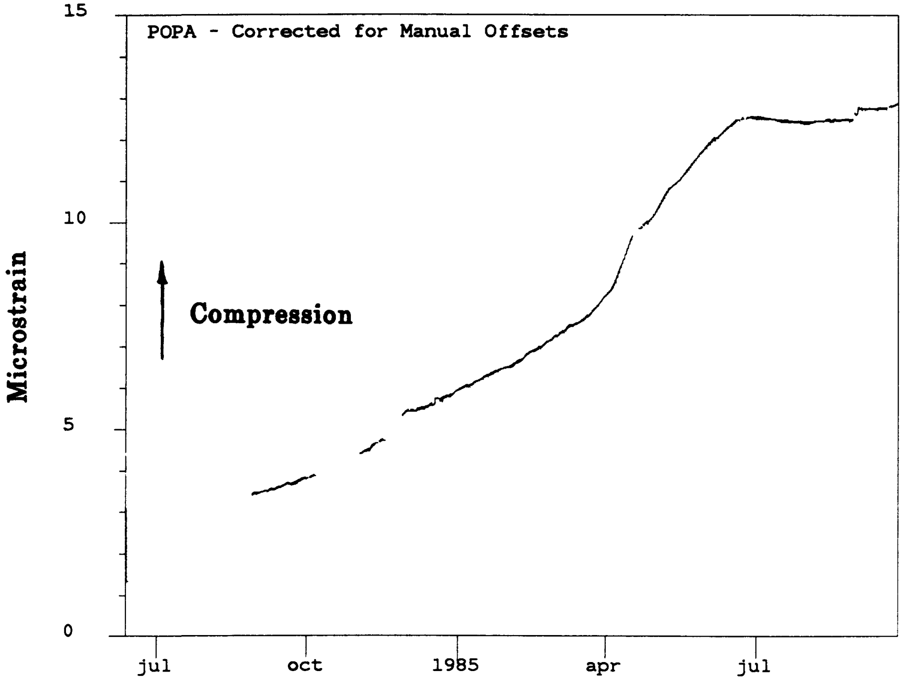

Figure 1: Dilatation measured by Sacks-Evertson dilatometer at the Devil's Postpile, California.

Experimental Rock Mechanics

9960-01180

Stephen H. Kirby
Branch of Tectonophysics
U.S. Geological Survey, MS/977
345 Middlefield Road
Menlo Park, California 94025
(415) 323-8111, Ext. 2872

Investigations

1. Effects of polymorphic phase transformations on mechanical instabilities and strain localization in shear zones.

2. Water weakening of crustal rocks with emphasis on quartz.

3. Constraints placed on the shear stresses supported by the continental lithosphere by the rheological laws of crustal and upper-mantle rocks.

4. Deep lithosphere accommodation of large-scale faulting as studied from deformation structures in mantle xenoliths brought up by basalts that issue from major intraplate fault zones.

5. The rheology of basal slip in single crystal biotite as a guide to the rheology of sheet-silicate-rich shear zones.

Results

1. Two important discoveries have been made in our investigations of phase changes in fault zones. First, trace amounts (< 0.1%) of serpentine reduce the coefficient of friction of an olivine rock by 50% at 400°C compared to samples previously annealed at 600°C above the dehydration temperature of serpentine and then subsequently tested at 400°C. This underscores the potential role of hydration-dehydration reactions in the upper continental crust at $T \leq 600°C$. Second, the polymorphic phase changes ice $I_h \rightarrow$ ice II and tremolite → diopside + talc are now implicated in the shear instabilities observed in ice I_h and tremolite (Kirby, 1985b). The transformations are apparently localized in the shear zones that develop in tests on these materials. Similar polymorphic phase changes occur in deeply-subducted lithosphere and this physical mechanism of shear instability may be in part responsible for the occurrence of deep earthquakes.

2. We have completed a landmark study (Kronenberg, Kirby, Aines, and Rossman, 1985) of the chemical and mechanical interactions of quartz and water under hydrothermal conditions (T = 700-900°C; P_{H_2O} = 400-1560 MPa; t = 10^4-4×10^6 s). After hydrothermal treatment, the initially dry quartz single crystals were examined by infrared spectroscopy. No significant change in water content was observed and the samples remained strong in subsequent tests, in conflict with the discovery experiments of Griggs and Blacic (1964, 1965). We have concluded that the simple diffusional uptake of H_2O is very slow and that microcracking is an important non-equilibrium agent for H_2O uptake in the earlier experiments by others and that such non-equilibrium processes may be also important in the upper crust and limiting the shear stresses in seismogenic zones along faults (Kronenberg and Kirby, 1985).

3. A major review of the rock mechanics literature on crustal and mantle rocks (Kirby, 1985a) indicates that the Moho is likely to be a rheological discontinuity with shear strength increasing discontinuously below the discontinuity. The geological, geophysical and rock mechanics literatures are reviewed with reference to shear zones and strain localization and it is concluded that the state of stress and limiting deviatoric stresses may be controlled by the special rheology of shear zones and faults rather than the bulk rheology of rocks.

4. Kirby, B. C. Hearn, and their Chinese colleagues have discovered peridotite ultramylonite xenoliths in a basaltic volcanic field along the Tancheng-Lujiang fault zone, a major plate-scale rift zone in Eastern China. The chemistries of similar rocks place their depth of origin at 30 to 80 km and their very fine grain size indicates high tectonic stresses in the lower lithosphere in the aseismic depth range in the fault zone (Kirby et al., 1985).

5. Layer-silicate-rich shear zones are commonly observed in fault zones deformed under low- to mid-grade metamorphic conditions and subsequently exhumed by erosion. They typically display a strongly-developed schistosity parallel to the plane of shear and it is likely that intracrystalline slip parallel to (001) contributes to the overall rheology of these shear zones. Kronenberg, Kirby, and Pinkston (1985) and Kronenberg, Pinkston, and Kirby (1985) have completed a preliminary study of the plasticity and rheology of biotite single crystals and salient results are as follows:

   a) Biotite deforming by basal slip exhibits a nearly perfectly plastic behavior with very low strain-rate and temperature sensitivity.

b) No evidence of non-basal slip is observed in compression directions that tend to suppress basal slip.

c) Closure of asymmetric cracks is responsible for the limited plasticity observed in crystals compressed normal to the basal plane.

These results, while preliminary, suggest that the rheology of sheet-silicate-rich shear zones may be remarkably simple, requiring little extrapolation in shear stress.

Reports

Kirby, S. H., 1985a, Rock mechanics observations pertinent to the rheology of the continental lithosphere and the localization of strain along shear zones: Tectonophysics (in press).

Kirby, S. H., 1985b, Localized polymorphic phase transformations as mechanisms for deep earthquakes: Trans. Am. Geophys. Union, v. 66 (in press).

Kirby, S. H., Hearn, B. C., He, Y., and Lin, C., 1985, Geophysical implications of mantle xenoliths: evidence for fault zones in the deep lithosphere: Trans. Am. Geophys. Union, v. 66 (in press).

Kronenberg, A. K., and Kirby, S. H., 1985, The hydrolytic weakening defect in quartz: equilibrium or metastable: Trans. Am. Geophys. Union, v. 66 (in press).

Kronenberg, A. K., Kirby, S. H., Aines, R. D., and Rossman, G. R., 1985, Solubility and diffusional uptake of hydrogen in quartz at high pressures: implications for hydrolytic weakening: Journal of Geophysical Research (in review).

Kronenberg, A. K., Kirby, S. H., and Pinkston, J. C., 1985, Compression of biotite single crystals perpendicular to cleavage: Trans. Am. Geophys. Union, v. 66 (in press).

Kronenberg, A. K., Pinkston, J., and Kirby, S. H., 1985, Rheology of basal slip in biotite, Trans. Am. Geophys. Union, v. 66, p. 366.

3-D Fault Behavior with Rate Dependant Fault Constitutive Laws and Coupling to the Asthenosphere.

14-08-0001-22043

Victor C. Li
Department of Civil Engineering
Massachusetts Institute of Technology
Cambridge, MA 02139
(617) 253-7142

Investigations

Development of numerical procedures for the analysis of surface deformations at plate boundaries, with specific focus on the influence of fault geometry and fault material properties.

Results

1) In the last funding period a quasi-three dimensional model was used to study tectonic scale earthquake rupture in a strike-slip environment. A limited comparison between the San Andreas "free slipping" zone and the numerical model was undertaken in order to demonstrate the soundness of the approach. The model gave plausible values for surface strain rates as well as for slip rates.

The three-dimensional model is that of a slip front penetrating through an elastic lithosphere under the effect of tectonic plate movement, the coupling of the lithosphere to the viscous asthenosphere is not included in the model. The physical approximation of the problem thus formulated is solved by means of a line spring model which reduces part-through crack problems in plates to two two-dimensional problems.

The current focus was on the effect of along strike and depth strength inhomogeneities on the control of the rupture processes. Two limiting cases of variation along strike were discussed in detail. The two cases are: i) An asperity zone imbedded in a uniform strength fault, ii) A free slipping zone separating two uniform strength fault regions.

The time and spatial evolution of fault slip, fault stress and surface strain, and rates of these quantities for each case was studied in relation to slip penetration into the seismogenic zone leading to an earthquake instability (see e.g. figures 1-4). The calculated results provide plausible interpretation of precursory seismicity and location of nucleation of earthquake ruptures, such as stress unloading, increased slippage rates and change in the variation of slippage rates along strike just prior to instability. However, detailed comparisons of the numerical results with field data must await further work in parametric studies. In addition, strong limitations of interpretation of numerical results may be expected due to negligence of coupling of the lithosphere to the asthenosphere.

The above work indicates the soundness of the use of instability models in analyzing pre-seismic behavior, but requires further refinement. Current efforts are directed towards including the effect of the asthenosphere in a full three-dimensional model of slippage surfaces penetrating an elastic plate that is underlain by a visco-elastic foundation.

Results of the above effort was presented by Li and Fares in an invited paper at the 5th Maurice Ewing Symposium on Earthquake Source Mechanics.

2) A numerical technique for solving two-dimensional problems containing discontinuity lines with finite or infinite boundaries was developed. The accuracy and versatility of the method in solving multiple crack problems having infinite boundaries and nonlinear boundary conditions along the crack was demonstrated. The method was found to be not very efficient when finite boundaries were involved although acceptable results were obtained.

The method is based on a modified indirect boundary element method having dislocation dipoles as the fundamental Green's function that is used to build up the elements. The type of elements used was allowed to be very general through the use of a specialized numerical integration technique. Some of the elements formulated were found to be especially useful and efficient, for example an "ellipse multiplied by a polynomial expansion" element was found to yield excellent results when studying multiple sharp cracks in infinite space, and "zero slope cracktip" elements were used for the simulation of slip-weakening zones. The method was used as a basis to treat quasi three-dimensional problems dealing with plate boundary deformations as described above.

Extensions of the above work to full three-dimensional time-dependent layered medium problems is under investigation. In addition, the coupling of the above technique to a finite element hybrid scheme developed by Cleary et al. (1981-1985) to handle the finite boundary effects more efficiently is currently being developed.

Reports and Publications

Li, V.C. and N. Fares, Control of rupture processes by asperities and creep zones, 5th Maurice Ewing Symposium on Earthquake Source Mechanics, July 1985.

Fares, N., Solution of 2-D crack problems by a superposition method - application to part-through cracks, S.M. thesis, MIT, 1985.

Fares, N. and V.C. Li, An indirect boundary element method for 2-D finite/infinite regions with multiple displacement discontinuities, in preperation, 1985.

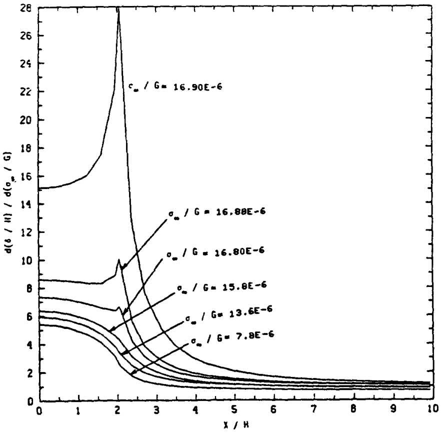

Figure 1

Distribution of slip rates at various times for the creep zone case. The parabolic shape is disturbed by the slip acceleration at the edge of the creep zone towards the later part of the earthquake cycle.

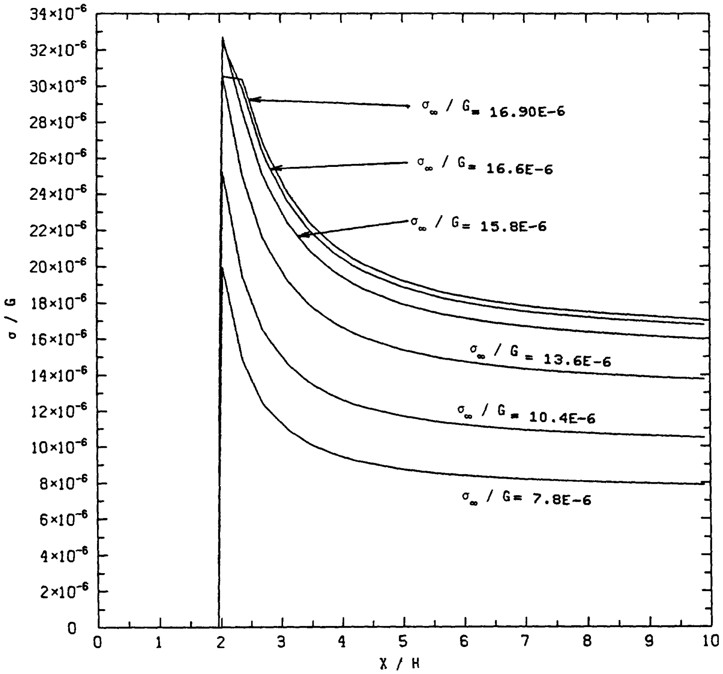

Figure 2

Stress concetration at the edge of a creep segment, eventually leading to failure at this location. The last two time steps shown indicate softening just outside the creep zone. The stress decays to the remote level at large X.

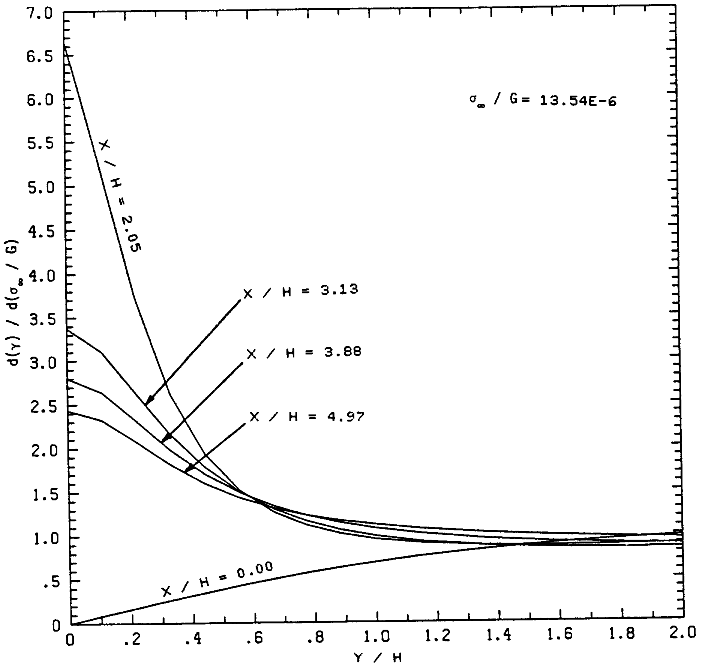

Figure 3

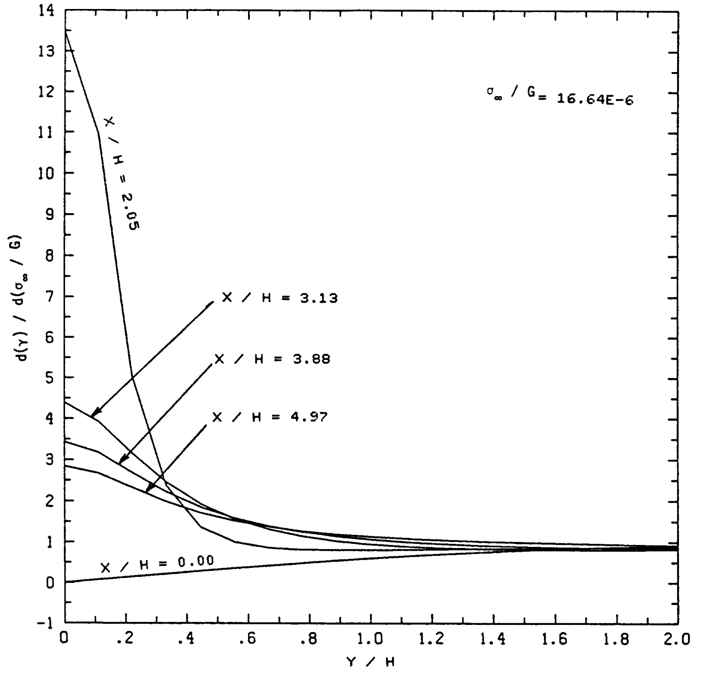

Figure 4

Surface shear strain rate profiles at five locations and at two time frames for the creep zone case.

ANALYSIS OF REFLECTION SURVEY DATA ON THE SAN ANDREAS FAULT ZONE FOR VELOCITY AND ATTENUATION PROPERTIES

Grant 14-08-0001-G-950

T. V. McEvilly
J. Scheiner

Seismographic Stations
Department of Geology and Geophysics
University of California, Berkeley

FINAL REPORT SUMMARY

The crustal velocity and attenuation profiles in the San Benito, California region have been carefully and extensively studied using several different methods and approaches. The data set used has been a deep seismic reflection survey conducted by CGG in 1978; conventional reflection processing for the velocity study using Digicon's software package, DISCO, has been complemented by the inversion procedure set forth by May and Covey (1981). The resulting velocity models of this report and of Feng and McEvilly (1983) are consistent with those of previous investigations. These models generally indicate a rather strongly heterogeneous structure characterized most prominently by a low velocity fault zone surrounded by the bounding crusts of Gabilan granite to the west and the Franciscan melange in the Diablo range to the east. There is evidence of structural and/or compositional contrast at mid-crustal depth, ($\sim$9 km) in the granitic crust; Lynn et al. (1981) have proposed that this represents the basal contact of the granitic batholith and that the transition itself can be explained as resulting from reaction melting and cumulative layering. Continued study of this feature using wide-angle reflection and refraction data is proposed in order to constrain the structure above and below the transition.

Reflectivity is generally poor in the Franciscan crust and it has been suggested that this is due in part to the heterogeneity characteristic of this melange. The attenuation profile of the two crusts and the fault zone has been studied under a weak scattering hypothesis as well as with a diffusion approach. The apparent coda Q factor tends under both models to decrease slightly eastward; however, the effect is not unambiguous. Both methods of inversion depend on good signal to noise ratio as well as the existence of strong spatially coherent reflectors to serve as primary arrivals of energy from which the coda decay. Results using filtered data show a consistent increase of apparent Q with frequency; there is a slight tendency for this frequency dependence to be stronger in the granitic crust than in the Franciscan crust. This very interesting result may be indicative of the dominant attenuation mechanism; however, the difficult question of partitioning of the intrinsic and (elastic) scattering attenuation mechanisms remains since either may be frequency dependent.

The results of this study serve to illuminate the velocity and attenuation profiles of this very important seismically active segment of the San Andreas fault zone and its bounding crusts. It is essential that a refinement of the velocity structure be accomplished using many different methods; it is hoped that hypocenter location problems, distortions in radiation patterns, and travel time and slowness anomalies may be understood more completely given such a refinement. Finally, the attenuation characteristics of this region are poorly understood; comparison of these results with those of other investigations in this and other regions using both natural and artificial sources is imperative if we are to comprehend the effects of attenuation on seismic data.

REFERENCES

Feng, R. and T. V. McEvilly (1983). Interpretation of seismic reflection profiling data for the structure of the San Andreas fault zone, Bull. Seism. Soc. Am., 73, 1701-1720.

Lynn, H. B., L. D. Hale and G. A. Thompson (1981). Seismic reflections from the basal contacts of batholiths, J. of Geophys. Res., 86, 10633-10638.

May, B. T. and J. D. Covey (1981). An inverse ray method for computing geologic structures from seismic reflections - zero offset case, Geophysics, 46, 268-287.

Stressing, Seismicity and Rupture of Slip-Deficient Fault Zones

14-08-0001-G-823

J.R. Rice (P.I.) and R. Dmowska
Division of Applied Sciences and
Department of Geological Sciences,
Harvard University
Cambridge, MA 02138
(617) 495-3445

Investigations

1. Continuing our work on stress accumulation and instability modelling, a depth-variable description of strike slip, modelled by using a laboratory constrained slip rate, slip history and temperature dependent frictional law for Westerly granite and a Lachenbruch-Sass San Andreas fault geotherm, is extended to study the different slipping processes and stressing interactions on the fault surface resulting from different frictional slip properties and inclusion of dynamic overshoot in stress drop during an instability.

2. An elementary mechanical model of stress accumulation along a subducting slab and stress transfer to the thrust zone during the whole earthquake cycle is being considered. This is based on a one-spatial-dimension Elsasser type model for the slab, subjected to steady gravitational sinking forces, with the great thrust zone earthquakes appearing as sudden stress relieving displacements of an otherwise fixed end of the slab. Results are being interpreted in terms of stress replenishment by migration of extensional deformation upwards along the slab, and correlations are sought with seismicity systematics throughout the cycle as discussed recently by McNally and co-workers for the Middle American Trench.

3. Stress drops of moderate foreshocks and aftershocks related to the Petatlan, Mexico (March 14, 1979, Ms=7.6) earthquake and their relation to precursory deformation are being studied. The work aims at comparison of stress drops of moderate ($5.4 \leqslant M \leqslant 5.8$) earthquakes, preceding the main shock by 1.5 months and forming a cluster at one end of seismically quiet zone, with stress drops of earthquakes of similar magnitude coming from the same area, but occurring during other parts of the earthquake cycle (many years before or after the main shock).

Results

1. The constitutive law, which was developed by Dieterich, Ruina and others, is characterized by a positive instantaneous rate sensitivity and an exponential (monotonic) decay of stress towards a steady state stress at fixed slip speed over a characteristic slip distance L. A uniform strike-slip fault is simulated by two oppositely sliding elastic plates with top and bottom surfaces traction free. Remote stress, originating from deeper mantle motions, is applied consistently with an appropriate relative plate velocity (35 mm/yr). An improved and fast numerical scheme is also implemented. Many multi-cycle earthquake simulations were performed to study the effects of different frictional slip properties and dynamic overshoot in stress. Fig. 1 shows the depth distributions of slip from an earthquake simulation for the case C2L40L00 (i.e., L=40 mm, levelling off of steady state stress at speed above 0.1 mm/sec and without dynamic overshoot in stress) for a time history of three earthquake

cycles. Each line represents a constant time. Fig. 1 shows the features such as the shallow depth region being locked for most of the cycle time, the rupture initiation at about 7 km, stopping of rupture at about 14 km, rapid post-seismic slip below and extending to about 18 km and the region at greater depth being only modestly perturbed by rupture above. The results indicate the shallow depth confinement of seismicity and the overall features are compatible with those observed along the San Andreas fault. Fig. 2 to Fig. 4 show examples of other simulations with dynamic overshoot in stress (30%, Fig. 2) and different frictional slip properties (such as L=10 mm in Fig. 3; smaller $B-A=-d\tau^{ss}/d\ln V$ in the shallow crust in Fig. 4). In general, smaller L gives rise to smaller pre-seismic slip and shorter cycle time. Inclusion of dynamic overshoot in stress during an instability generally increases the cycle time, seismic slip, rupture extent, etc. Also, a larger portion of total slip dissipated as pre-seismic slip is predicted for smaller B-A (compare Fig. 4 to Fig. 1). Simulations were also performed with L ranging from 160 mm down to 5 mm for the particular frictional slip properties distributions and loading environment. For L above 160 mm, no earthquakes are produced even with large perturbations from steady slip. Between 80 and 160 mm, slipping is transitional indicating a possible creep event. Below 80 mm, earthquake instability always occurs. With depth variations of the frictional slip properties such that there is velocity strengthening near the Earth's surface, a confined earthquake at some depth (i.e., no surface break) can possibly be simulated. The results of the simulations also provide information on the surface deformations. Mid-cycle surface shear strain rates near the fault are compatible with those summarized recently by Thatcher (1983 JGR), and predicted precursory strain signals are being examined.

2. In our present model of a gravitationally sinking slab at a subduction zone, motion is resisted by the surrounding viscoelastic upper mantle and is prohibited, except during earthquakes, by contact with the over-riding plate at the brittle stick-slipping thrust zone. At some large depth the mantle resistance is in steady state equilibrium with the gravitational forces and the slab sinks with uniform velocity V, equated to the relative plate velocity. An elementary first model has been developed which treats the slab as a one-dimensional continuum and approximates mantle shear interactions at the slab surfaces in a generalized Elsasser sense. The present model ignores or simplifies much interesting physics (slab bending, thermal stressing, slab-mantle interactions) and particularly simplifies conditions at the contact zone. Nevertheless, we feel that it is a useful first model to study the time-dependence of stress accumulation throughout the earthquake cycle and to seek correlations with times and locations at which intermediate depth extensional and thrust zone seismicity becomes active or inactive. (An interesting data set for comparison has been assembled recently by McNally et al. based on a composite of recent seismicity from several zones along the Middle American Trench, with time axis shifted and normalized to a given cycle time so that whole-cycle trends can be revealed).

The extensional stress $\sigma(x,t)$ in a slab of thickness H, subjected to a steady down-slab component of gravity force $f(x)$ from density mis-match and to resisting shear stresses $\tau(x,t)$ at both faces, must satisfy

$$\partial\sigma/\partial x + f = 2\tau/H \ .$$

For plane strain extension σ is related to displacement $u(x,t)$ by

$$\sigma = [2\mu/(1-\nu)]\partial u/\partial x \quad (\mu = \text{shear modulus, } \nu = \text{Poisson ratio})$$

and, within a generalized Elsasser model for slab interaction with a Maxwellian viscoelastic mantle,

$$\partial u/\partial t = (b/\mu)(\partial \tau/\partial t + \tau/t_r)$$

where b is an effective shear interaction length scale and t_r a shear relaxation time. (Results for the time-dependence of stressing are unchanged by replacing $\partial u/\partial t$ by $\partial u/\partial t - v_o(x)$, where $v_o(x)$ is the effectively steady mantle flow velocity at some distance b from the slab). The boundary condition is that at x=0, representing the thrust contact zone,

$$u(o,t) = VT\sum_m U(t-mT) \ , \quad m = \ldots,-2,-1,0,1,2,\ldots$$

where T is cycle time and U the unit step function; VT is the earthquake displacement.

By Fourier analysis methods we have shown that the solution for $\sigma(x,t)$ consists of the sum of a steady time-independent part $\sigma_s(x)$ and a periodic part $\sigma_p(x,t)$, with zero time average over the cycle, given by

$$\sigma_p(x,t) = -\ [2\mu VT/(1-\nu)L]\ \mathrm{Im}\left[\sum_n (\rho_n/\pi n)\exp(-\rho_n x/L+2\pi int/T)\right] ,$$

n = 1,2,3,... . Here $L^2 = Hb/(1-\nu)$ and ρ_n denotes the set of complex numbers, with $\mathrm{Re}(\rho_n) > 0$, given by

$$\rho_n = [2\pi in/(2\pi in + T/t_r)]^{1/2} .$$

Currently we are evaluating the series, after introducing measures to accelerate its painfully slow convergence (related to the step changes induced in σ at the time of each earthquake). Fuller results will be given in a subsequent report.

3. The objective of this part of our work is the comparison of stress drops of moderate earthquakes preceding the main shock and forming a cluster, with stress drops of earthquakes of similar magnitude coming from the same area but occurring during other parts of the earthquake cycle. Our purpose is to search for possible evidence of higher stresses present in the region of the future main shock during the precursory stage of the earthquake cycle. The cluster earthquakes that are being analyzed are located at the southeast end of the then quiet zone (three earthquakes that occurred on 26 Jan. 1979, with magnitudes m_b=5.4, 5.4 and 5.8). The comparison earthquakes come from the area of up to 100 km distant from the cluster events and include earthquakes of m_b=6.0 (9 Dec. 1965), m_b=5.9 (2 July 1968) and m_b=5.6 (16 July 1973), which occurred before the main Petatlan shock (14 March 1979), and two earthquakes that occurred after the main shock: m_b=5.4 (18 March 1979) and m_b=5.4 (2 Jan. 1982).

We are collecting and beginning to analyze the data. For the evaluation of the dynamic stress drops, the method introduced by Boatwright (1980) and used by Mori (1983) and Shimazaki (1985) will be followed, based on the slope of the initial rupture phase on the velocity recording. However, due to very limited number of good digital recordings of our events, we will complement the stress-drop estimates by Brune's stress drops, with the use of WWSSN records and measurements of moment and duration of displacement pulse. Work is in progress.

Publications

Dmowska R., V.C. Li and J.R. Rice, Nonuniform stressing in the Parkfield region from interactions between adjacent creeping and locked fault zones (abstract), *EOS, Trans. Am. Geophys. Union*, 66, in press, 1985.

Gao, H. and J.R. Rice, Shear stress intensity factors for a planar crack with slightly curved front, submitted to *J. Appl. Mech.*, 1985.

Rice, J.R. and S.T. Tse, Dynamic motion of a single degree of freedom system following a rate and state dependent friction law, *J. Geophys. Res.*, in press, 1985.

Rice, J.R., First-order variation in elastic fields due to variation in location of a planar crack front, *J. Appl. Mech.*, 52, N.3, pp. 571-579, 1985.

Tse, S.T., R. Dmowska and J.R. Rice, Stressing of locked patches along a creeping fault, *Bull. Seism. Soc. Am.*, 75, N.3, pp. 709-736, 1985.

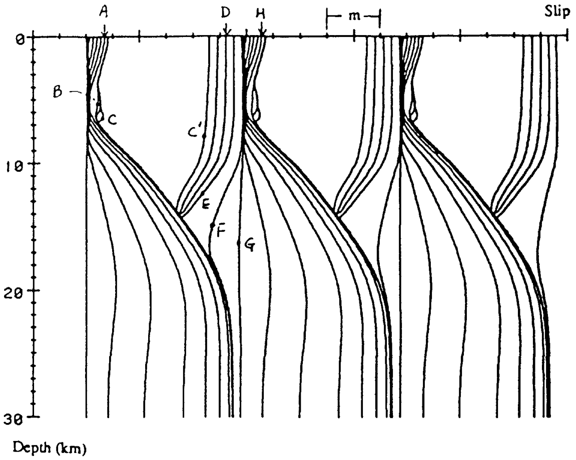

	Time Interval
A to B	2.4 yrs.
B to C	4.6 hrs.
C to C'	instantaneous
C' to D	4 secs.
D to E	3.5 mins.
E to F	77.8 days
F to G	3.6 yrs.
G to H	77.2 yrs.

$T_{cy} = 83.8$ yrs.

C2L40L00

FIG.1.

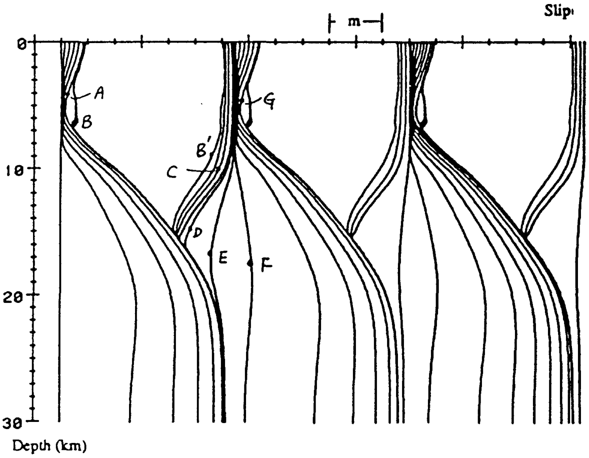

	Time Interval
A to B	300 days
B to B'	intantaneous
B' to C	2.5 mins.
C to D	4.2 days
D to E	1.9 yrs.
E to F	9.1 yrs.
F to G	82.5 yrs.

$T_{cy} = 92.9$ yrs.

C2L40L30

FIG.2.

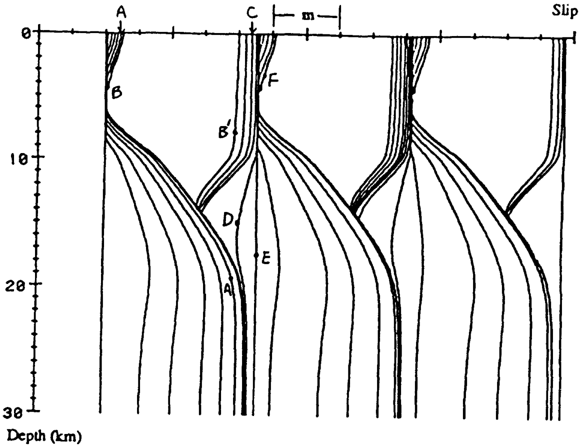

	Time Interval
A to B	4.9 yrs.
B to B'	instantaneous
B' to C	12 secs.
C to D	296 days
D to E	2.9 yrs.
E to F	61.6 yrs.

$T_{cy} = 65.3$ yrs.

C2L10L00

FIG. 3.

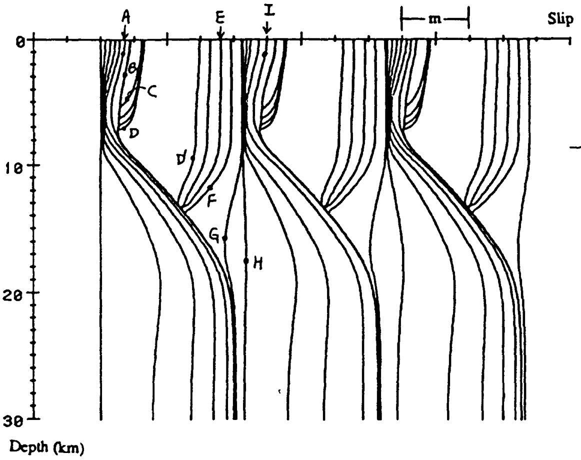

	Time Interval
A to B	107 days
B to C	10.3 hrs.
C to D	1.3 mins.
D to D'	instantaneous
D' to E	7 secs.
E to F	12 mins.
F to G	305 days
G to H	3.2 yrs.
H to I	56.5 yrs.

$T_{cy} = 60.8$ yrs.

C1L40L00

FIG. 4.

Rock Deformation

9950-00409

Eugene C. Robertson
Branch of Engineering Geology and Tectonics
U. S. Geological Survey
922 National Center
Reston, VA 22092
(703) 860-7404

Investigations

Tests of 23 samples of granite, 28 of basalt, and 12 of limestone in a torsion pendulum at 50 to 88 percent of their average tensile strengths were made to observe their anelastic and elastic behavior with advent of fracturing to failure.

Results

In carrying out the study of recovery of linear and nonlinear torsional deformation of granite, basalt, and limestone samples, many of them were carried to failure, in about 10 successive increments of strain (each about 1×10^{-4} units) from 0.1×10^{-4} to 10×10^{-4} strain units. In each run the sample oscillations (at 5 Hz) were allowed to decay from the initial strain to some very low strain. The failures were all in tension on a spiral surface, very close to the theoretical 45-degree angle from the shear plane, which lies between the maximum tensile and compressive stresses. Tensile strengths of rock are about 10 times less than compressive strengths, which accounts for the failure mode. Average tensile strengths of about 10 samples of each rock were as follows: basalt, 400 bars; granite, 300 bars; and limestone, 200 bars. The standard deviation is about 30 bars for each. Two examples can provide details of behavior.

In a fatigue study of a granite sample, 10 successive experiments were each initially deflected to 4×10^{-4} strain units, at about 50 percent of the tensile strength. After the tenth run, the sample failed. There was no perceptible residual strain in the sample after each run, and the rigidity recovered to within 0.05 percent of its low-strain value (0.3990 Mb). A possible permanent weakening was indicated by a decrease of 0.6 percent of the initial deflection rigidity from the first to the tenth run.

This weakening under the initial high strain with full recovery at the end of the run, at a very low strain, was observed in more detail in a series of 58 runs on a sample of basalt. The results are shown in Figure 1: cycle 1 of pairs of runs to 65 percent of tensile strength, cycle 2 of pairs of runs to 88 percent of tensile strength, and cycle 3 of single runs to 88 percent of the strength. The stress-strain curve ($\sigma - \gamma$)

shows representative points from strains of 10^{-5} to $6x10^{-4}$ strain units; above $6x10^{-4}$ units, there was a nonlinear strain hardening from cycle 1 to cycle 2 to cycle 3, indicating a memory of the previous deformation history. The rigidity (G) decreases with increasing load increments; it also shows a stengthening increase from cycles 1 to 3. Finally, the attenuation (α) also increases anomalously at strains above $6x10^{-4}$ in cycles 1,2, and 3. After each of the 58 runs, the rigidity and attenuation recovered their low-strain values, all runs returning down the same curves as the stress decayed. The nonlinear anelastic deformation, under tensile stresses of 50 to 88 percent of the strength, is recovered, but the history of the deformation is imprinted, and when tested to higher stresses would eventually lead to failure.

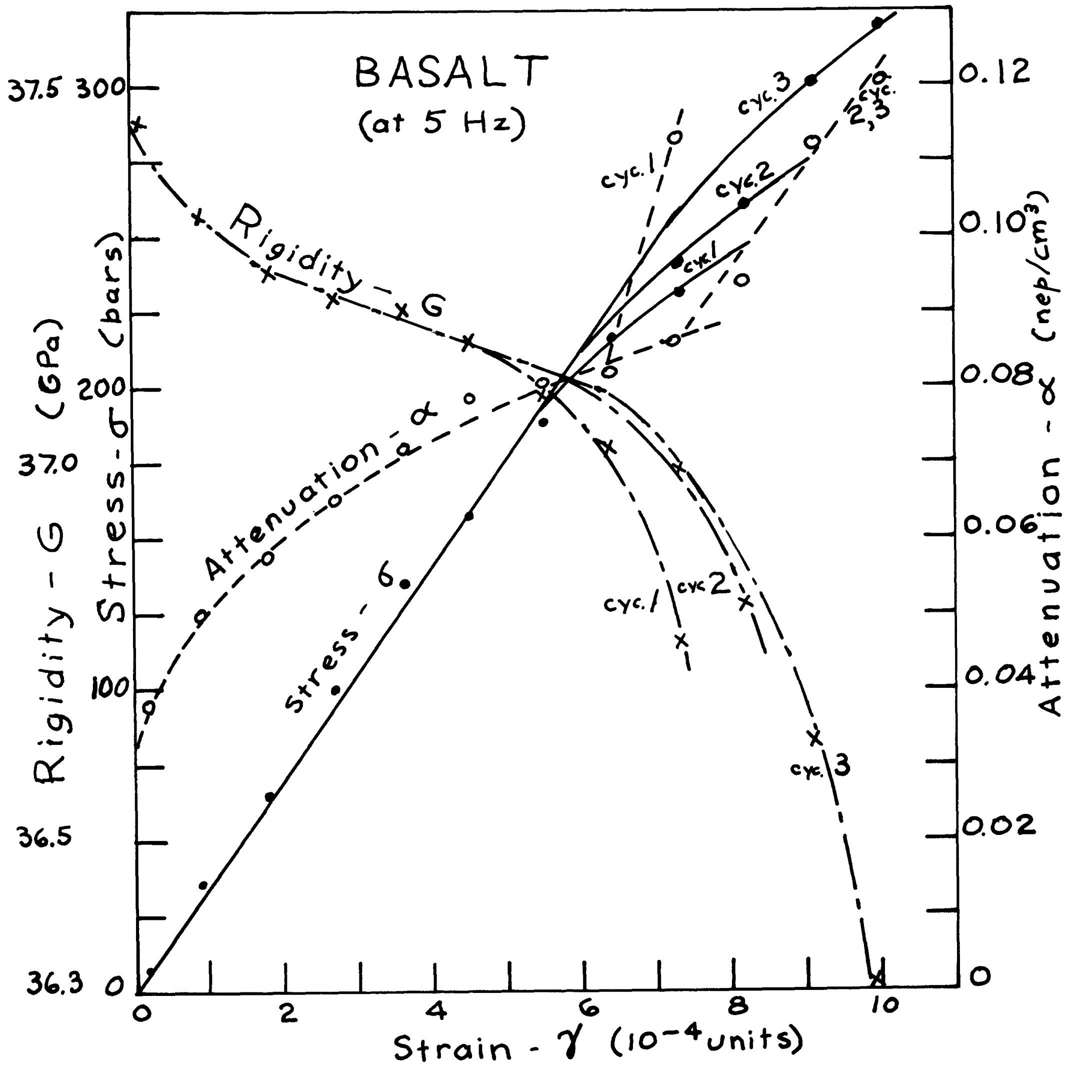

Heat Flow and Tectonic Studies
9960-01177

John H. Sass
Branch of Tectonophysics
U.S. Geological Survey
2255 North Gemini Drive
Flagstaff, Arizona 86001
(602) 527-7226
FTS: 765-7226

Arthur H. Lachenbruch
Branch of Tectonophysics
U.S. Geological Survey
345 Middlefield Road
Menlo Park, California 94025
(415) 323-8111, ext. 2272
FTS: 467-2272

Investigations:

1. Heat flow and tectonics of the Western United States.

Four wells were drilled to ~200 m in the SE Mojave Block along the original CALCRUST Vibroseis line (Figure 1).

Temperature measurements disturbed to an unknown extent by clean-out operations were obtained to a depth of nearly 1 km in the Cajon Pass well.

Temperature measurements were obtained in several key areas of the Mojave and Sonoran deserts in California and Arizona from holes drilled by mining and industry sources.

A hoist unit was modified and equipped with a high-temperature (320°C) corrosion-resistant single-conductor cable for deployment of instruments during the Salton Sea Scientific Drilling Project (SSSDP).

An Appolo-era lab trailer was also refitted for use as Science Headquarters for the SSSDP.

2. Heat flow, climatic history, and tectonics of Alaska.

Simple, one-dimensional climatic models may be used to infer amplitudes and durations of climatic disturbances during the past century or so from curvature of temperature profiles in the upper 100 meters of the permafrost of the North Slope of Alaska.

Heat-flow estimates from wells in the National Petroleum Reserve, Alaska (NPRA) are complete, and studies of the structure and hydrology of the basin have been initiated.

Results:

1. Heat flow and tectonics of the Western United States. Thermal conductivity measurements have not been completed, but preliminary gradients indicate heat flows from the new sites in SE California (Figure 1) compatible with the map of Lachenbruch and others (1985). The Salton Sea Scientific Drilling Program (SSSDP) involves a research well situated near the southeast end of the Salton Sea in the Salton trough, a tectonic depression within the

transition zone between the spreading centers of the Gulf of California and the San Andreas transform fault. The drill site is near the hottest part of the Salton Sea Geothermal Field as deduced from temperatures in previously drilled deep wells and temperatures extrapolated from shallow (~50-100 m) wells. The well is being drilled using standard technology but is different from conventional exploration or production wells in a number of ways, chief among which is the priority of scientific over economic objectives. The primary goals are to study the processes involved in an active, magmatically driven hydrothermal system. The temperatures, pressures and salinities in the well provide an opportunity for the evaluation of geothermal energy potential and a convenient laboratory for the study of greenschist metamorphism and hydrothermal ore formation in situ.

2. Heat flow and hydrology of Yucca Mountain tuffs. Heat flow in the unsaturated zone varies systematically over the Yucca Mountain area. The proposed repository site (near USW G-4, Figure 2) is in the center of a large low (<40 $\mathrm{mWm^{-2}}$). To the south, heat flows are greater than 60 $\mathrm{mWm^{-2}}$, typical of Basin and Range conductive heat fluxes. The abnormally low heat fluxes seem to be controlled by fluid movement in the saturated tuffs and the underlying Paleozoic basement rocks.

3. Heat flow, climatic history, and tectonics of Alaska.

Temperature profiles we have measured in permafrost on the Alaskan North Slope usually have anomalous curvature in the upper 100 meters or so. When analyzed by heat-conduction theory, they indicate a variable but widespread secular warming of the permafrost surface, generally in the range of 2°-4°C over the last few decades to a century. Although details of the form of the change are not resolvable with existing data, there is little doubt of the general magnitude of these quantities; heat transfer in cold permafrost is exclusively by conduction which allows few alternative explanations. As models of greenhouse warming predict that early warnings will be most observable in the arctic, and might in fact be in progress already, it is important to understand the rapidly changing thermal regime in this region. A manuscript on the problem is in preparation.

Heat flow increases systematically from about 50 $\mathrm{mWm^{-2}}$ the North Slope of of the Brooks Range to about 90 $\mathrm{mWm^{-2}}$ near the Coast between Point Barrow and Atigaru Point. This distribution of heat flows cannot be related to either climatic history or to Late Tertiary-Quaternary tectonic activity. We are presently investigating the structural and hydrologic regimes of the Basin in an attempt to find an explanation for the observed heat flow.

Reports:

Bills, D. J., and Sass, J. H., 1985, Hydrologic and near-surface thermal regimes of the San Francisco volcanic field: U.S. Geological Survey Professional Paper, in press.

DeRito, R. F., Cozzarelli, F. A., and Hodge, D. S., 1986, A forward approach to the problem of temperature and the long-term thickness of the mechanical lithosphere (Branch approval, May 1985).

Lachenbruch, A. H., Sass, J. H., and Galanis, S. P., Jr., 1985, Heat flow in southernmost California and the origin of the Salton Trough: Journal of Geophysical Research, v. 90, p. 6709-6736.

Pollack, H. N., and Sass, J. H., 1985, Thermal regime of the lithosphere, _in_ Haenel, R., Rybach, L., and Stegna, L., eds., Handbook of Terrestrial Heat-Flow Density Determination (Guidelines and Recommendations of the International Heat Flow Commission), in press.

Sass, J. H., Hendricks, J. D., Priest, S., and Robison, L., 1986, The Salton Sea Scientific Drilling Program--A progress report (abstract): Submitted to McKelvey Symposium on Energy Resources.

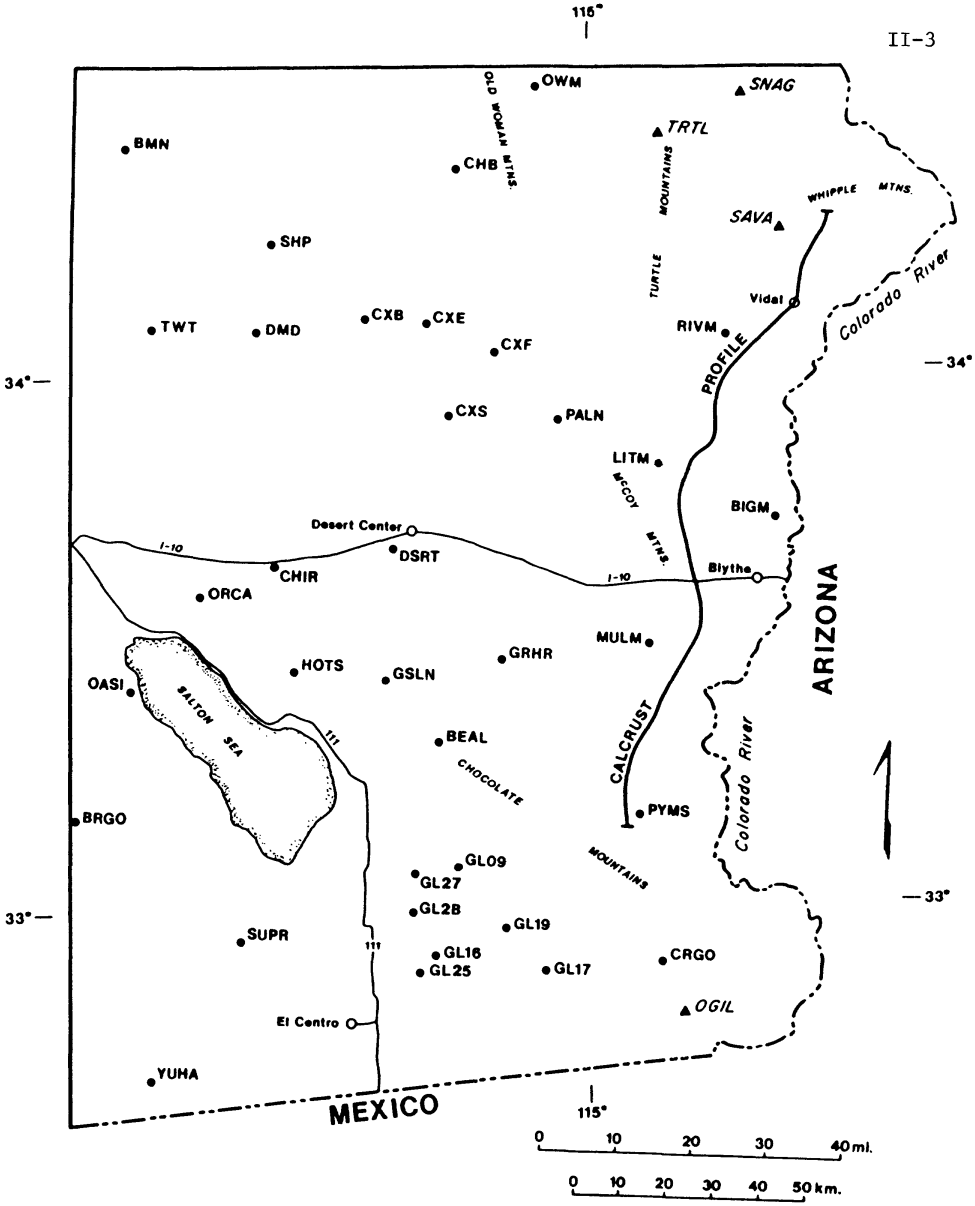

Figure 1. Sketch map of southeasternmost California with existing heat flow control (dots), the CALCRUST profile, and new sites in crystalline rock (triangles).

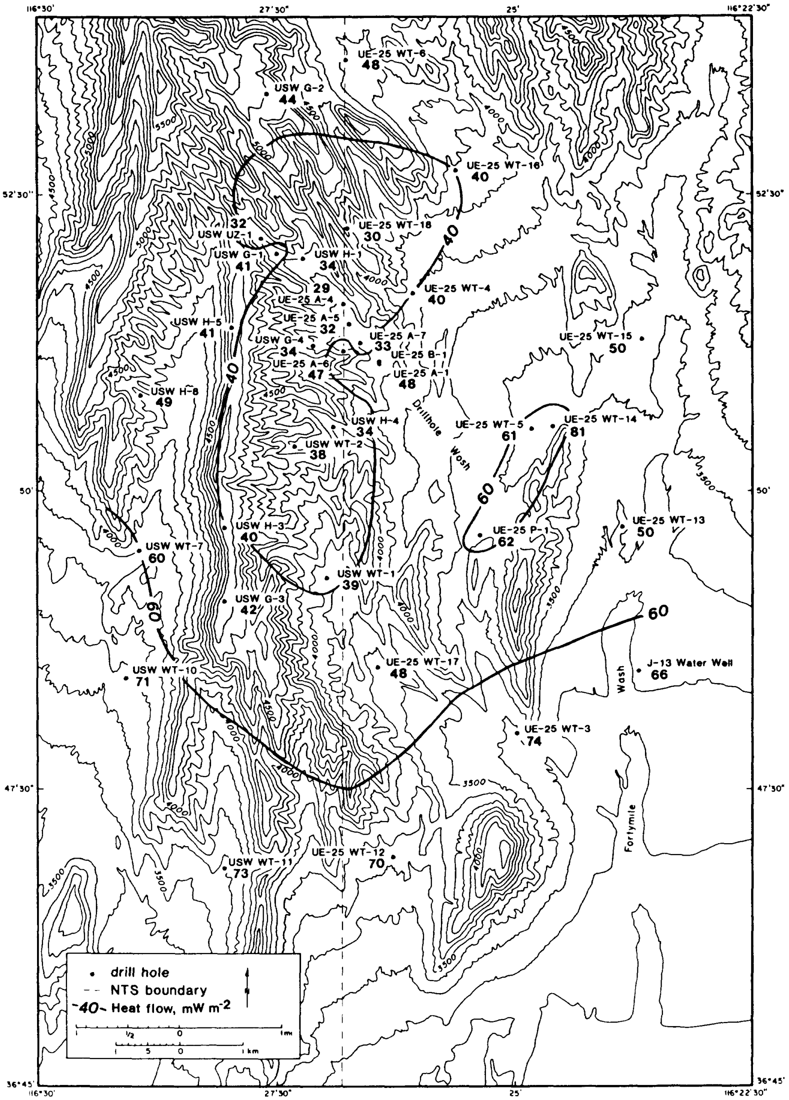

Figure 2. Heat flow in the unsaturated zone, Yucca Mountain, Nevada.

Systems Analysis of Geologic Rate Processes

9980-02798

Herbert R. Shaw and Anne E Gartner
Branch of Igneous and Geothermal Processes, U. S. Geological Survey
MS-910, 345 Middlefield Road, Menlo Park, CA 94025
(415) 323-8111, X4169, X4170

Objective: The work on this project has the objective of dynamic interpretation of paleoseismic data compiled by Shaw and others (1981). An aspect is the interpretation of self-similarity and fractal geometry of fault sets.

Results: The fractal character of faulting has now been measured in several different ways by us and other workers (e.g., Shaw and others, 1981; Shaw and Gartner, 1981; Shaw and Gartner, 1984; Shaw and Gartner, 1985; King, 1984; Okubo and Aki, in press; Aviles, written communication, 9 Aug. 1985). We conclude that no single-valued fractal dimension can be expected for a given set of faults, a single fault, or even for a single segment of a well-defined fault. The fractal concept applied to the earthquake process is of complex geometric and dynamic character, hence the fractal dimension is a property of spatial sets that change with time at different rates at different scales of measurement.

Scale invariance (or self-similarity) defined either on the basis of standard Euclidian or fractal geometries is a special condition that can be approximated only within limited spatial domains and/or time windows of behavior. In this sense quantification of the geometrical properties of fault systems has a closer resemblance to the problem of defining the structure of clouds over different scales of time and size than it does the measurement of coastline lengths of islands at different scales. The latter is a frequently cited metaphor for the application of fractal geometry to fault systems.

The problem of variable fractal dimensions in the earthquake process is illustrated in Figure 1. There, self-consistent fractal dimensions are plotted versus the b-value of the frequency-magnitude relation and the c-value of the moment-magnitude relation based on the relationship derived by Aki (1981). The Aki relation is given by the identity $D = 3\ b/c$, where D is the fractal dimension relative to a maximum topological dimension of 3; D attains this value only if the special condition defined by $b = c$ can be realized. This condition depends both on the branching character of coseismic faulting at different scales and the way the magnitude moment is defined (e.g., Hanks and Boore, 1984). That is to say, the Aki relation essentially expresses a proportionality between coseismic fault lengths and the source volume for the seismic moment. Some interesting paradoxes emerge from these comparisons. Fractal self-similarity is represented by lines of constant D in Figure 1. But any generalized history of fault-related earthquakes describes a variable path through fractal space. A simple kind of deviation sometimes observed is represented by an oscillation between high and low b-values at a constant c-value. However, if the c-values increase at the larger moments and magnitudes, as inferred by Hanks and Boore (1984), a zig-zag oscillation progresses from generally high to generally low fractal dimensions for typical b-values ($D = 3$ represents activations that effectively "fill" a seismic volume over all dimensional scales, whereas $D < 1$ represents fractally "less-than-linear" discontinuous activations). However, if b-values are also allowed to approach a limit near 3, the fractal path can first decrease then increase again to the vicinity of the volume-filling set. This upper fractal limit corresponds to the concept of an ultimate earthquake event (U.E. in Figure 1) according to any correlation resembling that of Hanks and Boore (1984). If such an event can be realized it represents a unique condition in the earthquake process.

References Cited:

Aki, Keiiti, 1981, A probabilistic synthesis of precursory phenomena: in Earthquake Prediction, D. W. Simpson and P. G. Richards, eds., Washington D. C., American Geophysical Union, p 566-574.

Hanks, T. C., and D. M. Boore, 1984, Moment magnitude relations in theory and practice: Journal of Geophysical Research, v. 89, p 6229-6235.

King, G., 1984, The accommodation of large strains in the upper lithosphere of the earth and other solids by self-similar fault systems: the geometrical origin of b-value: Pageoph., v. 121, p 761-815.

Okubo, P. G., and K. Aki, in press, Fractal geometry in the San Andreas fault system: Jour. Geophys. Res.

Shaw, H. R., and A. E. Gartner, 1981, Statistical data on faulting rates in the United States and deduced seismicity: Geol. Soc. Am., Abstracts w. Programs, v. 13, p 552.

Shaw, H. R., and A. E. Gartner, 1984, Empirical laws of order among rivers, faults, and earthquakes: U. S. Geol. Surv., Open-file Report 84-356, 51 pp.

Shaw, H. R., and A. E. Gartner, 1985, Systems analysis of geologic rate processes: U. S. Geological Survey Open File Report 85-464, p 199-201.

Shaw, H. R., A. E. Gartner, and F. Lusso, 1981, Statistical data for movements of young faults of the conterminous United States; paleoseismic implications and regional earthquake forecasting: U. S. Geological Survey Open File Report 81-946, 353 pp.

Reports:

Shaw, H. R., and A. E. Gartner, in review, On graphical interpretation of paleoseismic data.

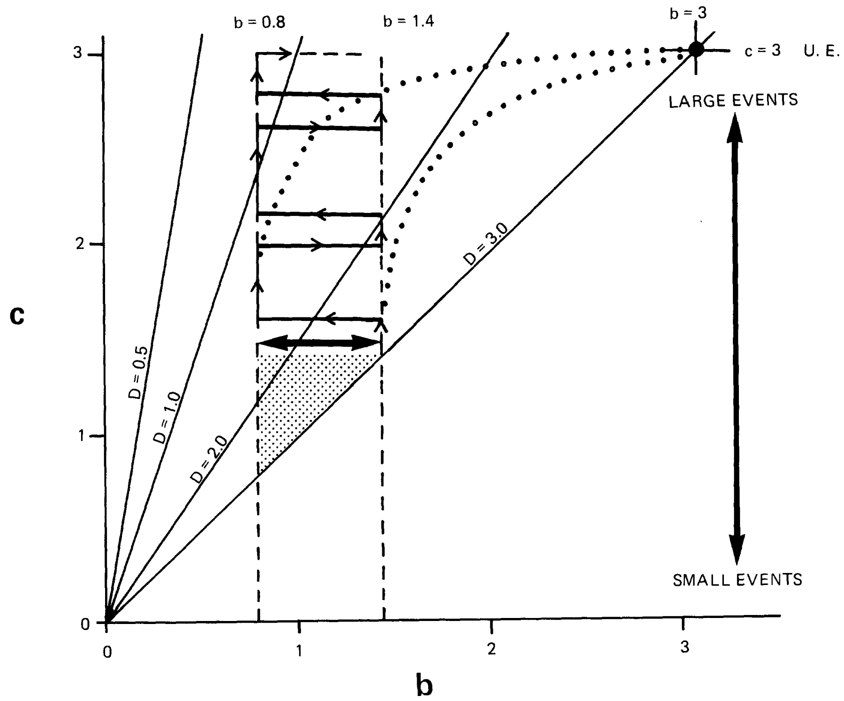

Figure 1. Fractal dimension paths.

Lines of constant fractal dimensions, D, limited to topological dimension 3, plotted vs variable values of b and c (defined in the text) according to the relation $D = 3\ b/c$. The solid lines with arrows schematically indicate the paths of fractal dimensions for two different assumptions concerning stepwise progressions of seismic frequency-magnitude data, as in Japan (Shaw and Gartner, 1985): (1) the heavy horizontal line with arrows indicates the alternations of D corresponding to alternations of b between the limiting slopes of the fractogram of Shaw and Gartner (1985) for a constant value of $c = 1.5$, and (2) the orthogonal zigzag line with arrows indicates the same alternations, but with c increasing in the larger events according to the correlation of Hanks and Boore (1984). There are two important qualifications of these idealized sequences: (i) when c increases, the equations relating fault length, moment, and magnitude are also modified, so that b also increases; in the extreme limit, b might approach the value 3 for a hypothetical ultimate magnitude (in this case the upper part of the zigzag path is skewed to the right toward the fractal limit $D = 3$, as indicated by U. E. and the dotted lines) and (ii) if the log number-length relation from Shaw and others (1981) has a slope near -1, the fractogram degenerates to a nearly single-valued slope, so that the range of b-values shrinks toward zero difference. In the second case, the ultimate event implies a very large length scale and a fixed b-value at a c-value near 3. The data for faulting in California quantified and illustrated by Shaw and others (1981), including the San Andreas system, may sometimes approximate this case. The stippled area represents the range of conditions for small to intermediate earthquakes where volume-filling activations are possible (i.e., $D = 3$); at larger magnitudes, D first decreases then increases toward an ultimate event (U. E.). Evidently the ultimate event must be one that engages a large volume domain at the scale of Plate Tectonics.

Fault Patterns and Strain Budgets

9960-02178

Robert W. Simpson
U.S. Geological Survey
Branch of Tectonophysics
345 Middlefield Road, MS/977
Menlo Park, California 94025
415-323-8111, ext. 4256

Investigations

Simulations were made of the creeping section of the San Andreas fault between San Juan Bautista and Parkfield using the two-dimensional Displacement Discontinuity program of Crouch. Tests of the effects of various events, including the 1983 Coalinga earthquake and the 1906 San Francisco earthquake, upon the locked patch at Parkfield were carried out.

Results

Although the two-dimensional plane strain elastic model used by Crouch's program is undoubtedly too simple to adequately describe many aspects of the earthquake generation process, the very simplicity seems to offer some advantages. It is quite an easy matter to enter the data needed to evaluate complex two-dimensional fault geometries, and the computation times are small enough that for many tests the program can be run interactively. This ease of operation encourages experimentation which helps to develop an intuition for the relative importances of the parameters being tested. The results are expected to be of qualitative and order-of-magnitude validity - only those results which are relatively insensitive to changes in geometries and parameters are considered robust enough to warrant comparison to the real world. The greatest oversimplification inherent in the model is probably its assumption of uniform properties and displacements with depth. Thus, results need to be thought of as averaged over depth.

The creeping segment of the San Andreas fault between San Juan Bautista and Parkfield was simulated by a series of end-to-end, 10-km-long discontinuities subjected to a remote shear field. The displacements on the discontinuities were calculated assuming no friction for the creeping zone and also assuming a viscous response to the applied shear stress. A persistent regularity in the deformations (noted earlier by Paul Segall) was the tendency of the creeping section to rotate counter-clockwise with time. This observation is naively consistent with the change in trend of the fault near Parkfield if elastic displacements are not 100 percent recoverable, but are incrementally adding up to permanent deformations.

A discontinuity was inserted near Coalinga to simulate the horizontal convergence accompanying reverse faulting in the 1983 Coalinga earthquake. For a viscous behavior on the creeping part of the San Andreas fault, the initial creep near Parkfield in response to the Coalinga earthquake is predicted to be in a left-lateral sense, in agreement with the reversal of creep observed at the Middle Mtn creepmeter. The net effect of the Coalinga earthquake on the Parkfield locked patch is to relieve the stresses slightly, possibly delaying the next Parkfield earthquake on the order of several years if similar deformations in the Coalinga area have not been a part of every Parkfield recurrence cycle.

Another earthquake that might have disrupted the 22-year Parkfield earthquake recurrence cycle would be the 1906 San Francisco earthquake. The 1906 coseismic slip, which was probably confined to the upper 10 km of crust, seems not to have extended south of San Juan Bautista. The coseismic displacements would not by themselves produce much of an instantaneous effect at Parkfield. If, however, the creeping zone could transfer these displacements southward with time, acting somewhat as a propagating crack, then the increased load on the Parkfield locked patch could be a significant fraction of the load required to break the locked patch. The ~22 year Parkfield earthquake recurrence cycle (1881, 1901, 1922, 1934, 1966) does not seem to have been immediately disturbed by the 1906 earthquake. It is conceivable that the effects of the 1906 earthquake did not reach Parkfield until the next cycle (perhaps traveling as a kinematic wave as described by Savage in 1971), causing the 1934 earthquake to occur ~10 years early. An answer to the question as to whether or not the 1906 earthquake affected the Parkfield recurrence cycle may offer some insights into the slip laws operating at depth in the lithosphere.

Earthquake Forecast Models

9960-03419

William D. Stuart
Branch of Tectonophysics
U.S. Geological Survey
Pasadena, California 91106
(818) 405-7816

Investigations

1. Development and testing of a procedure for predicting earthquakes using an earthquake instability model and repeated measurements of fault slip and ground deformation.

2. Estimate the change in magnetic field before and during a moderate Parkfield earthquake.

Results

1. The properties and results of the model are reported in Stuart (1985b) and in the last two Technical Summaries. In brief, the model represents the San Andreas, Imperial, Cerro Prieto, and San Jacinto faults by flat vertical planes in an elastic half space. The fault is divided into 640 rectangular cells, each of uniform slip. In most of the cells, slip and stress are computed results and vary with position and time. In the remaining cells, which occupy steadily creeping areas, fault slip rate is imposed as a boundary condition. The main free parameter in the problem is the variation of brittle fault strength along strike. The fault is assumed to be brittle from the ground surface to about 12 km depth between Parkfield and the Salton Sea. The strength of the brittle zone has been adjusted by trial until slips and times of instabilities (the earthquake analogs) agree with measured fault offsets since 1080 reported by K. Sieh and others. The brittle zone is found to be made of five contiguous sections of alternately low and high strength. The section ends, north to south, are near Parkfield, Bitterwater Valley, Lake Hughes, San Bernardino, Palm Springs, and the Salton Sea.

   Since the last Technical Summary the model has been refined in the following ways: (1) The number of fault cells was increased from 551 to 640, with a corresponding decrease in the size of the smallest cells. (2) An entirely new algorithm was devised to solve the system of simultaneous nonlinear equations. The new algorithm is substantially faster than the prior one. (3) The equation for the fault stress-slip law was improved to more realistically represent strain hardening. (4) The fault law stiffness now varies as the Gaussian of depth, independent of position along fault strike. This assumption allows the bottom of the brittle fault to fail stably before overall instability. (5) The strength of the fault between Palm Springs and the Salton Sea was altered to accommodate new field measurements by K. Sieh.

All of these changes result in better agreement between theoretical and observed dates of earthquakes, and in changes of a few years for instabilities predicted to occur in the near future. The next two instabilities predicted by the model occur within a decade between Parkfield and Bitterwater Valley and between Palm Springs and the Salton Sea. Computed fault creep and lengths of trilateration lines in the vicinity of the two fault sections show rate changes starting several years before instability. Some of the anomalous rate changes are large enough to detect by existing geodetic procedures.

2. In a recent paper Stuart et al. (1985) used an instability model to compute changes of fault creep and ground surface motion that might occur before a moderate earthquake near Parkfield. For the same model S.-W. Liu and I are trying to estimate magnetic field changes that would be caused by stress-induced changes of rock magnetic susceptibility. Preliminary calculations indicate that the change of total field near Parkfield would be less than one gamma during instability. During the precursory period of about one year, the anomalous magnetic field would be a fraction of the change during instability.

Reports

Stuart, W. D., R. J. Archuleta, and A. G. Lindh, Forecast model for moderate earthquakes near Parkfield, California, J. Geophys. Res., 90, 592-604, 1985.

Stuart, W. D., Theoretical line length changes before great earthquakes in southern California (abs.), EOS Trans. Am. Geophys. Un., 66, 383, 1985a.

Stuart, W. D., Instability model for recurring large and great earthquakes in southern California, Pure Appl. Geophys., 122, 793-811, 1985b.

SHEAR FRACTURE GEOMETRY OF PSEUDOTACHYLYTE GENERATION ZONES AND THE INTERNAL STRUCTURE OF BRITTLE SEISMIC FAULT SYSTEMS

14-08-001-G-1106

Mark T. Swanson
Department of Geosciences
University of Southern Maine
Gorham, Maine, 04038
(207)-780-5350

INVESTIGATIONS:

Detailed outcrop mapping of a pseudotachylyte locality within the Precambrian Rye Formation at Kittery Point in southern Maine is in progress. The study area, known as the Fort Foster Brittle Zone (Swanson, 1985), consists of a continuous coastal outcrop 200 meters long and 20-30 meters wide. The exposures contain abundant pseudotachylyte and minor breccia within a complex system of brittle strike-slip shear fractures that cut the near-vertical mylonitic fabric of the host rocks. The study area is interpreted to represent an oblique section through a 60 meter wide brittle seismic fault system developed during the reactivation of a major ductile mylonitic fault zone within the Rye Formation.

This study was designed to elucidate the overall geometry and cross-cutting relations within this complex shear fracture system. The layer parallel slip surfaces are most frequently arranged in pairs that create structural zones up to about a meter in width (Figure 1a). These are termed pseudotachyltye generation zones after Grocott (1981) and Swanson (1985). Each zone has a distinctive but variable internal structure of minor shear and extension fractures. It is this internal fracture geometry and the paired relationship of the bounding layer-parallel slip surfaces that is under investigation in this study. The development of a distinctive fracture geometry associated with the production of pseudotachylyte suggests a possible relationship between a recognizable mechanism of faulting and seismicity.

Mapping is proceeding on three scales, 1:4800 for the distribution of lithotectonic units within the Rye Formation of Gerrish Island (after Hussey, 1980); 1:240 for the structure and lithology within the Southern Ultramylonite Zone and 1:60 for the orientation and distribution of brittle structures within the Fort Foster Brittle Zone. The outcrop configuration and major slip surfaces within this brittle zone have been mapped using a plane table and alidade. Detailed minor fault patterns were added by grid mapping of the outcrop surface. To date, over 1200 shear fractures have been mapped, including nearly 100 individual layer-parallel pseudotachylyte-bearing slip surfaces.

Detailed structural analysis is proceeding from this base map and will include the orientation of fault surfaces as well as the sense and magnitude of their cross-cutting relations. Sequences of shear fracture development deduced from these outcrops will be used in the interpretation of the nature, significance and evolution of these distinctive fault zone geometries. Thin section analysis of fabric development in relation to metamorphism within the mylonitic rocks, photomosaic mapping of selected structural areas and K-Ar dating of the pseudotachylyte are also planned.

RESULTS:

The Fort Foster Brittle Zone was found to consist of a complex network of layer-parallel and oblique strike-slip surfaces (Figure 1) containing abundant pseudotachylyte and subordinate amounts of fault breccia. The development of pseudotachylyte generation zones defined by paired layer-parallel slip surfaces (Figure 1a) is characteristic. Individual pseudotachylyte generation zones can now be followed for as much as 100 meters.

The internal structural development within these zones was found to vary from intact, undamaged host rock (no internal structure) to total disruption in the formation of localized fault breccias. The coherent disruption of the internal zones generally takes the form of an assemblage of shear fractures that indicate the development of both layer-parallel extension and layer-parallel compression (Figure 1a) during slip on the layer-parallel bounding surfaces that define the pseudotachylyte generation zones.

The nature of the internal structures within each zone was found to vary along strike. Layer-parallel extension would cause thinning of the intervening host rock fault slab possibly leading to the formation of fault breccia.

Layer-parallel compression would cause thickening of the host rock fault slab that may create an asperity contact along the layer-parallel slip surface. Cross-cutting relationships within this internal zone also indicate a temporal sequence of layer-parallel compression and layer-parallel extension within the host rock fault slab. This structural relationship may reflect separate slip events or progressive development during a single slip event.

The characteristic development of zonal fault structures within the Fort Foster Brittle Zone suggests an effective decoupling of host rock fault slabs between contemporaneous layer-parallel slip surfaces. The overall geometry of the NW boundary (Figure 1b) as well as the entire 60 meter wide brittle strike slip fault system is also zonal in nature similar to the smaller scale pseudotachylyte generation zones found in these outcrops.

Strain concentration at the outer boundaries of the fault system is indicated by the intense development of layer-parallel slip surfaces, most of which are arranged in pairs as zones, along the outer margins of the mylonitic units undergoing the brittle deformation. The NW boundary of the fault system (Figure 1b) is delineated by the development of approximately 26 individual layer-parallel slip surfaces in a 10 meter section. This configuration appears to degenerate along strike to about half the number of slip surfaces by the development of a cascade of oblique shear fractures that have propagated into the interior of the fault system. These oblique shear fractures appear to merge with an internal zone of prominent layer-parallel slip surfaces creating a zonal structure at this NW boundary (Figure 1b).

The SE boundary of the fault system also shows a prominent strain concentration by the abundance of layer-parallel slip surfaces. There is also evidence of several phases of an earlier deformation concentrating strain at this boundary. This is indicated by an abundance of dark wispy layering interpreted as ductilly deformed pseudotachylyte. The host rock in the outer 10 meters of the fault system at this SE boundary is also an extremely well indurated fault breccia representing an earlier fault episode.

Finally, the pseudotachylyte and associated intricate fault geometries are preserved in these exposures because of the limited amounts of slip developed within this fault system. Any regionally significant offsets in the brittle mode along this zone would most certainly have destroyed the structures under study in a chaotic assemblage of gouge and breccia. The characteristic slip increment for surfaces within this brittle deformation zone is, so far, everywhere less than one meter. This suggests that the fault system under study represents a brief history of moderate seismicity as a final phase in the development of a major regional fault structure. Multiple earthquake sequences are recorded in these exposures by the preservation of the intricate fault structures and mechanisms associated with this seismicity. Interpretation of these structures is continuing in terms of coupled en echelon fault relations, rupture zone termination and lateral displacement transfer in brittle fault systems.

REFERENCES:

Grocott, J. 1981, Shear fracture geometry of pseudotachylyte generation zones: a study of shear fractures formed during seismic events, Jour. Struct. Geol., V. 3, #2, 169-178.

Hussey, A.M., 1980, The Rye Formation of Gerrish Island, Kittery, Maine: a reinterpretation, The Maine Geologist, Vol. 7, #2, p. 2-3.

Swanson, M.T., 1985, Pseudotachylyte generation zones of southern Maine and New Hampshire, Geol. Soc. Amer. Abstracts with Programs, V. 17, #1, p. 65.

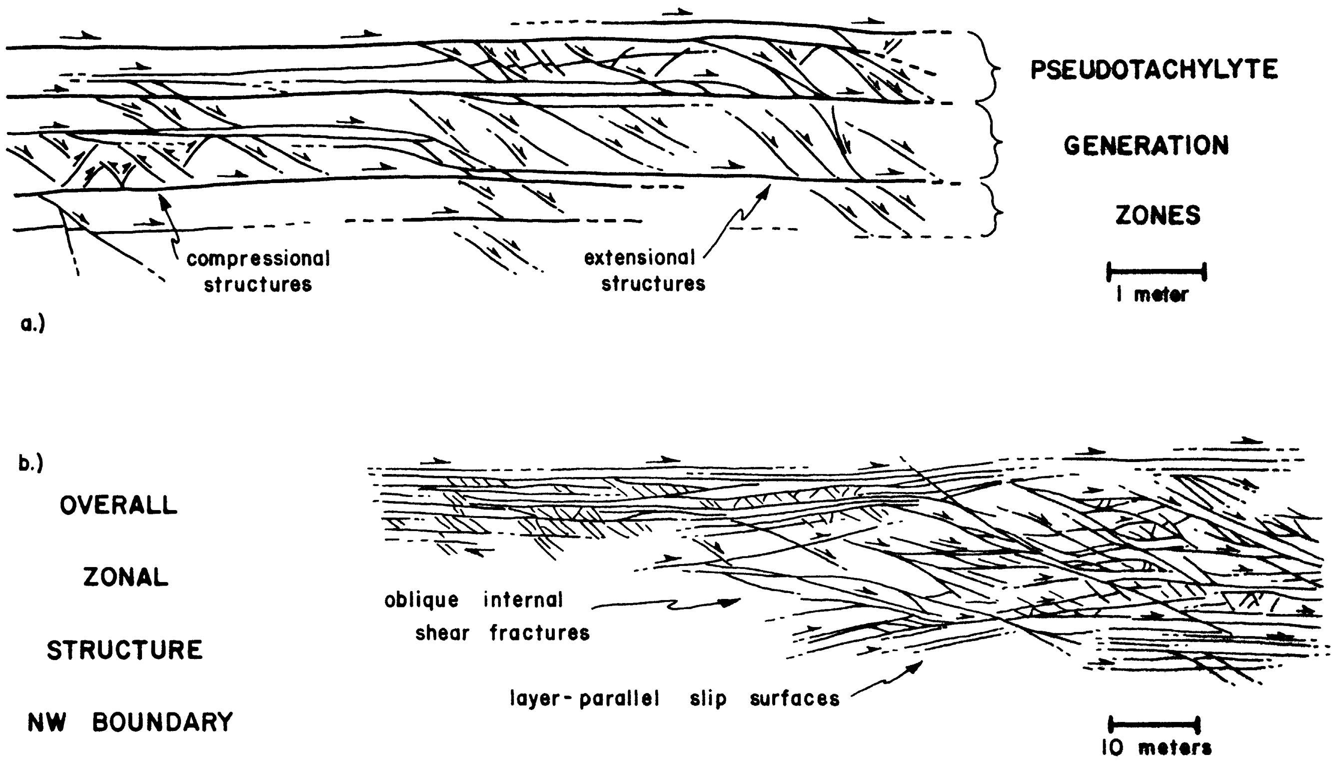

FIGURE 1 : a.) Configuration of pseudotachylyte generation zones as pairs of layer parallel slip surfaces and typical internal shear fracture patterns
b.) Fault patterns at the NW boundary of the Fort Foster Brittle Zone.

EXPERIMENTS OF ROCK FRICTION CONSTITUTIVE LAWS APPLIED TO EARTHQUAKE INSTABILITY ANALYSIS

USGS Contract 14-08-0001-G-821

Terry E. Tullis
John D. Weeks
Department of Geological Sciences
Brown University
Providence, Rhode Island 02912
(401) 863-3829

Investigations

1. We have started work on determining the detailed constitutive behavior for frictional sliding of calcite marble, kaolinate clay and artificial crushed granite gouge.

2. We have continued our theoretical investigation of the stability of a spring-and-slider block frictional system, using the theories developed by Gu, et al. (1984). Since our modeling of experimental data has shown that two state variables are needed to match our experimental results, we are examining how changes of the values of the constitutive parameters affects the stability of a frictional system characterized by two state variables.

Results

1. We have performed experiments on calcite marble at normal stresses of 75 MPa and 15 MPa, with samples exposed to room humidity of up to 65 per cent. At 75 MPa, while the bulk of the sample displacement was on the pre-cut sliding surface, the sample suffered pervasive cataclasis. At 15 MPa we have performed several velocity stepping sequences covering six and a half orders of magnitude in load point velocity, ranging from 10^{-3} μm s^{-1} (3.15 cm per year!) up to 3163 μm s^{-1}. The peak frictional strength observed in this experiment was a coefficient of friction of 0.99 at small displacement, a level significantly higher than the level predicted by "Byerlee's Law" and in strong contrast to measurements made on dolomite which showed peak friction as low as 0.3. The velocity stepping tests reveal two things: There is a strong dependence of the constitutive parameters on velocity that is not included in constitutive laws developed so far, with a change from velocity weakening at low velocity (0.01 μm s^{-1} and below) to velocity strengthening at high velocity. There is also a strong long term effect that does not evolve with displacement alone but may have some dependence on time. This long term effect can obscure the velocity weakening observed at low velocities by superimposing a downward drift as the sample displaces. This long term effect is also shown by the fact that velocity stepping sequences from low to high velocity and back to low show strong hysteresis. Samples have been prepared for experiments on kaolinite clay and crushed granite artifical gouge.

2. We have continued our numerical investigation of the stability and behavior of a frictional system in which two state variables describe the frictional response of the sliding surface. Our experiments have shown that for particular conditions the constitutive parameters are nearly constant over several orders of magnitude in sliding velocity. Here we discuss how changes in the values of L_1 and L_2, the characteristic decay distances associated with the two state variables ψ_1 and ψ_2, affect frictional stability and behavior. Frictional behavior may be represented on three-dimensional plots with axes of frictional resistance μ, log sliding velocity V, and ψ_2, the more slowly evolving state variable (Figures 1a, b). Evolution of the system with time can be represented by trajectories in this phase space. On these plots a stability surface separates a region of

stability below from instability above. Steady state and constant state behavior are shown by the heavy diagonal lines.

Figure 1a uses the stiffness of our rotary shear apparatus and parameter values we have found experimentally to describe the sliding of granite. Figure 1b uses a lower dimensionless stiffness value, only slightly higher than the critical stiffness for the system. Lowering the stiffness lowers the surface to a small distance above the origin and brings the drop-off at low velocity to a lower value of the state variable. Both effects severely limit the range of imposed changes in load velocity and/or normal stress which will remain stable, and limits the behavior possible subsequent to such changes.

Due to the coupling between the elastic loading system and the sliding surface, lowering the dimensionless stiffness K may be accomplished either by lowering the machine stiffness, or by decreasing L_1 and L_2 while keeping their ratio constant; the effect is identical. Allowing the ratio of L_1 and L_2 to change varies the slope of the stability surface along the ψ_2 axis as well.

Reference

Gu, J. C., Rice, J. R., Ruina, A. L., and Tse., S., Slip motion and stability of a single degree of freedom elastic system with rate and state dependent friction, *J. Mech. Phys. Solids, 32,* 167-196, 1984.

Report

Weeks, J. D., and T. E. Tullis, Frictional sliding of dolomite: an interesting variation in constitutive behavior, *J. Geophys. Res., 90,* 7821-7826, 1985.

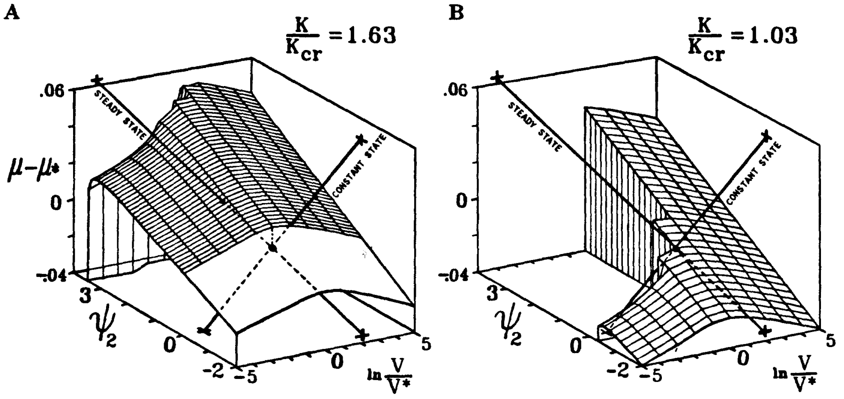

Figure 1. Stabilty for a frictional system described by a two state variable law, showing the effect of changing the dimensionless stiffness K. The steady state and constant state lines have been drawn in and dotted where they lie below the stability surface. The origin is indicated by a dot at the intersection of these lines. In both cases the parameter values are $a = 0.004$, $b_1 = 0.0075$, $b_2 = 0.01454$, and the critical stiffness $K_{cr} = 10.663$. (**a**) $L_1 = 8\ \mu m$, $L_2 = 150\ \mu m$, $K = 17.379$, $K/K_{cr} = 1.63$, the values experimentally determined for granite. (**b**) $L_1 = 5.06\ \mu m$, $L_2 = 94.875\ \mu m$ (ratio remains constant), $K = 11.0$, $K/K_{cr} = 1.03$. These changes are equivalent to lowering the system stiffness to 63% of its value in **a**.

PERMEABILITY OF FAULT ZONES

9960-02733

James Byerlee
Branch of Tectonophysics
U.S. Geological Survey
345 Middlefield Road, MS/977
Menlo Park, California 94025
(415) 323-8111, ext. 2453

Investigations

Laboratory studies of the permeability of rocks and gouge are carried out to provide information that will assist us in evaluating whether in a given region fluid can migrate to a sufficient depth during the lifetime of a reservoir to trigger a destructive earthquake. The results of the studies also have application in the solution of problems that arise in nuclear waste disposal.

Results

Permeability measurements of the Topopah Spring Member of the Paintbrush Tuff and the Bullfrog Member of the Crate Tuff have been made at room-temperature and in a temperature gradient. The room-temperature permeabilities of the samples ranged from 0.8 x 10^{-18} m^2 to 64 x 10^{-18} m^2 for the Topopah Spring Member and 0.5 x 10^{-18} m^2 to 8.4 x 10^{-18} m^2 for the Bullfrog Member. These variable permeabilities probably reflect differences in crack and void configurations among the samples. The permeability of a given sample was only slightly affected by heating to maximum temperatures between 90°C and 250°C during experiments of up to 5 weeks duration. The observed lack of permeability change suggests that the disposal of nuclear waste in tuff units in the unsaturated zone at the Nevada Test Site would not have a large effect on the permeability of the host rock. The fluids discharged from the tuff samples during the experiments were mostly dilute solutions of nearly neutral pH, whose compositions differed only slightly from the starting J13 ground water composition. Waters of this type should be relatively non-corrosive to stainless steel waste canisters.

Reports

C. Morrow, D. Moore and J. Byerlee, 1985, Permeability changes in crystalline rocks due to temperature: Effect of mineral assemblage, Mat. Res. Soc. Symp. Proc., v. 44, p. 467-474.

STRESS AND PORE PRESSURE CHANGES DUE TO ANNUAL WATER LEVEL CYCLES IN SEISMIC RESERVOIRS

Contract 14-08-0001-22022

Evelyn Roeloffs, Taechin F. Cho and Bezalel C. Haimson
University of Wisconsin, Madison
1509 University Avenue
Madison, WI 53706
(608) 262-2563

INVESTIGATIONS

Completion of theoretical study of strength changes produced by a periodic load on the surface of a porous elastic half-space.

Two-dimensional finite element modeling of strength changes produced by an arbitrarily time-varying reservoir load on a porous elastic crust with non-uniform material properties.

In both investigations, work is focused on two quantitative questions regarding the mechanism of reservoir induced seismicity. First, we seek improved estimates of the sizes of strength changes produced by reservoir impoundment. Second, we seek to explain common features of the correlation between seismic event frequency and reservoir water level.

RESULTS

Work has been completed on the strength changes accompanying periodic variations in water level on the surface of a uniform porous elastic half space. Frequency enters the coupled stress and pore pressure solutions through a dimensionless quantity ($\Omega = \omega L_1^2/c$) that ranges from 0.002 to 200.0, assuming an annual period, diffusivities (c) of 0.1 to 100.0 m^2/s, and reservoir widths (L_1) from 1 to 10 km. ω is the radian frequency of the loading. Pore pressure induced by compression can cause weakening at high dimensionless frequencies to be comparable to that at lower frequencies. Thus, uncoupled calculations that do not include compression-induced pore pressure will underestimate strength changes under these circumstances. No situations were identified in which peak coupled strength changes occurred more than several days after the high or low water level, so this model does not offer a simple explanation for observed lags as long as several months between peak water level and peak seismic event frequency.

Using a two-dimensional finite element program that solves the coupled equations of elasticity and fluid flow, we have the capability of incorporating nonuniform porous elastic crustal models and arbitrary variations of water level with time. Although information about _in situ_ values of porous elastic material properties is inadequate, layered models can be based on plausible assumptions about their variation with depth. In particular, as depth increases, it is reasonable to assume that diffusivity, Skempton's constant, and the difference between drained and undrained Poisson's ratios will also decrease. Model calculations show that near-surface layers with relatively high diffusivity and Skempton's constant quickly equilibrate to relatively high pore pressures and are the sites of broad zones of weakening for all fault orientations. The pressure of such near-surface layers also decreases the time required for deeper, less permeable layers to experience elevated pore pressure. For the layered models considered so far, the largest strength changes are comparable in size to those in a uniform half-space, but may be more or less extensive.

The introduction of layering complicates the time dependence of strength changes, with longer lags between peak water level and peak strength changes in layers of low diffusivity and Skempton's constant. Thus more elastic crustal models may be important for understanding the observed timing at activity peaks in relation to water level peaks.

REPORT

Roeloffs, E. A., 1985, Stress and Pore Pressure Changes Due to Annual Water Level Cycles in Seismic Reservoir, (abstract), EOS, Trans. Am. Geophys. Union, Vol. 66, No. 18.

Mechanics of Faulting and Fracturing

9960-02112

Paul Segall and Ruth Harris
Branch of Tectonophysics
U.S. Geological Survey
345 Middlefield Road, MS/977
Menlo Park, California 94025

Investigations

1. Inversion of trilateration data to determine slip distribution on the Parkfield-Cholame section of the San Andreas fault.

2. Field and microstructural investigation of fault and shear zone formation in granitic rocks.

3. Continued study of deformation and seismicity induced by subsurface fluid extraction and injection.

Results

1. Inversion of Parkfield Geodetic Data

The section of the San Andreas fault near Parkfield, CA, lies in the transition between the central creeping zone and the southern locked zone that last ruptured in 1857. Parkfield has been the site of frequent M6 earthquakes, with an average recurrence interval of 22 ± 5 yrs. Trilateration surveys in the region commenced prior to the last earthquake in 1966 and have continued to the present. These data can be used to estimate the distribution of buried fault slip during the coseismic and interseismic periods. For the interseismic period (1966-1984), average rates of survey-line length change have been calculated for the 31 lines with 4 or more measurements. Each line has been resurveyed an average of 11 times between 1970 and 1984. The rates of line-length change have been inverted to determine the distribution of slip rate on the fault. The shallow slip rate is specified to be consistent with creepmeter, alinement array, and small-aperture geodetic data. The slip rate northwest of Middle Mountain is assumed to be 25 mm/yr, while the rate below the seismogenic zone (i.e., below 12 to 16 km) is taken to be 33 mm/yr. A striking result of the inversions is that all solutions which provide acceptable fits to the data have little or no slip in the rupture zone of the 1966 earthquake (Figure 1). From the difference between the long-term rate of 33 mm/yr and the calculated slip rate we derive a moment deficit rate. Representative moment deficit rates range from 3.1 to 3.6 x 10^{24} dyne-cm/yr. The cumulative deficit from 1966 to the present is 5.9 to 6.8 x 10^{25} dyne-cm. This is comparable to geodetic estimates of the moment of the 1966 quake, which range from 4.7 to 6.3 x 10^{25} dyne-cm. The geodetic data suggest that sufficient slip deficit has accumulated for a repeat of the 1966 earthquake.

2. Nucleation of Shear Zones

Small shear zones in granitic rocks of the Sierra Nevada, California, and near Roses, NE Spain, display features which indicate that dilatant fracturing preceded the localization of ductile shear deformation. Many zones have sharp, nearly planar boundaries between their highly deformed interiors and the undeformed wall rock. The Roses shear zones narrow continuously to hairline fractures at their ends. Mineralized microcracks oriented parallel to the shear zones, cluster near the zone boundaries and are interpreted as relicts of the earlier fracturing episode. Dynamic recrystallization of minerals filling these microcracks demonstrate that fracturing predated the ductile deformation. Gradients in ductile strain suggest that deformation spread laterally into the wall rocks following nucleation of the shear zones. We suggest that cracks enhance the wall rock ductility by increasing local fluid fluxes, thereby promoting chemical alteration and/or hydrolytic weakening.

Reports

Segall, P., Stress and subsidence resulting from subsurface fluid withdrawal in the epicentral region of the 1983 Coalinga earthquake, J. Geophys. Res., v. 90, p. 6801-6816, 1985.

Segall, P., and J. W. Rudnicki, Stress and pore pressure changes resulting from fluid extraction and injection: Application to the 1983 Coalinga, California, earthquake, Earthquake Notes, v. 55, no. 1, p. 17, 1985.

Harris, R. and P. Segall, Determination of the slip deficit along the Parkfield, California section of the San Andreas fault from the inversion of trilateration data, Trans. Amer. Geophys. Union Fall Meeting, 1985.

Segall, P. and C. Simpson, Nucleation of ductile shear zones on dilatant fractures, Geology, in press, 1985.

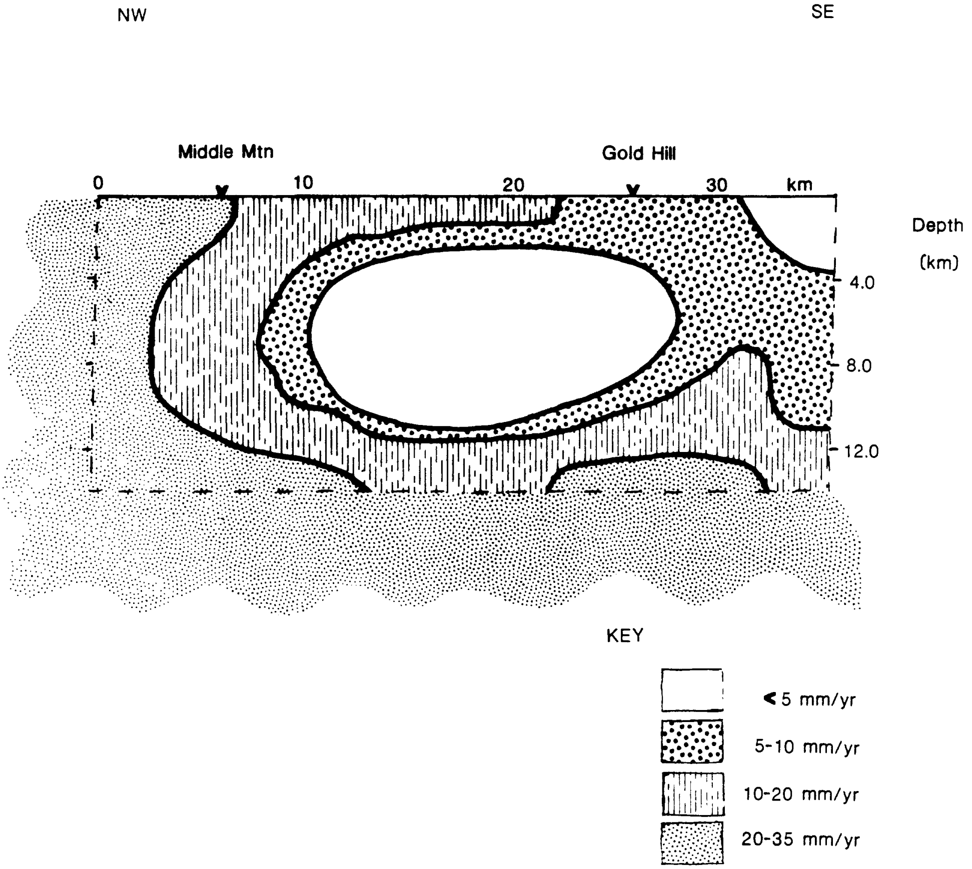

Figure 1. Interseismic slip-rate on the San Andreas fault near Parkfield projected onto a longitudinal cross-section of the fault. Slip rate is assumed to be 25 mm/yr 6 km NW of Middle Mountain, and 33 mm/yr everywhere below 14 km. Slip rate in the seismogenic zone (0-14 km) is determined from an inversion of trilateration data.

Deep Hole Desalinization of the Dolores River

9920-03464

William Spence
National Earthquake Information Center
U.S. Geological Survey
Denver, Federal Center
Box 25046, Mail Stop 967
Denver, Colorado 80225
(303) 236-1506

Investigations

This project relates to monitoring the seismicity of the region of the intersection of the Delores River and Paradox Valley, southwest Colorado. The project is a component of the Paradox Valley Unit of the Colorado River Basin Salinity Control Project and is being performed for the U.S. Bureau of Reclamation with support from the Induced Seismicity program of the USGS. In this desalinization project it is proposed to pump approximately 30,000 barrels/day from brine-saturated rocks beneath the Dolores River through a borehole to the Madison-Leadville limestone formation of Mississippian age, some 15,000 feet below the surface. There is a possibility of seismicity being induced by this desalinization procedure, especially in the long term. The project objectives are to establish a pre-pumping seismicity baseline and, during the pumping phase, to closely monitor the discharge zone for possible induced seismicity. If induced seismicity does occur it should be possible to relate it to formation characteristics and to the pumping pressure and discharge rates.

Results

A ten-station seismograph network is centered at the location of the proposed injection well. This high-gain network has a diameter of about 80 kilometers, and has been in operation since September, 1983. Seismic data are brought to Golden, Colorado, via microwave and phone line transmission. These data are fed through an A/D converter and then through an event detection algorithm. The network has operated at high quality, except for two periods when it was decommissioned by lighting strikes. Analysis procedures have been considerably complicated by a high rate of blasting activity in the region but means have been developed to distinguish the occurrence of natural earthquakes to good reliability.

Notable regional earthquake activity are a swarm of shallow events (maximum magnitude 3.2) near Carbondale, Colorado, and a magnitude 3.4 shallow earthquake near Blue Mesa Reservoir, Colorado. In the vicinity of the network, the earthquake catalog is complete to about magnitude 2.0. Most of the seismicity in the area of the network is in the shallow crust. However about 10 earthquakes have focal depths greater than 20 km, with several events at the depth intervals 30-35 km and 50-55 km. These results indicate that microearthquakes are distributed throughout the crust of the Colorado Plateau, with an occasional event in the upper mantle. The shallow and deeper earthquakes follow a diffuse north-south trend, parallel to the eastern boundary of the Colorado Plateau. These early results, combined with a lack of historical seismicity at the zone of the Paradox Valley seismic network, indicate that any seismicity induced by deep-well injection near Paradox Valley should be identifiable as such.

Report

Spence, W., and Chang, P-S., 1985, Seismic monitoring in the region of the Paradox Valley, Colorado (Annual report, July 1984 - June 1985, U.S. Bureau of Reclamation, Deep well injection site, Paradox Valley Unit, Colorado River Basin Salinity Control Project), 11 p.

Study of Reservoir Induced Seismicity and Earthquake Prediction in South Carolina

Contract No. 14-08-0001-22010

Pradeep Talwani
Geology Department
University of South Carolina
Columbia, S.C. 29208
(803) 777-6449

Investigations

1. Monitor seismicity near Monticello Reservoir, Rion, Newberry, Lake Jocassee and the Savannah River Plant in South Carolina.

2. Develop theoretical model for RIS.

Results

1. Continued monitoring at Monticello Reservoir has indicated a dramatic rise in seismicity during the first half of 1985. From a low of 3 events per week in 1984, the level currently stands at 16 events per week, which is comparable to the seismicity level in 1979, (Figure 1). Fifteen events had magnitudes greater than 1.0, two were of magnitude 2.0. The seismicity in 1980-83 had shown evidence of deepending. However, the seismicity in 1985 was shallow (87% within the uppermost 2 kilometers) and occurred in several discrete swarms.

   The epicentral area has remained constant after the initial spread of seismicity. In the period 1980-84 a large fraction of the seismicity was on the periphery of the reservoir - an observation consistent with shallow thrust fault RIS. However, most of the activity in 1985 is within the reservoir (Figure 2). This spatial change together with the rapid increase in the level of seismicity suggests a major change in the hypocentral stress condition and bears further monitoring.

   A study of temporal changes in b-values at Monticello Reservoir has been initiated to determine the temporal effect of impoundment on the mechanical properties of the seismogenic region. The study will cover the period from December, 1977 through December, 1985.

A new source of activity has been noted near Rion, approximately 20 km east of Monticello Reservoir. Seismicity began during the end of April, 1985 and peaked during May and June with a total of 16 events. Magnitudes of the events were all low, less than 2.0.

A seismotectonic model for the shallow seismicity near Newberry, 20 km west of Monticello Reservoir, is nearing completion and continued monitoring reflects an average level of one event per two weeks.

Lake Jocassee seismicity has been monitored continuously for 10 years, first with portable instruments, currently with three permanent stations. The activity for the first six months of 1985 was low, averaging less than two events per week. The largest event of the period was local magnitude 1.7 on April 9. Epicentral locations (Figure 3) are scattered throughout the area.

An earthquake of magnitude 2.6 occurred at the Savannah River Plant, approximately 100 km southwest of Columbia. The event was felt over an area of 130 sq. km, within the plant boundary, with a maximum intensity III (M.M.). The earthquake was shallow, 0.96 km, and located at the intersection of the northeast trending Dunbarton Triassic basin and an unidentified northwest trending feature noted on the aeromagnetic map. The fault plane solution suggests left lateral strike slip motion on the basin border fault.

2. A FORTRAN algorithm has been developed to calculate changes in pore pressure and stress within the lithosphere resulting from the filling of a reservoir of finite dimensions. The algorithm, based in linear Biot theory, models induced stresses and pore pressures along a plane of finite length and orientation for a particular filling history. The model is being tested against the pattern of seismicity observed at Monticello Reservoir following initial impoundment.

Presentation

Acree, S.C. and Talwani, P. Spatial and temporal variation of induced seismicity at Monticello Reservoir, paper presented at the Spring Meeting of the American Geophysical Union, Baltimore, MD, May, 1985.

Publications

Talwani, P. and Acree, S. Pore pressure diffusion and the mechanism of induced seismicity, *Pure and Appl. Geophys.*, **172**, 947-965, 1984/85.

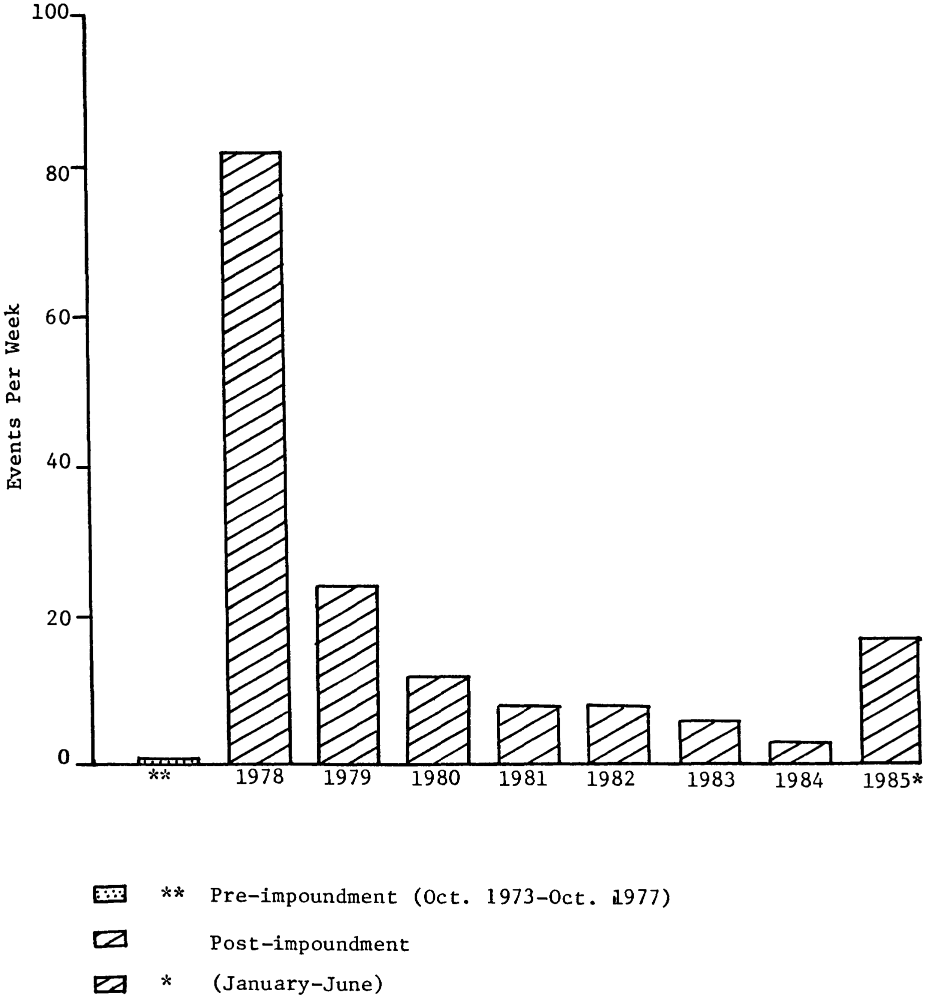
Events Per Week
100
80
60
40
20
0
**
1978
1979
1980
1981
1982
1983
1984
1985*
** Pre-impoundment (Oct. 1973-Oct. 1977)
Post-impoundment
* (January-June)

Figure 1

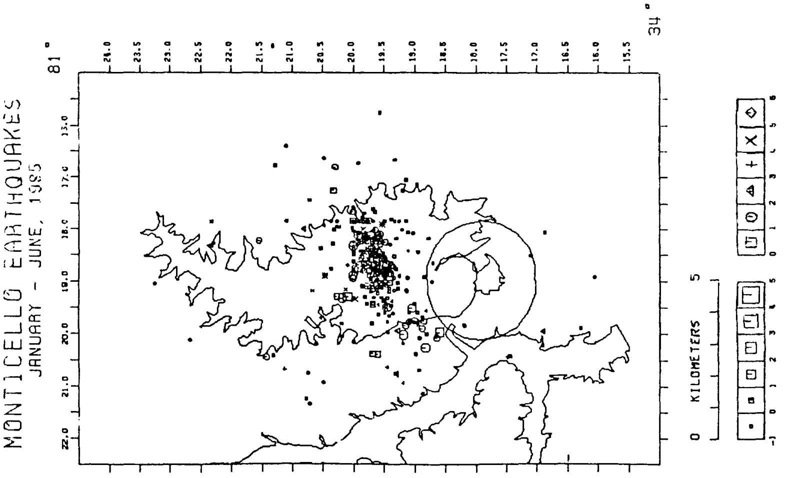

Figure 2

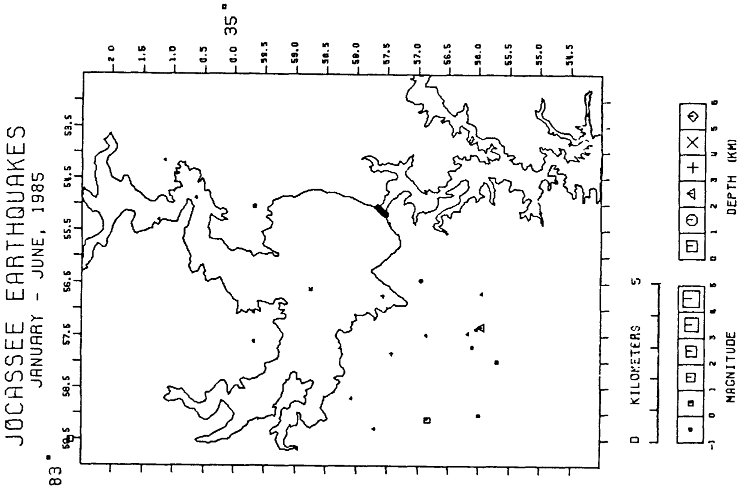

Figure 3

Regional and National Seismic Hazard and Risk Assessment

9950-01207

S. T. Algermissen
Branch of Engineering Geology and Tectonics
U.S. Geological Survey
Denver Federal Center, MS 966
Denver, CO 80225
(303) 236-1611

Investigations

1. Continued analysis of seismic source zone boundary uncertainty and the incorporation of this uncertainty into probabilistic seismic hazard evaluation.

2. Investigation of statistical treatment of errors in converting earthquake intensities to magnitudes in catalogs containing historical earthquake data.

3. Development of a technique for generalizing ground motions from a catalog of historical earthquakes in lieu of specifying seismic source zones.

4. Completion of an investigation as to the usefulness of pattern-recognition techniques in identifying earthquake-prone areas.

5. Documentation of existing auxiliary computer programs being used in support of probabilistic seismic hazard analyses.

Results

1. Comparing probabilistic accelerations calculated at sites along a line through (and past the boundary of) a source region, using, (1) median values in the Joyner and Boore attenuation function, (2) the values in the Schnabel and Seed curves, and (3) these relationships with standard deviation of $\sigma=0.5$ in $\log_e$-acceleration shows that including variability in the attenuation functions increases the difference in acceleration levels at sites near a boundary. The results demonstrate dramatic changes in probabilistic levels of acceleration at sites a short distance apart, and should serve to convince seismic hazard analysts that (a) significant differences in calculated probabilistic acceleration levels at sites a short distance apart (e.g., 50-80 per cent change in calculated accelerations at sites 20 km apart near a source zone boundary) result from the hard-edge boundary, and cannot be mitigated by taking acceleration variability into account; and (b) because there may be a significant difference in acceleration levels calculated at sites a few km apart, if one is interested in the hazard at a single site, one should also calculate probabilistic accelerations at a set of nearby sites, to determine how stable the answers are as a function of site location.

2. It is commonly believed that if $m=a+bI$, then $I=c+dm$, where $b=1/d$ and $a=-bc$. However, when these coefficients are fit by the least squares regression method to a set of earthquake magnitudes (when there are no observational errors), the relationships $b=1/d$ and $a=-bc$ do not hold. One

should never fit $I=c+dm$ but always use $m=a+bI$. Fitting both forms and averaging the results to obtain a better answer actually worsens the result. The relationship $\overline{m}_k=a+bI_k$ gives the mean magnitude for intensity I_k, but does not give us the magnitude range for that intensity. It is usually assumed that $\overline{m}_k$ is the midpoint of the magnitude interval (or possibly the lower endpoint), but this is wrong. If magnitudes in the range $m_k<m<m_{k+1}$ correspond to intensity I_k, and if $N(I_k)$ is the number of earthquakes with intensity I_k, it cannot be said that $\sum_{j \geq k} Nj$ is the number of earthquakes exceeding magnitude $\overline{m}_k$. When there are (normally distributed) errors in "observed" intensities (with standard deviation σ_i) the mean magnitude for an intensity decreases by $\beta\sigma_i^2$ (where $\beta \exp(-\beta m)$ is the density of earthquakes of magnitude m). If the magnitude-intensity relationship is fitted to a set of "observed" (magnitude, intensity) pairs, the standard deviation in the magnitude associated with a given intensity depends on the standard deviations in the original magnitudes and intensities and any corrections for magnitude or frequency must differentiate between the various errors.

3. Using programs and techniques developed for the source-zone boundary investigations above, a new program for generalizing ground motions from a catalog of historical earthquakes has been devised. The program permits the mapping of expected ground motions from, (1) past earthquakes, (2) past earthquakes with "fuzzed" locations, and (3) past earthquakes whose magnitudes are generalized over a specific range. Maps of these sorts will be useful in assessing the credibility of maps produced by the more usual techniques of estimating probabilistic ground motion in which more subjective choices of source zones and zonal seismicity rates must be used. The program will be tested in the northeastern United States, where the large amount of historical data should serve to define a stable product.

4. A manuscript entitled "Usefulness of Patter-Recognition Techniques for Identifying Earthquake Prone Areas" by B. Bender, M. Jones-Cecil and D. M. Perkins has been submitted for internal review.

5. A report entitled "Auxiliary Programs for Support of Seismic Hazard Analyses" has been submitted for Director's approval.

Reports

Campbell, K. W., 1985, Strong-motion attenuation relations: A ten-year perspective (1974-1984): Earthquake Spectra, v. 2, no. 1, November (in press).

Campbell, K. W., 1986, An empirical estimate of near-source ground motion for a major (m_b=6.8) earthquake in the eastern United States: Bulletin of the Seismological Society of America, v. 76, no. 1, February (in press).

Highland, L. M., 1985, Earthquake hazards to domestic water distribution systems in Salt Lake County, Utah, Proceedings American Water Works Association: Seattle, Wash., Distribution Symposium, Sept. 9-11, 1985 (in press).

Hopper, M. G., ed., 1985, Estimation of earthquake effects associated with large earthquakes in the New Madrid seismic zone: U.S. Geological Survey Open-File Report 85-457, 140 p.

Regional and Local Hazards Mapping in the Eastern Great Basin

9950-01738

R. Ernest Anderson
Branch of Engineering Geology and Tectonics
U.S. Geological Survey
Box 25046, MS 966, Denver Federal Center
Denver, CO 80225
(303) 236-1684

Investigations

1. Continued field mapping and analysis of data pertaining to earthquake hazards along the Wasatch fault zone. (Machette, Nelson, Personius, Scott)
2. Continued analysis of surface-rupture data and other effects of the 1983 Borah Peak, Idaho, earthquake. (Crone, Machette, and Bucknam)
3. Continued analysis and interpretation of exploratory trenching across the Lost River fault, Idaho. (Schwartz and Crone)
4. Studied Mackay segment of the Lost River fault, Idaho. (Crone, Haller and Bucknam)
5. Began installation of sets of control points at selected sites along the Lost River fault, Idaho, as a basis for monitoring post-faulting modification and the processes that cause them. (Crone and Bucknam)
6. Continued analysis of data bases that might reflect segmentation of the Wasatch fault zone. (Wheeler)
7. Began development of statistical procedures to identify significant concentrations and alignments of epicenters. (Wheeler)
8. Completed analysis of fault-slip data from south of the Wasatch fault in the central Sevier Valley area and compiled attitudes of Neogene strata adjacent to Sevier Valley. (Anderson and Barnhard)
9. Completed analysis of fault-slip data from the easternmost transition zone and westernmost Colorado Plateau, Wayne Co., Utah. (Anderson and Barnhard)
10. Began detailed study of late Quaternary surface deformation in two areas of southwest-central Utah where earthquakes are concentrated--the Elsinore and Annabella areas. (Anderson)
11. Began geologic study of the structural setting of the 1966 Clover Mountains earthquake Nevada. (Anderson and Barnhard)

Results

1a. As a result of detailed mapping of Quaternary deposits, studies of soils, and topographic profiling of Quaternary fault scarps along the northern Wasatch fault zone (WFZ), Personius and Nelson have differentiated two new segments of the fault zone, here named the Brigham City and Kaysville segments. The Brigham City segment extends north from a previously unrecognized segment boundary near the Pleasant View salient northwest of North Ogden, UT, to the Jim May Canyon reentrant northeast of Honeyville, UT. This segment contains the southern part of the Collinston segment and the northern part of the Ogden segment as previously described by Schwartz and Coppersmith (1984). The Kaysville segment comprises the remaining 50 km of the former Ogden segment.

Movement on the Brigham City segment is characterized by high slip rates and short recurrence intervals during the latest Pleistocene and early Holocene (similar to slip rates on other WFZ segments to the south), but the segment has been relatively inactive in middle and late Holocene time. Variation in the size of Quaternary scarps along the segment indicates that the highest rates of tectonic activity are along the central part (from Brigham City to Willard), whereas lower rates are typical to the north and south.

A vertical exposure in a late Holocene fault scarp along the Kaysville segment near Ogden shows three fault-produced colluvial wedges capped by organic-rich A horizons. Wedge thicknesses suggest three displacement events of about 1-2 m stratigraphic displacement each. All three events are probably <6 ka, but ^{14}C analysis of the A horizons will provide better age control. These and other data indicate that the Kaysville segment has a high mid- to late-Holocene slip rate in contrast to the Brigham City segment. Also, scarp heights indicate that post-Bonneville slip rates on the Kaysville segment are somewhat higher (1 m/kyr) than rates on segments to the north. As with the Brigham City segment, slip rates appear to decrease near the boundaries of the segment.

1b. The Provo segment of the WFZ, as recognized by Schwartz and Coppersmith (1984) extends from the Traverse Range northwest of Alpine, UT, south about 55 km to Payson Canyon, south of Payson, UT. This segment bounds the fairly linear front of the Wasatch Mountains as far south as Springville, UT, but then forms a convex-west arc in the Spanish Fork embayment of the southern Utah Valley. Preliminary interpretation from detailed mapping and morphometric analysis of fault scarps along the Provo segment suggest that it is two discrete segments that join north of Springville.

The northern part of the "Provo segment" is herein named the American Fork segment for the excellent scarps preserved on the southern part of the American Fork delta (a Bonneville-age feature). The southern part of the "Provo segment" is herein named the Spanish Fork segment; it includes Woodward-Clydes trench sites near Hobble Creek and William M. Davis' type locality of faceted spurs. The junction between the two newly differentiated segments has the geometric form of an inverted Y, the southwestern arm extends 3.5 km southwest from the mountain front along the west edge of Springville, UT. The southeastern arm is the northern end of the Spanish Fork segment. The southern part of the Spanish Fork segment has been traced along the front of Loafer Mountain, southward into Payson Canyon where it extends an undetermined but probably short distance (2 km?). Using this subdivision, the American Fork and Spanish Fork segments are 25 and 37 km long, respectively (the distances along trace are 31 and 39 km, respectively).

1c. The new data on fault segmentation described above suggests that the Wasatch Fault Zone (WFZ) consists of at least eight segments. Machette, Personius, and Nelson tentatively suggest the following segments for the WFZ:

	This report		Schwartz and Coppersmith	
	Segment	Length (km)	Segment	Length (km)
A	Collinston	15	Collinston	≥ 30
B	Brigham City	33	Ogden	70
C	Kaysville	50	Ogden	70
D	Salt Lake City	35	Salt Lake City	35
E	American Fork	37	Provo	55
F	Spanish Fork	25	Provo	55
G	Nephi	35	Nephi	35
H	Levan	40	Levan	40

Our analysis shows that (1) most of the eight segments have lengths of 25 km to 40 km; (2) these values are comparable to the rupture lengths of 30-40 km that are commonly associated with earthquakes in the magnitude range of 6.75-7.5; (3) the boundaries between segments have four forms: abut (A-B, B-C, E-F), en echelon overlap (C-D, F-G), Y-junction (E-F), and barren gap (G-H); and (4) the boundaries generally coincide with either changes in range front trend, general altitude of the range, or major structures that crosscut the WFZ.

2. The surface effects of the 1983 Borah Peak earthquake, Idaho, are documented in detail in the three reports marked by *. These and other data will serve as benchmarks not only for monitoring post-faulting effects such as those caused by erosional modification but also for comparison with the effects of other earthquakes.

3. The 1983 Borah Peak earthquake is seen as a calibration event for quantifying earthquake recurrence and fault behavior on normal faults in the eastern Great Basin. Exploratory trenching across the Lost River fault and 1983 surface displacements at Doublespring Pass Road show that (1) only one surface-faulting event occurred along this fault between the time of formation of the surface of a Pinedale-age outwash fan (approximately 15,000 yrs ago) and the 1983 earthquake, (2) fault displacement for the pre-1983 and 1983 events is nearly identical, and

(3) the analysis of scarp-derived colluvial deposits provides an accurate basis for quantifying recurrence of surface-faulting earthquakes on normal-slip faults. The similarity in the slip distribution between the 1983 and pre-1983 events along the length of the surface rupture suggests that the 1983 event is a characteristic earthquake for this segment of the Lost River fault. The relationship between the timing of individual past surface-faulting events and bedrock structure of the Lost River Range has the potential to provide important insights into processes of fault-zone segmentation.

4. Study of late Quaternary faulting along the Mackay segment of the Lost River fault, Idaho, provides data that are critical to understanding the segmentation of that fault. Surface faulting associated with the 1983 Borah Peak earthquake occurred mainly along the Thousand Spring (TS) segment of the Lost River fault. No 1983 faulting occurred along the 24-km-long Mackay segment to the southeast, yet fault scarps displace late Pleistocene and probably early Holocene alluvium. Higher scarps in older deposits attest to recurrent late Quaternary movement. Scarps on the Mackay segment at Upper Cedar Creek are morphologically similar to the pre-1983 scarps on the TS segment near Doublespring Pass road, suggesting that either the last prehistoric faulting on the TS and Mackay segments were closely spaced in time (few thousand years), or one event produced faulting on both segments.

   A 4-km-long gap in scarps along the Lost River fault separates the Mackay segment from the 1983 surface faulting along the TS segment. The boundary between these segments is probably located within this gap. The gap also coincides with a 55° change in the trend of the range, which suggests a bend or a discontinuity in the fault. Bends and discontinuities may play an important role in the initiation and termination of coseismic ruptures. The unilateral nature of the 1983 rupture and the temporal pattern of the aftershocks suggest that a large strain differential may exist across this segment boundary. A large strain differential at a major bend or discontinuity in the fault could be the nucleation site for a future earthquake on the Mackay segment.

5. No results yet.

6. No results yet.

7. Inspection of epicenters in the west-central United States by K. G. Brill, Jr., and O. W. Nuttli suggested to them that seismicity over the past century is concentrated in the Colorado lineament. This suggestion is evaluated by analyzing overlapping subsamples, mapping independent cells that are significantly overpopulated by epicenters, and arguing that the sample is representative of the population from which it was drawn. Results support the suggestion. Vectors connecting nearest-neighbor earthquakes show no significant preferred orientation. The epicenters cluster at several places in the lineament, but nearest neighbors do not align along it.

8. Analysis of fault-slip and other structural data from the central Sevier Valley area has led to formulation of a framework for neotectonic deformation that is broadly consistent with the earthquake record from the area. Large amounts of horizontal deformation concentrated on strike-slip faults and related folds in Neogene rocks cannot, on the basis of available data, be projected along strike into older rocks, thus requiring that the deformed rocks be structurally detached from the older rocks. Low-angle detachment is inferred. Block motions are primarily southwestward on integrated systems of strike-slip and inferred detachment faults. This style of deformation is consistent with the two main characteristics of the seismicity: (1) a predominance of strike-slip focal mechanisms with a conspicuous element of slip incompatibility indicated by interchangeable P and T axes, (2) hypocenter frequencies that fall off sharply at depths of 5-6 km, suggesting deformation above planes of structural compensation. For much of the study area, structural data do not allow for significant east-west extension on normal faults--a startling discovery considering the conventional characterization of neotectonic deformation in this region.

9. Fault-slip data were gathered from the Thousand Lake fault, the easternmost main fault zone of the transition zone. Faults that parallel the main fault show mainly dip slip, but many faults in the zone strike oblique to it and show strike slip or dip slip. Analysis of the predominantly dip-slip faults indicates a west-northwest/east-southeast (285°) least principal stress/strain axis that we interpret as the neotectonic extension direction for the area. The distribution of faults with slickenlines known to have formed during Laramide compression indicates that there has been a nominal amount of Neogene fault reactivation in the westernmost part of the Colorado Plateau interior. The easternmost limit of significant Cenozoic extensional deformation is sharply defined by the Thousand Lake fault. That fault has an estimated minimum of 85 m of Pleistocene (post early Wisconsin) throw suggesting that it is currently serving as a remarkably sharp strain boundary.

10. Late Quaternary surface faulting in the Elsinore and Annabella areas was documented by Anderson and Bucknam (1979). In the Annabella area, some of that deformation appears to be reactivation of Pliocene and younger faults that are linked structurally to uplift along the Sanpete-Sevier anticline, suggesting that the anticline is still active. Where the Sevier River crosses the trace of late-Quaternary fault scarps in the Elsinore area, its channel pattern appears to be out of equilibrium. The channel-pattern anomalies are consistent with the displacement directions implied by fault scarps and tilted geomorphic surfaces. Future studies will be conducted to test these relationships, and an attempt will be made to analyze the results in terms of the historic seismic record.

11. A reconnaissance study of structures in bedrock and basin-fill alluvium in the vicinity of the 1966 Clover Mountains earthquake and aftershock zone reveals two modes of Neogene deformation, neither of which is consistent with the focal mechanism and preferred nodal plane for that earthquake. The youngest deformation evident in the vicinity of the seismicity is a major episode of late Tertiary east-northeast/west-southwest extension. The area northwest of the seismicity includes

significant dextral shear on northwest-trending faults. Neither is consistent with dextral shear on a northerly trending plane indicated by the seismicity.

References Cited

Anderson, R. E., and Bucknam, R. C., 1979, Map of fault scarps on unconsolidated sediments, Richfield 1° by 2° quadrangle, Utah: U.S. Geological Survey Open-File Report 79-1236, 17 p., 1 pl.

Schwartz, D. P., and Coppersmith, K. J., 1984, Fault behavior and characteristic earthquakes--Examples from the Wasatch and San Andreas fault zones: Journal of Geophysical Research, v. 89, no. B7, p. 5681-5698.

Reports

*Crone, A. J., 1986 (in press), Surface faulting associated with the 1983 Borah Peak earthquake at Doublespring Pass Raod, east-central, Idaho: Geological Society of America, Decade of North American Geology, Centennial Field Guide Volume, 10 p.

Crone, A. J., and Harding, S. T., 1984, Near-surface faulting associated with Holocene fault scarps, Wasatch Fault Zone, Utah--A preliminary report, _in_ Hays, W. W., and Gori, P. L., eds., Proceedings of Conference XXVI--A workshop on "Evaluation of regional and urban earthquake hazards and risk in Utah:" U.S. Geological Survey Open-File Report 84-763, p. 241-265.

*Crone, A. J. and Hait, M. H. Jr., 1985, Fault scarps, landslides, and other features associated with the Borah Peak Earthquake on October 28, 1983, central Idaho--A field trip quide, _in_ Stein, R. S., and Bucknam, R. C., eds., Proceedings of Workshop XXVII on the Borah Peak, Idaho, Earthquake: U.S. Geological Survey Open-File Report 85-290, v. B, 23 p., 3 plates, 1:24,000 scale.

Crone, A. J., Haller, K. M., Bucknam, R. C., and others, 1985 (in press), Late Quaternary faulting along the Mackay segment of the Lost River fault, central Idaho [abs.]: EOS [American Geophysical Union]

Crone, A. J., Machette, M. N., Bonilla, M. G., Lienkaemper, J. J., Pierce, K. L., Scott, W. E., and Bucknam, R. C., 1985, Characteristics of surface faulting accompanying the Borah Peak Earthquake, central Idaho, _in_ Stein, R. S., and Bucknam, R. C., eds., Proceedings of Workshop XXVII on the Borah Peak, Idaho, Earthquake: U.S. Geological Survey Open-File Report 85-290, v. A, p. 43-58.

*Crone, A. J., and Monger, K. A., 1985, Variations in the morphology of 1983 fault scarps at Borah Peak, Idaho [abs.]: Geological Society of America Abstracts with Programs, v. 17, no. 4, p. 215.

Crone, A. J., and Pierce, K. L., 1985, The Borah Peak earthquake of October 28, 1985--Surface faulting, mass movements and Quaternary tectonic setting: Geological Society of America Field Trip Guide, 1985 Rocky Mountain Section Meetings, Boise, Idaho.

Machette, M. N., 1984, Preliminary investigations of late Quaternary slip rates along the southern part of the Wasatch Fault Zone, central Utah, in Hays, W. W., and Gori, P. L., eds., Proceedings of Conference XXVI--A workshop on "Evaluation of regional and urban earthquake hazards and risk in Utah": U.S. Geological Survey Open-File Report 84-763, p. 391-406.

Machette, M. N., 1985, Documentation for bechmark photographs showing some effects of the 1983 Borah Peak Earthquake with considerations for studies of scarp degradation, in Stein, R. S., and Bucknam, R. C., eds., Proceedings of Workshop XXVII on the Borah Peak, Idaho, Earthquake: U.S. Geological Survey Open-File Report 85-290, v. A, p. 97-109.

Machette, M. N., 1985, Calcic soils of the southwestern United States, in Weide, D. L., ed., Soils and Quaternary Geology of the Southwestern United States: Geological Society of America Special Paper 203, p. 1-21.

Machette, M. N., 1985, Late Cenozoic Geology of the Beaver Basin, southwestern Utah: Brigham Young University Geology Studies, v. 32, part 1, p. 19-37.

Machette, M. N., 1986 (in press), History of Quaternary offset and paleoseismicity along the La Jencia fault, central Rio Grande rift, New Mexico: Bulletin of the Seismological Society of America (23 manuscript pages, 3 tables, 5 figures).

Machette, M. N., Personius, S. F., Menges, C. M., and Pearthree, P. A., 1986 (in press), Map of Pliocene and Quaternary faults in the Silver City 1° x 2° quadrangle and Douglas 1° x 2° quadrangle, southeastern Arizona and southwestern New Mexico: U.S. Geological Survey Miscellaneous Field Studies Map MF-1465-C, scale 1:250,000 (Branch approval).

Schwartz, D. P., and Crone, A. J., 1985, The 1983 Borah Peak Earthquake--A calibration event for quantifying earthquake recurrence and fault behavior on Great Basin normal faults, in Stein, R. S., and Bucknam, R. C., eds., Proceedings of Workshop XXVII on the Borah Peak, Idaho, Earthquake: U.S. Geological Survey Open-File Report 85-290, v. A, p. 153-160.

Wheeler, R. L., 1985, Evaluating point concentrations on a map--Earthquakes in the Colorado Lineament [abs.]: Geological Society of America Abstracts with Programs, v. 17, no. 4, p. 271.

Wheeler, R. L, 1986 (in press), Evaluating point concentrations on a map: Earthquakes in the Colorado Lineament: Geology.

Wheeler, R. L., Van Gosen, B. S., Bedinger, G. M., and Wenrich, K. J., 1985, Methods for evaluating alignments of epicenters and other mapped points [abs.]: Earthquake Notes, v. 55, no. 1, p. 19.

Implementation of Research Results and Information Systems for Regional and Urban Earthquake Hazards Evaluation, Southern California

9950-03836

William M. Brown III
Branch of Engineering Geology and Tectonics
345 Middlefield Road, MS-998
Menlo Park, California 94025
(415) 856-7112/7119

Investigations:

This project is part of a long-range regional earthquake hazards evaluation for Southern California, directed by the U.S. Geological Survey. This phase of the project is oriented towards (1) Summarizing results of recent earth-science research on evaluating earthquake hazards; (2) Presenting examples of ongoing earthquake-hazard reduction efforts; and (3) Determining what additional scientific and technical information is needed and which hazard-reduction techniques are most effective. This phase draws upon research results published in U.S. Geological Survey Professional Paper 1360 (1985), and is intended to direct future research efforts based upon evaluation of those results.

The evaluation began during April-September 1985 with distribution of materials from Professional Paper 1360 and selective invitations for written statements on earthquake hazards evaluation. The distribution was directed to a multidisciplinary group of about 80 people from a variety of professions involved with the earthquake hazard for Southern California. These people were requested to prepare formal responses to those matérials, and to present their analyses and recommendations at a major multidisciplinary workshop convened during November 12-13, 1985.

The bulk of work during April-September, 1985 was directed toward coordinating and convening the workshop. This work was directed primarily by Joseph I. Ziony, William J. Kockelman, and William M. Brown III of the Office of Earthquakes, Volcanoes, and Engineering, U.S.G.S., Menlo Park, CA. The work is supported by the U.S. Geological Survey, National Science Foundation, Federal Emergency Management Agency, California Seismic Safety Commission, California Governor's Office of Emergency Services, California Department of Conservation/Division of Mines and Geology, Southern California Association of Governments, and the Southern California Earthquake Preparedness Project.

The workshop, "Future Directions in Evaluating Earthquake Hazards of Southern California" focuses on (1) Evaluating earthquake and surface-faulting potential; (2) Predicting seismic intensities for response planning and loss estimation; (3) Predicting ground motion for earthquake-resistant design; (4) Predicting major earthquakes for preparedness planning; (5) Evaluating earthquake ground-failure potential for development decisions; and (6) Evaluating the shaking hazard for redevelopment decisions. Each of these elements will be introduced from a scientific perspective, which in turn will be evaluated by those who would apply the scientific information. This format is intended to determine whether (1) the scientific information is understandable to those who need to use it; (2) the scientific information is appropriate to specific user needs; and (3) there should be redirection of research efforts to accommodate specific needs. The workshop will generate abundant written statements, commentary, and recommendations on these topics that will be published separately as a proceedings volume during 1986.

Results:

1. Development of a tight, formal program of 80 presenters, moderators, panelists, and commentators for an intensive two-day session involving a plenary session and three workshops each day. Total participation is about 300. Those on the program represent a significant aggregation of the most prominent workers in earthquake hazards evaluation, reduction, and response for Southern California. The program and all associated materials are available on request from the address at the head of this article.

2. Development of financial, logistical, and other support of sponsoring agencies to convene the workshop and produce the proceedings.

Reports:

Ziony, J. I., ed., 1985, Evaluating earthquake hazards in the Los Angeles Region--An earth-science perspective: U.S. Geological Survey Professional Paper 1360, 505 p.

Seismic Hazards of the Hilo 7 1/2′ Quadrangle

9950-02430

Jane M. Buchanan-Banks
Branch of Engineering Geology & Tectonics
U. S. Geological Survey
David A. Johnston Cascades Volcano Observatory
5400 MacArthur Boulevard
Vancouver, Washington 98661
(206) 696-7996

Investigations

1. Continued geologic mapping, field checking, compilation of geology on stable base, and writing of text for geologic map of Hilo quadrangle.

2. Revised reviewed manuscript on structural damage and ground failures from November 1983 Kao′iki earthquake.

3. Attendance at the 1985 Scientific Assembly on Potassic Volcanism - Mt. Etna Volcano.

Results

1. Completion of geologic mapping and field checking was hampered by continued inclement weather and preparations for a change-of-duty station to Vancouver in July. Transferring of geology from air photos to a stable base is nearly completed, and the text to accompany the GQ is being written.

2. A manuscript on structural damage and ground failures from the 1983 Kao′iki earthquake was revised, and received Director′s approval.

3. Attended the 1985 Scientific Assembly on Potassic Volcanism-Mt. Etna Volcano, sponsored by C.N.R., International Institute of Volcanology, Italy, and International Association of Volcanology and Chemistry of the Earth′s Interior. Several meeting sessions were devoted to descriptions of geologic settings, monitoring techniques, eruptive behavior and geologic hazards of various volcanoes of the world. The pre-meeting field trip provided an opportunity to view Italian volcanoes in a variety of seismotectonic settings, and to examine the types and extent of their products and the volcanic hazards they represent. Mid- and post-meeting field trips emphasized the volcanic hazards of Mt. Etna Volcano and the attempts undertaken to mitigate the hazards, particularly lava barriers used in a successful lava-flow diversion attempt in 1983.

Reports and Publications

Buchanan-Banks, J. M., 198_, Structural damage and ground failures from the Kao'iki Earthquake, Island of Hawai'i, November 16, 1983, in Decker, R. W. and Wright, T. L., eds., Hawai'ian Volcanism: U.S. Geol. Survey Prof. Paper 1350

Geology and Tectonic Evolution of the Western Transverse Ranges, California

9950-99924

R. H. Campbell
Branch of Engineering Geology and Tectonics
U.S. Geological Survey National Center, MS 922
Reston, Virginia 22092
(703) 860-7874

Investigations and Results:

Faunal lists from Middle and Lower Miocene strata of the central and western Santa Monica Mountains have been correlated with physical stratigraphy, combined, and listed by stratigraphic unit according to the nomenclature of Yerkes and Campbell, 1979. Cross-referencing according to collection locality and generation of a combined locality map in ADP format is in preparation. Following is the combined listing, which has had preliminary review and revision:

VAQUEROS FORMATION

Gastropods

- *Austrotrophon* sp.
- *Bittium* sp.
- *Crepidula princeps* Conrad
- *Crepidula* sp.
- *Forreria gabbiana* (Anderson)
- *Forreria* sp.
- Muricid
- Naticid
- *Neverita* sp.
- *Ocenebra topangensis* Arnold
- *Ocenebra* sp.
- *Rapana vaquerosensis* (Arnold)
- *Searlesia* sp.
- *Solenosteira* sp.
- *Thylaeodus* sp.
- *Trochita* sp.
- *Trophon kernensis* Anderson
- *Turritella inezana* Conrad
- *Turritella inezana* Conrad unnamed variant
- *Turritella inezana bicarina* Loel and Corey
- *Turritella inezana equisriata* Merriam
- *Turritella inezana hoffmani* Gabb
- *Turritella inezana santana* Loel and Corey

- *Turritella inezana sespeensis* Arnold
- *Turritella inezana n. subsp.*
- *Turritella ocoyana* Conrad
- *Turritella tritschi* Hertlein
- *Turritella variata* Conrad
- *Turritella* sp.

Pelecypods

- *Aequipecten andersoni* (Arnold)
- *Amiantis* sp.
- *Anadara santana* (Loel and Corey)
- *Anadara* sp.
- *Anadara?* sp.
- Arcid?
- *Atrina venturaensis* Yates in Cooper
- *Chione* sp.
- *Chlamys hericia* (Gould
- *Chlamys sespeensis* (Arnold)
- *Chlamys* sp.
- *Clementia* sp.
- *Crassostrea titan subtitan* Loel and Corey
- *Diplodonta* sp.
- *Dosinia* sp.
- *Glycymeris?* sp.
- *Here excavata* Carpenter
- Lucinid
- *Lucinoma* sp.
- *Lyropecten estrellanus* (Conrad)
- *Lyropecten miguelensis* (Arnold)
- *Lyropecten* sp.
- *Macoma nasuta* Conrad
- *Macoma* sp.
- *Macoma?* sp.
- *Macrochlamys magnolia* (Conrad)
- *Miltha sanctaecrucis* Arnold
- *Miltha* sp.
- *Mytilus expansus* Arnold
- *Mytilus* sp.
- *Ostrea eldridgei ynezana* Loel and Corey
- *Ostrea vespertina loeli* Hertlein
- *Ostrea* sp.
- *Panopea abrupta* (Conrad)
- *Pecten* sp.
- Pectinid
- *Saxidomus vaquerosensis* Arnold of Loel and Corey (1932)
- *Saxidomus* sp.
- *Semele* n. sp.
- *Spisula catillformis* Conrad
- *Spondylus perrini* Wiedey
- *Spondylus*
- *Tagelus gabbianus* (Anderson and Martin)
- *Tivela* sp.
- *Trachycardium vaquerosensis*
- *Trachycardium vaquerosensis* (Arnold)
- *Vertipecten nevadanus* (Conrad)
- *Vertipecten perrini* (Arnold)
- *Vertipecten* sp.
- Undet

Scaphopod

- *Dentalium* sp.

Echinoids

Vaquerosella vaquerosensis (Kew)
Undet

Bryozoan

Undet

Barnacles

Balanus concavus Bronn
Balanus gregarius (Conrad)
Balanus sp.
Balanus? sp.
Undet

Foraminfera

Bathysiphon sp.
Bolivina advena Cushman
Bolivina advena advena Cushman
Bolivina advena striatella Cushman
Bolivina conica Cushman
Bolivina marginata Cushman
Bolivina marginata marginata Cushman
Bolivina tumida Cushman
Bolivina tumida tumida Cushman
Bolivina sp.
Bulimina sp.
Buliminella curta Cushman
Buliminella subfusiformis Cushman
Buliminella sp.
Cassidulina crassa d'Orbigny
Dentalina sp.
Epistominella relizensis (Kleinpell)
Epistomella subperuviana subperuviana Cushman
Fursenkoina californiensis (Cushman)
Fursenkoina californiensis californiensis Cushman
Globigerina bulloides d'Orbigny
Globigerina dubia Egger
Globigerina hexagona Natland
Globigerina sp.
Nonion costiferum (Cushman)
Nonion incisum Cushman
Nonion sp.
Siphogenerina branneri (Bagg)
Siphogenerina sp.
Uvigerinella obesa Cushman
Undet arenaceous

Fish

Carangidae sp.
Cycloepoides tuberculatus David
Cynoscion sp.
Etringus 66
Etringus 75
Etringus sp.
Etrumeus sp.
Ganolytes sp.
Sciaenidae sp.
Scomber miocenicus
Sparidae sp.
Xyne luisensis
Xyne sp.

Sharks

- *Carcharhinus?* sp.
- undet tooth

Cetacean

- *Squalodon? bariensis* Jourdan

TOPANGA CANYON FORMATION

Gastropods

- *Anachis* sp.
- *Antillophos dumbleanus* (Anderson in Hanna)
- *Antillophos posunculensis* (Anderson and Martin)
- *Astraea morani* Loel and Corey
- *Astraea topangensis* (Arnold)
- *Austrotrophon* sp.
- *Batillaria ocoyana* (Anderson and Martin)
- *Bittium topangensis* (Arnold)
- *Bruclarkia barkeriana* (Cooper)
- *Bruclarkia orgonensis* (Conrad)
- *Bruclarkia yaquinana* (Anderson and Martin)
- *Bulla cantuaensis* Anderson and Martin
- *Bulla* sp.
- *Calicantharus* sp.
- *Calyptraea* sp.
- *Calyptraea coreyi* Addicott
- *Calyptraea filosa* (Gabb)
- *Calyptraea inornata* (Gabb)
- *Calyptraea* sp.
- *Cancellaria dalliana* Anderson
- *Cancellaria oregonensis* (Conrad)
- *Cancellaria posunculensis* Anderson and Martin
- *Cancellaria simplex* Anderson
- *Cancellaria* (*Crawfordia*) n. sp.
- *Cancellaria* (*Euclia*) n. sp.
- *Cancellaria* sp.
- *Cantharus* (*Hanetia*) n. sp.
- *Cerithium arnoldi* Anderson and Martin
- *Cerithium topangensis* Arnold
- *Cerithium* sp.
- *Conus haysei* Arnold
- *Conus owenianus*
- *Conus owenianus* Anderson
- *Conus* sp.
- *Corbula* sp.
- *Crepidula praerupta* Conrad
- *Crepidula princeps* Conrad
- *Crepidula* sp.
- *Crucibulum* sp.
- *Cymatium* n. sp.
- *Epitonium* sp.
- *Ficus* (*Trophosycon*) *kerniana* (Cooper)
- *Kelletia* sp.
- *Megasurcula keepi* (Arnold)
- *Melongena californica* Anderson and Martin
- *Mitrella* sp.
- Muricid
- *Nassarius antiselli* (Anderson and Martin)
- *Nassarius arnoldi* (Anderson)
- *Nassarius* sp.
- *Naticid*
- *Neverita alta* (Arnold)

Nerverita andersoni (Clark)
Neverita (Glossaulax) sp.
Neverita sp.
Nucella edmondi (Arnold)
Nucella sp.
Ocenebra topangensis Arnold
Ocenebra wilkesana (Anderson)
Ocenebra n. sp.
Ocenebra sp.
Oliva californica Anderson
Oliva californica futheyana Anderson
Olivella pedroana subpedroana Loel and Corey
Olivella subpedroana Loel and Corey
Olivella sp.
Ophiodermella sp.
Polinices sp.
Scalina whitei (Keen)
Scaphander jugularis (Conrad)
Tegula dalli (Arnold)
Tegula dalli (Arnold) var.
Tegula dalli inornata (Arnold)
Tegula dalli subnodosa (Arnold)
Terebra cooperi Anderson
Terebra sp.
Trochita spirata (Forbes)
Trochita trochiformis (Born)
Trophon kernensis Anderson
Trophon sp.
Turbo topangensis Arnold
Turricula buwaldana (Anderson and Martin)
Turricula ochsneri (Anderson)
Turricula piercei (Arnold)
Turricula wilsoni (Anderson and Martin)
Turricula sp.
Turritella moodyi Merriam
Turritella ocoyana Conrad
Turritella ocoyana topangensis Merriam
Turritella temblorensis Wiedey
Turritella sp.

Pelecypods

Acila conradi (Meek)
Acila sp.
Amiantis mathewsoni (Gabb)
Amussiopecten vanvlecki (Arnold)
Anadara sp.
Cardiid
Chione temblorensis (Anderson)
Chione (Chionista) sp.
Chione sp.
Clementia conradiana (Anderson)
Clementia pertenuis (Gabb)
Clementia sp.
Corbula sp.
Crassostrea sp.
Diplodonta buwaldana Anderson and Martin
Diplodonta harfordi Anderson
Diplodonta sp.
Dosinia mathewsoni (Gabb)
Dosinia merriami Clark
Dosinia sp.
Felaniella harfordi (Anderson)
Glycymeris sp.
Here excavata Carpenter
Heteromacoma rostellata (Clark)

Leptopecten andersoni (Arnold)
Leptopecten arnoldi (Anderson)
Lucinisca sp.
Lucinoma acutilineata (Conrad)
Lucinoma sp.
Lyropecten crassicardo (Conrad)
Lyropecten estrellanus (Conrad)
Lyropeceten miguelensis (Arnold)
Lyropecten sp.
Macoma arctata (Conrad)
Macoma copelandi Wiedey
Macoma nasuta (Conrad)
Macoma panzana Wiedey
Macoma sp.
Miltha sanctaecrucis (Arnold)
Miltha sp.
Modiolus sp.
Mya sp.
Mytilus expansus Arnold
Mytilus sp.
Nuculana sp.
Ostrea sp.
Pectinid
Pholadid
Psephidia sp.
Sanquinolaria sp.
Saxidomus vaquerosensis Loel and Corey
Securella sp.
Solecurtus gabbianus (Anderson and Martin)
Solen curtus Conrad
Solen gravidus Clark
Solen sp.
Spisula catilliformis Conrad
Tellina idae Dall
Tellina piercei (Arnold)
Tellinid
Teredo sp.
Trachycardium schencki (Wiedey)
Trachycardium vaquerosensis (Arnold)
Trachycardium sp.
Tresus nuttalli (Conrad)
Tresus sp.
Vertipecten nevadanus (Conrad)
Zirfaea sp.
Zirphaea dentata Gabb

Brachiopod
  Discinisca sp.

Echinoids
  Vaquerosella coreyi Durham
  Vaquerosella sp.

Barnacles
  Balanus sp.

Ostracods
  Undet

Foraminifera
  Angulogerina sp.
  Anomalina salinasensis Kleinpell
  Bathysiphon sp.
  Bolivina advena advena Cushman
  Bolivina advena striatella Cushman
  Bolivina californica Cushman
  Bolivina imbricata Cushman
  Bolivina marginata adelaidana

Bolivina marginata marginata Cushman
Bolivina parva Cushman and Galliher
Bolivina perrini Kleinpell
Bolivina tumida Cushman
Bolivina vaughani Natland
Bolivina yneziana Kleinpell
Bolivina sp.
Bucella sp.
Bulimina montereyana delmonteensis Kleinpell
Buliminella curta Cushman
Buliminella elegantissima (d'Orbigny)
Buliminella subfusiformis Cushman
Buliminella sp.
Cancris sp.
Cassidulina crassa d'Orbigny
Cassudulina monicana Cushman and Kleinpell
Cibicides sp.
Elphidium sp.
Epistominella capitanensis Cushman and Kleinpell
Epistominella gyroidinaformis (Cushman and Goudkoff)
Epistominella relizensis (Kleinpell)
Epistominella subperuviana (Cushman)
Eponides sp.
Florilus sp.
Fursenkoina bramlettei Galloway and Morrey
Fursenkoina californiensis (Cushman)
Fursenkoina californiensis californiensis (Cushman)
Gaudryina sp.
Globigerina bulloides

Globigerina bulloides bulloides d'Orbigny
Globigerina sp.
Globobulimina ovula
Globobulimina sp.
Gyroidina sp.
Hanzawaia sp.
Haplophragmoides sp.
Lagena sp.
Lenticulina sp.
Nonion incisum Cushman
Nonion mediocostatum (Cushman)
Nonion ynezianum Kleinpell
Nonionella costifera
Nonionella miocenica Cushman
Nonionella sp.
Pullenia miocenica Kleinpell
Quinqueloculina sp.
Siphogenerina sp.
Spiroplectammina sp.
Uvigerina hootsi, Rankin
Uvigerinella californica Cushman
Uvigerinella californica perparva Bandy and Arnal
Uvigerinella obesa (Cushman)
Uvigerinella sp.
Valvulinera araucana (d'Orbigny)
Valvulineria californica Cushman

Valvulineria californica appressa Cushman
Valvulineria depressa Cushman
Valvulineria miocenica Cushman
Valvulineria sp.
Undet. arenaceous

Diatoms
Undet.

Radiolaria
Undet.

Sponges
Undet. spicules

Fish
Atherinidae 1 Sp no 1 of David
Atherinidae 2
Atherinidae 4
Atherinidae sp.
Carangidae sp.
Cynoscion sp.
Decapterus sp.
Embiotocoidae sp.
Etringus 66
Etringus sp. (Round herring)
Etrumeus sp. (Round herring)
Ganolytes sp.
Harengula sp.
Paralabrax piccolus
Plectrites sp.
Salmonidae sp.
Sciaenidae sp.
Scomber "miocaenicus"
Scomber "miocaenicus" (Undescribed ARCO nos 47, 47a)
Scomber miocenicus
Scomber elongatus Ayres
Sebastodes sp.
Seriola sp.
Sparidae sp.
Xyne "luisensis" (Undescribed ARCO type no 36)
Xyne luisensis
Xyne sp.

Shark
Carcharodon branneri Jordan

Mammals
Merychippus tehachapiensis Buwaldana and Lewis

Plants
Undet. fragments

CALABASAS FORMATION
(Indigenous fossils)

Gastropods
Astraea topangensis (Arnold)
Astraea sp.
Bittium topangensis (Arnold)
Bulla cantuaensis Anderson and Martin
Calyptraea filosa (Gabb)
Calyptraea inornata (Gabb)
Cerithid
Conus haysei Arnold

- *Conus* sp.
- *Ficus* (*Trophosycon*) *kerniana* (Cooper)
- *Miopleniona* sp.
- *Naticid*
- *Ocenebra topangensis* Arnold
- *Tegula dalli* (Arnold)
- *Tegula dalli subnodosus* (Arnold)
- *Terebra* sp.
- *Turricula buwadana* (Anderson and Martin)
- *Turritella ocoyana* Conrad
- *Turrtella ocoyana topangensis* Merriam
- *Turritella temblorensis* Wiedey
- Undet.

Pelecypods

- *Amiantis* sp.
- *Amussiopecten* sp.
- *Clementia pertenuis* (Gabb)
- *Crassostrea* sp.
- *Dosinia* sp.
- *Glycymeris* sp.
- *Lucinisca* sp.
- *Macoma* sp.
- *Mytilus* sp.
- *Ostrea* sp.
- Pectinid
- *Solen* sp.
- Tellinid
- *Tivela* sp.
- *Trachycardium schencki* (Wiedey)
- *Trachycardium vaquerosensis* (Arnold)
- Venerid
- *Vertipecten nevadanus* (Conrad)
- Undet.

Scaphopods

- *Dentalium* sp.

Echiniod

- *Vaquerosella*? (or *Kewia*?); fragment

Ostracods

- Undet.

Foraminifera

- *Baggina californica* Cushman
- *Baggina subinaequalis* Kleinpell
- *Bathysiphon* sp.
- *Bolivina advena advena* Cushman
- *Bolivina advena striatella* Cushman
- *Bolivina brevior* Cushman
- *Bolivina californica* Cushman
- *Bolivina guadalupae* Parker
- *Bolivina imbricata imbricata* Cushman
- *Bolivina marginata* Cushman
- *Bolivina marginata marginata* Cushman
- *Bolivina modeloensis* Cushman and Kleinpell
- *Bolivina parva* Cushman and Galliher
- *Bolivina rankini* Kleinpell
- *Bolivina seminuda* Cushman
- *Bolivina tumida* Cushman
- *Bolivina vaughani* Natland

Bolivina sp.
Bucella mansfieldi (Cushman)
Buccella sp.
Bulimina pseudotorta Cushman
Bulimina uvigerinaformis Cushman and Kleinpell
Buliminella curta Cushman
Buliminella elegantissima (d'Orbigny)
Buliminella subfusiformis Cushman
Cassidulina panzana Kleinpell
Cibicides fletcheri Cushman
Cibicides floridanus (Cushman)
Cibicides sp.
Dentalina obliqua (Linne)
Elphidium crispum (Linne)
Elphidium sp.
Epistominella capitanensis Cushman and Kleinpell
Epistominella gyroidinaformis Cushman and Goudkoff
Epistominella relizensis (Kleinpell)
Epistominella subperuviana Cushman
Epistominella sp.
Fursenkoina californiensis
Fursenkoina californiensis californiensis Cushman
Fursenkoina californiensis grandis (Cushman and Kleinpell)
Globigerina bulloides d'Orbigny
Globigerina hexagona Natland
Globigerina sp.
Globorotalia scitula (Brady)
Globorotalia sp.
Gyroidina rotundimargo Stewart and Stewart
Hanzawai illingi (Nuttall)
Hanzawaia sp.
Haplophragmoides sp.
Nonionella costifera (Cushman)
Nonionella miocenica Cushman
Pullenia miocenica
Rotalia sp.
Stilostomella advena (Cushman and Laiming)
Uvigerina hootsi Rankin
Uvergerina subperegrina Cushman and Kleinpell
Uvigerinella californica Cushman
Uvigerinella californica gracilis Cushman and Kleinpell
Uvigerinella californica perparva Bandy and Arnal
Valvulineria alicia Pierce
Valvulineria californica Cushman
Valvulineria californica obesa Cushman
Valvulineria depressa Cushman
Valvulineria miocenica Cushman
Valvulineria miocenica depressa Cushman
Valvulineria miocenica miocenica Cushman
Valvulineria sp.

Diatoms
Undet.

Sponges

- Undet spicules

Fish

- *Atherinidae 4*
- *Atherinidae* sp.
- *Carangidae* sp.
- *Cynoscion* sp.
- *Etringus scintullanus* Jordan
- *Etringus* sp.
- *Etrumeus* sp.
- *Ganolytes cameo* Jordan
- *Ganolytes* sp.
- *Harengula* sp.
- *Lompoquia culveri* (Jordan)
- *Lompoquia* sp.
- *Pseudoseriola* sp.
- *Salmonidae* sp.
- *Sciaenidae* sp.
- *Scomber "miocaenicus"* (Undescribed ARCO type nos 47, 47a)
- *Scomber miocenicus*
- *Scomber* sp.
- *Sebastodes elongatus* Ayres
- *Sebastodes elongatus*
- *Seriola* sp.
- *Sparidae* sp.
- *Xyne "luisensis"* (ARCO type no 36)
- *Xyne luisiensis*
- *Xyne* sp.
- Undet.

Plants

- Undet *Anacardiaceaen*; fragment of trunk

CALABASAS FORMATION:

(Reworked fossils from horizons other than Stokes Canyon Breccia)

Gastropods

- *Amaurellina clarki* Stewart
- *Amaurellina moragai lajollaensis* Stewart
- *Amaurellina multiangulata* Vokes
- *Amaurellina* sp.
- *Amauropsis martinezensis* Dickerson
- *Ampullela schencki* Vokes
- *Cerithium cliffensis* Hanna
- *Cerithium* sp.
- *Coalingodea tuberculiformis* (Hanna)
- *Conus* sp.
- *Cylichna*
- *Cymatium* (*Lampusia*) n. sp. Vokes
- *Cymatium* n. sp.
- *Ectinochilus supraplicaus* (Gabb)
- *Eocernina hannibali* (Dickerson)
- *Ficopsis meganosensis packardi* Merriam and Turner
- *Ficopsis remondi crescentensis* Weaver and Palmer
- *Heteroterma gabbi* Stanton
- *Naticid*
- *Pseudoliva lineata* Cabb
- *Pseudoliva* n. sp.

Ranellina pilsbryi Stewart

Retipirula crassitesta (Gabb)

Scahphander costatus (Gabb)

Sinum obliquum (Gabb)

Surculites mathewsoni (Gabb)

Surculites n. sp.

Tornatellaea pingulis (Gabb)

Turricula califia Nelson

Turritella andersoni Dickerson s. l.

Turritella pachecoensis Stanton

Turritella uvasana etheringtoni Merriam

Turritella sp.

Undet.

Pelecypods

Arcoid

Cardiid

Corbula sp.

Crassatella sp.

Crassostrea sp.

Glycymeris sp.

Macrocallista sp.

Miltha packi (Dickerson)

Modiolus sp.

Nemocardium linteum (Conrad)

Nemodon morani (Waring)

Nuculana (Saccella) sp.

Ostrea idraensis Gabb

Pitar sp.

Schedocardia breweri (Gabb)

Spisula sp.

Tellina simiensis Nolan

Tellinid

Venericardia domenginica Vokes

Undet.

CALABASAS FORMATION; STOKES CANYON BRECCIA

(Reworked fossils-- S.C. Brec. only)

Gastropods

Amauropsis martinezensis Dickerson

Ampullospirid

Architectonica simiensis Nelson

Brachysphingus sinuatus Gabb

Brachysphingus sp.

Calyptraea sp.

Conus sp.

Cyclichna

Cylichna costata Gabb

Ectinochilus macilentus (White)

Eocernina hannibali (Dickerson)

Fusinus sp.

Gyrodes robustus Waring

Gyrodes sp.

Heteroterma gabbi Stanton

Lyria hannibali Waring

Lyria sp.

Mesalia martinezensis (Gabb)

Naticid

Priscoficus caudata (Stanton)

Pseudoliva howardi (Dickerson)

Retipirula crassitesta (Gabb)

Scaphander costatus (Gabb)

Surculites mathewsoni (Gabb) Dickerson 1914

Surculites sp.
Trochid
Turritella andersoni lawsoni secondaria Merriam
Turritella buwaldana Dickerson
Turritella infragranulata Gabb
Turritella pachecoensis Stanton
Turritella pachecoensis waringi Merriam
Turritella pachecoensis renodata Merriam
Turritella sp.
Woodsalia martinezensis (Gabb)
Undet.

Pelecypods

Acila sp.
Callocardia simensis Nelson
Crassatella branneri (Waring)
Crassatella sp.
Cucullaea mathewsoni Gabb
Cucullaea sp.
Diplodonta sp.
Glycymeris veatchi major (Stanton)
Lucinid
Macrocallistra furlongi Nelson
Macrocallista hornii (Gabb)
Macrocallista sp.
Nemocardium linteum (Gabb)
Nemocardium sp.
Nuculana sp.
Nuculanid
Ostrea sp.
Pitar sp.
Pitarinid
Saxolucina muirensis (Dickerson)
Schedocardia breweri (Gabb)
Septifer sp.
Spisula sp.
Tellina simensis Nelson
Tellina undulifera Gabb
Tellina sp.
Tellinid
Venericardina sp.
Undet.

Cephalopods

Eutrephoceras stephensoni (Dickerson) Miller and Downs

Scaphopods

Dentalium cooperi Gabb

References Cited

Yerkes, R.F., and Campbell, R. H., 1979, Stratigraphic nomenclature of the central Santa Monica Mountains, Los Angeles County, California; U.S. Geological Survey Bulletin 1457-E, 31 p.

Investigations of Intraplate Seismic-Source Zones

9950-01504

W. H. Diment
Branch of Engineering Geology and Tectonics
U.S. Geological Survey
Box 25046, MS 966, Denver Federal Center
Denver, CO 80225

Investigations

1. Interpretation of 320 km of seismic-reflection profile data in the upper Mississippi embayment.
2. Reprocessing of seismic-reflection data to investigate deep structure.
3. Quantitative geomorphic study of stream profiles in the southeastern part of the Ozark Mountain.
4. Processing and interpretation of seismic-reflection data recorded on the Mississippi River.
5. Analysis of level line data in the upper Mississippi embayment and environs.
6. Logging and interpretation of two trenches excavated across the scarp of the Meers Fault in Comanche County, Okla., in conjunction with personnel from the Oklahoma Geological Survey.
7. Interpretation of trench excavated near Blytheville, Ark., in 1982.
8. Analysis of high-resolution reflection data obtained across the Meers Fault.
9. Effects of earthquakes on two perennially boiling wells in the Long Valley caldera, Mono County , Calif.

Results

1. A report by A. J. Crone, F. A. McKeown, S. T. Harding, R. M. Hamilton, D. P. Russ, and M. D. Zoback describing a structurally disrupted zone along the axis of the Reelfoot Rift has been published in Geology.

2. Reprocessing of field tape records of seismic-reflection profiles to 11 s two-way traveltime has been completed on four profiles. An open-file report on them is being prepared. Two abstracts have been submitted (Dwyer and Harding, 1985 and Harding, 1985).

3. A draft report entitled "Analysis of stream-profile data for the eastern Ozark Mountains region and their geologic implications," by F. A. McKeown, M. J. Cecil, B. L. Askew, and M. B. McGrath, has been technically reviewed. Revisions are now being made and it will be sumitted to BCTR for publication as a USGS Bulletin.

4. Progress on the interpretation of the seismic-reflection data recorded on the Mississippi River continued to be slow because of unanticipated redirection of the work of the investigators.

5. Compilation and analysis of level line data for the upper Mississippi Embayment and vicinity was completed by Richard Dart and an open-file report is ready for technical review.

6. The two trenches across the Meers fault indicate that the scarp was formed by a reverse fault that dips to the northeast in the shallow subsurface. Nearly all of the deformation in the alluvium is accomplished by warping and flexing with only a small component of brittle deformation. Stratigraphic units in the trenches have a net vertical throw of more than 3 m. Preliminary interpretation of the trenches indicates one surface-faulting event since late Pleistocene time; however, this surface faulting is probably mid-Holocene or younger. There is no evidence in the trenches that supports a large component of lateral slip.

7. The trench, excavated across prominent linear features in the Blytheville, Ark., area of the New Madrid seismic zone, failed to expose any near-surface faults but did reveal numerous liquefaction-induced sandblows that were probably produced by the 1811-1812 earthquakes. An unusual feature observed in this trench was liquefied sand that rose toward the surface through the soil until it encountered the root-bound turf in the A horizon. The turf of the A horizon delaminated from the underlying parts of the soil and a lens of sand was injected laterally beneath the A horizon. Eventually the pressure accumulated in the lens-ruptured turf and the sand and water flowed onto the ground, burying the soil. A more detailed description of the results of this study has been technically reviewed for publication as a U.S. Geological Survey Miscellaneous Field Studies Map. No additional work has been done on this study because of other commitments.

8. A short, high-resolution seismic-reflection line was conducted across the Meers fault in Oklahoma. This data has been processed and shows a fault at approximately 271 m in depth which can be connected to the surface faulting. This fault has a displacement of about 30 m (Harding, 1985).

9. Temperature logs obtained in Chance No. 1 (south moat of the Long Valley caldera, Mono County, Calif.) in 1976, 1982, 1983, and 1985 show a progressive cooling in the uncased part of the hole. Examination of the rate of change suggests that the cooling began to accelerate about the time of the strong earthquakes of May 1980 (Diment and Urban, 1985). Temperature logs from Mammoth No. 1 (near Casa Diablo Hot Springs, 3 km west of Chance No. 1) obtained in 1979, 1982, and 1983 are also being processed and examined for seismically induced phenomena (Urban and Diment, 1984; 1985).

Reports

Crone, A. J., McKeown, F. A., Harding, S. T., Hamilton, R. M., Russ, D. P., and Zoback, M. D., 1985, Structure of the New Madrid seismic source zone in southeastern Missouri and northeastern Arkansas: Geology, v. 13, p. 547-550.

Diment, W. H., 1984, Earthquake hazards in northeastern United States, in Management of earthquake hazards in New England--a regional conference: Federal Emergency Mangement Agency, Region I and New England Governor's Conference, Inc., Boston, Massachusetts, p. 19.

Diment, W. H., and Urban, T. C., 1985, Temperature variations with time in a perennially boiling well in the Long Valley caldera, Mono County, California: Observations in Change No. 1 (1976-83): Geothermal Resources Council Transactions, v. 9, part 1, p. 417-422.

Dwyer, R. A., and Harding, S. T., 1985, Mid-crustal seismic reflections from part of the New Madrid seismic zone: Earthquake Notes, v. 55, p. 26.

Harding, S. T., 1985, Preliminary results of a high-resolution reflection survey across the Meers Fault, Comanche County, Oklahoma: Earthquake Notes, v. 55, p. 2.

Harding, S. T., 1985, The use of seismic-reflection data to interpret the earthquake history associated with intracratonic earthquakes: Geophysics (in press).

McKeown, F. A., 1984, New Madrid seismic zone, Part I, Historical review of studies; Part II, Contemporary studies by the U.S. Geological Survey, in Proceedings of the New Madrid seismic zone symposium, Cape Girardeau, Missouri, April 27-28, 1984: U.S. Geological Survey Open-File Report 84-770, p. 6-32.

Thenhaus, P. C., Ziony, J. I., Diment, W. H., Hopper, M. G., Perkins, D. M., Hanson, S. L., Algermissen, S. T., 1985, Probabilistic estimates of maximum seismic horizontal ground acceleration of rock in Alaska and the adjacent outer Continental Shelf: Earthquake Spectra, v. 1, p. 285-306.

Urban, T. C., and Diment, W. H., 1984, Precision temperature measurements in a deep geothermal well in the Long Valley caldera, Mono County, California: EOS [American Geophysical Union Transactions], v. 65, p. 1084-1085.

Urban, T. C., and Diment, W. H., 1985, Convection in boreholes: limits on interpretation of temperature logs and methods for determining anomalous fluid flow, in Proceedings National Water Well Association Conference on surface and borehole geophysical methods in ground-water investigations: National Water Well Association, Worthington, Ohio, p. 399-414.

Seismic Hazard Studies, Anchorage, Alaska

9950-03643

A. F. Espinosa
Branch of Engineering Geology and Tectonics
U.S. Geological Survey
Box 25046, MS 966, Denver Federal Center
Denver, CO 80225
(303) 236-1597

Investigations

1. A "completeness" of the seismicity catalogue is being investigated in order to use lower magnitude thresholds in (a) spatial and magnitude-temporal distribution of shallow ($h \leq 33$ km) and intermediate ($33 < h \leq 100$ km) seismicity ($M_S \geq 5.5$) occurring within a specified area in the period of time which uses (a) historical and (b) instrumentally recorded earthquakes. This effort is part of the seismicity study being carried out in this project for the Anchorage and vicinity region in Alaska.

2. A damage evaluation for the City of Anchorage, sustained from the 1964 Alaskan earthquake, is in preparation with damage data that have not been published previously. This information and local surficial geological data is planned to be used in order to evaluate transfer-function amplification curves in Anchorage and to ascertain any existing correlation between damage and soil conditions in the area.

3. A suite of seismicity maps and depth cross sections for the Anchorage and vicinity region in Alaska are being prepared. A technique has been developed to map the subducting plate on a three-dimensional finite-difference display for Anchorage and vicinity. ISC, USGS, and Menlo Park's local seismicity data files are used to perform the geometrical mapping of the lithosphere in this region.

4. The intensity catalogue covering the period 1900 through 1981 for the State of Alaska has undergone a very careful editing process during last year and a half. A total of 14 isoseismal maps have been compiled and drawn for Alaska, and attenuation laws are being derived from the above data set.

5. A report describing geologic materials from shot holes drilled in 1984 for the Trans-Alaska Crustal Transect project has been finished. The most significant finding of this work is that deposits in the central part of the Copper River basin are dominantly lacustrine silt and clay with thinner intervening units of alluvial gravel and sand. No diamicton or other evidence of glacial deposits was found in the central basin. These findings support the controversial concept that during each of several glaciations the center of the basin was not occupied by glacier ice but instead was the site of glacial Lake Atna and its predecessors throughout the glaciation. These observations further bring into question the direct glacial origin of any diamictons exposed along river bluffs in the central part of the basin.

6. A model which incorporates the concept of seismotechnistratigraphic cells as a method for delineation of subsurface geology beneath Anchorage, Alaska, and its application to seismic hazards studies is under study.

7. A report is being prepared that describes the difficulties encountered in testing relatively weak, nonhomogeneous rocks, in contrast to standard techniques that have been developed for either high modulus, homogeneous rocks or low modulus soils. Most of the problems encountered are discussed and derived from drill core samples from the west side of Cook Inlet but are equally applicable to similar rocks of the same formation that underlie the Anchorage area.

8. A study has been performed which describes volcanic debris flows of the Copper River basin, based on work undertaken several years ago. At least five flows are now recognized, and interpretated to have accompanied lengthy periods of active volcanism in the western Wrangell Mountains that occurred within Pleistocene time; two of the flows may have resulted from lateral-blast eruptions similar to the one that occurred at Mount Saint Helens, Washington, in 1980.

9. Two papers were presented at the workshop, "Evaluation of Regional and Urban Earthquake Hazards and Risk in Alaska", convened in Anchorage, Alaska, on September 1985. One of the papers described the accomplishments and aims of the present project, and the other reviewed the history of engineering geology research in the Anchorage area from 1948 to the present, displaying selected products of those efforts.

10. The geologic map of the northwestern quarter of the Tyonek A-4 quadrangle at 1:31,680 scale has been revised and completed. Also, the geologic map of the Tyonek B-4 quadrangle has been reviewed. These two maps will be released shortly.

11. A report describing the geology and geophysics of the Tikishla Park hole, drilled in Anchorage in 1984, has been completed.

12. A draft of an invited paper describing Tertiary to Holocene glaciation of Cook Inlet region has been completed. The paper discusses new ideas that have evolved during studies undertaken over the past several years and embodies the concept of glacioestuarine associations as a means of classifying both stratigraphically and geomorphically evidenced depositional units.

13. An open-file report describing cuttings from shot holes drilled for the Trans-Alaska Crustal Transect Project in the Copper River basin in 1985 has been completed.

14. The first draft of a USGS Professional Paper interpreting results from geotechnical testing of cores from four drill holes in the Tyonek Formation has been completed.

15. Contributions consisting of surficial geology input to the geologic map of the Gulkana B-1 quadrangle, covering about half of the map (which is being prepared as an adjunct to the Trans-Alaska Crustal Transect Project), have been nearly completed.

16. The northeastern sheet of the three-sheet geologic materials map of the Municipality of Anchorage has been checked following drafting of line work and is in the process of undergoing minor cartographic revision.

17. An abstract was prepared for a paper to be presented at the Fifth Congress of the International Association of Engineering Geologists to be held in 1986. This paper discusses the development of the technique of preparing a map that portrays the subsurface geology in the Anchorage metropolitan area based on the concept of seismotechnistratigraphic cells.

Reports

Espinosa, A. F., Schmoll, H. R., Brockman, S. R., Yehle, L. A., Odum, J. K., Michael, J. A., and Rukstales, K. S., 1985, Seismic hazard studies, Anchorage, Alaska, in Hays, W. W., and Gori, Paula, eds., Evaluation of regional and urban earthquake hazards and risk in Alaska: U.S. Geological Survey Open-File Report 85- , 17 p.

Nichols, D. R., and Yehle, L. A., 1985, Volcanic debris flows, Copper River basin, Alaska, in Committee for International Exchange of Landslide Technique (eds.), Proceedings of IVth International Conference and Field Workshop on Landslides: The Japan Landslide Society, Tokyo, p. 365-372.

Odum, J. K., 1985, Difficulties in characterizing weak Tertiary rocks using field and laboratory geotechnical tests--the Tyonek Formation, Cook Inlet region, Alaska, as an example: Geological Society of America Abstracts with Programs, v. 17, no. 7, p. 680.

Schmoll, H. R., 1985, USGS engineering geology products in the Anchorage area, Alaska: A review, in Hays, W. W., and Gori, Paula, eds., Evaluation of regional and urban earthquake hazards and risk in Alaska: U.S. Geological Survey Open-File Report 85- , 18 p.

Schmoll, H. R., Odum, J. K., and Espinosa, A. F., 1985, Seismotechnistratigraphic cells: an approach to the analysis of subsurface geology at Anchorage, Alaska, for use in seismic zonation studies: Geological Society of America Abstracts with Programs, v. 17, no. 7, p. 710.

Yehle, L. A., Odum, J. K., and Reneau, David, 1985, Generalized interpretation of geologic materials from shot holes drilled for the Trans-Alaska Crustal Transect project, Copper River basin and adjacent regions, Alaska, May-June 1984: U.S. Geological Survey Open-File Report 85-582, 33 p.

Soil Development as a Time-Stratigraphic Tool

9540-03852

Jennifer W. Harden
Branch of Western Regional Geology
U.S. Geological Survey
345 Middlefield Road, MS 975
Menlo Park, California 94025
(415) 323-8111 ext. 2039

Investigations

1. The first objective of this project is to use soil development as age control for studies on the recency and timing of tectonic events. Geomorphic surfaces that have been offset by faults are correlated across the fault and approximately dated by the degree of soil development. In some studies, the surfaces include both Pleistocene and Holocene deposits, thereby providing information on the evolution of fault activity.

2. The second objective is to develop methods for sampling and data analysis to (a) establish rates of soil development in areas where soils have been studied and dated radiometrically; (b) test comparability of development rates between different geographical and geologic settings; and (c) establish statistical methods for estimating the ages of deposits based on soil development and calibration curves.

3. These methods are to be applied in areas along faults such as the San Andreas and Calaveras (in conjunction with J.C. Matti and M.M. Clark, U.S. Geological Survey; FY-85, 86).

Results

1. Two stream terraces along the Calaveras fault provided age calibration for soil development near Tres Pinos, California. These two terraces, approximately 20 and at least 40 ka old, were excavated in June, and three soil profiles were sampled from each unit. Soil samples are currently being analyzed at the University of California. These samples will provide a means to test whether rates of soil development are significantly different from rates near Merced, California, where there is extensive age control (in conjuction with K.K. Harms, and M.M. Clark, U.S. Geological Survey).

2. Four alluvial fan deposits were described and sampled in the Owens Valley along the eastern flank of the Sierra Nevada. Age constraints for the fans were provided by stratigraphic and mapping relationships with basalt flows dated by K/Ar and $Ar^{39/40}$. Soil samples are currently being analyzed at Humboldt State University. These samples will provide calibrated data for deposits along the eastern Sierra and for regional data sets that combine and compare dated soils from a variety of climates and parent materials.

The data from this region are summarized as follows (conjunction with Alan Gillespie, University of Washington, R.M. Burke, Humboldt State Univ., and K.K. Harms and M.M. Clark, U.S. Geological Survey).

map unit	K/Ar, $Ar^{39/40}$ age, ka	soil horizons	maximum color	maximum texture and (parent material)
VIII	10-15?	A/Bw/Cox	10YR 5/6	SL (SL)
VII	10-30	A/Bw/Cox	10YR 5/4	SL (SL)
III	250-750?	A/Bt/BC	10YR 5/4	CL (L)
II	<1200, >750	A/Btq/BC	7.5YR 7/8	CL (SL-L)
I	>1800	A/Bt/BC	7.5YR 5/8	CL (SL)

3. Mapping of Quaternary deposits near Yucaipa, California was continued. Twenty-two soils were described in the field (June). From these and previous data, there appear to be four fluvial units distinguishable by soil field studies. Preliminarily, the ages of these units are approximately 50 to 1,000 years; 1,000 to 3,000 years; 15,000 to 40,000 years; and 70,000 to 140,000 years. These dates are based on calibration to soils near Merced, California. Geographically, the most extensive unit is the third oldest (15 to 40 ka) unit. There appears to be considerable variability in this unit, and we hypothesize that there are multiple terraces within this age-range, possibly as a result of basin subsidence near the Crafton Hills. Soil data from these units may be summarized as follows (conjunction with C. Terhune and J.C. Matti, U.S. Geological Survey).

map unit	soil horizons	maximum color	thickness of B+ horizon, cm	soil development index*
1	A/Cox/C	10YR 5/3	0	2
2	A/AC/Cox	10YR 5/4	0	6
3	A/Bt_j or Bt/Cox	7.5YR 5/6, 5YR 5/4	20-60	20-40
4	A/Bt/BC/Cox	5YR 5/6-8	100-200	40-60

*Using rubification, total-texture, clay films and dry consistence

4. Calibration of soils to dated deposits is fundamental to the use of soils as dating tools. We have devised two methods to test whether soils develop at comparable rates between two areas (conjunction with P. Switzer, Stanford Univ., and R. Mark, U.S. Geological Survey). Subsequently, if rates are similar in the two areas, calibration in one area can be used in the other area where dates are less abundant. The first method requires dated soils in both study areas, in which calibration curves with dated soils are tested for similarity. For example, the slope of the linear Holocene curve for soil-development-index versus time is 1.85 ± .52 near Merced, California (data of Harden) and 1.40 ± .26 near Cajon Pass (preliminary data of McFadden and Weldon). The second method requires calibration in one area, but only a few dated deposits are needed in the second area. In this method, the one calibration curve is used to estimate the age of deposits in the second area. If the estimated (soil) age agrees with one or two independent dates in the second area, then rates of soil development are probably similar. Dated soils near Merced, California were used to estimate ages of deposits in five regions (fig. 1) that had a few dates available for comparison. "Soil ages",

meaning the ages that were estimated by calibration to Merced, agreed with independent dates for soils near Cajon Pass. The soils near Merced and Cajon Pass probably have somewhat similar rates of development, at least with respect to field properties. Soils that had significantly different rates of development include those from andesitic detritus in the Sacramento Valley (data of Busacca) and Mt. Shasta, California (data of Harden, Christiansen and Miller) and granitic glacial moraines from E. Washington (data of Harden and Waitt) and the Sierra Nevada (data of Burke and Birkeland). It appears that andesitic deposits weather more rapidly, and glacial moraines weather less rapidly than granitic outwash in the Central Valley near Merced. Another factor affecting soils on Sierran moraines is climate; there may be less effective precipitation on the eastern Sierra Nevada than at the calibration site near Merced.

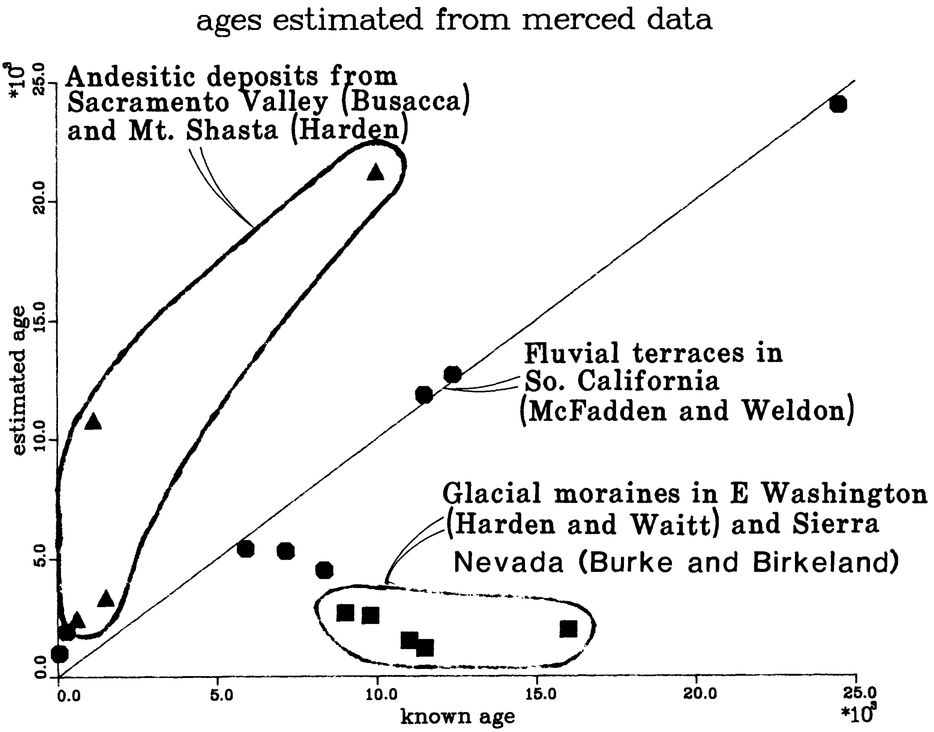

Publications

Harden, J.W., Harms, K.K., Mark, R.K., and Clark, M.M., 1986, Soil development as a tool for studying seismogenic faults, Soil Science Society of America Abstracts; Annual Meeting, Chicago, Illinois, December 4-9.

Harden, J.W., Sarna-Wojcicki, A.M., and Dembroff, G., in press, Soils developed on coastal and fluvial terraces near Ventura, California in Harden, J.W., (ed): A series of soil chronosequences in the western United States, U.S. Geological Survey Bulletin 1590.

Harden, J.W., in press, Chemical differentiation by soils: elemental and mineralogical changes in a soil chronosequence. Submitted to Geology 10/85.

Seismic Slope Stability
9950-03391

Edwin L. Harp
Branch of Engineering Geology and Tectonics
345 Middlefield Road, MS 998
Menlo Park, CA 94025
(415) 856-7124

Investigations

1.Conducted investigations assessing the fracture and joint characteristics of rock slopes along the Wasatch Front near Salt Lake City to evaluate their seismic slope stability.

2. Summarized research products and capabilities of Regional Landslide Research Group of U.S.G.S. over past 10 years to highlight state-of-the-art knowledge about earthquake-induced landslides.

Results

1. A modified version of the Rock Mass Quality designation has been employed to assess the fracture and joint characteristics of rock slopes and their susceptibility`to seismic-induced failure in the Wasatch Front near Salt Lake City, Utah. Preliminary results of this study have revealed several areas of marginal rock slope stability near rapidly developing residential areas within the section of the Wasatch Front studied which stretches from Mill Creek Canyon south to Little Cottonwood Canyon.

Several cliffs composed of rocks of the Big Cottonwood Formation at the mouth of Heughs Canyon are likely to form rock falls from an earthquake in which Modified Mercalli shaking intensities exceed VI or in which Arias intensities exceed 0.15 m/sec. The slopes beneath these cliffs are sufficiently steep that rocks falling from the cliffs would probably travel into an area where future residences are planned.

Similar problems exist near the mouth of Big Cottonwood Canyon where near-vertical cliffs in Little Cottonwood quartz monzonite have sufficiently open fractures and loose boulders to produce rock falls. A steep, open grassy slope of about 200 m separates the cliffs from luxury homes with no apparent obstacles in the intervening slope to provide diversion or obstruction. Several other areas of high susceptibility to seismic-induced rock fall have been documented in the study area.

2. A summary of current knowledge and capabilities of the Regional Landslide Research Group of the U.S.G.S. concerning seismic-induced landslides is in preparation. This summary illustrates the progress of the group over a 10-year period and assesses its present understanding of landslide mechanisms and their relationships to seismic input, and the present ability to predict the regional occurrence of seismic-induced landslides.

Reports

Harp, Edwin L., and Keefer, David K., 1985 (in press), Landslides triggered by the September 4, 1984, Nagano-Ken-Seibu earthquake in Japan, Geological Society of America National Meeting, in Abstracts With Programs.

Keefer, David K., and Harp, Edwin L., Iwasaki, Toshio, Sasaki, Yasushi, Yoshimatsu, Hiroyuki, Oyagi, Norio, and Tanaka, Kohei, 1985 (in press), Earthquake-induced rock avalanche and soil flows in the Japan Alps: submitted to Geological Society of America Bulletin, 13p., 3 figures.

Urban Hazards Seismic Field Investigations

9950-01919

Kenneth W. King
Branch of Engineering Geology and Tectonics
U.S. Geological Survey
Box 25046, MS 966, Denver Federal Center
Denver, CO 80225
(303) 236-1591; 776-1591 (FTS)

Investigations

The basic objective of this project is to improve the fundamental knowledge on how the ground response is affected by local geology. The investigations are presently concentrating in the LA/Wasatch areas. An investigation of the feasibility of using a high resolution reflection method to identify soil parameters and shallow displacements (faults?) is now in progress. Shallow reflection profiles have been made at all the Salt Lake City strong-motion sites, and the data have been processed. Shallow reflection profiles using both P-waves and S-waves were also made at high, medium and low response sites in the Los Angeles area, and in the Springfield-Provo, Utah area. These data are being analyzed at this time. Progress on the Wasatch strong-motion program continues in cooperation with the Utah Geological and Mineral Survey and the University of Utah.

Seismic field studies for the Bureau of Indian Affairs are in progress to investigate seismic effects produced by nearby industrial activities on the town of Paguate, N.M.

Results

1. Several field methods have evolved from the past field efforts in high-resolution shallow reflection methods. The best energy sources found to date are a 12 gauge or 50 cal slug for compression waves and a hydraulic plate system for shear waves. Frequencies from 200 to 300 Hz have been found to be the most useful to map beds in the 20 to 50 foot depth range.

2. Tailoring the in-put software to the Disco programs to process the shallow reflection data is finished. The normal data entry methods had to be modified to achieve the desired resolution for the shallow targets. A procedure is now being developed on the Disco system to calibrate the Mini Sosie System.

3. Test reflection data collected at the Denver Federal Center indicate the feasibility of mapping beds in unconsolidated sediments with a shallow water table in the 20 to 100 foot depth ranges. A report is in peer review.

4. A seismoscope array has been planned and permitted in the Ogden area to supplement the existing SMA-1 array. This is the second seismoscope array sited in the Wasatch area.

5. The new 3-channel seismic field systems (DR-200) were calibrated on the U.S. Bureau of Mines shaking table. A report is now in peer review.

6. Shallow reflection data in Provo have been analyzed. The data have shown folding and faulting in the unconsolidated sediments within 5 meters of the surface. The data also indicate a possible correlation difference between sites of low ground motion response and sites of high ground motion response. The report is being reviewed.

7. Preliminary analysis of experimental shallow reflection data indicate that the developed process may be a viable method to map the bottom of certain types of landslides.

8. Reports on the national park seismic investigations are finished. The Chaco Canyon report has been published as an open-file and the Hovenweep report is in review.

References

Hays, W. W., and King, K. W., 1985, Evaluation of the ground shaking hazard in Utah urban areas [abs.]: Seismological Society of America, Eastern Section, Austin, Texas.

King, K. W., Algermissen, S. T., and McDermott, P. J., 1985, Seismic and vibration hazards investigation of Chaco Culture National Historical Park: U.S. Geological Survey Open-File Report 85-529.

Determining Landslide Ages and Recurrence Intervals

9950-03789

Richard F. Madole
Branch of Engineering Geology and Tectonics
U.S. Geological Survey
P.O. Box 25046, MS 966
Denver, Colorado 80225
(303) 236-1617

Investigations

Study of the distribution of slope failures in the Rocky Mountains and plateaus to the west, including the High Plateaus of central Utah, shows that earth flows are by far the most extensive form of slope failure in the region. Moreover, field studies indicate that of the various slope movement types, earth flows have the greatest potential for determining recurrence intervals of slope failure and for evaluating the relationship between slope failure and climatic change and earthquakes. Hence, during the latter part of FY 1985, study was focused on lateral ridges associated with large earth flows. The Manti landslide in Sanpete County, Utah, was the principal study area and, in addition, a reconnaissance study was made of the Slumgullion earth flow near Lake City, Colorado. Earth flows in both areas have complex histories wherein slope failures have produced lateral ridges at different times, possibly even at the same times. A part of the 1985 field season was devoted to a detailed study of features exposed in a 25-m long trench excavated across a lateral ridge along the northeast side of the Manti landslide.

Results

Lateral ridges formed by earth flows closely resemble lateral moraines. The lateral ridges examined along the Manti landslide and Slumgullion earth flow are 3-6 m high and 20-40 m wide. Some ridge segments are broad, others are sharp-crested. The variations in shape appear to be related to conditions of formation rather than to differences in age. Data obtained from the trench study, from natural exposures at two other localities along the northeast side of the Manti landslide, and on lateral ridges of the Slumgullion earth flow suggest the following about lateral ridges:

1. They are the products of large magnitude slope movements and the larger the event, the larger the lateral ridge.

2. The material composing lateral ridges flowed or was thrust over the surface adjacent to the slide or flow path thereby burying materials capable of providing maximum ^{14}C ages for the time of ridge formation. The bottom contact of the material composing lateral ridges was observed at four different localities, including the trench. At all four localities, the ridge-forming diamicton overlies a well preserved soil.

3. Segments of lateral ridges of different ages can be distinguished by relative soil-profile development and, to some degree, by form (height, width, and slope angles).

4. A single lateral ridge may include deposits related to more than one slope movement and the ridge associated with a given slope movement may be discontinuous. Hence, at one locality, deposits related to two or more events may be superposed, whereas a short distance away, the ridge may be formed by a single deposit. Consequently, the number of major slope movements cannot be determined simply by counting ridges on aerial photographs. Examination on the ground, including reconnaisance study of soil-profile development is required to identify the number of slope movement events.

5. The innermost lateral ridge along the northeast side of the Manti landslide comprises deposits and ridge segments related to at least four slope movements that are estimated to range in age from early Holocene to the present (^{14}C age determinations of three deposits are pending). Other ridges of Pleistocene age lie just beyond the distal edge of the inner lateral ridge but have not yet been studied in detail.

The soils buried by lateral ridges intersect the surface at the base of the distal edge of the ridge. Merger of the buried soil and the surface soil along the outer edge of the ridge gives rise locally to a markedly overthickened A horizon. Part of the overthickening is due to additions of sheetwash from the flank of the ridge. The sheetwash origin of some of the soil is apparent from the general absence of large rock fragments such as are abundant in the material composing the lateral ridges. The lateral ridges typically are composed of matrix-supported cobble and boulder diamicton. The overthickened A horizons are predominantly clayey silt and contain only a small percentage of angular and subangular pebble-size fragments.

Reports

No reports have been published yet, but one on the history of the Manti earthflow will be prepared as soon as ^{14}C ages are completed.

Effects of Site Geology on Ground Shaking in the Wasatch Front Urban Area

9950-03788

Albert M. Rogers
Branch of Engineering Geology and Tectonics
U.S. Geological Survey
Box 25046, MS 966, Denver Federal Center
Denver, CO 80225
(303) 236-1585; 776-1585 (FTS)

Investigations

The principal effort in this reporting period was to establish operational computer programs to process digital data collected in Salt Lake City with Sprengnether DR-200 portable recorders. These programs read the data into the VAX 780 computer, display the data, compute spectra and spectral ratios. The DR-200 systems were also calibrated on a shake table at the Bureau of Mines Twin Cities Research Center Laboratory. A report presenting the details of this calibration is nearly complete. As a result of these efforts, we have transferred and processed the data collected in Salt Lake City region last Spring to the VAX computer. These data are being used to supplement data previously collected in this region.

Source Properties of Great Basin Earthquakes

9950-03835

Arthur C. Tarr
Branch of Engineering Geology and Tectonics
U.S. Geological Survey
Box 25046, MS 966, Denver Federal Center
Denver, CO 80225
(303) 236-1605; (FTS) 776-1605

Investigations

Three investigations were continued during this reporting period:

1. Analysis of digital data recorded at the Nevada Test Site.
2. Analysis of digital data recorded by portable seismic systems in Wyoming.
3. Information systems element of the Wasatch Front regional and Urban Hazards Evaluation.

The objective of the first investigation was to analyze digital seismic data that had been recorded in 1981 by DR-100 portable seismic systems and in subsequent years by the permanent Southern Great Basin Seismic Network (SGBSN). One goal in this investigation was to implement software for the rapid spectral analysis of large quantitites of digital waveform data. Another goal was to compare source parameters, such as stress drop, from earthquakes in different seismic regimes at the Nevada Test Site. This investigation is in support of the Southern Great Basin Seismic Studies project (9950-02151).

The objective of the second investigation was to determine source parameters of aftershocks of the widely-felt October 18, 1984 Laramie Mountains, Wyoming earthquake recorded on MCR-600 digital field seismic systems. The magnitude 5.5 mainshock was interesting because of its depth (about 24 km) and its location in a low heat flow area. This investigation is in support of Seismic Field Investigations project (9950-01539).

The objective of the third investigation was to contribute to the information systems element of the Wasatch Front Regional and Urban Hazards Evaluation study. The information delivery system has been described in previous reports and is scheduled to be completed in FY 1986.

Results

Extensive software revision was performed during the reporting period to streamline the increasing data processing load resulting from voluminous digital data sets acquired during the last year. This software and assistance were provided for the digital seismic data analyses of four projects: South Carolina Seismic Network (9950-01195); Regional and National Seismic Hazard and Risk Assessment (9950-01207); Urban Hazards Seismic Field Investigations (9950-01919); and Chaco Seismology

Study (9950-03816). In addition, computer programs used for computing seismic moment, stress drop, and other source parameters were improved during the reporting period. The effect of the improvements was to reduce the scatter of the moment and stress drop estimates and consequently, to provide more accurate values of moment magnitude M_L.

The source parameters of ten small earthquakes recorded in 1981 at Jackass Flats were updated, using the revised program for computing source parameters. The coda duration magnitudes M_d ranged from 0.1 to 1.8 and depths ranged from 0.5 km to 16.1 km. Seismic moments computed from displacement spectra yielded moment magnitudes M_L which closely matched SGBSN M_d magnitudes; the mean deviation of M_L from M_d was only +0.04 units. Equivalent Wood-Anderson magnitudes M_{WA} computed from maximum amplitudes measured on displacement seismograms were, on average, 0.26 units greater than the corresponding M_d magnitudes. Stress drops were small, ranging from 0.006 MPa for the smallest event and about 0.1 MPa for the largest event. Small stress drops were also computed for several small ($M_d < 1.0$) earthquakes located near Yucca Mountain and for a $M_d = 1.7$ Pahute Mesa event.

Fourteen aftershocks of the Laramie Mountains earthquake were analyzed in detail. Focal depths ranged from 21 km to 24.5 km. The M_d magnitudes ranged from 2.5 to 3.5, about 0.6 magnitude units greater than the corresponding magnitude determined from the seismic moment, probably because California constants were used in the coda duration magnitude formula. Stress drops ranged from about one MPa to about 27 MPa; stress drop tended to increase with increasing seismic moment. A reviewed draft Open-File Report has been completed.

Activity in the third investigation consisted principally of contributing material to the "Wasatch Front Forum" in the form of summaries of Semi-Annual Technical Reports appropriate to the Wasatch front studies. In addition, a copy of the UGMS bibliography was reviewed.

Quaternary Framework for Earthquake Studies
Los Angeles, California

9540-01611

John C. Tinsley
Branch of Western Regional Geology
U.S. Geological Survey
345 Middlefield Road, MS 975
Menlo Park, California 94025
(415) 323-8111, x 2037

Investigations

1. Completed editing of text galleys and of proofs of maps and illustrations pertaining to chapters 5 and 11, U.S. Geological Survey Professional Paper 1360 "Evaluating earthquake hazards in the Los Angeles region -- an earth science perspective: J.I. Ziony, editor, (J.C. Tinsley).

2. Completed initial studies of the deformation of late Holocene floodplain deposits of Los Gatos Creek, near Coalinga, CA. (B. Atwater, J. Tinsley, R. Stein and D. Trumm).

3. Continued collection of geologic and geotechnical data to characterize relative ground motion in terms of site geology at about 70 instrument sites along the Wasatch Front, from Logan, Utah to Provo, Utah. (J. Tinsley, D. Cower, K. Parrish and D. Trumm).

4. Compiled P-wave and S-wave velocity data at 4 sites in the Los Angeles region and at 5 sites in the Wasatch region, where high-resolution reflection profiles were subsequently recorded.

5. Initiated study of late Quaternary deposits in the San Gorgonio Pass area, with the objective of determining slip rates on reverse faults that are an unevaluated component in the fault systems of the region.

6. Initiated drilling and subsurface sampling program in the Provo, Utah, area, to obtain site-specific geologic and geotechnical data pertinent to making improved predictions, of site-response and earthquake-generated ground motion in the Wasatch region.

Results

1. Publication of U.S. Geological Survey Professional Paper 1360 is anticipated by November, 1985.

2. Late Holocene deformation of the Coalinga Anticline, at a location about 10 km southeast of the epicenter of the $M_L = 6.7$ Coalinga earthquake of 2 May, 1983, was studied to improve estimates of late Holocene earthquake recurrence. Buried alluvial plains exposed in the banks of Los Gatos Creek were correlated using radiocarbon dating of 25 measured stratigraphic sections which were located using a 3rd order geodetic survey. Datums at 500, 2000, and 2500 years extend from the Pleasant

Valley syncline across the Coalinga anticline and into the San Joaquin Valley syncline. The buried 2000 yr BP and 2500 yr BP alluvial plains, traced discontinuously for 20 km, nearly parallel the present alluvial plain. We can demonstrate no deformation during the past 2500 yrs, and infer a minimum earthquake repeat time of 250 yrs. A 5000 yr BP alluvial plain is identified and correlated in the axis of the Coalinga anticline. If it can be identified in the adjacent synclinal basins, a 500 yr BP datum will enable improved estimates of Late Holocene deformation and earthquake recurrence in this region.

3. Collected geologic data including water well logs and foundation investigations from public agencies and private consultants, for all USGS relative ground-motion instrument stations located in the Logan, Salt Lake City and Provo, Utah areas. Compilation of data for stations in the Ogden area will be completed this spring. This effort was greatly facilitated by Loren D. Anderson, Professor of Geotechnical Engineering, Utah State University, Logan, UT, who has maintained files of geotechnical data compiled during studies to evaluate liquefaction in the Wasatch region. The objective is to predict relative ground response for the Wasatch region in terms of sets of geologic properties of materials beneath the instrument sites. Measurements of P-wave and S-wave velocities were completed using down-hole techniques (K. W. King). These geologic and geotechnical data are to be correlated with ground-motion amplification data, to comprise a regional evaluation of the ground shaking hazard in the Wasatch region. The data base will include in-situ data at as many of our ground-motion instrument sites as possible (20 to 40 sites, eventually), from Logan, UT to Provo, UT.

4. Detailed reflection profiles were recorded using as P-wave sources a 0.30-caliber rifle, 0.50 caliber rifle, and 12 ga (slug) shotgun. The initial results are promising (see report by K. W. King, this volume, for additional details.).

5. Initial field reconnaissance and photogeologic studies of Quaternary deposits and landforms in the San Gorgonio Pass area, California, indicate that scarps up to 20 m high are associated with reverse faults in the Millard Canyon area, Cabezon, CA 7.5' quadrangle. Landforms and late Quaternary terraces of Millard Creek are characterized by poorly developed but well-preserved pedogenic soils, indicating that the deposits are not older than middle Holocene. Further studies are planned, including trenching, to obtain radiometric age estimates for the deposits, determining the slip rates of the faults, assessing the number of faulting events and the elapsed time since the latest event.

6. U.S. Geological Survey personnel from the Engineering Branch (Denver) completed drilling, sampling, and casing of shallow exploratory boreholes at 3 sites: Spanish Fork Airport, Provo Airport, and near Springville, Utah (600 N 700 W). Holes were drilled using the USGS Mobile B52 drill rig, and hollow stem continuous flight augers. Back-to-back 30" Shelby-type samples (3" diameter) were used to obtain samples of deposits from 25% of the section drilled. Depths reached were 100 ft (Spanish Fork airport) 125 ft (Provo Airport) and 105 ft (600 N , 700 W). Holes were cased with 4" PVC casing and the casing was grouted into place. Particle size distribution, Atterburg limits,

consolidation tests, bulk density and dry P measurements were completed in the soils engineering facilities at Bringham Young University (Scott L. Hardman).

Reports

Atwater, B.F., Tinsley, J.C., Stein, R.S., Trumm, D.A., Tucker, A.B.[1], Donahue, D.J.[2], Jull, A.J.T.[2] and Payen, L.A.[3], 1982, Alluvial plains and earthquake recurrence art the Coalinga anticline, *in* Rymer, M.J., and Ellsworth, W.L., eds., The Coalinga Earthquake of 2 May 1983: USSG Professional Paper ____ (Passed Peer Review 8/85).

Atwater, B.F., Tinsley, J.C., Stein, R.S., Trumm, D.A., Tucker, A.B., Donohue, D.J., and Jull., A.J.T., 1985, Progress toward estimation of earthquake recurrence at Coalinga anticline, California: (Abstract submitted to 1985 Fall American Geophysics Union meeting, San Francisco)

[1] Department of Physics, San Jose State University, San Jose, California 95192

[2] National Science Foundation Facility for Radioisotope Dating, University of Arizona, Tucson, Arizona 85721

[3] Radiocarbon Laboratory, Department of Anthropology, University of California, Riverside, California 92521

Worldwide Standardized Seismograph Network (WWSSN)

9920-01201

Russ Wilson
Branch of Global Seismology and Geomagnetism
U.S. Geological Survey
Albuquerque Seismological Laboratory
Building 10002, Kirtland AFB-East
Albuquerque, New Mexico 87115-5000
(505) 844-4637

Investigations

1. Technical and operational support were provided to each station in the Worldwide Standardized Seismograph Network (WWSSN) as needed and required.

2. One hundred and forty (140) nodules and components were repaired, and 300 separate items were shipped to support the network during this period.

3. Several emergency shipments of photographic paper and chemicals were made during this period.

Results

1. A continuous flow of high-quality seismic data from the cooperating stations within the network is provided to the users in the seismological community.

2. One hot pen conversion kit (for converting photographic recorders to hot pen recorders) was designed, built, and tested (using corvilinear stylus). The results of the testing were excellent.

3. Six hot pen conversion kits were built and sent to Kingsbay, Spitsbergen (KBS). During the month of September 1985, Dr. Robert Hutt moved the (DWWSSN) station from Bergen, Norway (BER) to (KBS) and converted the photographic recorders to hot pen recorders. Results are excellent.

4. During this period, a contract field engineer, Mr. Juan Nieto, made maintenance and calibration visits to the following WW stations: AFI, LEM, POO, KOD, NDI.

5. September 23, 1985 through October 4, 1985, Mr. Joe Beaulieu from Reston, Virginia, and Mr. Bill Conover from Rolla, Missouri, were trained to operate the (SPA) WW station during the winter-over period.

Geophysical and Tectonic Investigations of the Intermountain Seismic Belt

9930-02669

Mary Lou Zoback
U.S. Geological Survey
Branch of Seismology
345 Middlefield Road, Mail Stop 977
Menlo Park, California 94025
(415) 323-8111, Ext 2367

Investigations

1. Analysis of the state of stress and modern deformation of the northern Basin and Range province.

2. Investigations of tectonic stress in the eastern U.S.

Results

1. The current stress regime of the actively extending northern Basin and Range province has been constrained using a variety of observations. The data include deformation data (focal mechanisms and fault slip studies), in-situ stress (hydraulic fracturing) measurements, borehole elongation ("breakouts") analyses and alignment of young volcanic vents. Integrated, the data indicate significant regional and temporal variations both in principal stress orientations and magnitudes, as well as relative magnitude variations with depth. Approximately E-W extension appears to characterize both the eastern and western margins of the province, whereas a NW to N 60°W least principal stress orientation characterizes the active parts of the interior of the province. Abundant strike-slip focal mechanisms from many areas in the province suggest a stress regime in which the maximum horizontal stress and the vertical stress have similar magnitudes. Temporal fluctuations in the relative magnitudes of these stresses can produce much of the observed deformation patterns such as relatively abundant strike-slip focal mechanisms along the Sierran front, a region which has experience profound relative vertical uplift in the last 3 m.y. State of stress in the Wasatch front region appears to be a major exception to the general stress state where the maximum horizontal stress and the vertical stress are of similar magnitude. In the Wasatch front area the two horizontal stresses currently appear to be approximately equal, fault slip data suggest this stress state may be time-varying, on the time-scale of a major earthquake cycle (1,000-5,000 years). Measured stress magnitudes, focal mechanisms, and slip in historic major earthquakes in the province suggest classic frictional faulting theory can be applied to faulting in the brittle crust. Interaction between the "classic" relatively steep normal faults and low-angle normal faults known throughout the province from geologic mapping and seismic reflection profiling remains to be investigated, hopefully by drill-hole examination of an in-situ example.

2. Available in situ stress data indicate that, with the exception of the Western Cordillera, the entire mid-plate region of the North American plate is characterized by a NE to ENE maximum compressive stress

orientation. New stress data cast serious doubt on the existence of a previously proposed Atlantic Coast stress province characterized by a NW compressive stress orientation. The evidence for a distinct coastal stress province included poorly constrained earthquake focal mechanisms and late Tertiary reverse (?) fault offsets. The new stress data include: 1) better-constrained earthquake focal mechanisms in the Charleston, South Carolina area (Talwani, 1982 GEOLOGY, v. 10, p. 654-658) and for intraplate events in the Western Atlantic (Nishenko and Kafa, 1982, JGR, v. 87, p. 3929-3941), as well as new mechanisms and a re-analysis and error assessment (Quittmeyer and others, 1985, Earthquake Notes, in press) of earlier focal mechanisms in the New York-New Jersey area that suggested NW-compression (Yang and Aggarwal, 1981, JGR, v. 86, 4981-4998), 2) well bore elongations ("breakouts") by Plumb and Cox (1984, EOS, v. 65, p. 1081-1082), Prodrouzek and Bell (1985, Geol. Survey of Canada, paper 85-1B, p. 59-62), as well as our own data from wells in the Atlantic coast region including the continental shelf, and 3) hydraulic fracturing data from the Ramapo fault zone in the New York-New Jersey area and several holes near the Georgia-South Carolina border.

Reports

Zoback, M. L., Zoback, M. D., and Dart, R., 1985, Reassessment of the state of stress in the Atlantic Coast region: Geological Society of America abstracts with Programs, v. 7, no. 7, p. 759.

Zoback, M. L., and Zoback, M. D., 1985, Uniform NE to ENE maximum horizontal compressive stress throughout mid-plate North America: EOS (Transactions American Geophysical Union), v. 66, in press.

SIGNIFICANT DRILL HOLES OF THE WASATCH FRONT VALLEYS INCLUDING CACHE AND TOOELE

Contract Number 14-80-001-G991

William F Case
Utah Geological and Mineral Survey
606 Black Hawk Way, Salt Lake City, Utah (801) 581-6831

A set of lithologic logs of 268 "significant" drill holes in valleys of the Wasatch Front has been compiled. Drill holes were designated as being significant if: A) they extended at least 300 m into valley fill, or B) they encountered consolidated bedrock, or C) the lithologic logs were geologically complete. Depth to bedrock, thickness of valley fill, and various sedimentologic, hydrologic, and lithologic parameters from wells in the data file are useful for geophysical and ground response studies of the valleys of the Wasatch Front. In addition to sediment and lithologic descriptions, some well logs include mention of potentially dateable materials such as shells, plant debris, paleosoils, and volcanic rocks.

The area covered is the main valley areas of the Wasatch Front from Township 12 North to Township 11 South from Range 3 East to Range 5 West (SLBM) and includes Cache, and Tooele Valleys (fig. 1). The wells were drilled after 1940. Most of the well logs are from Water Well Application Forms which are filed with the Utah Division of Water Rights. Water well lithologic logs are filed by drillers, therefore, the reliablity of the data presented represents a spectrum ranging from worse than poor to acceptable. The noted presence of water and measured flow data should be quite reliable because the reason for drilling the well is water-related. An experienced geologist should be able to judge the reliability of the data and will find a large volume of data in water well driller's logs that are useful for geologic studies. Research, geothermal, and exploration well logs were obtained from governmental, private, and academic sources.

Rock types reported in the lithologic logs include pre-Tertiary, consolidated sedimentary and metamorphic rocks. Tertiary rocks represented in the lithologic logs are intrusive and extrusive igneous rocks. Tertiary sediments such as conglomerates, volcanic ashes, sands, and limestones are usually at some stage of consolidation as compared to normally unconsolidated Quaternary rocks. The Quaternary exceptions are hardpan, tufa, marl, caliche, oolitic sandstone, and tillite.

Well log descriptions in the data file consist of well location by Township and Range and, if given, USGS well location nomenclature; well owner; well log reference citation; surface elevation (if given); arbitrary well number; and lithologic log which includes size classification (clay through gravel/conglomerate), and remarks on hydrology, lithology, and drilling.

The data file is located on the Utah Geological and Mineral Survey WANG VS-80 computer. The file can be searched for user-picked keywords. The file is to be updated as new well logs become available. A hard copy of the data file is published by the Utah Geological and Mineral Survey as an open-file report and the file will shortly be made available on 5.25 inch floppy diskettes.

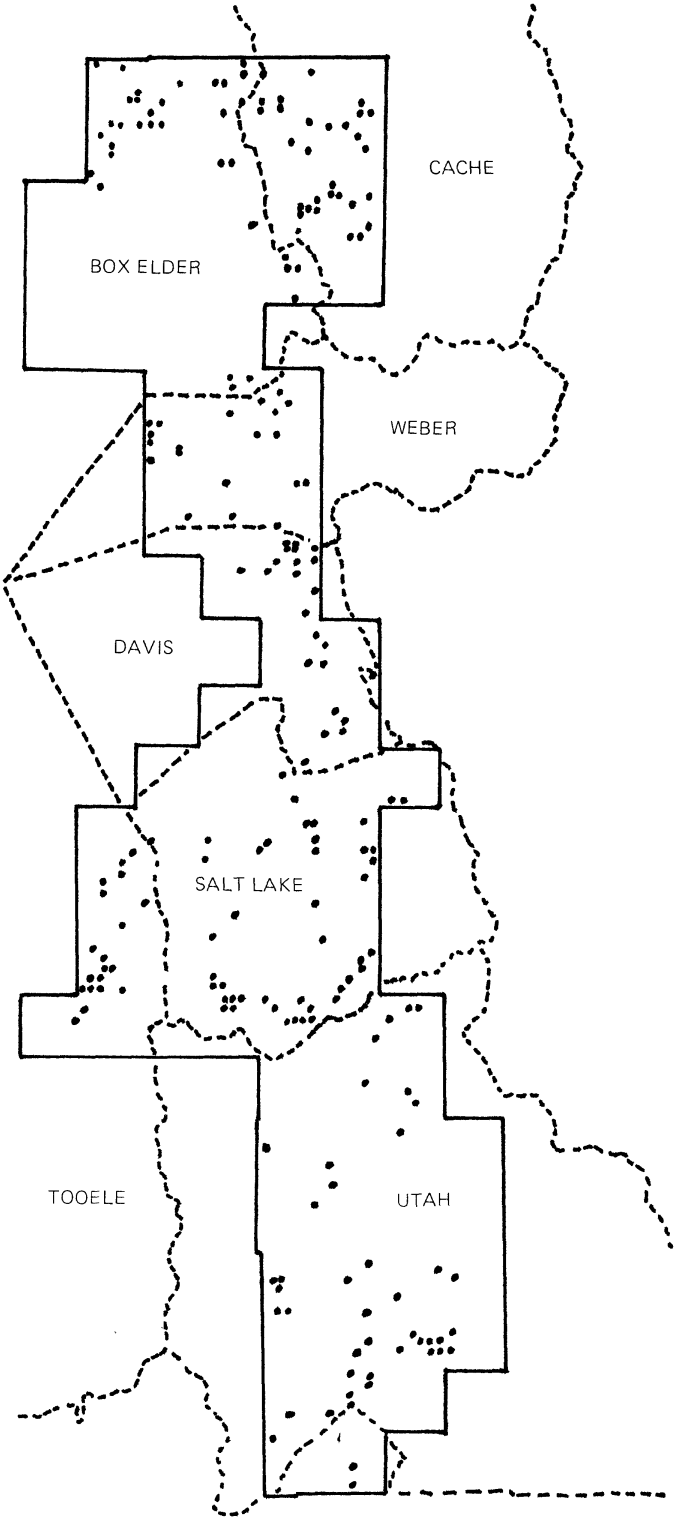

Figure 1: Location map of study area and drill hole sites in Wasatch Front counties, Utah

Development of Seismic Hazard Maps for Puget Sound

USGS Contract No. 14-08-0001-21306

Steven M. Ihnen and David M. Hadley
Sierra Geophysics, Inc.
15446 Bell-Red Road
Redmond, WA 98052
(206) 881-8833

Investigations

Previous work on this contract (Ihnen and Hadley, 1984, 1986a) demonstrated the importance of focusing and soils effects on ground shaking in Puget Sound. In this contract period, emphasis was on incorporating these effects into statistical estimates of risk and preparation of seismic risk maps.

Results

A "base risk" map has been prepared using the program SEISRISK (NOAA) which is an extension of the risk assessment technique of Cornell (1974). The "base risk" map is computed by assigning earthquake frequency-magnitude (f-M) curves to user-specified seismic zones. The program computes the risk at any given point by summing the effects of the seismic zones using a relationship between earthquake magnitude and peak ground acceleration (PGA) at a given distance from the source. The result is an estimate of the PGA for which there is an X percent probability of not being exceeded in Y years, where X and Y are user-settable. This map is termed a "base risk" map because the effects of soils and focusing have not yet been included.

We have modeled the seismicity of Puget Sound using three different seismic zones, shown in Figure One. Zone One models seismicity associated with the subducted Juan de Fuca Plate. The total area of this zone is about 150,000 square kilometers and the recurrence relation used is:

$$\log N = 3.67 - 0.73\,M$$
$$M_{max} = 8.0$$

The second zone, of 75,000 square kilometers, at 15 km depth, models the general shallow background seismicity. The recurrence relation is:

$$\log N = 4.53 - 1.02\,M$$
$$M_{max} = 7.0$$

Finally a smaller shallow zone of 7400 square kilometers, also at 15 km depth, reflects the higher seismicity of the central Puget Sound region. It has been assigned the recurrence relation:

$$\log N = 3.61 - 1.02 M$$
$$M_{max} = 7.0$$

In each case the f-M curves rolls off at M_{max} so that no events larger than that magnitude occur. Recurrence relations were calculated to match the b-values and seismicity rates determined by Crossen (1983).

In this preliminary work we have used the preferred attenuation relation of Campbell (1981) which is:

$$PGA(R,M) = 0.0185\exp(1.28M)[R+0.147\exp(0.732M)]^{-1.75}$$

when PGA is expressed as a fraction of g. To simplify the calculation, earthquakes are taken as point sources and R is the epicentral distance in km. We take this relationship to be suitable for rock sites.

The risk map resulting from these calculations is shown in Figure 2 for the case of 95% non-exceedence. PGAs in the figure are around 30% of g.

References

Campbell, K.W., 1981, Near-source attenuation of peak horizontal acceleration, Bull. Seism. Soc. Amer., 71, pp. 2039-2070

Cornell, C.A., 1974, Seismic design decision anaysis: A seismic risk analysis of Boston: MIT-CE P74-2, publication No. 392, 29p

Crossen, R.S., 1983, Review of seismicity in the Puget Sound region from 1970 through 1978, Proceedings of Workshop XIV Earthquake hazards of Puget Sound Region, Washington, USGS Open File Report, OFR 83-19, pp. 6-18

National Oceanic and Atmospheric Administration, 1982, Development and initial application of software for seismic exposure evaluation, Volume 1, Software Description

Reports

Ihnen, S.M. and D.M. Hadley, 1984, Prediction of strong ground motion in the Puget Sound region: the 1965 Seattle earthquake, Sierra Geophysics Report SGI-R-84-113

Ihnen, S.M. and D.M. Hadley, 1986a, Prediction of strong ground motion in the Puget Sound region: the 1965 Seattle earthquake, accepted for publication in Bull. Seism. Soc. Amer.

Ihnen, S.M. and D.M. Hadley, 1986b, Seismic risk maps for the Puget Sound Region, Washington, in preparation

Ihnen, S.M. and D.M. Hadley, 1986c, Effects of soils and subsurface focusing on seismic risk in the Puget Sound Region, Washington, in preparation for Proceedings of the American Society of Civil Engineers

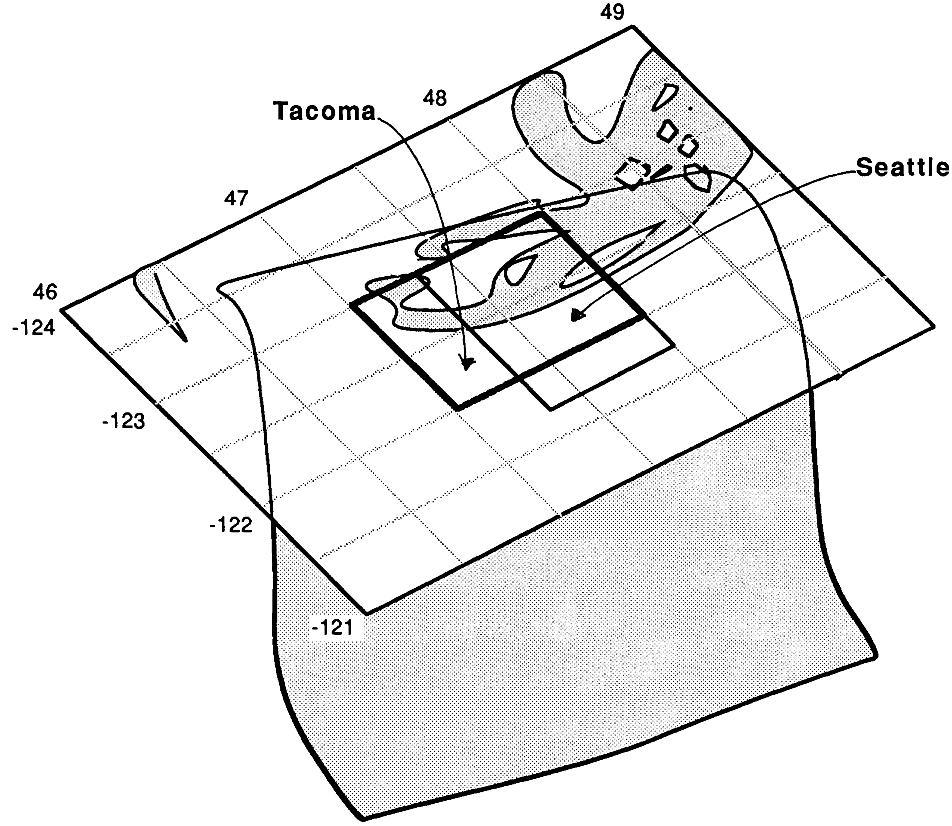

FIGURE ONE - Seismic zones used in risk modeling procedure. Zone One (Juan de Fuca plate) is the dipping shaded area. Zone Two, the shallow seismicity, extends from 46 to 49 N and from 121 to 124 W. The E-W rectangle near the center is the zone of higher seismicity (Zone 3) and the rectangle between 47 and 48 N and 122 and 123 W outlines the study area.

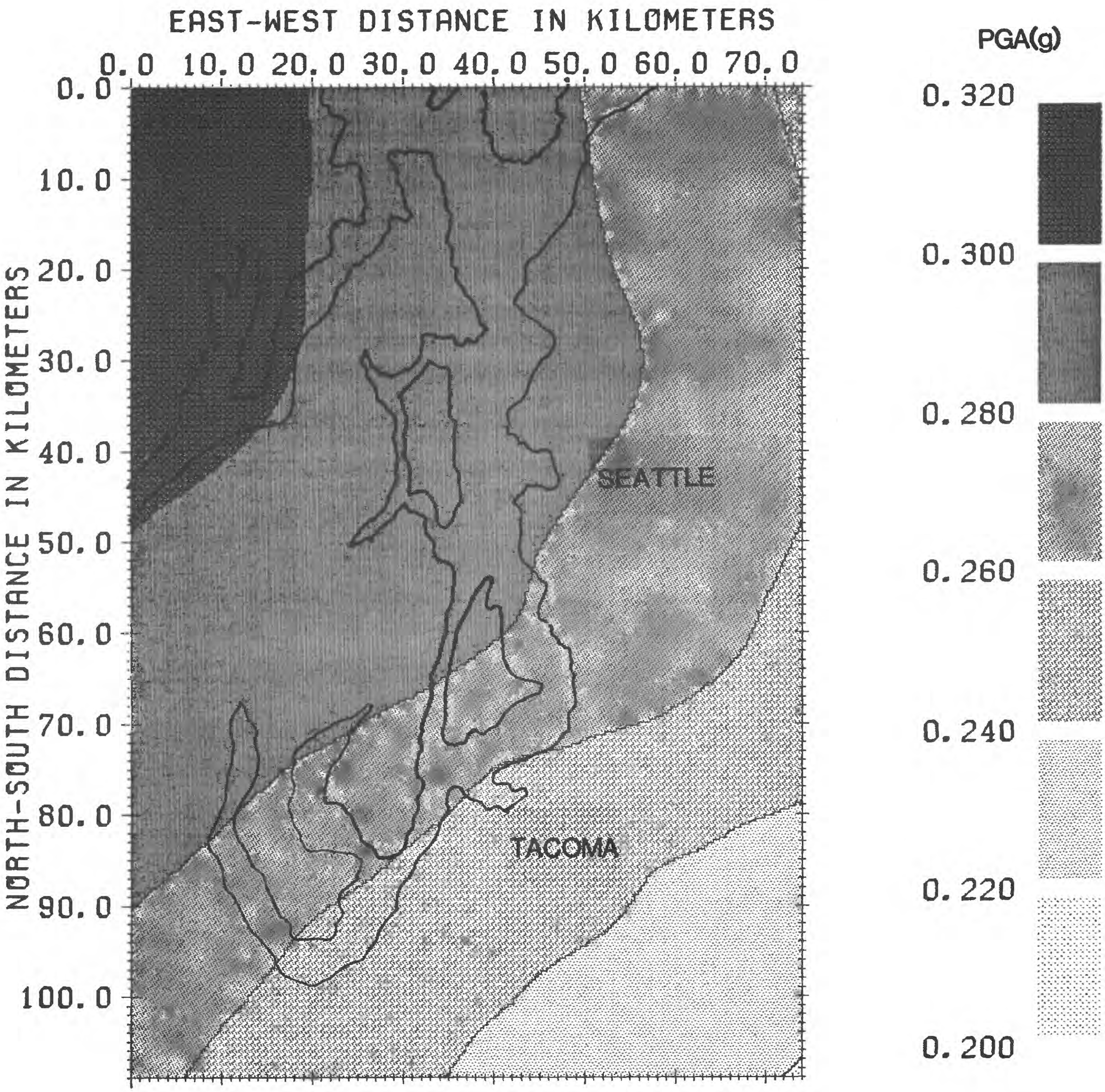

FIGURE TWO - Contour map of peak horizontal ground acceleration in Puget Sound region. Shades represent the PGA for which there is a 95% chance of non-exceedence in 250 years. The shores of Puget Sound are outlined for reference.

Socorro Magma Bodies

9920-03379

Lawrence H. Jaksha
U.S. Geological Survey
Geoscience Department
New Mexico Institute of Mining and Technology
Socorro, New Mexico 87801
(505) 835-5501

Investigations

1. Seismicity.

2. Crustal structure.

Results

1. Seismicity near Socorro, New Mexico, was up sharply during the report period due primarily to a lengthy swarm located about 19 km NE of WTX (fig. 1) and a magnitude 4.0 shock (with its associated aftershocks) located 10-km south of the swarm activity. Preliminary data suggest strike-slip faulting for the magnitude 4 event and intensity V-VI (Modified Mercalli) in and around Socorro. Two papers summarizing our seismicity studies during 1983 were submitted to "U.S. Earthquakes."

A paper summarizing the results of seismic monitoring near Albuquerque, New Mexico, during 1976-1981 has been accepted for publication in the Journal of Geophysical Research. The report suggests that most Rio Grande rift seismicity occurs near Socorro and within metropolitan Albuquerque (fig. 2). Some areas within the city limits of Albuquerque are seismicially active, and because of this proximity, even a small magnitude earthquake (~4.0) has done substantial property damage.

2. We recorded a large military detonation on the White Sands Missile Range (code named MINOR SCALE) for use in two crustal-structure studies. Eight temporary stations were deployed interior to the permanent USGS/New Mexico Tech. network (fig. 1) to observe the P_g phase from this shot. The data will be used in a time-term study of the upper crustal velocity structure near Socorro.

P_n arrivals from MINOR SCALE were observed on a seven-element array (aperature ~100 km) deployed in the transition zone between the Colorado Plateau and the Basin and Range provinces. The array straddles the New Mexico-Arizona border near 34.5° N. latitude. Preliminary results of this experiment suggest crustal thickening both to the north and east of Springerville, Arizona, and a P_n velocity of 7.9-8.0 km/s.

Reports

Jaksha, L. H., 1985, Earthquakes near Albuquerque, New Mexico, 1976-1981: Journal of Geophysical Research, in press.

Jaksha, L. H., 1985, P_n velocity beneath western New Mexico and eastern Arizona, in Papers presented to the conference on heat and detachment in crustal extension on continents and planets: Lunar and Planetary Institute, Houston, Texas, p. 55-57.

Sanford, A., Jaksha, L., and Cash, D., 1985, Seismicity of New Mexico, 1983, in U.S. earthquakes, 1983: U.S. Geological Survey Circular, in press.

Sanford, A., Ake, J., Jarpe, S., and Jaksha, L., 1985, New Mexico area earthquakes, 1983, in U.S. earthquakes, 1983: U.S. Geological Survey Circular, in press.

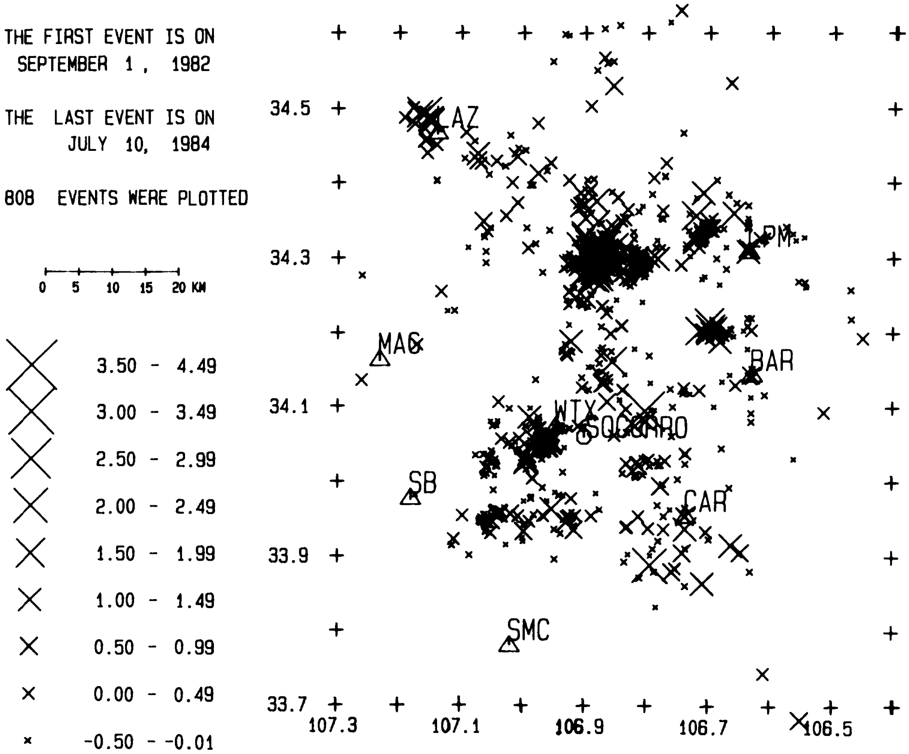

Fig. 1.—Seismicity map of the Socorro, NM area. Seismic stations are shown as open triangles. The magnitudes range from negative values up to 4.1.

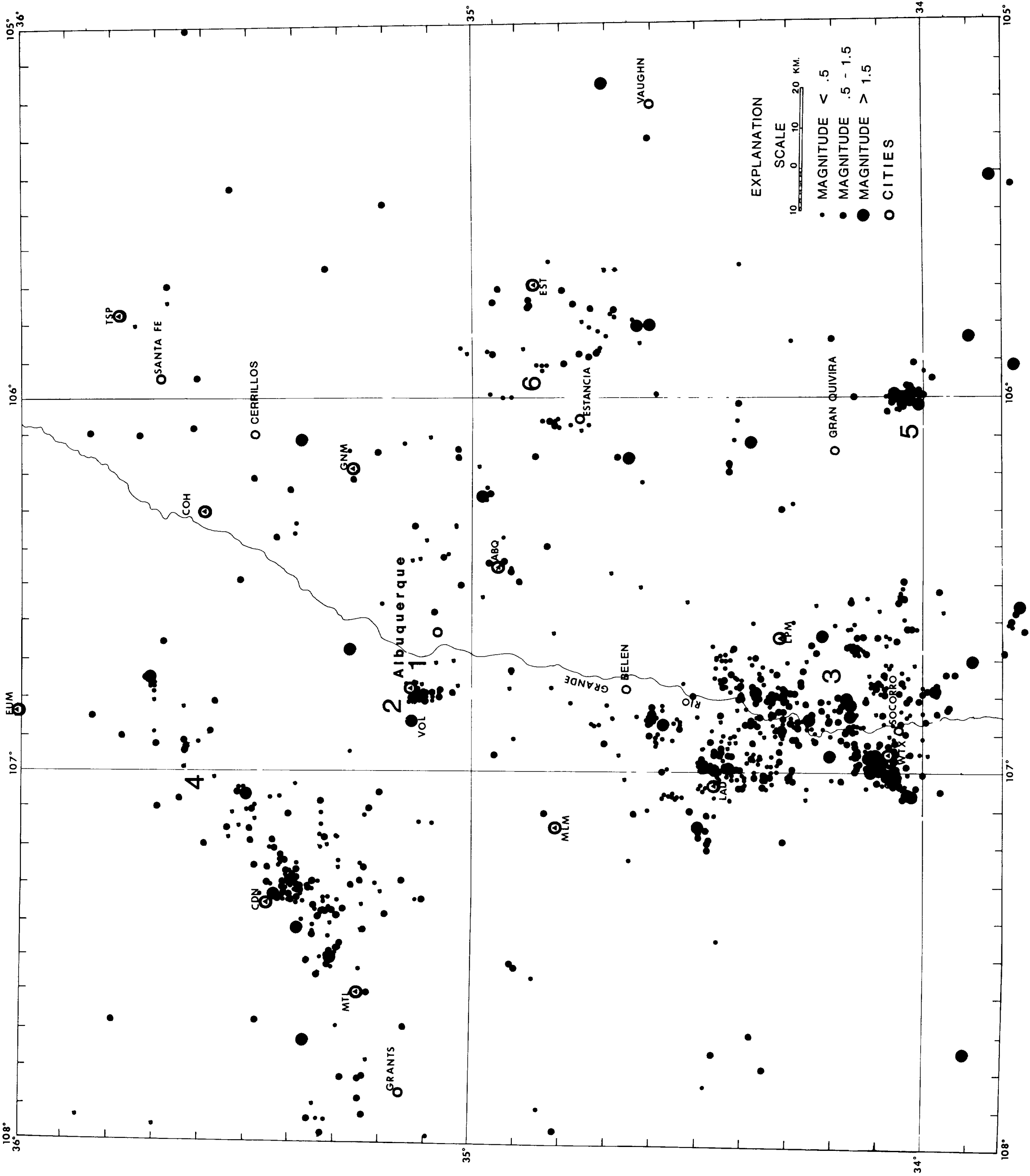

Fig. 2.--Seismicity map derived by U.S. Geological Survey from a seismic network centered on Albuquerque, NM. The study covered a 66-month period between Jan. 1976 and Nov. 1981. Approximately 1,000 epicenters are plotted, and the magnitudes range up to 3.2.

Earthquake Hazards Studies, Upper Santa Ana Valley and Adjacent Areas, Southern California

9540-01616

Jonathan C. Matti
Branch of Western Regional Geology
U. S. Geological Survey
345 Middlefield Road, MS 975
Menlo Park, California 94025
(415) 323-8111 ext. 2358, 2353

Investigations

1. Neotectonic studies of the Crafton Hills, San Gorgonio Pass, and San Andreas fault zones. The study has focused on: (a) mapping fault strands that deform crystalline basement rocks, Tertiary sedimentary rocks, and Quaternary surficial units; (b) identification of Quaternary units to establish Quaternary depositional patterns, relative ages of displacements along various fault strands, and rates of Quaternary fault slip; and (c) interpreting kinematic relations between the San Gorgonio Pass fault complex and the modern trace of the San Andreas fault.

Results

1. J.C. Matti, J.W. Harden, and C. Terhune continued an investigation of the faulting history of the Yucaipa Valley region--an area where the modern trace of the San Andreas fault has a complex surface geometry and is associated with normal dip-slip faults of the Crafton Hills horst-and-graben complex. During this work period, we continued a program of data collection and analysis from pedogenic soils that cap multiple alluvial units (see Harden, this volume), and mapped the distribution of distinctive bedrock units that occur as cobbles in the alluvial units. The bedrock-mapping is designed to constrain the distance that the alluvial units have been displaced from their bedrock sources by the modern trace of the San Andreas fault.

2. J.C. Tinsley and J.C. Matti initiated field studies designed to evaluate neotectonic history and rates of convergence within the San Gorgonio Pass fault zone. Reconnaissance mapping by Matti shows that multiple nested alluvial-fan units in the San Gorgonio Pass region can be correlated by using a local soils chronosequence established by L.D. McFadden (U. of New Mexico, Albuquerque). The alluvial-fan succession is traversed by thrust-fault scarps of the San Gorgonio Pass complex, which provides an opportunity to assess rates of slip within this zone of compressional convergence. A key element in the study is a 20-m high scarp formed in alluvium of Millard Canyon. Although we do not yet have numerical-age control for the deposits, reconnaissance soils studies by McFadden, Tinsley, and Matti show that the soil that caps the faulted alluvium is trivial and has minimal development that is similar to that of soils found on deposits dated elsewhere in the Transverse Ranges at less than 5000 years. Impressively high slip-rates of 10-15 mm/yr or greater are implied. Future studies will focus on trenching the Millard Canyon scarp in order to obtain radiometric ages estimates for the faulted (and unfaulted) alluvial units and to determine slip rates, the number of faulting events, and the elapsed time since the latest event.

Tectonic Analysis of Active Faults

9900-01270

Robert E. Wallace
Office of Earthquakes, Volcanoes and Engineering
345 Middlefield Road, MS 977
Menlo Park, California 94025
(415) 323-8111, ext. 2751

Investigations

1. Evaluation of fault scarps and tectonics of the central Nevada and eastern California seismic belts.

2. Active Tectonics--Impact on Society. A Project under the auspices of the Geophysics Study Group, National Research Council, National Academy of Sciences. Serve as chairman of study group.

3. International Geological Correlation Program (IGCP) - Project 206 - Active Faults of the World.

4. Investigations of active faults in Ningxia and Gansu Province, PRC. Cooperative program in earthquake studies: U.S. Geological Survey/State Seismological Bureau, People's Republic of China.

Results

1. The volume "Active Tectonics" is completed and will soon go to press at the National Academy Press.

2. Twelve maps of the San Andreas fault were gatnered and reproduced at 1:2,000,000 scale for presentation to the IGCP Project 206. A working group meeting was held in Beijing, PRC, in November, 1985. Among the twelve maps are two different geologic, two different seismologic, a fault map, LANDSAT, both false color and black and white, a synthesized relief map from digital topographic data, and a slip rate map. These maps represent products from many parts of the USGS. These maps should set a goal for other countries to achieve.

3. A final draft of a paper on faults in Ningxia Hui Autonomous Region was completed. Progress was made on comparison papers relating to Gansu Province and on an archaeological paper about the Great Wall of China.

Reports

Hill, David P., Wallace, Robert E., and Cockerham, Robert S., 1985, Review of Evidence on the potential for major earthquakes and volcanism in the Long Valley-Mono Craters-White Mountains Regions of Eastern California: Earthquake Prediction Research 3, Tokyo, Japan.

Evaluation of Quaternary Fault Slip-Rate Data as a Basis for Assessing Seismic Hazard in California

Steven G. Wesnousky and Kerry E. Sieh

Division of Geological and Planetary Sciences
California Institute of Technology
Pasadena, California 91125

14-08-0001-21980

The purpose of the proposed work is to examine existing data describing the rate of slip across active faults and use that data to construct maps that depict the long-term average seismic hazard in California. Much of the initial effort has thus been toward the identification and systematic cataloguing of published slip-rate data into a computer-useable format. The primary data base for this compilation effort are the work of Anderson (1979), Bird and Rosenstock (1984), and Clark et al. (1984). In the table of Clark et al. (1984), only information on slip rates derived from displaced Quaternary deposits are listed. Anderson (1979) and Bird and Rosenstock (1984) consider slip rate information determined from displaced Pliocene and Miocene deposits as well. Figures 1 provide a synopsis of the information regarding slip-rate that is presently available. The distribution of onshore faults that displace Quaternary deposits is shown in Figure 1a. The location of the onshore faults is based principally on the work of Jennings (1975) and Clark et al. (1984). Also shown in Figure 1a is the distribution of major offshore fault structures that are known from marine seismic reflection or drillhole studies to break surface on near surface deposits and, hence, may well also displace Quaternary deposits. Figure 1b shows all the faults in California for which some information on slip rate has been inferred from displaced Quaternary or younger deposits. Figure 1c displays all Quaternary faults for which some information on slip rate, including that derived from offset Pliocene and Miocene units, is available. It is evident from Figure 1c that estimates of slip rate exist for most of the major fault zones, though there still remain a large number of faults for which we have no information other than that they have broken Quaternary beds (Figure 1d). Rates of slip determined from older Pliocene and Miocene deposits may be less representative of present rates of seismic activity than are rates assessed from the offset of younger deposits. In this work, slip rates derived from offset Pliocene and Miocene beds are used only when rates determined from younger deposits are not available.

Information on fault slip rate enables an estimate of the moment release rate $\dot{M}_0$ characteristic of each mapped fault. The seismic moment rate provides a $(\dot{M}_0)$ characterization of the average rate of seismic activity on a fault. The release of seismic moment on a fault occurs, however, in the discrete form of earthquakes. Hence, seismic hazard analysis requires an estimate of both the expected size and the occurrence rate of earthquakes on faults in a region of interest. Toward that end, source parameter data have also been compiled from the literature for about 50 earthquakes from California and similar tectonic environments to establish the relationship between seismic moment M_0 and fault rupture length l. The seismic moment M_0 versus rupture length l of each event is plotted in Figure 2. The data form a trend, though the scatter is quite large. Representative error bars are presented in the upper left hand portion of the plot. The horizontal bar corresponds to a factor of 3 in seismic moment, whereas the vertical bar indicates 50% of the fault length. The earthquakes are divided according to the estimated geologic slip rate of the fault zone on which they occurred. The closed circles in Figure 2 indicate events that occurred on major plate bounding faults characterized by slip rates of a centimeter per year or more. The open circles represent earthquakes that occurred on faults with lesser slip rates. Though scatter exists, the two groups form distinct populations. Empirically, the separation indicates that, for two faults of similar length, earthquakes rupturing the more slowly slipping fault will produce a greater amount of slip, and hence, a greater seismic moment. For the purposes of this study, lines of the form $\text{Log } M_0 = a + b \times \text{Log } l$ are fit through the two groups of data, and shall provide the basis for estimating the expected earthquake size from mapped fault length.

Estimates of the occurrence rate of earthquakes on faults, from geologic data of fault length and fault slip rate, require the assumption of a fault model. It is initially assumed in this analysis that the average expected return time of earthquakes on a fault that is described by the maximum magnitude model can be approximated to equal

$$T = M_o^e / \dot{M}_o^g \qquad (1)$$

years, where the seismic moment M_o^e of the expected event on the fault is proportional to the fault length, and the geologically assessed moment rate M_o^g of the fault is a function of the fault slip rate, (e.g., Wesnousky et al., 1983, 1984). Approximation of average earthquake return times in this manner is conceptually consistent with the elastic rebound concept of fault behavior originally proposed by H. F. Reid in 1910. That now generally accepted concept simply states that strain along a fault accumulates slowly through time and upon reaching a critical level is released as sudden slip during an earthquake. The repeated buildup and release of strain is the earthquake cycle. Implicit to the theory, rupture will occur on a fault at the point in time when strain has accumulated to the level released in the prior earthquake. Hence, in equation (1) , M_o^e is a measure of the average strain drop during an earthquake and M_o^g is a function of the strain accumulation rate, and it is assumed that the two parameters remain constant for each fault through time.

The size distribution of earthquakes in a region generally obeys the relationship $\text{Log } N = a - c \times \text{Log } M_o$, where N is the number of events with seismic moment $\geq M_o$ and a and c are empirical constants. A correct analysis of regional seismic hazard should incorporate this observation. The expected moment-frequency distribution of earthquakes resulting from slip on all mapped faults in California may be computed from existing information of fault length and slip rate. The seismic moment M_o^e expected for an earthquake rupturing the entire length of each fault or fault segment in Table A1 is considered a function of fault length, and computed with the empirical relations in Figure 2. The moment rate $M_o^g = \mu l w \dot{u}$ of each fault is a function of the mapped fault length l and the respective fault slip rate $\dot{u}$, and determined assuming that the width w of each fault is 15 km and that the shear modulus μ of the crust is equal to 3×10^{11}dyne/cm^2. Insertion of the estimates of M_o^e and M_o^g into equation 1 defines the average repeat time T of M_o^e earthquakes for each of the mapped faults. The cumulative rate of seismicity resulting from slip on all mapped faults may then be summed and depicted in a plot of N versus M_o. Thus, in Figure 3, the open circles represent the expected frequency distribution of earthquakes resulting from slip on all mapped Quaternary faults and, for comparison, the closed circles represent the historical record of seismicity during the last 150 years. Preliminary results show that the observed and predicted earthquake frequency distributions exhibit a similar shape, and indicate earthquake occurrence rates that generally agree to within a factor of 2 of the observed values. Speculation as to the cause of the differences in the predicted versus observed curves is not warranted, since the differences are small with respect to the uncertainties associated with this analysis. The cumulative seismic moment rate $\sum M_o$ predicted from the geologic data (2.1×10^{25} dyne-cm/year) is also found to differ by less than a factor of 2 from the rate computed from the historical record (1.5×10^{25} dyne-cm/year). The similarity between the observed and predicted values of $\sum M_o$ as well as the earthquake frequency distributions computed with the two data sets is encouraging, for it is in accord with the hypothesis that present knowledge of Quaternary fault offsets provides sufficient information to predict both the average spatial and size distribution of earthquakes in California through time. The result also indicates that the observation that seismicity over a broad region satisfies a b-value distribution does not require that seismicity on a particular fault also satisfy a b-value distribution. Future effort will be placed toward combining the estimates of M_o^e and M^g for each fault with empirical relations between M_o, source-to-site distance, and strong ground motion to construct maps that depict the average expected occurrence rate of various levels of strong ground motion in California. A more detailed account of the methodology is found in Wesnousky et al. (1984).

References

Anderson, J. G., Estimating the seismicity from geological structure for seismic-risk studies, *Seismol. Soc. Amer., Bull., 69* p. 135-158, 1979.

Bird, P. and R. W. Rosenstock, Kinematics of present crust and mantle flow in southern California, *G.S.A.B., 95,* p. 946-957, August 1984.

Clark, M., M.., J. J. Lienkaemper, D. S. Harwood, K. R. Lajoie, J. C. Matti, J. A. Perkins, M. J. Rymer, A. M. Sarna-Wojcicki, R. V. Sharp, J. D. Sims, J. C. Tinsley and J. I. Zoiny, Preliminary slip-rate table for late Quaternary faults of California, *U.S. Geol. Surv. Open-File Report 84-106,* 1984.

Wesnousky, S. G., C. H. Scholz, K. Shimazaki, and T. Matsuda, Earthquake frequency distribution and the mechanics of faulting, *J. Geophys. Res., 88,* p. 9331-9340, 1983.

Wesnousky, S. G., C. H. Scholz, K. Shimazaki, and T. Matsuda, Integration of geological and seismological data for the analysis of seismic hazard: a case study of Japan, *Seismol. Soc. Amer. Bull., 74,* p.687-700, 1984.

Wesnousky, S. G., Seismic hazard in sourthern California due to earthquakes on mapped Quaternary faults, *EOS, 45,* p. 988, 1984. (presented at Fall meeting of AGU, December, 1984)

Wesnousky, S. G., Quaternary faulting and seismic hazard in California, *Earthquake Notes, 55,* p.29, 1985. (presented at Spring meeting of SSA, March, 1985)

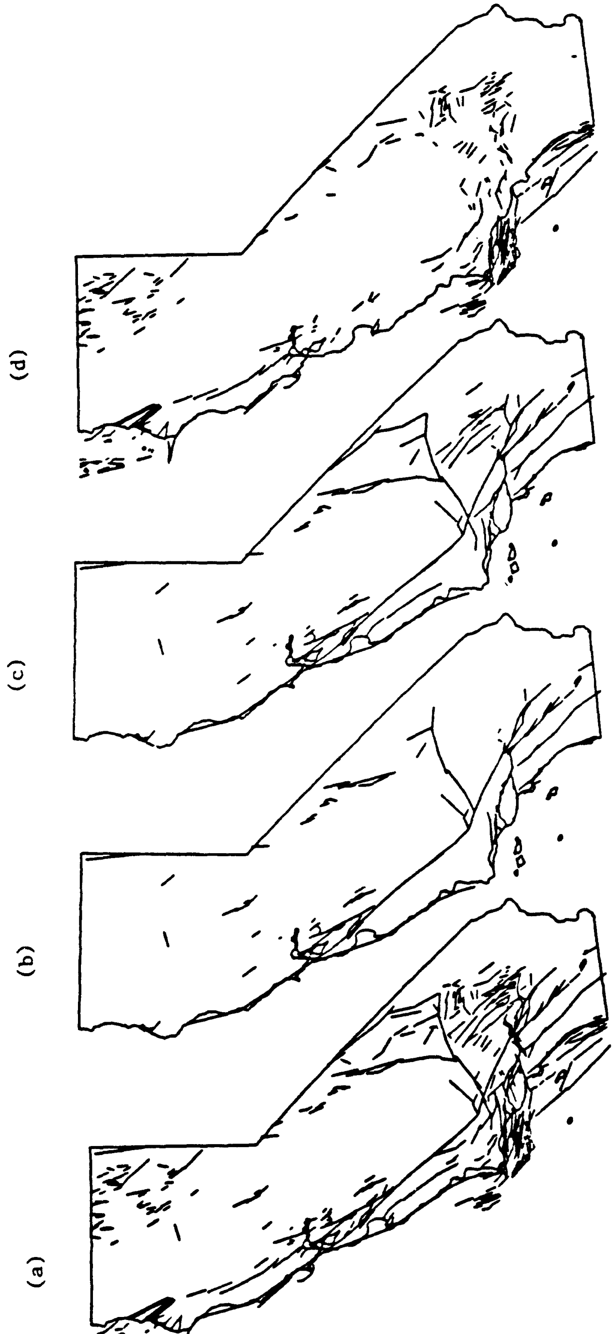

Figure 1. Distribution of faults (a)that displace onshore Quaternary beds and near surface marine deposits, (b) with information on slip rate determined from displaced Quaternary deposits, (c) with information on slip rate determined from displaced Quaternary deposits, as well as older Pliocene to Miocene strata, (d) with no information on slip rate but are known to displace Quaternary beds.

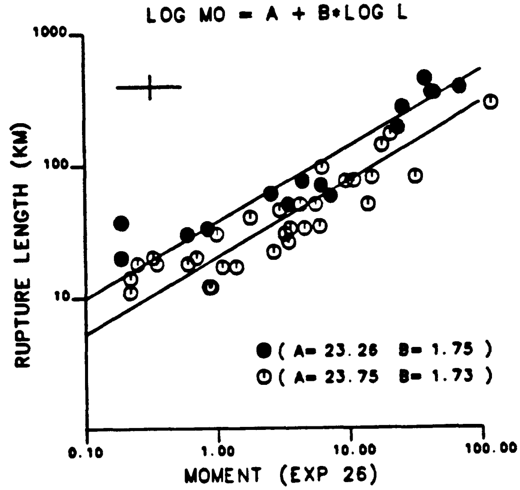

Figure 2. Seismic moment M_o versus rupture length l for earthquakes in California and similar tectonic environments. Earthquakes that occurred on faults with geologic slip rates estimated to be greater than and less than about 1 cm/yr are displayed in (a) as closed and open circles, respectively,

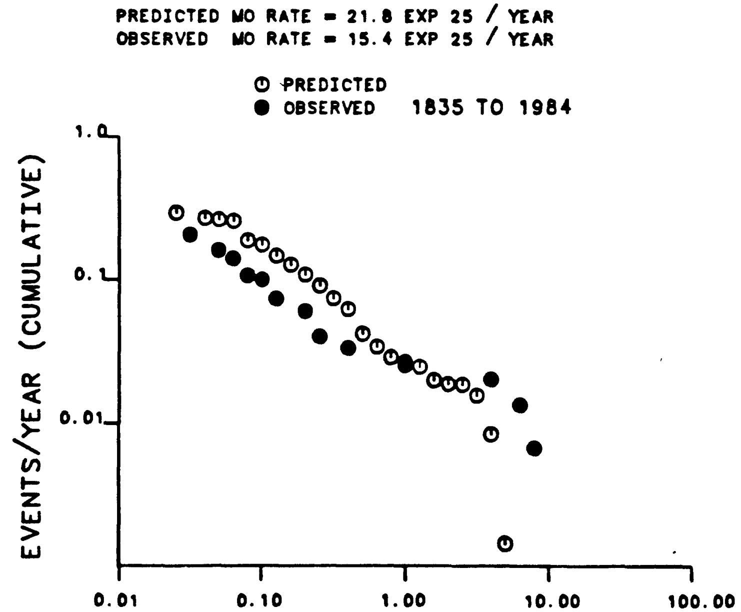

Figure 3. Observed earthquake frequency distribution (closed circles) versus distribution predicted from geologic data with the maximum magnitude model of fault behavior (open circles).

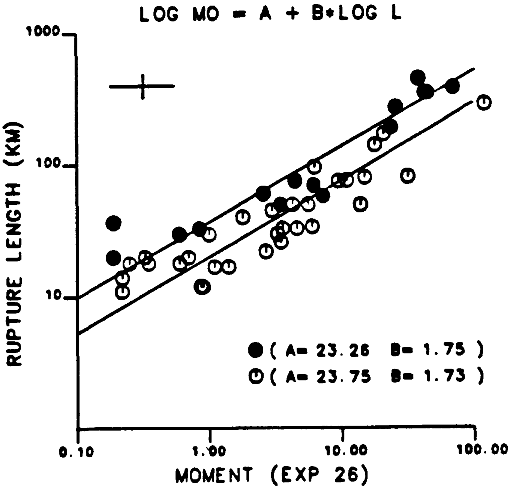

Figure 2. Seismic moment M_0 versus rupture length l for earthquakes in California and similar tectonic environments. Earthquakes that occurred on faults with geologic slip-rates estimated to be greater than and less than about 1 cm/yr are displayed in (a) as closed and open circles, respectively,

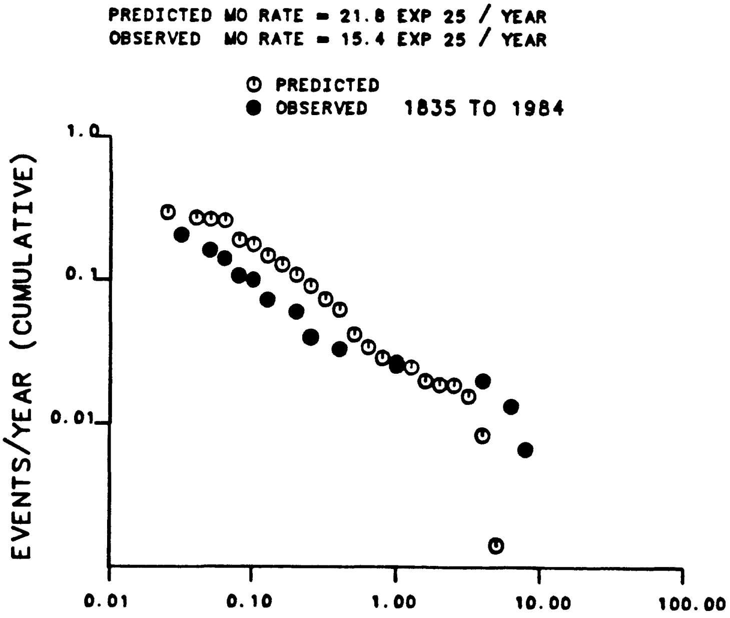

Figure 3. Observed earthquake frequency distribution (closed circles) versus distribution predicted from geologic data with the maximum magnitude model of fault behavior (open circles).

Earthquake Hazards Studies, Metropolitan Los Angeles-Western Transverse Ranges Region

9540-02907

R. F. Yerkes
Branch of Western Regional Geology
345 Middlefield Road MS 975
Menlo Park, California 94025
(415) 323-8111 x2350

Investigations and results

1. Historic earthquake data (W.H.K. Lee and P. Levine). Several steps have been required to efficiently relocate earthquakes in the Los Angeles metropolitan region. Each of the steps is well in hand. (A). The HYPO71 earthquake location program is being revised for interactive processing because of the need to modify station weighting during analysis of single events. Because the phase data were obtained from other institutions many inconsistencies in data and format required correction. (B). A station-operation history of the CalTech-USGS Southern California Seismic Network was prepared and computerized. (C). Phase data were extracted from CalTech tapes for January to March 1984; many discrepancies were corrected and the data converted to HYPO71 format.

2. Earthquake hazards studies (Yerkes and Levine). (A) Two chapters of Coalinga Professional Paper were revised to include the August 1985 earthquake sequence and then completed through peer and Office of Earthquakes, Volcanoes, and Engineering review: "Tectonic Setting" and "Abnormally high fluid pressures in the region of the....earthquakes and their significance". The August 4, 1985 M_L 5.5 thrust/reverse earthquake occurred 17 km southeast of the 1983 main shock at a depth of about 12 km and after-shocks extended south and southwest. In section the sequence forms a gently southwest-dipping detachment beneath Kettleman North Dome (Eaton, 1985, written comm.) and coincides with the Franciscan-basement boundary previously mapped by seismic profiling. The 1985 sequence thus greatly strengthens the interpretation that the Coalinga earthquakes occurred on a southwest-dipping detachment that ruptured downward, implying an inverse relation between depth and crustal strength, a relation that could be caused by abnormally high fluid pressures at seismogenic depths. (B). The investigation of abnormally high fluid pressures was extended to the western Transverse Ranges, well known for its effects of severe north-south compression. Abnormally high fluid pressures are much more extensive than previously reported, and have been identified in several localities along the general trend of the Pitas Point-Red Mountain-San Cayetano zone of thrust/reverse faults. An Open-File Report on this investigation has been prepared and released (Levine and Yerkes). (C). Dated marine terrace deposits along the Ventura-Santa Barbara coast have been uplifted to elevations of about 1150 ft over the last 40,000 years. Implied rates of uplift, about 8 mm/yr, are about the same as those inferred for the axis of the Ventura-Rincon anticline itself. The anticlinal trend extends eastward more than 20 km from the northeast Santa Barbara Channel, and is segmented by numerous reverse faults, which divide the trend into several separate structures that contain oil fields. The overall surface and subsurface structure of this zone has never been examined in an integrated

study, nor have the uplifted terraces been related to specific faults. Since the zone is seismically active, we expect that a detailed examination will identify active structures that may explain the loci of both the uplift and the extreme horizontal convergence across the province. (D). The April 7, 1981 reverse-fault surface rupture and M_L 2.5 earthquake at the Lompoc, California, diatomite quarry (see SUMMARIES, vol. XIII, p. 74; Geology, vol. 11, p. 287-291, 1983) was followed on April 9, 1985 by a second reverse-fault rupture, and on September 30, 1985 by a third reverse-fault rupture. The 1985 ruptures formed on the south limb of the main syncline that underlies the quarry, instead of on the north limb as in 1981; however, it is reported that the same geologic unit ruptured as in 1981. The core and south limb of the syncline have been quarried vigorously since 1981, whereas the north limb has not been quarried since the 1981 event. Although both 1985 rupture events were reportedly accompanied by appreciable local shaking, careful search of CIT/USGS network records revealed no seismologic evidence of either event.

3. Quaternary stratigraphy, chronology, and tectonics, Ventura area (A.M. Sarna-Wojcicki, Branch of Western Regional Geology, and Kris McDougall, Branch of Paleontology and Stratigraphy). Continued investigations previously reported (SUMMARIES, Vol. XX, p. 128, 1985).

Reports

Harden, J.W., Sarna-Wojcicki, A.M., and Dembroff, Glenn, Soil development on coastal terraces near Ventura, California in: a series of soils chronosequeces in the Western U.S., J.W. Harden, editor, U.S. Geological Survey Bulletin 1590.

Levine, Paia, and Yerkes, R.F., 1985, Distribution of abnormally high pore pressures in the western Transverse Ranges, California: U.S. Geological Survey Open-File Report 85-522, text, tables, and map at 1:250,000.

Sarna-Wojcicki, A.M., Morrison, S.D., Meyer, C.E., and Hillhouse, J.W., Correlation of upper Cenozoic volcanic ash beds in sediments of the western United States and northeastern Pacific Ocean, and comparison with biostratigraphic and magnetostratigraphic data, prepared for GSA Bulletin.

SHALLOW SHEAR WAVE VELOCITY AT THE EL CENTRO STRONG MOTION SITES BOND'S CORNER AND DIFFERENTIAL ARRAY

Contract No. 14-08-0001-22045

Terrance G. Barker and Jeffry L. Stevens

S-CUBED
P. O. Box 1620
La Jolla, California 92038
(619) 453-0060

The objective of this project is to extend the work reported in Barker and Stevens (1983), in which the shallow shear wave velocity and Q structure were found for sites E05, E06 and E07 of the U. S. Geological Survey (USGS) El Centro Strong Motion Accelerograph Sites. In that project, a weight drop was used to generate Rayleigh waves which were recorded on linear arrays of geophones. Generalized linear inversion was used to infer the shear velocity structure from phase and group velocity dispersion, and to infer the Q structure from the Rayleigh wave attenuation coefficients. In the current project, we are applying the inversion procedure to data recorded at Bond's Corner (BCR) and the differential array (DFA). The final objective of the project is to correlate the responses of the structures at these five sites with observations of strong ground motion caused by the 1979 Imperial Valley earthquake.

Reference:

Barker, T. G. and J. L. Stevens (1983), "Shallow Shear Wave Velocity and Q Structures at the El Centro Strong Motion Accelerograph Array," *Geophys. Res. Letters,* 10(9), pp. 853-856.

STRONG GROUND MOTION OF THE LOS ANGELES BASIN

0001 - 22023

Marijan Dravinski
Department of Mechanical Engineering
University of Southern California
Los Angeles, California 90089 - 1453
(213) 743-2309

Objectives

The goals of this investigations are (i) to study diffraction of elastic waves by an alluvial valley which contain dipping layers of arbitrary shape and (ii) to evaluate the surface ground motion atop the alluvial valley of the Los Angeles basin.

Investigations

The problem of amplification of the surface strong ground motion by dipping layers of arbitrary shape has been investigated by using an indirect boundary integral equation approach in the frequency domain. The method requires numerical evaluation of the Green functions for line loads within a viscoelastic half-space. An extensive testing of the Green functions has been completed and the results of these investigations can be found in two reports by Dravinski and Mossessian.

Plane strain model for diffraction of a plane harmonic elastic P, SV, or Rayleigh waves by a stack of dipping layers of arbitrary shape has been developed and tested. The results pertinent to special geometry of the alluvial valley show very good agreement with those available in literature.

The results indicate that the amplification effects due to presence of the dipping layers depend upon number of parameters present in the problem,such as, nature and frequency of the incoming wave, contrast in material properties between the layers, geometry of the layers, location of the observation point at the surface, and the component of the displacement field being measured. A typical result of a surface displacement spectra atop a cross-section of the Los Angeles basin is shown by Fig. 1. It is apparent from the figure that the presence of the subsurface irregularity may increase the surface strong ground motion significantly in comparison to the free-field which would be present in the absence of the irregularity. The surface displacement spectra have been evaluated for various cross-sections of the Los Angeles basin and for a range of physical parameters present in the problem.

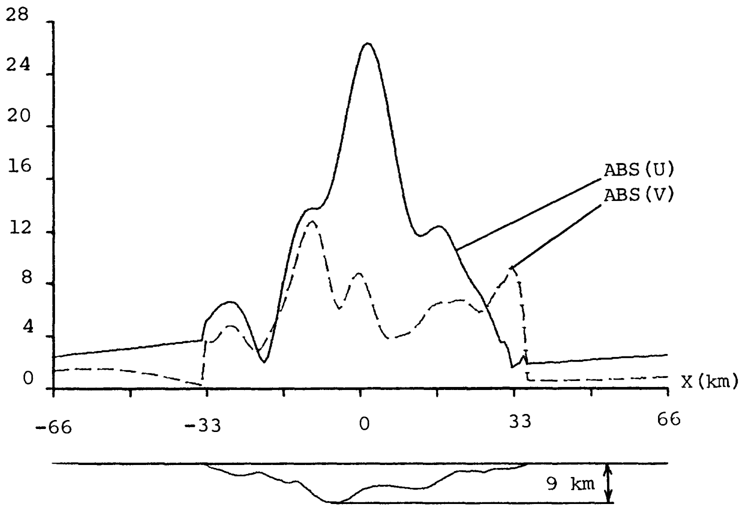

Fig. 1 Surface displacement amplitude spectra for a cross-section of the Los Angeles basin and for incident plane harmonic SV-wave. The following parameters have been assumed: Angle of incidence 30° off vertical axis from left to right; circular frequency of incident wave 0.718 1/s. Ratios of (bedrock vs. alluvium)shear moduli, shear wave speeds, and dilatational wave speeds are assumed to be 1:0.045; 1:0.3; and 2:0.6, respectively. Attenuation for P and S waves is assumed to be 25 and 50, respectively.

The Graphics Package

Since the future research should incorporate the three dimensional analysis of the basin a set of programs have been developed to model alluvial valley of the Los Angeles basin. As reported earlier, the package works in the following way: The data points specifying the alluvial depth of the valley are provided from the existing maps. It is assumed that the set of data is sparse. Through the data a bidirectional cubic spline surface patches are fitted so that the continuity of the interface surface and its derivatives is preserved between the patches. Therefore, the interface and the corresponding normals can be evaluated numerically with sufficient accuracy at any point of the interface between the valley and the bedrock. This will facilitate evaluation of the displacement and the traction fields along the interface of a three dimensional model. All programs were written in FORTRAN IV. The programs require a graphic terminal or a computer plotter. As an illustrative example a cross-section of the basin is presented by Fig. 2.

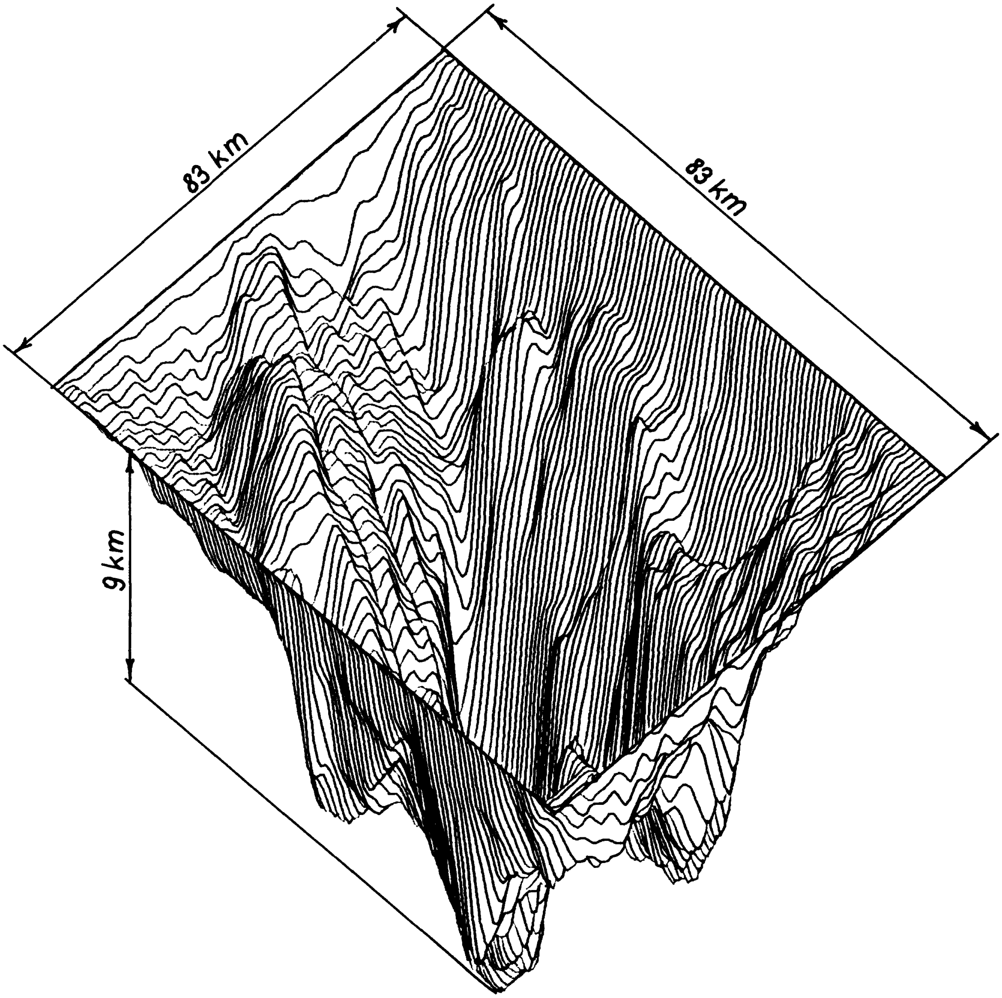

Fig. 2. Alluvial valley of the Los Angeles basin modeled by a set of bidirectional cubic spline patches.

Future Research

It is planned to extend the analysis to a set of three-dimensional dipping layers. This model should be more realistic than the two-dimensional one and should provide us with some insight in the amplification of the strong ground motion by dipping layers in an actual basin.

Experimental Investigation of Liquefaction Potential

9910-01629

Thomas L. Holzer

Branch of Engineering Seismology and Geology
U.S. Geological Survey
345 Middlefield Road, MS 977
Menlo Park, CA 94025
(415) 323-8111, ext. 2760

Investigations

1. Shallow seismic refraction, cone penetration testing, and standard penetration testing were completed near Parkfield, California, in the Cholame Valley south of Jack Ranch and north of Highway 41. The purpose is to find a site to install a system of piezometers and accelerometers to measure both pore-water pressures in sands and the shallow vertical variation of acceleration during the predicted Parkfield earthquake ($M_L = 5.6$).

2. Evaluation of the dependency of liquefaction during strong ground motion on crustal stress state in the earthquake source region.

Results

1. Exploratory drilling has found a stratum of medium to coarse-grained saturated sand, parts of which appear to have potential to generate excess pore pressures during the predicted Parkfield earthquake. The thickest accumulation of sand, 6.5 m, was found at 35°47'41" N and 120°20'12" W. This location is 0.54 km southwest of the active trace of the San Andreas fault. The top of the sand body is at a depth of 5 m. The deposit is confined by a 3-m thick clayey silt. Modified blow counts (SPT) in the sand stratum ranged from 20 to 30, with the lowest values occurring in its upper part. Hydrogeologic considerations suggest that the sand is permanently saturated. The area is adjacent to the Cholame Creek, an intermittent stream which recharges the shallow valley fill. Depth to the water table was about 2 m in July 1985.

2. The empirical correlation of peak accelerations during strong ground motion with liquefaction forms the basis for both site specific and regional evaluations of liquefaction hazards. Dependency of peak acceleration on crustal stress state as well as magnitude suggests that the state-of-the-art for liquefaction hazard evaluation could be improved by considering crustal stress state in addition to earthquake magnitude. Data relating distance from an earthquake to which liquefaction is observed versus magnitude were analyzed. They suggest that there is a dependency on the type of faulting (and stress state). Earthquakes

associated with normal faults (extension areas) do not cause liquefaction to as great a distance as do earthquakes on reverse faults (compressive areas).

Reports

Bennett, M.J., 1985, Subsurface investigation of ground failure at the San Fernando Valley Juvenile Hall, Sylmar, California: Association of Engineering Geologists, 28th Annual Meeting, Winston-Salem, N.C., Abstracts with Programs, p. 57.

Youd, T.L., Harp. E.L., Keefer, D.K., and Wilson, R.C., 1985, Liquefaction generated by the 1983 Borah Peak, Idaho, earthquake in U.S. Geological Survey Open-File Report 85-290, p. 625-634.

Youd, T.L., 1985, Landslides caused by earthquakes: discussion: Geological Society of America Bulletin, v. 96, p. 1091-1094.

Tinsley, J.C., Youd, T.L., Perkins, D.M., and Chen, A.T.F., 1985, Evaluating liquefaction potential in U.S. Geological Survey Professional Paper 1360, p. 263-315.

Near Surface Lithologic and Seismic Properties

9910-01168

W. B. Joyner
J. F. Gibbs

Branch of Engineering Seismology and Geology
U.S. Geological Survey
345 Middlefield Road, MS 977
Menlo Park, California 94025
(415) 323-8111, Ext. 2754, 2910

Investigations

Measurement of seismic velocity and attenuation to determine the effect of local geology on strong ground motion and to aid in the interpretation of seismic source parameters.

Results

Downhole shear velocity data were obtained at recording sites for the Coalinga earthquake sequence.

Reports

Fumal, T. E., Gibbs, J. F., and Roth, E. F., 1985, Near-surface geology and seismic wave velocities at six strong-motion stations near Gilroy, California, *in* Hoose, S. N. (ed.), The Morgan Hill, California, earthquake of April 24, 1984, *U.S. Geological Survey Bulletin 1639.*

Fumal, T. E., and Tinsley, J. C., 1985, Mapping shear-wave velocities of near-surface geologic materials, *in* Ziony, J. I. (ed.), Evaluating earthquake hazards in the Los Angeles region, *U.S. Geological Survey Professional Paper 1360*, 127–149.

Fumal, T. E., Tinsley, J. C., and Joyner, W. B., 1985, Correlations between shear-wave velocity and other geotechnical properties of near-surface geologic materials in California (abstract), Association of Engineering Geologists, 1985 annual meeting.

Fumal, T. E., Warrick, R. E., Etheredge, E. C., and Archuleta, R. J., 1985, Downhole geology, seismic velocity structure, and instrumentation at the McGee Creek, California, recording site (abstract), *Earthquake Notes* **55**, 5.

Joyner, W. B., and Fumal, T. E., 1985, Predictive mapping of earthquake ground motion, *in* Ziony, J. I. (ed.), Evaluating earthquake hazards in the Los Angeles region, *U.S. Geological Survey Professional Paper 1360*, 203–220.

Tinsley, J. C., and Fumal, T. E., 1985, Mapping Quaternary sedimentary deposits for areal variations in shaking response, *in* Ziony, J. I. (ed.), Evaluating earthquake hazards in the Los Angeles region, *U.S. Geological Survey Professional Paper 1360*, 101–125.

Regional Syntheses of Earthquake Hazards in Southern California

9910-03012

Joseph I. Ziony

Branch of Engineering Seismology and Geology
U.S. Geological Survey
345 Middlefield Road, MS 977
Menlo Park, CA 94025
(415) 323-8111, ext. 2944

Investigations

Our efforts focused on:

1. Final coordination of the Los Angeles earthquake hazards professional paper, chiefly involving review and correction of page proofs.

2. Organizing a workshop, Future Directions in Evaluating Earthquake Hazards of Southern California, to be held November 12 and 13, 1985, that will summarize recent results of earth-science research on hazard-prediction methods, and will identify priorities for future research in the southern California region.

Results

1. U.S. Geological Survey Professional Paper 1360, Evaluating Earthquake Hazards in the Los Angeles Region--An Earth-Science Perspective, was published. This 505-page report summarizes current knowledge of the geologically controlled earthquake hazards of the region and presents methods for predicting strong ground shaking, surface faulting, liquefaction, landsliding, and tsunamis from future earthquakes. The report contains the following chapters:

   Introduction, by J.I. Ziony and W.J. Kockelman.

   Geologic and Seismologic Setting, by R.F. Yerkes

   Evaluating Earthquake and Surface-Faulting Potential, by J.I. Ziony and R.F. Yerkes.

   Predicting Earthquake Ground Motion: An Introduction, by R.D. Borcherdt.

   Mapping Quaternary Sedimentary Deposits for Areal Variations in Shaking Response, by J.C. Tinsley and T.E. Fumal.

   Mapping Shear-Wave Velocities of Near-Surface Geologic Materials, by T.E. Fumal and J.C. Tinsley.

Predicting Seismic Intensities, by J.F. Evernden and J.M. Thomson.

Predictive Mapping of Earthquake Ground Motion, by W.B. Joyner and T.E. Fumal.

Predicting Relative Ground Response, by A.M. Rogers, J.C. Tinsley, and R.D. Borcherdt.

Predicting Earthquake Ground-Motion Time Histories, by P.A. Spudich and S.H. Hartzell.

Evaluating Liquefaction Potential, by J.C. Tinsley, T.L. Youd, D.M. Perkins, and A.T.F. Chen.

Predicting Areal Limits of Earthquake-Induced Landsliding, by R.C. Wilson and D.K. Keefer.

Identifying Potentially Active Faults and Unstable Slopes Offshore, by S.H. Clarke, Jr., H.G. Greene, and M.P. Kennedy.

Evaluating Tsunami Potential, by D.S. McCulloch.

Predicted Geologic and Seismologic Effects of a Postulated Magnitude 6.5 Earthquake Along the Northern Part of the Newport-Inglewood Zone, by J.I. Ziony, J.F. Evernden, T.E. Fumal, E.L. Harp, S.H. Hartzell, W.B. Joyner, D.K. Keefer, P.A. Spudich, J.C. Tinsley, R.F. Yerkes, and T.L. Youd.

Using Earth-Science Information for Earthquake Hazard Reduction, by W.J. Kockelman.

Reports

Ziony, J.I., editor, 1985, Evaluating earthquake hazards in the Los Angeles region--an earth-science perspective: U.S. Geological Professional Paper 1360, 505 p.

Ziony, J.I., and Kockelman, W.J., 1985, Introduction, in Ziony, J.I., ed., Evaluating earthquake hazards in the Los Angeles region--an earth-science perspective: U.S. Geological Professional Paper 1360, p. 1-23.

Ziony, J.I., and Yerkes, R.F., 1985, Evaluating earthquake and surface potential in Ziony, J.I., ed., Evaluating earthquake hazards in the Los Angeles region--an earth-science perspective: U.S. Geological Professional Paper 1360, p. 43-91.

Ziony, J.I., Evernden, J.F., Fumal, T.E., Harp, E.L., Hartzell, S.H., Joyner, W.B., Keefer, D.K., Spudich, P.A., Tinsley, J.C., Yerkes, R.F., and T.L. Youd, 1985, Predicted geologic and seismologic effects of a postulated magnitude 6.5 earthquake along the northern part of the Newport-Inglewood Zone, in Ziony, J.I., ed., Evaluating earthquake hazards in the Los Angeles region--an earth-science perspective: U.S. Geological Professional Paper 1360, p. 415-442.

Development Of A
Seismic Slope Stability Map
Of The Urban Corridor Of
Davis And Salt Lake Counties, Utah

14-08-0001-21913

Jeffrey R. Keaton
Dames & Moore
250 East Broadway, Suite 200
Salt Lake City, Utah 84111
(801) 521-9255

Loren R. Anderson
Department of Civil & Environmental Engineering
Utah State University
Logan, Utah 84322
(801) 750-2780

INVESTIGATIONS

1. Completed parametric analyses to identify ranges of critical slope angle as a function of material strength parameters for several values of slope height for two horizontal ground acceleration values and dry and fully saturated ground water conditions.
2. Nearly completed compilation of existing landslides.
3. Have acquired digital topographic data (vector format) for 19 quadrangles (about 75% of study area).
4. Have written program to convert vector format digital topographic data to 30 m x 30 m grid format.
5. Have gridded digital topographic data and created files with 1) elevation, 2) slope aspect, 3) slope gradient, 4) down slope curvature, and 5) across slope curvature for each 30 m grid cell for all 19 quadrangles.
6. Have assessed uniformity of geotechnical and geologic conditions in study area and began digitizing geoproperties to match 30 m grid for computer calculation.

RESULTS

By using the digital topographic and geoproperties data, we will be able to compute horizontal acceleration values required to reduce calculated factors of safety to unity (assumed failure) for each 30 m grid. The acceleration values will be used as index values to rank slope instability (failure) potential into qualitative terms of High, Moderate, Low, and Very Low.

High slope instability potential will correspond to those accelerations which have a 50% or greater probability of occurring in a 100-year period. Probabilistic acceleration values in the Davis and Salt Lake City area have been developed for several projects and will be used in this study in the same manner that they were used in recent and on-going liquefaction potential analyses.

Moderate potential will correspond to acceleration values with probability between 50% and 10% in a 100-year period. Low potential will correspond to acceleration values between 10% and 5% probability in 100 years. Very low potential corresponds to accelerations with less than 5% probability of occurring in 100 years.

The differences associated with dry and fully saturated conditions will be incorporated into the slope instability indexes.

A Systems Approach to Wasatch Front Seismic Risk Problems

14-08-001-22013

Craig Taylor and John Wiggins
J.H. Wiggins Company/NTS
1650 South Pacific Coast Highway
Redondo Beach, CA 90277
(213) 316-2257

Investigations

1. Develop a data base structure, including selection of a basic geographic reference and microzonation scheme, and construct building data and lifeline network component data formats for earthquake risk studies.

2. For Salt Lake and Davis Counties, Utah, gather and input data on State-owned buildings, natural gas supply facilities, culinary water supply facilities, and local geoseismic hazards.

3. Using seismic energy sources mapped at depth, develop seismic risk procedures and programs that will produce figures of merit for State insurance analysis and that will estimate expected pipeline breaks in natural gas and culinary water systems.

4. Produce figures of merit for State building earthquake insurance analysis and evaluate expected pipeline breaks in natural gas and culinary water systems inventoried.

Results

Based on its extensive use in local municipal and utility planning, the township-and-range geographic reference system was selected for basic data collection and for microzonation construction. Over six hundred microzones (township-and-range sections) were determined to have potential exposures among facilities surveyed. Basic formats for data input were developed. Data were gathered on State-owned buildings, natural gas system facilities, and at least 16 culinary water systems. These data were then systematically input except that time permitted only five culinary water systems (including two major wholesalers) to be prepared for analysis.

Liquefaction susceptibility data were supplied by Dames & Moore and Utah State University. Dynamic amplification data were derived from reports by Hays, Rogers, Miller, and others. Surface fault rupture data were derived from recent U.S.G.S. Salt Lake County studies along with previous Woodward-Clyde fault trace maps. Computer files were developed for microzone hazard data. Fault displacement sensitivity records were also developed to indicate percent of facilities in the Wasatch fault zone.

Fifty-two events were then defined to provide a representative sample of damaging areal seismicity. Smaller events were randomized on north-south trending lines. New techniques allow damage outputs from these events to be used to estimate overall expected damage from smaller magnitude events. (See Taylor, Legg, Haber, Wiggins, 1985). The larger (M_S > 6.4) twelve of those events were associated with a three-dimensional model of the Wasatch normal fault, which dips and plunges under facilities. For the Salt Lake segment of the Wasatch fault, the model used was based on preliminary findings by Bruhn and others. For the Ogden segment, this model was constructed on the assumption of constant plunge and trend angles. For each of the twelve larger events, distances from seismogenic planes to microzones were calculated and found to be very short--illustrating the near-field nature of the seismic risk problem in this region.

Rapid procedures were then constructed to calculate expected fault displacements, shaking intensities, and liquefaction probabilities. Shaking intensities were based on Ken Campbell's near-field horizontal peak ground velocity attenuation function converted into a continuous Modified Mercalli intensity attenuation function. Dynamic amplification factors were assigned to each microzone to account for intensity increases implied by ongoing U.S.G.S. relative ground response studies. Raw data on water table depths, critical boring count values, and critical accelerations were combined with procedures incorporating magnitude level and estimated peak horizontal ground acceleration to assess liquefaction probabilties.

These procedures were augmented with categorization of the seismic vulnerability of buildings surveyed--categorization based on date of construction, frame/exterior wall system raw data, and familiarity with many of the buildings surveyed as well as with local earthquake design and construcion practices as they have evolved. Building loss algorithms were based on previous NSF findings. Casualty estimation procedures were based on in-house earthquake insurance work. Pipe vulnerability models were based on previous NSF results supplemented by engineering judgment on pipeline types not previously modeled.

Preliminary results show that building losses and casualty ratios (percent of casualties per population exposed) are significant in the largest (7.0 > M_S > 7.5) two events studies--one each on the Ogden and Salt Lake segments respectively. Derived shaking intensity values are high, largely as a result of the short distances to seismogenic planes and the size of these two earthquakes. So far, shaking even appears to be the major cause of pipeline failure in these events. These findings, however, still require interpretation. For instance, in smaller events to be evaluated, it is expected that liquefaction will be the dominant factor affecting pipe break estimates--especially in Davis and northern Salt Lake County with widespread high liquefaction susceptible regions.

References

Taylor, C.E., M.R. Legg, J.M. Haber, and J.H. Wiggins "New Lifeline Multiscenario Seismic Risk Techniques with a Model Application," *Civil Engineering Systems*, pp. 77-83, vol. 2, June 1985.

Earthquake hazards research applications

9900-90022

Walter W. Hays, Paula L. Gori, and William J. Kockelman
Office of Earthquakes, Volcanoes, and Engineering
905 National Center
Reston, VA 22092
(703) 860-6471; 928-6471 (FTS)

Investigations

Since fiscal year 1978, the USGS Earthquake Hazards Reduction Program has sponsored an active program to foster implementation of research results at all levels of government and in the private sector. The objectives of the program are to:

- Establish "good neighbor" partnerships with Federal, State, and local government agencies and private organizations in the United States to work on the National Earthquake Hazards Reduction Program (NEHRP).
- Strengthen local expertise in every part of the Nation, stimulate interested persons to accelerate their research about earthquake hazards, and to foster the implementation of seismic safety policies.
- Disseminate research results and information produced by the USGS to all users, including Federal, State and local government agencies, engineers and scientists, professional organizations, model building code groups, and others who can incorporate and utilize them it in their programs.

Results

In FY 1985, this program supported many diverse activities throughout the United States to meet the above objectives. The principal activities which this program supported are summarized below.

Workshops

The USGS, in cooperation with FEMA and other Federal Agencies, has convened 20 regional workshops since Fiscal Year 1978 in earthquake-prone areas of the United States to focus research on specific problems and to foster implementation of loss-reduction measures. These workshops have brought together scientists and representatives from all levels of government, academia, and the private sector. They have 1) reviewed the state-of-knowledge of the regional earthquake hazard; 2) determined the need for additional scientific, engineering, and societal-response information to increase knowledge and to devise and implement effective earthquake hazards loss-reduction programs; and 3) created practical plans for achieving research, mitigation, response, and recovery goals in a 3-5 year time frame. These meetings have stimulated researchers and research users and have resulted in the formation of several regional seismic safety commissions and improved policies on seismic safety.

Five workshops held in Fiscal Year 1985 in Albany, New York; Dorado, Puerto Rico; Salt Lake City, Utah; and Anchorage, Alaska, are summarized below:

1) Workshop on "Continuing Actions to Reduce Potential Losses from Future Earthquakes in New York and Nearby States," December 12-14, 1984. Eighty-five geologists, scientists, engineers, social scientists, emergency planners, and public officials met in Albany, New York, on December 12-14, 1985, to discuss "Continuing Actions to Reduce Potential Losses from Future Earthquakes in New York and Nearby States." The workshop was sponsored by the USGS, FEMA, New York Geological Survey, and New York State Division of Military and Naval Affairs. Although the probability of a major earthquake occurring in the near future in New York or in Canada or a nearby State is quite low, the geological and seismological record indicates that damaging, moderate-to-severe earthquakes have occurred in the vicinity of New York in the past and will recur in the future. The workshop was convened just after the formation of the New York Earthquake Advisory Council and the implementation of an earthquake preparedness program in New York. The workshop reinforced the commitment of the scientific/technical and public-policymaking communities to seek effective ways to improve research, mitigation, response, and recovery activities and to set realistic goals of loss reduction. The participants unaminously adopted a resolution in support of the New York Earthquake Advisory Council and other important research and mitigation goals.

2) Workshop on "Reducing Potential Losses from Earthquake Hazards in Puerto Rico," May 30-31, 1985. One hundred earth scientists, social scientists, engineers, architects, urban planners, and emergency management specialists met in Dorado, Puerto Rico, on May 30-31, 1985, to formulate measures to stimulate current research on earthquake hazards in the Puerto Rico region and to design action plans to reduce potential losses from future earthquakes in the region. With the experience of the March 3, 1985, Chile earthquake (a subduction zone earthquake) fresh in their minds, the Dorado workshop participants reiterated the desire expressed at a geologic hazards workshop in 1984 that Puerto Rico must take steps to reduce potential losses from earthquake hazards. The recurrence interval for a $M = 7.5$ earthquake (like that of 1918) in the Puerto Rico area is now estimated to be about 80 years. The results of a preliminary vulnerability study of the San Juan area were presented, showing that the potential losses from such an earthquake could be very high. The participants recommended that the study be expanded to include other parts of Puerto Rico and completed as soon as possible. Other recommendations included specific proposals to upgrade the strong-motion accelerograph network, to complete the seismic source zone and probabilistic ground-shaking hazard maps, and to adopt an updated building code reflecting state-of-the-art seismic design and hazard assessment methodologies. A third geologic hazards workshop is planned for May 1986 in San Juan, Puerto Rico, and will incorporate results of the September 19, 1985, Mexico earthquake, another subduction zone earthquake.

3 and 4) Workshops on "Earthquake and Landslide Hazards in the Wasatch Front Region of Utah," July 10-11, 1985; July 30-August 1, 1985. The USGS, FEMA, Utah Geological and Mineral Survey (UGMS), Utah Division of Comprehensive Emergency Management (CEM), and the University of Utah jointly sponsored the 1985 workshops on earthquake hazards and risks in Utah. Continuing a planning process begun at the first conference in 1984, two earthquake hazards workshops were convened in Salt Lake City during July-August 1985. The goal was to increase the capability of UGMS and CEM to meet the needs of government officials, private industry, academic institutions, and engineers and architects in Utah to incorporate earthquake and landslide hazards information in their porgrams. The first of the two workshops which was held at the UGMS office in Salt Lake City on July 10-11, 1985, was attended by twenty-five scientists, emergency managers, architects, and engineers. In this workshop, the UGMS, with the assistance of the workshop participants, identified viable roles and responsibilites of the State Survey in the creation of basic data systems, hazard monitoring, loss estimation studies, and postearthquake investigations. Several agencies and groups were identified who could assist or who could share these responsibilities. At the conclusion of the two-day workshop, all participants recognized the urgency of institutionalizing the relationships and activities of all of the partners in a hazards reduction program for Utah and requested that UGMS take the long-term role of coordinator of hazards information focusing on collection, translation, and dissemination of hazards information, as well as the process of preparing for postearthquake investigations.

The second workshop, which was held July 30-August 1, 1985, was designed to assist CEM, USGS, and cities and counties in the State to increase their use of hazards information and to devise and implement loss-reduction measures. For two days, 60 emergency managers, urban planners, and county geologists participated in discussions of earthquake and landslide hazards identification and risk analysis, and the use of hazards and risk information (maps, reports, data) in land-use and emergency response planning. Communication was greatly improved by the spirited interaction between geologists, seismologists, and social scientists (who collect and translate hazard information) and urban planners, emergency managers, and architects and engineers, (who need to use the information in their communities and for their clients). On the third day of the workshop, the participants took a field trip to see landslides, fault scarps, and examples of appropriate land use in earthquake- and landslide-prone areas. Two weeks later, UGMS and USGS collaborated in a training exercise on fault identification and excavated a trench across the Wasatch fault zone as a dynamic laboratory exercise. An ad hoc working group on Utah seismic zoning was created to evaluate the seismic zoning map for Utah.

5) Workshop on "Evaluation of Regional and Urban Earthquake Hazards and Risk in Alaska," September 5-7, 1985. Seventy-five earth scientists, social scientists, engineers, planners, and emergency management specialists participated in a 3-day workshop on "Evaluation of Regional and Urban Earthquake Hazards and Risk in Alaska." This workshop, held in Anchorage, Alaska, on September 5-7, 1985, was

sponsored by the U.S. Geological Survey, Federal Emergency Management Agency, Alaska Division of Geological and Geophysical Surveys, and Alaska Office of Emergency Services. Alaska is a classic example of the problem of earthquake hazards mitigation in the Western United States where the earthquake threat, stated in terms of the relative seismicity, is roughly 75 times worse than in the Pacific West, but little is being done. The threat is well known to the public, because the 1964 Prince William Sound earthquake was either experienced by or its effects are well known to a large percentage of the 400,000 residents of Alaska. Nevertheless, very little has been done to institutionalize and implement loss-reduction measures in Alaska even though relevant information is available and practical measures have been identified and proposed. A repeat of the great 1964 earthquake or a less severe earthquake near a populated region has the potential for causing much greater losses due to the increase in population and capital improvements since 1964. Many more tall buildings, offshore platforms, and other facilities exist now. To stimulate future advances, the workshop participants formulated action plans for the next 3-5 years to increase the scientific knowledge in a way that will minimize the controversy about where and how often earthquakes are likely to occur in the future and to strengthen the options available to local, State, and Federal governments, as well as businesses and private citizens, to prepare for future earthquakes. A meeting to evaluate progress is being planned in Anchorage for 1989, the year of the 25th anniversary of the 1964 earthquake.

Other Activities to Foster Application of Research

In addition to convening State and regional workshops, the program sponsored activities of Federal and State organizations and other groups to increase the application of earthquake hazards research. These activities included:

- State-wide earthquake hazards conferences were held in Redlands, Wyoming and Murray, Kentucky.
- Assistance was provided to the American Institute of Architects who convened workshops for architects and related building professionals on earthquake-resistant design and construction in Charleston, South Carolina; Salt Lake City, Utah; and Seattle, Washington.
- Assistance was provided to the Building Seismic Safety Council to conduct workshops and to create educational materials for building officials and professionals to dissiminate information about the seismic safety provisions of the ATC model building code and to foster their adoption. Workshops were held in Charleston, South Carolina; Memphis, Tennessee; Seattle, Washington; and St. Louis, Missouri.
- A training session on "Understanding the history, cause, and effects of earthquakes in the United States," was designed for 30 regional and national Federal Emergency Management Agency personnel and held in Menlo Park, California.

- Support was provided for the seismic safety activities of Colorado, South Carolina, and Utah State Geological Surveys. The activities of the Utah Geological and Mineral Survey are reported elsewhere in this report.
- Support was provided for activities of the Interagency Committee on Seismic Safety in Construction which has a goal of recommending procedures and standard practices for evaluating the seismic hazards of ground shaking, surface fault rupture, earthquake-induced ground failure, tectonic deformation, and tsunamis at all Federal construction sites.
- Workshop on "The Borah Peak, Idaho, Earthquake," which was attended by 70 scientists, was convened to discuss what was learned from the 1983 event and to define additional research and application programs in the Great Basin.

Reports

Building Seismic Safety Council, Committee on the Societal Implications of Using New or Improved Seismic Safety Design Provisions, 1985, Societal implications: A community handbook: Federal Emergency Managment Agency, Earthquake Hazards Reduction Series 13, 54 p.

Building Seismic Safety Council, Committee on the Societal Implications of Using New or Improved Seismic Safety Design Provisions, 1985, Societal implications: Selected readings: Federal Emergency Managment Agency, Earthquake Hazards Reduction Series 14, 105 p.

Gori, P. L., ed., 1984, Primer on Improving the state of earthquake hazards mitigation and preparedness: U.S. Geological Survey Open-File Report 84-772, 219 p.

Gori, P. L., and Hays, W. W., eds., 1984, Proceedings of conference XXIV, a workshop on "Geologic hazards in Puerto Rico:" U.S. Geological Survey Open-File Report 84-761, 160 p.

_______________, 1984, Proceedings of conference XXV, a workshop on "Earthquake hazards in the Virgin Islands Region:" U.S. Geological Survey Open-File Report 84-762, 140 p.

Hays, W. W., and Gori, P. L., eds., 1984, Proceedings of conference XXVI, a workshop on "Evaluation of Regional and Urban Earthquake Hazards and Risk in Utah:" U.S. Geological Survey Open-File Report 84-763, 790 p.

_______________, 1985, Proceedings of conference XXVIII, a workshop on "Continuing actions to reduce potential losses from future earthquakes in New York and nearby States:" U.S. Geological Survey Open-File Report 84-386, 172 p.

Hays, W. W., 1985, An introduction to technical issues in the evaluation of site hazards. Interagency Committee on Seismic Safety in Construction TR-6: U.S. Geological Survey Open-file Report 85-371, 102 p.

Interagency Committee on Seismic Safety in Construction, 1985, Tsunami: Hazards definition and effects on facilities, ICSSC TR-8: U.S. Geological Survey Open-File Report 85-533, 140 p.

Stein, R. S., and Bucknam, R. C., 1985, Proceedings of Conference XXVIII on the Borah Peak, Idaho, Earthquake, Vol. A and B: Open-File Report 85-290, 686 p.

Brown, R. D., and Kockelman, W. J., 1983, Geologic principles for prudent land use: U.S. Geological Survey Professional Paper 946, 97 p.

Digital Data Analysis

9920-01788

Ray Buland
Branch of Global Seismology and Geomagnetism
U.S. Geological Survey
Denver Federal Center
Box 25046, Mail Stop 967
Denver, Colorado 80225
(303) 236-1506

Investigations

1. Moment Tensor Inversion. Apply methods for inverting body phase waveforms for the best point source description to research problems.

2. Computation of Free Oscillations. Study the effects of anelasticity on free oscillation eigenfrequencies and eigenfunctions.

3. Earthquake Location Technology. Study techniques for improving the robustness, honesty, and portability of earthquake location algorithms.

4. Real Time Earthquake Location. Experiment with real time signal detection, arrival time estimation, and event location for regional earthquakes.

5. ScS Studies. Use multiple ScS phases to study lateral heterogeneity, attenuation, and scattering in the Western Pacific.

6. Data Collection Center. Develop a state-of-the-art data collection center to handle digital waveform data collection for the next decade.

7. Network Day/Event Tapes. Support and enhance portable software for retrieving data from the Global Digital Seismograph "Network Day Tapes." Create and distribute Network "Event Tapes."

8. NEIS Monthly Listing. Contribute both fault plane solutions (using first-motion direction) and moment tensors (using long-period body-phase waveforms) for all events of magnitude 5.8 or greater when sufficient data exist. Contribute waveform/focal sphere figures of selected events.

Results

1. Moment Tensor Inversion. A catalogue of moment tensors for all sufficiently large events during 1981-1983 is being prepared for publication. Special studies have been done for the 51 IASPEI events and for the March 3, 1985 Chilean earthquake. For the Chilean event, it was determined that neglecting the complexity of the event resulted in a routine result that was too deep and had large non-double-couple and strike slip components.

2. Computation of Free Oscillations. A journal article describing comparisons of exact calculations and first order perturbation theory is being prepared. A new result has been obtained which seems to imply that a layer of extremely low Q can mechanically decouple wave propagation above and below the layer.

3. Earthquake Location Technology. A location program based on R-estimator was tested against the program used by the NEIS to produce the monthly listing. In this test, all published events for March 1985 were relocated neglecting analyst instructions for P waves. Overall, the R-estimator preformed very well. The few descrepancies discovered remain to be analysed.

4. Real-time Earthquake Location. The real-time system developed in cooperation with the Instituto Nazionale di Geofisica (Italian Government) is being implemented in Golden, Colorado, for the United States' seismic network. The system is being generalized to handle both digital and analogue telemetry, different sample rates, and asynchronous channel timing. Dedicated microcomputer hardware has been procured for the near-real-time back end system. Software for regional and teleseismic on-line event location is being tested. The current prototype is processing 128 analogue channels.

5. ScS Studies. The Tonga-Fiji to Hawaii path has been chosen for study, a suite of deep focus events have been selected, and digital seismic waveform and gravity anomaly data have been collected. Software for waveform processing and synthetic seismogram generation has been developed and tested.

6. Data Collection Center. A new data collection system for the Albuquerque Seismological Laboratory has been discussed. By basing the hardware on 32-bit microcomputer and local area network technologies, it appears to be possible to achieve low cost, high reliability, and the flexibility to economically expand the capacity of the system from today's modest requirements to the full output of the proposed IRIS network a decade hence. Several strategies have been developed to protect the system from the vageries of emerging technologies. In particular, redundant data paths employing different technologies will be employed in the network. Also, the mass storage and archival media will be isolated from the system by means of a special purpose file server node.

7. Network Day/Event Tapes. Event tapes are being routinely produced and distributed to 18 data centers. Production and distribution is complete for 1980 to the present. Software is being developed to add data from NARS, Graefenberg, NORESS, Geoscope, and USSR stations to the event tapes. Also, waveform catalogues summarizing the contents of the event tapes are being prepared for montly publication. They will cover January 1985 to the present.

8. NEIS Monthly Listing. Since May 1981, fault plane solutions for large events have been contributed to the Monthly Listing. Beginning in November 1982, moment tensors and waveform/focal sphere plots are also being contributed. In the last six months the fault plane solutions and moment tensors of approximately 80 events were published. A catalogue of all fault plane

solutions for 1981-83 along with first motion data has been prepared for publication as a U.S. Geological Survey Bulletin. In this three-volume set, each volume covers a different geographical region. A new three-volume set is planned every two years.

Reports

Buland, R. P., Yuen, D. A., Konstanty, K., and Widmer, R., 1985, Source phase shift: a new phenomenon in wave propagation due to anelasticity: Geophysical Research Letters, v. 12, 569-572.

Gordon, D. W., and Needham, R. E., 1985, Recent seismicity in eastern and central Wyoming: Earthquake Notes, in press.

Needham, R. E., 1985, First motion focal mechanism solutions for the IASPEI earthquakes: U.S. Geological Survey Open-File Report 85-458.

Needham, R. E., 1985, Catalogue of first motion fault plane solutions, volumes I-III: U.S. Geological Survey Bulletin, submitted.

Sipkin, S. A., 1985, Moment tensor analysis of the 1985 Chilean earthquake mainshock: EOS, in press.

Zirbes, M. D., Lishner, J. M., and Moon, B. J., 1985, NEIC waveform catalogue, Jan.-Mar., 1985: U.S. Geological Survey Open-File Report, submitted.

U.S. Seismic Network

9920-01899

Marvin A. Carlson
Branch of Global Seismology and Geomagnetism
U.S. Geological Survey
Denver Federal Center
Box 25046, Mail Stop 967
Denver, Colorado 80225
(303) 236-1506

Investigations

U.S. Seismicity. Data from the U.S. Seismic Network are used to obtain a preliminary location and magnitude of significant earthquakes throughout the United States and the world.

Results

As an operational program, the U.S. Seismic Network operated normally throughout the report period. Data were recorded continuously in real time at the NEIS main office in Golden, Colorado. At the present time, 100 channels of SPZ data are being recorded at Golden on develocorder film. This includes data telemetered to Golden via satellite from both the Alaska Tsunami Warning Center, Palmer, Alaska, and the Pacific Tsunami Warning Center, Ewa Beach, Hawaii. A representative number of SPZ channels are also recorded on Helicorders to give NEIS real time monitoring capability of the more active seismic areas of the United States. In addition, 15 channels of LPZ data are recorded in real time on multiple pen Helicorders.

Data from the U.S. Seismic Network are interpreted by record analysts and the seismic readings are entered into the NEIS data base. The data are also used by NEIS standby personnel to monitor seismic activity in the United States and worldwide on a real time basis. Additionally, the data are used to support the Alaska Tsunami Warning Center and the Pacific Tsunami Warning Service. At the present time, all earthquakes large enough to be recorded on several stations are worked up using the "Quick Quake" program to obtain a provisional solution as rapidly as possible. Finally, the data are used in such NEIS publications as the "Preliminary Determination of Epicenters" and the "Earthquake Data Report."

Development is continuing on an Event Detect and Earthquake Location System to process data generated by the U.S. Seismic Network. We expect the new system to be ready for routine operational use by early 1986. At that time, the use of develocorders for data storage will be discontinued. Ray Buland and David Ketchum have been doing most of the developmental programming for the new system. A Micro Vax II has been ordered and will be used as the primary computer of the Event Detect and Earthquake Location System. It will replace the VAX 750 which has been used for system development.

Earth Structure and its Effects upon Seismic Wave Propagation

9920-01736

George L. Choy
Branch of Global Seismology and Geomagnetism
U.S. Geological Survey
Denver Federal Center
Box 25046, Mail Stop 967
Denver, Colorado 80225
(303) 236-1506

Investigations

1. Use of body wave pulse shapes in infer attenuation in the Earth. We have developed a method of generating synthetic waveforms that can incorporate the frequency-dependent effects of source finiteness as well as propagation. We applied this method to modeling P- and SH-type body waves in order to obtain frequency-dependent constraints on Q_α and Q_β of the Earth. Resolution of frequency-dependent effects requires analysis of frequencies over a continuous frequency band from several Hz to tens of seconds. We have obtained broadband records either directly or through multichannel deconvolution of digital data from the GDSN, RSTN, and GRF array.

2. Source parameters from broadband data. We are developing methods to extract source parameters from digitally recorded data by applying propagation corrections to waveforms. These corrections are most important for the midband frequencies (0.1-1.0 Hz), in which is located the corner frequency of most well-recorded teleseismic events (m_b>5.5).

Results

1. The source parameters of a deep earthquake were derived by modeling the P waveforms using a model of Q_α that was allowed to be frequency dependent. Using the derived rupture process enabled us to derive the t_β^* operators for SH-type body waves. A distinct variation as a function of distance and frequency between the t_β^* operators of S and ScS provided strong constraints on Q_β. The mid-mantle between depths of 400 and 1,600 km contributes primarily to the attenuation of low frequencies (0.01 to 0.1 Hz). Below the mantle depth of 2,000 km, the P and SH waveforms suggest little or no attenuation exists in the band of 0.01 to 5 Hz for the paths investigated.

2. We are incorporating into an algorithm for computing radiated energy a feature for correcting spectral information for the effects of frequency-dependent attenuation. Application of the method to two recent earthquakes

(the Coalinga earthquake of May 2, 1983, and the Borah Peak earthquake of October 28, 1983) indicates that spectral information above the corner frequency must be included in the energy estimate. It is also in this frequency band that attenuation corrections are most important.

Reports

Boatwright, J., and Choy, G. L., 1985, Teleseismic estimates of the energy radiated by shallow earthquakes: Journal of Geophysical Research, in press.

Choy, G. L., and Cormier, V. F., 1985, Direct measurement of the mantle attenuation operator from broadband P and S waveforms: Journal of Geophysical Research, submitted.

Systems Engineering

9920-01262

Harold Clark
Branch of Global Seismology and Geomagnetism
U.S. Geological Survey
Albuquerque Seismological Laboratory
Building 10002, Kirtland AFB-East
Albuquerque, New Mexico 87115-5000
(505) 844-4637

Investigations

1. Design, develop, and test microprocessor-based seismic instrumentation.

2. Design, develop, procure, and test special electronic systems required by seismic facilities.

3. Design, develop, and test microprocessor/computer software programs for seismic instrumentation and seismic recording systems.

Results

1. The China Digital Seismic Network (CDSN) power systems have arrived in the People's Republic of China. The first CDSN power system was installed at the Beijing Seismic Station. The second CDSN power system was installed at the Shanghai Seismic Station. During the Beijing installation, the People's Republic of China service company that will install the remaining CDSN power systems was trained on power system installation. Robert Young from the Albuquerque Seismological Laboratory directed the two CDSN power system installations and conducted the power system training. The installation and training time took five days for the Beijing system and three days for the Shanghai system. The remaining CDSN power systems are being installed at the CDSN station sites by the People's Republic of China service company.

2. The 3M HCD-75 tape drive software to provide for read-after-write has been completed. All of the event detector software has been completed. Both software programs were developed under contract with Western Programmers of Albuquerque, New Mexico. The "Demonstration" CDSN Digital Recording System is in final software checkout and system performance evaluation. The present goals are to install the "Demonstration" CDSN Digital Recording System in Beijing during late November 1985. During this same time period, the remaining CDSN Digital Recording Systems will be shipped to the People's Republic of China. The complete nine-station network installation will begin during March 1986. Final installation should be complete in one to two months from the start of installation. During the March 1986 time period, the final depot repair training will be completed.

Reanalysis of Instrumentally-Recorded U.S. Earthquakes

9920-01901

J. W. Dewey
Branch of Global Seismology and Geomagnetism
U.S. Geological Survey
Denver Federal Center
Box 25046, Mail Stop 967
Denver, Colorado 80225
(303) 236-1506

Investigations

1. Relocate instrumentally recorded U.S. earthquakes using the method of joint hypocenter determination (JHD) or the master event method, using subsidiary phases (Pg, S, Lg) in addition to first arriving P-waves, using regional travel-time tables, and expressing the uncertainty of the computed hypocenter in terms of confidence ellipsoids on the hypocentral coordinates.

2. Evaluate the implications of the revised hypocenters on regional tectonics and seismic risk.

Results

1. Dave Gordon and Russ Needham have determined focal mechanisms for three 1984 shocks in eastern Wyoming that had magnitudes of 5.0 and greater, and they have relocated by joint hypocenter determination the hypocenters of about forty regionally recorded shocks that occurred in Wyoming east of longitude 110 degrees west. The three focal mechanisms correspond to strike-slip faulting with the axes of maximum compression being oriented approximately east-west. Some hypocenters are reliably located at focal depths of more than 20 km.

2. Jim Dewey has reviewed hypotheses on the cause of the 1886 Charleston, South Carolina, earthquake and on the likelihood of future large earthquakes occurring at other locations of the Southeastern Seaboard. The hypotheses are classified into three categories: (A) hypotheses on the specific geologic structures that might cause large earthquakes in the Southeastern Seaboard; (B) hypotheses on the seismotectonic zones in which large earthquakes might occur; and (C) hypotheses on temporal variations of seismicity in the Southeastern Seaboard. When data are interpreted in the ways that currently seem to be the most straightforward, the hypotheses that are supported by one kind of evidence are usually opposed by another kind of evidence. Reaching a consensus on the cause of the Charleston earthquake, and on the likelihood of such an earthquake occurring at other locations of the Southeastern Seaboard, will therefore probably require the reconciliation of what currently appear to be contradictory pieces of evidence. In addition, most of the individual hypotheses do not predict that large Southeastern Seaboard earthquakes will occur only in a small region near Charleston. The ability to define small source regions in the Southeastern Seaboard may require simultaneous consensus on the specific geologic

structures capable of causing large earthquakes, on the broader seismotectonic zones within which conditions are favorable for eventual activation of the specific structures, and on the temporal variations of seismicity in small source regions.

Reports

Dewey, James W., 1985, Instrumental seismicity of central Idaho, in Stein, R. S., and Bucknam, R. C., eds., Proceedings of Workshop XXVIII on the Borah Peak, Idaho, Earthquake: U.S. Geological Survey Open-File Report 85-290, 264-284.

Dewey, James, W., 1985, A review of recent research on the seismotectonics of the Southeastern Seaboard and an evaluation of hypotheses on the source of the 1886 Charleston, South Carolina, earthquake: published by the Nuclear Regulatory Commission as NUREG Technical Report NUREG/CR-4339, 52 p.

Gordon, D. W., and Needham, R. E., 1985, Recent seismicity in eastern and central Wyoming [abs.]: accepted for presentation at the annual meeting of the Eastern Section of the Seismological Society of America, Knoxville, October 16-18, 1985.

Global Seismology

9920-03684

E. R. Engdahl
and
J. W. Dewey

Branch of Global Seismology and Geomagnetism
U.S. Geological Survey
Denver Federal Center
Box 25046, Mail Stop 967
Denver, Colorado 80225
(303) 236-1506

Investigations

1. Depth Phases. Develop procedure for the global analyses of earthquake depth phases and source characteristics using broadband seismograms of body waves.

2. Earthquake Location in Island Arcs. Develop practical methods to accurately locate earthquakes in island arcs.

3. Subduction Zone Structure. Develop techniques to invert seismic travel times simultaneously for earthquake locations and subduction zone structure.

4. Global Synthesis. Synthesize recent observational results on the seismicity of the earth and analyze this seismicity in light of current models of global tectonic processes.

Results

1. Depth Phases. Displacement and velocity records of body waves with frequency content from 0.01 to 5 Hz can now be routinely obtained for most earthquakes with $m_b>5.5$. These records are obtained either directly or by multichannel deconvolution of waveforms from digitally recording seismograph stations such as those of the GDSN (Global Digital Seismograph Network), RSTN (Regional Seismic Test Network), and GRF-array (Graefenberg Seismological Observatory). Once the distortion of the seismograph filter is removed, the seismograms often show the source-time functions of the direct and surface-reflected phases, even for shallow events where depth phases may overlap the direct wave. A systematic procedure is under development for analyzing broadband seismograms that identifies depth phases and subevents (for complex earthquakes). A natural benefit of the procedure is that better resolution of the focal mechanism can be obtained from the polarities of depth phases. In particular, the phase sP, which is also more clearly defined, provides additional valuable constraints on focal mechanism determinations. Because most large earthquakes are complex events, depth phases recorded on conventional seismograms are often incorrectly read and reported. It is now possible for reporting agencies, such as the NEIC (National Earthquake Information Center), to utilize digital waveforms

routinely to obtain better estimates of focal depth, to identify subevents in complex earthquakes, and to improve focal mechanism determinations.

2. Earthquake Location in Island Arcs. Joint Hypocenter Determination is used to compute locations of teleseismically well-recorded earthquakes (magnitude 4.5 or larger) that occurred from 1964 through March 1985, in and near the aftershock zone of the Chilean earthquake of March 3, 1985. The 1985 mainshock nucleated in a region that had experienced a swarm of teleseismically recorded earthquakes that began 10 days before the main shock. The most precisely located foreshock epicenters fall in an equidimensional area of about 20 km that is free of, but surrounded by, the most precisely located 1985 aftershock epicenters. This distribution of seismicity is consistent with foreshock activity occurring as preliminary failure of an asperity that ruptured completely in the course of the mainshock. The seismically active thrust interface appears to consist of a shallow thrust zone and the deep thrust zone separated by 20 km in the plane of the interface. The low seismicity region between the two thrust zones is centered at a depth of approximately 35 km. A similar pairing of deep and shallow thrust zones has been documented for northern Honshu, Japan, by Kawakatsu and Seno (JGR, v. 88, p. 4215). Both the deep and shallow Chilean thrust zones may be activated in large earthquakes. 1985 aftershocks of magnitude less than 6.0 were heavily concentrated in the shallow thrust zone, and the 1985 mainshock nucleated near the downdip extremity of the shallow thrust zone. The deep thrust zone produced at least one, and probably two, aftershocks of magnitude 6.0 or greater the first day after the 1985 mainshock, but few shocks of magnitude between 4.5 and 5.9. The large thrust-fault earthquake of July 1971, nucleated in the deep thrust zone at the north end of the 1985 aftershock zone; virtually all of its aftershocks were in the shallow thrust zone.

3. Subduction Zone Structure. A combined location and velocity inversion technique is applied to travel-time data from 151 well-recorded central Aleutian earthquakes. The data include P and S arrivals at stations of a local network and P, pP, and sP arrivals at teleseismic stations. After correction for upper crustal structure at the reflection points, the depth phases pP and sP provide important constraints on subduction zone structure not ordinarily resolved by other data types. The structure is parameterized with cubic splines that provide a specification of velocity at each point of a gridded arc cross section. To avoid ray tracing, it is assumed that the velocity part of the problem is linear. First attempts to invert the central Aleutian data set have provided important new preliminary information about earthquake locations and structure in this subduction zone, and about the inversion approach in general. Delineation of a well-defined gap in seismicity between earthquake activity near the trench and a 70-km wide continuous band of shallow-depth thrust earthquakes along the plate interface confirms results of previous studies. Deeper earthquakes appear to occur within a narrow downdip zone near the top of the descending slab, in comparison to previous locations which are more central to the slab. A slab thickness of 60-80 km and a downdip length of about 400 km, well below the deepest seismic activity, seem to be indicated. The slab is characterized by seismic velocities as much as 11 percent higher than the surrounding mantle in its upper portions and 4-6 percent higher at depth. A sharp

velocity gradient and lower velocities occur directly beneath the volcanic arc near the top of the slab. In these preliminary inversions, the slab anomaly appears to spread out and fall off very slowly with depth. Non-linearity, requiring three-dimensional ray tracing, and/or poor resolution at depth may be the cause, and future work will focus on these problems.

4. Global Synthesis. The sythesis study is currently in outline form. Approximately half the synthesis is outlined in full sentences or paragraphs that are intended to be included directly into the final publication. The other half is outlined with a skeleton listing of topics that will be covered. Related work continues on a review of the seismicity of the United States and on a project to produce a map of the seismicity of North America for the Geological Society of America's Decade of North American Geology series.

Reports

Dewey, J. W., Choy, G. L., and Nishenko, S. P., 1985, Asperities and paired thrust zones in the focal region of the Chilean earthquake of March 3, 1985 [abs.]: EOS, Trans. American Geophysical Union, v. 66, in press.

Engdahl, E. R., and Choy, G., 1985, Global analyses of earthquake depth phases and source characteristics using broadband seismograms of body waves [abs.]: 23rd IASPEI General Assembly, Tokyo, Japan.

Engdahl, E. R., and Kind, R., 1985, Interpretation of broadband seismograms from central Aleutian earthquakes: Ann. Geophysicae, in press.

Engdahl, E. R., and Gubbins, D., 1985, Simultaneous travel-time inversion for earthquake location and subduction zone structure [abs.]: EOS, Trans. American Geophysical Union, v. 66, in press.

Engdahl, E. R., and Billington, S., 1986, Focal depth determination of central Aleutian earthquakes: Bulletin of the Seismological Society of America, in press.

Seismic Observatories

9920-01193

Leonard Kerry
Branch of Global Seismology and Geomagnetism
U.S. Geological Survey
Denver Federal Center
Box 25046, Mail Stop 967
Denver, Colorado 80225
(303) 236-1506

Investigations

Recorded and provisionally interpreted seismological and geomagnetic data at observatories operated at Newport, Washington; Cayey, Puerto Rico; and Agana, Guam. Continued operation of the Puerto Rican Seismic Telemetry Network from the main base located in Cayey, Puerto Rico. Operated advanced equipment for gathering research data for universities and other agencies at Cayey, Puerto Rico and Agna, Guam. At Agana, Guam, a 24-hour standby duty was maintained to provide input to the Tsunami Warning Service operated at Honolulu Observatory by NOAA and to support the Early Earthquake Reporting function of the National Earthquake Information Service.

Results

Provided data on an immediate basis to the National Earthquake Information Service and the Tsunami Warning Service. Continued to send seismograms obtained from the WWSSN Systems to NEIS for use in the ongoing USGS programs. Analog seismic records and digital seismic tape records were obtained from the SRO system and forwarded to ASL for use in ongoing USGS and other users' programs. Data from advanced research equipment was forwarded to universities or other agencies working in conjunction with USGS. Seismic data from the Puerto Rican net was provided on a continuing basis to the University of Puerto Rico for their use in studying and research of the seismicity of the Puerto Rican area.

Responded to requests from the public, interested scientists, universities, state, and Federal agencies regarding geophysical data and phenomena.

Global Seismograph Network Evaluation and Development

9920-02384

Jon Peterson
Branch of Global Seismology and Geomagnetism
U.S. Geological Survey
Albuquerque Seismological Laboratory
Building 10002, Kirtland AFB-East
Albuquerque, New Mexico 87115-5000
(505) 844-4637

Investigations

Work continued on the development and testing of hardware and software for the China Digital Seismograph Network.

Investigations and activities related to GDSN network improvements included the testing of a new version of the KS 36000 borehole seismometer, the purchase of component parts for a prototype data logger, and assisting IRIS in the development of plans for upgrading the digital networks.

Results

Progress in the assembly and testing of the CDSN instrumentation is proceeding rapidly following the resolution of several major hardware and software problems related to the writing and playback of 3M HCD-75 cartridge data. Sensor systems and power systems are currently being installed at the station sites in China. Data system and data management system hardware assembly at Albuquerque is complete; software is being tested and debugged at the present time.

A modified version of the KS 36000 borehole seismometer that provides a broadband (.25 - 200 s) velocity output was tested by comparison with a standard KS 36000. Noise levels are comparable. The principal advantages of the modified seismometer are the greater bandwidth and much improved dynamic range, especially in the short-period band.

Component parts were purchased for the assembly of a new datalogger that will be used as a test bed for the development and testing of a new station processor and peripherals. The hardware and software selected is based on a 68000 microcomputer, VME bus, and a UNIX-like operating system designed for real-time operations.

The project chief attended meetings of the IRIS GSN standing committee during which design goals were formalized and initial plans were made to upgrade some stations in the GDSN.

Global Digital Network Operations

9920-02398

Robert D. Reynolds
Branch of Global Seismology and Geomagnetism
U.S. Geological Survey
Albuquerque Seismological Laboratory
Building 10002, Kirtland AFB-East
Albuquerque, New Mexico 87115-5000
(505) 844-4637

Investigations

The Global Network Operations continued to provide technical and operational support to the SRO/ASRO/DWWSSN observatories which include operating supplies, replacement parts, repair service, redesign of equipment, training and on-site maintenance, recalibration and installation. Maintenance is performed at locations as required, when the problem cannot be resolved by the station personnel. The Bendix O&M contract personnel level has been increased to one team leader, six field engineers, and one digital technican.

The SRO enhancement program continued at the SRO stations. These enhancements consist of adding the two short-period horizontal components to the digital data, removal of the six-second notch from the long-period filters, and installation of clip detectors on each seismometer module.

The following station maintenance activity was accomplished:

ANMO - Albuquerque - SRO
One maintenance visits

ANTO - Ankara, Turkey - SRO
One maintenance visit

BCAO - Bangui, C.A.R. - SRO
Three maintenance visits

BOCO - Bogota, Columbia - SRO
One maintenance visit

CHTO - Chiang Mai, Thailand - SRO
Two maintenance visits

GRFO - Grafenberg, W. Germany - SRO
Two maintenance visits

SHIO - Shillong, India - SRO
Two maintenance visit

SNZO - Wellington, New Zealand - SRO
One maintenance visit

TATO - Taipei, Taiwan - SRO
One maintenance visit

KONO - Kongsberg, Norway - ASRO
Three maintenance visits

MAJO - Matsushiro, Japan - ASRO
Two maintenance visits

DWWSSN

AFI - Afiamalu, W. Samoa
One maintenance visit

COL - College, Alaska
One maintenance visit

WWSSN

KOD - Kodaikanal, India
One maintenance visit

NDI - New Delhi, India
One maintenance visit

POO - Poona, India
One maintenance visit

RAB - Rabaul, New Guinea
One maintenance visit

ASL Repair Facility

As much routine repair as possible was done during this period to support the field maintenance activity.

Special Activity

An SRO system was refurbished and tested in preparation for shipment to Isreal.

Tests were started on a Teledyne-Geotech model 44000 borehole seismometer during this period.

A seismic noise site survey was started in South Africa.

Results

The digital network continues with a combined total of 29 SRO/ASRO/DWWSSN stations. The main effort of this project is to perform as much on-site maintenance and training as possible in order to provide the highest quality digital data for the worldwide digital data base.

Seismicity and Tectonics

9920-01206

William Spence
Branch of Global Seismology and Geomagnetism
U.S. Geological Survey
Denver Federal Center
Box 25046, Mail Stop 967
Denver, Colorado 80225
(303) 236-1506

Investigations

Studies carried out under this project focus on detailed investigations of large earthquakes, aftershock series, tectonic problems, and earth structure. Studies in progress have the following objectives:

1. Provide tectonic setting for and analysis of the 1977 Sumba earthquake series (W. Spence).

2. Generalize the role of the slab pull force in determining the primary tectonic features at subduction zones and in contributing to stresses that cause subduction zone earthquakes (W. Spence).

3. Provide tectonic setting for and analysis of the 1974 Peru gap-filling earthquake (W. Spence and C. J. Langer).

4. Examine the source properties (focal mechanism and depth) of aftershocks following large thrust earthquakes in subduction regions by using digital surface-wave data (C. Mendoza).

5. Determine the maximum depth and degree of velocity anomaly beneath the Rio Grande Rift and Jemez Lineament by use of a 3-D, seismic ray-tracing methodology (W. Spence and R. S. Gross).

Results

1. The great ($M_o = 4 \times 10^{28}$ dyne-cm), normal-faulting Sumba earthquake of 1977 occurred at the Java Trench, just west of the zone where the Australian continental lithosphere is in collision with the Java arc. Aftershocks of the Sumba earthquake have been relocated by the joint hypocenter method and occur in two zones: an east-west trending zone, mostly east of the main shock, and a triggered northwest- southeast-trending zone located about 180 km northwest of the main shock. Both sets of earthquakes are confined to the 40-km-thick brittle portion of the oceanic lithosphere. Focal mechanism data for the aftershocks in the main shock zone and in the triggered zone, interpreted in the context of the detailed tectonic setting, support the conclusion that both earthquake groups occurred directly as a result of slab pull forces. Slab pull forces have led to limited and very slow subduction of Australian lithosphere whereas more rapid subduction of oceanic lithosphere occurs at the western Java arc. This differential in subduction rate

causes a right lateral torque in lithosphere subducted at the zone of the Sumba earthquake and explains the right-lateral faulting of earthquakes in the triggered zone.

2. In spite of the recognized strong influence of the slab pull force in moving tectonic plates, the influence of this force in causing tectonic phenomena occurring on the order of days to several years generally has been neglected. In addition to reviewing evidence that the slab pull force is responsible for most steady-state features associated with mature subduction zones, this study considers a time-dependent model that describes the slab pull force and the weaker ridge push force through a cycle of great subduction zone earthquakes. The steady-state and short-term behaviors of a predominant slab pull force are demonstrated to be consistent with most seismic and tectonic data that exist for mature subduction zones. Slab pull forces can explain double seismic zones associated with old, rapidly subducting plates, the transition from extensional faulting in the upper mantle to compressional faulting below depths of about 300 km, the sudden increase in curvature of subducted plate at depths of 20-40 km, and possibly can provide some of the excitation function for the Chandler wobble.

3. The great 1974 Peru thrust earthquake (M_S 7.8, M_W 8.1) occurred in a documented seismic gap, between two earthquakes each with magnitude of about 8, occurring in 1940 and 1942. Additional major earthquakes occurred in this region in 1966 and in 1970; all but the 1970 shock represent thrust faulting. The stress release of the October 3, 1974 main shock and aftershocks occurred in a spatially and temporally irregular pattern. The multiple-rupture main shock produced a tsunami with wave heights of 0.6 ft at Hawaii and which was observed, for example, at Truk Island and at Crescent City. The aftershock series essentially was ended with the occurrence of a M_S 7.1 aftershock on November 9, 1974. The several years of preseismicity data to this earthquake include an unusually clear example of the "Mogi donut" pattern.

4. Love and Rayleigh-wave signals recorded by the Global Digital Seismograph Network provide source-parameter information for moderate-magnitude aftershocks that followed the large (M_S 7.7) Colombia earthquake of 12 December 1979. Love/Rayleigh amplitude ratios observed in a 30-80 second passband are compared against theoretical values calculated for a suite of source models fixed at independently determined depths. In addition, a reference earthquake with known focal mechanism and depth is used to calibrate the procedure and to minimize the path and size effects. Source mechanisms compatible with the amplitude data and observed P-wave first motions are obtained. These mechanisms serve to identify subsidiary faulting not associated with the main shock rupture.

Similar surface-wave techniques are being implemented in the analysis of the aftershock sequence that followed the large (M_S 7.8) Chile earthquake of 3 March 1985. The earthquake ruptured about 1/3 of the rupture length inferred for the great (M_S 8.2-8.4) Valparaiso earthquake of 1906. By comparing the spectra observed in a 20-50 second period range, focal depths can be estimated and source mechanisms can be computed for the aftershocks.

The aftershock properties should provide additional constraints on the faulting geometry produced by the main shock of 3 March 1985.

5. To a depth of about 160 km, the upper mantle P-wave velocity beneath the Rio Grande rift and Jemez lineament is 4-6 percent lower than beneath the High Plains Province. A 3-D, P-wave velocity inversion shows scant evidence for pronounced low P-wave velocity beneath the 240-km-long section of the Rio Grande rift covered by our array. However, the inversion shows a primary trend of 1-2 percent lower P-wave velocity underlying the northeast-trending Jemez lineament, down to a depth of about 160 km. The Jemez lineament is defined by extensive Pliocene-Pleistocene volcanics and late Quaternary faults. The upper mantle low-velocity segment beneath the Jemez lineament is at most 100 km wide and at least 150-200 km long, extending in our inversion from Mt. Taylor through the Jemez volcanic center and through the Rio Grande rift. A Backus-Gilbert resolution calculation indicates that these results are well-resolved.

Reports

Mendoza, C., 1985, Aftershock source properties from digital surface-wave data: The 1979 Colombia sequence: AGU 1985 Fall Meeting, Dec. 9-13, abstract accepted.

Spence, W., 1985, The 1977 Sumba earthquake series: direct evidence for slab pull: Journal of Geophysical Research (in press).

Spence, W., 1985, Slab pull: Journal of Geophysical Research, submitted.

Spence, W., 1985, Can slab pull cause shallow, decouping earthquakes?: AGU 1985 Fall Meeting, Dec 9-13, abstract accepted.

United States Earthquakes

9920-01222

Carl W. Stover
Branch of Global Seismology and Geomagnetism
U.S. Geological Survey
Denver Federal Center
Box 25046, Mail Stop 967
Denver, Colorado 80225
(303) 236-1500

Investigations

1. One hundred and two earthquakes in 15 states and Puerto Rico were canvassed by a mail questionnaire for felt and damage data. Fifty-one of these occurred in California, and 22 in Alaska. The most significant event was one southeast of Coalinga, California, near Avenal, on August 4, 1985, which was located at 36.211°N., 120.177°W., at a depth of about 5 km, magnitude 5.4 mb, 5.9 MS, and 5.4 ML, and a maximum intensity of VI.

2. Earthquakes in the United States for the period April 1, 1985, through September 30, 1985, have been located and the hypocenters, magnitudes, and maximum intensitites have been published in the Preliminary Determination of Epicenters.

Results

A maximum Modified Mercalli intensity of VI was assigned to Avenal, Kettleman City, and Lemoore, California, for the August 4, 1985 earthquake. Six people were injured in Avenal where the shaking was reported strongest and the damage was the most widespread, although minor.

United States Earthquakes, 1982 (Bulletin 1655) has received director's approval and is being printed. The Seismicity Map of the State of Wyoming (MF-1798) has been printed. It lists the earthquake history of Wyoming through 1981.

Reports

Reagor, B. G., Stover, C. W., and Algermissen, S. T., 1985, Seismicity map of the state of Wyoming: U.S. Geological Survey Miscellaneous Field Studies Map MF-1798.

National Earthquake Catalog

9920-02648

J. N. Taggart
Branch of Global Seismology and Geomagnetism
U.S. Geological Survey
Denver Federal Center
Box 25046, Mail Stop 967
Denver, Colorado 80225
(303) 236-1506

Investigations

1. Continued investigation of path-dependent attenuation of L_g waves.

2. Continued development of a national earthquake event list database.

Results

1. Measurements of maximum and sustained amplitudes and associated periods of L_g were obtained from vertical and horizontal short-period seismograms from Canadian and WWSSN stations for a suite of earthquakes ($M \geq 5$) and their larger aftershocks that occurred in eight focal regions from New Brunswick to California. Because the earthquakes have large trace amplitudes, the nearest stations with readable L_g peaks are generally at epicentral distances greater than 10 degrees. As a result, periods of less than 1.0 sec are not obvious at the arrival times of the maximum amplitudes or in the L_g codas. The codas, which presumably consist mainly of reflected surface waves at epicentral distances greater than 10 degrees, are much less affected by frequency-dependent attenuation than the higher frequency L_g codas recorded within three degrees from the earthquakes.

2. The Alaska earthquake database file has been brought on-line in the HDS hypocenter search routine. This version of the Alaska database does not include local network listings. The HDS routine is available to anyone with access to the USGS VAX-A computer at 1711 Illinois in Golden, Colorado.

Taggart compared the overlap and advantages of each of several USGS hypocenter databases in a paper presented at the IASPEI 23rd General Assembly in Tokyo.

Responsibility for the Historical Seismogram Filming Project has been transferred from NOAA to the U.S. Geological Survey, National Earthquake Information Center and will be incorporated into this project effective October 1, 1985.

China Digital Seismic Network

9920-02217

John Hoffmann
Branch of Global Seismology and Geomagnetism
U.S. Geological Survey
Albuquerque Seismological Laboratory
Building 10002, Kirtland AFB-East
Albuquerque, New Mexico 87115-5000
(505) 844-4637

Investigations

1. Data Management Center for the China Digital Seismograph Network. All of the computer hardware has been purchased, installed, and thoroughly checked. Several software programs still have to be debugged using the field tapes which will be available during the first week of October. The system is scheduled for shipment to China during the first week of November.

2. Data Processing for the Global Digital Seismograph Network. All of the data received from the Global Network and other contributing stations are reviewed and checked for quality.

3. Network-Day Tape Program. Data from the Global Network stations are assembled into network-day tapes which are distributed to regional data centers and other government agencies.

Results

1. Data Management Center for the China Digital Seismograph Network. A problem developed with the cartridge tape drive recording systems during April and May 1985, which required replacing the units with new ones from a different manufacturer. This delayed the checkout procedure for several months. The new units have proved very satisfactory, and we are presently in the final stages of checking the software programs with field cartridge tapes. This checkout will be completed by the end of October; the computer will then be shipped via air freight to the People's Republic of China, where it will be installed in early December.

2. Data Processing for the Global Digital Seismograph Network. During the past six months, 514 digital tapes (171 SRO/ASRO, 230 DWWSSN, and 113 RSTN) from the Global Network and other contributing stations were edited, checked for quality, corrected when feasible, and archived at the Albuquerque Seismological Laboratory (ASL). The Global Network is presently comprised of 11 SRO stations, 4 ASRO stations, and 14 DWWSSN stations. In addition, there are six contributing stations which include Glen Almond, Canada, plus the five RSTN stations which are supported by Sandia National Laboratories.

3. Network-Day Tape Program. The network-day tape program is a continuing program which assembles all of the data recorded by the Global Digital Seismograph Network plus the contributing stations for a specific calendar day onto one magnetic tape. This tape includes all the necessary station parameters, calibration data, frequency response, and time correction information for each station in the network. A seventh edition of the National Earthquake Information Center Newsletter containing information on the various digitally recording seismograph stations was distributed in July 1985. These newsletters are published twice a year, and copies are forwarded to all digital data users.

Reports

Hoffman, J. P., Buland, R., and Zirbes, M., July 1985, National Earthquake Information Center Newsletter, v. 4, no. 1, 8 p.: Available from Albuquerque Seismological Laboratory, Albuquerque, New Mexico.

Seismic Review and Data Services

9920-01204

R. P. McCarthy
Branch of Global Seismology and Geomagnetism
U.S. Geological Survey
Denver Federal Center
Box 25046, Mail Stop 969
Denver, Colorado 80225
(303) 236-1513

Investigations and Results

Technical review and quality control were carried out on 472 station-months of seismograms from the World-Wide Standardized Seismograph Network (WWSSN). Seventy-four station-months of Seismic Research Observatory (SRO & ASRO) seismograms were provided to the National Earthquake Information Service (NEIS) for their PDE programs on a current basis. An average of thirty-six WWSSN current station-months were supplied monthly for the NEIS fault plane solution program.

Annual WWSSN Station Performance Reports were sent to 46 station directors. These cover instrumental and operational details which include timing precision, calibrations, damping, noise, recording quality, label data, backlogs, and any other problems that may require attention. Timing precision is still being maintained with many stations, averaging daily errors well below 50 milliseconds. Overall operational standards remain at high levels. There are 96 operational stations and 8 questionables.

Monthly reports covering the analog and digital records received from the WWSSN, DWWSSN, SRO, and ASRO networks were distributed to officials and researchers in the USGS, DOD, and NOAA. Advice and consultations still are provided to users, government officials, researchers, and the private sector.

As of July 1, 1985, the USGS assumed the WWSSN microfilming transferred from NOAA. Filming, while still on microfiche (105 x 148 mm), has been reformatted from the columnar to the row sequence with only the SPZ and the three long periods being filmed. Announcement of this service has been sent to all users. A considerable reduction in costs for both blanket and special orders has been put into affect. Pricing structure for the Canadian and other networks are being worked out.

The microfilming quality control and operational overview will be carried out through this project along with monitoring and responding to user requests. Upon completion of the filming, the seismograms will be returned through our Data Services. Additional functions may also be undertaken as the complete transfer of these NOAA services progresses.

Data Processing, Golden

9950-02088

Robert B. Park
Branch of Engineering Geology and Tectonics
U.S. Geological Survey
Box 25046, MS 966, Denver Federal Center
Denver, CO 80225
(303) 236-1638

Investigations

The purpose of this project is to provide the day-to-day management and systems maintenance and development for the Golden Data Processing Center. The center supports Golden-based Office of Earthquakes, Volcanoes, and Engineering investigators with a variety of computer services. The systems include a PDP 11/70, several PDP 11/03′s and PDP 11/23′s, a VAX/750, a VAX/780 and two PDP 11/34′s. Total memory is 12 mbytes and disk space will be approximately 3.8 G bytes. Peripherals include five plotters, ten mag-type units, an analog tape unit, five line printers, 5 CRT terminals with graphics and a Summagraphic digitizing table. On order is a laser disk to be used for archiving data. Dial-up is available on all the major systems and hardwire lines are available for user terminals on the upper floors of the building. Users may access any of the systems through a Gandalf terminal switch. Operating systems used are RSX11 (11/34′s), Unix (11/70), RT11 (LSI′s) and VMS (VAX′s).

The three major systems are shared by the Branch of Global Seismicity and Geomagnetism and the Branch of Engineering Geology and Tectonics.

Results

Computation performed is primarily related to the Global Seismology and Hazards programs; however, work is also done for the Induced Seismicity and Prediction programs as well as for DARPA, ACDA, MMS, U.S. Bureau of Reclamation and AFTAC, among others.

In Global Seismology and Geomagnetism, the data center is central to nearly every project. The monitoring and reporting of seismic events by the National Earthquake Information Service is 100 percent supported by the center. Their products are, of course, a primary data source for international seismic research and have implications for hazard assessment and prediction research as well as nuclear test ban treaties. Digital time series analysis of Global Digital Seismograph Network data is also 100 percent supported by the data center. These data are used to augment NEIS activities as well as for research into routine estimation of earthquake source parameters. The data center is also intimately related to the automatic detection of events recorded by telemetered U.S. stations and the cataloging of U.S. seismicity, both under development.

In Engineering Geology and Tectonics, the data center supports research in assessing seismic risk and the construction of national risk maps. It also provides capability for digitizing analog chart recordings and maps as well as analog tape. Also, most, if not all, of the research computing related to the hazards program are supported by the data center.

The data center also supports equipment for online digital monitoring of Nevada seismicity. Also, it provides capability for processing seismic data recorded on field analog and digital cassette tape in various formats. Under development is a portable microprocessor-based system to be used by the field investigations group to do preliminary analysis and editing of temporary local networks and the GOES Satellite Event Detect System. Recent acquisitions include the VAX/750, laser plotter, three additional tape drives, two HP plotters, DECNET/ETHERNET, and 400 MB of disk storage. A VAX-based accounting system has been developed for an up-to-date reporting capability on branch projects.

National Earthquake Information Center

9920-01194

Waverly J. Person
Branch of Global Seismology and Geomagnetism
U.S. Geological Survey
Denver Federal Center
Box 25046, Mail Stop 967
Denver, Colorado 80225
(303) 236-1500

Investigations and Results

The Quick Epicenter Determinations (QED) became available in November to individuals and groups having access to a 300-baud terminal with dial-up capabilities to a toll-free WATS number or a commercial telephone number in Golden, Colorado. The time period of data available in the QED is approximately three weeks--from about two days behind real time to the current PDE in production. Since the QED program became available, we have had approximately 265 users. The QED program is available on a 24-hour basis, 7 days a week.

The weekly publication, Preliminary Determination of Epicenters (PDE) continues to be published, averaging about 90 earthquakes per issue. The PDE Monthly Listing and Earthquake Data Report (EDR) continue to be prepared on the VAX/1180 with very little down time encountered.

We continue to receive telegraphic data from the USSR in a very timely manner on magnitude 6.5 or greater earthquakes and some smaller damaging earthquakes in the USSR and bordering countries. Data from the People's Republic of China via the American Embassy are also being received in a very timely manner and in time for the PDE publication. We continue to receive 4 stations on a weekly basis from the State Seismological Bureau of the People's Republic of China and about 22 by mail, which are in time for the Monthly. We have rapid data exchange (alarm quakes) with Centre Seismologique European-Mediterranean (CSEM), Strasbourg, France and Instituto Nazionale de Geofisica, Rome, Italy and data by telephone from Mundaring Geophysical Observatory, Mundaring, Western Australia.

The Monthly Listing of Earthquakes is up to date. As of September 30, 1985, the Monthly Listing and Earthquake Data Report (EDR) were completed through May 1985. A total of 6,252 events were published for the 6-month period. Solutions continue to be determined when possible and published in the Monthly Listing and EDR for any earthquake having an m_b magnitude ≥ 5.8. Centroid moment tensor solutions from Harvard University continue to be published in the Monthly Listing and EDR. Moment tensor solutions are being computed by the U.S. Geological Survey and are also published in the above publications. Waveform plots are being published for selected events having m_b magnitudes ≥ 5.8.

The Earthquake Early Alerting Service (EEAS) continues to provide information on recent earthquakes on a 24-hour basis to the OEVE, scientists, news media, other government agencies, foreign countries, and the general public. Sixty-eight releases were made from April 1, 1985 through September 30, 1985. The largest during this period was the magnitude 8.1 Mexico earthquake. This earthquake created more media interest than any earthquake we have had since the EEAS begain in 1966.

Reports

Quick Epicenter Determination (QED) (daily).
Preliminary Determination of Epicenters (PDE)
    26 weekly publications from April 4, 1985 to September 26, 1985--Numbers 11-85 through 36-85. Compilers: Willis Jacobs, Leonard Kerry, John Minsch, W. Person, B. Presgrave, W. Schmieder.
Monthly Listing of Earthquakes and Earthquake Data Reports (EDR)
    6 publications from December 1984 through May 1985.
    Compilers: Willis Jacobs, L. Kerry, John Minsch, R. Needham, W. Person, B. Presgrave, W. Schmieder.
Seismological Notes, BSSA, Waverly J. Person
    Vol. 75, No. 3--July-August 1984; Vol. 75, No. 4--September-October 1984; Vol. 75, No. 5--November-December 1984.
Presgrave, Bruce, 1985, Phase data catalogue for IASPEI events: U.S. Geological Survey Open-File Report 85-398.

Digital Data Acquisition for Strong Motion Seismology

9910-02089

Roger D. Borcherdt
James F. Gibbs

Branch of Engineering Seismology and Geology
345 Middlefield Road, MS 977
Menlo Park, CA 94025
(415) 323-8111, ext. 2910

Investigations

Cooperative seismological and engineering studies to extend bandwidth and detection thresholds for a variety of active and passive experiments including: near-source strong motion, source mechanisms for aftershock sequences, velocity and Q^{-1} structure for crust and upper mantle, short-period earth strain, high-frequency wave propagation from downhole arrays, local-site amplification studies for improved estimates of source parameters and earthquake engineering, near-surface shear-wave velocity structure, and response of engineered structures. This project, during the report period, has been responsible for the maintenance, operation, and deployment of wide dynamic range, broad band digital recorders (General Earthquake Observation System, GEOS) to acquire data sets for the cooperative studies indicated. This project has been conducted in conjunction with project 9910-03009 (see Maxwell and Borcherdt).

Results:

1. Maintenance laboratory; several improvements in laboratory maintenance procedures have been implemented in cooperation with G. Maxwell, J. Sena, and C. Dietel, including: hardware modifications and tests to restrict least count noise levels to least significant bit at 60 dB gain, recording system and sensor calibration test procedures for each of the 50 amplifier and filter settings on each channel, field check-out and instrument operation procedures.

2. High-frequency downhole array studies - In cooperation with Ralph Archuleta of the University of California, Santa Barbara (UCSB), three GEOS were deployed with assistance from J. Gibbs, C. Dietel, G. Maxwell, and J. Sena, for 10 days at McGee Creek near Bishop, California to record 18 components of a downhole array installation. The array is comprised of three-component velocity and acceleration sensors installed at the surface and at depths of 35 m and 166 m. With an alluvium-rock interface at about 33 m, near surface amplification and attenuation effects are readily apparent on comparing uphole and downhole observations (Archuleta, 1985).

3. Soil response on a downhole array near Coalinga - M. Andrews and T. Hanks, in cooperation with L. Wennerberg, R. Warrick, and T. Fumal, initiated the installation of two downhole arrays (80 and 100 m) near Coalinga following the Kettleman Hills earthquake of August 4, 1985. These six-component arrays, recorded on GEOS for approximately six weeks, yielded high quality digital recordings of about 40 events for study of the influence of local site conditions on source parameter estimates (see M. Andrews, this report).

4. High frequency downhole array studies with emphasis on earthquake prediction - In cooperation with P. Malin at UCSB, six-component downhole arrays have been recorded on three GEOS since installation in July 1985. This project is focussing on extending bandwidth and signal resolution thresholds for seismic detection near Parkfield, California. Each sensor component has been calibrated and adjusted to 0.5 v/cm/s sensitivity with the installation of appropriate S and T resistors by R.E. Warrick and R. Frye. Since installation, several hundred event files have been processed by G. Glassmoyer. Preliminary analyses show that downhole backnoise levels are about 15 dB less in power spectral density than those at the surface in the band 5-20 Hz. A larger improvement in signal to noise ratios is apparent for frequencies in the 20-100 Hz interval. Significant near-surface amplification (up to 20 dB in amplitude) is apparent for signals (5-15 Hz) recorded at each of the sites. Utilization of low-noise 16 bit digital recorders together with the 2 Hz downhole arrays has permitted extensions of both the bandwidth and detection thresholds for seismic signals. Uphole and downhole time-histories for an event of M ~ 124 and an event of M ~ -0.1 are shown for the sites SJC and VNC (Figures 1 and 2), respectively. Amplitude spectra computed for a signal-to-noise ratio of greater than 2 (in power) suggests that signal detection bandwidth for the M ~ 1.24 event was about 70-75 Hz uphole and 80-85 Hz downhole (Figure 3).

5. Short Period Earth-Strain - In cooperation with M. Johnston and D. Myren of USGS, Earth strain noise has been measured using GEOS over the period band 10^5 - 10 s at 9 sites for which Sacks'-Evertson dilatometers have been installed in a cooperative project with A. Linde and S. Sacks of Carnegie Institution of Washington. At four of the sites GEOS have been deployed in a long-term deployment configuration to simultaneously record the output of the downhole dilatometer and three component colocated seismometers. Operating the systems in event trigger mode, several hundred event files have been processed. Earth strain noise levels are measured over the period band 10^7-10^2 Hz at sites near Hollister, California, and are shown in Figure 4. Utilization of 16 bit recorders has permitted extensions of both the resolution and bandwidth of signals detected by the Sacks'-Evertson dilatometers. The time history and spectrum for a M ~ 3.7 event recorded at a distance less than 10 km near Palmdale, California, is shown in Figures 5 and 6. The spectrum suggests that seismic energy up to 25 Hz was detected on the dilatometer.

6. Local geologic, topographic, and structural response studies near Santiago, Chile - As the result of a project initiated by M. Celebi and S.T. Algermissen with support from Agency for International Development, eight GEOS systems were deployed on two different occasions by G. Sembera, C. Dietel, and M. Celebi for studies of soil and structural response, and the influence of steep topography in the vicinity of Viña del Mar, Chile, using aftershocks of the M ~ 8.0 earthquake of March 3, 1985. With 100% reliability reported for instrumentation, a large data base was acquired documenting variations in ground response that correlate with topography, type of local geologic deposit, and in some cases, observed damage patterns (Algermissen, *et al.*, 1985; Celebi, 1985).

7. Seismic refraction studies near Parker, Arizona - In cooperation with G. Fuis and W. Mooney of USGS, a program was undertaken to collect three-

component wide angle mantle reflection data to augment the Cal-Crust cooperative studies near Parker, Arizona. Eleven six channel GEOS systems were utilized to augment and calibrate the recordings obtained on colocated cassette recorders and the multi-channel array system developed by P. Malin of UCSB. On scale records were obtained for 31 explosions at each of the recording locations with the assistance of G. Sembera, L. Wennerberg, and C. Dietel. Data playback has been completed. Interpretation of the data set in conjunction with L. Wennerberg, G. Fuis, and W. Mooney will commence during next report period.

8. High frequency near-source attenuation - In support of a project funded by DARPA to study variations in high-frequency attenuation for active and passive seismic sources, six GEOS were utilized to record nearby quarry blasts at 400 sps. This experiment being conducted by W. Lee and J. Pfluke yielded broad band on-scale recordings at each of the sites with detectable near-source seismic energy exceeding 100 Hz as analyzed by C. Dietel.

Reports

Algermissen, S.T., Kausel, E., Mueller, C., Borcherdt, R.D., Thenhaus, P.C., 1985, Preliminary analysis of ground response and observed intensity *in* Algermissen, S.T. (ed.), *Preliminary report of investigations of the central Chile Earthquake of March 3, 1985.*

Archuleta, R.J., 1985, Strong ground motion recorded downhole: *EOS*, v. 66, no. 46, p. 976.

Askew, B., Mueller, C., Converse, A., Watson, J., Algermissen, S.T., Borcherdt, R., and Tarr, A., 1985, Site spectra and spectral ratios *in* Algermissen, S.T. (ed.), Site spectra and spectral ratios: *Preliminary report of investigations of the Central Chile Earthquake of March 3, 1985.*

Boatwright, J., 1985, Characteristics of the aftershock sequence of the Borah Peak, Idaho, Earthquake determined from digital recordings of the events: *Seismological Society of America Bulletin*, **75**.

Borcherdt, R.D., 1985, Implications of recent advances in instrumentation for strong-motion studies: *17th Joint Panel on Wind and Seismic Effects (UJNR)*, Tsukuba, Japan.

Celebi, M., 1985, Preliminary evaluation of performance of structures *in* Algermissen, S.T. (ed.), *Preliminary report of investigation of the central Chile Earthquake of March 3, 1985: U.S. Geological Survey Open-File Report 85-* .

Cranswick, E., Wetmiller, R., Boatwright, J., 1985, High-frequency observations and source parameters of microearthquakes recorded at hard rock sites: *Seismological Society of America Bulletin*, December 1985.

Johnston, M.J.S., Borcherdt, R.D., and Linde, A.T., 1985, Measurements of short period strain (0.1-$10^{5}{}_{s}$): near source strainfield for an earthquake (M_L 3.2) near San Juan Bautista, California: *EOS*, v. 66, no. 46, p. 1093.

Malin, Peter E., 1985, Initial results from downhole/surface seismometer pairs near Parkfield, California: *EOS*, v. 66, no. 46, p. 982.

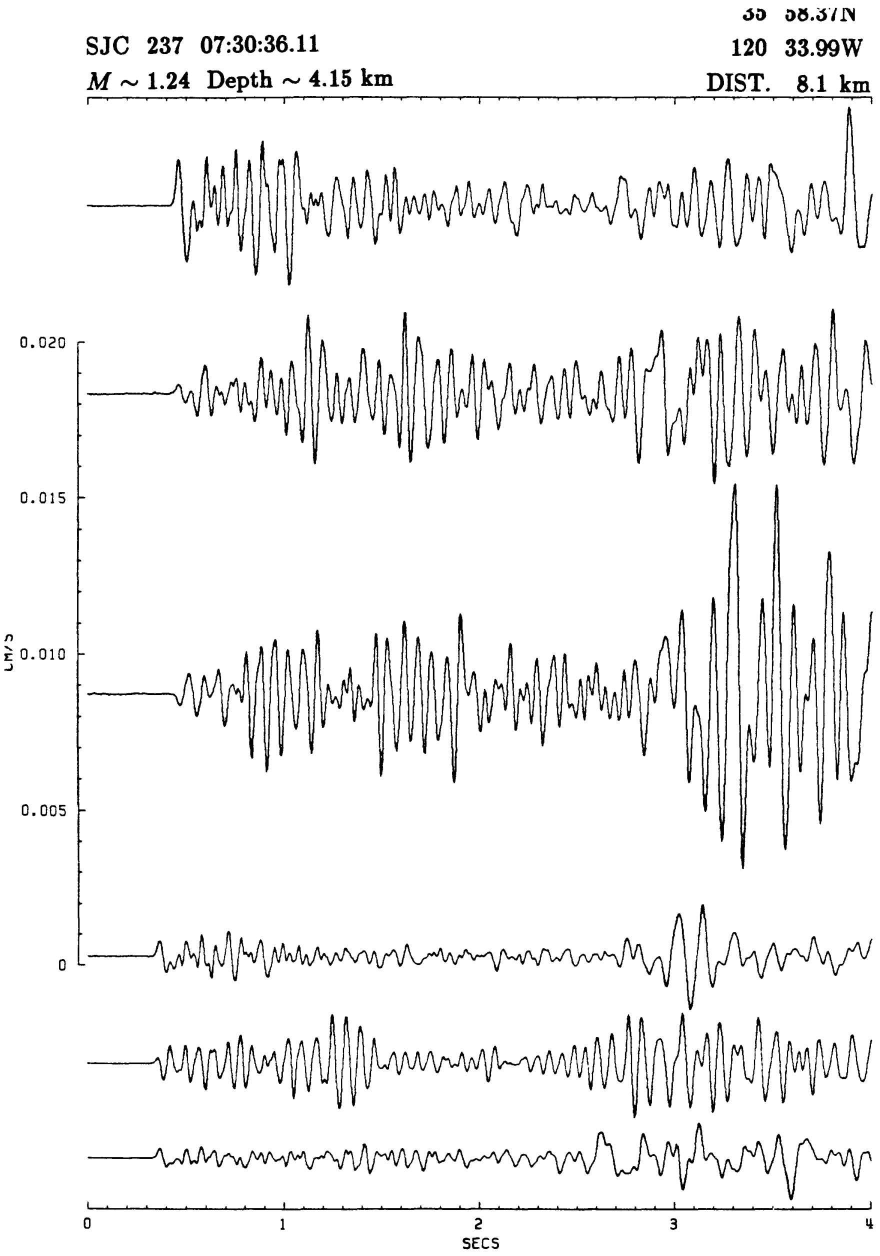
35 58.37N
SJC 237 07:30:36.11
120 33.99W
M ~ 1.24 Depth ~ 4.15 km
DIST. 8.1 km
0.020
0.015
CM/S 0.010
0.005
0
0
1
2
3
4
SECS

Figure 1

SJC 276 07:31:43

$M \sim -0.1$

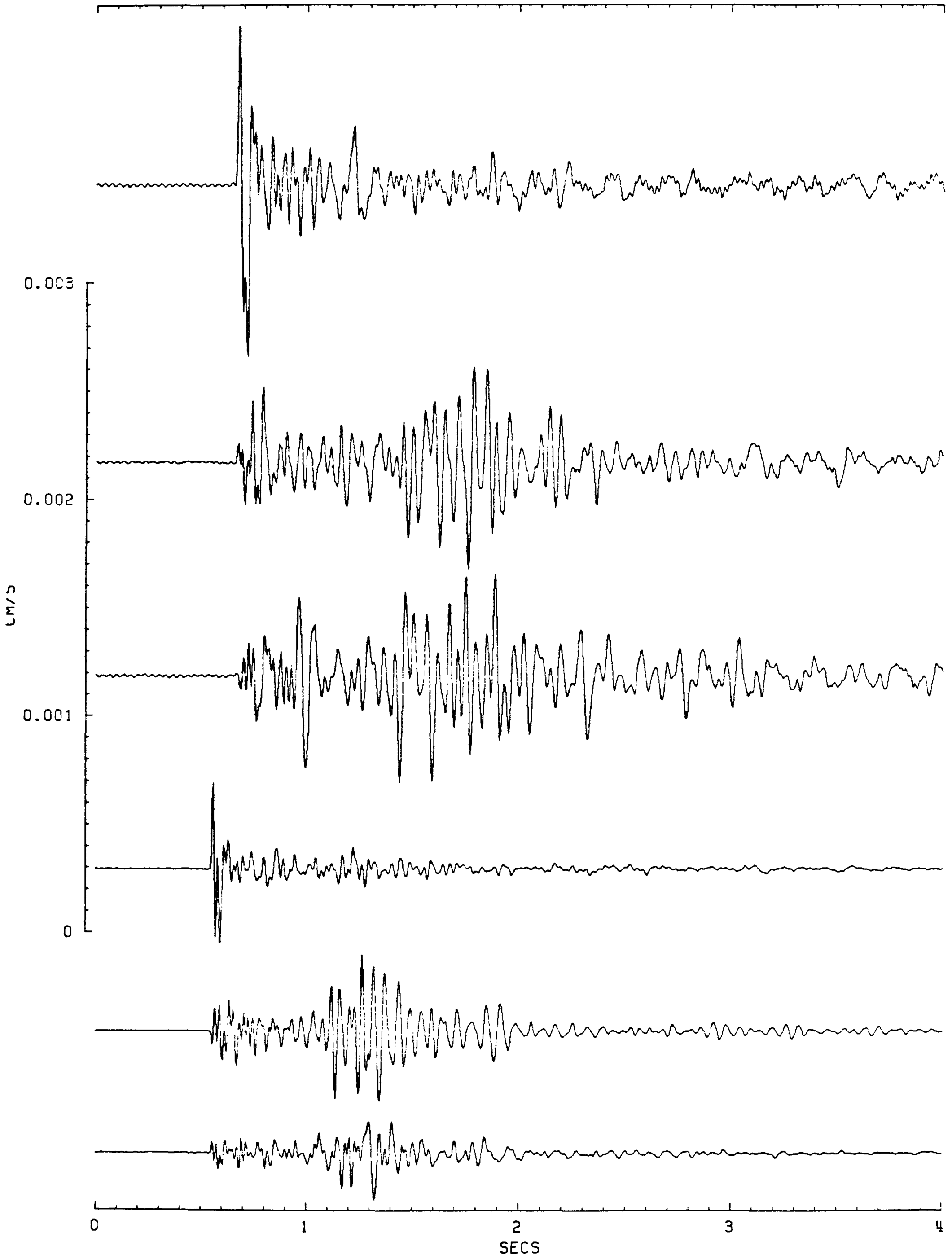

Figure 2

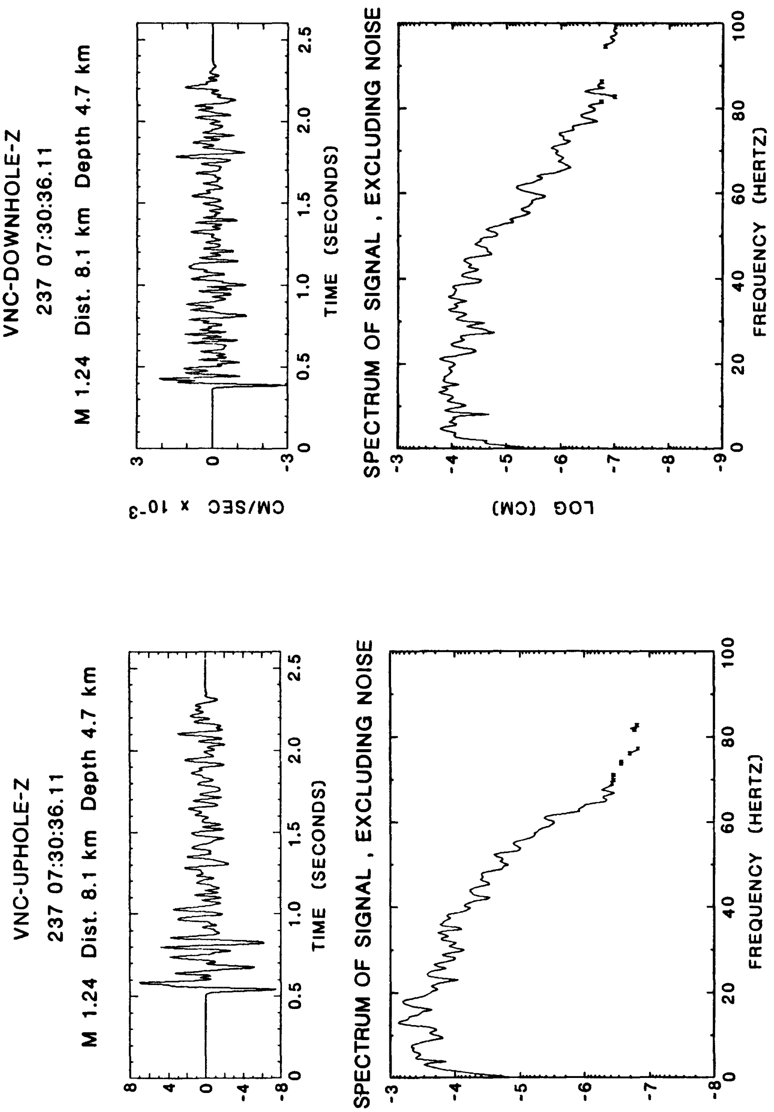

VNC-UPHOLE-Z
237 07:30:36.11
M 1.24 Dist. 8.1 km Depth 4.7 km

VNC-DOWNHOLE-Z
237 07:30:36.11
M 1.24 Dist. 8.1 km Depth 4.7 km

Figure 3

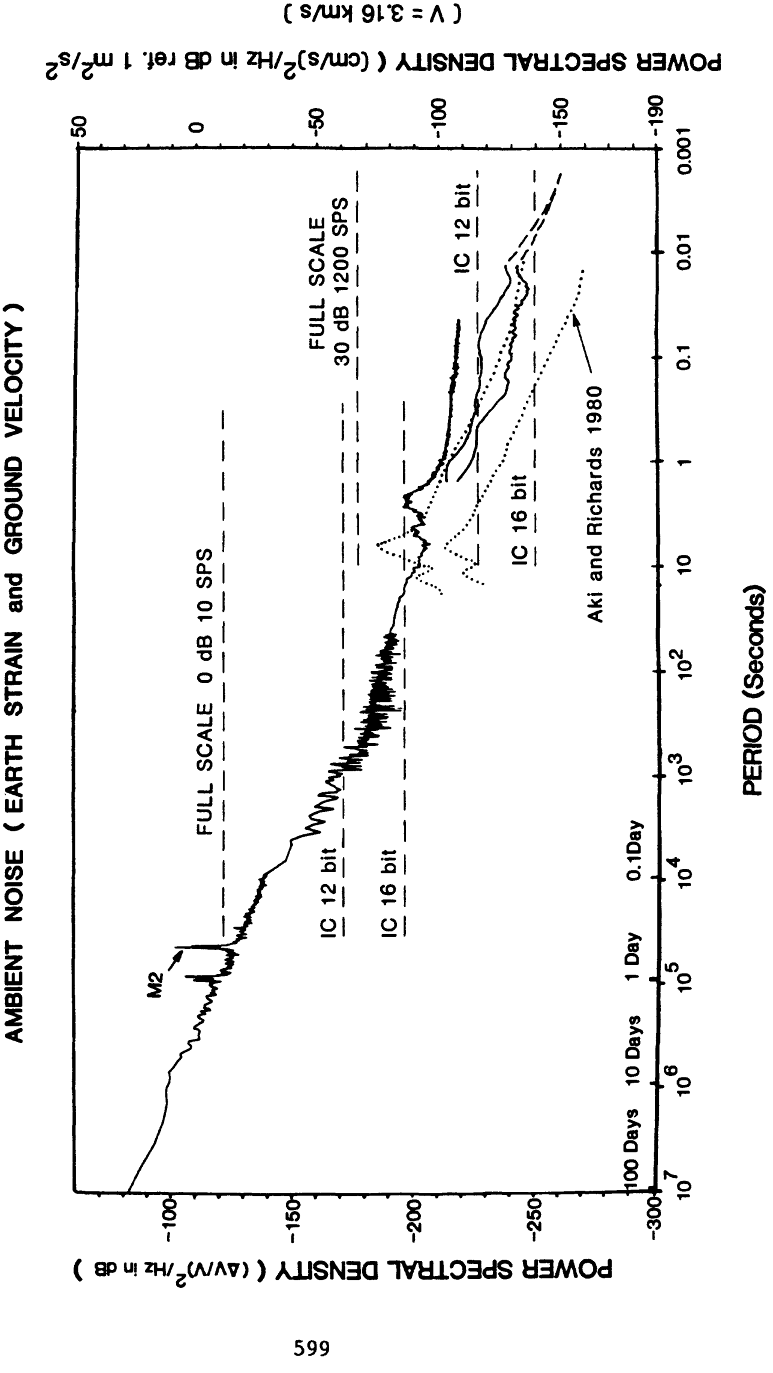
AMBIENT NOISE (EARTH STRAIN and GROUND VELOCITY)
POWER SPECTRAL DENSITY ((cm/s)^2/Hz in dB ref. 1 m^2/s^2
(V = 3.16 km/s)
50
0
-50
-100
-150
-190
POWER SPECTRAL DENSITY ((ΔV/V)^2/Hz in dB)
-100
-150
-200
-250
-300
PERIOD (Seconds)
10^7
10^6
10^5
10^4
10^3
10^2
10
1
0.1
0.01
0.001
100 Days
10 Days
1 Day
0.1Day
M2
FULL SCALE 0 dB 10 SPS
IC 12 bit
IC 16 bit
FULL SCALE 30 dB 1200 SPS
IC 12 bit
IC 16 bit
Aki and Richards 1980

Figure 4

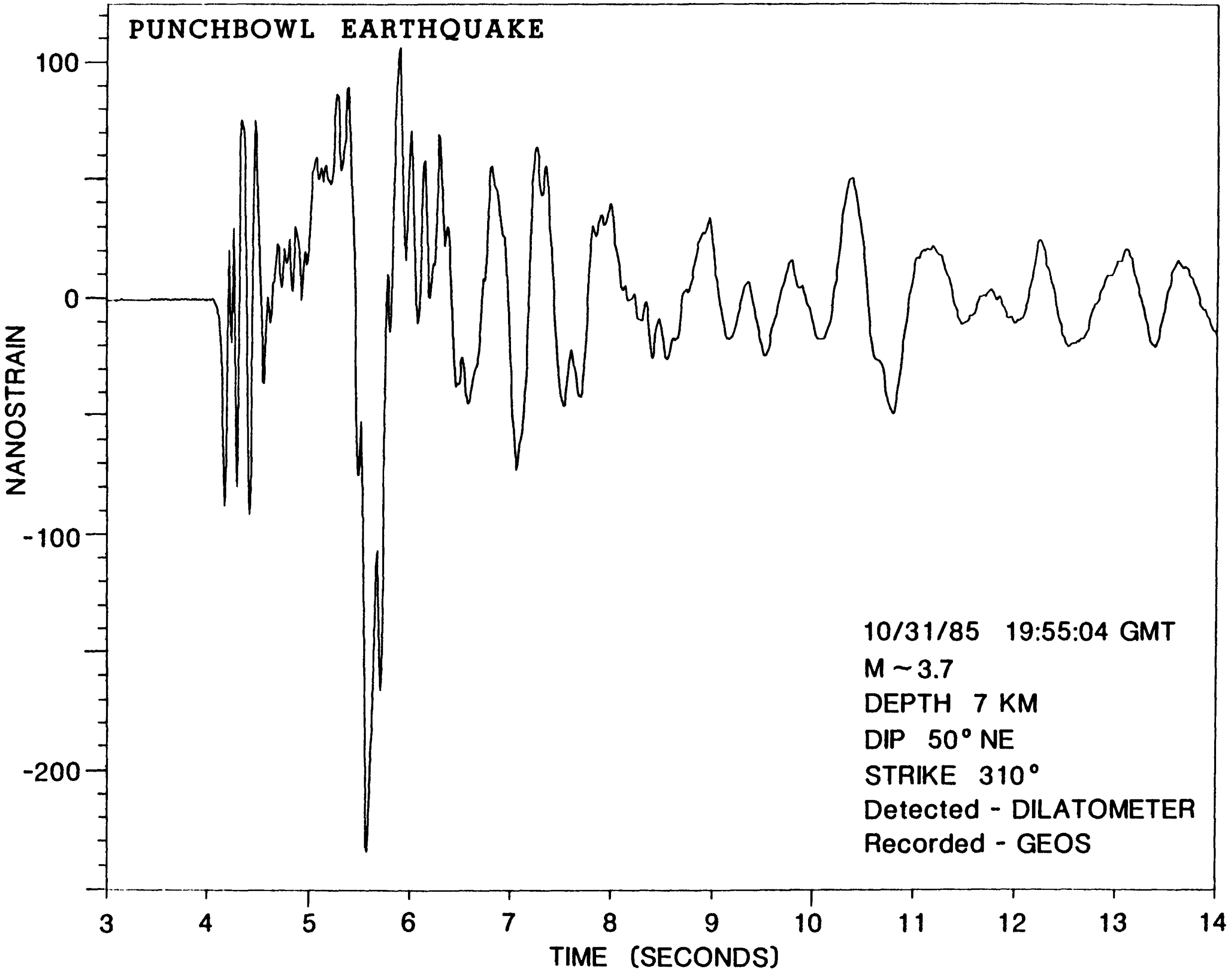
PUNCHBOWL EARTHQUAKE
NANOSTRAIN
100
0
-100
-200
3
4
5
6
7
8
9
10
11
12
13
14
TIME (SECONDS)
10/31/85 19:55:04 GMT
M ~ 3.7
DEPTH 7 KM
DIP 50° NE
STRIKE 310°
Detected - DILATOMETER
Recorded - GEOS

Figure 5

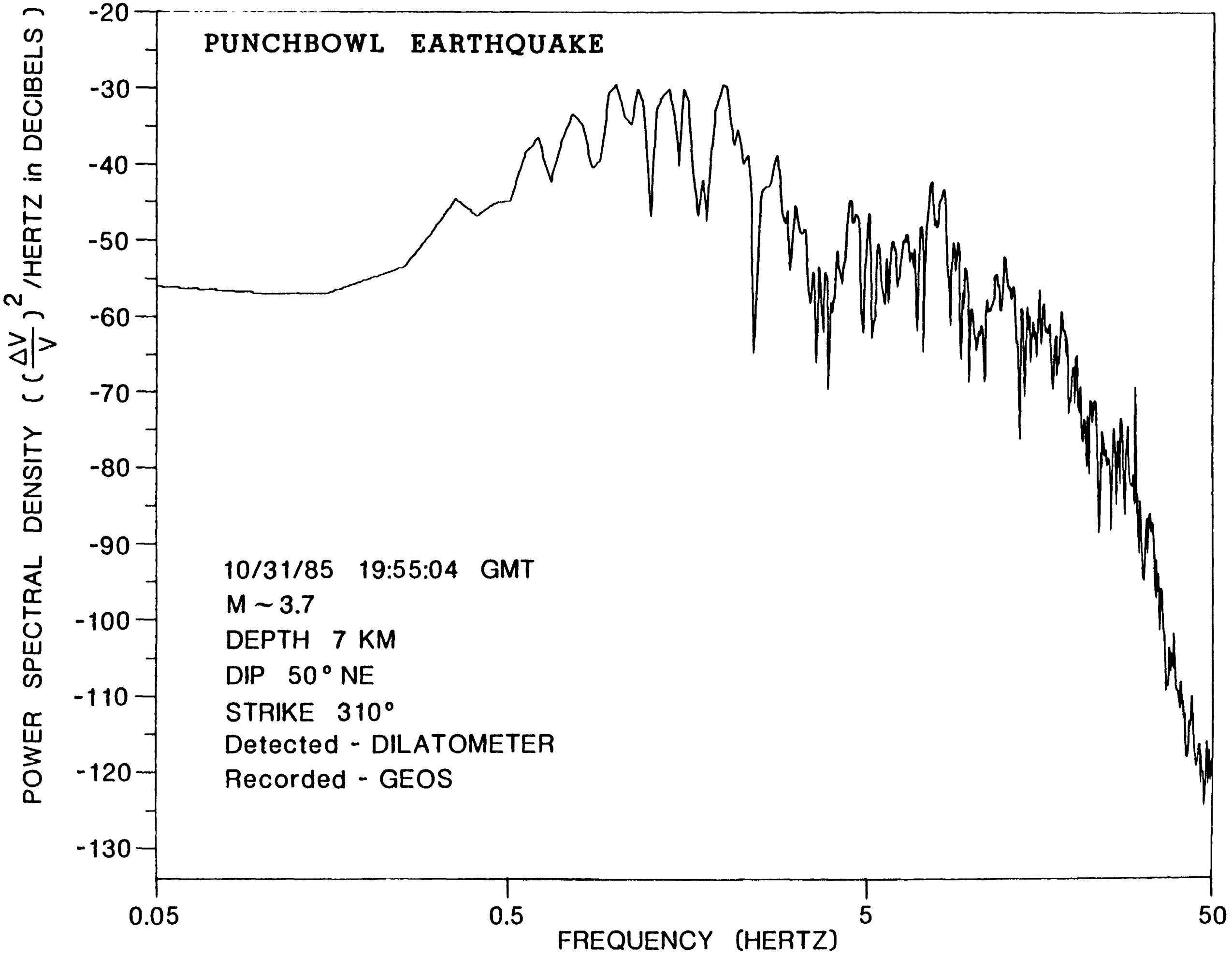
PUNCHBOWL EARTHQUAKE
10/31/85 19:55:04 GMT
M ~ 3.7
DEPTH 7 KM
DIP 50° NE
STRIKE 310°
Detected - DILATOMETER
Recorded - GEOS
POWER SPECTRAL DENSITY ($(\frac{\Delta V}{V})^2$/HERTZ in DECIBELS)
-20
-30
-40
-50
-60
-70
-80
-90
-100
-110
-120
-130
FREQUENCY (HERTZ)
0.05
0.5
5
50

Figure 6

Strong Motion Data Management

9910-02757

A.G. Brady
Branch of Engineering Seismology and Geology
U.S. Geological Survey
345 Middlefield Road, MS 977
Menlo Park, California 94025
(415) 323-8111, ext. 2881

Investigations

Optimum long-period selection for noise removal continues to be a prime concern in preparation of corrected data. A summary of the strong motion data from both USGS and CDMG networks from the Morgan Hill earthquake of April 24, 1985 has been prepared in cooperation with CDMG.

Improvements continue in our standard data processing package named AGRAM. An updated user manual to replace Version 2.0 (July 1984) will result from this effort.

The threat to discontinue running, early in 1986, of the Multics computer in Denver, where our SMIRS (Strong Motion Information Retrieval System) data base resides, is forcing us to move the whole data base to Menlo Park. We are taking the opportunity to revise the entire data base structure and will use INGRES on the DEC VAX.

Results

Routine digitizing (indicated by D), computer processing (indicated by P), and report preparation (indicated by R), of strong motion earthquake recording continues: 4 records (D, P, R), southern Alaska, January 1, 1975; 6 records (P) Imperial Valley aftershock, October 15, 1979, 2317:40 UTC; 6 records (P) Imperial Valley aftershock, October 15, 1979, 2318:20 UTC.

Reports

Brady, A.G., and Shakal, A.F., 1985, The Morgan Hill Earthquake of April 24, 1984--Strong Motion Records, *Earthquake Spectra*, Vol. 1, No. 3, May 1985.

Silverstein, B.L., 1985, Processed strong-motion records from the Coalinga aftershock of July 9, 1983, 0740 UTC: *U.S. Geological Survey Open-File Report 85-584*.

National Strong Motion Data Center

9910-02085

Howard Bundock
Branch of Engineering Seismology and Geology
U. S. Geological Survey
345 Middlefield Road, MS 977
Menlo Park, California 94025
(415) 323-8111, ext. 2982

INVESTIGATIONS

The objectives of the National Strong Motion Data Center are to:

Maintain a strong capability for the processing, analysis and dissemination of all strong motion data collected on the National Strong Motion Network and data collected on portable arrays;

Support research projects in the Branch of Engineering Seismology and Geology by providing programming and computer support including digitizing, graphics, processing and plotting capabilities as an aid to earthquake investigations;

Manage and maintain computer hardware and software so that it is ready to process data rapidly in the event of an earthquake.

The Center's facilities include a VAX 11/750 computer operating under VMS Version 4.2, a PDP 11/70 and two PDP 11/73 computers running RSX-11M+. The Center's computers are part of a local area network with other branch, OEVE, Geologic Division, and ISD computers, and we have access to computers Survey-wide over Geonet. Project personnel join other office branches and ISD in the support of the OEVE VAX 11/780.

Investigations during the last six months of FY85 include research into advanced technologies for high resolution printing for text processing and reports, networks and communication, the use of high speed computer processors, and system management software. Also, the project has an ongoing policy to remain current with available operating systems, network, and other software. Currently available system hardware upgrades to speed processing have been investigated, and user written programs have been studied and expanded to better use existing graphics and digitizing hardware.

RESULTS

As a result of these investigations, the project has:

Purchased, installed, and trained branch personnel in the use of a high resolution laser printer and related software;

Surveyed branch personnel and coordinated with the Information Systems Division for a fast and efficient changeover to the new, Survey-wide voice and data communications network;

Ordered a highly cost efficient terminal serving device which will link a number of terminals with any computer on our existing local area network, as well as any computer on Geonet. Savings over other methods such as direct cabling are substantial;

Obtained information concerning and advised the Information Systems Council in Reston on ways to obtain access to a proposed San Diego Supercomputer Center. A link to this center is needed by scientists needing high speed processing for modelling, and to keep U.S.G.S. scientists current with new processing methods;

Surveyed branch scientists on complaints and concerns about the OEVE VAX 11/780 and advised ISD in Reston of our plan to upgrade it to a higher speed 11/785 processor;

Upgraded our VAX 11/750 to VMS Version 4.2, Fortran 4.3, INGRES Database Management System Version 3.0/23c with patches and fixes to other system and device software;

Installed hardware which doubles the physical memory on our VAX 11/750 for faster processing and higher user capacity;

Wrote software to digitize maps, graphs, etc. so that resulting data is formatted for three existing plotting programs;

Managed and maintained system hardware and software.

REPORTS

none

Structural Performance Investigations
Using Strong Motion Instrumentation

9910-02759

Mehmet Celebi, A. Gerald Brady, Erdal Safak, and Richard Maley
Branch of Engineering Seismology and Geology
U.S. Geological Survey
345 Middlefield Road, MS 977
Menlo Park, California 94025
(415) 323-8111, ext. 2394

Investigations

1. Development of instrumentation schemes for structures in seismically active regions of the United States.

2. Through advisory committees, development of list of recommended structures for implementation.

3. Study of performance of structures through available strong motion records of post earthquakes.

Results

1. Four unique structures in the San Francisco Bay Area have been instrumented and are now operational. Two structures in San Bernardino and one in Charleston, South Carolina are being instrumented.

2. In addition to the San Francisco Bay Area and San Bernardino, California, active committees in Boston, St. Louis, and Anchorage are developing recommendations for their respective regions.

3. Records from a bridge deck in San Jose, California and a gymnasium roof diaphragm are currently being studied.

Reports

Celebi, M., *et al.*, 1985, Report on recommended list of structures for seismic instrumentation in San Bernardino County, California: *U.S. Geological Survey Open-File Report 85-583.*

Celebi, M., Safak, E., Brady, A.G., Maley, R., and Sotoudeh, V., 1985, Integrated instrumentation plan for assessing seismic response of structures - A review of current USGS Programs: *U.S. Geological Survey Circular 947.*

Celebi, M., and Brady, G., 1985, Earthquake performance of a bridge deck and abutment: *Proceedings, Second International Conference on Soil Dynamics and Earthquake Engineering*, Southampton, July 1985.

STRONG-MOTION INSTRUMENTATION NETWORK
DESIGN, DEVELOPMENT, AND OPERATIONS

9910-02763, 02764, 02765

Richard P. Maley
Edwin C. Etheredge

Branch of Engineering Seismology and Geology
345 Middlefield Road, MS 977
Menlo Park, CA 94025
(415) 323-8111, ext. 2881

Investigations

The Strong-Motion laboratory, in concert with several federal, state, and local agencies and advisory engineering committees, designs, develops, and operates an instrumentation program in 41 states and Puerto Rico. Program goals include: (1) recording of potentially damaging ground motion in regional networks and in closely spaced sensor arrays; and (2) monitoring the structural response of buildings, bridges and dams with sensors placed in critical locations. The present coordinated network consists of more than 1,000 recording units installed at approximately 600 ground sites, 52 buildings, 5 bridges, 54 dams, and 2 pumping plants.

Recent structural arrays completed

1) A 19 channel strong-motion system was installed in the 49-story (plus 11 story empty "loft") Transamerica building (figure 1) in San Francisco. Transducers are located at the following levels: third basement, first basement, and first, 5th, 21st, 29th, and 49th floors.

2) A 13 channel strong-motion system was installed in the 11-story Hayward City Hall (figure 2) with sensors located in the basement and at the 1st, 3rd, 6th and 11th floors. Free-field accelerograph stations were established north and south of the building in small fiberglass shelters. The three recorders are interconnected in real time by the use of WWVB receivers.

3) McPhee dam in southwestern Colorado, was instrumented for the Bureau of Reclamation in the following configuration:

Triaxial downhole accelerometers at depths of 8 and 21 m below
center crest and down 3 m at mid-slope.
A surface accelerograph is located at center crest.

Ground Motion Instrumentation

1) An array of 7 permanent strong-motion stations was established near Anza in south-central California (figure 3) in a recognized seismic gap segment of the San Jacinto fault. Instrumentation consists of older-model RFT-350 accelerographs modified to conform to modern accelerograph standards. Each station is equipped with a WWVB receiver to provide a real time base on the records.

2) Five strong-motion instruments were installed at various sites in California in conjunction with structural instrumentation projects and at ground sites important to the total instrumentation network.

3) A third triaxial accelerometer module was added to the downhole system located at McGee Creek near Mammoth Lakes, California. Strong-motion instrumentation consists of 15 sensors, 3 triaxial transducers located at depths of 1, 35, and 165 m, and two at the surface.

Results

More than 25 accelerograms were recovered in California and processed for inclusion into the SMIRS data base.

Bear Valley Region	5	records
Coalinga	10	records
Palm Springs	1	record
Pleasant Valley Pump Plant	5	records
McGee Creek	24	channels of data (2 events)

Reports

None

STRUCTURAL DRAWING

STATION NAME: TRANSAMERICA PYRAMID BUILDING

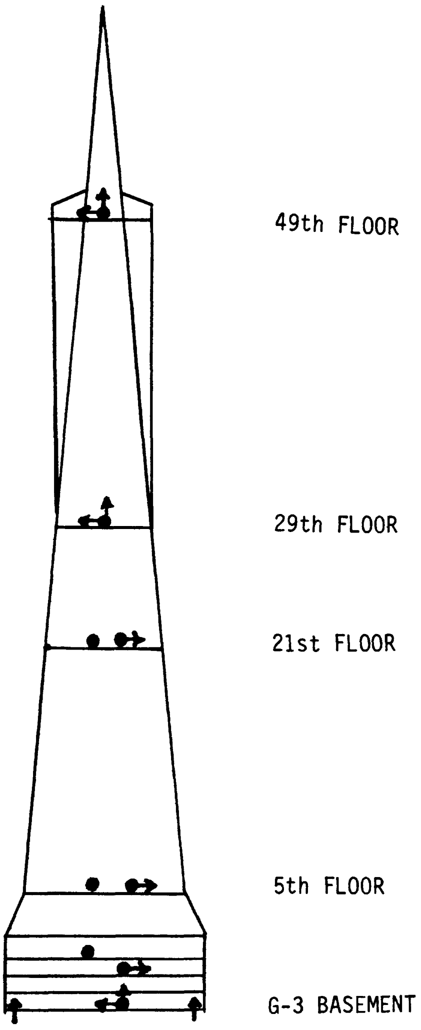

FIGURE 1

STRUCTURAL DRAWING
ELEVATION VIEW

STATION NAME: HAYWARD CITY HALL
22300 FOOTHILL BLVD.

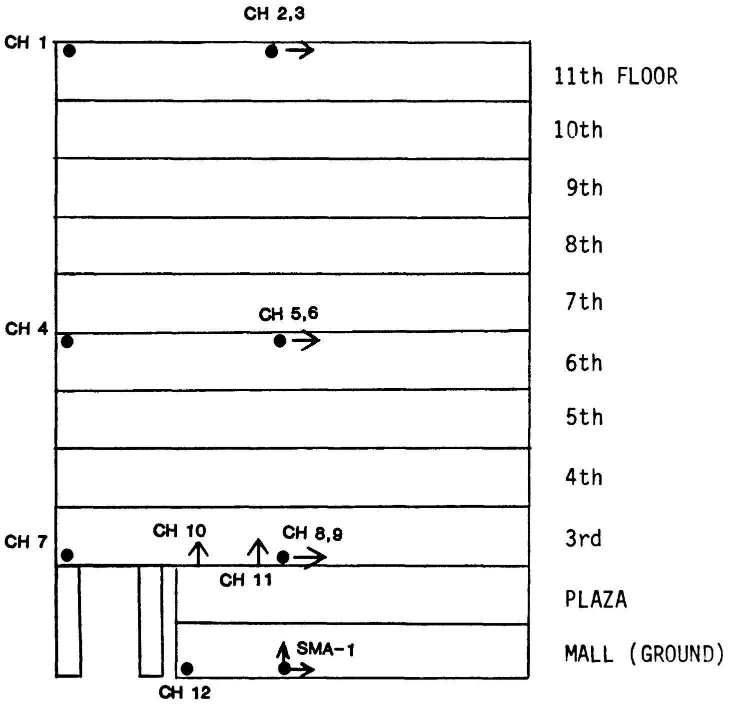

TRANSDUCER LOCATION
VIEW NORTH

FIGURE 2

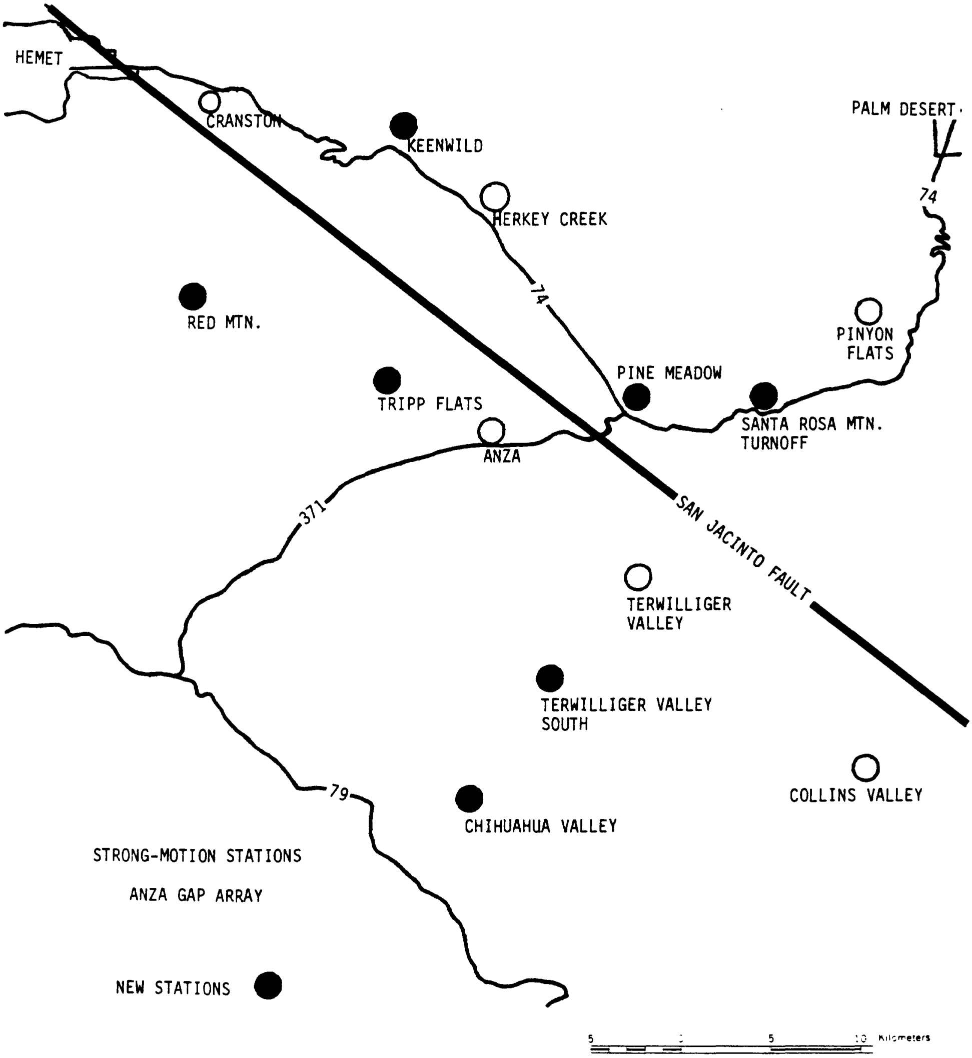
HEMET
CRANSTON
KEENWILD
PALM DESERT
74
HERKEY CREEK
74
RED MTN.
PINYON
FLATS
PINE MEADOW
TRIPP FLATS
SANTA ROSA MTN.
TURNOFF
ANZA
371
SAN JACINTO FAULT
TERWILLIGER
VALLEY
TERWILLIGER VALLEY
SOUTH
COLLINS VALLEY
79
CHIHUAHUA VALLEY
STRONG-MOTION STATIONS
ANZA GAP ARRAY
NEW STATIONS ●
5 0 5 10 Kilometers

FIGURE 3

General Earthquake Observation System (GEOS)
General Analysis and Playback Systems (GAPS)

9910-03009

Gary L. Maxwell and Roger D. Borcherdt
Branch of Engineering Seismology and Geology
U.S. Geological Survey
345 Middlefield Road, MS 977
Menlo Park, California 94025
(415) 323-8111 ext. 2910

Investigations

1. Development and construction of a portable, broad band, high-resolution digital data acquisition capability for seismology and engineering (GEOS).
2. Development of mini- and micro-computer systems (hardware and software) for retrieval, processing, and archival of large volumes of digital data (GAPS).
3. Development of hardware and software components to improve functionality, versatility, and reliability of digital data acquisition and retrieval systems.

Results

Design features and modifications incorporated in the General Earthquake Observation System (GEOS) during this report period with assistance from J. Sena, C. Dietel, G. Jensen, and J. VanSchaack include:

1. Refinement and modification of digital and analog electronics to restrict rms noise levels for 16 bit resolution to lsb at 60 dB gain (Implementation and tests completed on thirty-five systems during report period).
2. Development of internal sensor and recorder calibration procedures to permit complete relative system calibration without operator intervention.
3. Design and installation of initial voltage detection switch to prevent low-voltage damage to internal power cells.
4. Enhancement of GEOS software to improve watchdog environment for long-term operation.

Longer term development efforts that are nearing completion during this report period include:

1. Design and implementation of comparative bandpass detection algorithm for use in discrimination of teleseisms. (H.Y. Iyer, J. Evans, R. Cutler).

2. Development of new EPROM/RAM memory module to expand program memory by a factor of 2.5 to 56 K bytes.

3. Development and incorporation of hardware multiply capability to significantly increase computational speed of CPU. This arithmetic assist module is instrumental in extending digital computational capabilities of GEOS CPU and in implementation of teleseismic detection algorithm based on digital filters.

4. Extension of internal mass storage capability of GEOS to 25 Mbytes. Acquisition of high density (10,000 BPI), low power cartridge tape decks is expected to be completed for 50 units within next report period.

5. Final construction of 270 channel high resolution (16 bit, 96 dB), broad band (DC-500 Hz) data acquisition capability should be completed within next report period.

Enhancements completed on the GEOS analysis and playback systems (GAPS) includes:

1. Hardware enhancements for field deployable playback systems based on a PDP 11/73 CPU, including increase in on-line disc storage capability, reduction in weight, and an extension in library of field portable seismic analysis programs.

2. Software development to permit transfer of data fiels from remote field locations to National Strong Motion Data Center via telephone.

Reports

Borcherdt, R.D., Fletcher, J.B., Jensen, E.G., Maxwell, G.L., VanSchaack, J.R., Warrick, R.E., Cranswick, E., Johnston, M.J.S., and McClearn, R., 1985, A general earthquake-observation system (GEOS): *Bulletin, Seismological Society of Americal*, **75**, no. 6.

Maxwell, G.L., Borcherdt, R.D., Johnston, M.J.S., Malin, P.R., Sacks, I.S., Myren, R., Renaker, R., and Glassmoyer, G., 1985, On extending bandwidth and resolution for near-source seismic observations near Parkfield, California: *EOS*, **66**, no. 46, p. 986.

Database Management

9910-03975

Charles S. Mueller
Branch of Engineering Seismology and Geology
U.S. Geological Survey
345 Middlefield Road, MS 977
Menlo Park, California 94025
(415) 323-8111, ext. 2989

Investigations

1. Development of techniques for data playback, processing and management, with emphasis on large datasets collected with portable digital event-recording seismographs.

2. Design and implement a prototype relational database for aftershock and special-experiment data. The goal of the database is to enhance researcher access to diverse Branch datasets.

Results

1a. The following datasets have been processed and archived:

Simultaneous digital recording of co-sited dilatometer and geophone at various localities in California (January 1984 - continuing)
Chile aftershock experiment (March 1985)
Chile aftershock experiment (July 1985)

1b. FORTRAN software has been developed to enhance data processing and archival procedures.

2a. The first priority was to conceptually design database tables based primarily on seismological considerations - these table designs have been completed.

2b. Based on the tables designed in 2a, prototype applications to update and retrieve data have been implemented using INGRES software.

Reports

Algermissen, S.T. (ed.), 1985, Data processing and computation of seismograms *in* Preliminary investigation of the March 1985 Chile earthquake: *U.S. Geological Survey Open-File Report*, in press.

Soil-Structure and Structural Response Studies

9910-02760

A.G. Brady and G.N. Bycroft

Branch of Engineering Seismology and Geology
U.S. Geological Survey
345 Middlefield Road, MS 977
Menlo Park, California 94025
(415) 323-8111, ext. 2881

Investigations

1. *Differential ground motion.* A method of satisfactorily integrating acceleration records to determine differential displacements has been developed. An electronic spike has been found in the records of the Morgan Hill earthquake from the Hollister differential array. This has enabled the records to be synchronized in time and the differential motions between the stations to be determined. A fundamental model of a structure which responds to both inertial loading and differential strains has been developed and the differential motions from the Morgan Hill earthquake applied to it. In certain cases it has been shown that the effect of the differential strains compared to the inertial loading is substantial, and two reports are in preparation describing these results. Basic investigations into other soil structure interaction problems is continuing.

2. *Time dependent structural response to ground level excitation.* Investigations continue into the displacements attained by structures exhibiting elasto-plastic force-displacement characteristics.

3. *Analysis of structural records.* A modal analysis has been completed to the extent possible with the 15 channels of acceleration data from the three-span freeway bridge during the Morgan Hill earthquake of April 24, 1984. (A report is forthcoming). Although all the structural channels are from the first of the three spans, the relative displacement mode shapes for this span clearly indicate how the remainder of the bridge probably moved.

   The roof diaphragm of the West Valley College gymnasium has also been studied using records from the Morgan Hill earthquake, available from the Strong Motion Instrumentation Program of CDMG. Much information comes from the original record, but processing for corrected displacements gives a clear picture of the in-plane shearing and bending suffered by the flat roof diaphragm. Maximum amplitudes at the center of the roof, with respect to the displacements at the roof edge, are of the order of 5 mm.

Reports

Celebi, M., Brady, A.G., Safak., E., and Converse, A., Performance of an earthquake excited roof diaphragm: submitted to *3rd ASCE Engineering Mechanics Specialty Conference on Dynamic Response of Structures*, UCLA, March 31, 1986.

Ground Motion Prediction for Critical Structures

9910–01913

D. M. Boore
W. B. Joyner

Branch of Engineering Seismology and Geology
U.S. Geological Survey
345 Middlefield Road, MS 977
Menlo Park, California 94025
(415) 323–8111, Ext. 2698, 2154

Investigations

1. A method for adding small earthquakes to make big ones, such that predefined scaling relations hold, was developed.
2. The influence of a magnitude-independent, high-frequency cutoff on the scaling of various measures of ground motion and on derived source properties was investigated.
3. Work on a definitive study of the magnitude and distance dependence of response spectra was initiated.
4. Predictions were made of ground motion in eastern North America, using a stochastic fault model.

Results

1. Simulation of ground motion from large earthquakes has been attempted by a number of authors using small earthquakes (subevents) as Green's functions and summing them, generally in a random way. We present a simple model for the random summation of subevents to illustrate how seismic scaling relations can be used to constrain methods of summation. In the model η identical subevents are added together with their start times randomly distributed over the source duration T and their waveforms scaled by a factor κ. The subevents can be considered to be distributed on a fault with later start times at progressively greater distances from the focus, simulating the irregular propagation of a coherent rupture front. For simplicity the distance between source and observer is assumed large compared to the source dimensions of the simulated event. By proper choice of η and κ the spectrum of the simulated event deduced from these assumptions can be made to conform at both low- and high-frequency limits to any arbitrary seismic scaling law. For the ω-squared model with similarity (that is, with constant $M_0 f_0^3$ scaling, where f_0 is the corner frequency), the required values are $\eta = (M_0/M_{0e})^{4/3}$ and $\kappa = (M_0/M_{0e})^{-1/3}$, where M_0 is the simulated event moment and M_{0e} is the subevent moment. The spectra resulting from other choices of η and κ will not conform at both high and low frequency. If η is determined by the ratio of the rupture area of the simulated event to that of the

subevent and $\kappa = 1$, the simulated spectrum will conform at high frequency to the ω-squared model with similarity, but not at low frequency. Because the high-frequency part of the spectrum is generally the important part for engineering applications, however, this choice of values for η and κ may be satisfactory in many cases. If η is determined by the ratio of the moment of the simulated event to that of the subevent and $\kappa = 1$, the simulated spectrum will conform at low frequency to the ω-squared model with similarity, but not at high frequency. Interestingly, the high-frequency scaling implied by this latter choice of η and κ corresponds to an ω-squared model with constant $M_0 F_0^4$—a scaling law proposed by Nuttli, although questioned recently by Haar and others.

2. A breakdown of similarity is generally observed in earthquake sequences below a magnitude of about 5. Although usually manifested as an upper limit on observed corner frequencies (and therefore a decrease of calculated stress drop with decreasing moment), the apparent breakdown can also be seen by changes in the slope of various peak motions when plotted against moment. The effect can be explained by a moment-independent high-frequency limit on the band of the recorded signal without specifying whether the limit is imposed by the source, the propagation path, the local site, or the recording instrument. With such a limit, the logarithm of peak acceleration, peak velocity, peak displacement, response spectra, apparent stress, and stress drop will scale for small earthquakes at 1.0 log M_0, in contrast to the lesser dependence on moment exhibited for larger earthquakes. Using an ω-squared, constant stress parameter spectral model and a previously published simulation method (Boore, 1983), seismograms were simulated for two cases, one with the upper limit to the spectral band spanning a wide range of frequencies and the other with parameters appropriate for the aftershock sequence of the 1983 Coalinga, California, earthquake sequence. In the first case, the simulations reproduced the general observations with respect to the moment dependence of corner frequencies, stress parameters, and the various measures of peak ground motion. In the second case, the simulations are consistent with the observed data of McGarr *et al.* (1985) for peak acceleration and peak velocity of both P and S waves, although a rather high stress parameter is required: around 30 or 80 MPa (300 or 800 bars), depending on whether or not amplification due to the decreasing seismic velocity near the earth's surface is included.

Reports

Boore, D. M., The effect of finite bandwidth on seismic scaling relationships, *Proc. Fifth Ewing Symposium on Earthquake Source Mechanics*, Harriman, NY, submitted, 1986.

Haar, L. C., Mueller, C. S., Fletcher, J. B., and Boore, D. M., Comments on "Some recent *Lg* phase displacement spectral densities and their implications with respect to prediction of ground motions in eastern North America" by R. Street, *Bull. Seismol. Soc. Am.* **76**, in press, 1986.

Joyner, W. B. and Boore, D. M., On simulating large earthquakes by Green's function addition of smaller earthquakes, *Proc. Fifth Ewing Symposium on Earthquake Source Mechanics*, Harriman, NY, submitted, 1986.

Anelastic Wave Propagation
9910-02689

Roger D. Borcherdt
Branch of Engineering Seismology and Geology
U.S. Geological Survey
345 Middlefield Road, MS 977
Menlo Park, California 94025
(415) 323-8111, ext. 2755

Investigations:

1. Physical characteristics of inhomogeneous waves in general low-loss anelastic solids.
2. Effects of anelastic boundaries on the physical characteristics of inhomogeneous P, elliptical S, and linear S waves.
3. Anelastic studies of short period strain (10^5 - 10^{-1}s) and high frequency (50+ Hz) radiation near seismic sources.

Results:

1. Working in conjunction with L. Wennerberg the physical characteristics for general plane-wave radiation fields in an arbitrary linear viscoelastic solid were derived. Expressions for the characteristics of inhomogeneous wave fields, derived in terms of those for homogeneous fields were utilized to specify the characteristics and a set of reference curves for general P and S wave fields in arbitrary viscoelastic solids as a function of wave inhomogeneity and intrinsic material absorption. The expressions show that an increase in inhomogeneity of the wave fields causes the velocity to decrease, the fractional-energy loss (Q^{-1}) to increase, the deviation of maximum energy flow with respect to phase propagation to increase, and the elliptical particle motions for P and type-I S waves to approach circularity. Q^{-1} for inhomogeneous type-I S waves is shown to be greater than that for type-II S waves with the deviation in general increasing with inhomogeneity. The mean energy densities (kinetic, potential and total), the mean rate of energy dissipation, the mean energy flux, and Q^{-1} for inhomogeneous waves are shown to be greater than corresponding characteristics for homogeneous waves, with the deviations increasing as the inhomogeneity is increased for waves of fixed maximum displacement amplitude. For inhomogeneous wave fields in low-loss solids, only the tilt of the particle motion ellipse for P and type-I S waves is independent to first order of the degree of inhomogeneity. Quantitative estimates for the characteristics of inhomogeneous plane body waves in layered low-loss solids are derived and guidelines established for estimating the effect of inhomogeneity on seismic body waves and a Rayleigh-type surface wave in low-loss media.
2. Working in conjunction with G. Glassmoyer and L. Wennerberg a general computer code (WAVES) has been utilized to calculate anelastic reflection-refraction coefficients, energy flow, and the physical characteristics of plane waves reflected and refracted by general P, type-I S, and type-II S waves incident on anelastic boundaries. Consideration of homogeneous and inhomogeneous linear S waves incident on anelastic boundaries with significant intrinsic absorption, illustrates reductions in phase and energy speeds, increases in maximum attenuation and Q^{-1}, and directions of maximum energy flow distinct from phase propagation, with each of these

changes being dependent on angle of incidence. Finite relaxation times for anelastic media result in energy flow due to interaction of superimposed radiation fields and contribute to energy flow across anelastic boundaries for all angles of incidence. Agreement of theoretical and numerical results with laboratory measurements for acoustic waves incident on a liquid-solid boundary argues for the validity of the theoretical and numerical formulations, attests to the applicability of the exact anelastic model, and helps confirm the characteristics predicted for corresponding P and elliptical S waves in anelastic media. The exact anelastic formulation with no low-loss approximations predicts the existence of an anelastic Rayleigh window, which accounts for the discrepancy noted by Brekovskikh (1960) between measured reflection data and predictions based on classical elasticity theory. Characteristics of the anelastic Rayleigh window are expected to be evident in certain sets of wide-angle ocean-bottom reflection data and to be useful in estimating Q^{-1} for some ocean-bottom reflectors. Reflection data from the North Atlantic Transect, provided by J. Mutter (LDGO), is being examined for evidence of this "Rayleigh window".

An extended version of Snell's Law has been utilized by L. Wennerberg and G. Glassmoyer to compare the influence of elastic and anelastic boundaries on phase velocity, ray geometry, travel time, and attenuation coefficient. A computer code has been developed by L. Wennerberg to calculate the influence of anelastic boundaries on incident beams with a Gaussian intensity profile.

3. In conjunction with M. Johnston and A.T. Linde an interpretation has begun on short-period strain signals recorded with resolution up to 16 bits on recorders deployed at four sites with deep borehole dilatometers. In conjunction with P. Malin, interpretation has begun on high resolution seismic signals recorded at the sites of three downhole seismometer arrays. Theoretical expressions have been derived for the displacement field and the volumetric strain associated with the passage of an inhomogeneous dilational wave in an anelastic half-space. The expressions suggest techniques for using colocated sensors recorded with 16 bit resolution at high sampling rates to resolve *in-situ* Q^{-1}. The signals recorded to date show that the bandwidth for detection of seismic radiation fields can be extended with presently installed sensors to cover the range of 10^{-2} to 10^{5} seconds and down to volumetric strain levels of 10^{-11}.

Reports

Borcherdt, R.D., Glassmoyer, G., and Wennerberg, L., 1986, Influence of anelastic boundaries on energy flow and characteristics of general P, type-I S and type-II S waves, for submission: *Journal of Geophysical Research*, in press.

Borcherdt, R.D., Glassmoyer, G., and Wennerberg, L., 1985, On physical phenomena associated with the reflection and refraction of anelastic waves: *EOS*, v. 66, p. 984.

Borcherdt, R.D., and Wennerberg, L., 1985, General P, type-I S, and type-II S waves in anelastic solids: Inhomogeneous wave fields in low-loss solids: *Bulletin, Seismological Society of America*, v. 75.

Johnston, M.J.S., and Borcherdt, R.D., 1985, Measurements of short period strain ($0.1-10^5$s): Near source strain field for an earthquake (M_L~3.2) near San Juan Batista, California: for submission: *Journal of Geophysical Research*, in press.

Wennerberg, L., and Glassmoyer, G., 1985, Snell's law applied to rays in layered viscoelastic media: *EOS*, v. 66, p. 984.

Wennerberg, L., and Glassmoyer, G., 1986, Some absorption effects on plane waves in layered media: *Bulletin, Seismological Society of America*, in press.

NORTHWEST U.S. SUBDUCTION ZONE
RISK ASSESSMENT
9930-03790

Thomas H. Heaton and Stephen H. Hartzell
Branch of Seismology
U.S. Geological Survey
525 S. Wilson Avenue
Pasadena, CA 91106
(818) 405-7823

The purpose of this project is to assess the potential seismic hazard due to large shallow thrust earthquakes along the Cascadia subduction zone of the northwestern United States. Although there is good evidence for a convergence rate of 3 to 4 cm/yr, there have been no large historic earthquakes. Interplate slip along this 1000 km interface may be occurring aseismically, however, the Cascadia subduction zone has many characteristics with other young subduction zones that have experienced great shallow thrust earthquakes.

Under this project, of the 1984 Morgan Hill, California, earthquake has also been studied.

INVESTIGATIONS

1. The physical characteristics of world-wide subduction zones have been compared with those of the Juan de Fuca subduction zone of the northwestern United States. Through these comparisons source characteristics have been estimated for hypothetical subduction earthquakes in the northwestern United States. Finally, estimates of potential strong ground motions are made for the postulated earthquakes.

2. Near-source strong motion velocity records are modeled to obtain the spatial and temporal distribution of slip for the 1984 Morgan Hill earthquake. Both forward modeling and constrained, least-squares inversion techniques are used to interpret the velocity waveforms in the frequency range of 0.2 Hz to 5.0 Hz.

RESULTS

1. Compared with other world-wide subduction zones, the Cascadia subduction zone seems most similar to southern Chile, the Nankai Trough, and Colombia, each of which have experienced very large historic earthquake sequences. Table I compares physical characteristics of the Cascadia subduction zone with other zones in which young oceanic lithosphere is subducted. The length of the subducting margin along the Cascadia subduction zone probably exceeds

1000 km and if the zone is locked, then earthquakes of very large size must be considered. Several observations seem compatible with a model in which great earthquake sequences occur with an average repeat time of 400 to 500 years, but because of the nature of this data, we consider this hypothesis to be highly speculative.

Since no large historic, shallow thrust earthquakes have occurred on the Cascadia subduction zone, potential ground motions are estimated by indirect methods. A comparison study has been completed of the strong ground motions and teleseismic time functions for world-wide subduction zone earthquakes of moment magnitude greater than 7.0. Results indicate that the existing data set of strong motion records from shallow subduction earthquakes of $M_w < 8\frac{1}{4}$ can be used to make meaningful estimates of potential ground motions in the northwestern U.S. Figure 1 shows some of the available response spectra, grouped according to epicentral distance, for earthquakes of $M_w < 8\frac{1}{4}$. Some of the large scatter seen in Figure 1 can be attributed to site effects. Grouping of response spectra from the same stations but for different events shows strong corrrelations at some sites.

To estimate strong ground motions for earthquakes of $M_w > 8\frac{1}{4}$ for which there is no data, a summation procedure is adopted using the records from smaller events. The summation process is constrained by the requirement that it fit teleseismic broad-band recordings from earthquakes of the same desired moment. Results indicate that a significant fraction of the total moment for earthquakes of $M_w > 8\frac{1}{4}$ is in long-period radiation (> 60 sec), which does not produce damaging shorter-period strong ground motion. The proper transfer function for the summation, as indicated by the teleseismic data, is obtained by introducing randomness having the correct distribution.

2. Figure 2 shows the contours of strike-slip dislocation in centimeters obtained from the inversion of the Morgan Hill strong motion data. Each of the three frames shows the cumulative dislocation which occurs in time windows separated by 0.2 sec. The first frame is tied to a rupture velocity of nine tenths of the local S-wave velocity. The Morgan Hill earthquake is almost entirely a unilateral rupture originating at a depth of about 8.5 km near Halls Valley and propagating to the southeast 25 km along the Calaveras Fault. Significant slip is terminated near the Coyote Lake Dam station at the northern end of Coyote Lake. The average rupture velocity is approximately nine tenths of the local shear wave velocity. To first approximation, the Morgan Hill rupture consists of two main source regions separated by about 4.3 sec, one in the north near the hypocenter and a second larger source located under Anderson Reservoir. The idealized, uniform rupture with a "starting-phase" and a "stopping phase" is rejected. The source region under Anderson Reservoir is approximately 3 times larger in moment than the initial source, with a maximum dislocation of about 1 meter. On a finer scale, both of these source regions have structure of their own, and should not be viewed as two simple point sources. Resolution of this fine structure is hindered by a complex velocity structure with strong lateral heterogeneity. The surface expression of the

Calaveras Fault zone is very complex in the region of Anderson Reservoir, with many small bifurcated faults. This complexity may be a manifestation of an asperity at depth, which apparently broke during the Morgan Hill earthquake, but which hampers the formation of a simple through-going fault. The total moment is estimated from the inversion of the strong motion data to be 2.1×10^{25} dyne-cm.

Reports

Hartzell, S.H. and T.H. Heaton (1985). Rupture history of the 1984 Morgan Hill, California, earthquake from the inversion of strong motion records, *Bull. Seism. Soc. Am.*, submitted.

Heaton, T.H. and S.H. Hartzell (1985). Source characteristics of hypothetical subduction earthquakes in the northwestern United States, *Bull. Seism. Soc. Am.*, submitted.

Heaton, T.H. and S.H. Hartzell (1985). Ground motion estimates for hypothetical earthquakes on the Cascadia subduction zone, EOS, in press.

TABLE I.

	Cascadia	Southern Chile	Nankai Trough	Alaska	Colombia	Mexico (Rivera Plate)
Age (m.y.) of subducted plate	10	5 to 30	18 to 24	40 to 50	10 to 15	10?
Convergence rate (cm/yr)	3.3 to 4.3	9	3.3 to 4.3	5.7	8	2.3
Character of trench	shallow sediment filled	shallow sediment filled	shallow sediment filled	shallow sediment filled	shallow sediment filled	shallow few sediments
Free-air gravity anomaly	small 50 mgal	small 50 mgal	moderate 100 mgal	moderate 100 mgal	small 50 mgal	moderate 100 mgal
Background seismicity	very low	very low	low	moderate	low	?moderate?
Heat flow	high 1-2 HFU	high 1-2 HFU	high 1-2 HFU			
Quaternary volcanism	yes	yes	no	varies along the trench	yes	yes
Inland sea or valley	yes	yes	yes	yes	?no?	no
Width of continental margin	30-120 km	100 km	110 km	180 km	130 km	80 km
Largest historic earthquakes M_W	none in 150 yr.	9.5 (1960)	8.1 (1944,1946) ?8.5? (1707)	9.2 (1964)	8.8 (1906)	8.2 (1932)
Average repeat time	?400 yr.?	128 yr.	180 yr.	?800 yr.?	unknown	?50 yr.?

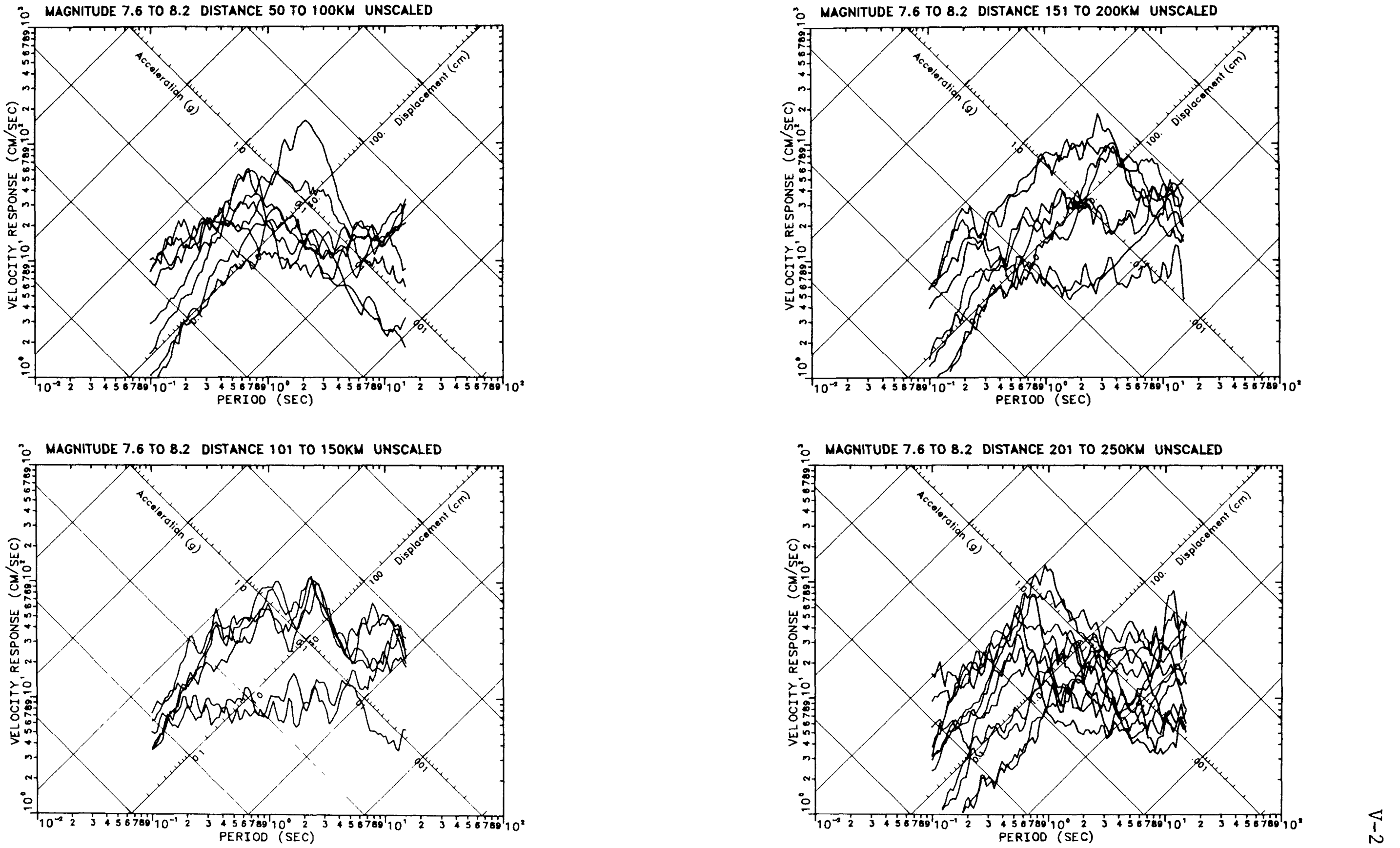

MAGNITUDE 7.6 TO 8.2 DISTANCE 50 TO 100KM UNSCALED

MAGNITUDE 7.6 TO 8.2 DISTANCE 151 TO 200KM UNSCALED

MAGNITUDE 7.6 TO 8.2 DISTANCE 101 TO 150KM UNSCALED

MAGNITUDE 7.6 TO 8.2 DISTANCE 201 TO 250KM UNSCALED

Figure 1. Response spectra (5% damping) from large shallow subduction earthquakes.

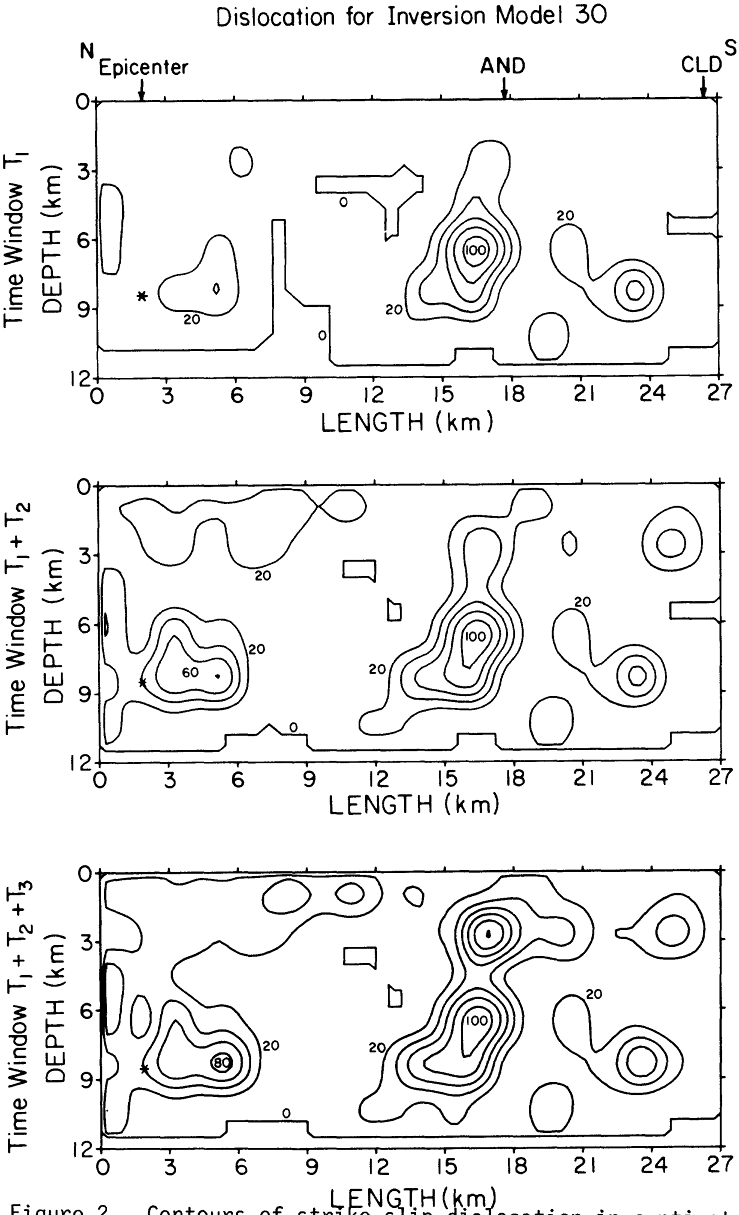

Figure 2. Contours of strike-slip dislocation in centimeters for the 1984 Morgan Hill earthquake.

PRECISE VELOCITY AND ATTENUATION MEASUREMENTS IN ENGINEERING SEISMOLOGY

9910-02413

Hsi-Ping Liu
Branch of Engineering Seismology and Geology
U. S. Geological Survey
345 Middlefield Road, Mail Stop 977
Menlo Park, California 94025
(415) 323-8111, ext. 2731

Investigations

1. Continued data analysis of the results obtained for dynamic testing of Monticello Dam, Lake Berryessa, California. The test was conducted for the purpose of improving upon the current methods of dynamic dam testing by firing a 656 cm^3 volume air gun at pressures up to 13.8 MPa in the reservoir as the excitation source and recording the dam response at various locations on the dam with three-component 1 Hz electromagnetic geophones.

2. Construction and testing of a pneumatically driven shear wave generation device. The objective is to develop a horizontally polarized seismic snear wave source in order to measure seismic wave attenuation in shallow crust to a depth of several hundred meters. The near-surface shear wave attenuation data are needed for seismic safety site evaluation of engineering structures and for determination of earthquake source parameters from records obtained at the earth's surface.

3. Design and construction of a low-cost, 3-component, 2 Hz electromagnetic borehole geophone which can be leveled after downhole emplacement. Such an instrument would provide calibrated seismograms recorded below the earth's weathered layer for earthquake focal mechanism studies.

Results

1. A dynamic testing method, which employs an air gun firing in the reservoir as the excitation source, has been used to identify more than ten natural frequencies of a concrete-arch dam (Monticello Dam near Sacramento, California). Data recorded at three crest locations using three-component geophones show that all modes except one have three-dimensional motion. The exceptional mode has motion predominantly in the vertical direction. These modes were substantially excited by the wide-band and relatively high-energy air-gun source. Peak responses in the Fourier amplitude spectra of the recorded motions were used to identify the natural frequencies of the dam. Comparisons of these responses with previous results, in which modes were determined by forced-vibration tests using rotating-mass shakers, show good agreement. Additionally, several modes not previously identified by experimental methods were determined using these tests. The results show that this method alleviates some of the limitations of other dynamic testing

methods for mode identification. While ambient-vibration tests utilize unpredictable excitation sources (e.g., wind and water waves) and vibrations are usually limited to low amplitudes, the air gun provides an impulsive force to the structure, after which the free-vibration response is several times greater than the ambient response. These free-vibration motions are easily analyzed to give quick and reliable estimates of modal parameters.

2. In collaboration with Richard E. Warrick, a shear wave generator which puts out a repeatable signal has been constructed to measure shear wave velocity and attenuation for site response studies in engineering seismology. The driving force of the generator comes from a double-acting air cylinder. When in use the device is firmly held on the soil surface and the two hammers, attached to the ends of the air-cylinder piston and sliding on low-friction tracks, impact alternately two anvils clamped between two aluminum channels at the ends. The resulting traction exerted on the soil surface produces a repeatable wave field whose S to P amplitude ratio exceeds 10. The motions recorded by horizontal geophones oriented parallel to the shear wave generator show negligible P-wave motion and the polarity of the entire wave train is reversed when the direction of impact is reversed. Signals generated by the new device are highly repeatable. We hope that with digital recording and stacking, the new device can be used for shear wave measurements over an extended distance, which would lead to a number of interesting applications.

3. Based on a leveling method used in an ocean bottom seismometer and by using miniature frictionless hinges, a low-cost, 3-component, 2 Hz electromagnetic borehole geophone which can be leveled after emplacement has been designed. It is now under construction at the U. S. Geological Survey.

Reports

H.-P. Liu, J. J. Fedock, J. B. Fletcher, and E. D. Sembera, Dynamic air-gun test of arch dam: vertical motion, submitted to Journal of the Structural Engineering Division, ASCE, 1985.

H.-P. Liu, J. J. Fedock, and J. B. Fletcher, Mode identification by dynamic air-gun test of an arch dam, Abstract, submitted to the Third U. S. National Congress on Earthquake Engineering, 1985.

H.-P. Liu, R.E. Warrick, and R. E. Westerlund, A pneumatic shear-wave generator with repeatable signal, Abstarct, submitted to American Geophysical Union Fall Annual Meeting, 1985.

Strong Ground Motion Prediction in Realistic Earth Structures

9910-03010

P. Spudich
Branch of Engineering Seismology and Geology
U.S. Geological Survey
345 Middlefield Road, MS 977
Menlo Park, California 94025
(415) 323-8111, ext. 2395
April 1, 1985 to September 30, 1985

Investigations

1. Development of improved methods for analysis of seismograph array data.

2. Investigation of wave scattering effects in the source region of the 1984 Morgan Hill, California, earthquake.

Results

1. We developed a new technique for suppressing spurious side lobes and aliases obtained from frequency/wave-number transforms of seismic data. By analyzing frequency/wave-number transforms in slowness and by stacking over frequency, spurious signals can be effectively suppressed relative to the true signal.

   The power of this technique derives from working in the slowness plane instead of the wave-number plane. Direct body waves arrive at a constant slowness for all frequencies, whereas the side lobes and aliases of the array impulse response appear to arrive at different slownesses, depending on frequency. Thus, if the slowness planes calculated at different frequencies are stacked, peaks corresponding to signals stack constructively, whereas the side lobe and alias peaks do not.

   The range of frequencies over which the stack is taken depends on the aperture of the array and the frequency content of the signal. The lower-frequency limit is determined by the width of peaks in the slowness plane, which is a function of the array aperture. The upper-frequency limit for stacking is determined only by the upper-frequency limit of spectral content of the signal. This method may be used at higher frequencies where conventional methods would be too contaminated with aliases to be useful.

   Tests with synthetic data have shown the method to be effective in distinguishing peaks corresponding to real signals from spurious peaks and to be robust with respect to multiple signals arriving at similar slownesses and azimuths--conditions under which the high-resolution methods of Capon becomes difficult to interpret.

2. The reciprocity relation for Green's functions tells us that the time series obtained in the following two experiments would be identical: (1)

measurement of the $\hat{a}$ component (where $\hat{a}$ is an arbitrarily oriented unit vector) of ground displacement at location x caused by a unit dislocation $\hat{d}$ at y on a fault surface A. and (2) measurement of the $\hat{d}$ component of stress acting across A at buried point y. caused by an instantaneous force applied in direction $\hat{a}$ at location x on the ground. This means that simply by recording earthquakes on a single seismograph we obtain *exactly* the same time series as if we had buried stress meters deep within the earth and recorded a surficial source on them. In particular, recording an earthquake swarm or aftershock sequence is identical to having a buried instrument array. Consequently, any analysis method appropriate for surface arrays may be applied to earthquake clusters. As an example we applied frequency/wave-number analysis to aftershocks of the 1984 Morgan Hill earthquake in order to decompose the waves impinging upon the earthquake cluster (in the sense of experiment 2) into their plane wave constituents. From such a decomposition we recover the take-off angles of both the direct and scattered waves that travel from the cluster to the surface. Using this technique we have found that much of the large amplitude S wave coda consists of waves reverberated very near the seismographs.

Reports

Bostwick, T., and Spudich, P., 1985, Suppressing aliases and side lobes in frequency/wave-number transforms through slowness and frequency stacking: *EOS*, **66**, p. 313.

Spudich, P., and Bostwick, T., 1985, Use of earthquake clusters as deeply buried seismograph arrays, *EOS*, **66**, p. 313.

Late Pleistocene-Holocene Soil Chronology for Evaluating Tectonic Framework and Events, Transverse Ranges, California

14-08-0001-21829

E. A. Keller, R. L. Zepeda, D. M. Laduzinsky,
D. B. Seaver and E. X. Zhao
Department of Geological Sciences
University of California
Santa Barbara, California 93106
(805) 961-4207

with assistance from

D. L. Johnson
Department of Geography
University of Illinois
Urbana, Illinois 61801
(217) 333-0589

T. K. Rockwell
Department of Geological Sciences
California State University
San Diego, California 92182
(619) 265-4441

OBJECTIVES

Research objectives are: 1) Develop a chronology for Holocene and late Pleistocene deposits based upon relative development of soils; and 2) apply the chronology to evaluate late Pleistocene and Holocene tectonic framework and events in three study areas: 1) Wheeler Ridge south of Bakersfield, California; 2) the northern front of the San Emigdio Mountains west of Wheeler Ridge, and 3) Frazier Mountain near Gorman, California.

INVESTIGATIONS

The primary task is the development of soil chronosequences for the three study areas. A secondary activity is the application of the soil chronosequence work to develop preliminary rates of uplift associated with folding on the upper plates of concealed reverse faults.

RESULTS

Soil Chronosequences: Soils in the Wheeler Ridge-San Emigdio area vary from AC profiles on Holocene surfaces to well developed argillic B and petrocalcic horizons on Pleistocene surfaces (Table 1). The soil chronosequence suggests that with increasing age, soils thicken, colors redden, structure becomes more strongly developed, clay and $CaCO_3$ contents increase, number and thickness of clay films increases, and stage of carbonate morphology increases. General characteristics of Holocene soils are relatively pale colors (Hue = 2.5Y-10YR), poorly developed structure, no clay films, and stage I-II carbonate morphology. Pleistocene soils are redder (Hue = 7.5YR), struc-

Table I. Wheeler Ridge - San Emigdio Soil Chronosequence

Geomorphic Surface		Solum Thickness (m)	B Horizon					Carbonate Stage[b]	Estimated Age (10^3 ybp)[c]
Wheeler Ridge	San Emigdio		Type	Moist Color[a]	Texture	Structure	Clay Films		
Q1	Q1 Q2 Q3 Q3b	0.5-0.8	AC to cambic B	10YR 3/3	Sandy to sandy loam	Primary fluvial stratification to massive	None	Weak I-II	Holocene
Q2	-	2.4+	Argillic	10YR 4/4	Sandy loam	Moderate coarse subangular blocky	Many thin and moderately thick on pebble-matrix interfaces	I-II	16.5 - 28.5
Q3	-	2.7+	Argillic	10YR 4/4	Loam to sandy loam	Weak medium subangular blocky	Many moderately thick on pebble-matrix interfaces	II	28.5 - 59
Q4	Q4a	2.0-3.1+	Argillic	7.5YR 4/6	Sandy loam to sandy clay loam	Massive breaking to fine subangular blocky	Continuous thick on pebble-matrix interfaces	II-III	93 - 146.5
-	Q4b	2.5-3.1+	Argillic	7.5YR 4/6	Sandy clay loam	Strong angular blocky to columnar	Many to continuous thick	Weak IV	~130
Q5	-	NA	B horizon stripped					Strong IV	218-254

[a] Color terms follow Munsell notation.

[b] Carbonate stage terms follow Gile, Peterson and Grossman (1966).

[c] Age control for Holocene soils is from ^{14}C dates. Mid- to late-Pleistocene age estimates are from assumed rates of uplift and present elevations of geomorphic surfaces (see text for discussion).

ture is blocky to columnar, clay films are thick and continuous, and stage III-IV carbonate development is present.

Soils in the Hungry Valley-Frazier Mountain area vary from young AC profiles with minimum development to well developed soils with argillic B horizons (Table 2). Soils in the Hungry Valley-Frazier Mountain chronosequence suggest that as the soils age, colors redden, structure becomes better developed, and number and thickness of clay films increases. Holocene age soils have relatively light colors (Hue = 10YR), poorly developed structure, and none to few, thin clay films. Pleistocene soils are redder (Hue = 7.5YR-5YR), structure is angular blocky, and clay films are medium and continuous. High geomorphic surfaces on the southeast side of Frazier Mountain have apparent anomalously weakly developed soils compared to soils on high surfaces on the northwest side of the mountain. We hypothesize that soil forming processes on the southeast side of Frazier Mountain may be retarded by erosional events or bioturbation.

Age control for the soil chronosequences is from: (1) ^{14}C dates on charcoal and carbonate rinds of clasts for Holocene soils; (2) rates of uplift derived from deformed Holocene soils and extrapolated to deformed Pleistocene surfaces; and, (3) correlation with other chronosequences in the San Joaquin Valley (this was primarily done for the Hungry Valley-Frazier Mountain area).

Active Tectonics at the San Emigdio Front: The north flank of the San Emigdio Mountains is underlain by the westward extension of the White Wolf-Wheeler Ridge fault system (Davis, 1983). A significant feature of this fault system is that it is not exposed at the surface. Late Pleistocene, Q4b gravel deposits are steeply folded at the front however, indicating that faulting at depth is accompanied by folding at the surface.

Surveying of terrace surfaces in San Emigdio Canyon indicates that Holocene deposits are deformed both at the present range front and at the Los Lobos folds on the adjacent San Joaquin Valley floor. Geomorphic evidence suggests that the Pleito fault defined the position of the San Emigdio range front during the late Pleistocene, and that the range front has migrated northward approximately 5 km, consuming the adjacent valley floor in the process. The position of the Los Lobos folds may mark the initiation of a northward step in rangefront migration (Figure 1).

The rate of uplift at the present front is determined by surveying of deformed Holocene surfaces. Survey results show that the Holocene stream terraces diverge toward the axis of uplift, and the overall morphology of the deformed surface is such that the terrace gradient is reduced upstream from the axis, and increased downstream.

Detailed profiles in San Emigdio Canyon suggest there is 8.5 m of vertical uplift at the point of maximum deformation of the 4300 ybp Q3 surface. This provides an uplift rate of 2.0 mm/yr. Assuming a one meter displacement per event suggests the recurrence interval for such events is about 500 years (Table 3).

At the Los Lobos folds, the Q4b surface emerges from beneath the Holocene deposits and is folded into two broad anticlines on the San Joaquin Valley floor. The Q4b soil, exposed along San Emigdio Creek, is buried by Q2 and Q3

Table 2. Characteristic Soil Properties of Hungry Valley - Frazier Mountain Chronosequence

Geomorphic Surface	Solum Thickness (m)	B Horizon					Carbonate Stage[b]	Estimated Age (10^3 ybp)
		Type	Color[a]	Texture	Structure	Clay Films		
Q1	0.2	AC Profile				None	None	<1[c]
Q2	1.3	Cambic	10YR 5/4	Sandy loam	Massive	Few, thin discontinuous	None	5-10[d]
Q3	1.3-1.9	Argillic	10YR 5/4- 7.5YR 5/6	Clay loam	Moderate to medium angular blocky	Common, thin-med., discontinuous	None	20-40[d]
Q4	0.7	Cambic-dispersed	10YR 5/4	Loam	Massive	Few, thin discontinuous	None	Not known
Q5	1.9	Argillic	5YR 4/6	Clay loam	Moderate angular blocky	Many, medium continuous	Weak II	100-200[d]

[a] Color terms follow Munsell notation.

[b] Carbonate stage terms follow Gile, Peterson, and Grossman (1966).

[c] ^{14}C date.

[d] Based on correlation with San Joaquin Valley chronosequences of Harden (1982).

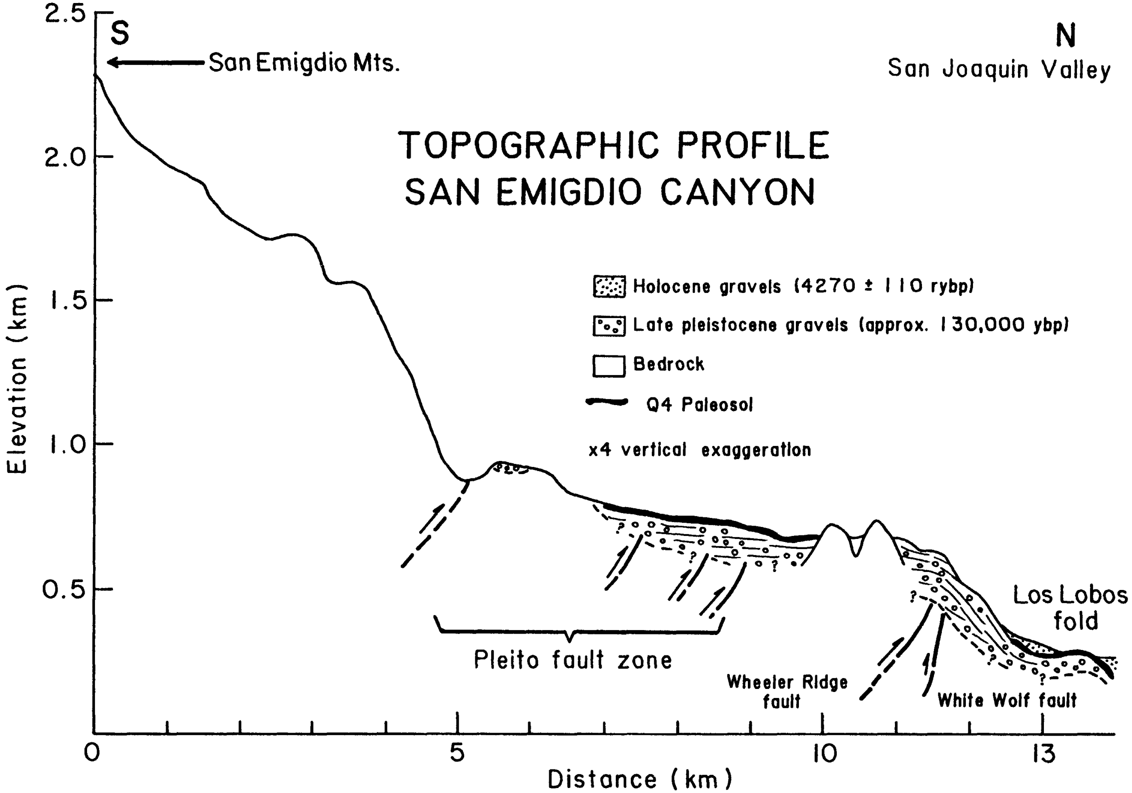

Figure 1. Topographic profile of the San Emigdio Canyon.

Table 3. Comparison of possible recurrence intervals for Wheeler Ridge (White Wolf-Wheeler Ridge faults, Ms = 7.3, 1952) with the 1983 (Ms = 6.5) event below Anticline Ridge near Coalinga. Data for the Coalinga event after Stein and King, 1984. Also listed are possible recurrence intervals for an assumed Ms = 7.3 event with 1 m of surface uplift for the White Wolf-Wheeler Ridge faults below the San Emigdio Front and Los Lobos folds.

	(A) Surface uplift per event (m)	(B) Fault slip per event (m)	Uplift Rate mm/yr.	Slip Rate mm/yr.	Recurrence Interval (Yrs.)
Coalinga (Anticline Ridge) Ms = 6.5	0.6	1.8	1-4	3-12	150-600
Wheeler Ridge Ms = 7.3	1.0	2.1[a]	0.6-2.1	1.3-4.5	450-1600
Los Lobos folds Ms = 7.3 (assumed)	1.0 (assumed)	2.1[a]	1.6	3.6	600
San Emigdio Front Ms = 7.3 (assumed)	1.0 (assumed)	2.1[a]	2.0	4.3	500

[a] Based on a buried fault that dips at 28° as in the case with the Wheeler Ridge fault (Medwedeff, 1984).

deposits which are in turn deformed as they cross the fold. Survey results shown on Figure 2, suggest an uplift rate of 1.6 mm/yr for the Q3 surface, and 1.7 mm/yr for the Q2 surface. Assuming an uplift of 1 m per event provides a recurrence interval of about 600 years for the buried fault that probably underlies the Los Lobos folds (Table 3).

Although the Pleito fault is an active structure at Grapevine Canyon, 25 km to the east (Hall, 1984), the active uplift at San Emigdio Canyon occurs 5 km north of the Pleito fault on the buried White Wolf-Wheeler Ridge fault system, and even further to the north along probable thrust faults concealed beneath the Los Lobos folds.

Active Tectonics at Wheeler Ridge: The 1952 Kern County, California earthquake (Ms = 7.3) had a source several kilometers deep below Wheeler Ridge on the buried White Wolf-Wheeler Ridge fault system (Gutenberg, 1955). Ground rupture and displaced features were observed along a 64 km long zone following the earthquake, but in the epicentral region near Wheeler Ridge the major surficial expression consisted of fractures orientated obliquely to the east-west anticlinal structure that forms the ridge. Major displacement which occurred at depth did not reach the surface at Wheeler Ridge (Buwalda and Amand, 1955).

Interpretation of the tectonic framework based on limited soil chronology and radiocarbon dates in suggests that Wheeler Ridge is an active anticline on the upper plate of the White Wolf-Wheeler Ridge faults. The fold is growing to the east at about 2 mm/year, and uplift, tilting, and faulting associated with the growth of the fold is denoted by geomorphic surfaces that are higher and older to the west of the eastern terminus of the structure (Figure 3).

We can demonstrate Holocene activity at the eastern end of the fold. Figure 4 shows the present course of Salt Creek which crosses the anticlinal axis and two older surfaces that are folded. Analysis of this data suggests that in the last 12,000 years the rate of uplift is constrained between 0.6 and 2.1 mm/year. Estimated uplift, slip rate, and recurrence intervals for the 1952 event are shown on Table 3. It is premature to suggest that these data are adequate for earthquake hazards reduction planning. The basic assumption is that the surface uplift per event is related to the fault slip per event. Surface uplift associated with Wheeler Ridge during the 1952 event was 1 m (Stein and Thatcher, 1981). Assuming the dip of the fault is 28° (Medwedeff, 1984), the fault slip per event is about 2.1 m. Thus, our calculated uplift rate of 0.6 to 2.1 mm/year corresponds to a slip rate of 1.3 to 4.5 mm/year with a recurrence interval of 450 to 1600 years for the Ms = 7.3 event. Using an average slip rate of 1.4 mm/year which is a compromise between a minimum and a maximum, suggests a recurrence interval of about 700 years for a 1952-type event.

REFERENCES

Buwalda, J. P., and St. Amand, P., 1955, Geological effects of the Arvin-Tehachapi earthquake (in) Earthquakes in Kern County, California during 1952: California Division of Mines Bulletin, v. 181, p. 41-66.

Davis, T. L., 1983, Late Cenozoic structure and tectonic history of the western "Big Bend" of the San Andreas fault and adjacent San Emigdio Mountains: Unpublished Ph.D. dissertation, University of California, Santa Barbara, 508 p.

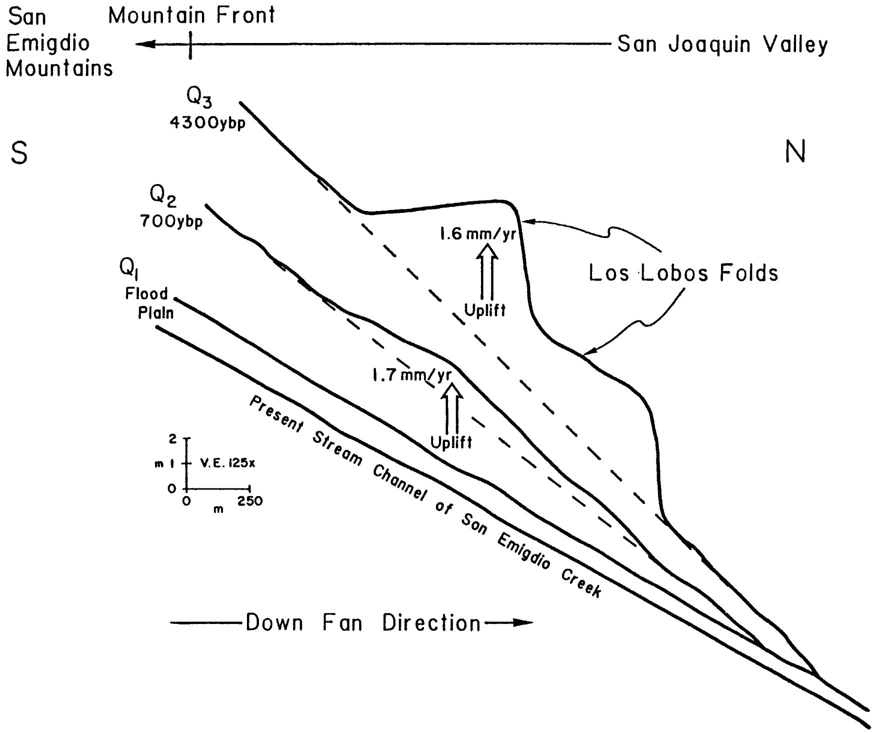

Figure 2. Deformation of the Q2 and Q3 geomorphic surfaces and associated rates of uplift over the Los Lobos folds.

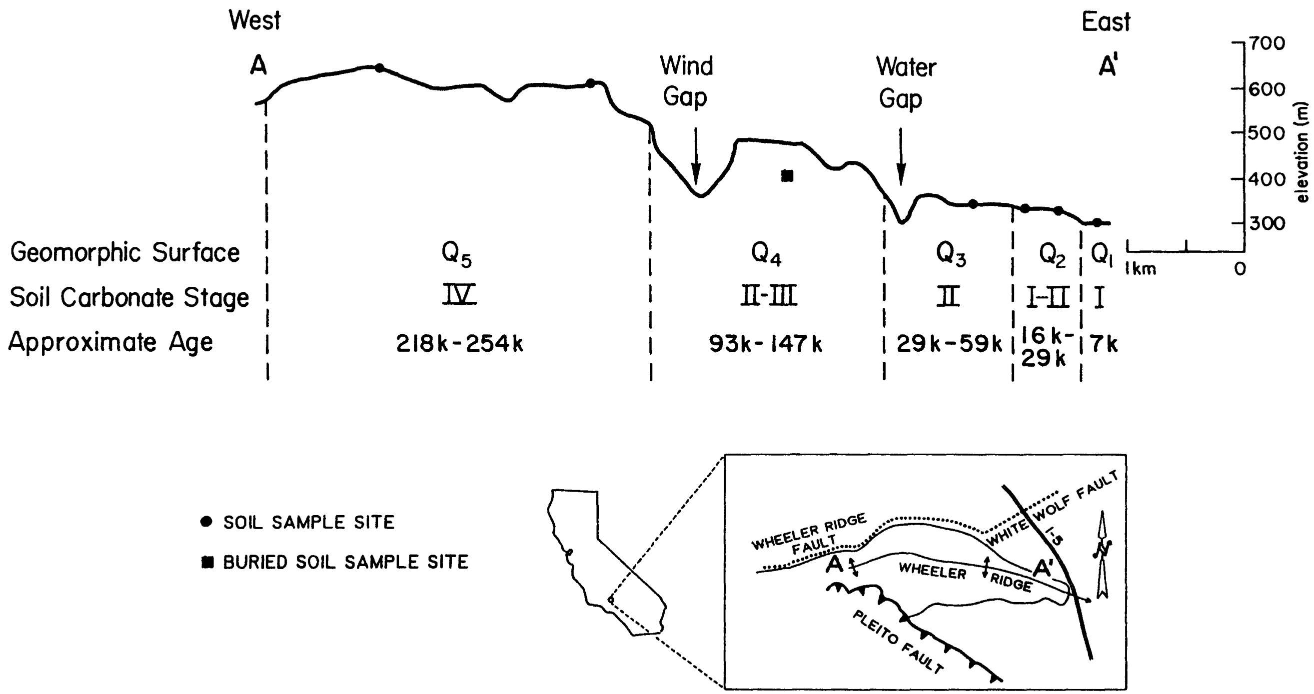

Figure 3. Topographic profile along the crest of Wheeler Ridge, showing five distinct geomorphic surfaces.

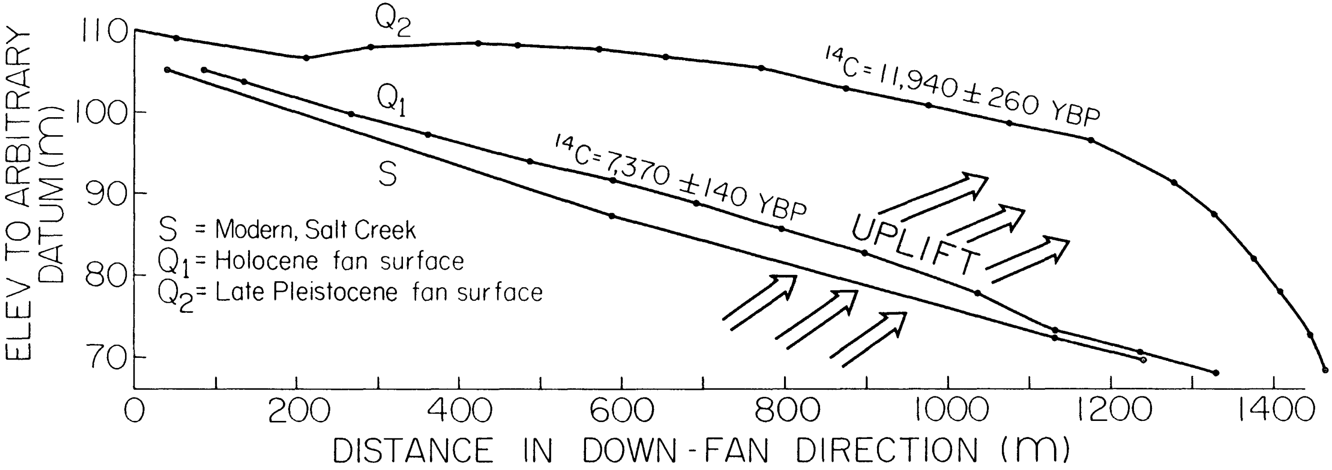

Figure 4. Surveyed profiles of deformed Q1 and Q2 surfaces at the eastern end of Wheeler Ridge.

Gile, L. H., Peterson, F. F., and Grossman, R. B., 1966, Morphological and genetic sequences of carbonate accumulation in desert soils: Soil Science, v. 10, p. 347-360.

Gutenberg, B., 1955, Epicenter and origin time of the main shock on July 21 and travel times of major phases, (in) Earthquakes in Kern County, California during 1952: California Division of Mines Bulletin, v. 181, p. 165-175.

Hall, N. T., 1984, Late Quaternary history of the eastern Pleito thrust fault, northern Transverse Ranges, California: Unpublished Ph.D. dissertation, Stanford University.

Harden, J. W., 1982, A quantitative index of soil development from field descriptions: Examples from a chronosequence in central California: Geoderma, v. 28, p. 1-28.

Medwedeff, D. A., 1984, Structural analysis of Wheeler Ridge, San Emigdio Mountains, California: Unpublished manuscript.

Stein, R. S., and King, C. P., 1984, Seismic potential revealed by surface folding: 1983 Coalinga, California earthquake: Science, v. 244, p. 869-872.

Stein, R. S., and Thatcher, W., 1981, Seismic and aseismic deformation associated with the 1952 Kern County, California, earthquake and relationship to the Quaternary history of the White Wolf fault: Journal of Geophysical Research, v. 86, p. 4913-4928.

STUDY OF SEISMIC ACTIVITY BY SELECTIVE TRENCHING ALONG THE ELSINORE FAULT ZONE, SOUTHERN CALIFORNIA

Contract 14-08-0001-21376

T. K. Rockwell
Geology Department
San Diego State University
San Diego, CA 92182

and

D. L. Lamar
Lamar-Merifield Geologists, Inc.
1318 Second Street, Suite 25
Santa Monica, CA 90401
Telephone: (213) 395-4528

Investigations

Study and logging of exposures in trenches across the Glen Ivy North fault, a strand of the Elsinore fault zone between Corona and Lake Elsinore, have continued. Displaced peat layers have been dated by Carbon 14 methods and dendrochronologically corrected. Additional peat layers have been submitted for carbon 14 dating.

Results

No new results will be available until dating of the additional carbon 14 samples is obtained.

Biological Premonitors of Earthquakes: A Validation Study

14-08-0001-16784
14-08-0001-19112

Leon S. Otis and William H. Kautz
SRI International
Menlo Park, CA 94025
(415) 859-3194

This prospective research project investigated the validity of the hypothesis that at least some members of one or more animal species may sense and react with unusual behavior to one or more earthquake precursors. Although this hypothesis has been strongly supported by anecdotal reports since antiquity, the scientific evidence supporting its validity is scant and is based mostly on retrospective studies. Interest in further investigation of the animal hypothesis by the USGS was generated in the late 1970s following the successful short-term prediction of several earthquakes in the People's Republic of China. A principal element of the Chinese program is reports of unusual behavior of animals by volunteer observers.

The SRI International project, modeled somewhat after the Chinese volunteer program, was initiated on January 12, 1978 and was renewed annually through October 31, 1982. The behavior of pets as well as domesticated and feral animals was observed by volunteers recruited from selected seismically active areas of California. Volunteer observers, because of their vocation or avocation, owned or were around one or more animals on a regular basis.

Most of the observers were concentrated in regions identified as the most likely populated sites of future major earthquakes, predicted on the basis of computer simulation of postulated observer locations relative to seismicity in California from 1945 to 1974. Most lived and/or worked in Humboldt County, the Greater San Francisco Bay Area (north to Santa Rosa, east to Livermore, and south to Santa Cruz and Hollister), the northern Los Angeles area (particularly around San Fernando), and the San Diego area.

The primary responsibility of each volunteer was to immediately call a dedicated toll-free telephone number (hot line) whenever he or she observed unusual animal behavior whose cause was not immediately observable and obvious. The hot line was operational 24 hours/day, 7 days/week. Each report was automatically tape-recorded and the date and time it was received were also recorded.

In addition, volunteer observers were required to call the hot line once a week, on a designated day, to check in. The check-in call was unrelated to whether or not an unusual animal response had been observed; it functioned to indicate each observer's continued participation in the project. Observers were also required to complete a daily check list to log the behavior of their animals and to mail the log to SRI monthly. (SRI provided self-addressed envelopes.) Observers' performance in meeting these responsibilities was monitored biweekly using specially written computer programs.

These two latter requirements functioned to permit the project leaders to quantify the degree of observer participation in the project, as well as to maintain observer interest and motivation. In addition, observers received a monthly newsletter which was both didactic (vis-à-vis earthquake phenomena, theories, and research) and informative (project results to date).

A computer-programmed model and analysis procedure that treated earthquakes and reports as independent events in time was developed during 1979 to evaluate the statistical significance of report frequency preceding earthquakes.

Data analysis required that a set of parameters be chosen to describe the period of time before an earthquake and the distance within which an observation of animal behavior could be considered (called the forespace) and the time and distance after an earthquake in which observations could not be considered (the afterspace). The sizes of the forespace and afterspace and the allowable magnitude thresholds were defined for each earthquake and a "control cylinder" was selected to define a baseline measure of "normal" reporting. For each earthquake evaluated, the data analysis enumerated the number of reports received in the forespace relative to the number received in the control space--the control cylinder minus the portions of all afterspaces and all other forespaces contained within it. This ratio was then compared with the volume ratios of the two regions being tallied. A binomial test was applied to test the null hypothesis: that the report density in the forespace was merely a random extrapolation of that observed in the control space cylinder.

Initially, preliminary sets of parameters were employed in the model to report provisional results to the USGS. A final set was selected in 1981 and applied to 13 candidate earthquakes of magnitude greater than

Richter 4.0 ($M > 4.0$) that occurred during 1979, 1980, and 1981.* Although none of the 13 earthquakes occurred within areas of heavy observer concentrations, they were selected for analysis because they were either large or appeared graphically to be preceded by a relatively greater number of reports from observers residing near the epicenters (i.e., less than 160 miles) as compared with the baseline report level. Seven significant correlations with null hypothesis probabilities ranging from 0.03 to < 0.00005 were found.

Although encouraging, these results are not conclusive. Scientific evidence that unequivocally establishes that the reported instances of unusual animal behavior resulted from precursory earthquake phenomena (as yet unidentified), and not from other causes, is not available.

Because a number of our findings were statistically significant, however, and because anomalous animal responses represent one of the few sources of observable data that may be useful, along with geophysical data, to predict an *imminent* earthquake, it would appear desirable to continue investigations of the animal hypothesis. In addition to collecting data from volunteer observers, it is recommended that research efforts be expended to identify the earthquake precursors to which selected species of animals (e.g., those most frequently reported as displaying unusual behavior) may be responding, and to test animal sensitivities to these precursor energy levels in rigorously controlled laboratory studies.

---

*Because the project was renewed without funding from January 1 through October 31, 1982, funds were not available to analyze the 1982 data. A preliminary analysis, however, suggested that none of the 1982 earthquakes of $M > 4.0$ were preceded by a sufficient number of reports to warrant further statistical analysis.

INDEX 1

INDEX ALPHABETIZED BY PRINCIPAL INVESTIGATOR

INDEX 2

INDEX ALPHABETIZED BY INSTITUTION